Gerd Czycholl

# Solid State Theory, Volume 1

## Basics: Phonons and Electrons in Crystals

Springer

# Solid State Theory, Volume 1

Gerd Czycholl

# Solid State Theory, Volume 1

## Basics: Phonons and Electrons in Crystals

Springer

Gerd Czycholl
Institut für Theoretische
Physik Universität Bremen
Bremen, Germany

ISBN 978-3-662-66134-5 ISBN 978-3-662-66135-2 (eBook)
https://doi.org/10.1007/978-3-662-66135-2

© The Editor(s) (if applicable) and The Author(s), under exclusive license to Springer-Verlag GmbH, DE, part of Springer Nature 2023
This work is subject to copyright. All rights are solely and exclusively licensed by the Publisher, whether the whole or part of the material is concerned, specifically the rights of translation, reprinting, reuse of illustrations, recitation, broadcasting, reproduction on microfilms or in any other physical way, and transmission or information storage and retrieval, electronic adaptation, computer software, or by similar or dissimilar methodology now known or hereafter developed.
The use of general descriptive names, registered names, trademarks, service marks, etc. in this publication does not imply, even in the absence of a specific statement, that such names are exempt from the relevant protective laws and regulations and therefore free for general use.
The publisher, the authors, and the editors are safe to assume that the advice and information in this book are believed to be true and accurate at the date of publication. Neither the publisher nor the authors or the editors give a warranty, expressed or implied, with respect to the material contained herein or for any errors or omissions that may have been made. The publisher remains neutral with regard to jurisdictional claims in published maps and institutional affiliations.

Responsible Editor: Tobias Kompatscher
This Springer imprint is published by the registered company Springer-Verlag GmbH, DE, part of Springer Nature.
The registered company address is: Heidelberger Platz 3, 14197 Berlin, Germany

# Preface to the Fourth (German) Edition

The great innovation in the long-planned new edition of the book "Solid State Theory" is the division into 2 volumes. This also takes into account the change in the German physics study program into Bachelor and Master degrees. The present volume 1 deals with the classical fields of theoretical solid state physics (Born-Oppenheimer approximation, electrons and phonons in periodic potentials, Bloch theorem, Hartree-Fock approximation, density functional theory, electron-phonon interaction). Only the basic lectures on theoretical physics (classical mechanics, electromagnetism, non-relativistic quantum mechanics and statistical physics) which already occur in the Physics Bachelor program are required. Volume 1 is therefore already suitable for students in the Bachelor program who want to gain an insight into an application area of theoretical physics, in particular quantum theory, in addition to the basic courses in "Theoretical Physics". The content of volume 1 is therefore suitable for an elective course "Theoretical (Solid State) Physics" in the Bachelor's degree program and as a basis for a Bachelor thesis. Every experimental solid state physicist should have knowledge of theoretical solid state physics to the extent of volume 1. Together with a book or script on experimental solid state physics, the content can therefore also be the basis for an elective course "Solid State Physics" or, together with the content of volume 2, the basis for an elective course "Theoretical (Solid State) Physics" in the Master program. However, for a Master thesis on theoretical solid state physics, knowledge beyond the content of volumes 1 and 2 is required, in particular special methods of many-particle theory.

The solutions to the exercise problems, which previously were only available in the Internet, are now included in the book. This sets a new focus on the exercise problems by taking up almost a third of the book. Since solving exercises is generally an essential part of teaching and learning of theoretical physics, the book thus gains an additional value. Some interesting results (e.g. tight-binding dispersions and density of states for fcc or bcc lattices or for graphene) can now be found in the solutions to the exercise problems. There are also some new exercise problems, so that Volume 1 now contains over 60 problems. The examples used in the exercises can be easily modified and extended to more realistic models, so that they can also serve as the basis for, for example, a bachelor's thesis.

Of course, my coworkers and research assistants contributed essentially to the exercise problems, testing them for physical sense and solvability with reasonable effort. I cannot list all the coworkers who have supervised the exercises to my solid state theory lectures over the years (now even decades). On behalf of all of them, I would like to mention here by name Dr. Ilan Schnell, whose study project has become an exercise problem and from whose other scientific work some figures are used, Dr. Claudia Schneider, to whom I am indebted for the suggestion to treat the numerically solvable exercise problems using Matlab, and Dr. Daniel Mourad, who has drawn my attention to various remaining errors and shortcomings in the 2nd and 3rd editions. I would also like to thank all colleagues, students and readers who have drawn my attention to individual errors that could be corrected in the new edition.

Bremen Gerd Czycholl
in July 2015

# Extract from the Preface to the First German Edition

This book is based on lectures (Solid State Theory I and II, each 4 h) which I have given since 1986 first at the University of Dortmund and RWTH Aachen and from 1991 several times at the University of Bremen. These lectures were not strictly based on one of the existing and well-known solid state physics or solid state theory books. Since the individual chapters were changed and revised several times when repeating the lecture, it is today no longer possible to specify exactly which book was followed in which chapters. Therefore, in the bibliography, I have only given the books in which I myself looked during the lecture preparation; the bibliography therefore by no means provides a complete overview of the existing solid state physics textbooks. In addition to these mentioned books, I had lecture manuscripts of my colleagues (or former teachers) Prof. Dr. E. Müller-Hartmann (University of Cologne), Prof. Dr. H. Keiter (University of Dortmund), Prof. Dr. P. H. Dederichs (RWTH Aachen) and my own transcript of the lecture by Prof. Dr. B. Mühlschlegel (University of Cologne, on superconductivity) while preparing the lectures. Since the handwritten manuscript became unreadable over time due to the constant revision, I rewrote everything from about 1995 and then immediately typed it in LaTeX and distributed it to the students as a script. The figures were first photocopied and glued in; when repeating the lecture, the figures were gradually produced by myself in Postscript format, a few were scanned, so that an entirely electronic version of the lecture script was available. From this script, the present book has emerged after further revision.

It is impossible to give a complete overview of solid state theory in a single book or in a two-semester solid state theory lecture intended for students in their 7th and 8th semesters. Therefore, only the most important basics can be covered here, and with regard to applications and current research topics in theoretical solid state physics, only a elementary introduction can be given each time. Even then, not everything can be addressed, and the selection of material is—at least as far as the topics beyond the basics presented in Volume 1 are concerned—somewhat subjective; other lecturers or authors would probably set different priorities and accents here depending on what they consider to be particularly interesting and important themselves. In any case, these more specific and current topics can only serve to spark interest in such an introduction, and for details one must refer to more specialized literature or to corresponding special lectures. Only the standard knowledge in theoretical physics, in particular quantum mechanics and statistical physics, as one learns about it in the introductory physics courses at German universities up to the 6th semester, is assumed in this book. Although (at least from Chap. 6 on) the occupation number representation ("2nd Quantization") is used, the more specialized methods of many-particle theory are not used or introduced here; therefore, the treatments of current topics and interaction effects remain on the level of molecular field approximations. The book is therefore intended overall for physics students from the 7th semester and also for students or physicists who work in experimental solid state physics. For theoretical solid state physicists, however, the book is usually not sufficient on its own, in particular because it does not yet contain enough many-particle theory (and also no group theory).

Bremen
in March 2000

Gerd Czycholl

# Contents

**1 Introduction** . . . . . . . . . . 1

**2 Periodic Structures** . . . . . . . . . . 5
- 2.1 Crystal Structure, Bravais Lattice, Wigner-Seitz Cell . . . . . . . . . . 5
  - 2.1.1 Crystallization of Solids . . . . . . . . . . 5
  - 2.1.2 Crystal System and Crystal Lattice . . . . . . . . . . 6
  - 2.1.3 Symmetry Group of the Crystal Systems . . . . . . . . . . 10
  - 2.1.4 Bravais Lattice, Primitive Unit Cell and Wigner-Seitz Cell. . . . . . . . . . . 11
  - 2.1.5 Crystal Structures. . . . . . . . . . . 14
- 2.2 The Reciprocal Lattice, Brillouin Zone . . . . . . . . . . 17
- 2.3 Periodic Functions . . . . . . . . . . 19
- 2.4 Problems for Chap. 2 . . . . . . . . . . 22

**3 Separation of Lattice and Electron Dynamics** . . . . . . . . . . 25
- 3.1 The General Solid-State Hamiltonian Operator. . . . . . . . . . . 25
- 3.2 Adiabatic Approximation (Born-Oppenheimer Approximation) . . . . . . . . . . 27
- 3.3 Bonding and Effective Nuclear-Nuclear Interaction . . . . . . . . . . 31
- 3.4 Problems for Chap. 3 . . . . . . . . . . 37

**4 Lattice Vibrations (Phonons)** . . . . . . . . . . 41
- 4.1 Harmonic Approximation, Dynamic Matrix and Normal Coordinates . . . . . . . . . . 41
- 4.2 Classical Equations of Motion. . . . . . . . . . . 44
- 4.3 Periodic or Born-von-Kármán Boundary Conditions . . . . . . . . . . 47
- 4.4 Quantized Lattice Vibrations and Phonon Dispersion Relations . . . . . . . . . . 50
- 4.5 Thermodynamics of Lattice Vibrations (Phonons), Debye and Einstein Model . . . . . . . . . . 54
- 4.6 Phonon Spectra and Densities of States. . . . . . . . . . . 62
  - 4.6.1 Example: Simple Cubic Lattice. . . . . . . . . . . 62
  - 4.6.2 Phonon Density of States. . . . . . . . . . . 66
- 4.7 Long Wavelength Limit . . . . . . . . . . 73
  - 4.7.1 Acoustic phonons and elastic waves . . . . . . . . . . 73

4.7.2 Long Wavelength Optical Phonons and Electromagnetic Waves, Polaritons . . . . . . . . . . . . . . . . . 78
4.8 (Neutron) Scattering on Crystals (Phonons), Debye-Waller Factor . . . . . . . . . . . . . . . . . . . . . . . . . . . . . . . . . 82
4.9 Anharmonic Corrections . . . . . . . . . . . . . . . . . . . . . . . . . . . . . . 88
4.10 Problems for Chap. 4 . . . . . . . . . . . . . . . . . . . . . . . . . . . . . . . . . . 89

**5 Non-interacting Electrons in the Solid State** . . . . . . . . . . . . . . . . . . . . 101
5.1 Electron in periodic potential, Bloch theorem . . . . . . . . . . . . . . . . 102
5.2 Nearly Free Electron Approximation . . . . . . . . . . . . . . . . . . . . . . . . 108
5.3 Effective mass tensor, group velocity and $\boldsymbol{k} \cdot \boldsymbol{p}$-perturbation theory . . . . . . . . . . . . . . . . . . . . . . . . . . . . . . . . . . . . . . . . . . . . . 114
5.4 Tight binding model, Wannier states . . . . . . . . . . . . . . . . . . . . . . . 117
5.5 Basic ideas of numerical methods for calculating the electronic band structure . . . . . . . . . . . . . . . . . . . . . . . . . . . . . . . . . 126
5.5.1 Cellular method . . . . . . . . . . . . . . . . . . . . . . . . . . . . . . . . 126
5.5.2 Expansion in plane waves . . . . . . . . . . . . . . . . . . . . . . . . 129
5.5.3 APW-(“Augmented Plane Waves”)-Method . . . . . . . . . . 129
5.5.4 Green function method by Korringa, Kohn and Rostoker, KKR method . . . . . . . . . . . . . . . . . . . . . . . . . . . 130
5.5.5 OPW-(“orthogonalized plane waves”)-method . . . . . . . . 132
5.5.6 Pseudopotential method . . . . . . . . . . . . . . . . . . . . . . . . . . . 134
5.6 Electronic classification of solids . . . . . . . . . . . . . . . . . . . . . . . . . . 135
5.7 Electronic density of states and Fermi surface . . . . . . . . . . . . . . . 141
5.8 Quantum statistics and thermodynamics of solid-state electrons . . . . . . . . . . . . . . . . . . . . . . . . . . . . . . . . . . . . . . . . . . . . . . 147
5.9 Statistics of electrons and holes in semiconductors . . . . . . . . . . . . 154
5.10 Problems for Chapter 5 . . . . . . . . . . . . . . . . . . . . . . . . . . . . . . . . . 158

**6 Electron–Electron Interaction** . . . . . . . . . . . . . . . . . . . . . . . . . . . . . . . 167
6.1 Occupation Number Representation (“Second Quantization”) for Fermions . . . . . . . . . . . . . . . . . . . . . . . . . . . . . 168
6.2 Models of Interacting Electron Systems in Solid State Physics . . . . . . . . . . . . . . . . . . . . . . . . . . . . . . . . . . . . . . . . . . . . . . . . 175
6.3 Hartree-Fock Approximation . . . . . . . . . . . . . . . . . . . . . . . . . . . . . 182
6.3.1 Derivation from the Ritz Variation Principle . . . . . . . . . . 182
6.3.2 Derivation from a Variational Principle for the Grand Canonical Potential . . . . . . . . . . . . . . . . . . . . . . . . . . . . . 189
6.4 Homogeneous Electron Gas in Hartree-Fock Approximation . . . . 195
6.5 Basic Ideas of Density Functional Theory . . . . . . . . . . . . . . . . . . . 201
6.6 Elementary Theory of Static Screening . . . . . . . . . . . . . . . . . . . . . 210
6.6.1 Thomas-Fermi Theory of Screening . . . . . . . . . . . . . . . . 211
6.6.2 Lindhard Theory of Screening . . . . . . . . . . . . . . . . . . . . . 213
6.6.3 Static Screening in Semiconductors . . . . . . . . . . . . . . . . 217
6.7 Excitations in the Homogeneous Electron Gas, Plasmons . . . . . . 219
6.8 Excitons in Semiconductors . . . . . . . . . . . . . . . . . . . . . . . . . . . . . . 225

6.9 Quasiparticles and Landau Theory of the Fermi Liquid . . . . . . . . 233
6.10 Problems for Chap. 6 . . . . . . . . . . . . . . . . . . . . . . . . . . . . . . . . . . 236

**7 Electron-phonon Interaction** . . . . . . . . . . . . . . . . . . . . . . . . . . . . . . 247
7.1 Hamiltonian of the Electron-Phonon Interaction . . . . . . . . . . . . . . 247
7.2 Renormalization of the Effective Electron Mass . . . . . . . . . . . . . . 253
7.3 Screening Effects on Phonon Dispersion and Electron-Phonon Interaction . . . . . . . . . . . . . . . . . . . . . . . . . . . . . 255
7.4 Electron-Phonon Interaction in Ionic Crystals . . . . . . . . . . . . . . . . 260
7.5 The Polaron . . . . . . . . . . . . . . . . . . . . . . . . . . . . . . . . . . . . . . . . . 262
7.6 Problems for Chap. 7 . . . . . . . . . . . . . . . . . . . . . . . . . . . . . . . . . . 266

**8 Solutions to the Exercise Problems** . . . . . . . . . . . . . . . . . . . . . . . . . 269
8.1 Solution of the Problems for Chap. 2 . . . . . . . . . . . . . . . . . . . . . . 269
8.2 Solution to Exercise Problems for Chap. 3 . . . . . . . . . . . . . . . . . . 274
8.3 Solution of the Exercise Problems for Chap. 4 . . . . . . . . . . . . . . . 281
8.4 Solution of the Problems for Chap. 5 . . . . . . . . . . . . . . . . . . . . . . 313
8.5 Solution to the Problems of Chap. 6 . . . . . . . . . . . . . . . . . . . . . . . 355
8.6 Solution to Problems in Chap. 7 . . . . . . . . . . . . . . . . . . . . . . . . . 389

**References** . . . . . . . . . . . . . . . . . . . . . . . . . . . . . . . . . . . . . . . . . . . . 399

# Introduction

# 1

Solid state physics deals with the properties of matter in the solid state, in particular with the structure, the electronic and the thermal properties of solids. A solid consists, like all condensed matter, i.e. matter as we find it under normal conditions (pressures and temperatures on earth), of atoms which are held together by chemical bonds. It differs from a molecule only in that the number of participating atoms is so large that the solid is a macroscopic object as a whole. While in a molecule the number of participating atoms is between 2 and a few 1000, a macroscopic solid consists of an unimaginably large number of constituents, of the order of $10^{23}$ atoms.

After what has been said, it is clear which physical methods we must use to describe the properties of a solid microscopically; since it consists of atoms and the chemical bond between atoms can be understood by the fact that there can be energetically more favorable electron states in the overlap potential of two atoms than in the isolated (far apart) individual atoms, we have to use quantum mechanics. And since we are dealing with a system of very many atoms (with also very many electrons), the solid (in addition to the ideal gas) is the standard example of a system to which we have to apply the methods of statistical physics. Solid State Theory is therefore nothing fundamentally new, but consists in the application of quantum theory and statistical physics to a specific physical problem or to a specific Hamiltonian operator.

In solid state physics, we are in the fortunate situation that we know the Hamiltonian exactly. Of the four known elementary interactions (weak interaction, strong interaction, electromagnetic interaction and gravitation), only one plays a role in solid state physics (as well as in atomic and molecular physics), namely the electromagnetic interaction, and we know the decisive potential quite exactly, namely the Coulomb potential. While in elementary particle physics one deals with the weak interaction mediated by massive bosons, the unified electro-weak or the strong interaction mediated by gluons, and in nuclear physics there is an

© The Author(s), under exclusive license to Springer-Verlag GmbH, DE, part of
Springer Nature 2023
G. Czycholl, *Solid State Theory, Volume 1*,
https://doi.org/10.1007/978-3-662-66135-2_1

effective (short-ranged) nuclear potential due to the exchange of pions, the exact spatial dependence of which (and analytical expression) we do not know in detail, we can safely neglect most interactions in solid state physics except for the well-known Coulomb interaction. Also, we can often neglect relativistic effects. Only for special effects one sometimes has to take into account other interactions (of relativistic origin) such as the spin-orbit interaction.

Nevertheless, the fundamental problem of solid state physics is difficult and not solvable in full generality. The reason for this is the fact that we are dealing with very many particles, which is why we also have to use the methods of statistical physics. But these methods are relatively easy to apply only if we are dealing with non-interacting particles, as is (almost) always the case for the examples dealt with in the introductory course on statistical physics. However, the particles (electrons and atomic nuclei) that make up a solid are anything but non-interacting, but they interact precisely via the (long-range) Coulomb interaction. At first it seems hopeless again to be able to at least partially treat or solve this complicated and complex many-particle problem of $10^{23}$ particles interacting with each other.

To get any further here, the development of new methods and approaches was therefore necessary within the framework of quantum theory of the (already restricted) solid state problem. These methods follow from their concept the principle of abstraction and modeling always used in theoretical physics. One tries to consider only certain partial aspects of the general solid state problem, which one assumes – on the basis of physical considerations – to already contain the most important contributions to a certain physical effect or phenomenon; mathematically this means that we make certain approximations and simplifications in the general solid state Hamiltonian operator in order to derive an effective Hamiltonian suitable for a specific sub-problem, which we can then (in contrast to the original) treat (if possible even solve exactly). The concept of approximating and simplifying the Hamiltonian operator to such an extent that certain elementary excitations can be formally represented as interaction-free quasiparticles (with Fermi or Bose character) occurs in solid state theory in many different places. The simplest example of this concept of quasiparticle description of elementary excitations are the phonons: First, one separates the lattice (i.e. atomic nucleus or ionic core) components from the electron component in the general Hamiltonian operator, makes the harmonic approximation for the lattice component, i.e. one expands to 2nd order around the equilibrium positions and thus finds an effective Hamiltonian operator, which describes coupled harmonic oscillators. This can be diagonalized by a principle axis transformation and by introducing the oscillator raising and lowering operators (well known from elementary quantum mechanics), and is formally brought into the form of a Hamilton operator, which describes non-interacting (quasi-)bosons, which we refer to as phonons. And this effective phonon Hamiltonian operator we can relatively easily treat and understand with the methods of elementary quantum statistics. But this quasiparticle concept also plays a role in other places in solid state physics; there are numerous quasiparticle descriptions of elementary excitations in the solid state, e.g. magnons for the description of spin waves, polarons (electrons with lattice polarization), excitons (bound electron-hole pairs) in semiconductor physics, polaritons, plasmons, etc.; if we use the concept of non-interacting electrons, which we can do for many aspects with some justification and good success, the solid state electrons are in fact also fermionic quasiparticles, since we have put the (always strong and never really negligible) interactions into effective parameters of a (non-interacting) one-particle model.

In addition to describing the special and most important solid state phenomena, the aim of this treatise is therefore also to introduce the special form of simplification and modeling, and in particular the quasiparticle concept, in order to learn the special working method and language of the solid state physicist.

# Periodic Structures

# 2

## 2.1 Crystal Structure, Bravais Lattice, Wigner-Seitz Cell

### 2.1.1 Crystallization of Solids

It is an experimental fact that the most stable state of matter is generally the crystalline state in which the atoms or the molecular groups are periodically arranged. It is physically clear that for a system of several or very many atoms or molecules in a solid, which are bound to each other and therefore interact with each other, there must be an equilibrium configuration that corresponds to the absolute minimum of the interaction potential. At sufficiently low temperatures, the atoms (or building blocks) are in this equilibrium configuration. If a system consists of very many identical atoms or other molecular building blocks and is overall macroscopically large, the environment of each building block looks the same from each position, which makes it understandable that a periodic, translationally invariant arrangement results. In addition, it is clear that a periodic arrangement is the more ordered state with the greater symmetry and thus the lower entropy, so that the crystalline state is most stable in thermodynamic equilibrium at low temperatures.

There are also non-crystalline solids, and these are precisely the ones that are particularly interesting and also the subject of current research. Examples include glasses, amorphous semiconductors, polymers, metallic glasses, random alloys, vapour-deposited layers, etc. In many of these systems, there is still a short-range order, i.e. the number and arrangement of the nearest neighbours is still similar to that in the crystal, but the long-range order has been lost. Many of these amorphous systems are obtained by rapidly solidifying them from the melt, i.e. from the liquid state, and it can be assumed that, by doing so, the atomic arrangement in the liquid is frozen and the system is not given the opportunity, by cooling rapidly, to reach the thermodynamically more stable state. Amorphous systems such as glasses are therefore usually not in the absolute minimum of the potential energy

© The Author(s), under exclusive license to Springer-Verlag GmbH, DE, part of Springer Nature 2023
G. Czycholl, *Solid State Theory, Volume 1*,
https://doi.org/10.1007/978-3-662-66135-2_2

but only in a relative (local) minimum, from which they cannot escape at sufficiently low temperatures because a thermally unattainable potential barrier has to be overcome. The amorphous state is therefore a metastable state and not the thermodynamically most favourable state.

In the introduction to solid state theory, we can restrict ourselves to the consideration of the crystalline state, in particular since the translational invariance enormously simplifies the theoretical description. For example, precisely because of the translational symmetry, the normal vibrations of crystals and, therefore, a system of $10^{23}$ particles can be determined in many cases exactly, as we will see in Chap. 4, while this is already more difficult for a much smaller molecule consisting of 100–1000 atoms. Since the crystalline state is so important for solid state physics, a brief overview of the possible lattices and crystal structures will be given in this chapter and the terms and notations commonly used for the description of crystals will be introduced.

### 2.1.2 Crystal System and Crystal Lattice

An ideal crystal is infinitely extended, that is, it occupies the entire three-dimensional space, and consists of a strictly periodic repetition of the same building element, i.e. the same atom or the same group of atoms. First, one distinguishes between **crystal system**, **crystal lattice** and **crystal structure**. A crystal lattice consists of lattice points in space, which are described by the position vector to these points. These lattice vectors can be represented in dimension $d$ as an integer linear combination of $d$ linearly independent basis vectors:

$$\boldsymbol{R}_{\boldsymbol{n}} = \sum_{i=1}^{d} n_i \boldsymbol{a}_i$$

where $\boldsymbol{n} = (n_1, \ldots, n_d)$ denotes a d-tuple of integers. The basis vectors $\boldsymbol{a}_i$ span the **unit cell** whose periodic continuation fills the whole space. The basis vectors do not have to be orthogonal to each other, the angles between them are denoted by $\alpha_i$. The volume $V_{ez}$ of the unit cell is therefore given for $d=2$ by $V_{ez} = |\boldsymbol{a}_1 \times \boldsymbol{a}_2|$, for $d=3$ by the scalar triple product $V_{ez} = |\boldsymbol{a}_1(\boldsymbol{a}_2 \times \boldsymbol{a}_3)|$.

The **primitive unit cell** is the smallest unit cell, the periodic repetition of which fills space. Unit cells cannot be chosen arbitrarily, but they must have a certain symmetry. For example, in 2 dimensions it is not possible to have regular pentagons as unit cells, as it is not possible to fill the whole plane with pentagons. On the other hand, this can be done with squares, rectangles, parallelograms and regular hexagons. It can be mathematically rigorously proven and immediately seen visually that for $d = 2$ and $d = 3$ there can only be crystal lattices with 2-, 3-, 4- or 6-fold symmetry[1].

According to the mentioned symmetry, one first distinguishes between different **crystal systems**. For $d = 2$ there are 4 crystal systems, namely

1. the square system with $a_1 = a_2, \alpha_1 = 90°$, so that the unit cell consists of squares and the lattice has a 4-fold rotational symmetry, reflection at 2 axes and inversion as symmetry operations,

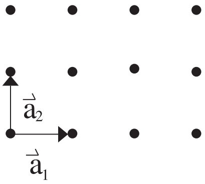

2. the rectangular system with $a_1 \neq a_2$, $\alpha_1 = 90°$, so that the unit cell consists of rectangles and the lattice only has reflection at 2 axes and inversion as symmetry operations,

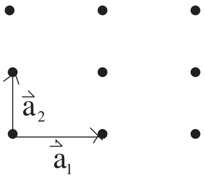

3. the hexagonal system (triangular lattice) with $a_1 = a_2$, but $\alpha_1 = 60°$, so that the unit cells are rhombuses and the lattice has 6-fold rotational symmetry, reflections at 3 axes, and inversion as symmetry operations,

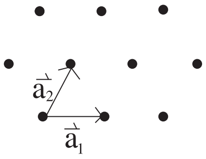

4. the obliquely angled lattice with $a_1 \neq a_2, \alpha_1 \neq 90°$, so that the unit cells are parallelograms and only inversion exists as a symmetry operation.

---

[1] It was therefore all the more surprising that in 1982, during X-ray diffraction measurements of special aluminum-manganese alloys, Israeli materials scientist D. Shechtman (* 1941, Chemistry Nobel Prize 2011) observed a 5-fold symmetry; such systems are now called quasicrystals.

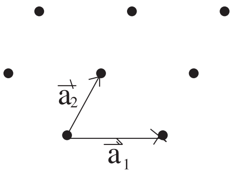

To each crystal **system** there may belong several **(crystal) lattices** or **Bravais lattices**[2]. In 2 dimensions there exists, for example, in addition to the simple rectangular lattice, the **centered rectangular** lattice, in which there is additionally a lattice point in the center of each rectangle.

This lattice could be considered as a special oblique lattice, but since it has all the symmetry properties of the rectangular system, it is considered as its own lattice type, as its own Bravais class, within the rectangular crystal system.

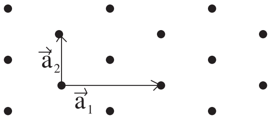

After the term crystal system and crystal lattice has been illustrated for the example of $d=2$, we want to state without proof which crystal systems are possible in 3-dimensional Euclidean space. For $d=3$ there are 7 crystal systems and 14 Bravais lattices, namely

1. the **cubic** system with a cube as (conventional) unit cell, i. e. $a_1 = a_2 = a_3 = a$ , $\alpha_1 = \alpha_2 = \alpha_3 = 90°$, and 3 associated Bravais lattices (simple cubic *sc*, face-centered cubic *fcc*, body-centered cubic *bcc*),

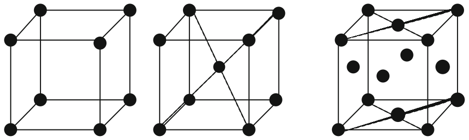

simple cubic body-centered cubic cubic face-centered

2. the **tetragonal** system with a cuboid with a square base as the unit cell, i. e. $a_1 = a_2 \neq a_3, \alpha_1 = \alpha_2 = \alpha_3 = 90°$, and two Bravais lattices (simple tetragonal and tetragonal-bodycentered or space-centered),

---

[2] Auguste Bravais, 1811–1863, French natural scientist, professor at the Polytechnicum in Paris, worked on crystal physics and optics and discovered in 1850 the 14 space lattices for $d=3$.

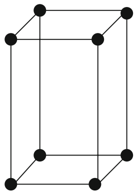

simply tetragonal

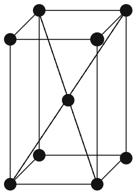

tetragonal space-centered

3. the **(ortho)rhombic** system with an abritary cuboid as the unit cell, i. e. $a_1 \neq a_2 \neq a_3 \neq a_1, \alpha_1 = \alpha_2 = \alpha_3 = 90^\circ$, and four Bravais lattices (simple, base-centered, face-centered, and body(space)-centered),

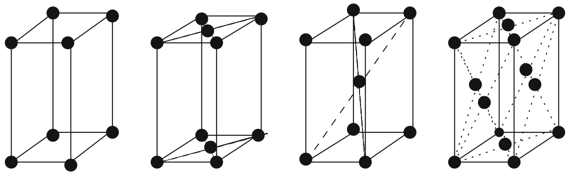

rhombic

simply base-centered body-centered face-centered

4. the **monoclinic** system with a parallelepiped with a rectangular base as the unit cell, i. e. $a_1 \neq a_2 \neq a_3, \alpha_1 = \alpha_3 = 90^\circ \neq \alpha_2$, and two Bravais lattices (simple or “primitive” and base-centered),

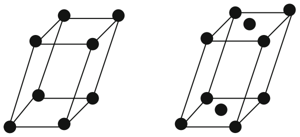

monoclinic

simply base-centered

5. the **rhombohedral** system with a rhombohedron as the unit cell (with equilateral rhombuses as the side faces), i. e. $a_1 = a_2 = a_3, \alpha_1 = \alpha_2 = \alpha_3 \neq 90^\circ$, and only one Bravais lattice,

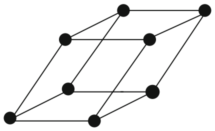

6. the **hexagonal** system with a parallelepiped with 2 rhombuses as base faces and 4 rectangles as side faces, i.e. $a_1 = a_2 \neq a_3, \alpha_1 = \alpha_2 = 90^\circ, \alpha_3 = 120^\circ$ and only one Bravais lattice,

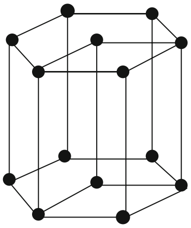

7. the **triclinic** system with any parallelepiped as the unit cell, i. e. $a_1 \neq a_2 \neq a_3, \alpha_1, \alpha_2, \alpha_3 \neq 90°$ and only one Bravais lattice.

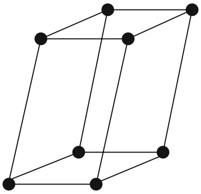

### 2.1.3 Symmetry Group of the Crystal Systems

The classification into the crystal systems is carried out according to the symmetry of the lattice. Every ideal, infinitely extended lattice always has translational invariance with respect to all lattice vectors to begin with. In addition, the lattices have **point symmetries**, i.e. there are certain discrete operations which transform the lattice into itself while keeping a point (the origin) fixed, e.g. rotations about certain axes and discrete angles, reflections at a lattice plane or axis, inversion (transformation $\boldsymbol{r} \to -\boldsymbol{r}$). These symmetry operations form a group mathematically with respect to their consecutive execution, namely the so-called **point group**. Each of the 7 listed crystal systems has a characteristic point group. All symmetry operations of the lattice (i.e. lattice translations plus point group operations including combinations of both) form the so-called **space group** of the lattice.

A detailed description of the point groups for all 7 listed crystal systems is omitted here. As an example, we only briefly describe the point group for the cubic system, which is the most important crystal system next to the hexagonal system. The following operations transform a cube and thus a cubic lattice into itself: Rotations by $90° = \frac{2\pi}{4}$ around 3 fourfold axes (through the midpoints of the cube sides), rotations by $120° = \frac{2\pi}{3}$ around 4 threefold rotation axes (space diagonals), and rotations by $180° = \pi$ around 6 twofold axes (around the diagonals through two opposite edge midpoints), and these 24 operations together form the so-called **Octahedral Group** $\boldsymbol{O}$, in addition there is inversion (point reflection at the origin), so that the cubic symmetry group $O_h$ (octahedral group plus inversion) contains 48 elements. This can be made clear independently in the following way: All relevant functions $f(x,y,z)$ must remain invariant in the event of cubic symmetry when exchanging the coordinates $(x, y, z)$: $f(x, y, z) = f(y, z, x) = \ldots = f(y, x, z)$, which corresponds to 6 operations, in addition they must be invariant against sign change: $f(x, y, z) = f(-x, y, z) = f(x, -y, z) = \ldots = f(-x, -y, -z)$, which corresponds to $2^3 = 8$ operations; in total there are $8 * 6 = 48$ symmetry operations, since both basic operations can be combined arbitrarily.

The group-theoretical classification of the crystal system and the associated symmetry can be of great importance in practice. All point symmetry operations have a natural representation as $3 * 3$ -matrices and each element corresponds to an operator in Hilbert space. Since the Hamiltonian for the crystalline solid also has the symmetry of the lattice, it commutes with the corresponding operators, which are therefore conserved quantities, and from quantum mechanics it is known that with such conservation laws, for example, special degeneracies can be connected. If the symmetry is lost or disturbed, such degeneracies are then lifted, which can be predicted and understood if the group-theoretical classification of the crystal symmetry and the resulting eigenvalues has been considered.

### 2.1.4 Bravais Lattice, Primitive Unit Cell and Wigner-Seitz Cell

As mentioned in Sect. 2.1.2, there are several Bravais lattices for some crystal systems, namely the cubic, orthorhombic, monoclinic and tetragonal system. These can be imagined to have arisen in that, in addition to the characteristic conventional unit cell of the system, there are also lattice points located either spatially in the center of the cell (space-or body-centered) or in the centers of the 6 surfaces of the cell (face-centered) or in the centers of the two base surfaces (base-centered). The primitive (i.e. smallest possible) unit cell of these centered lattices is no longer the (for the crystal structure and its symmetry) characteristic **conventional unit cell**. This shall be briefly explained for the three cubic lattices:

- **simple cubic (simple-cubic, sc) lattice:**
  There are 6 nearest-neighbor lattice sites for each lattice point. The natural primitive unit cell corresponds to the **conventional** unit cell (i.e. the unit cell characteristic for the system) and is thus a cube with edge length $a$, the three linearly independent unit vectors spanning this primitive elementary cell are connecting vectors to nearest-neighbor lattice points and are given with respect to the corresponding cartesian coordinate system by

$$\boldsymbol{a}_1 = a \begin{pmatrix} 1 \\ 0 \\ 0 \end{pmatrix} \quad \boldsymbol{a}_2 = a \begin{pmatrix} 0 \\ 1 \\ 0 \end{pmatrix} \quad \boldsymbol{a}_3 = a \begin{pmatrix} 0 \\ 0 \\ 1 \end{pmatrix},$$

the volume of the primitive unit cell is

$$V_{pEZ} = \boldsymbol{a}_1(\boldsymbol{a}_2 \times \boldsymbol{a}_3) = \det \begin{pmatrix} a & 0 & 0 \\ 0 & a & 0 \\ 0 & 0 & a \end{pmatrix} = a^3$$

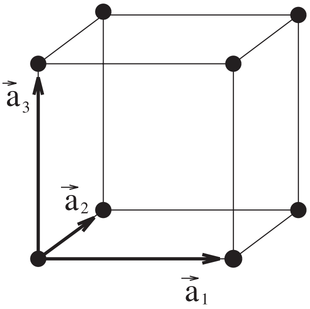

- **cubic face-centered (face-centered cubic, fcc) lattice:**
  A possible primitive unit cell is spanned by three linearly independent connection vectors to nearest-neighbor lattice sites; in total, there are 12 nearest neighbors for each lattice point. With respect to the Cartesian coordinate system, possible $\boldsymbol{a}_i$ are therefore

$$\boldsymbol{a}_1 = \frac{a}{2}\begin{pmatrix}1\\1\\0\end{pmatrix} \quad \boldsymbol{a}_2 = \frac{a}{2}\begin{pmatrix}1\\0\\1\end{pmatrix} \quad \boldsymbol{a}_3 = \frac{a}{2}\begin{pmatrix}0\\1\\1\end{pmatrix}$$

The volume of the primitive unit cell is therefore

$$V_{pEZ} = \boldsymbol{a}_1(\boldsymbol{a}_2 \times \boldsymbol{a}_3) = \frac{a^3}{8}\left|\det\begin{pmatrix}1&1&0\\1&0&1\\0&1&1\end{pmatrix}\right| = \frac{a^3}{4}$$

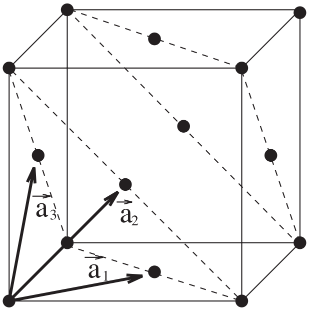

The fact that the volume of the primitive unit cell is only one fourth of the volume of the conventional unit cell (i.e. the cube of edge length $a$) expresses that there are effectively 4 lattice points per conventional unit cell. This can be seen by the following consideration: The eight vertices of the cube each belong to 8 unit cells, the 6 face centers each belong to 2 unit cells, so in total there are $8 \cdot \frac{1}{8} + 6 \cdot \frac{1}{2} = 4$ lattice points per conventional elementary cell (cube of edge length $a$).

- **cubic-space-centered (body-centered cubic, bcc) lattice:**
  For this lattice there are 8 nearest neighbors, namely the vertices of the cube with edge length $a$ surrounding the site at the center of this cube. Three linearly independent vectors connecting these nearest neighbors can again be chosen as basis vectors for the primitive unit cell. A possible choice is therefore:

$$\boldsymbol{a}_1 = \frac{a}{2}\begin{pmatrix}1\\1\\1\end{pmatrix} \quad \boldsymbol{a}_2 = \frac{a}{2}\begin{pmatrix}1\\-1\\1\end{pmatrix} \quad \boldsymbol{a}_3 = \frac{a}{2}\begin{pmatrix}-1\\1\\1\end{pmatrix}$$

$$V_{pEZ} = \boldsymbol{a}_1(\boldsymbol{a}_2 \times \boldsymbol{a}_3) = \frac{a^3}{8}\left|\det\begin{pmatrix}1 & 1 & 1\\ 1 & -1 & 1\\ -1 & 1 & 1\end{pmatrix}\right| = \frac{a^3}{2}$$

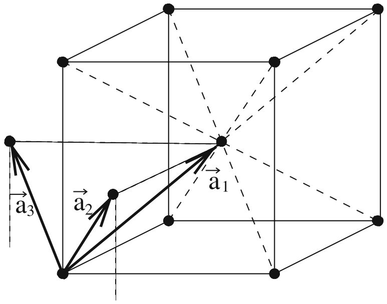

This again expresses that there are 2 lattice points per conventional unit cell, namely the central point with weigt 1 and the 8 corners of the cube with the weight $\frac{1}{8}$.

Another common cell in crystal lattices is the so-called **Wigner-Seitz**[3]-cell. It is centered around a lattice point and can be defined as the set of all points whose distance to this lattice point is smaller than to any other lattice point. The Wigner-Seitz cell can be constructed geometrically according to the following procedure: Draw the connecting lines from the lattice point under consideration to other lattice points (not just nearest neighbors) and construct the perpendicular bisector planes to these lines. Then the smallest body enclosed by the different planes forms the Wigner-Seitz cell. Only for the simple cubic lattice does the Wigner-Seitz cell have the shape of a cube again, in general more complicated figures result. The illustrations show the Wigner-Seitz cells for some two-dimensional lattices and for the fcc and bcc lattices. For the face-centered lattice, a rhombic dodecahedron results (with 12 faces in the form of equilateral rhombi corresponding to the 12 nearest neighbors), for the space-(body-)centered lattice a “truncated” octahedron results (8 faces of the mean perpendiculars to the connecting lines to 8 nearest neighbors, the 6 vertices of the equilateral octahedron are “truncated” by the perpendicular bisector planes on the connecting lines to the 6 next-nearest neighbors).

---

[3] Named after E.P. Wigner (* 1902 in Budapest, † 1995 in Princeton, famous theoretical physicist, pioneer in applications of symmetry principles and group theoretical methods in quantum theory, Nobel Prize 1963 for his contributions to theoretical nuclear physics) and F. Seitz (American physicist, * 1911 in San Francisco, † 2008 in New York, received his PhD under Wigner in Princeton, wrote one of the first solid state theory textbooks „Modern Theory of Solids" in 1940, later president of Rockefeller University in New York).

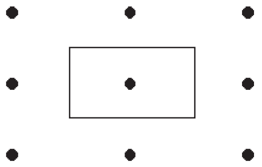

Wigner-Seitz cell of the 2d rectangular lattice

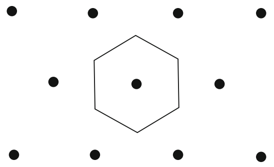

Wigner-Seitz cell of the 2d triangular lattice

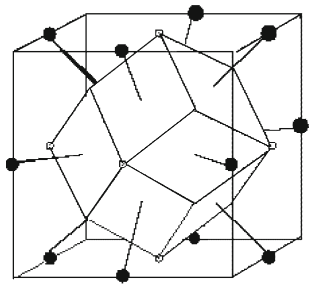

Wigner-Seitz cell of the 3d face-centered cubic lattice

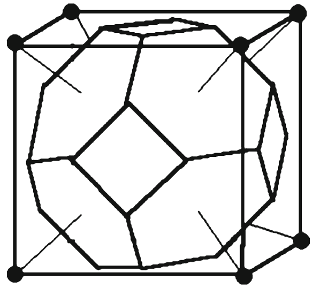

Wigner-Seitz cell of the 3d body-centred cubic lattice

Despite their different shapes, the volume of the Wigner-Seitz cell is equal to that of the primitive unit cell.

### 2.1.5 Crystal Structures

So far, we have only discussed the possible types of lattices and their symmetries and elementary cells. Nothing has been said about the arrangement of atoms in the elementary cell. Only with this additional information do we get the actual **crystal structure**. In addition to the type of lattice, we also need to specify the so-called **basis**. In a real crystal structure, there are usually several atoms per primitive elementary cell. To specify the basis, we need to know the position of the individual atoms within the elementary cell. The atom positions are then described by $\boldsymbol{R}_{n\mu} = \boldsymbol{R}_n + \boldsymbol{R}_\mu$ where $\boldsymbol{R}_n$ is a lattice vector and $\boldsymbol{R}_\mu$ indicates the position of the μ-th atom in the individual elementary cell; $\boldsymbol{R}_\mu$ is therefore restricted to the individual elementary cell. Here we will forego an overview of all possible crystal structures and instead only present some important examples of crystal structures.

- **Sodium chloride structure**
  This crystal structure consists of a face-centered cubic lattice with a two-atom basis (e.g., NaCl) with one atom (or ion, e.g., $Na^+$) at point $(0,0,0)$ and the other atom (ion, e.g., $Cl^-$) at $(\frac{1}{2},\frac{1}{2},\frac{1}{2})$ (with respect to the conventional elementary cell). If the two atoms in the elementary cell were identical, one would obtain a simple cubic lattice with lattice constant $a/2$. In particular, for NaCl the lattice constant is $a = 5.6$ Å. This is the characteristic order of magnitude for lattice constants. In addition to NaCl, other substances that crystallize in this structure include, for example, AgBr, KCl, PbS, etc.

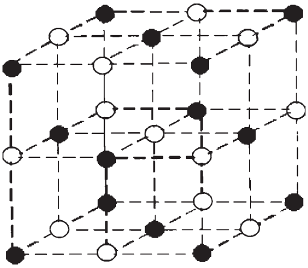

- **CsCl structure**
  This structure consists of a simple cubic lattice with a two-atom basis and one atom (ion, e.g. $Cs^+$) at $(0,0,0)$ and the other atom (ion, e.g. $Cl^-$) at $(\frac{1}{2},\frac{1}{2},\frac{1}{2})$. If the two atoms were identical, one would obtain a cubic-centered lattice. The lattice constant for CsCl is $a = 4.11$ Å. In addition to CsCl, other substances such as TlBr, CuZn, and AgMg also crystallize in this structure.

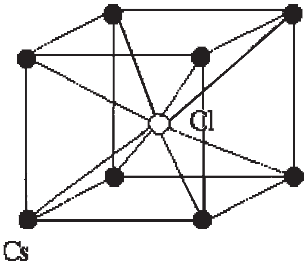

- **Diamond structure**
  The diamond structure is a face-centered cubic lattice with a two-atom basis of **identical** atoms (e.g., C) at $(0,0,0)$ and $(\frac{1}{4},\frac{1}{4},\frac{1}{4})$ (with respect to the conventional elementary cell). Therefore, there are 8 atoms in each conventional unit cell (4 lattice points of the fcc lattice $*2$). Each atom has only 4 nearest neighbors and 12 next-nearest neighbors. The four nearest neighbors of an atom have a distance of $\frac{\sqrt{3}}{4}a$ from it and form an (equal-sided) tetrahedron with edge length $a/\sqrt{2}$. In addition to carbon (diamond), silicon and germanium crystallize in the diamond structure.

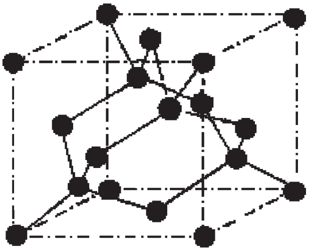

- **Zinc blende structure**

  The zinc blende structure also consists of an fcc lattice with a two-atom basis at $(0, 0, 0)$ and $(\frac{1}{4}, \frac{1}{4}, \frac{1}{4})$, in contrast to the diamond structure, the basis consists of 2 different atoms (ions), e.g. Zn and S. So each Zn atom is tetrahedrally surrounded by 4 S atoms and vice versa. In the ZnS structure, many of the (technologically important) III-V and II-VI semiconductors crystallize, in addition to ZnS, in particular GaAs, InAs, ZnSe, CdS, etc.

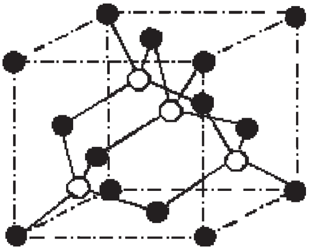

- **The hexagonal close-packed structure**

  The crystal structure of the “hexagonal close-packed” (hcp) structure consists of a hexagonal lattice with a basis of two identical atoms at $(0, 0, 0)$ and $(\frac{2}{3}, \frac{1}{3}, \frac{1}{2})$ with respect to the unit cell of the hexagonal lattice. It can be shown that in the fcc structure and in the hcp structure with a ratio $\frac{a_3}{a_1} = \sqrt{\frac{8}{3}}$ the smallest possible volume is occupied if the lattice points are occupied with spheres of finite radius $a_1/2$. This is where the name “close packed” comes from. Many elemental solids, e.g. Mg, Zn, Cd, etc. crystallize in the hcp-structure.

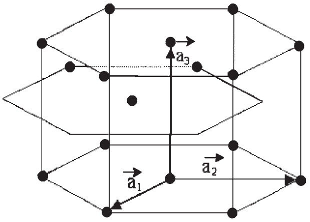

## 2.2 The Reciprocal Lattice, Brillouin Zone

Each Bravais lattice can be assigned a **reciprocal lattice**, so that its basis vectors $\boldsymbol{b}_j$ are orthogonal to the basis vectors $\boldsymbol{a}_i$ of the real lattice, by the following rule:

$$\boldsymbol{b}_1 = \frac{2\pi}{V_{pEZ}}(\boldsymbol{a}_2 \times \boldsymbol{a_3}), \quad \boldsymbol{b}_2 = \frac{2\pi}{V_{pEZ}}(\boldsymbol{a}_3 \times \boldsymbol{a_1}), \quad \boldsymbol{b}_3 = \frac{2\pi}{V_{pEZ}}(\boldsymbol{a}_1 \times \boldsymbol{a_2}) \tag{2.1}$$

where

$$V_{pEZ} = |\boldsymbol{a}_1 \cdot (\boldsymbol{a}_2 \times \boldsymbol{a}_3)| \tag{2.2}$$

is the volume of the primitive unit cell of the real lattice. For two-dimensional lattices, use the above definition accordingly with $\boldsymbol{a}_3 = (0,0,1)$. Each lattice point of the reciprocal lattice is then given by

$$\boldsymbol{G} = k_1\boldsymbol{b}_1 + k_2\boldsymbol{b}_2 + k_3\boldsymbol{b}_3 \tag{2.3}$$

with an integer triple $(k_1, k_2, k_3)$. The basis vectors of the direct and reciprocal lattices then satisfy the orthogonality relation

$$\boldsymbol{a}_i\boldsymbol{b}_j = 2\pi\,\delta_{ij}. \tag{2.4}$$

The scalar product of any lattice vector $\boldsymbol{R_n}$ with any reciprocal lattice vector is always an integer multiple of $2\pi$

$$\boldsymbol{R_n} \cdot \boldsymbol{G} = \sum_{i=1}^{3} n_i\boldsymbol{a}_i \sum_{j=1}^{3} k_j\boldsymbol{b}_j = 2\pi \sum_{i=1}^{3} n_i k_i. \tag{2.5}$$

Conversely, any vector $\boldsymbol{G}$ that yields an integer multiple of $2\pi$ as the scalar product with all lattice vectors $\boldsymbol{R}$ is a reciprocal lattice vector; because otherwise it would have a representation $\boldsymbol{G} = \sum_j x_j\boldsymbol{b}_j$ with non-integer $(x_1, x_2, x_3)$, since the $\boldsymbol{b}_j$ definitely form a basis; let $x_j$ be not an integer, then for the special direct lattice vector $\boldsymbol{a}_j$ also $\boldsymbol{G}\boldsymbol{a_j} = 2\pi x_j$ the scalar product is not an integer multiple of $2\pi$, contradiction.

The volume of the (primitive) elementary cell of the reciprocal lattice is given by

$$V_{rEZ} = |\boldsymbol{b}_1 \cdot (\boldsymbol{b}_2 \times \boldsymbol{b}_3)| = \left(\frac{2\pi}{V_{pEZ}}\right)^3 (\boldsymbol{a}_2 \times \boldsymbol{a}_3)((\boldsymbol{a}_3 \times \boldsymbol{a}_1) \times (\boldsymbol{a}_1 \times \boldsymbol{a}_2))$$

$$= \left(\frac{2\pi}{V_{pEZ}}\right)^3 (\boldsymbol{a}_2 \times \boldsymbol{a}_3)[\boldsymbol{a}_1 \cdot (\boldsymbol{a}_3 \cdot (\boldsymbol{a}_1 \times \boldsymbol{a}_2)) - \boldsymbol{a}_3 \cdot ((\boldsymbol{a}_1 \times \boldsymbol{a}_2) \cdot \boldsymbol{a}_1)]$$

$$= \frac{(2\pi)^3}{V_{pEZ}}. \tag{2.6}$$

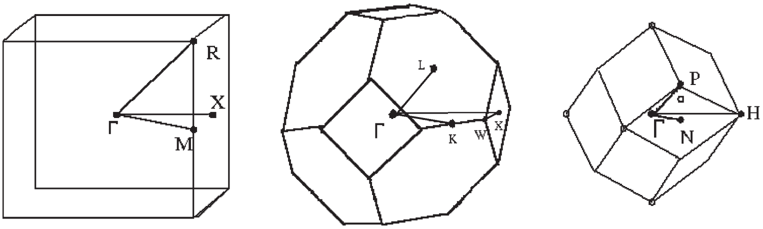

**Fig. 2.1** The first Brillouin zone for the simple-cubic, the fcc, and the bcc lattice; also depicted are the special symmetry points between which one usually plots the course of phonon dispersions and electronic energy bands

The Wigner-Seitz cell of the reciprocal lattice is called the **first Brillouin zone**[4]. The reciprocal lattice of the simple cubic lattice is again a simple cubic lattice, the reciprocal lattice of the fcc lattice is the bcc lattice and vice versa. Therefore, the first Brillouin zone of the fcc lattice corresponds to the Wigner-Seitz cell of the bcc lattice and vice versa. The reciprocal lattice of the reciprocal lattice is again the direct lattice. In Fig. 2.1 the first Brillouin zones of the three cubic lattices are shown; here also special symmetry points are indicated, which are conventionally denoted by special letters: thus the center of the 1st Brillouin zone is also called "Gamma point" $\Gamma = (0,0,0)$, the point $\frac{\pi}{a}(1,0,0)$ is also called X point for the simple cubic or fcc lattice and H of the bcc lattice, and for the simple cubic system the point $\frac{\pi}{a}(1,1,0)$ is denoted by N and $\frac{\pi}{a}(1,1,1)$ by R. The names of the analogous symmetry points in the fcc and bcc lattice can be taken from the figure. It is customary to represent the phonon dispersion relation and the electronic energy bands along special symmetry directions within the first Brillouin zone between these special points (cf. Chap. 4 and 5).

Reciprocal lattice vectors uniquely describe families of parallel lattice planes. Namely, each reciprocal lattice vector is perpendicular to a family of lattice planes of the direct Bravais lattice. A lattice plane of a Bravais lattice is spanned by three lattice points not lying on a straight line, a family of lattice planes is the set of lattice planes parallel to each other. Namely, to a given family of parallel lattice planes,

$$\boldsymbol{G} = \frac{2\pi}{d}\boldsymbol{n} \tag{2.7}$$

describes a reciprocal lattice vector if $\boldsymbol{n}$ is the normal unit vector on the family of lattice planes and $d$ is the distance of adjacent ones. Then, for two lattice vectors $\boldsymbol{R}_1, \boldsymbol{R}_2$ to lattice points from the same plane it is valid:

$$\boldsymbol{G} \cdot (\boldsymbol{R}_1 - \boldsymbol{R}_2) = 0$$

---

[4] Named after L. Brillouin, * 1889 in Sevres (France), † 1969 in New York, French physicist, professor in Paris, from 1942 in the USA, worked on approximation methods in quantum mechanics (including the WKB method), solid state physics and quantum statistics.

for $\boldsymbol{n} \perp (\boldsymbol{R}_1 - \boldsymbol{R}_2)$. But if $\boldsymbol{R}_1, \boldsymbol{R}_2$ are lattice vectors to points from different planes of the same family, having distance $ld$, then

$$\boldsymbol{n} \cdot (\boldsymbol{R}_1 - \boldsymbol{R}_2) = ld$$

and therefore

$$\boldsymbol{G} \cdot (\boldsymbol{R}_1 - \boldsymbol{R}_2) = 2\pi l.$$

Since the origin is also contained in each family of parallel lattice planes, the following applies to each lattice vector $\boldsymbol{R}$

$$\boldsymbol{G} \cdot \boldsymbol{R} = 2\pi l \tag{2.8}$$

with an integer $l$, which shows that the $\boldsymbol{G}$ defined above is actually a reciprocal lattice vector. This is also already the shortest reciprocal lattice vector that has this property, because if there were a shorter one in the same direction $\boldsymbol{n}$, then for $\boldsymbol{R}_1, \boldsymbol{R_2}$ from adjacent planes in the family $|\boldsymbol{G} \cdot (\boldsymbol{R}_1 - \boldsymbol{R}_2)| < 2\pi$, i.e. there would be lattice vectors for which the scalar product with $\boldsymbol{G}$ would not be an integer multiple of $2\pi$, contradiction. Conversely, for every reciprocal lattice vector $\boldsymbol{G}$ there is a lattice plane and thus also a family of lattice planes to which $\boldsymbol{G}$ is orthogonal, for example, let

$$\boldsymbol{G} = h\boldsymbol{b}_1 + k\boldsymbol{b}_2 + l\boldsymbol{b}_3 \tag{2.9}$$

with an integer triple $(hkl)$. Then $\boldsymbol{G}$ is obviously orthogonal to, for example, the linearly independent lattice vectors

$$\boldsymbol{R}_1 = k\boldsymbol{a}_1 - h\boldsymbol{a}_2, \quad \boldsymbol{R}_2 = l\boldsymbol{a}_1 - h\boldsymbol{a}_3.$$

By $\boldsymbol{R}_1, \boldsymbol{R}_2$ a lattice plane is spanned and by shifting to endpoints of different lattice vectors a family of parallel lattice planes is determined, on which $\boldsymbol{G}$ is orthogonal.

Thus, any reciprocal lattice vector uniquely determines a family of parallel planes in the direct lattice. It is customary to classify lattice planes by specifying the so-called **Miller indices** $(hkl)$ ; this means that $\boldsymbol{G} = h\boldsymbol{b}_1 + k\boldsymbol{b}_2 + l\boldsymbol{b}_3$ is the shortest reciprocal lattice vector orthogonal to the lattice planes. The distance between adjacent lattice planes is then

$$d = \frac{2\pi}{|\boldsymbol{G}|}. \tag{2.10}$$

## 2.3 Periodic Functions

Many physical quantities and functions relevant to a solid or crystal, such as the potential $V(\boldsymbol{r})$, the (electron or ion) density $\rho(\boldsymbol{r})$, etc., have the translational invariance of the lattice, i.e. they satisfy

$$f(\boldsymbol{r}) = f(\boldsymbol{r} + \boldsymbol{R}) \tag{2.11}$$

for any lattice vector $\boldsymbol{R}$ of the Bravais lattice. It is therefore sufficient to know the functions within a single elementary cell (or the Wigner-Seitz cell) in order to know them throughout space. Such functions can of course be represented as a Fourier series:

$$f(\boldsymbol{r}) = \sum_{\boldsymbol{G}} f_{\boldsymbol{G}} e^{i\boldsymbol{G}\boldsymbol{r}} \tag{2.12}$$

with discrete Fourier coefficients

$$f_{\boldsymbol{G}} = \frac{1}{V_{EZ}} \int_{EZ} d^3r f(\boldsymbol{r}) e^{-i\boldsymbol{G}\boldsymbol{r}}, \tag{2.13}$$

where $V_{EZ}$ denotes the volume of the (primitive) unit cell . From the condition $f(\boldsymbol{r}) = f(\boldsymbol{r}+\boldsymbol{R})$ it follows that

$$e^{i\boldsymbol{G}\boldsymbol{R}} = 1 \rightarrow \boldsymbol{R}\boldsymbol{G} = 2\pi n \tag{2.14}$$

with integer $n$ for all lattice vectors $\boldsymbol{R}$, so the Fourier series runs over the reciprocal lattice vectors.

The function system $\left\{ \frac{1}{\sqrt{V_{EZ}}} e^{i\boldsymbol{G}\boldsymbol{r}} \right\}$ forms a basis on the space of square-integrable functions on the unit cell of the real lattice, if $\boldsymbol{G}$ runs through all points of the reciprocal lattice; this basis is periodic with respect to lattice vectors $\boldsymbol{R}$ of the real lattice. The following orthonormality relations apply:

$$\frac{1}{V_{EZ}} \int_{EZ} d^3r e^{i(\boldsymbol{G}-\boldsymbol{G}')\boldsymbol{r}} = \delta_{\boldsymbol{G}\boldsymbol{G}'} \tag{2.15}$$

$$\sum_{\boldsymbol{G}} e^{i\boldsymbol{G}\boldsymbol{r}} = V_{EZ} \sum_{\boldsymbol{R}} \delta(\boldsymbol{r}-\boldsymbol{R}). \tag{2.16}$$

To prove this, we represent $\boldsymbol{r}, \boldsymbol{G}$ with respect to the basis vectors of the primitive unit cells of the real and reciprocal lattices; then it applies:

$$\boldsymbol{r} = \sum_{i=1}^{3} x_i \boldsymbol{a}_i, \boldsymbol{G} = \sum_{j=1}^{3} h_j \boldsymbol{b}_j$$

with $0 \leq x_i \leq 1$, since $\boldsymbol{r} \in EZ$, but integer $h_j$. This implies:

$$\frac{1}{V_{EZ}} \int_{EZ} d^3r e^{i\boldsymbol{G}\boldsymbol{r}} = \prod_{i=1}^{3} \int_0^1 dx_i e^{i2\pi x_i h_i} = \begin{cases} 0 & \text{if there is one } h_i \neq 0 \\ 1 & \text{if all } h_i = 0 \end{cases}.$$

Furthermore, for an arbitrary (thus not necessarily lattice-periodic) function $f(\boldsymbol{r})$

$$\begin{aligned} \int d^3r f(\boldsymbol{r}) \sum_{\boldsymbol{G}} e^{i\boldsymbol{G}\boldsymbol{r}} &= \sum_{\boldsymbol{R}} \sum_{\boldsymbol{G}} \int_{EZ} d^3r' f(\boldsymbol{R}+\boldsymbol{r}') e^{i\boldsymbol{G}(\boldsymbol{R}+\boldsymbol{r}')} = \\ &= \sum_{\boldsymbol{R}} \sum_{\boldsymbol{G}} \int_{EZ} d^3r' g^{\boldsymbol{R}}(\boldsymbol{r}') e^{i\boldsymbol{G}\boldsymbol{r}'} = \sum_{\boldsymbol{R}} \sum_{\boldsymbol{G}} V_{EZ} g^{\boldsymbol{R}}_{-\boldsymbol{G}} = \\ &= V_{EZ} \sum_{\boldsymbol{R}} g^{\boldsymbol{R}}(\boldsymbol{r}=0) = V_{EZ} \sum_{\boldsymbol{R}} f(\boldsymbol{R}). \end{aligned}$$

Here $g^{\boldsymbol{R}}(\boldsymbol{r})$ denotes the one lattice-periodic function that agrees on the unit cell around $\boldsymbol{R}$ just with the arbitrary function $f(\boldsymbol{r})$. Because of the arbitrariness of $f(\boldsymbol{r})$, (2.16) is thus proved.

Since the direct lattice is again the reciprocal lattice of the reciprocal lattice, we can formulate the relations (2.15), (2.16) accordingly for the reciprocal lattice:

$$\frac{V_{EZ}}{(2\pi)^3}\int_{1.BZ} d^3k e^{i\boldsymbol{k}(\boldsymbol{R}-\boldsymbol{R}')} = \delta_{\boldsymbol{R},\boldsymbol{R}'} \tag{2.17}$$

$$\frac{V_{EZ}}{(2\pi)^3}\sum_{\boldsymbol{R}} e^{i\boldsymbol{k}\boldsymbol{R}} = \sum_{\boldsymbol{G}} \delta(\boldsymbol{k}-\boldsymbol{G}). \tag{2.18}$$

**Example of application: Crystal structure analysis using X-ray diffraction**

When free particles (e.g. photons), which can be described as a plane wave $e^{i\boldsymbol{k}\boldsymbol{r}}$, hit a crystal, they are scattered at a lattice-periodic potential, which fulfills $V(\boldsymbol{r}) = V(\boldsymbol{r}+\boldsymbol{R})$ for all lattice vectors $\boldsymbol{R}$, and pass into a state $\boldsymbol{k}'$. As is known from quantum mechanics and will be used explicitly in later chapters (cf. e.g. Sect. 4.8), for quantities such as the transition probability (e.g. in Born's approximation), the matrix element $\langle \boldsymbol{k}'|V(\boldsymbol{r})|\boldsymbol{k}\rangle$ must be determined in any case. This is calculated as follows:

$$\langle \boldsymbol{k}'|V(\boldsymbol{r})|\boldsymbol{k}\rangle = \frac{1}{V}\int d^3r e^{-i\boldsymbol{k}'\boldsymbol{r}}V(\boldsymbol{r})e^{i\boldsymbol{k}\boldsymbol{r}} \tag{2.19}$$

$$= \frac{1}{V}\int d^3r \sum_{\boldsymbol{G}} V_{\boldsymbol{G}} e^{i(\boldsymbol{k}+\boldsymbol{G}-\boldsymbol{k}')\boldsymbol{r}} = \sum_{\boldsymbol{G}} V_{\boldsymbol{G}}\delta_{\boldsymbol{k}'-\boldsymbol{k},\boldsymbol{G}}.$$

For scattering on crystals, therefore, the selection rule

$$\boldsymbol{k}' = \boldsymbol{k}+\boldsymbol{G} \tag{2.20}$$

with $\boldsymbol{G}$ a reciprocal lattice vector applies. The wave vector of the scattered and incident quantum must therefore differ by a reciprocal lattice vector. In particular, for elastic scattering with $k^2 = k'^2$, this leads to the condition

$$2\boldsymbol{k}\boldsymbol{G} + \boldsymbol{G}^2 = 0. \tag{2.21}$$

We have seen that the absolute value of reciprocal lattice vectors can always be represented as $|\boldsymbol{G}| = \frac{2\pi n}{d}$ with $d$ distance of parallel lattice planes on which $\boldsymbol{G}$ is orthogonal. The photon wave vector is also given by $k = \frac{2\pi}{\lambda}$, if λ is the wavelength of the light used. Then it follows:

$$2\frac{4\pi^2 n}{d\lambda}\cos(\sphericalangle(\boldsymbol{k},\boldsymbol{G})) + \frac{4\pi^2 n^2}{d^2} = 0. \tag{2.22}$$

This results in the **Bragg condition**[5]:

$$2d\sin\theta = n\lambda \tag{2.23}$$

Here, θ is the angle between the incident beam and the lattice plane, therefore $\sphericalangle(\boldsymbol{k},\boldsymbol{G}) = \frac{\pi}{2}+\theta$ applies.

## 2.4 Problems for Chap. 2

**Problem 2.1** ***Sphere packing in crystal structures***

Estimate for the simple cubic crystal structure, for the fcc structure, the bcc structure and the hcp structure, which packing ratio one obtains, if one occupies the atomic sites with hard spheres of maximum possible radius (hard spheres, which may only touch and may not penetrate each other).

*Note*: In the hcp structure ("hexagonal close-packed") there is a hexagonal lattice with a ratio $\frac{c}{a}=\sqrt{\frac{8}{3}}$ and a basis consisting of 2 atoms at $(0,0,0)$ and $\frac{1}{3}\boldsymbol{a}_1+\frac{1}{3}\boldsymbol{a}_2+\frac{1}{2}\boldsymbol{a}_3$, if $\boldsymbol{a}_1,\boldsymbol{a}_2,\boldsymbol{a}_3$ span the primitive unit cell of the hexagonal lattice. With respect to a Cartesian coordinate system, these primitive translations can, for example, be the row vectors.

$$\boldsymbol{a}_1=\left(a,0,0\right), \quad \boldsymbol{a}_2=\left(\tfrac{1}{2}a,\tfrac{\sqrt{3}}{2}a,0\right), \quad \boldsymbol{a}_3=\left(0,0,\sqrt{\tfrac{8}{3}}a\right)$$

To determine the packing ratio for a given structure, you only need to consider how many spheres with which radius per primitive (or conventional) unit cell are possible, and then divide the volume of these spheres by the volume of this unit cell.

**Problem 2.2** ***Direct and reciprocal lattices***

a) Show that the reciprocal lattice of the reciprocal lattice is the original lattice again.
b) Show that fcc and bcc lattices are reciprocal to each other.

---

[5] W.H. Bragg (* 1862 in Westward (England), † 1942 in London) and his son W.L. Bragg (* 1890 in Adelaide (Australia), † 1971 in Ipswich, England) developed the X-ray diffraction method for crystal structure analysis and the Bragg equation together 1912-13, shared Nobel Prize 1915.

### Problem 2.3 *Centered Rectangular Lattice*

a) Determine the reciprocal lattice of a centered rectangular lattice. Which Bravais lattice is obtained?

b) Draw the first Brillouin zone of the centered rectangular lattice.

### Problem 2.4 *Crystal Structure of $La_2CuO_4$*

$La_2$ $CuO_4$ has a tetragonal space-(body-)centered structure; with respect to the conventional unit cell (with a square of length $a_1 = a_2 = a \approx 3.8$ Å as the base and $a_3 = c \approx 13.2$ Å) the atoms are arranged as follows:

Cu at $(0, 0, 0)$ and $(\frac{1}{2}, \frac{1}{2}, \frac{1}{2})$

O at $(\frac{1}{2}, 0, 0)$, $(0, \frac{1}{2}, 0)$, $(0, 0, \frac{1}{6})$, $(\frac{1}{2}, \frac{1}{2}, \frac{1}{3})$, $(1, \frac{1}{2}, \frac{1}{2})$, $(\frac{1}{2}, 1, \frac{1}{2})$, $(\frac{1}{2}, \frac{1}{2}, \frac{2}{3})$, $(1, 1, \frac{5}{6})$

La at $(0, 0, \frac{1}{3})$, $(\frac{1}{2}, \frac{1}{2}, \frac{1}{6})$, $(\frac{1}{2}, \frac{1}{2}, \frac{5}{6})$, $(1, 1, \frac{2}{3})$.

a) Sketch this structure by representing the atomic distribution in one (and up to four) conventional elementary cells.

b) How many formula units are there per conventional and per primitive elementary cell?

c) Convince yourself that each copper ion is surrounded by an (in $c$-direction slightly stretched) octahedron of 6 oxygen ions.

d) Convince yourself that at a distance of $\frac{c}{2}$ $CuO_2$ layers form and determine the lattice and basis of these two-dimensional layers.

### Problem 2.5 *Wurtzite structure*

The Wurtzite structure, which occurs in some II-VI semiconductors and III-nitride semiconductors (e.g. GaN) – in addition to the zinc blende structure – corresponds to a hcp structure with a basis of 2 atoms A and B at a distance $\frac{3}{8}|\boldsymbol{a}_3|$ in the z-direction. So what Bravais lattice and what basis are there in total? Show that (similar to the zinc blende structure) each B atom is tetrahedrally surrounded by 4 A atoms at a distance $\frac{3}{8}|\boldsymbol{a}_3|$ (and vice versa).

# Separation of Lattice and Electron Dynamics

# 3

## 3.1 The General Solid-State Hamiltonian Operator

We begin with the explicit specification of the general solid-state Hamiltonian operator mentioned in the introduction. A solid consists of $N_\mathrm{K}$ atomic nuclei of masses $M_k$ and nuclear charges $Z_k$ (i. e. charge $Z_k e$), where $e$ denotes the (positive) elementary charge, and $N_\mathrm{e}$ electrons of charge $-e$. Because of charge neutrality, one has

$$N_\mathrm{e} = \sum_{k=1}^{N_\mathrm{K}} Z_k \; . \tag{3.1}$$

If $N_\mathrm{K}$ identical atomic nuclei with mass $M$ and nuclear charge $Z$ are present, one has $N_\mathrm{e} = Z N_\mathrm{K}$.

Under the assumption that one can neglect relativistic effects, the Hamiltonian operator (in “1st Quantization”) can be written as:

$$H = T_\mathrm{K} + T_\mathrm{e} + V_\text{K-K} + V_\text{e-e} + V_\text{e-K} \tag{3.2}$$

where

$$T_\mathrm{e} = \sum_{i=1}^{N_\mathrm{e}} \frac{\boldsymbol{p}_i^2}{2m} \tag{3.3}$$

denotes the kinetic energy of the electrons,

$$T_\mathrm{K} = \sum_{k=1}^{N_\mathrm{K}} \frac{\boldsymbol{P}_k^2}{2M_k} \tag{3.4}$$

© The Author(s), under exclusive license to Springer-Verlag GmbH, DE, part of Springer Nature 2023

G. Czycholl, *Solid State Theory, Volume 1*,
https://doi.org/10.1007/978-3-662-66135-2_3

the kinetic energy of the atomic nuclei,

$$V_{\text{e-e}} = \sum_{i<j} v_{\text{e-e}}\left(\boldsymbol{r}_i - \boldsymbol{r}_j\right) \tag{3.5}$$

the interaction of the electrons with each other,

$$V_{\text{K-K}} = \sum_{k<l} v_{\text{K-K}}(\boldsymbol{R}_k - \boldsymbol{R}_l) \tag{3.6}$$

the interaction of the nuclei with each other and

$$V_{\text{e-K}} = \sum_{i,k} v_{\text{e-K}}(\boldsymbol{r}_i - \boldsymbol{R}_k) \tag{3.7}$$

the (attractive) interaction between the positive atomic nuclei and the negatively charged electrons.

Here, $\boldsymbol{P}_k$ and $\boldsymbol{R}_k$ are the momentum and position of the $k$-th nucleus, and $\boldsymbol{p}_i$ and $\boldsymbol{r}_i$ are the momentum and position of the $i$-th electron. In the general form above (3.2)–(3.7), the Hamiltonian operator can also describe the situation where the heavy particles are not the bare atomic nuclei, but the ions, i.e. atomic nuclei plus inner shells, which can often be considered as rigidly connected to the nucleus. Then the interaction potentials $v_{\text{e-K}}, v_{\text{K-K}}$ would not be the free Coulomb potentials, but rather the effective potentials screened by the inner electron shells between the ions or between a positive ion and outer electrons. However, if we consider the bare nuclei, all three interaction potentials $v_{\text{e-e}}, v_{\text{e-K}}, v_{\text{K-K}}$ are given by the elementary Coulomb interaction, so the repulsive interaction between 2 electrons at the locations $\boldsymbol{r}, \boldsymbol{r}'$ is:

$$v_{\text{e-e}}\left(\boldsymbol{r} - \boldsymbol{r}'\right) = \frac{e^2}{|\boldsymbol{r} - \boldsymbol{r}'|}\ , \tag{3.8}$$

the repulsive interaction between the bare atomic nuclei $k, l$:

$$v_{\text{K-K}}(\boldsymbol{R}_k - \boldsymbol{R}_l) = \frac{Z_k Z_l e^2}{|\boldsymbol{R}_k - \boldsymbol{R}_l|} \tag{3.9}$$

and the attractive interaction between the ($Z_k$-fold) positively charged nucleus $k$ and a negatively charged electron at the location $\boldsymbol{r}$:

$$v_{\text{e-K}}(\boldsymbol{r} - \boldsymbol{R}_k) = \frac{-Z_k e^2}{|\boldsymbol{r} - \boldsymbol{R}_k|} \tag{3.10}$$

In order to estimate the relative magnitude of the individual contributions to (3.2), we use **atomic units**. Radii of atoms and thus also the distance of atoms in condensed matter are of the order of a few Å. The natural unit of length is therefore the Bohr radius $a_0 = \hbar^2/me^2 = 0.5\,\text{Å} = 0.5 \times 10^{-8}\,\text{cm}$, and accordingly we measure energies in units of $E_0 = me^4/\hbar^2 = e^2/a_0 = 0.43 \times 10^{-10}\,\text{erg} = 2\,\text{Ry} = 27.2\,\text{eV}$. We therefore replace position vectors according to $\boldsymbol{r} = a_0\boldsymbol{r}$ with dimensionless vector $\boldsymbol{r}$, position derivatives (the nabla operator) by $\nabla_r = \frac{\partial}{\partial \boldsymbol{r}} = \frac{1}{a_0}\partial/\partial\boldsymbol{r}$. Thus we obtain after simple conversion the dimensionless Hamiltonian operator

$$H/E_0 = -\frac{1}{2}\sum_i \frac{\partial^2}{\partial \boldsymbol{r}_i^2} - \frac{1}{2}\sum_k \frac{m}{M_k}\frac{\partial^2}{\partial \boldsymbol{R}_k^2} + \sum_{i<j}\frac{1}{|\boldsymbol{r}_i - \boldsymbol{r}_j|} \tag{3.11}$$

$$+\sum_{k<l}\frac{Z_k Z_l}{\left|\boldsymbol{R_k} - \boldsymbol{R_l}\right|} - \sum_{i,k}\frac{Z_k}{\left|\boldsymbol{r_i} - \boldsymbol{R_k}\right|}\ .$$

Obviously, this only depends on the nuclear charge numbers $Z_k$ and the mass ratios $m/M_k$. In particular, the relative magnitude of the contribution of the kinetic energy of the atomic nuclei (or ions) is exactly this factor $m/M_k$ smaller than the other contributions to the Hamiltonian operator. Since $m/M_k$ is of the order of $10^{-4}$–$10^{-5}$, an expansion in this parameter and thus in the kinetic energy of the atomic nuclei suggests itself. In lowest approximation one will therefore consider the nuclei to be motionless and thus consider electrons in the potential of the nuclei at fixed positions and take into account the influence of the movement of the nuclei (or ions) only perturbatively. This smallness of the parameter $m/M_k$ is thus the decisive reason why we can consider lattice and electron motion in lowest order as decoupled from each other (i.e. lattice vibrations, i.e. phonons, and electrons can be treated independently of each other in lowest order), and corrections to this (i.e. the electron-phonon interaction) can be considered perturbatively. This decoupling of lattice and electron degrees of freedom, which we can understand qualitatively with the above simple dimensional argument, will be discussed in more quantitative terms in the following section.

## 3.2 Adiabatic Approximation (Born-Oppenheimer Approximation)

The considerations of the last section suggest that the kinetic energy of the (heavy) nuclei should be considered as a perturbation and neglected in lowest order. We therefore decompose the solid-state Hamiltonian operator (3.2) according to:

$$H = H_0 + T_\mathrm{K}$$

$$H_0 = T_\mathrm{e} + V_\text{e-K}(\underline{\boldsymbol{r}}, \underline{\boldsymbol{R}}) + V_\text{e-e}(\underline{\boldsymbol{r}}) + V_\text{K-K}(\underline{\boldsymbol{R}}) \tag{3.12}$$

where $\underline{\boldsymbol{r}} = (\boldsymbol{r}_1, \ldots, \boldsymbol{r}_{N_\mathrm{e}})$ is the $3N_\mathrm{e}$-dimensional vector of electron positions and $\underline{\boldsymbol{R}} = (\boldsymbol{R}_1, \ldots, \boldsymbol{R}_{N_\mathrm{K}})$ is the $3N_\mathrm{K}$-dimensional vector of all atomic nucleus positions. We now assume that we can solve the Schrödinger equation associated with $H_0$; this Schrödinger equation is only a differential equation with respect to the electron positions $\underline{\boldsymbol{r}}$, since the nuclear impulses do not occur in $H_0$. Therefore, the nuclear positions only enter the Schrödinger equation associated with $H_0$ as parameters. In other words, $H_0$ describes the quantum mechanical problem of $N_\mathrm{e}$ (interacting) electrons in the static potential that is generated by $N_\mathrm{K}$ atomic nuclei at fixed positions $\underline{\boldsymbol{R}}$. These fixed nuclear positions therefore only enter as parameters in the electronic wave functions $\{\phi_\alpha(\underline{\boldsymbol{r}}; \underline{\boldsymbol{R}})\}$ and eigenvalues $\varepsilon_\alpha(\underline{\boldsymbol{R}})$:

$$H_0\phi_\alpha(\underline{\boldsymbol{r}};\underline{\boldsymbol{R}}) = \varepsilon_\alpha(\underline{\boldsymbol{R}})\phi_\alpha(\underline{\boldsymbol{r}};\underline{\boldsymbol{R}}) \tag{3.13}$$

where $\{\alpha\}$ describes a complete set of electronic quantum numbers. For each configuration $\underline{\boldsymbol{R}}$ of the nuclei, the $\{\phi_\alpha(\underline{\boldsymbol{r}};\underline{\boldsymbol{R}})\}$ form a complete set of basis functions. A general wave function $\psi(\underline{\boldsymbol{r}},\underline{\boldsymbol{R}})$ of the full solid-state Hamiltonian operator $H$, i.e. a solution of the eigenvalue problem

$$H\psi(\underline{\boldsymbol{r}},\underline{\boldsymbol{R}}) = E\psi(\underline{\boldsymbol{r}},\underline{\boldsymbol{R}}) \tag{3.14}$$

can, therefore, be expanded for each fixed $\underline{\boldsymbol{R}}$ in terms of the basis functions $\phi_\alpha(\underline{\boldsymbol{r}};\underline{\boldsymbol{R}})$, i.e.:

$$\psi(\underline{\boldsymbol{r}},\underline{\boldsymbol{R}}) = \sum_\alpha \chi_\alpha(\underline{\boldsymbol{R}})\phi_\alpha(\underline{\boldsymbol{r}};\underline{\boldsymbol{R}})\ . \tag{3.15}$$

Inserting this into (3.14) yields:

$$(H-E)\psi(\underline{\boldsymbol{r}},\underline{\boldsymbol{R}}) = \sum_\alpha (H_0 + T_\mathrm{K} - E)\chi_\alpha(\underline{\boldsymbol{R}})\phi_\alpha(\underline{\boldsymbol{r}};\underline{\boldsymbol{R}}) = \tag{3.16}$$

$$= \sum_\alpha (\varepsilon_\alpha(\underline{\boldsymbol{R}}) + T_\mathrm{K} - E)\chi_\alpha(\underline{\boldsymbol{R}})\phi_\alpha(\underline{\boldsymbol{r}};\underline{\boldsymbol{R}}) = 0$$

If one multiplies from the left by $\phi^*_\beta(\underline{\boldsymbol{r}};\underline{\boldsymbol{R}})$ and integrates over all electron positions $\underline{\boldsymbol{r}}$, one obtains

$$(T_\mathrm{K} + \varepsilon_\beta(\underline{\boldsymbol{R}}))\chi_\beta(\underline{\boldsymbol{R}}) + \sum_\alpha A_{\beta,\alpha}(\underline{\boldsymbol{R}})\chi_\alpha(\underline{\boldsymbol{R}}) = E\chi_\beta(\underline{\boldsymbol{R}}) \tag{3.17}$$

with

$$A_{\beta,\alpha}(\underline{\boldsymbol{R}}) = -\sum_l \frac{\hbar^2}{2M_l}\int d\underline{\boldsymbol{r}}\left[\phi^*_\beta(\underline{\boldsymbol{r}};\underline{\boldsymbol{R}})\frac{\partial^2}{\partial {\boldsymbol{R}_l}^2}\phi_\alpha(\underline{\boldsymbol{r}};\underline{\boldsymbol{R}})\right.$$

$$\left. +2\phi^*_\beta(\underline{\boldsymbol{r}};\underline{\boldsymbol{R}})\left(\frac{\partial}{\partial \boldsymbol{R}_l}\phi_\alpha(\underline{\boldsymbol{r}};\underline{\boldsymbol{R}})\right)\frac{\partial}{\partial \boldsymbol{R}_l}\right]\ . \tag{3.18}$$

The product rule

$$\frac{\partial^2}{\partial {\boldsymbol{R}_l}^2}(\phi_\alpha(\underline{\boldsymbol{r}};\underline{\boldsymbol{R}})\chi_\alpha(\underline{\boldsymbol{R}})) = \phi_\alpha(\underline{\boldsymbol{r}};\underline{\boldsymbol{R}})\frac{\partial^2}{\partial {\boldsymbol{R}_l}^2}\chi_\alpha(\underline{\boldsymbol{R}}) + 2\frac{\partial}{\partial \boldsymbol{R}_l}\phi_\alpha(\underline{\boldsymbol{r}};\underline{\boldsymbol{R}})\frac{\partial}{\partial \boldsymbol{R}_l}\chi_\alpha(\underline{\boldsymbol{R}})$$

$$+\ \chi_\alpha(\underline{\boldsymbol{R}})\frac{\partial^2}{\partial {\boldsymbol{R}_l}^2}\phi_\alpha(\underline{\boldsymbol{r}};\underline{\boldsymbol{R}}) \tag{3.19}$$

and the completeness and orthonormality of the $\{\phi_\alpha(\underline{\boldsymbol{r}};\underline{\boldsymbol{R}})\}$ were used here. If one now neglects the contributions $A_{\beta,\alpha}(\underline{\boldsymbol{R}})$, i.e. transition matrix elements between different electronic quantum numbers $\alpha,\beta$, one obtains

$$(T_\mathrm{K} + \varepsilon_\beta(\underline{\boldsymbol{R}}))\chi_\beta(\underline{\boldsymbol{R}}) = E\chi_\beta(\underline{\boldsymbol{R}})\ . \tag{3.20}$$

This is obviously a Schrödinger equation for the atomic nuclei in the effective potential $\varepsilon_\beta(\underline{\boldsymbol{R}})$; the electronic eigenenergies therefore determine (via their parametric dependence on the nuclear positions $\underline{\boldsymbol{R}}$) the effective potential for the nuclei (into which the bare Coulomb repulsion $V_{\text{K-K}}$ enters additively). All effects of the chemical binding of the ions (nuclei) to each other and the energetic favoring of the formation of the crystal structure must be contained therein and is a consequence of the fact that $\varepsilon_\beta(\underline{\boldsymbol{R}})$ has a minimum for special positions $\underline{\boldsymbol{R}}_0$.

In order to get an idea of the order of magnitude of the eigenenergies $E$ in (3.20) of the pure nuclear motion, we can imagine that we expand the $\varepsilon_\alpha(\underline{\boldsymbol{R}})$ around these equilibrium positions $\underline{\boldsymbol{R}}_0$ to second order in the displacements, as one does anyway in the harmonic approximation (discussed in the next chapter). Then one has to deal with (coupled) harmonic oscillators, for which the ($\underline{\boldsymbol{R}}$-dependence of) electronic eigenenergies form the harmonic potential. The lattice energies $E$ are known to be of the order of the eigenfrequency $E \sim \hbar\omega \sim \sqrt{K/M}$, where the effective spring constant is given by $K \sim \partial^2\varepsilon/\partial R^2$. Thus, for the eigenenergies $E$ or the frequencies of the nuclear motion, the order of magnitude estimate

$$E_k^2 = \hbar^2\omega^2 \sim \frac{K}{M} \sim \frac{E_e}{M\Delta R^2} \sim \frac{E_e m^2 e^4}{M\hbar^4} = \frac{m}{M}E_e^2$$

is valid, where it was used that displacements from the equilibrium positions are of the order of the Bohr radius: $\Delta R \sim a_0 = \hbar^2/me^2$. So for the motion (vibration) of the atomic nuclei, typical energies are to be expected to be smaller by a factor $\sqrt{m/M}$ than typical electronic energies.

We now have to convince ourselves that it is justified to neglect the (in the space of the wave functions $\chi_\alpha(\underline{\boldsymbol{R}})$ still as an operator acting) contributions $A_{\beta\alpha}(\underline{\boldsymbol{R}})$. Since in the Schrödinger equation (3.13) for the electrons the core-core interaction $V_{\text{K-K}}$ only occurs as an additive constant to the Hamilton operator, the $\underline{\boldsymbol{R}}$-dependence of the wave functions $\phi_\alpha(\underline{\boldsymbol{r}},\underline{\boldsymbol{R}})$ essentially results from the electron-nucleus interaction $V_{\text{e-K}}$. Therefore, only a dependence on the relative positions $|\boldsymbol{r}_i - \boldsymbol{R}_k|$ is to be expected, which is why $\frac{\partial}{\partial \boldsymbol{R}_l}$ can be rewritten as $\frac{\partial}{\partial \boldsymbol{r}_i}$. This makes the first contribution to $A_{\beta\alpha}$ in (3.18) essentially $\frac{m}{M}\langle\phi_\beta|T_e|\phi_\alpha\rangle$, this contribution is therefore by a factor of the order of magnitude $m/M$ smaller than the kinetic energy of the electrons and thus the purely electronic eigenenergies $\varepsilon_\alpha$ and still by a factor $\sqrt{m/M}$ smaller than the eigenenergies of the nuclear motion. The magnitude of the second contribution to $A_{\beta\alpha}(\underline{\boldsymbol{R}})$ can be estimated analogously as follows:

$$\begin{aligned}
\frac{\hbar^2}{2M}\int d\underline{\boldsymbol{r}}\,\phi_\beta^*(\underline{\boldsymbol{r}},\underline{\boldsymbol{R}})\frac{\partial}{\partial\underline{\boldsymbol{R}}}\phi_\alpha(\underline{\boldsymbol{r}},\underline{\boldsymbol{R}})\frac{\partial}{\partial\underline{\boldsymbol{R}}}\chi_\alpha(\underline{\boldsymbol{R}}) &\sim \frac{\hbar}{M}\langle\phi_\beta|p_e|\phi_\alpha\rangle\frac{\partial}{\partial\underline{\boldsymbol{R}}}\chi_\alpha(\underline{\boldsymbol{R}}) \\
&\sim \frac{1}{M}\langle p_e\rangle\cdot\langle P_{\text{k}}\rangle \sim \frac{1}{M}\sqrt{mE_e}\sqrt{ME_{\text{k}}} \\
&= \sqrt{\frac{m}{M}\left(\frac{m}{M}\right)^{\frac{1}{2}}E_e^2} = \left(\frac{m}{M}\right)^{\frac{3}{4}}E_e \,.
\end{aligned} \tag{3.21}$$

This neglected energetic contribution is therefore by a factor $(m/M)^{3/4}$ smaller than the purely electronic energies and still by a factor $(m/M)^{1/4}$ smaller than the characteristic energies of the movement of the nuclei in the effective potential. This factor $(m/M)^{1/4}$ is of the order of $10^{-1}$–$10^{-2}$.

The **adiabatic approximation** (Born-Oppenheimer approximation) consists in neglecting the $A_{\beta\alpha}$-terms in the – in principle exact – equation (3.17). This separates the electron and the atomic nuclei motion from each other. In principle, one therefore has to proceed as follows:

1. First, for given nuclear positions $\underline{\boldsymbol{R}} = (\boldsymbol{R}_1, \ldots, \boldsymbol{R}_{N_K})$, the Schrödinger equation (3.13) for the electron problem has to be solved. The energy eigenvalues $\varepsilon_\alpha(\underline{\boldsymbol{R}})$ depend on these nuclear positions.
2. Then, for each given electronic quantum number α, the Schrödinger equation (3.20) has to be solved, where the electronic eigenenergies $\varepsilon_\alpha(\underline{\boldsymbol{R}})$ form the effective potential for the atomic nuclei.

The physical motivation for this approach is the idea that the electron system adapts practically instantaneously to the nuclear motion. Even if the atomic nuclei are in motion, the electronic system sees a static potential, as if the nuclei were fixed at the locations $\boldsymbol{R}_k$. This is not the case in reality and would only be fulfilled if the nuclei had an infinitely large mass in comparison to the electrons, from which it can be seen again that the mass ratio $m/M$ is the decisive parameter for the justification of the approximation. One can also argue with the different time scales on which the electron motion and the movement of the atomic nuclei or ions takes place. The decoupling is justified if the movement of the nuclei takes place so slowly that the "much faster" electron system has enough time to adjust to the new nuclear positions and the nuclear system behaves like a time-independent, static system on the electronic time scale. Therefore, one also speaks of "adiabatic approximation", since the nuclear system changes over time so slowly that the state of fixed, quasi-static nuclear positions is always established for the electron system.

The fact that the simplest correction to the complete separation of electron and nuclear dynamics according to the above estimate is of the order of magnitude $\left(\frac{m}{M}\right)^{1/4} \approx 10^{-1}$–$10^{-2}$ already shows that its influence is not completely negligible and that the coupling of electron and lattice dynamics plays an important role. However, the existence of a small parameter justifies a perturbative treatment of this contribution, which is explicitly carried out in the later chapter on electron-phonon coupling.

The principle of the adiabatic approximation has been developed shortly after the development of quantum mechanics for molecules (Born[1] and

---

[1] M. Born, * 1882 in Breslau (Germany, now Polish Wroclaw), † 1970 in Göttingen, PhD 1906 in Göttingen, from around 1910 work on lattice dynamics in crystals, from 1921 as a professor in Göttingen groundbreaking work on the formulation and the foundations of quantum mechanics, 1933 emigrated, from 1936 professor in Edinburgh, work on quantum electrodynamics and again on lattice dynamics in crystals, 1953 returned to Germany, Nobel Prize 1954.

Oppenheimer[2] 1927). The goal was the quantum mechanical explanation of the chemical bond and thus the formation of molecules. The reason why we can use this method here practically unchanged in solid state physics is that solids are ultimately nothing else but macroscopically large macromolecules.

For each electronic quantum number α there is a corresponding functional dependence of the eigenenergy $\varepsilon_\alpha$ on the nuclear positions. If chemical bonding occurs, it is to be expected that these functions will have minima for special configurations $\{\boldsymbol{R}_k\}$. For solids, the crystal structures should then automatically result as the energetically most favorable configurations. In practice, however, this Born-Oppenheimer method is hardly feasible in full generality. In any case, one is usually only interested in the electronic ground state $\varepsilon_0(\underline{\boldsymbol{R}})$. Effective and successful methods have been developed in recent years and decades for the calculation of the electronic ground state energy of solids, namely the density functional method to be discussed in Sect. 6.5 in connection with the band structure calculation methods to be discussed in Sect. 5.5. With these methods, one can in principle also calculate the crystal structure. However, it is not possible to calculate the full dependence of the ground state energy on $\underline{\boldsymbol{R}}$ and then read off the crystal structure from the absolute minimum of this function, but one can specify the known crystal structures as configurations and then compare the resulting ground state energies with each other to determine which structure is energetically favored at least at low temperatures.

Since one cannot calculate the dependence of $\varepsilon_0(\boldsymbol{R_1}, \ldots, \boldsymbol{R}_{N_\text{K}})$ on the nuclear positions, one also does not know the effective potential in which the atomic nuclei move as a result of the binding mediated by the electrons. For this effective potential, therefore, semi-empirical model approaches are often made, and the common models for the description of the effective nuclear-nuclear potential are discussed in the next section.

## 3.3 Bonding and Effective Nuclear-Nuclear Interaction

Since one does not know the effective potential $V_\text{eff}(\boldsymbol{R}_1, \ldots, \boldsymbol{R}_{N_\text{K}})$, in which the atomic nuclei move, which ultimately holds the nuclei together, and which – at least for the equilibrium configuration, i.e. for low temperatures – should ultimately follow from the dependence of the electronic ground state energy $\varepsilon_0(\boldsymbol{R}_1, \ldots, \boldsymbol{R}_{N_\text{K}})$ on the nuclear positions according to the previous section, one often resorts to model approaches for this. Here, ideas about the dominant type of chemical bond flow into the model approaches. In this section, the most important types of bonds and associated model approaches for nuclear-nuclear interaction potentials are summarized.

---

[2] J. R. Oppenheimer, * 1904 in New York, † 1967 in Princeton, basic studies at Harvard University, PhD 1927 with M. Born in Göttingen, in the USA further work on quantum theory, later head of the Manhattan Project, which was carried out from 1943 at his instigation in Los Alamos (New Mexico), from 1947 at Princeton University.

Strictly speaking, there are no fundamentally different types of chemical bonds, but there is a chemical bond which is mediated by the electrons in that they can lower their energy in the potential of several nuclei. When we speak here of different types of bonds, then different conceivable limiting cases of the chemical bond are meant, which differ, for example, in whether the electrons are more localized at one ion or whether the electronic wave function is approximately evenly distributed over all ion positions.

Almost all approaches to effective potentials assume that the effective potential for $N$ mutually interacting particles can be represented as a sum of two-body potentials. For these two-body potentials, the additional assumption is then justified that they only depend on the distance between the two interaction partners. Thus one has

$$V(\boldsymbol{R}_1, \ldots, \boldsymbol{R}_N) = \sum_{n<m} v(|\boldsymbol{R}_n - \boldsymbol{R}_m|) = \frac{1}{2} \sum_{n \neq m} v(|\boldsymbol{R}_n - \boldsymbol{R}_m|) \ . \tag{3.22}$$

All relevant two-body potentials $v(R)$ are qualitatively of the form shown in Fig. 3.1. They therefore have in particular a strong repulsive component for sufficiently small distances, which prevents two atoms from getting too close to each other. The repulsive component is physically due on the one hand to the Coulomb repulsion of the nuclei and on the other hand to the Pauli exclusion principle and the Coulomb repulsion of the electrons. This repulsive component then becomes effective when the two atoms come so close to each other that the electron shells begin to overlap. Then the electrons have to occupy higher lying antibonding orbitals because of the Pauli principle, which leads to a strong increase in energy.

The pair interaction potential therefore becomes positive (repulsive) as soon as the distance of the atoms becomes smaller than the sum of the atomic radii. In good approximation one could assume a "hard-core" potential here, i.e.

$$v(r) = \infty \quad \text{für} \quad r < r_{at1} + r_{at2} \ , \tag{3.23}$$

**Fig. 3.1** Qualitative behavior of an effective two-body potential between two ions with distance $R = |\boldsymbol{R}_1 - \boldsymbol{R}_2|$

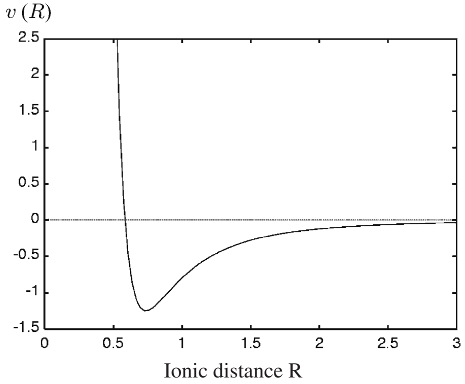

then one would consider the individual atoms or ions involved in the bond as hard spheres with atomic radii $r_{at1}$ and $r_{at2}$.

In addition, a somewhat realistic pair potential also has an attractive component (as in the sketch) and in particular an absolute minimum at a certain distance $r_0$, and it vanishes for large distances. $r$. The energetically most favorable distance $r_0$ then corresponds to the equilibrium distance, which is of the order of magnitude $2r_{at}$, and in the case of a solid, this is also the order of magnitude of the lattice constants $a$. The common model approaches for the pair potential are listed below

- **Van der Waals bond**
  Even noble gases, which, due to their closed shells, hardly participate in any chemical reactions and therefore can only have very weak interactions with other atoms, crystallize for sufficiently low temperatures (with the exception of helium, which only does so under high pressure, and thus is the only substance which, at normal pressures, does not have a crystalline state). There must therefore also be an interaction potential for noble gas atoms. The physical origin of such an interaction between noble gas atoms is the fact that, despite of the closed atomic electron shells, there are instantaneous atomic electric dipole moments due to the inneratomic charge distribution. The resulting dipole-dipole interaction leads to an attractive potential $\sim -\frac{1}{r^6}$, as can be explained by quantum mechanical perturbation theory. This is also referred to as the **Van der Waals interaction**. In addition, there is a repulsive component for small distances, which is simulated in noble gas crystals by an empirical $\frac{1}{r^{12}}$ law. Probably there exists no physical explanation for the $r^{-12}$ -behavior at small distances, but this choice is motivated only to ensure that for small $r$ the repulsive component can dominate and for larger $r$ the attractive $r^{-6}$ part so that the minimum and thus the equilibrium distance can be easily calculated. The resulting overall potential is the **Lennard-Jones potential:**

$$v(r) = 4\varepsilon\left(\left(\frac{\sigma}{r}\right)^{12} - \left(\frac{\sigma}{r}\right)^{6}\right) . \tag{3.24}$$

  For the equilibrium distance one obtains:

$$r_0 = 2^{\frac{1}{6}}\sigma . \tag{3.25}$$

  The effective potential of a crystal with $N$ atoms is

$$V_{\text{eff}}(\boldsymbol{R}_1, \ldots, \boldsymbol{R}_N) = 4\varepsilon \sum_{i<j}\left(\left(\frac{\sigma}{R_{ij}}\right)^{12} - \left(\frac{\sigma}{R_{ij}}\right)^{6}\right) . \tag{3.26}$$

  At temperature $T = 0$ the atoms occupy the positions of a Bravais lattice; in particular, in the case of noble gas crystals, an fcc structure is the rule, i. e. the $\boldsymbol{R}_{ij}$ in the above equation then run through the lattice vectors of an fcc lattice. If one sets $R_{ij} = ap_{ij}$, where $a$ is the lattice constant of the conventional unit cell, then the $p_{ij}$ are numbers which are characteristic for the lattice type. One obtains for the ground state energy:

$$E_0(a) = 2N\varepsilon\left(\left(\frac{\sigma}{a}\right)^{12} \cdot C_{12} - \left(\frac{\sigma}{a}\right)^{6} \cdot C_6\right) \tag{3.27}$$

where the $C_n$ are characteristic sums

$$C_n = \sum_{j \neq i} p_{ij}^{-n} \tag{3.28}$$

for the respective lattice type. In particular, for fcc lattices one obtains $C_{12} = 12.13$, $C_6 = 14.45$. The lattice constant $a_0$ assumed at $T = 0$ is determined by the condition that $E_0$ is minimal, and this results

$$a_0 = \left(2\frac{C_{12}}{C_6}\right)^{\frac{1}{6}} \sigma = 1.09\,\sigma\ . \tag{3.29}$$

The ground state energy corresponding to this value of the lattice constant is

$$E_0(a_0) = -\frac{1}{2} N\varepsilon \frac{C_6^2}{C_{12}} = -8.6\,N\varepsilon\ . \tag{3.30}$$

This is therefore the ground state energy under the assumption that the atoms are at rest at the lattice sites of an fcc lattice with lattice constants $a_0$. It corresponds to the cohesion energy ("cohesive energy"), i.e. the binding energy of the crystal, which was calculated classically here; quantum corrections are added when the zero point energy is taken into account correctly.

- **Ionic Bond**
  In ionic bonding, it is imagined that one or more electrons from the outer shell of atom $A$ are used to fill the atomic shells of atom $B$, so that positively charged $A^{n+}$ cations and negatively charged $B^{n-}$ anions are formed which are bound to each other by electrostatic attraction. The interaction potential between two ions 1 and 2 with charges $Q_1$ and $Q_2$ at a distance $r$ is then

$$v(r) = \frac{Q_1 Q_2}{r} + \frac{B}{r^n}\ . \tag{3.31}$$

For differently charged ions (cation and anion), the first summand is attractive, the second summand heuristically describes repulsion for small distances $r$. Here, $n$ and $B$ are free parameters that should actually be calculated quantum mechanically, but are usually determined empirically by fitting to measured quantities (ion distance, compressibility). Another common approach for the heuristic, short-range repulsive component is $v_{\text{rep}}(r) = \lambda e^{-r/\sigma}$. If crystallization occurs under ionic bonding, the binding energy can be estimated analogously to the procedure for the Van der Waals interaction as follows:

At $T = 0$ the masses (ions) are assumed to be at the equilibrium positions, i.e. the lattice vectors $\boldsymbol{R}_{i0}$; if $a$ denotes the lattice constant of the conventional unit cell for cubic lattices and assuming that the repulsive component can only be effective between nearest neighbors, then it follows:

$$E_0 = V_{\text{eff}}(\boldsymbol{R}_{10}, \ldots, \boldsymbol{R}_{N0}) = N\left(Zv_{\text{rep}}(p_{12}a) - \alpha\frac{Q^2}{a}\right) \tag{3.32}$$

where $Z$ is the number of nearest neighbors (coordination number) and $Q$ is the ionic charge. Here, $\alpha$ is again (analogously as before $C_n$) a constant characteristic of the lattice, which is determined by the following lattice sum:

$$\alpha = \sum_{j \neq i} \frac{\text{sign}(Q_i \cdot Q_j)}{p_{ij}} \,. \tag{3.33}$$

The $p_{ij}$ are again numerical values characteristic for the lattice, which one obtains from $R_{ij} = p_{ij} \cdot a$. $\alpha$ is also called the **Madelung constant**[3]. The explicit calculation yields for the NaCl structure $\alpha_{\text{NaCl}} = 1.74$, and for the CsCl structure $\alpha_{\text{CsCl}} = 1.76$.

- **Covalent Bond**
  The covalent bond can only be understood quantum mechanically and originates from the formation of new molecular orbitals in the superposition potential of the atoms involved in the binding; these molecular orbitals are bonding or antibonding, depending on whether the corresponding eigenenergy is lowered or raised compared to that of the free atoms. The actual covalent or homopolar bond is found in particular between atoms of the same kind, e.g. in the $H_2$ molecule. It is usually formed by 2 electrons, each of which comes from one of the atoms involved in the bond. The electronic occupation probability in a molecular orbital is usually particularly high in the intermediate range between the atoms; then the two electrons must have antiparallel spin because of the Pauli principle (singlet state). One then usually has a directed bond. Covalent bonding is particularly common in solids with a diamond structure. The fact that the nearest neighbors are arranged tetrahedrally around a lattice point already shows that four equivalent directions from each atom are preferred for the bond. In C, Si, Ge, atoms of the same kind are on adjacent sites, i.e. ionic bonding cannot play a role, the bond must be purely covalent. The valence electrons involved in the bond no longer belong to one atom but to both atoms to an approximately equal extent and with an approximately equal probability.

  For simple hydrogen-like atoms, the molecule formation and the binding energy can be calculated as a function of the distance quantum-mechanically, either perturbatively or by means of suitable approaches for the **molecular orbital**, that is, the molecular wave function (for example, as a linear combination of atomic wave functions). This then yields approximately explicit, but relatively complex expressions for the electronic ground state energy depending on the atomic distance and, thus, for the effective pair potential between the hydrogen atoms[4]

---

[3] First calculated in 1918 by E. Madelung, * 1881 in Bonn, † 1972 in Frankfurt, PhD 1905 in Göttingen, developed already around 1910 lattice models for crystals, 1921–1949 Professor for Theoretical Physics in Frankfurt and work on atomic physics and quantum theory, his son O. Madelung (*1922 †, 2017) also became a solid state (semiconductor) theorist (Professor in Marburg) and is the author of the solid state theory textbook 9.

$$V_{\text{eff}}(R) = \frac{Q(R) + A(R)}{1 + S^2(R)}$$

$$Q(R) = \frac{e^2}{R} e^{-2R/a} P_1(R/a)$$

$$A(R) = \frac{e^2}{a} \left( F_1(R) + e^{-2R/a} P_2(R/a) + F_2(R) \right)$$

$$S(R) = P_3(R/a) e^{-R/a} \tag{3.34}$$

with certain polynomials$P_i$ and tabulated functions$F_i$, where$a$ now denotes the Bohr radius. Qualitatively, the binding contribution again results in a potential exactly of the type sketched in Fig. 3.1.

Because of the complexity of these expressions, and because it was only derived for the simplest conceivable, but for solids not very interesting $H_2$ molecule, one often uses simplified, empirical model approaches, for instance the **Morse potential**

$$V_{\text{eff}}(R) = D \left( e^{-2\alpha(R-r_0)} - 2e^{-\alpha(R-r_0)} \right), \tag{3.35}$$

which has three adjustable parameters $(\alpha, D, r_0)$, where $r_0$ is the equilibrium distance and - $D$ is the corresponding binding energy.

While in the $H_2$ molecule and accordingly in all molecules out of the same atoms and in solids in those with diamond structure, the pure covalent bond is present, there are numerous systems in which the chemical bond has both ionic and covalent character. This is especially true for solids with zinc-blende structure, in which there is still a tetrahedral coordination, but to different atoms, as in the III–V and II–VI compounds such as GaAs, ZnS. With decreasing valence of the partners, the bond character becomes increasingly ionic, i.e. the electron occupation probability is no longer evenly distributed over the bonding partners but the electron is more localized near the anion. The transition between ionic and covalent bonding is therefore fluent, there are no fundamentally different chemical bonds.

- **Metallic Bonding**

  The bonding of metals also comes about because valence electrons do not only belong to one atom. In contrast to covalent bonding and ionic bonding, however, there is no specific neighbor to which the electron belongs with the same occupation probability as to the starting atom or to which the electron is given off. The occupation probability of the electrons is not only significantly different from 0 over two or a few atoms or the space in between, but evenly distributed over the whole solid. The electrons that cause solidification are therefore freely movable within the crystal. The valence electrons of the individual atoms become the conduction electrons of the metal. In transition metals, the partially filled inner d-shells also contribute significantly to the bond. Since the atomic d-orbitals are relatively strongly localized at the individual atom (lattice point), the contribution of the d-orbitals to the bond already has a covalent character again. The transition between metallic and covalent bonding is therefore also fluent.

---

[4] F. Schwabl, Quantum Mechanics, Chapt. 15, Springer, Berlin, Heidelberg (2007)

- **Spring models**
  As repeatedly emphasized, the effective interaction potential between two atomic nuclei is qualitatively always of the form shown in Fig. 3.1 for all conceivable bonds. There is therefore always a repulsive component at small distances and an attractive component and a minimum of the potential that corresponds to the equilibrium distance. If one considers that for not too high temperatures $T$ only small deviations from this equilibrium position are to be expected, one can expand the potential around this equilibrium position up to second order in the displacement, i. e. one approximates the potential curve near $r_0$ by a parabolic potential. This is equivalent to the fact that one imagines the interaction between each two atomic nuclei to be mediated by effective "springs". The effective interaction potential is then simply

$$V_{\text{eff}}(R) = V_0 + \frac{K}{2}(R - r_0)^2 \tag{3.36}$$

  with $V_0 = V_{\text{eff}}(r_0)$, $K = \frac{\partial^2}{\partial R^2} V_{\text{eff}}(R)|_{R=r_0}$. Such effective spring models are often used in specific calculations of the characteristic properties (eigenfrequencies and eigenmodes) of lattice vibrations (phonons) for certain crystal structures, which will be discussed in more detail in the following chapter.

## 3.4 Problems for Chap. 3

**Problem 3.1 Born-Oppenheimer approximation**
Given the Hamiltonian operator

$$H = \frac{p_1^2}{2M} + \frac{p_2^2}{2m} + \frac{K}{2}x_1^2 + \frac{k}{2}(x_1 - x_2)^2$$
$$\text{with} \quad [p_l, x_k] = \frac{\hbar}{i}\delta_{lk}$$

($(x_l, p_l)$ canonical conjugate position and momentum coordinates)

a) Determine the exact eigenvalues of $H$.
   (Keyword: coupled harmonic oscillators)
b) Solve the problem in Born-Oppenheimer approximation assuming that for $m \ll M$

$$T_A = \frac{p_1^2}{2M}$$

as "atomic" kinetic energy can be neglected (to lowest order), and solve the "electronic" problem

$$\frac{p_2^2}{2m} + \frac{K}{2}x_1^2 + \frac{k}{2}(x_1 - x_2)^2$$

for fixed "parameter" $x_1$ ( calculate the eigenvalues $\varepsilon_{n_1}(x_1)$) and then solve the atomic problem

$$\frac{p_1^2}{2M} + \varepsilon_{n_1}(x_1).$$

c) Compare the approximate solution from b) with the exact solution from a).

**Problem 3.2** ***1-dimensional "hydrogen molecule ion"***

A one-dimensional model Hamiltonian operator for 2 simply positively charged atomic nuclei of mass $M$ at $R_1$ and $R_2$ and a negatively charged electron at $x$ can be written as

$$H = \frac{P_1^2}{2M} + \frac{P_2^2}{2M} + \frac{p^2}{2m} - v(x - R_1) - v(x - R_2) + v(R_1 - R_2)\ .$$

For the "Coulomb" interaction in one dimension, we make the model assumption:

$$v(x) = \frac{e^2}{|x| + \delta}$$

where the parameter $\delta$ was introduced to avoid a singularity.

According to the concept of the Born-Oppenheimer approximation, the electronic Schrödinger equation is to be solved first for fixed nuclear positions $R_1$ and $R_2$. If one chooses the origin of the coordinate system in the middle between $R_1$ and $R_2$, i. e. $R_1 = -a$, $R_2 = +a$, $|R_1 - R_2| = 2a$, then the following electronic Schrödinger equation

$$-\frac{\hbar^2}{2m}\frac{d^2}{dx^2}\psi(x) - \left(\frac{e^2}{|x - a| + \delta} + \frac{e^2}{|x + a| + \delta}\right)\psi(x) = E\psi(x)$$

is to be solved.

a) Convince yourself that with $a_0 = \frac{\hbar^2}{me^2}$ and $x = a_0\tilde{x}$ you get to the dimensionless Schrödinger equation

$$-\frac{1}{2}\psi''(\tilde{x}) - \left(\frac{1}{|\tilde{x}-\tilde{a}|+\tilde{\delta}} + \frac{1}{|\tilde{x}+\tilde{a}|+\tilde{\delta}}\right)\psi(\tilde{x}) = \tilde{E}\psi(\tilde{x})$$

with

$$\tilde{E} = \frac{E}{(me^4/\hbar^2)} = \frac{Ea_0}{e^2} .$$

In the following, the "tildes" are omitted and energies are measured in units of $\frac{me^4}{\hbar^2} = \frac{e^2}{a_0} = 2\,\mathrm{Ry}$ and lengths in units of $a_0 = 0.5\,\text{Å}$.

b) Discretize the above differential equation for 201 grid points on the interval $[-10.,10.]$ according to $x_i = -10. + (i-1) * 0.1$, choose $\delta = 0.1$ and show that you get the following difference equation:

$$\begin{aligned}&-\psi(x_{i+1}) - \psi(x_{i-1}) + 2. * \psi(x_i) - 2. * V_i * 0.01 * \psi(x_i)\\&= E * 0.02 * \psi(x_i)\end{aligned}$$

with

$$V_i = V(x_i) = \frac{1}{|x_i - a| + 0.1} + \frac{1}{|x_i + a| + 0.1} .$$

c) Show that you have to diagonalize a matrix of the form

$$\begin{pmatrix} h_1 & -1. & 0 & 0 & \dots & 0 \\ -1. & h_2 & -1. & 0 & \dots & 0 \\ 0. & -1. & h_3 & -1. & 0. & \dots \\ 0. & 0. & \ddots & \ddots & \ddots & 0. \\ 0. & \dots & 0. & -1. & h_{200} & -1. \\ 0. & \dots & 0. & 0. & -1. & h_{201} \end{pmatrix} \text{with } h_i = 2. * (1. - V_i * 0.01)$$

and from its eigenvalues $E_w(n)$ $(n = 1, \dots, 201)$ you get the eigenvalues of the one-dimensional Schrödinger equation approximately $E_n = E_w(n)/0.02$.

d) Diagonalize the matrix from c) numerically (using an appropriate routine for tridiagonal matrices), give the lowest 4 energy eigenvalues $E_1, \dots, E_4$ and plot the corresponding eigenstates for $a = 1$ and $a = 7$. Interpret the result physically.

e) Now determine numerically the dependence of the lowest two eigenvalues on $a$ or the distance $|R_1 - R_2| = 2a$ and plot for $n = 1,2$ $E_n(2a) = E_n(|R_1 - R_2|)$.

f) According to the Born-Oppenheimer approximation, the effective potential for the two atomic nuclei is given by

$$V_{\text{eff}}(|R_1 - R_2|) = E_n(|R_1 - R_2|) + \frac{1}{|R_1 - R_2| + 0.1} \ .$$

Plot the course of this effective potential for $n = 1{,}2$.

# Lattice Vibrations (Phonons)

# 4

## 4.1 Harmonic Approximation, Dynamic Matrix and Normal Coordinates

We consider in this chapter $N$ mass points (nuclei or ions) that interact with each other via an effective potential $V_{\text{eff}}(\boldsymbol{R}_1, \ldots, \boldsymbol{R}_N)$ of the type discussed in the previous chapter. The Hamilton operator or the classical Hamilton function has the form:

$$H = \sum_{l=1}^{N} \frac{\boldsymbol{P}_l^2}{2M_l} + V_{\text{eff}}(\boldsymbol{R}_1, \ldots, \boldsymbol{R}_N) \ . \tag{4.1}$$

There should be certain equilibrium positions $\underline{\boldsymbol{R}}^{(0)} = (\boldsymbol{R}_1^{(0)}, \ldots, \boldsymbol{R}_N^{(0)})$ that correspond to the absolute minimum of the potential. For small deviations from equilibrium, the potential can be expanded to second order around the equilibrium positions. If one sets

$$\boldsymbol{R}_l = (R_{l1}, \ldots, R_{ld}) = \boldsymbol{R}_l^{(0)} + \boldsymbol{u}_l \tag{4.2}$$

($d$ dimension), then expanding yields:

$$V_{\text{eff}}(\boldsymbol{R}_1, \ldots, \boldsymbol{R}_N) = V\left(\underline{\boldsymbol{R}}^{(0)}\right) + \sum_{l,\alpha} \left.\frac{\partial V}{\partial R_{l\alpha}}\right|_{\underline{\boldsymbol{R}}^{(0)}} \cdot u_{l\alpha}$$

$$+\frac{1}{2} \sum_{l,m,\alpha,\beta} \left.\frac{\partial^2 V}{\partial R_{l\alpha} \partial R_{m\beta}}\right|_{\underline{\boldsymbol{R}}^{(0)}} \cdot u_{l\alpha} u_{m\beta} + \ldots \tag{4.3}$$

© The Author(s), under exclusive license to Springer-Verlag GmbH, DE, part of Springer Nature 2023

G. Czycholl, *Solid State Theory, Volume 1*,
https://doi.org/10.1007/978-3-662-66135-2_4

The **harmonic approximation** consists in truncating the expansion after this term, which is quadratic in the extensions. The linear term vanishes because at the equilibrium positions, i.e. at the absolute minimum of the potential, the partial derivatives $\frac{\partial V}{\partial R_{l\alpha}}(\underline{\boldsymbol{R}}^{(0)}) = 0$ must be zero. The

$$\Phi_{l\alpha,m\beta} = \left.\frac{\partial^2 V}{\partial R_{l\alpha}\partial R_{m\beta}}\right|_{\underline{\boldsymbol{R}}^{(0)}} \tag{4.4}$$

form a symmetric, positive definite $dN * dN$-matrix; that it is positive definite follows immediately from the requirement that at $\underline{\boldsymbol{R}}^{(0)}$ there is a minimum (and not a saddle point or maximum). With the definition

$$\tilde{u}_{l\alpha} = \sqrt{M_l}u_{l\alpha}, \tilde{p}_{l\alpha} = \frac{1}{\sqrt{M_l}}P_{l\alpha} \tag{4.5}$$

the Hamilton operator or the Hamilton function (4.1) can be written in harmonic approximation as:

$$H_{\text{harm}} = \frac{1}{2}\left(\underline{\tilde{\boldsymbol{p}}}^{\text{t}} \cdot \underline{\tilde{\boldsymbol{p}}} + \underline{\tilde{\boldsymbol{u}}}^{\text{t}} \cdot \underline{\underline{D}} \cdot \underline{\tilde{\boldsymbol{u}}}\right) \tag{4.6}$$

with the column or row vectors

$$\underline{\tilde{\boldsymbol{u}}} = \begin{pmatrix} \tilde{u}_{11} \\ \vdots \\ \tilde{u}_{Nd} \end{pmatrix}, \quad \underline{\tilde{\boldsymbol{u}}}^{\text{t}} = (\tilde{u}_{11}, \ldots, \tilde{u}_{Nd})$$

and the $dN * dN$-matrix

$$\left(\underline{\underline{D}}\right)_{l\alpha,m\beta} = \frac{1}{\sqrt{M_l M_m}}\Phi_{l\alpha,m\beta} \; . \tag{4.7}$$

The matrix $\underline{\underline{D}}$ is called **dynamic matrix**, it is (like $\underline{\underline{\Phi}}$) a real, symmetric, positive definite $dN * dN$-matrix, which can be diagonalized. There exists an orthogonal transformation (or a unitary transformation, if we allow complex displacement vectors $\underline{\tilde{\boldsymbol{u}}}$), which diagonalizes the matrix, i.e. there exists an orthogonal (unitary) $dN * dN$-matrix $\underline{\underline{C}}$ with

$$\underline{\underline{C}} \cdot \underline{\underline{D}} \cdot \underline{\underline{C}}^{\dagger} = \underline{\underline{\Omega}} = \begin{pmatrix} \omega_1^2 & 0 & \ldots & 0 \\ 0 & \omega_2^2 & \ldots & \vdots \\ \vdots & 0 & \ddots & 0 \\ 0 & \ldots & 0 & \omega_{Nd}^2 \end{pmatrix} . \tag{4.8}$$

diagonal matrix with positive diagonal elements (because of the positive definiteness); because of the orthogonality or unitarity one has

$$\underline{\underline{C}}^{\dagger} \cdot \underline{\underline{C}} = \underline{\underline{1}} \tag{4.9}$$

(identity matrix). By the corresponding orthogonal (unitary) coordinate transformation (rotation in the $dN$-dimensional space)

$$\underline{\bar{\boldsymbol{p}}} = \underline{\underline{C}} \cdot \underline{\tilde{\boldsymbol{p}}} \ , \quad \underline{\bar{\boldsymbol{u}}} = \underline{\underline{C}} \cdot \underline{\tilde{\boldsymbol{u}}} \tag{4.10}$$

we come to new generalized, canonically conjugate momenta $\underline{\bar{\boldsymbol{p}}} = (\bar{p}_1, \ldots, \bar{p}_{dN})$ and coordinates $\underline{\bar{\boldsymbol{u}}} = (\bar{u}_1, \ldots, \bar{u}_{dN})$, with respect to which the Hamilton matrix is diagonal:

$$\begin{aligned} H_{\text{harm}} &= \frac{1}{2}\left(\underline{\bar{\boldsymbol{p}}}^{\mathrm{t}} \cdot \underline{\bar{\boldsymbol{p}}} + \underline{\bar{\boldsymbol{u}}}^{\mathrm{t}} \cdot \underline{\underline{\Omega}} \cdot \underline{\bar{\boldsymbol{u}}}\right) \\ &= \frac{1}{2} \sum_{i=1}^{Nd} \left(\bar{p}_i^2 + \omega_i^2 \bar{u}_i^2\right) \ . \end{aligned} \tag{4.11}$$

This is the Hamilton function or the Hamilton operator of $dN$ independent harmonic oscillators.

So far, the classical and quantum mechanical treatment is identical. Classically, it is the “small oscillations” problem (coupled harmonic oscillators) known from mechanics, which can be solved by transition to normal coordinates, in which the oscillators are decoupled. Quantum mechanically, the displacements $u_{l\alpha}$ and the impulses $P_{m\beta}$ fulfill the usual commutation relations

$$[u_{l\alpha}, P_{m\beta}] = i\hbar \delta_{lm} \delta_{\alpha\beta} \ . \tag{4.12}$$

Then also the transformed generalized (normal) coordinates $\bar{u}_i$ and impulses $\bar{p}_j$ fulfill the analogous commutator relation

$$[\bar{u}_i, \bar{p}_j] = i\hbar \delta_{ij} \quad (i,j = 1, \ldots, dN) \ . \tag{4.13}$$

Then one can introduce the usual raising and lowering operators, as it is known from the lecture (or textbooks) on elementary quantum mechanics for the one-dimensional harmonic oscillator problem:

$$b_j = \sqrt{\frac{\omega_j}{2\hbar}} \bar{u}_j + i \sqrt{\frac{1}{2\hbar\omega_j}} \bar{p}_j \ , \quad b_j^\dagger = \sqrt{\frac{\omega_j}{2\hbar}} \bar{u}_j - i \sqrt{\frac{1}{2\hbar\omega_j}} \bar{p}_j \tag{4.14}$$

which fulfill the commutation relation

$$\left[b_j, b_k^\dagger\right] = \delta_{jk} \ , \quad \left[b_j, b_k\right] = \left[b_j^\dagger, b_k^\dagger\right] = 0 \tag{4.15}$$

, and the Hamiltonian operator can be written as

$$H_{\text{harm}} = \sum_{j=1}^{Nd} \hbar\omega_j \left(b_j^\dagger b_j + \frac{1}{2}\right) \ . \tag{4.16}$$

So far the treatment is standard and has nothing to do with solid state physics yet. The treatment of molecular vibrations proceeds in principle in the same way.

The problem is the diagonalization of the dynamic matrix; although one knows mathematically that the dynamic matrix is diagonalizable, i.e. that normal coordinates exist, the concrete finding of the latter, i.e. the concrete diagonalization and thus the calculation of the eigenvalues $\omega_j$ can still be very difficult, especially if $N$ is large. Even for slightly larger molecules this should be quite unpleasant, at least if one cannot reduce the problem by symmetry considerations. If one wants to exploit such symmetries systematically, one has to resort to methods of group theory. But even if all symmetries are exploited, one may still have to resort to numerical diagonalization.

In solid-state physics, the problem seems to be even more difficult at first glance than for molecules, because due to $N = 10^{23}$ the dynamic matrix is extremely large. However, it turns out that for solids one can at least partially explicitly carry out the diagonalization analytically if one only uses one symmetry characteristic of solids, namely the translational invariance with respect to lattice vectors. So far we have not made any assumptions about the equilibrium positions (rest positions) $(\boldsymbol{R}_{10}, \ldots, \boldsymbol{R}_{N0})$ of the atoms. We will assume in the following that they can be represented by lattice vectors of a Bravais lattice plus possibly still individual position vectors within the elementary cell (in a crystal structure with a multi-atomic basis).

## 4.2 Classical Equations of Motion

From this section on, we assume the existence of a crystal structure. So we assume that a Bravais lattice exists, described by fixed lattice vectors $\boldsymbol{R}_{n0}$ and a basis of $r$ atoms, whose position is described by vectors $\boldsymbol{R}_\mu$ $(\mu = 1, \ldots, r)$ within an elementary cell and whose masses $M_\mu$ are, in general, different. But with respect to the lattice vectors $\boldsymbol{R}_{n0} - \boldsymbol{R}_{n'0}$ there is translational invariance, i. e. the same group of atoms is periodically repeated. The vectors $\boldsymbol{R}_{n0} + \boldsymbol{R}_\mu$ denote the equilibrium position of the μ-th atom in the elementary cell $n$. The atoms oscillate around their equilibrium positions, then their current (time-dependent) position is given by

$$\boldsymbol{R}_{n\mu} = \boldsymbol{R}_{n0} + \boldsymbol{R}_\mu + \boldsymbol{u}_{n\mu} \tag{4.17}$$

(see Fig. 4.1 for a 2-d illustration of the notation). $\boldsymbol{u}_{n\mu}$ therefore denotes the displacement of the μ-th atom in the $n$-th elementary cell from its equilibrium position. The potential is given in harmonic approximation by

$$\begin{aligned} V &= \tfrac{1}{2} \textstyle\sum_{n\mu\alpha, n'\mu'\alpha'} \frac{\partial^2 V}{\partial R_{n\mu\alpha} \partial R_{n'\mu'\alpha'}} u_{n\mu\alpha} u_{n'\mu'\alpha'} \\ &= \tfrac{1}{2} \textstyle\sum_{n\mu\alpha, n'\mu'\alpha'} \Phi_{n\mu\alpha, n'\mu'\alpha'} u_{n\mu\alpha} u_{n'\mu'\alpha'} \end{aligned} , \tag{4.18}$$

where we have chosen the potential corresponding to the equilibrium position (that is, the classical ground state energy) to be 0; the $\alpha, \alpha'$ denote as in Sect. 4.1the ($d$ or 3 cartesian) coordinates.

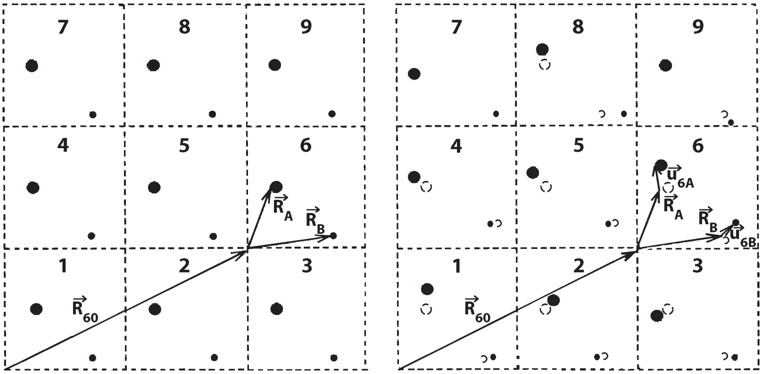

**Fig. 4.1** Square lattice with two-atom basis in equilibrium and with displacements

As a classical equation of motion one obtains

$$M_\mu \ddot{u}_{n\mu\alpha} = -\frac{\partial V}{\partial u_{n\mu\alpha}} = -\sum_{n'\mu'\alpha'} \Phi_{n\mu\alpha,n'\mu'\alpha'} u_{n'\mu'\alpha'} \ . \tag{4.19}$$

$\Phi_{n\mu\alpha,n'\mu'\alpha'} u_{n'\mu'\alpha'}$ is thus the force in the α-direction that the atom μ experiences in the $n$-th elementary cell as a result of the atom $\mu'$ in the $n'$-th elementary cell being displaced in the $\alpha'$-direction by $u_{n'\mu'\alpha'}$. The $\Phi_{n\mu\alpha,n'\mu'\alpha'}$ is therefore also called a force constant. The elementary symmetry properties of the matrix $\underline{\underline{\Phi}}$ are, on the one hand, the symmetry (with respect to the indices), which was already established in the previous section:

$$\Phi_{n\mu\alpha,n'\mu'\alpha'} = \Phi_{n'\mu'\alpha',n\mu\alpha} \ . \tag{4.20}$$

On the other hand, if all atoms have the same displacement vector, only the whole crystal is displaced, but this must not cause any force between the mass points. Therefore, it must apply:

$$\sum_{n'\mu'} \Phi_{n\mu\alpha,n'\mu'\alpha'} = 0 \ . \tag{4.21}$$

Finally, because of the translational invariance, the force constant matrix must not depend on the Bravais lattice vectors $\boldsymbol{R}_{n0}, \boldsymbol{R}_{n'0}$ individually, but it can only depend on the relative distance $\boldsymbol{R}_{n0} - \boldsymbol{R}_{n'0}$, i.e.

$$\Phi_{n\mu\alpha,n'\mu'\alpha'} = \Phi_{\mu\alpha,\mu'\alpha'}(\boldsymbol{R}_{n0} - \boldsymbol{R}_{n'0}) \ . \tag{4.22}$$

From each lattice point, the system must look the same. Here the translational invariance with respect to displacements by Bravais lattice vectors is exploited.

The solution of the equation of motion (4.19) can now be carried out in the following steps. First we make the ansatz for the time dependence:

$$u_{n\mu\alpha}(t) = \frac{1}{\sqrt{M_\mu}} v_{n\mu\alpha} e^{-i\omega t} \ . \tag{4.23}$$

Then for the time-independent coefficients $v_{n\mu\alpha}$ the following equation results

$$\omega^2 v_{n\mu\alpha} = \sum_{n'\mu'\alpha'} D_{\mu\alpha,\mu'\alpha'}(\boldsymbol{R}_{n0} - \boldsymbol{R}_{n'0}) v_{n'\mu'\alpha'} \quad \text{with} \quad \underline{\underline{D}} = \frac{1}{\sqrt{M_\mu M_{\mu'}}} \underline{\underline{\Phi}} \ . \tag{4.24}$$

This is now an eigenvalue equation for the symmetric matrix $\underline{\underline{D}}$, the **dynamic matrix**, which for $N$ elementary cells (lattice sites) is a $dNr * dNr$-matrix. Therefore there exist also $dNr$ positive eigenvalues. For the dependence on the lattice vector $n$ the ansatz

$$v_{n\mu\alpha} = w_{\mu\alpha} e^{i\boldsymbol{q}\boldsymbol{R}_{n0}} \tag{4.25}$$

can be made. Substitution into the eigenvalue equation leads to

$$\omega^2 w_{\mu\alpha} = \sum_{\mu'\alpha'} \sum_{n'} D_{\mu\alpha,\mu'\alpha'}(\boldsymbol{R}_{n0} - \boldsymbol{R}_{n'0}) e^{i\boldsymbol{q}(\boldsymbol{R}_{n'0} - \boldsymbol{R}_{n0})} w_{\mu'\alpha'} \ . \tag{4.26}$$

Instead of the sum over all elementary lattice cells $n'$ or lattice vectors $\boldsymbol{R}_{n'0}$ one can also sum over all difference vectors, which are also lattice vectors. If one then defines

$$D_{\mu\alpha,\mu'\alpha'}(\boldsymbol{q}) = \sum_{n} D_{\mu\alpha,\mu'\alpha'}(\boldsymbol{R}_{n0}) e^{-i\boldsymbol{q}\boldsymbol{R}_{n0}} \tag{4.27}$$

then obviously the Fourier transformed dynamic matrix fulfills the eigenvalue equation

$$\omega^2 w_{\mu\alpha} = \sum_{\mu'\alpha'} D_{\mu\alpha,\mu'\alpha'}(\boldsymbol{q}) w_{\mu'\alpha'} \ . \tag{4.28}$$

This is for each $\boldsymbol{q}$ only a $dr * dr$-eigenvalue problem; in 3 dimensions, for example, only a $3 * 3$-matrix has to be diagonalized for a one-atom basis, which is relatively unproblematic. For each $\boldsymbol{q}$ there are therefore in general (dimension $d$ and $r$ atoms per elementary cell) $dr$ eigenvalues $\omega_j(\boldsymbol{q})$ ($j = 1, \ldots, dr$) and corresponding $dr$-dimensional eigenvectors ($e^{(j)}_{\mu\alpha}$); each of these $dr$-dimensional eigenvectors can be decomposed into $r$ ordinary $d$-dimensional vectors $\boldsymbol{e}^{(j)}_{\mu}$, which can be chosen as unit vectors and whose directions designate the directions of displacement of the $\mu$-th atom, and these vectors are also called **polarization vectors**.

In total, we have thus found as special solutions of our original equation of motion (4.19)

$$\boldsymbol{u}^{(j)}_{n\mu} = \frac{1}{\sqrt{M_\mu}} \boldsymbol{e}^{(j)}_{\mu} e^{i\left(\boldsymbol{q}\boldsymbol{R}_{n0} - \omega_j(\boldsymbol{q})t\right)} \ . \tag{4.29}$$

The general solutions result as linear combinations of these special solutions for the displacement of the atom $\mu$ in the $n$-th elementary cell.

So we have partially carried out the diagonalization of the dynamic $dNr * dNr$-matrix analytically here and reduced it to the diagonalization of a $dr * dr$-matrix. In doing so, we have explicitly used translational invariance by assuming that the dynamic matrix $\underline{\underline{D}}(\boldsymbol{R}_{n0}, \boldsymbol{R}_{n'0})$ only depends on the difference vector $\boldsymbol{R}_{n0} - \boldsymbol{R}_{n'0}$. This allowed the Fourier transformation, i.e. the transition to the $\boldsymbol{q}$-dependent dynamic matrix $\underline{\underline{D}}(\boldsymbol{q})$, which is only a $dr * dr$-matrix. The unitary transformation mentioned in the previous chapter therefore has the special form

$$C_{\boldsymbol{R},\boldsymbol{q}} \sim e^{i\boldsymbol{q}\boldsymbol{R}} \tag{4.30}$$

if $\boldsymbol{R}$ denotes lattice vectors. Since we use complex displacement vectors by means of the complex exponential function for the time dependence of the displacements, a unitary transformation must be used for diagonalization. As is known from classical mechanics, one could also work with real approaches (e.g. $\cos(\omega t)$-time dependence), but the complex approach is more convenient for calculation. But this also depends on the boundary conditions used, and the next section is devoted to the possible and the boundary conditions usually used in solid state theory, which are used everywhere (e.g. for electronic eigenstates) and not only here for lattice vibrations.

## 4.3 Periodic or Born-von-Kármán Boundary Conditions

In this section, the so-called Born-von-Kármán[1] -boundary conditions, which are generally used in solid state theory, will be discussed and motivated. Of course, every real solid is finite, so there is a finite number$N$ of elementary cells and a surface that can have very interesting effects. But if you want to consider the realistic surface, the translational invariance, which simplifies many concrete calculations, is lost. Translational invariance with respect to lattice vectors only exists for an infinitely extended Bravais lattice that fills the whole space;if there are surfaces, individual lattice points or elementary cells are closer to the surface than others and strictly speaking there is no translational invariance anymore. On the other hand, it is physically clear that, far inside the crystal, it should not matter how far the surface is away. Since the crystal is very large on the atomic length scale, the surface should not be noticeable for “most” atoms and lattice cells.

In order to take both into account, on the one hand the finiteness of the system, the finite total number $N$ of atoms, and on the other hand full translational invariance and full equality of all lattice cells, one usually uses **periodic boundary conditions** (also called “cyclic boundary conditions”). You can imagine continuing and repeating the whole finite crystal periodically and thus filling the whole space, or you can imagine considering the first and last atom layer as coupled to each other; in one dimension this would correspond to closing the linear chain to a ring, where you couple the first and the $N$-th atom to each other and make them neighbors. In two dimensions, periodic boundary conditions can also be illustrated, you then bend the finite surface to a torus. In three dimensions, a geometric illustration is no longer possible if periodic boundary conditions are required in all three directions $(x, y, z)$.

---

[1] T. von Kármán, * 1881 in Budapest, † 1963 in Aachen, important aerodynamicist, works on fluid mechanics, airfoil profiles etc., 1909 professor of mechanics and aerodynamics at RWTH Aachen, studied the vibrations of lattice atoms with M.Born around 1912, 1930-1949 at Caltech in California.

This means that, if $L_\alpha$ denotes the dimension (length) of the system in the α-direction, all functions relevant to the system must satisfy the boundary condition

$$f(\ldots, x_\alpha + L_\alpha, \ldots) = f(\ldots, x_\alpha, \ldots). \tag{4.31}$$

In solid state physics, the interesting functions (e.g. the displacements $\boldsymbol{u}_{n\mu}$) will depend on the elementary cell index $n$ or the corresponding lattice vector $\boldsymbol{R}_n$ : $f_n = f(\boldsymbol{R}_n)$. If this is described by the integer tuple $(n_1, \ldots, n_d)$ with respect to a basis $\boldsymbol{a}_1, \ldots, \boldsymbol{a}_d$ of primitive translations, and let $N_\alpha a_\alpha$ be the length of the entire crystal in the α-direction, then

$$f(\boldsymbol{R}_n) = f(\boldsymbol{R}_n + N_\alpha \boldsymbol{a}_\alpha) \quad (\alpha = 1, \ldots, d) \ . \tag{4.32}$$

applies for periodic boundary conditions. The total number of unit cells is then

$$N = \prod_{\alpha=1}^{d} N_\alpha \ .$$

Between functions $f_n = f(\boldsymbol{R}_n)$ defined on the lattice and their Fourier transforms, the following relationship applies for periodic boundary conditions:

$$f(\boldsymbol{q}) = \sum_n f(\boldsymbol{R}_n) e^{-i\boldsymbol{q}\boldsymbol{R}_n}$$

$$f(\boldsymbol{R}_n) = \frac{1}{N} \sum_{\boldsymbol{q}} e^{i\boldsymbol{q}\boldsymbol{R}_n} f(\boldsymbol{q}) \ . \tag{4.33}$$

It then follows from (4.32)

$$N_\alpha \boldsymbol{q} \cdot \boldsymbol{a}_\alpha = 2\pi q_\alpha N_\alpha = 2\pi l_\alpha, \quad \text{with integer } l_\alpha \text{ and} \quad \boldsymbol{q} = \sum_{\alpha=1}^{d} q_\alpha \boldsymbol{b}_\alpha \tag{4.34}$$

was set and the $\{\boldsymbol{b}_\alpha, \alpha = 1, \ldots, d\}$ are the (to $\boldsymbol{a}_\alpha$ associated) primitive unit vectors of the reciprocal lattice. Apparently, the allowed Fourier coefficients take only discrete values:

$$q_\alpha = \frac{l_\alpha}{N_\alpha} \ . \tag{4.35}$$

It is sufficient to restrict the $\boldsymbol{q}$ to the **first Brillouin zone** (or the primitive elementary cell of the reciprocal lattice), i. e.

$$l_\alpha \in \{1, \ldots, N_\alpha\} \quad \text{or} \quad l_\alpha \in \left\{-\frac{N_\alpha}{2}, \ldots, \frac{N_\alpha}{2} - 1\right\} \tag{4.36}$$

because adding a reciprocal lattice vector $\boldsymbol{G}$ to $\boldsymbol{q}$ (because of $\exp(i\boldsymbol{G}\boldsymbol{R}_n) = 1$) does not give anything new. There are therefore exactly $N$ different, discrete (not equivalent) $\boldsymbol{q}$ values. For $\boldsymbol{q}, \boldsymbol{q}' \in$ 1st Brillouin zone the following rule applies:

$$\frac{1}{N} \sum_n e^{i(\boldsymbol{q}-\boldsymbol{q}')\boldsymbol{R}_n} = \delta_{\boldsymbol{q},\boldsymbol{q}'} \tag{4.37}$$

as can be easily proved: For

$$\boldsymbol{R}_n = \sum_{\alpha=1}^{d} n_\alpha \boldsymbol{a}_\alpha, \boldsymbol{q} = \sum_{\beta=1}^{d} \frac{l_\beta}{N_\beta} \boldsymbol{b}_\beta \ .$$

it follows because of $\boldsymbol{a}_\alpha \cdot \boldsymbol{b}_\beta = 2\pi \delta_{\alpha\beta}$

$$\begin{aligned} \frac{1}{N} \sum_n e^{i\boldsymbol{R}_n(\boldsymbol{q}-\boldsymbol{q}')} &= \prod_{\alpha=1}^{d} \frac{1}{N_\alpha} \sum_{n_\alpha=1}^{N_\alpha} \exp\left(i2\pi n_\alpha \frac{l_\alpha - l'_\alpha}{N_\alpha}\right) \\ &= \begin{cases} 0 \text{ if } l_\alpha \neq l'_\alpha & \text{for at least one} \quad \alpha \in \{1, \ldots, d\} \\ 1 \text{ if } l_\alpha = l'_\alpha & \text{for all} \quad \alpha \in \{1, \ldots, d\} \end{cases} , \end{aligned}$$

because of

$$\sum_{n=1}^{N} a^n = \frac{1 - a^N}{1 - a} \cdot a \quad \text{and} \quad e^{2\pi i l} = 1 \ .$$

For a real, finite crystal, rigid boundary conditions would be more realistic than the periodic boundary conditions presented and discussed here. With regard to the lattice vibrations, for example, rigid boundary conditions are the requirement that the surface atoms are no longer deflected. Then standing waves arise in the crystal to be described, for example, by a $\sin(\boldsymbol{q}\boldsymbol{R})$-like dependence on position, which can satisfy the rigid boundary conditions for suitable $\boldsymbol{q}$. Even then, there are $N$ discrete, but closely spaced allowed $\boldsymbol{q}$-values from the first Brillouin zone. Boundary conditions in a finite crystal cause the wave vectors $\boldsymbol{q}$ (and thus the wavelengths) to assume only discrete values. But it is physically clear that the macroscopic properties do not depend on the exact boundary conditions. In particular, the dispersion relation $\omega(\boldsymbol{q})$ does not depend on the boundary conditions, which can be easily calculated for the example of the linear chain. With periodic boundary conditions, one considers running lattice waves instead of standing waves, which mathematically results in the complex e-function $e^{i\boldsymbol{q}\boldsymbol{R}}$ instead of $\sin(\boldsymbol{q}\boldsymbol{R})$ describing the dependence on position. However, the quantization condition for the $\boldsymbol{q}$ depends on the boundary conditions. Since the $\boldsymbol{q}$-values are very close together in the first

Brillouin zone, this does not play a role for the macroscopic physical properties. In any case, one usually replaces the actually occurring discrete $\boldsymbol{q}$-sums by integrals, i.e.:

$$\sum_{\boldsymbol{q}\in 1.BZ} f(\boldsymbol{q}) \rightarrow \frac{N}{V_{1.BZ}} \int_{1.BZ} d^3q f(\boldsymbol{q}) \ . \tag{4.38}$$

Here $V_{1.BZ}$ is the ($k$-space) volume of the 1st Brillouin zone, $\frac{N}{V_{1.BZ}} d^3q$ is therefore the number of $\boldsymbol{q}$-values in the "infinitesimal" $\boldsymbol{q}$-space volume $d^3q$ around $\boldsymbol{q}$. According to equation (2.6) one has (for dimension $d = 3$)

$$V_{1.BZ} = \frac{(2\pi)^3}{V_{pEZ}}$$

and since $N \cdot V_{pEZ} = V$ is the total volume of the system (crystal),

$$\sum_{\boldsymbol{q}\in 1.BZ} f(\boldsymbol{q}) = \frac{V}{(2\pi)^3} \int_{1.BZ} d^3q f(\boldsymbol{q}) \ . \tag{4.39}$$

This replacement of the $\boldsymbol{q}$-sums by integrals is explicitly used in many practical calculations in solid state physics; integrals are usually easier to calculate than discrete sums. The replacement is justified if the $\boldsymbol{q}$-values in the Brillouin zone are sufficiently dense (close together), that is, for large $N$. The relationship is mathematically exact only in the **thermodynamic limit** $N \to \infty, V \to \infty, \frac{N}{V} = \text{const}$ . At least then, when the thermodynamic limit is justified, the difference between periodic and more realistic boundary conditions is no longer relevant.

## 4.4 Quantized Lattice Vibrations and Phonon Dispersion Relations

We now consider a crystal structure consisting of a Bravais lattice of $N$ primitive unit cells with periodic boundary conditions and a basis of $r$ atoms per unit cell, so the total number of atoms is $N * r$. According to Sect. 4.3 there are exactly $N$ non-equivalent $\boldsymbol{q}$-values in the 1st Brillouin zone, and according to Sect. 4.2for each $\boldsymbol{q}$ the (Fourier transformed) dynamic matrix $\underline{\underline{D}}(\boldsymbol{q})$ (a $dr * dr$-matrix) is to be diagonalized and has $dr$ positive eigenvalues $\omega_j^2(\boldsymbol{q})$. In total, there are exactly $dNr$ eigenfrequencies $\omega_j(\boldsymbol{q})$, as it must be according to the considerations from Sect. 4.1. Thus, the unitary transformation that partially diagonalizes the dynamic matrix (i.e., with respect to the lattice vector index) is just the discrete Fourier transform, the matrix elements of the corresponding matrix $\underline{\underline{C}}$ (according to the notation of Sect. 4.1) are thus:

$$C_{\boldsymbol{q},\boldsymbol{R}} = \frac{1}{\sqrt{N}} e^{i\boldsymbol{q}\boldsymbol{R}} \ . \tag{4.40}$$

The Hamiltonian operator in harmonic approximation is then written according to (4.16) as

$$H_{\text{harm}} = \sum_{\boldsymbol{q}} \sum_{j=1}^{dr} \hbar\omega_j(\boldsymbol{q}) \left( b_{\boldsymbol{q}j}^{\dagger} b_{\boldsymbol{q}j} + \frac{1}{2} \right) . \tag{4.41}$$

Hereby the oscillator-raising-and lowering-operators $b_{\boldsymbol{q}j}^{(\dagger)}$ fulfill, according to (4.15), the commutation relation

$$\left[ b_{\boldsymbol{q}j}, b_{\boldsymbol{q}'j'}^{\dagger} \right] = \delta_{\boldsymbol{q}\boldsymbol{q}'} \delta_{jj'} \ , \quad \left[ b_{\boldsymbol{q}j}^{\dagger}, b_{\boldsymbol{q}'j'}^{\dagger} \right] = [b_{\boldsymbol{q}j}, b_{\boldsymbol{q}'j'}] = 0 \ . \tag{4.42}$$

These are the commutation relations for Bose[2] -creation and annihilation operators. Thus, the elementary excitations of the Hamilton operator in harmonic approximation, i.e. the quantized normal oscillations, behave like those of a system of **interaction-free bosons**. These are also called **phonons**. Phonons are not real particles but **quasiparticles**. In particular, there is no particle number conservation (and therefore no chemical potential). Phonons behave analogously to photons (quantum of the electromagnetic field) in this respect as well. Indeed, the thermodynamics of phonons (quantized lattice waves) also shows a close analogy to the thermodynamics of a photon gas (cavity radiation, quantized electromagnetic waves).

The possible total energies of the lattice vibrations, i.e. the eigenenergies of $H_{\text{harm}}$, are (including the zero point energy) given by:

$$E = \sum_{j\boldsymbol{q}} \hbar\omega_j(\boldsymbol{q}) \left( n_{\boldsymbol{q}j} + \frac{1}{2} \right) . \tag{4.43}$$

Here, the **occupation numbers** (quantum numbers of the individual harmonic oscillator $j\boldsymbol{q}$) $n_{\boldsymbol{q}j}$ are integers. The individual states of the lattice vibration spectrum can therefore be occupied an arbitrary number of times. This again reflects the bosonic character of the excitations.

For each of the (closely lying) $\boldsymbol{q}$ values, there are $dr$ $\omega_j(\boldsymbol{q})$, $(j = 1, \ldots, dr)$. So you get $dr$ different **dispersion relations**, that is $dr$ **branches of the phonon spectrum**. All $\omega_j(\boldsymbol{q})$ are periodic with respect to reciprocal lattice vectors $\boldsymbol{G}$ :

$$\omega_j(\boldsymbol{q}) = \omega_j(\boldsymbol{q} + \boldsymbol{G}) \ . \tag{4.44}$$

This follows directly from the corresponding relation for the $\boldsymbol{q}$-dependent dynamical matrix $\underline{\underline{D}}(\boldsymbol{q})$, equation (4.27) (because of $e^{i\boldsymbol{G}\boldsymbol{R}} = 1$), because $\omega_j(\boldsymbol{q})$ is an eigenvalue of this matrix. Furthermore, there are $d$ phonon branches for which

---

[2] Named after S.N. Bose, * 1896 in Kalkutta, † 1974 ibid, Indian physicist, important work on statistical thermodynamics, founded Bose-Einstein statistics for photons in 1924.

$\omega_j(\boldsymbol{q}) \to 0$ for $q \to 0$, and these special dispersions go linearly with $q$ towards 0. This follows directly from the following consideration:

Consider special displacements of the atoms of the crystal, so that all atoms oscillate in the same coordinate direction $\alpha$ and the displacements of all $r$ atoms of a single lattice cell are exactly the same; the displacements $\boldsymbol{u}_{n\mu}^{(j)}$ according to (4.29) are then not dependent on the atom index $\mu$ for these special branches $j$ and only one coordinate direction $\alpha$ occurs. From the equation of motion (4.19) or the eigenvalue equation (4.26) we then get

$$M_\mu \omega_j^2(\boldsymbol{q}) u_\alpha e^{i\boldsymbol{q}\boldsymbol{R}_n} = \sum_{n'\mu'} \Phi_{n\mu\alpha,n'\mu'\alpha} u_\alpha e^{i\boldsymbol{q}\boldsymbol{R}_{n'}} \; . \tag{4.45}$$

All atoms are thus displaced in the same direction, within an elementary cell the displacements are even exactly the same, but from elementary cell to elementary cell they have a phase shift according to the $e^{i\boldsymbol{q}\boldsymbol{R}_n}$ factor. If we now expand both sides of this equation for small $q$, then we get:

$$M_\mu \left(\omega_j(0) + \nabla_{\boldsymbol{q}} \omega_j(\boldsymbol{q})|_{\boldsymbol{q}=0} \cdot \boldsymbol{q} + \ldots\right)^2 \tag{4.46}$$

$$= \sum_{\boldsymbol{R}\mu'} \Phi_{\mu\alpha,\mu'\alpha}(\boldsymbol{R}) \left(1 - i\boldsymbol{q}\boldsymbol{R} - \frac{1}{2}(\boldsymbol{q}\boldsymbol{R})^2 + \ldots\right) .$$

Now let's compare the different orders in $\boldsymbol{q}$ on the left and right sides, the following results:

- 0. Order in $\boldsymbol{q}$ :

  $$M_\mu \omega_j^2(0) = \sum_{\boldsymbol{R}\mu'} \Phi_{\mu\alpha,\mu'\alpha}(\boldsymbol{R}) = 0 \tag{4.47}$$

  because of equation (4.21). For these special phonon branches $j$, in which all atoms in the elementary cell are displaced in the same way, the vibration eigenfrequency must therefore go to 0 for $\boldsymbol{q} \to 0$ :

  $$\omega_j(\boldsymbol{q} = 0) = 0 \; . \tag{4.48}$$

  The physical reason is that in the limit $\boldsymbol{q} \to 0$, that is, in the extremely long-wavelength limit, there is also no modulation from one lattice cell to the next (the $e^{i\boldsymbol{q}\boldsymbol{R}}$ factor is approximated by 1), so all displacements become identical at a given time, which corresponds to a shift of the entire crystal, but cannot excite a lattice vibration.
- 1. Order in $\boldsymbol{q}$ :
  In linear order in $\boldsymbol{q}$ we find:

$$M_\mu 2\omega_j(0) \cdot \left(\nabla_{\boldsymbol{q}}\omega_j(\boldsymbol{q})|_{\boldsymbol{q}=0} \cdot \boldsymbol{q}\right) = \sum_{\boldsymbol{R}\mu'} \Phi_{\mu\alpha,\mu'\alpha}(-i\boldsymbol{q}\boldsymbol{R}) \ . \tag{4.49}$$

The left side still vanishes because of $\omega_j(0) = 0$, so the right side must also vanish. We therefore find another symmetry relation for the matrix $\underline{\underline{\Phi}}$ :

$$\sum_{\boldsymbol{R}\mu'} \Phi_{\mu\alpha,\mu'\alpha'}(\boldsymbol{R})\boldsymbol{R} = 0 \ . \tag{4.50}$$

- 2. order in $\boldsymbol{q}$ :
  In 2. order it results:

$$M_\mu \left(\nabla_{\boldsymbol{q}}\omega_j(\boldsymbol{q})|_{\boldsymbol{q}=0} \cdot \boldsymbol{q}\right)^2 = -\frac{1}{2}\sum_{\boldsymbol{R}\mu'} \Phi_{\mu\alpha,\mu'\alpha'}(\boldsymbol{R})(\boldsymbol{R}\boldsymbol{q})^2 \ . \tag{4.51}$$

This order generally does not disappear. It is recognized that $\omega_j(\boldsymbol{q})$ should go linearly with $\boldsymbol{q}$ against 0, more rigorously

$$\omega_j^2(\boldsymbol{q}) = \sum_{\alpha\alpha'} c_{\alpha\alpha'} q_\alpha q_{\alpha'} \quad \text{for small } |q| \ . \tag{4.52}$$

For the phonon branches, for which the atoms are displaced and oscillate evenly within an elementary cell, a linear dispersion relation and a vanishing of the eigenfrequencies for small $q$ is therefore to be expected. In dimension $d$ one expects $d$ such branches (corresponding to the $d$ spatial directions α). These phonon branches are also called **acoustic phonons**, because they correspond to the lattice vibrations that can be excited by sound waves and transport sound through the crystal. In total, $dr$ phonon branches are to be expected, and the remaining $d(r-1)$ branches are also called **optical phonons**. Intuitively, they correspond to vibration excitations in which the different atoms in an elementary cell do not oscillate in unison but against each other. In ionic crystals, in which the sites in an elementary cell are occupied by ions of different charge, such vibrations can be excited by electromagnetic fields, in particular by optical means, hence the name. The eigenfrequencies for such excitations do not vanish for $\boldsymbol{q} \to 0$. The term optical phonon is used more generally for lattice vibrations that are not necessarily optically excited, e.g. for those in crystals with covalent bonding and atoms of the same kind in the elementary cell, if they have the property that the atoms in the elementary cell oscillate against each other and the frequency does not vanish for $\boldsymbol{q} = 0$. In crystals with a one-atom primitive elementary cell, there are therefore only acoustic phonons.

In addition to the classification according to acoustic and optical phonons, a classification into transverse and longitudinal phonons is also common. At least for certain symmetry directions of the crystal, the displacements can be either parallel or perpendicular to the wave vector $\boldsymbol{q}$. Accordingly, one speaks of **longitudinal** or **transverse** phonon branches. In total, therefore, one distinguishes transverse-optical (TO), longitudinal optical (LO), transverse acoustic (TA) and longitudinal acoustic (LA) phonon branches. However, it should be noted that for arbitrarily chosen $\boldsymbol{q}$ directions, a classification as longitudinal or transverse is not always possible.

Typical dispersion curves $\omega(\boldsymbol{q})$ are calculated and discussed in Sect. 4.6.

## 4.5 Thermodynamics of Lattice Vibrations (Phonons), Debye and Einstein Model

The Hamiltonian operator (4.41) for the lattice vibrations in harmonic approximation describes formally non-interacting bosons. Therefore, if we want to calculate the thermal properties of a solid, which are due to the possible vibration excitations, we have to deal with a standard problem of statistical physics, namely that of non-interacting bosons. For such an ideal quantum gas, the occupation number representation and the grand canonical treatment are appropriate. However, since the phonons are quasiparticles, there is no particle number conservation and therefore no chemical potential. Therefore, the treatment is completely analogous to that of the photon gas (cavity radiation) from the lecture course on Statistical Physics. Alternatively, one can also treat the problem of $dNr$ uncoupled harmonic oscillators using the canonical ensemble. Due to the absence of a chemical potential, this canonical treatment and the grand canonical treatment are identical in the occupation number representation.

The internal energy of the phonon system is given by the expectation value of the Hamiltonian operator (4.41), that is:

$$E = \langle H_{\text{harm}} \rangle = \sum_{\boldsymbol{q}j} \hbar\omega_j(\boldsymbol{q}) \left( \left\langle b^{\dagger}_{\boldsymbol{q}j} b_{\boldsymbol{q}j} \right\rangle + \frac{1}{2} \right) . \tag{4.53}$$

Here, the thermal expectation value of the occupation number operator is given by the Bose function:

$$\left\langle n_{\boldsymbol{q}j} \right\rangle = \left\langle b^{\dagger}_{\boldsymbol{q}j} b_{\boldsymbol{q}j} \right\rangle = \frac{1}{e^{\frac{\hbar\omega_j(\boldsymbol{q})}{k_B T}} - 1} . \tag{4.54}$$

As usual, $T$ is the absolute temperature and $k_B = 1.38 \times 10^{-16}\,\text{erg/K} = 1.38 \times 10^{-23}\,\text{J/K} = 8.61 \times 10^{-5}\,\text{eV/K}$ is the Boltzmann constant. This result can also be derived elementary as follows:
The occupation probability for the state $n$ of a single oscillator is given by

$$P_n = \frac{e^{-\frac{E_n}{k_B T}}}{Z} = \frac{e^{-\frac{\left(n+\frac{1}{2}\right)\hbar\omega}{k_B T}}}{Z}$$

with the partition function

$$Z = \sum_n e^{-\frac{\left(n+\frac{1}{2}\right)\hbar\omega}{k_BT}} = e^{-\frac{\hbar\omega}{2k_BT}} \frac{1}{1-e^{-\frac{\hbar\omega}{k_BT}}} \, .$$

For the mean occupation number it follows

$$\begin{aligned}\langle n\rangle &= \frac{1}{Z}\sum_n \left(n\cdot e^{-\frac{(n+\frac{1}{2})\hbar\omega}{k_BT}}\right) = -\frac{k_BT}{\hbar}\frac{\partial}{\partial\omega}\ln\sum_n e^{-n\frac{\hbar\omega}{k_BT}} \\ &= -\frac{k_BT}{\hbar}\frac{\partial}{\partial\omega}\ln\frac{1}{1-e^{-\frac{\hbar\omega}{k_BT}}} = \frac{k_BT}{\hbar}\frac{\partial}{\partial\omega}\ln\left(1-e^{-\frac{\hbar\omega}{k_BT}}\right) = \frac{e^{-\frac{\hbar\omega}{k_BT}}}{1-e^{-\frac{\hbar\omega}{k_BT}}} \\ &= \frac{1}{e^{\frac{\hbar\omega}{k_BT}}-1} \, .\end{aligned}$$

By insertion of the Bose function one obtains explicitly for the internal energy:

$$E = \sum_{\boldsymbol{q},j} \hbar\omega_j(\boldsymbol{q}) \left(\frac{1}{e^{\hbar\omega_j(\boldsymbol{q})/k_BT}-1} + \frac{1}{2}\right) \, . \tag{4.55}$$

Here the finite zero point energy

$$E_0 = \sum_{\boldsymbol{q}j} \frac{1}{2}\hbar\omega_j(\boldsymbol{q}) \tag{4.56}$$

which is temperature-independent, still appears explicitly as an additive constant.

In two limiting cases one can calculate or estimate the ***q***-sums analytically:

- **high temperature limit**
  Since the phonon frequency spectra are bounded from above, there are temperatures that satisfy

  $$k_BT \gg \hbar\omega_j(\boldsymbol{q}) \quad \text{for all} \quad j, \boldsymbol{q} \tag{4.57}$$

  Then one obtains by expanding the exponential function

  $$\begin{aligned}E &= \sum_{\boldsymbol{q},j} \hbar\omega_j(\boldsymbol{q}) \left(\frac{1}{1+\hbar\omega_j(\boldsymbol{q})/k_BT+\ldots-1} + \frac{1}{2}\right) \\ &= \sum_{\boldsymbol{q},j} k_BT \left(1 + \frac{1}{2}\frac{\hbar\omega_j(\boldsymbol{q})}{k_BT} + \ldots\right) \, .\end{aligned} \tag{4.58}$$

  In leading order one obtains in dimension $d$ for a crystal made of $N$ unit cells and $r$ atoms per unit cell:

  $$E(T) = dNrk_BT \quad \text{for} \quad k_BT \gg \hbar\omega \tag{4.59}$$

This is precisely the

**Dulong-Petit Law**[3]

for the internal energy of $dNr$ classical harmonic oscillators. According to the laws of classical statistical mechanics (the Equipartition Theorem), each degree of freedom (each impulse or position coordinate that enters quadratically into the Hamilton function) contributes with $\frac{1}{2}k_BT$ to the internal energy. For example, this immediately results in the $\frac{3}{2}Nk_BT$-law for the classical, one-atom ideal gas or the $\frac{5}{2}Nk_BT$-law for two-atom ideal gases. A classical one-dimensional oscillator therefore has two degrees of freedom, one of kinetic and one of potential energy, and since the lattice vibrations of the $d$-dimensional crystal with $r$ atoms per unit cell can be described in harmonic approximation by $dNr$ uncoupled harmonic oscillators, an internal energy of $dNrk_BT$ is to be expected according to the Equipartition Theorem. In the limit of high temperatures, the classical result is therefore confirmed.[3]

- **Limit of low temperatures**
  For every low temperature $T$ there are eigenfrequencies $\omega_j(\boldsymbol{q})$ with $\hbar\omega_j(\boldsymbol{q}) < k_BT$, since at least the frequencies of the always present acoustic phonons go to 0 for $q \to 0$. Therefore, an assumption $k_BT \ll \hbar\omega$ and an expansion according to the corresponding small parameter is not possible, at least not for the acoustic phonon branches. However, one can assume that the temperature is so low that only acoustic phonons in the linear dispersion range $\omega \sim q$ can be thermally excited. Then, in the $\boldsymbol{q}$-sum only the $d$ acoustic branches occur as excited states and it applies:

$$E - E_0 = \sum_{\boldsymbol{q}s} \frac{\hbar c_s q}{e^{\hbar c_s q/k_BT} - 1} \; . \tag{4.60}$$

  Here, $s$ denotes the acoustic branches and $c_s$ the corresponding proportionality constant between frequency $\omega_s(\boldsymbol{q})$ and wave number $q$. This constant $c_s$ has the dimension of a velocity and is to be identified with the sound velocity. In general, however, one can expect different sound velocities for the different acoustic branches, in particular the propagation velocity for transverse and longitudinal branches are often different. If one replaces the $\boldsymbol{q}$-sum according to (4.39) by an integral, one obtains:

$$\begin{aligned} E - E_0 &= \frac{V}{(2\pi)^d} \sum_s \int d^d q \frac{\hbar c_s q}{e^{\hbar c_s q/k_BT} - 1} \\ &= \frac{V}{(2\pi)^d} \sum_s \frac{(k_BT)^d}{(\hbar c_s)^d} k_BT \int d^d x \frac{x}{e^x - 1} \; . \end{aligned} \tag{4.61}$$

---

[3] P.L. Dulong, 1785–1838, French chemist, found with Petit the classical law for the specific heat or heat capacity, further work on heat measurement, thermal expansion coefficients, etc.

Here, the substitution $x = \frac{\hbar c_s}{k_B T} \cdot q$ was made. The original $\boldsymbol{q}$-integral is to be extended over the first Brillouin zone or the primitive unit cell of the reciprocal lattice, if one disregards the fact that at the edge of the Brillouin zone, in fact, no longer a linear dispersion relation is valid; but this can be neglected because for sufficiently low $T$ for the states at the edge of the Brillouin zone $\hbar\omega \gg k_B T$ applies and therefore the occupation probability is exponentially small due to the Bose factor. The $d$ components $q_\alpha$ are therefore to be integrated in the limits of 0 to $\frac{\pi}{a}$, the by substitution resulting $x_\alpha$-integrals are to be extended accordingly from 0 to $\frac{\pi \hbar c_s}{a k_B T}$. For sufficiently low temperatures $T$, i.e. for

$$k_B T \ll \frac{\pi \hbar c_s}{a}, \tag{4.62}$$

the upper integration limit can therefore be approximated by $\infty$. Then, the $d$-dimensional integral can be reduced to a one-dimensional integral due to the isotropy of the integrand. In particular, for $d = 3$ one obtains:

$$E - E_0 = \frac{V}{(2\pi)^3} 3 \frac{(k_B T)^4}{(\hbar \bar{c}_s)^3} 4\pi \int_0^\infty dx \frac{x^3}{e^x - 1} = \frac{\pi^2}{10} \frac{V}{(\hbar \bar{c}_s)^3} (k_B T)^4 \ . \tag{4.63}$$

Here, the sum over the three possible branches was replaced by a factor 3 by introducing (in the case of anisotropic sound velocities) some average sound velocity $\bar{c}_s$; in addition, in the last step for the definite integral

$$\int_0^\infty dx \frac{x^3}{e^x - 1} = \frac{\pi^4}{15} \tag{4.64}$$

was used.
The contribution of the crystal's vibration excitations to the internal energy thus follows a characteristic $T^4$-law for low temperatures. This is completely analogous to the photon gas (black-body radiation), in which case, however, it applies throughout the whole temperature range. It is ultimately due to the linear dispersion $\omega \sim q$, which always exists for photons and for phonons for the energetically low-lying excitations, and to the Bose and quasiparticle character of the excitations.

The specific heat $C_V$ (per volume) can be directly determined from the internal energy. We thus obtain for three-dimensional systems for low temperatures:

$$C_V = \frac{1}{V} \frac{\partial E}{\partial T} = \frac{2}{5} \pi^2 k_B \left( \frac{k_B T}{\hbar c_s} \right)^3 , \tag{4.65}$$

for high temperatures

$$C_V = 3 \frac{N}{V} r k_B \ . \tag{4.66}$$

The lattice part of the specific heat thus shows a $T^3$-behavior for low temperatures $T$ and approaches a constant contribution for high $T$, if all vibration modes can be thermally excited. This is well confirmed by experiments.
A simplifying model that correctly contains both limiting cases and can be interpolating between them to a reasonable extent is the

**Debye-Model.**[4]

The following assumptions are made:

1. There is a linear dispersion relation
$$\omega(\boldsymbol{q}) = c_s q \ , \tag{4.67}$$
valid throughout the relevant $\boldsymbol{q}$-range,[4] with an appropriately chosen mean sound velocity $c_s$.
2. The Brillouin zone is replaced by a sphere of radius $q_D$. This "Debye wave number" $q_D$ is to be determined such that the number of states is equal to the number $N$ of atoms. Then this sphere has the same volume as the Brillouin zone it replaces. The purpose of introducing this "Debye sphere" is solely that all integrands and integration ranges then have spherical symmetry and the concrete calculation of the integrals is simplified. The Debye wave number is therefore defined by:
$$\sum_{\boldsymbol{q},|\boldsymbol{q}|\le q_D} 1 = N = \frac{V}{(2\pi)^3}\int_{|\boldsymbol{q}|\le q_D} d^3q \cdot 1 = \frac{V}{2\pi^2}\int_0^{q_D} dq q^2 = \frac{V}{2\pi^2}\frac{q_D^3}{3} \cdot \tag{4.68}$$
This results in:
$$q_D = \sqrt[3]{6\pi^2\frac{N}{V}} \ . \tag{4.69}$$
The Debye wave number is therefore solely determined by the density of atoms in the crystal, which remains finite even in the thermodynamic limit.

For the internal energy one obtains for 3 dimensions in the Debye model:

$$E - E_0 = 3\frac{V}{(2\pi)^3}\int_{|\boldsymbol{q}|\le q_D} d^3q \frac{\hbar c_s q}{e^{\hbar c_s q/k_BT} - 1} = 3\frac{V}{(2\pi)^3}4\pi\int_0^{q_D} dq \frac{\hbar c_s q^3}{e^{\hbar c_s q/k_BT} - 1}$$

---

[4] P. Debye, *1884 in Maastricht, †1966 in Ithaca (New York), Dutch Physicist and Physical Chemist PhD 1910 in Munich, Professor at the Universities Zürich, Utrecht, Göttingen and Leipzig, 1935 at the Kaiser-Wilhelm-Institute in Berlin, emigrated to the USA in 1940, Professor for Chemistry at Cornell-University in Ithaca (N.Y.), Nobel Prize for Chemistry 1936, proposed in 1916 to use pulverized samples for X-ray structure analysis of crystals (Debye-Scherrer-Method, powder diffraction), worked on dipole moments, atomic positions in molecules, light scattering, etc.,

$$= 3\frac{V}{2\pi^2}\left(\frac{k_BT}{\hbar c_s}\right)^3 k_BT\int_0^{x_D} dx\frac{x^3}{e^x-1} \tag{4.70}$$

where in the last step the substitution

$$x = \frac{\hbar c_s q}{k_BT}$$

was made again. A **Debye temperature** $\Theta_D$ and a **Debye frequency** $\omega_D$ are usually defined by

$$k_B\Theta_D = \hbar c_s q_D = \hbar\omega_D\ . \tag{4.71}$$

If one then uses$V = \frac{6\pi^2 N}{q_D^3}$, it follows:

$$E - E_0 = 9N\left(\frac{T}{\Theta_D}\right)^3 k_BT\int_0^{\Theta_D/T} dx\frac{x^3}{e^x-1}\ . \tag{4.72}$$

For the specific heat per volume, one then obtains analogously in the Debye model:

$$\begin{aligned} C_V = \frac{\partial}{\partial T}(E-E_0) &= \frac{3}{2\pi^2}\int_0^{q_D} dq\hbar c_s q^3\frac{\partial}{\partial T}\frac{1}{e^{\hbar c_s q/k_BT}-1} \\ &= \frac{3}{2\pi^2}\int_0^{q_D} dq\hbar c_s q^3\frac{\hbar c_s q}{k_BT^2}\frac{e^{\hbar c_s q/k_BT}}{(e^{\hbar c_s q/k_BT}-1)^2} \\ &= \frac{3}{2\pi^2}\left(\frac{k_BT}{\hbar c_s}\right)^3 k_B\int_0^{\Theta_D/T} dx\frac{x^4e^x}{(e^x-1)^2} \\ &= 9\frac{N}{V}\left(\frac{T}{\Theta_D}\right)^3 k_B\int_0^{\Theta_D/T} dx\frac{x^4e^x}{(e^x-1)^2}\ . \end{aligned} \tag{4.73}$$

For low temperatures one can again replace the upper integration limit by $\infty$ and it results because of

$$\int_0^\infty dx\frac{x^4e^x}{(e^x-1)^2} = \frac{4\pi^4}{15} = 25.97$$

$$C_V = 234\left(\frac{T}{\Theta_D}\right)^3\frac{N}{V}k_B\ . \tag{4.74}$$

For high temperatures, i.e.$\frac{\Theta_D}{T} \ll 1$ one can expand the integrand in powers of $x$ and thus obtain

$$C_V = 9\frac{N}{V}\left(\frac{T}{\Theta_D}\right)^3 k_B\int_0^{\Theta_D/T} dxx^2 = 3\frac{N}{V}k_B \tag{4.75}$$

So again the Dulong-Petit law for three acoustic branches, which are only considered in the Debye model, is obtained. For medium temperatures $T$ one must calculate the **Debye function**

$$D_n(x) = \int_0^x dy \frac{y^n}{e^y - 1}$$

for n=3 numerically resp. you can find them tabulated[5], so that a calculation of the full $T$ -dependence of the internal energy and specific heat becomes possible and the exact behavior is reproduced in the high and low temperature limit.

The Debye temperature can be determined for the various materials by adaptation to experimental results for the specific heat. $\Theta_D$ is typically of the order of $10^2$ $-10^3$ K. Such temperatures or the associated energies of $\sim 10^{-2}$ eV are characteristic of the phonons. This is also in agreement with the estimate from the Born-Oppenheimer approximation that lattice energies should be smaller than electronic energies by a factor of $10^{-2}$. Debye temperatures are tabulated for various materials and, for example: one finds for Al: $\Theta_D = 394\,\mathrm{K}$, C (diamond): $\Theta_D = 1860\,\mathrm{K}$, K: $\Theta_D = 100\,\mathrm{K}$. Closely related to this is the order of magnitude of the sound velocity, which is known to be at $c_s \sim 10^2 - 10^3\,\frac{\mathrm{m}}{\mathrm{s}}$. Because of $\hbar c_s q_D = k_B \Theta_D$ and $q_D \sim \frac{\pi}{a} \sim 10^8\,\mathrm{cm}^{-1}$, one finds

$$\Theta_D \sim \frac{10^{-15}\,\mathrm{eV\,s}\;10^3\,\mathrm{m\,s^{-1}}\;10^{10}\,\mathrm{m^{-1}}}{10^{-4}}\,\mathrm{eV\,K^{-1}} \sim 10^2\,\mathrm{K}$$

(because of $\hbar = 1.054 \times 10^{-34}\,\mathrm{Nm\,s} = 1.054 \times 10^{-27}\,\mathrm{erg\,s} = 6.59 \times 10^{-15}\,\mathrm{eVs}$). Another, much simpler model for lattice vibrations is the

### Einstein-Model.[6]

It makes the – in comparison to the Debye model – even simpler assumption[6]

$$\omega_j(\boldsymbol{q}) = \omega_0 \quad \text{for all } j, \boldsymbol{q} \,. \tag{4.76}$$

Then one obtains for the internal energy

$$E = E_0 + 3Nr \frac{\hbar\omega_0}{e^{\hbar\omega_0/k_B T} - 1} \tag{4.77}$$

---

[5] e.g. in: Abramowitz, Stegun: Handbook of Mathematical Functions, Dover Publications New York (1970).

[6] A. Einstein, * 1879 in Ulm, † 1955 in Princeton, one of the most important physicists of the 20th century, 1905 three groundbreaking works on kinetic gas theory (Brownian motion), special relativity and quantum theory of light, 1906 first quantum theory of lattice vibrations, which could explain the vanishing of the specific heat for very low temperatures, professor in Prague, Zurich and from 1914 in Berlin, 1916 general relativity, Nobel Prize in Physics 1921, emigrated 1933 and since then at the newly founded Institute for Advanced Studies at Princeton University in New Jersey.

and for the specific heat

$$C_V = \frac{1}{V}\frac{\partial}{\partial T}E = 3\,\frac{N}{V}r\frac{(\hbar\omega_0)^2}{k_BT^2}\,\frac{e^{\hbar\omega_0/k_BT}}{(e^{\hbar\omega_0/k_BT}-1)^2} \tag{4.78}$$

$$= 3\,\frac{N}{V}rk_B\left(\frac{\Theta_E}{T}\right)^2\frac{e^{\Theta_E/T}}{(e^{\Theta_E/T}-1)^2}\ .$$

The characteristic **Einstein temperature** for the phonon system was introduced here by

$$k_B\Theta_E = \hbar\omega_0\ . \tag{4.79}$$

In the limit of high temperatures ($T \gg \Theta_E$), the exponential function ($e^{\Theta_E/T} \approx 1 + \Theta_E/T + \ldots$) yields

$$E - E_0 = 3N\,rk_BT, \quad C_V = 3\,\frac{N}{V}rk_B \tag{4.80}$$

again, which is the Dulong-Petit law. In the limit of low temperatures ($T \ll \Theta_E$), the exponential function is very large, so that the 1 in the denominator can be neglected, i.e. the replacement $e^{\Theta_E/T} - 1 \approx e^{\Theta_E/T}$ is justified. This yields (see Fig. 4.2):

$$E - E_0 = 3\,Nrk_B\Theta_E e^{-\Theta_E/T}, \quad C_V = 3\,\frac{N}{V}rk_B\left(\frac{\Theta_E}{T}\right)^2 e^{-\Theta_E/T}\ . \tag{4.81}$$

Internal energy and specific heat therefore disappear exponentially for $T \to 0$. This is characteristic of systems with a gap in the excitation spectrum. In the

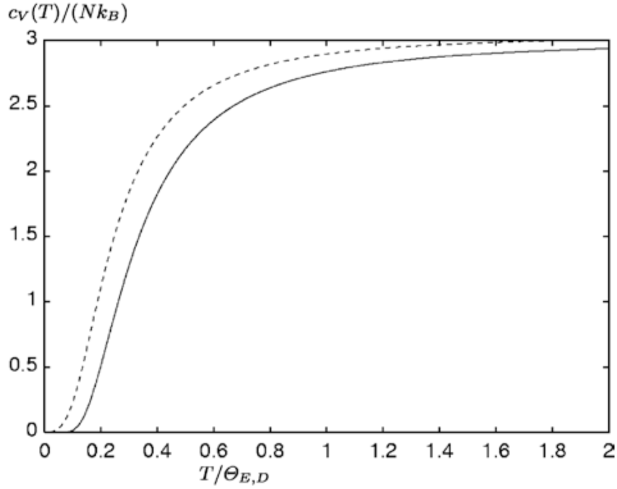

**Fig. 4.2** Temperature dependence of the lattice contribution to the specific heat in the Debye model (dashed curve) and in the Einstein model (full line)

Einstein model, there is precisely such a gap of $\hbar\omega_0 = k_B\Theta_E$, because this finite energy is neccessary to create a vibration excitation.

The experimentally confirmed characteristic $T^3$-law for the specific heat at low temperatures is therefore not included in the Einstein model. The reason for this is that the linear dispersion relation for acoustic phonons and the resulting disappearance of the excitation energy for $q \to 0$ is not taken into account, since a constant, $q$-independent $\omega_0$ was assumed. One could therefore conclude that the Einstein model is worse than the Debye model. But this is not the case, because there are vibration excitations whose frequency remains finite for $q \to 0$, namely the optical phonons. In fact, the $q$-dependence (dispersion) for optical phonons is also relatively small, so that the assumption of a $q$-independent frequency is not completely unrealistic for optical phonons. In summary, one can therefore say that the Einstein model gives a useful and physically meaningful approximation for the optical phonons, while the Debye model describes the acoustic phonons to a certain extent correctly.

## 4.6 Phonon Spectra and Densities of States

For more realistic, microscopic calculations than in the framework of the Debye model, model assumptions about the interaction potential are necessary and the diagonalization of the dynamic matrix is to be carried out concretely for a given crystal structure. The simplest examples of a one-atom and a two-atom linear chain can be found in almost all textbooks and scripts on experimental solid-state physics. Therefore, a not quite so simple example shall be discussed here, namely the phonon spectrum for a model of a three-dimensional lattice.

### 4.6.1 Example: Simple Cubic Lattice

We consider a one-atomic, simple cubic lattice with lattice constants $a$ and coupling of nearest and next-nearest neighbor atoms. These couplings can be thought of as mediated by springs of certain strength. If the atoms at lattice sites $\boldsymbol{R}_n$ and $\boldsymbol{R}_m$ are connected by a spring of spring constant $k$ and are displaced by $\boldsymbol{u}_n$ and $\boldsymbol{u}_m$ from their rest positions, then the corresponding contribution to the potential energy is given by:

$$V_{nm} = \frac{k}{2}\left(|\boldsymbol{R}_n + \boldsymbol{u}_n - \boldsymbol{R}_m - \boldsymbol{u}_m| - |\boldsymbol{R}_n - \boldsymbol{R}_m|\right)^2 \tag{4.82}$$

$$\approx \frac{k}{2}\left(\frac{1}{|\boldsymbol{R}_n - \boldsymbol{R}_m|}(\boldsymbol{R}_n - \boldsymbol{R}_m)\cdot(\boldsymbol{u}_n - \boldsymbol{u}_m)\right)^2 .$$

The spring should therefore be in the relaxed state when the atoms (mass points) occupy their equilibrium positions $\boldsymbol{R}_n, \boldsymbol{R}_m$. In the multidimensional case, not only the spring constants enter the dynamical matrix, but there are also anharmonic contributions despite the harmonic spring coupling, because the springs cannot only be stretched or compressed in the direction of the connecting vectors of the rest positions. Let us assume that nearest neighbors are coupled by springs of strength $k_1$, next-nearest neighbors by springs of strength $k_2$, then we get in harmonic approximation the following contribution to the potential:

$$V = \sum_R \frac{1}{4a^2} \left( k_1 \sum_{\Delta \mathrm{n.\,n.}} (\Delta \cdot (u_{R+\Delta} - u_R))^2 + \frac{k_2}{2} \sum_{\Delta' \mathrm{n.\,n.\,n}} \left( \Delta' \cdot (u_{R+\Delta'} - u_R) \right)^2 \right). \tag{4.83}$$

Here, the first factor $\frac{1}{2}$ corrects the double counting of the same coupling and the 2nd factor $\frac{1}{2}$ results from the spring potential. $\boldsymbol{\Delta}$ runs through the 6 vectors $(\pm a, 0, 0), (0, \pm a, 0), (0, 0, \pm a)$ and $\boldsymbol{\Delta}'$, the 12 vectors $(\pm a, \pm a, 0), (\pm a, 0, \pm a)$, $(0, \pm a, \pm a)$, $|\boldsymbol{\Delta}| = a$, $|\boldsymbol{\Delta}'| = \sqrt{2}a$. We denote the lattice vectors $\boldsymbol{R}$ by the integer triplets $(n, m, l)$ with respect to the cubic primitive unit vectors, then for $\boldsymbol{\Delta} = \pm a\boldsymbol{e}_x$ :

$$\boldsymbol{\Delta} \cdot (\boldsymbol{u}_{\boldsymbol{R}+\boldsymbol{\Delta}} - \boldsymbol{u}_{\boldsymbol{R}}) = a\left(u_{(n\pm1,m,l)x} - u_{(n,m,l)x}\right)$$

and correspondingly for the other nearest-neighbor vectors $\boldsymbol{\Delta}$. For $\boldsymbol{\Delta}' = (a, a, 0)$ we therefore have:

$$\boldsymbol{\Delta}' \cdot \left(\boldsymbol{u}_{\boldsymbol{R}+\boldsymbol{\Delta}'} - \boldsymbol{u}_{\boldsymbol{R}}\right) = a\left(u_{(n+1,m+1,l)x} - u_{(n,m,l)x} + u_{(n+1,m+1,l)y} - u_{(n,m,l)y}\right)$$

and analogous expressions for the other 11 possible connection vectors to next-nearest neighbors.

For the potential in harmonic approximation we therefore obtain

$$V = V_{\mathrm{n.n.}} + V_{\mathrm{n.\,n.\,n.}} \tag{4.84}$$

with

$$\begin{aligned} V_{\mathrm{n.n.}} &= \tfrac{1}{2} \textstyle\sum_{\boldsymbol{R}} \sum_{\boldsymbol{\Delta}\mathrm{n.n.}} \frac{k_1}{2|\boldsymbol{\Delta}|^2} \sum_{\alpha,\beta=1}^{3} \Delta_\alpha \Delta_\beta \left(2u_{\boldsymbol{R}\alpha} u_{\boldsymbol{R}\beta} - u_{\boldsymbol{R}\alpha} u_{\boldsymbol{R}+\boldsymbol{\Delta}\beta} - u_{\boldsymbol{R}+\boldsymbol{\Delta}\alpha} u_{\boldsymbol{R}\beta}\right) \\ &= \tfrac{1}{2} \textstyle\sum_{\boldsymbol{R}} \sum_{\boldsymbol{\Delta}\mathrm{n.n.}} \frac{k_1}{|\boldsymbol{\Delta}|^2} \sum_{\alpha,\beta=1}^{3} \Delta_\alpha \Delta_\beta \left(u_{\boldsymbol{R}\alpha} u_{\boldsymbol{R}\beta} - u_{\boldsymbol{R}\alpha} u_{\boldsymbol{R}+\boldsymbol{\Delta}\beta}\right) \end{aligned} \tag{4.85}$$

$$\begin{aligned} V_{\mathrm{n.\,n.\,n.}} &= \tfrac{1}{2} \textstyle\sum_{\boldsymbol{R}} \sum_{\boldsymbol{\Delta}'\mathrm{n.\,n.\,n.}} \frac{k_2}{2|\boldsymbol{\Delta}'|^2} \\ &\quad \times \textstyle\sum_{\alpha,\beta=1}^{3} \Delta'_\alpha \Delta'_\beta \left(2u_{\boldsymbol{R}\alpha} u_{\boldsymbol{R}\beta} - u_{\boldsymbol{R}\alpha} u_{\boldsymbol{R}+\boldsymbol{\Delta}'\beta} - u_{\boldsymbol{R}+\boldsymbol{\Delta}'\alpha} u_{\boldsymbol{R}\beta}\right) \\ &= \tfrac{1}{2} \textstyle\sum_{\boldsymbol{R}} \sum_{\boldsymbol{\Delta}'\mathrm{n.\,n.\,n.}} \frac{k_2}{|\boldsymbol{\Delta}'|^2} \sum_{\alpha,\beta=1}^{3} \Delta'_\alpha \Delta'_\beta \left(u_{\boldsymbol{R}\alpha} u_{\boldsymbol{R}\beta} - u_{\boldsymbol{R}\alpha} u_{\boldsymbol{R}+\boldsymbol{\Delta}'\beta}\right) . \end{aligned} \tag{4.86}$$

By comparison with (4.18) we can now read off the explicit form of the matrix elements $\Phi_{\alpha,\beta}(\boldsymbol{R})$ :

$$\Phi_{xx}(\boldsymbol{R} = 0) = 2k_1 + 4k_2, \quad \Phi_{xx}(\boldsymbol{R} = (a, 0, 0)) = -k_1,$$

$$\Phi_{xx}(\boldsymbol{R}=(a,a,0)) = -\frac{k_2}{2}$$

$$\Phi_{xy}(\boldsymbol{R}=0)=0, \quad \Phi_{xy}(\boldsymbol{R}=(a,0,0))=0, \quad \Phi_{xy}(\boldsymbol{R}=(a,\pm a,0)) = \mp\frac{k_2}{2}\ . \tag{4.87}$$

Using the cubic symmetry, the other matrix elements and their values for other connection vectors $\boldsymbol{R} \in \{\boldsymbol{\Delta}\text{n.n.}, \boldsymbol{\Delta}'\text{n.n.n.}\}$ can be concluded.
For the matrix elements of the $\boldsymbol{q}$-dependent dynamic matrix we therefore have:

$$D_{xx}(\boldsymbol{q}) = \frac{1}{M}\left[2k_1 + 4k_2 - k_1(e^{-iq_xa}+e^{iq_xa})\right. \tag{4.88}$$

$$-\frac{k_2}{2}\left(e^{iq_xa}e^{iq_ya} + e^{iq_xa}e^{-iq_ya} + e^{-iq_xa}e^{iq_ya} + e^{-iq_xa}e^{-iq_ya}\right.$$

$$\left.\left.+e^{iq_xa}e^{iq_za} + e^{iq_xa}e^{-iq_za} + e^{-iq_xa}e^{iq_za} + e^{-iq_xa}e^{-iq_za}\right)\right]$$

$$= \frac{1}{M}[2k_1(1-\cos(q_xa)) + 2k_2(2-\cos(q_xa)\cos(q_ya)$$

$$-\cos(q_xa)\cos(q_za))]$$

$$D_{xy}(\boldsymbol{q}) = -\frac{1}{M}\frac{k_2}{2}\left(e^{iq_xa}e^{iq_ya} - e^{iq_xa}e^{-iq_ya} - e^{-iq_xa}e^{iq_ya} + e^{-iq_xa}e^{-iq_ya}\right)$$

$$= \frac{1}{M}2k_2\sin(q_xa)\sin(q_ya)\ . \tag{4.89}$$

The remaining matrix elements of the $\boldsymbol{q}$-dependent dynamic matrix are obtained by exchanging the indices $x, y, z$ due to the cubic symmetry. To determine the eigenfrequencies $\omega_j^2(\boldsymbol{q})$, a $3 * 3$-matrix is now to be diagonalized for each $\boldsymbol{q}$ by solving the secular equation. $det\,(\underline{\underline{D}}(\boldsymbol{q}) - \omega^2\underline{\underline{1}}) = 0$. This leads to the solution of a cubic equation, which is still possible analytically, but leads to elongated, unreadable expressions. Therefore, the $3 * 3$-matrix was diagonalized numerically using standard algorithms[7]. In order to obtain a one-dimensional representation from which the essential properties of the frequency spectrum are already apparent, it is customary to vary $\boldsymbol{q}$ along certain symmetry directions of the Brillouin zone and to plot it. There are certain, special symmetry points in the Brillouin zone, for which a special nomenclature has been established, as was already discussed in Sect. 2.2

---

[7] E.g. the Matlab routine "eig".

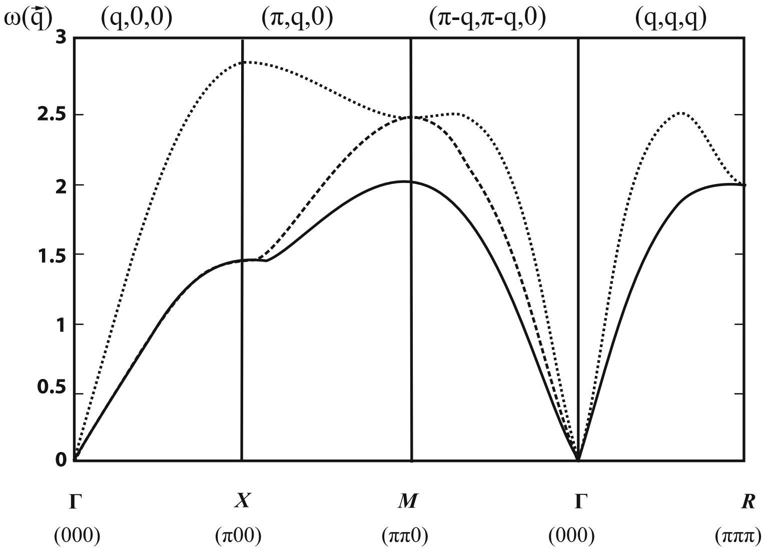

**Fig. 4.3** Phonon dispersions for a monatomic single-cubic lattice with nearest-neighbor and next-next-neighbor coupling along selected directions in the 1st Brillouin zone.

(see Fig. 2.1). For the simple cubic lattice, the Brillouin zone is also a cube in q-space of edge length $\frac{2\pi}{a}$, see also Fig. 2.1. A special symmetry point is therefore the center of the Brillouin zone, the so-called $\Gamma$ -point (000). Other special points are the X-point ($\frac{\pi}{a}$00), the M-point ($\frac{\pi}{a}\frac{\pi}{a}$0) and R-point ($\frac{\pi}{a}\frac{\pi}{a}\frac{\pi}{a}$), which is a corner point of the Brillouin zone. In Fig. 4.3 the dispersion curves $\omega_j(\boldsymbol{q})$ are shown, first for $\boldsymbol{q} = (q_x 00)$ varying from the $\Gamma$ point to the X point, so for $0 \leq q_x \leq \frac{\pi}{a}$, then for $\boldsymbol{q}$ from the X point to the M point varying, so for $\boldsymbol{q} = (\frac{\pi}{a} q_y 0)$ and $0 \leq q_y \leq \frac{\pi}{a}$, then from the M point back to the $\Gamma$ point, so for $\boldsymbol{q} = q(110)$ and $\frac{\pi}{a} \geq q \geq 0$ and finally again from the $\Gamma$ point to the R point, so along the space diagonal, so for $\boldsymbol{q} = q(111)$ and $0 \leq q \leq \frac{\pi}{a}$. The frequencies are measured in units of $\sqrt{k_1/M}$ and it was specifically assumed $k_1/k_2 = 2$.

One recognizes clearly that there are in general (for arbitrary directions in the Brillouin zone) three phonon branches. In particular, in (100)-direction, however, two branches are degenerate, namely the two transverse branches. This is physically immediately intuitively clear, since because of the cubic symmetry it must not matter whether for a transverse wave propagating in x-direction the mass points oscillate in y- or in z-direction. In particular, for this (100)-direction in the $\boldsymbol{q}$-space, the dispersion curve can also be given quite easily analytically, since for $q_y = q_z = 0$ the dynamic matrix $\underline{\underline{D}}(\boldsymbol{q})$ is already diagonal because of $\sin(q_y a) = \sin(q_z a) = 0$. Since in addition $\cos(q_y a) = \cos(q_z a) = 1$ is valid, we obtain according to (4.88) for $\boldsymbol{q} = (q_x 00)$ :

$$D_{xx}(\boldsymbol{q}) = \omega_l^2(\boldsymbol{q}) = \frac{2k_1 + 4k_2}{M}(1 - \cos(q_x a))$$

$$D_{yy}(\boldsymbol{q}) = D_{zz}(\boldsymbol{q}) = \omega_{t1,2}^2(\boldsymbol{q}) = \frac{2k_2}{M}(1 - \cos(q_x a)) \ . \tag{4.90}$$

For the chosen parameters $k_1 = 2k_2$ therefore the longitudinal branch varies from 0 to $2\sqrt{2}\sqrt{k_1/M}$, but the two transverse branches only from 0 to $\sqrt{2}\sqrt{k_1/M}$, as can be seen also from the figure; otherwise the dispersion (as in one dimension) follows a course according to $\sqrt{1 - \cos(q_x a)} = \sqrt{2}\sin(q_x a/2)$. The dispersion curves are linear in q apparently only in the vicinity of the Γ-point, which is also understandable, since only there the condition of small $q$ is fulfilled. But the increase is different in the different directions of the Brillouin zone and for longitudinal and transverse modes, so the sound velocity is not isotropic for more realistic lattice structures. The linear approximation for $\omega_j(\boldsymbol{q})$ seems to be usable in a relatively large range of the Brillouin zone. In addition, there is a maximum frequency at $\sqrt{\frac{2k_1+4k_2}{M}} = 2\sqrt{2}\sqrt{\frac{k_1}{M}}$.

### 4.6.2 Phonon Density of States

For many practical purposes, one is not interested in the full information that the detailed knowledge of the dispersion relations $\omega_j(\boldsymbol{q})$ provides. Often, it is enough to know whether there are vibration excitations at certain frequencies and, if so, how many. The size that contains this information and is characteristic of the phonon spectrum is the **density of states** $n(\omega)$. It is defined as the number of vibration states with eigenfrequency in the frequency interval $d\omega$ at ω $d\omega$ and per volume or per unit cell; both normalizations are common and only differ by a factor of atomic density $N/V$. In formulas, the definition of the density of states is:

$$n(\omega) = \frac{1}{N}\sum_j \sum_{\boldsymbol{q}} \delta(\omega - \omega_j(\boldsymbol{q})) = \frac{V}{N}\sum_j \int_{1.BZ} \frac{d^d q}{(2\pi)^d}\delta(\omega - \omega_j(\boldsymbol{q})) \ . \tag{4.91}$$

Obviously,

$$n(\omega)\Delta\omega = \int_\omega^{\omega+\Delta\omega} d\omega' n(\omega') = \frac{1}{N}\sum_{j\boldsymbol{q}} \int_\omega^{\omega+\Delta\omega} d\omega' \delta(\omega' - \omega(\boldsymbol{q})) \tag{4.92}$$

$$= \frac{1}{N} \cdot (\text{number of states between } \omega \text{ and } \omega + \Delta\omega) \ . \tag{4.93}$$

In total, the density of states is normalized to $dr$ :

$$\int_0^\infty d\omega n(\omega) = d \cdot r \; . \tag{4.94}$$

Because of

$$\lim_{\delta\to 0} \mathrm{Im} \frac{1}{x + i\delta} = -\pi\delta(x)$$

, the density of states can also be written as:

$$n(\omega) = -\frac{1}{\pi}\frac{1}{N}\sum_j \sum_{\boldsymbol{q}} \mathrm{Im} \frac{1}{\omega + i0 - \omega_j(\boldsymbol{q})} \; . \tag{4.95}$$

A major reason for the introduction of the density of states is the fact that many quantities ultimately only depend on frequency or energy; they depend on **q** only implicitly via $\omega_j(\boldsymbol{q})$. Such quantities (such as the internal energy) can be represented as:

$$\tilde{Q} = \sum_{j\boldsymbol{q}} Q(\omega_j(\boldsymbol{q})) \tag{4.96}$$

and should actually be calculated by calculating the $\boldsymbol{q}$ sum or the corresponding $d$-dimensional $\boldsymbol{q}$ integral. However, if one knows the density of states $n(\omega)$ corresponding to the vibration spectrum, it applies

$$\tilde{Q} = \int_0^\infty d\omega n(\omega) Q(\omega) \; . \tag{4.97}$$

Thus, only a one-dimensional integral over the density of states has to be calculated. Many measured quantities can thus be represented as a frequency integral over the product of density of states and a function characteristic for the measured quantity, and if the density of states is known once, only one-dimensional ω-integrals instead of multidimensional $\boldsymbol{q}$-integrals have to be carried out.

The equation

$$\omega_j(\boldsymbol{q}) = \omega \tag{4.98}$$

defines a surface $S(\omega)$ in the $\boldsymbol{q}$-space, namely the surface of the $\boldsymbol{q}$-points, for which the corresponding frequency is exactly ω. The density of states is therefore proportional to the volume of a shell in the $\boldsymbol{q}$-space, which is formed by the surfaces $S(\omega), S(\omega + \Delta\omega)$. It therefore applies

$$n(\omega)d\omega = \frac{V}{N}\sum_j \int_{S(\omega)} \frac{ds}{(2\pi)^d} dq_\perp \; , \tag{4.99}$$

where $ds$ denotes an surface element of $S(\omega)$ and $dq_\perp$ the distance to the surface $S(\omega + d\omega)$ at this point of the surface. Thus, the integral as a whole gives the desired shell volume. For the points on the shell $S(\omega + d\omega)$ it holds, if $\boldsymbol{q}$ is a point on $S(\omega)$:

$$\omega_j(\boldsymbol{q} + d\boldsymbol{q}) = \omega_j(\boldsymbol{q}) + \nabla_{\boldsymbol{q}}\omega_j(\boldsymbol{q}) \cdot d\boldsymbol{q} = \omega + d\omega \,. \tag{4.100}$$

From this it follows:

$$d\omega = \nabla_{\boldsymbol{q}}\omega_j(\boldsymbol{q}) \cdot d\boldsymbol{q} = |\nabla_{\boldsymbol{q}}\omega_j(\boldsymbol{q})| \cdot dq_\perp \,. \tag{4.101}$$

This gives the density of states

$$n(\omega) = \frac{V}{N}\sum_j \frac{1}{(2\pi)^d}\int_{S(\omega)} \frac{ds}{|\nabla_{\boldsymbol{q}}\omega_j(\boldsymbol{q})|} \,. \tag{4.102}$$

The density of states is thus given by a surface integral over the surface to constant ω. In one dimension, this is particularly simple, since the “surface” consists of only one point; therefore, only the derivative of the dispersion relation has to be calculated and $q$ has to be substituted by ω. For a one-atom linear chain with coupling (“spring” with spring constant $K$) to the next neighbor, the dispersion is given by

$$\omega^2(q) = \frac{2K}{M}(1 - \cos(qa)) = \frac{4K}{M}\sin^2\left(\frac{qa}{2}\right) . \tag{4.103}$$

From this it follows

$$\omega(q) = 2\sqrt{\frac{K}{M}}\left|\sin\frac{qa}{2}\right| \tag{4.104}$$

$$\left|\frac{d\omega}{dq}\right| = a\sqrt{\frac{K}{M}}\cos\left(\frac{qa}{2}\right) = a\sqrt{\frac{K}{M}\left(1 - \sin^2\left(\frac{qa}{2}\right)\right)} \,.$$

The one-dimensional phonon density of states is therefore (factor 2 due to same behavior for positive and negative $q$):

$$n_{1d}(\omega) = \frac{2a}{2\pi a\sqrt{\frac{K}{M} - \frac{\omega^2}{4}}} = \frac{2}{\pi}\frac{1}{\sqrt{\omega_m^2 - \omega^2}} \tag{4.105}$$

with the maximum frequency $\omega_m = 2\sqrt{\frac{K}{M}}$. This typical phonon density of states for a one-dimensional system with the characteristic (inverse square root) Van Hove singularity at $\omega_m$ for $d = 1$ is shown in Fig. 4.4.

The numerically calculated density of states for the simple cubic system with nearest and next-nearest neighbor coupling discussed in the previous section is shown in Fig. 4.5; the frequency is measured in units of $\sqrt{\frac{k_1}{M}}$, as in Fig. 4.3. A clear increase in the density of states proportional to $\omega^2$ for small ω is seen, but there is also a rich, structure characteristic for the lattice and the couplings

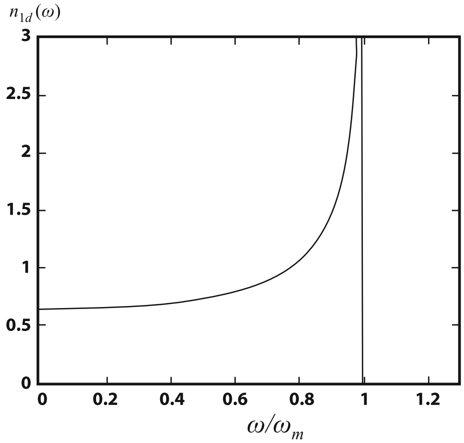

**Fig. 4.4** Phonon state density for a one-atom linear chain

considered in the middle frequency range. The spectrum ends at the frequency $\omega_m = 2\sqrt{2}$, as can be seen from the $\omega_j(\boldsymbol{q})$ dispersion curves in Fig. 4.3.

The behavior for small ω is a direct consequence of the linear dispersion relation; in the range of validity of the latter, $|\nabla_{\boldsymbol{q}}\omega_j(\boldsymbol{q})| = c_s$ and the surfaces of constant frequency are $d$-dimensional spheres. Therefore, for small ω, the following behavior of the density of states results:

$$\text{for} \quad d = 1 : n(\omega) = \frac{L}{N}\frac{1}{2\pi c_s} = \frac{a}{2\pi c_s} = \text{const.} \tag{4.106}$$

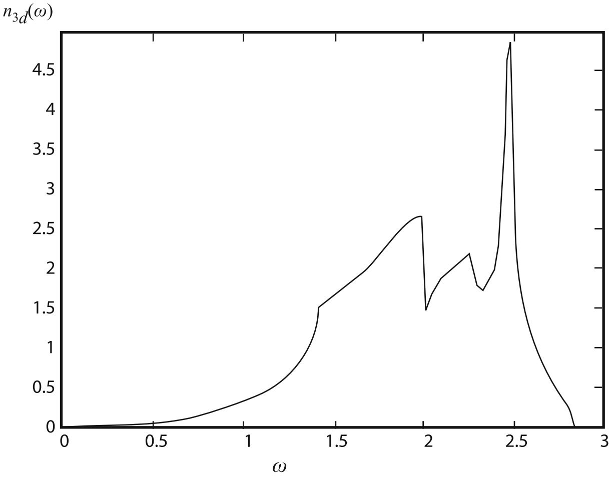

**Fig. 4.5** Phonon density of states for the 3-dimensional simple cubic system with nearest and next-nearest neighbor coupling

$$\text{for} \quad d = 2 : n(\omega) = 2\,\frac{F}{N} 2\pi \frac{q}{(2\pi)^2 c_s} = 2\,\frac{a^2}{2\pi c_s^2}\omega \tag{4.107}$$

$$\text{for} \quad d = 3 : n(\omega) = 3\,\frac{V}{N} 4\pi \frac{q^2}{(2\pi)^3 c_s} = \frac{3a^3}{2\pi^2 c_s^3}\omega^2 \; . \tag{4.108}$$

In particular, for the Debye model and $d = 3$, the calculated $\omega^2$ behavior of the density of states is valid in the whole range, i. e.

$$n_D(\omega) = \begin{cases} \frac{3a^3}{2\pi^2 c_s^3}\omega^2 & \text{for} \quad 0 \le \omega \le \omega_D \\ 0 & \text{else} \end{cases} \; . \tag{4.109}$$

This results in

$$\int_0^{\omega_D} n_D(\omega) d\omega = \frac{3a^3}{6\pi^2 c_s^3}\omega_D^3 = 3 \; , \tag{4.110}$$

where the relations (4.69) and (4.71) were used for the Debye frequency. The normalization to 3 corresponds to the three acoustic branches. The density of states of the Einstein model is even simpler and given by a delta function:

$$n_E(\omega) = d \cdot r \cdot \delta(\omega - \omega_0) \; . \tag{4.111}$$

A characteristic property of more realistic densities of states are singularities at certain frequencies $\omega_c$, which can be seen in the density of states shown in Fig. 4.5. This type of singularity is called a **Van-Hove singularity**[8]. They are characteristic of the dimension and the lattice type and occur exactly for the frequencies for which the dispersion relations $\omega_j(\boldsymbol{q})$ for certain branches $j$ have a horizontal tangent, i.e. $\nabla_{\boldsymbol{q}}\omega_j(\boldsymbol{q}) = 0$ is fulfilled. For the example discussed in the previous section, there are such singularities therefore in particular at $\omega_c = \sqrt{2}, 2, 2.5, 2\sqrt{2}$, as the dispersion curves of Fig. 4.3 show. It is easy to see that at the corresponding values $\omega_c$ there is a singular behavior of the density of states, cf. Fig. 4.5. Formally, this singular behavior can be traced back to the fact that in the representation (4.102) for the density of states the integrand diverges for special values of $\boldsymbol{q}$ for the corresponding values $\omega_c$.

The type of singularity can be estimated analytically. There are apparently two types of points in the $\boldsymbol{q}$-space with $\nabla_{\boldsymbol{q}}\omega_j(\boldsymbol{q}) = 0$, namely extrema (maxima or minima) of $\omega_j(\boldsymbol{q})$ and saddle points; for our example, at $\omega_c = \omega_m = 2\sqrt{2} = 2.82$ there is certainly a maximum, but at $\omega_c = \sqrt{2}$ a saddle point is present. Now the dispersion relation can be expanded in the vicinity of the critical point $\boldsymbol{q}_c$, where one has to go up to second order because of $\nabla_{\boldsymbol{q}}\omega_j(\boldsymbol{q}) = 0$. This leads for $d = 3$ to:

---

[8] L. van Hove, * 1924 in Brussels, † 1990, Belgian theoretical physicist, 1954 professor in Utrecht, works include quantum field theory, many-particle physics, theory of neutron scattering, phase transitions, transport theory, from 1961 head of the theory department at CERN in Geneva.

$$\omega = \omega(\boldsymbol{q}) = \omega(\boldsymbol{q}_c) + \nabla_{\boldsymbol{q}}\omega(\boldsymbol{q})|_{\boldsymbol{q}_c} \tag{4.112}$$
$$+\frac{1}{2}\sum_{i,j=1}^{3}\frac{\partial^2}{\partial q_i \partial q_j}\omega(\boldsymbol{q})|_{\boldsymbol{q}_c}(q_i - q_{ci})(q_j - q_{cj}) + \ldots$$

By a principal axis transformation (diagonalization of the symmetric $3 * 3$-matrix $(\frac{\partial^2}{\partial q_i \partial q_j}\omega(\boldsymbol{q})|_{\boldsymbol{q}_c})$ this can be brought into the following form:

$$\omega = \omega_c + \sum_{i=1}^{3}\varepsilon_i \kappa_i^2 \,. \tag{4.113}$$

Here now four cases are conceivable:

1. if all $\varepsilon_i > 0$, then there is a minimum,
2. if all $\varepsilon_i < 0$, then there is a maximum,
3. $\varepsilon_1, \varepsilon_2 > 0, \varepsilon_3 < 0$, then there is a saddle point of type 1,
4. $\varepsilon_1 > 0, \varepsilon_2, \varepsilon_3 < 0$, then there is a saddle point of type 2.

The behavior of the density of states in the vicinity of $\omega_c$ is then given according to (4.91) essentially by

$$n(\omega) \sim \int d^3\kappa\,\delta\left(\omega - \omega_c - \sum_i \varepsilon_i \kappa_i^2\right) . \tag{4.114}$$

In the case of the minimum, the substitution $x_i = \sqrt{\varepsilon_i}\kappa_i$ immediately leads to

$$\begin{aligned} n(\omega) &\sim \frac{1}{\sqrt{\varepsilon_1\varepsilon_2\varepsilon_3}}\int dxdydz\,\delta\left(\omega - \omega_c - x^2 - y^2 - z^2\right) \\ &= \frac{1}{\sqrt{\varepsilon_1\varepsilon_2\varepsilon_3}}4\pi\int dr r^2\delta\left(\omega - \omega_c - r^2\right) \\ &= \frac{1}{\sqrt{\varepsilon_1\varepsilon_2\varepsilon_3}}2\pi\int d\tilde{r}\sqrt{\tilde{r}}\,\delta(\omega - \omega_c - \tilde{r}) \\ &\sim \sqrt{\omega - \omega_c} \,. \end{aligned} \tag{4.115}$$

In the case of the maximum, the substitution $x_i = \sqrt{|\varepsilon_i|}\kappa_i$ leads analogously to

$$n(\omega) \sim \sqrt{\omega_c - \omega} \,. \tag{4.116}$$

In particular, the density of states vanishes at the upper edge of the spectrum for 3-dimensional systems as $\sqrt{\omega_c - \omega}$.

In the case of a saddle point, i.e. at critical points inside the spectrum, one can estimate the singular behavior analogously, e.g. by transition to cylindrical coordinates. If one substitutes at a saddle point of type 1 ($\varepsilon_1, \varepsilon_2 > 0, \varepsilon_3 < 0$): $x_i = \sqrt{|\varepsilon_i|}\kappa_i$ and then goes over to cylindrical coordinates, one obtains:

$$n(\omega) \sim \frac{2\pi}{\sqrt{|\varepsilon_1\varepsilon_2\varepsilon_3|}} \int drrdz\delta\left(\omega - \omega_c - r^2 + z^2\right) \tag{4.117}$$

$$\sim \int dr \frac{r}{\sqrt{r^2 + \omega_c - \omega}} \sim \sqrt{r^2 + \omega_c - \omega}\Big|_0^{r_m} = C - \sqrt{\omega_c - \omega}\,.$$

Analogously, one can estimate at a saddle point of 2nd order:

$$n(\omega) \sim C - \sqrt{\omega - \omega_c} \quad \text{for} \quad \omega > \omega_c\,. \tag{4.118}$$

There are also Van-Hove singularities of higher order, e.g. if $\varepsilon_i = 0$ applies. Analogous estimates about the type of singularity can also be made for 1- and 2-dimensional systems. For $d = 2$, jump singularities at the extrema of the dispersion relation arise, in particular at the upper edge of the spectrum, and logarithmic Van-Hove singularities within the spectrum are typical, for $d = 1$ one finds $\frac{1}{\sqrt{\omega}}$-singularities at the edge of the spectrum.

To conclude this section, Fig. 4.6 shows phonon dispersion curves and derived phonon densities of states for crystalline Ar and NaCl, which were measured

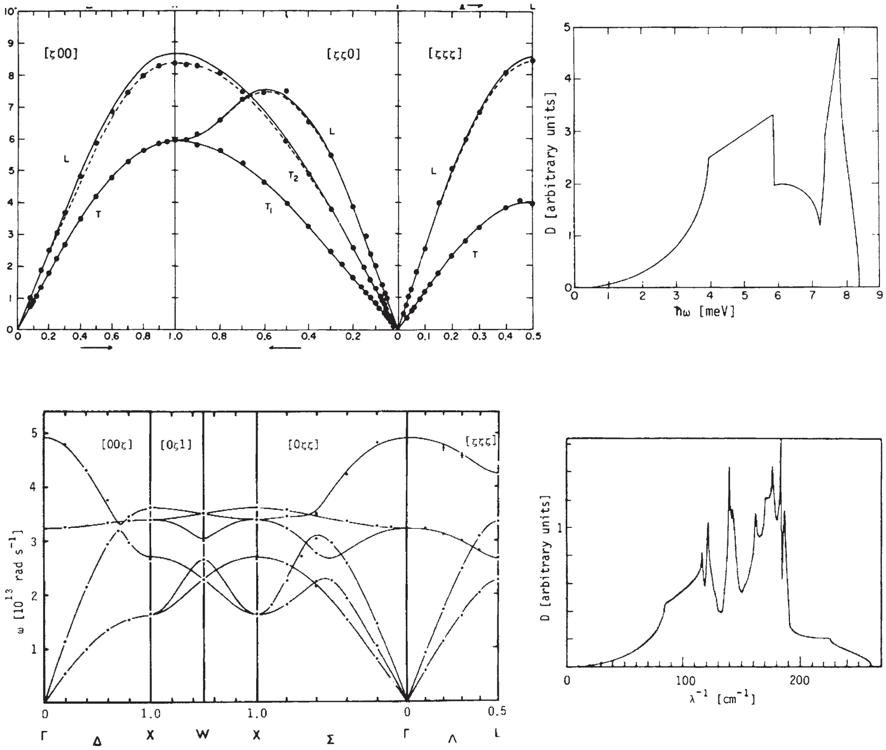

**Fig. 4.6** Measured and calculated phonon dispersion relations and state densities for Ar and NaCl (fcc lattice with one-atom or two-atom basis)

and calculated, respectively.[9] For the one-atom fcc system Ar, a clear qualitative similarity to the fcc spectrum calculated with the nearest-neighbor spring model is evident. In particular, the typical Van Hove singularities can be seen. For the two-atom fcc lattice of NaCl, the optical branches are also visible; however, in the density of states, these are not necessarily separated from the acoustic part of the phonon spectrum by a gap in three dimensions.

## 4.7 Long Wavelength Limit

### 4.7.1 Acoustic phonons and elastic waves

In the limit of large wavelength or small $q$ one can sometimes neglect the discrete, atomic structure and instead work in the continuum limit. This is justified if one is working on a length scale that is large compared to the lattice constant $a$, that is, on the order of the wavelength of the sound waves. This transition from the discrete lattice structure to the continuum limit in the limit $a \ll 1/q$ will be carried out in this section.

Since only acoustic phonons are considered, it is sufficient to work with a one-atom basis; otherwise, one can think of the different atoms of the unit cell as being united in the center of the unit cell. We then start from the classical equation of motion (4.19):

$$M\ddot{u}_{n\alpha} = -\sum_{n'\alpha'} \Phi_{n\alpha,n'\alpha'} u_{n'\alpha'} \; . \tag{4.119}$$

We now assume that only displacements $u_{n'\alpha'}$ at points $\boldsymbol{R}_{n'}$ in the vicinity of $\boldsymbol{R}_n$ exert a force on the mass there, as was already assumed in the models of coupling to nearest and next-nearest neighbors, etc. Furthermore, since over the distance of a few lattice vectors only a slow change of $\boldsymbol{u}_n$ is to be expected, an expansion is justified:

$$\begin{aligned} u_{n'\alpha'} = u_{\alpha'}(\boldsymbol{R}_{n'}) &= u_{\alpha'}(\boldsymbol{R}_n) + \sum_{\beta} \frac{\partial u_{\alpha'}(\boldsymbol{R}_n)}{\partial r_\beta}(R_{n'\beta} - R_{n\beta}) \\ &+ \frac{1}{2}\sum_{\beta\beta'} \frac{\partial^2 u_{\alpha'}(\boldsymbol{R}_n)}{\partial r_\beta \partial r_{\beta'}}(R_{n'\beta} - R_{n\beta})(R_{n'\beta'} - R_{n\beta'}) \; . \end{aligned} \tag{4.120}$$

If one inserts this expansion into (4.119) and uses the elementary symmetry relations (4.21) (or (4.47) and 4.50)) for the matrix $\underline{\underline{\Phi}}$, i.e.

---

[9] From: H. Biltz, W. Kress: Phonon Dispersion Relations in Insulators, Springer Series in Solid State Sciences 10 (1979).

$$\sum_{n'} \Phi_{n\alpha,n'\alpha'} = 0\,, \quad \sum_{n'} \Phi_{n\alpha,n'\alpha'} \cdot (\boldsymbol{R}_{n'} - \boldsymbol{R}_n) = 0\,, \tag{4.121}$$

one obtains:

$$M\ddot{u}_\alpha(\boldsymbol{R}_n) = -\frac{1}{2} \sum_{n'\alpha'\beta\beta'} \Phi_{n\alpha,n'\alpha'} \cdot (R_{n'\beta} - R_{n\beta})(R_{n'\beta'} - R_{n\beta'}) \frac{\partial^2 u_{\alpha'}(\boldsymbol{R}_n)}{\partial r_\beta \partial r_{\beta'}} \cdot \tag{4.122}$$

If one further divides by the volume of the unit cell, considers the displacements as a continuous displacement field $\boldsymbol{u}(\boldsymbol{r}, t)$, defines the density as $\rho = M/V_{EZ}$ and introduces the new constants

$$C_{\alpha\alpha',\beta\beta'} = -\frac{1}{2V_{EZ}} \sum_{n'} \Phi_{\alpha\alpha'}(\boldsymbol{R}_n - \boldsymbol{R}_{n'}) \cdot (R_{n'\beta} - R_{n\beta})(R_{n'\beta'} - R_{n\beta'}), \tag{4.123}$$

one finally obtains the wave equation

$$\rho \cdot \frac{\partial^2}{\partial t^2} u_\alpha(\boldsymbol{r}, t) = \sum_{\alpha'\beta\beta'} C_{\alpha\alpha',\beta\beta'} \frac{\partial^2}{\partial r_\beta \partial r_{\beta'}} u_{\alpha'}(\boldsymbol{r}, t)\,. \tag{4.124}$$

The coefficients $C_{\alpha\alpha',\beta\beta'}$ form a tensor of 4th degree $\underline{\underline{\underline{\underline{C}}}}$, the

**Tensor of elastic constants.**

The elements of this tensor satisfy certain symmetry relations, e.g.

$$C_{\alpha\alpha',\beta\beta'} = C_{\alpha'\alpha,\beta'\beta} = C_{\alpha\alpha',\beta'\beta}\,. \tag{4.125}$$

Already because of this relatively elementary symmetry, there are not 81 different elastic constants but at most 36 elastic constants. In fact, there are only 21 different elastic constants. By further symmetry considerations, these can be further reduced, e.g. for a cubic system only 3 different elastic constants remain, namely $C_{xx,xx}, C_{xx,yy}, C_{xy,xy}$. The elastic constants can therefore be traced back microscopically to the force constants $\Phi_{\alpha,\alpha'}$. Conversely, the elastic constants allow conclusions to be drawn about $\underline{\underline{\Phi}}$. The elastic constants determine, on the one hand, the elastic waves in a classical continuous medium, which can be regarded as the long-wavelength limit of the lattice waves and thus of the phonons. On the other hand, the elastic constants can also be obtained from static measurements, e.g. by measuring deformations under the influence of external forces or volume changes by applying pressure.

Since in the introductory course on theoretical mechanics usually no elasticity theory is treated anymore, the basics of elasticity theory shall be summarized briefly below: We consider a displacement field $\boldsymbol{u}(\boldsymbol{r}, t)$. In the elastic range, the displacements are overall relatively small compared to the dimensions of the system. Therefore, a linear relationship can be assumed:

$$u_\alpha = \sum_{\alpha'} v_{\alpha\alpha'} x_{\alpha'} \ . \tag{4.126}$$

The tensor $\underline{\underline{v}}$ can now be decomposed into a symmetric and an antisymmetric part according to

$$v_{\alpha\alpha'} = \frac{1}{2}(v_{\alpha\alpha'} + v_{\alpha'\alpha}) + \frac{1}{2}(v_{\alpha\alpha'} - v_{\alpha'\alpha}) = \varepsilon_{\alpha\alpha'} + \omega_{\alpha\alpha'} \ . \tag{4.127}$$

One can convince oneself that $\underline{\underline{\omega}}$ describes a pure rotation and $\underline{\underline{\varepsilon}}$ a deformation of the body. The symmetric tensor $\underline{\underline{\varepsilon}}$ is also called the **strain tensor**, the antisymmetric tensor $\underline{\underline{\omega}}$ only has 3 independent elements, which can also be regarded as components of a 3-dimensional (pseudo-) vector $\underline{\omega} = \boldsymbol{\omega}$, so that $\underline{\underline{\omega}} \cdot \underline{a} = \boldsymbol{\omega} \times \boldsymbol{a}$ applies.

**Examples**

1. The deformation described by

$$\underline{\underline{v}} = \begin{pmatrix} 0 & \varphi & 0 \\ 0 & 0 & 0 \\ 0 & 0 & 0 \end{pmatrix} \text{ i.e. } u_x = \varphi y \ , \quad u_y = u_z = 0$$

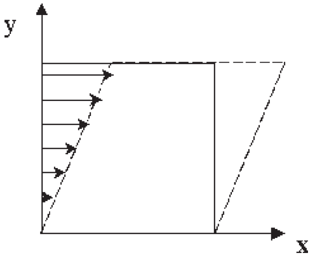

can be considered to be composed of a pure stretching,

$$\underline{\underline{\varepsilon}} = \begin{pmatrix} 0 & \frac{\varphi}{2} & 0 \\ \frac{\varphi}{2} & 0 & 0 \\ 0 & 0 & 0 \end{pmatrix} \text{ i.e. } u_x = \frac{\varphi}{2} y \ , \quad u_y = \frac{\varphi}{2} x \ , u_z = 0 \ ,$$

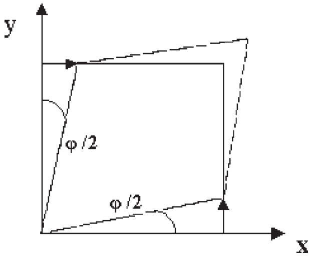

namely a shearing, and a rotation

$$\underline{\underline{\omega}} = \begin{pmatrix} 0 & \frac{\varphi}{2} & 0 \\ -\frac{\varphi}{2} & 0 & 0 \\ 0 & 0 & 0 \end{pmatrix} \text{ i.e. } u_x = \frac{\varphi}{2} y\,, \quad u_y = -\frac{\varphi}{2} x\,,$$

$$u_z = 0\,.$$

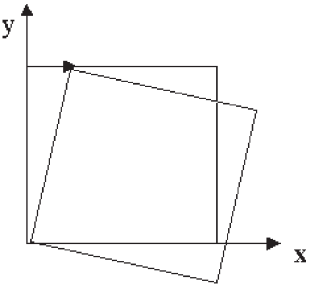

2. A simple one-dimensional extension is described by the tensor:

$$\underline{\underline{\varepsilon}} = \begin{pmatrix} \varepsilon_{11} & 0 & 0 \\ 0 & 0 & 0 \\ 0 & 0 & 0 \end{pmatrix} \text{ i.e. } u_x = \varepsilon_{11} x\,, \quad u_y = u_z = 0\,.$$

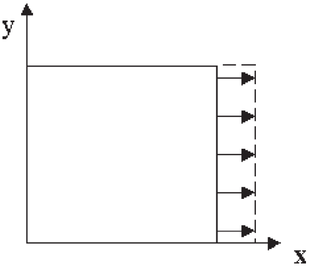

3. An (isotropic) compression is described by

$$\underline{\underline{\varepsilon}} = \begin{pmatrix} \varepsilon & 0 & 0 \\ 0 & \varepsilon & 0 \\ 0 & 0 & \varepsilon \end{pmatrix} \text{ d. h. } u_x = \varepsilon x\,, \quad u_y = \varepsilon y\,,$$

$$u_z = \varepsilon z\,.$$

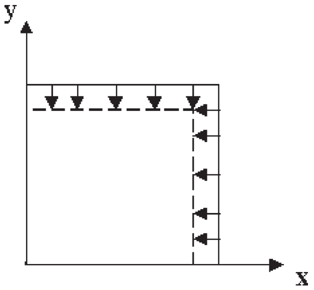

For general $\boldsymbol{u}(\boldsymbol{r})$ the elements of the strain tensor can be written as:

$$\varepsilon_{\alpha\beta} = \frac{1}{2}\left(\frac{\partial u_\alpha}{\partial x_\beta} + \frac{\partial u_\beta}{\partial x_\alpha}\right) . \tag{4.128}$$

In addition to the forces on the whole mass within a volume element (such as gravity), there are also internal forces exerted by other volume elements on this one in a continuous body with mass density $\rho(\boldsymbol{r})$. These forces can be considered as surface forces on the surfaces of the volume element; the forces per unit area are called tension or pressure. If $\boldsymbol{df}$ is the normal vector on a surface element $df$ that separates the considered $dV$ from an adjacent $dV'$, then the force acting on $df$ is not necessarily parallel to $\boldsymbol{df}$. For the internal force on $df$ therefore

$$d\boldsymbol{K} = \underline{\underline{\sigma}}\boldsymbol{df} , \tag{4.129}$$

applies, where $\underline{\underline{\sigma}}$ is the **stress tensor**. This is symmetric and in general dependent on location. In the absence of external (volume) forces, therefore, for a volume element $\Delta V$ of the body, the equation of motion holds:

$$\int_{\Delta V} \rho(\boldsymbol{r})\ddot{\boldsymbol{u}}(\boldsymbol{r},t)d^3r = \int_{O(\Delta V)} \underline{\underline{\sigma}}(\boldsymbol{r})\boldsymbol{df} . \tag{4.130}$$

Applying the Gauss theorem, this results in:

$$\rho\ddot{u}_\alpha(\boldsymbol{r},t) = \sum_\beta \frac{\partial}{\partial x_\beta}\sigma_{\alpha\beta}(\boldsymbol{r}) . \tag{4.131}$$

The stresses are often caused by strains, and the simplest assumption is to demand a linear relationship. This is just the generalization of the **Hooke's law**[10]. The general linear relationship between two second-order tensors (here stress and strain tensor) is described by a tensor of 4th order, and this is the tensor of elastic constants:

$$\underline{\underline{\sigma}} = \underline{\underline{\underline{\underline{C}}}} \cdot \underline{\underline{\varepsilon}} . \tag{4.132}$$

---

[10] Named after Robert Hooke (1635-1703), English polymath.

Since both the stress and strain tensors are symmetric, they both have a maximum of 6 independent matrix elements; the elasticity tensor between them can therefore have a maximum of 36 matrix elements; however, since it is itself symmetric, there are only a maximum of 21 elastic constants. From these, measurable quantities characteristic for the body and material can be calculated, such as the compression modulus or the shear modulus.

If we now insert (4.132), (4.128) in (4.131), we get:

$$\rho \ddot{u}_\alpha = \sum_{\alpha'\beta\beta'} C_{\alpha\alpha',\beta\beta'} \frac{\partial^2}{\partial x_\beta \partial x_{\beta'}} u_{\alpha'} \ . \tag{4.133}$$

This agrees with (4.124), which makes it clear that and how the elastic constants are to be determined from the microscopic parameters of the "force constant matrix" $\underline{\underline{\Phi}}$.

### 4.7.2 Long Wavelength Optical Phonons and Electromagnetic Waves, Polaritons

We consider an ionic crystal with two ions per elementary cell in this section. In such a system, there are optical phonon branches. In the long wavelength limit, the differently charged ions are deflected against each other in all elementary cells in the same way and oscillate against each other. First, it is physically plausible that for $q \to 0$ the longitudinal optical (LO) phonons must have a higher frequency or energy than the transverse optical (TO) phonons. For small $q$, after all, entire sublattices of the positive ions oscillate against the corresponding sublattice of the negative ions. This results in a surface charge and a macroscopic electric field. For LO phonons, this field also acts for small $q \neq 0$ so that it counteracts the displacement, thus working in addition to the usual restoring forces. But for TO phonons, this is no longer the case at least for macroscopically large crystals and small finite $q$ ; while there is still a field caused by the surface charges, it no longer causes a force in the transverse displacement direction. This consideration makes it plausible that for ionic crystals in general:

$$\omega_{LO}(\boldsymbol{q}) > \omega_{TO}(\boldsymbol{q}) \quad \text{for } q \to 0 \ . \tag{4.134}$$

Since the long-wavelength optical phonons generate macroscopic electric fields, a coupling to electromagnetic waves of the corresponding frequencies is to be expected. If one plots the (linear) dispersion relation for light (photons) into the phonon dispersion diagram, it is initially clear that the light line runs extremely steeply and intersects the optical phonon dispersions very close to $q = 0$. This is because in the photon dispersion relation $\omega = cq$ the speed of light is used instead of the speed of sound, which is about a factor of $10^5$ larger. Therefore, one can neglect the dispersion of the optical phonons and work with the frequencies of the LO or TO phonons at $q = 0$. As for the long-wavelength acoustic phonons, we consider a displacement vector $\boldsymbol{u}(\boldsymbol{r},t) = \boldsymbol{u}_+(\boldsymbol{r},t) - \boldsymbol{u}_-(\boldsymbol{r},t)$ which no longer depends on the discrete lattice vector but continuously on the position $\boldsymbol{r}$. In the presence of an electric field, an additional force is exerted on the charged ions, which enters as an inhomogeneity in the equations of motion. These are therefore of the form:

$$\ddot{\boldsymbol{u}} = -\omega_0^2 \boldsymbol{u} + e^* \boldsymbol{E} \; . \tag{4.135}$$

Here $e^*$ is an effective charge of the ions. The displacement of the differently charged ions against each other causes an electric dipole moment and, as we know from electrodynamics in matter, an additional explicit contribution to the polarization after averaging over microscopic regions. But even without the displacement of the ions, a polarization can already be present in the material due to the $\boldsymbol{E}$-field, caused, for example, by shifting the electrons in the (inner) shells of the ions. There are therefore two contributions to the polarization, i.e.:

$$\boldsymbol{P} = \beta \boldsymbol{u} + \gamma \boldsymbol{E} \; . \tag{4.136}$$

As solutions one can use the ansatz of plane waves as usual:

$$\boldsymbol{E} = \boldsymbol{E}_0 e^{i(\boldsymbol{qr}-\omega t)} \; , \quad \boldsymbol{P} = \boldsymbol{P}_0 e^{i(\boldsymbol{qr}-\omega t)} \; , \quad \boldsymbol{u} = \boldsymbol{u}_0 e^{i(\boldsymbol{qr}-\omega t)} \; . \tag{4.137}$$

This results in:

$$\boldsymbol{u} = \frac{e^*}{\omega_0^2 - \omega^2} \cdot \boldsymbol{E} \tag{4.138}$$

$$\boldsymbol{P} = \left( \frac{\beta e^*}{\omega_0^2 - \omega^2} + \gamma \right) \boldsymbol{E} = \frac{\varepsilon(\omega) - 1}{4\pi} \boldsymbol{E} \; , \tag{4.139}$$

where the latter equation corresponds to the standard definition of the (frequency-dependent) dielectric constant $\varepsilon$ from electrodynamics (in the cgs system). We therefore obtain:

$$\varepsilon(\omega) = 1 + 4\pi \left( \gamma + \frac{\beta e^*}{\omega_0^2 - \omega^2} \right) \; . \tag{4.140}$$

$\omega_0$ is supposed to be the frequency of the TO phonon here, ω is the frequency of the light, i.e. the electromagnetic field that forces the system to vibrate. The still unknown phenomenological constants can be expressed in terms of the dielectric constants for small and large frequencies. Obviously one has:

$$\varepsilon_0 = 1 + 4\pi \left( \gamma + \frac{\beta e^*}{\omega_0^2} \right) \; , \quad \varepsilon_\infty = 1 + 4\pi\gamma \; . \tag{4.141}$$

This results in:

$$\varepsilon(\omega) = \frac{\omega_0^2\varepsilon_0 - \omega^2\varepsilon_\infty}{\omega_0^2 - \omega^2} \; . \tag{4.142}$$

So we have determined the frequency dependence of the dielectric constant for small $q$ ; it is $\varepsilon(\omega = 0) = \varepsilon_0$ and $\varepsilon(\omega \to \infty) = \varepsilon_\infty$. for$\omega \to \infty$, strictly speaking only $\omega \gg \omega_0$ ; if ω has the order of magnitude of electronic excitations, there are further modifications.

We now have to consider the Maxwell equations with the found result for the dielectric function; due to the usual plane wave ansatz the Maxwell equations yield

$$\boldsymbol{q} \times \boldsymbol{B} = -\frac{\omega}{c}\varepsilon(\omega)\boldsymbol{E} \; , \quad \boldsymbol{q} \times \boldsymbol{E} = \frac{\omega}{c}\boldsymbol{B}$$

$$\boldsymbol{q} \cdot \boldsymbol{B} = 0 \; , \quad \varepsilon(\omega)\boldsymbol{q} \cdot \boldsymbol{E} = 0 \; . \tag{4.143}$$

Obviously, the electromagnetic fields are usually transverse, as usual, with one possible exception, namely if

$$\varepsilon(\omega) = 0 \tag{4.144}$$

applies. For this special frequency

$$\omega_l^2 = \frac{\varepsilon_0}{\varepsilon_\infty}\omega_0^2 \tag{4.145}$$

, the transmission of a longitudinal wave is possible if $\boldsymbol{B} = 0$ applies at the same time. This just corresponds to the LO phonon, i.e. $\omega_l = \omega_{LO}$, $\omega_0 = \omega_{TO}$. The above relationship (4.145) is also called the **Lyddane-Sachs-Teller relation**, which links the splitting between LO and TO phonons with the static and high-frequency dielectric constants. According to the consideration at the beginning of this subsection, $\omega_l > \omega_0$ and therefore also $\varepsilon_0 > \varepsilon_\infty$ apply.

For $\varepsilon(\omega) \neq 0$, the electromagnetic waves that can propagate through the crystal must be transverse as usual. It then follows that

$$\boldsymbol{q} \times (\boldsymbol{q} \times \boldsymbol{E}) = \boldsymbol{q} \cdot (\boldsymbol{q} \cdot \boldsymbol{E}) - q^2\boldsymbol{E} = \frac{\omega}{c}\boldsymbol{q} \times \boldsymbol{B} = -\left(\frac{\omega}{c}\right)^2 \varepsilon(\omega)\boldsymbol{E}$$

$$\left(\frac{\omega}{c}\right)^2 \frac{\omega_0^2\varepsilon_0 - \omega^2\varepsilon_\infty}{\omega_0^2 - \omega^2} = q^2 \; . \tag{4.146}$$

This is a quadratic equation for $\omega^2$ (and thus a biquadratic equation for ω) with the solution

$$\omega_{1,2}^2(\boldsymbol{q}) = \frac{1}{2\varepsilon_\infty}\left[c^2q^2 + \omega_0^2\varepsilon_0 \pm \sqrt{\left(c^2q^2 + \omega_0^2\varepsilon_0\right)^2 - 4c^2q^2\omega_0^2\varepsilon_\infty}\right] . \tag{4.147}$$

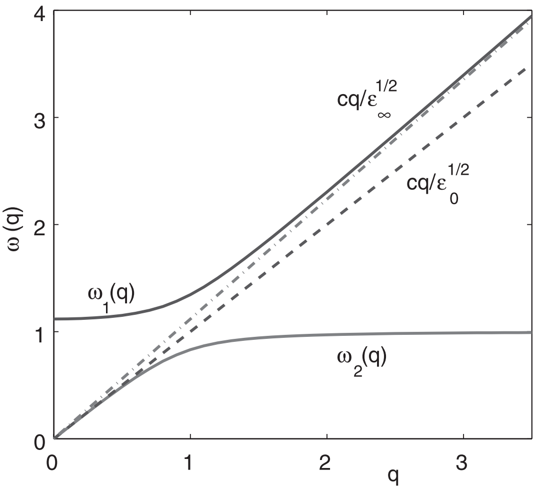

**Fig. 4.7** Dispersion curve of the (phonon-) polariton

There are therefore two branches of transverse excitations when an electromagnetic wave couples to the optical phonons, which are plotted in Fig. 4.7. This coupled excitation is also called a

**Polariton.**

A polariton is an excitation consisting of an electromagnetic wave and an optical lattice wave coupled together, or in the quantum picture, a superposition of a photon and a transverse optical phonon. For $q \to 0$, the upper branch apparently goes over into

$$\omega_1 \to \omega_0 \sqrt{\frac{\varepsilon_0}{\varepsilon_\infty}} = \omega_l = \omega_{LO} \ , \tag{4.148}$$

i.e. the frequency of the LO phonon. The second branch behaves for small $q$ like

$$\omega_2 \overset{q \to 0}{\to} \frac{cq}{\sqrt{\varepsilon_0}} \ . \tag{4.149}$$

This just corresponds to the propagation of an electromagnetic wave in the medium with the (static) dielectric constant $\varepsilon_0$, that is, the refractive index $n = \sqrt{\varepsilon_0}$. For large $q$, the polariton dispersions go over into

$$\omega_1 = \frac{cq}{\sqrt{\varepsilon_\infty}} \tag{4.150}$$

$$\omega_2 = \omega_0 = \omega_{TO} \ . \tag{4.151}$$

The first (upper) branch then behaves like a photon in the medium with dielectric constant $\varepsilon_\infty$, the second (lower) branch corresponds to the simple TO phonon. For frequencies between $\omega_{TO}$ and $\omega_{LO}$, there are no solutions propagating through the crystal (at least for small $q$, that is, for large wavelengths). In this forbidden frequency range, therefore, no waves can propagate through the crystal, neither electromagnetic waves nor lattice waves. An electromagnetic wave incident on the ionic crystal in this frequency interval will therefore not penetrate into the crystal and must be totally reflected.

## 4.8 (Neutron) Scattering on Crystals (Phonons), Debye-Waller Factor

Scattering experiments are a particularly important type of experiment that provides information about the physical properties of the sample. In particular, neutron scattering is very important in solid-state physics, because the momentum and energy of the neutrons are just of the right order of magnitude for excitations in the crystal. However, many of the formulas discussed in this section are also valid for other types of scattering experiments.

A monochromatic neutron beam consisting of neutrons with momentum $\hbar\boldsymbol{k}$ and thus with energy $E(\boldsymbol{k}) = \frac{\hbar^2 k^2}{2M_N}$ falls on a sample, i.e. on a crystal, whose physical properties are to be examined. Then, at a certain angle relative to the direction of incidence, a detector is set up and the number of neutrons scattered at this angle is measured. More information is obtained if one measures energy-resolved, i.e. the number of neutrons scattered at the angle with a certain energy. The measured quantity is then directly the

**double differential cross section**

$$\frac{d^2\sigma}{d\Omega d\omega} = \frac{N_s(\Omega,\omega)}{N_a d\Omega d\omega}\,, \tag{4.152}$$

where $N_s(\Omega,\omega)$ denotes the number of particles scattered per unit time into the solid angle element $d\Omega$ around $\Omega$ with energy transfer between $\hbar\omega$ and $\hbar(\omega + d\omega)$ and $N_a$ the number of particles per unit time and unit area incident; $d\Omega$ is a (infinitesimal) solid angle element and $d\omega$ an infinitesimal frequency interval. So it holds:

$$N_a = \text{incident particle current} = \frac{\hbar k}{M_N} \cdot n_N \tag{4.153}$$

$$N_s(\Omega,\omega) = N_s\big(\boldsymbol{k},\boldsymbol{k}'\big) = \sum_{i,f} \frac{e^{-E_i/k_BT}}{Z} \cdot W\big(\boldsymbol{k}i \to \boldsymbol{k}'f\big) n_N \frac{Vol^2}{(2\pi)^3} d^3k'\,. \tag{4.154}$$

Here, $n_N$ is the particle (neutron) density, $n_N Vol$ is therefore the number of neutrons, $W(\boldsymbol{k}i \to \boldsymbol{k}'f)$ is the (quantum mechanical) transition probability (per unit time) for a transition of the neutron from the state $\boldsymbol{k}$ to the state $\boldsymbol{k}'$ with simultaneous transition of the sample (of the crystal) from the initial state $i$ into the final state $f$, the statistical factor gives the thermodynamic probability that the (many-particle) state $i$ of the crystal is occupied ($Z$ is the partition function of the sample), and the factor $\frac{Vol}{(2\pi)^3}d^3k'$ is the number of neutron final states in the volume $Vol$. If one takes into account that $d^3k' = k'^2dk'd\Omega$ applies and because of the energy conservation

$$\hbar\omega = \frac{\hbar^2}{2M_N}(k'^2 - k^2) = E_i - E_f \ , \tag{4.155}$$

holds and that therefore $\hbar k'dk' = M_N d\omega$ follows, the scattering cross section turns into

$$\frac{d^2\sigma}{d\Omega d\omega} = \left(\frac{M_N}{2\pi\hbar}\right)^2 \frac{Vol^2}{2\pi}\frac{k'}{k}\sum_{i,f}\frac{e^{-E_i/k_BT}}{Z}W\big(\boldsymbol{k}i \to \boldsymbol{k}'f\big) \ . \tag{4.156}$$

For the quantum mechanical transition probability $W(\boldsymbol{k}i \to \boldsymbol{k}'f)$ (per unit time) we now use

**Fermi's golden rule[11]:**

$$W\big(\boldsymbol{k}i \to \boldsymbol{k}'f\big) = \frac{2\pi}{\hbar}\left|\left\langle \boldsymbol{k}i|V|\boldsymbol{k}'f\right\rangle\right|^2\delta(E_f - E_i + \hbar\omega) \ . \tag{4.157}$$

Here, $V$ is the interaction potential between neutrons and crystal. The neutron initial and final states are states of free particles, i.e. plane waves $e^{i\boldsymbol{k}\boldsymbol{r}}/\sqrt{Vol}$. Therefore it follows:

$$\left\langle \boldsymbol{k}i|V|\boldsymbol{k}'f\right\rangle = \frac{1}{Vol}\int d^3r e^{i(\boldsymbol{k}'-\boldsymbol{k})\boldsymbol{r}}\langle i|V|f\rangle \ . \tag{4.158}$$

Neutrons as neutral particles of the diameter of a nucleus interact on the one hand with the atomic nuclei, from which they can be scattered, at least if only such materials and neutron energies are used, in which no nuclear reactions occur, on the other hand, the spin of the neutrons also interacts with any magnetic moments present in the system. Here, the magnetic neutron scattering is not considered, then the interaction potential neutron-crystal is to be described by:

$$V(\boldsymbol{r}) = \sum_n v(\boldsymbol{r} - \boldsymbol{R}_n) = \sum_n v_0\delta(\boldsymbol{r} - \boldsymbol{R}_n) \ . \tag{4.159}$$

Here $v(\boldsymbol{r}) = v_0\delta(\boldsymbol{r})$ is the interaction potential neutron-atomic nucleus; This can be replaced by a delta potential, since the radius of the atomic nucleus ($\sim 10^{-13}$ cm) is extremely small compared to the length scale lattice constant ($\sim 10^{-8}$ cm $= 1$ Å), on which we work in solid state physics otherwise. Then it follows:

$$\left\langle \boldsymbol{k}i|V|\boldsymbol{k}'f\right\rangle = \frac{v_0}{Vol}\sum_n\left\langle i|e^{i\boldsymbol{q}\boldsymbol{R}_n}|f\right\rangle \ , \tag{4.160}$$

---

[11] Named after Enrico Fermi, see footnote 5.8.

where $\boldsymbol{q} = \boldsymbol{k}' - \boldsymbol{k}$ denotes the momentum transfer. For the scattering cross section one obtains:

$$\frac{d^2\sigma}{d\Omega d\omega} = \left(\frac{M_N}{2\pi\hbar}\right)^2 \frac{k'}{k} N \frac{v_0^2}{\hbar^2} S(\boldsymbol{q},\omega) \tag{4.161}$$

with the **dynamic structure factor**

$$\begin{aligned} S(\boldsymbol{q},\omega) &= \frac{\hbar}{ZN}\sum_{i,f} e^{-E_i/k_BT} \sum_{n,n'} \left\langle i | e^{i\boldsymbol{q}\boldsymbol{R}_n} | f \right\rangle \left\langle f | e^{-i\boldsymbol{q}\boldsymbol{R}_{n'}} | i \right\rangle \delta(E_f - E_i + \hbar\omega) \\ &= \frac{1}{N}\int_{-\infty}^{\infty} \frac{dt}{2\pi} e^{i\omega t} \sum_{n,n'} \left\langle e^{i\boldsymbol{q}\boldsymbol{R}_n} e^{iHt/\hbar} e^{-i\boldsymbol{q}\boldsymbol{R}_{n'}} e^{-iHt/\hbar} \right\rangle \\ &= \frac{1}{N}\int_{-\infty}^{\infty} \frac{dt}{2\pi} e^{i\omega t} \sum_{n,n'} \left\langle e^{i\boldsymbol{q}\boldsymbol{R}_n} \cdot e^{-i\boldsymbol{q}\boldsymbol{R}_{n'}}(t) \right\rangle , \end{aligned} \tag{4.162}$$

where the time dependence of operators in the Heisenberg picture has been used and it was used

$$\begin{aligned} \delta(\hbar\omega) &= \frac{1}{\hbar}\delta(\omega) = \frac{1}{2\pi\hbar}\int_{-\infty}^{+\infty} dt e^{i\omega t} \\ \langle A \cdot B(t)\rangle &= \frac{1}{Z}\sum_{i,f} e^{-E_i/k_BT} \langle i \,|\, A \,|f\rangle\langle f \,|\, e^{iHt/\hbar} B e^{-iHt/\hbar} |i\rangle \ . \end{aligned}$$

With neutron scattering one measures thus directly the dynamic structure factor of the crystal, and this is related to a certain correlation function of the type $\langle AB(t)\rangle$, where the operators $A, B$ are determined by the displacements.

The positions of the atomic nuclei are time-dependent in the case of lattice vibrations and are given by:

$$\boldsymbol{R}_n = \boldsymbol{R}_{n0} + \boldsymbol{u}_n \ , \tag{4.163}$$

where the $\boldsymbol{R}_{n0}$ are the fixed lattice vectors (equilibrium positions) and the $\boldsymbol{u}_n$ are the displacements. This implies:

$$S(\boldsymbol{q},\omega) = \frac{1}{N}\int_{-\infty}^{+\infty} \frac{dt}{2\pi} e^{i\omega t} \sum_{n,n'} e^{i\boldsymbol{q}(\boldsymbol{R}_{n0} - \boldsymbol{R}_{n'0})} \langle \exp(i\boldsymbol{q}\boldsymbol{u}_n) \cdot \exp(-i\boldsymbol{q}\boldsymbol{u}_{n'})(t)\rangle \ . \tag{4.164}$$

For further calculation, two operator relations are used which are useful and important not only here, but quite generally in solid state and quantum theory, namely the so-called

**Baker-Hausdorff formula:**

$$e^A e^B = e^{(A+B)} e^{[A,B]/2} \tag{4.165}$$

for any two operators

$$A, B \text{ with } [A,[A,B]] = [[A,B],B] = 0 \ .$$

**Proof:**
Define $f(x) = e^{-xB} A e^{xB}$. This fulfills: $f'(x) = [A,B]$ (independent of x), if $[B,[A,B]] = 0$. Thus: $f(x) = [A,B]x + A$, i. e.:

$$e^{-xB} A = (A + [A,B]x) e^{-xB} \ .$$

In particular, for $x = 1$ it follows:

$$e^{-B} A e^{B} = [A,B] + A \ .$$

Now define $g(x) = e^{x(A+B)} e^{-xB} e^{-xA}$. This fulfills: $g'(x) = e^{x(A+B)}(A + B - B)e^{-xB}e^{-xA} + e^{x(A+B)}e^{-xB}(-A)e^{-xA}$.

Thus: $g'(x) = e^{x(A+B)}[A, e^{-xB}]e^{-xA} = -\, e^{x(A+B)}[A,B]xe^{-xB}e^{-xA} = -\,[A,B]xg(x)$.

Thus: $g(x) = e^{-x^2[A,B]/2}$. In particular, for $x = 1$ it follows: $g(1) = e^{(A+B)}e^{-B}e^{-A} = e^{-[A,B]/2}$, which corresponds to the claim.

Furthermore, the following statement applies:

If $a, a^\dagger$ are Bose operators with $[a, a^\dagger] = 1$ and $L = xa + ya^\dagger$ a linear combination of these creation and annihilation operators, then one has for the thermodynamic expectation value with respect to an in the $a, a^\dagger$ diagonal Hamilton operator $h = \varepsilon a^\dagger a$ :

$$\left\langle e^L \right\rangle = e^{\left\langle L^2 \right\rangle /2} \ . \tag{4.166}$$

**Proof:**

First, using the Baker-Haussdorff formula:

$$\left\langle e^L \right\rangle = \left\langle e^{(xa+ya^\dagger)} \right\rangle = \left\langle e^{xa} e^{ya^\dagger} \right\rangle e^{-xy/2} \ .$$

Set: $k(x) = e^{-xa^\dagger a} a e^{xa^\dagger a}$. Then $k(0) = a$, $k'(x) = e^{-xa^\dagger a}(-a^\dagger a a + a a^\dagger a)e^{xa^\dagger a} = k(x)$. Thus: $k'(x) = k(x)$, so: $k(x) = ae^x$ or $e^{-xa^\dagger a} a = e^x a e^{-xa^\dagger a}$. This finally leads to $h(x) = \left\langle e^{xa} e^{ya^\dagger} \right\rangle$, $h'(x) = \frac{1}{Z} Sp(e^{-\varepsilon a^\dagger a/k_B T} a e^{xa} e^{ya^\dagger}) = \frac{1}{Z} Sp(e^{\varepsilon/k_B T} a e^{-\varepsilon a^\dagger a/k_B T} e^{xa} e^{ya^\dagger})$ $= \frac{1}{Z} e^{\varepsilon/k_B T} Sp(e^{-\varepsilon a^\dagger a/k_B T} e^{xa} e^{ya^\dagger} a)$

According to the rules derived above one has $e^{ya^\dagger} a = (a - y[a, a^\dagger])e^{ya^\dagger}$, from which finally follows:

$$h'(x) = e^{\varepsilon/k_B T}(h'(x) - yh(x)) \ ,$$

thus

$$h'(x) = \frac{y e^{\varepsilon/k_B T}}{e^{\varepsilon/k_B T} - 1} h(x) \ .$$

So: $h(x) = \exp\left[\frac{xye^{\varepsilon/k_BT}}{e^{\varepsilon/k_BT}-1}\right]$ and

$$\left\langle e^L \right\rangle = h(x)e^{-xy/2} = \exp\left[\frac{xy}{2}\frac{e^{\varepsilon/k_BT}+1}{e^{\varepsilon/k_BT}-1}\right] .$$

On the other hand:

$$\begin{aligned}\left\langle L^2 \right\rangle &= \left\langle (xa+ya^\dagger)^2 \right\rangle = xy\left\langle aa^\dagger + a^\dagger a \right\rangle = xy(2\left\langle a^\dagger a \right\rangle + 1)\\ &= xy\left(\frac{2}{e^{\varepsilon/k_BT}-1}+1\right) = xy\frac{e^{\varepsilon/k_BT}+1}{e^{\varepsilon/k_BT}-1} .\end{aligned}$$

Thus apparently:

$$\exp\left(\frac{1}{2}\left\langle L^2 \right\rangle\right) = \left\langle e^L \right\rangle \quad \text{q.e.d} .$$

If now $A, B$ both are operators, which can be represented as linear combinations of Bose creators and -annihilators, the combination of the two theorems yields:

$$\left\langle e^A e^B \right\rangle = \left\langle e^{A+B+\frac{1}{2}(AB-BA)} \right\rangle = e^{\frac{1}{2}\left(\left\langle (A+B)^2 \right\rangle + [A,B]\right)} = e^{\frac{1}{2}<A^2+2AB+B^2>} . \tag{4.167}$$

This leads to:

$$\left\langle e^{i\boldsymbol{q}\boldsymbol{u}_n} \cdot e^{-i\boldsymbol{q}\boldsymbol{u}_{n'}}(t) \right\rangle = e^{-2W} e^{\langle (\boldsymbol{q}\boldsymbol{u}_n)\cdot(\boldsymbol{q}\boldsymbol{u}_{n'}(t))\rangle} \tag{4.168}$$

with

$$2W = \left\langle (\boldsymbol{q}\boldsymbol{u}_n)^2 \right\rangle = \left\langle (\boldsymbol{q}\boldsymbol{u}_{n'}(t))^2 \right\rangle , \tag{4.169}$$

the so-called **Debye-Waller factor**. This gives for the dynamic structure factor:

$$S(\boldsymbol{q}, \omega) = e^{-2W} \int_{-\infty}^{+\infty} \frac{dt}{2\pi} e^{i\omega t} \sum_n e^{-i\boldsymbol{q}\boldsymbol{R}_{n0}} \exp\left[\langle (\boldsymbol{q}\boldsymbol{u}_0)(\boldsymbol{q}\boldsymbol{u}_n)(t)\rangle\right] . \tag{4.170}$$

Now we expand for small displacements, i. e. we approximate

$$\exp\left[\langle (\boldsymbol{q}\boldsymbol{u}_0)(\boldsymbol{q}\boldsymbol{u}_n)(t)\rangle\right] = 1 + \langle (\boldsymbol{q}\boldsymbol{u}_0)(\boldsymbol{q}\boldsymbol{u}_n)(t)\rangle . \tag{4.171}$$

Analyzing the contributions to the structure factor now individually, we obtain in 0th order in the displacements

$$S_{(0)}(\boldsymbol{q}, \omega) = e^{-2W}\delta(\omega)N\sum_{\boldsymbol{G}} \delta_{\boldsymbol{G},\boldsymbol{q}} , \tag{4.172}$$

where $\boldsymbol{G}$ runs through the reciprocal lattice vectors. The vector $\boldsymbol{q}$ is the momentum transfer of the neutron, $\boldsymbol{q}$ is therefore not limited to the first Brillouin zone. We therefore obtain the condition that in zeroth order in the displacements, that is, for the rigid lattice in the equilibrium positions, only neutron reflections occur, in which the momentum transferred corresponds to a reciprocal lattice vector. This is nothing else but the **Bragg reflection condition**. Purely elastic scattering can take place at the angles for which the momentum transfer corresponds to a reciprocal lattice vector. Elastic Bragg peaks are expected to occur at finite temperatures according to this calculation, the Debye-Waller factor determines the decrease in their intensity with increasing temperature.

In first order in the displacements we express them by phonon creat ion and annihilation operators according to:

$$\boldsymbol{u}_n = \frac{1}{\sqrt{N}} \sum_{\boldsymbol{k}j} \sqrt{\frac{\hbar}{2M\omega_j(\boldsymbol{k})}} \left(b_{\boldsymbol{k}j} + b^{\dagger}_{-\boldsymbol{k}j}\right) \boldsymbol{e}_j(\boldsymbol{k}) e^{i\boldsymbol{k}\boldsymbol{R}_{n0}} \,. \tag{4.173}$$

This gives:

$$\langle (\boldsymbol{q}\boldsymbol{u}_0)(\boldsymbol{q}\boldsymbol{u}_n)(t)\rangle = \frac{1}{N} \sum_{\boldsymbol{k}\boldsymbol{k}'jj'} \frac{\hbar}{2M\sqrt{\omega_j(\boldsymbol{k})\omega_{j'}\left(\boldsymbol{k}'\right)}} \tag{4.174}$$

$$\times \left\langle \left(b_{\boldsymbol{k}j} + b^{\dagger}_{-\boldsymbol{k}j}\right) \left(\boldsymbol{q}\boldsymbol{e}_j(\boldsymbol{k})\right) \left(\boldsymbol{q}\boldsymbol{e}_{j'}\left(\boldsymbol{k}'\right)\right) e^{i\boldsymbol{k}'\boldsymbol{R}_{n0}} \left(b_{\boldsymbol{k}'j'} + b^{\dagger}_{-\boldsymbol{k}'j'}\right)(t) \right\rangle$$

$$= \frac{1}{N} \sum_{\boldsymbol{k}j} \frac{\hbar}{2M\omega_j(\boldsymbol{k})} \left(\boldsymbol{q}\boldsymbol{e}_j(\boldsymbol{k})\right) \left(\boldsymbol{q}\boldsymbol{e}_j(-\boldsymbol{k})\right) \left( \left\langle b^{\dagger}_{-\boldsymbol{k}j} b_{-\boldsymbol{k}j}(t) \right\rangle + \left\langle b_{\boldsymbol{k}j} b^{\dagger}_{\boldsymbol{k}j}(t) \right\rangle \right) e^{-i\boldsymbol{k}\boldsymbol{R}_{n0}}.$$

We now take into account:

$$\left\langle b^{\dagger}_{\boldsymbol{k}j} b_{\boldsymbol{k}j}(t) \right\rangle = \left\langle b^{\dagger}_{\boldsymbol{k}j} b_{\boldsymbol{k}j} \right\rangle e^{-i\omega_j(\boldsymbol{k})t} \,, \left\langle b_{\boldsymbol{k}j} b^{\dagger}_{\boldsymbol{k}j}(t) \right\rangle = \left\langle b_{\boldsymbol{k}j} b^{\dagger}_{\boldsymbol{k}j} \right\rangle e^{+i\omega_j(\boldsymbol{k})t} \,.$$

Using

$$\sum_n e^{-i(\boldsymbol{q}+\boldsymbol{k})\boldsymbol{R}_{n0}} = N\delta_{-\boldsymbol{k},\boldsymbol{q}} \quad , \quad \int_{-\infty}^{+\infty} \frac{dt}{2\pi} e^{i\left(\omega \pm \omega_j(\boldsymbol{k})\right)t} = \delta\left(\omega \pm \omega_j(\boldsymbol{k})\right) \tag{4.175}$$

finally gives for the structure factor in 1th order in the displacements:

$$S_{(1)}(\boldsymbol{q},\omega) = e^{-2W} \sum_j \frac{\hbar}{2M\omega_j(\boldsymbol{q})} \left(\boldsymbol{q}\boldsymbol{e}_j(\boldsymbol{q})\right)^2 \left( \left\langle b^{\dagger}_{\boldsymbol{q}j} b_{\boldsymbol{q}j} \right\rangle \delta(\omega - \omega_j(\boldsymbol{q})) \right.$$

$$\left. + \left(1 + \left\langle b^{\dagger}_{-\boldsymbol{q}j} b_{-\boldsymbol{q}j} \right\rangle\right) \delta(\omega + \omega_j(\boldsymbol{q})) \right) \,. \tag{4.176}$$

As a function of ω, $S_{(1)}(\boldsymbol{q},\omega)$ therefore has sharp delta peaks exactly at the phonon eigenfrequencies $\omega_j(\boldsymbol{q})$. It is precisely for this reason that the phonon spectrum can be explicitly measured by measuring the structure factor with neutron scattering. The higher (so far neglected) contributions, on the other hand, give a continuous contribution from which the characteristic peaks stand out. The neutrons can therefore absorb or emit phonons during the scattering process in the crystal, then they are scattered inelastically, that is, they absorb or release energy to the crystal.

We want to end this chapter with comments on possible alternatives to neutron scattering experiments, that is, on scattering of other particles (quanta) on the crystal. In particular, **X-ray scattering** is possible. X-ray quanta have just the right wavelength of the right order of magnitude (as well as the relevant neutrons) of a few Å. Therefore, X-ray diffraction is at least as well suited for determining crystal structure as neutron diffraction. In principle, one can imagine that X-ray quanta are also able to absorb or emit phonons. But if it exists, it is extremely difficult to measure, and that is due to the relevant energy scale. X-ray quanta have an energy of about $10^3$ eV, by absorbing or emitting a phonon they experience a relative change in energy of $10^{-5}$, which is only difficult to measure and should disappear in the background (of the existing broadening of the elastic Bragg peak).

Another possibility is **light scattering**. Also visible light can be scattered by absorbing or emitting phonons. The scattered light quantum then has the energy

$$\hbar\omega' = \hbar\omega \pm \hbar\omega_j(\boldsymbol{q}) \; . \tag{4.177}$$

The relative energy transfer is then of the order of $10^{-2}$ and thus measurable (resolvable). However, the wave number of visible photons is much smaller than that of phonons; the wavelength of visible light is of the magnitude 10 $^3$Å, that is, it is larger by this factor than the lattice constant and thus a typical wavelength of lattice waves. Therefore, with light scattering, the Brillouin zone can only be measured in the area of very small $q$, while with neutrons the entire Brillouin zone and thus the entire phonon spectrum can be measured.

Light scattering on acoustic phonons is also called **Brillouin scattering**.

Scattering of light on optical phonons is also called **Raman scattering**.

In phonon absorption (energy increase of the scattered photons), one also speaks of the **anti-Stokes component** in the spectrum of the scattered light, in phonon emission the crystal has received energy and momentum from the photon; the corresponding part of the spectrum is also called the **Stokes component**.

## 4.9 Anharmonic Corrections

All considerations of this chapter were so far restricted to the **harmonic approximation**, i. e. the potential energy was expanded in a Taylor series according to the displacements, and this series was cut off after the second term. Of course, in principle, one can consider corrections to the harmonic approximation by taking into account the next orders in this series expansion. The 3rd order contribution in the displacements is of the form:

$$V^{(3)} = \frac{1}{6} \sum_{nml} \sum_{\alpha\beta\gamma} \frac{\partial^3}{\partial R_{n\alpha} \partial R_{m\beta} \partial R_{l\gamma}} |_0 u_{n\alpha} u_{m\beta} u_{l\gamma} \; . \tag{4.178}$$

Of course the displacements $u_{n\alpha}$ can still be written as linear combinations of phonon creation and annihilation operators according to (4.173), because the relationship between the $b_{\boldsymbol{q}j}, b^\dagger_{\boldsymbol{q}j}$ and the momenta and displacements $P_{n\alpha}, u_{m\beta}$ is merely a canonical transformation and has nothing to do with the harmonic approximation. In the harmonic approximation, however, this canonical transformation leads to the diagonalization of the Hamiltonian operator, which is no longer the case when considering anharmonic corrections. Expressed by the $b, b^\dagger$, $V^{(3)}$ is of the form

$$V^{(3)} = \sum_{\boldsymbol{k}_1 j_1 \boldsymbol{k}_2 j_2 \boldsymbol{k}_3 j_3} D^{j_1 j_2 j_3}_{\boldsymbol{k}_1 \boldsymbol{k}_2 \boldsymbol{k}_3} \left(b_{\boldsymbol{k}_1 j_1} + b^\dagger_{-\boldsymbol{k}_1 j_1}\right)\left(b_{\boldsymbol{k}_2 j_2} + b^\dagger_{-\boldsymbol{k}_2 j_2}\right)\left(b_{\boldsymbol{k}_3 j_3} + b^\dagger_{-\boldsymbol{k}_3 j_3}\right) \tag{4.179}$$

Obviously, three-phonon processes occur here explicitly, e. g. the mutual annihilation of two phonons under emission of a third phonon described by processes of the type $b^\dagger_{\boldsymbol{k}_1 j_1} b_{\boldsymbol{k}_2 j_2} b_{\boldsymbol{k}_3 j_3}$. The momenta (wave numbers) are not completely independent, but the total momentum is conserved in this "phonon splitting". The phonon number is no longer conserved when taking into account these corrections. In second order perturbation theory for $V^{(3)}$ and in first order in $V^{(4)}$, inter alia, a phonon-phonon scattering arises, the consideration of anharmonic corrections therefore leads to terms which are at least formally of the form of an interaction between the phonons.

At least for two realistic and important phenomena, the inclusion of anharmonic corrections is of decisive importance, namely for the understanding of thermal expansion and heat conduction. In the strictly harmonic system, there would be no thermal expansion of crystals, which contradicts experience. In a harmonic system, higher energy oscillator states are excited at higher temperatures, but they continue to oscillate around the same center, i.e. the mean value of the displacement (the original lattice site) remains unchanged. However, even when taking into account the simplest anharmonic contributions, the mean displacement becomes larger with increasing magnitude of the excitation, i.e. also with increasing temperature, at which the higher excitation is occupied. In addition, in the purely harmonic crystal there would be an infinitely good heat conductivity. To understand that heat conduction is finite, one must consider defects and just anharmonic corrections, which due to the finite lifetime of the phonons lead to a finite thermal conductivity through the possibility that a phonon is destroyed or split into two other phonons.

## 4.10 Problems for Chap. 4

**Problem 4.1** ***Vibrational modes of a (1-dimensional) molecule***

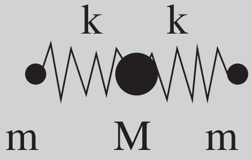

A linear 3-atomic molecule consists of 2 mass points of mass $m$, which are harmonic (e.g. over a spring of spring constant $k$) coupled to another mass $M$ between the masses $m$. This could model, for example, a $CO_2$ molecule; for simplicity, however, we only consider displacements in the direction of the molecular axis.

a) Write down the equations of motion if the 3 mass points are displaced by $u_i$ ($i \in \{1, 2, 3\}$) from their rest position.
b) Give the force constant matrix $\underline{\underline{\Phi}}$ and the dynamic matrix $\underline{\underline{D}}$ explicitly.
c) Diagonalize the dynamic matrix and determine the eigenfrequencies and eigenvectors analytically.
d) Discuss the 3 possible eigenvibrations physically and intuitively. How are the 3 atoms extended in each case in the eigenvibrations?
e) To practice programming: Solve the problem numerically as well, e.g. for $M = 2m$.

**Problem 4.2** ***Lattice waves on the square lattice***

Consider a square lattice of atoms of mass $M$ (with periodic boundary conditions). The potential energy has the form

$$V = \frac{\alpha}{2} \sum_{\boldsymbol{R}} \left[ \left( \boldsymbol{u}_{\boldsymbol{R}+\boldsymbol{a}_1} - \boldsymbol{u}_{\boldsymbol{R}} \right)^2 + \left( \boldsymbol{u}_{\boldsymbol{R}+\boldsymbol{a}_2} - \boldsymbol{u}_{\boldsymbol{R}} \right)^2 \right] ,$$

$$\text{with} \quad \boldsymbol{a}_1 = \begin{pmatrix} a \\ 0 \end{pmatrix} , \quad \boldsymbol{a}_2 = \begin{pmatrix} 0 \\ a \end{pmatrix}$$

which span the (primitive) elementary cell of the square lattice.

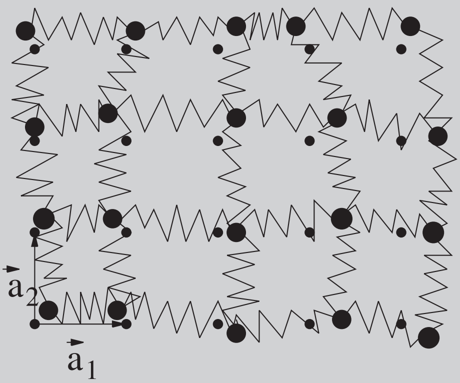

Determine the dispersion relation $\omega(\boldsymbol{q})$ of the possible lattice vibrations.

**Problem 4.3** ***Linear chain with 2 atom types per unit cell***
Consider a chain of 2 different atoms of masses $M$ and $m$, which are coupled by springs with spring constant $K$.

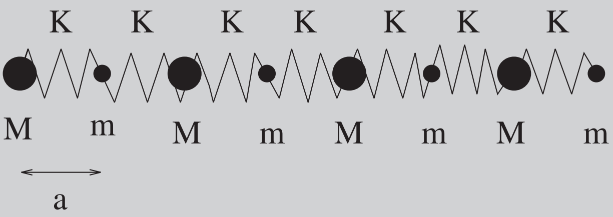

The equilibrium distance between two adjacent atoms be $a$ ; in the resting position, the system is thus periodic with lattice constant $2a$.

a) Show that the dispersion relation of the eigenvibrations is given by

$$\omega^2 = \frac{K}{Mm}\left[M + m \pm \sqrt{M^2 + m^2 + 2Mm\cos(2qa)}\right].$$

b) Discuss and sketch the dispersion relation; consider in particular the cases $qa \to 0$, $2qa \to \pi$.
c) Show that for $m = M$ the result of the monatomic chain is obtained.

**Problem 4.4** ***Linear chain with rigid boundary conditions***
Consider a linear chain of $N + 1$ atoms of mass $M$, which are coupled by equal springs (spring constant $k$) and have in the (relaxed) equilibrium state the distance of the lattice constants $a$ with rigid boundary conditions, i. e., the displacements $u_n$ of the $n$-th atom must fulfill the boundary condition $u_0 = u_N = 0$ ($N + 1$ atoms, but only the atoms $1, \ldots, N - 1$ can oscillate, while the atoms 0 and $N$ are held fixed). Set up the equations of motion and solve it with the ansatz

$$u_n = A\sin(nqa)e^{i\omega t} .$$

Determine the dispersion relation $\omega(q)$. Which $q$-values are allowed?

**Problem 4.5** ***Internal energy of the linear harmonic chain***
Consider again the model of $N$ mass points $m$ coupled by springs of spring constant $k$ with equilibrium distance (lattice constant) $a$ and periodic

boundary conditions. As is well known, the dispersion relation of the phonons is given by

$$\omega(q) = 2\sqrt{\frac{k}{m}}\left|\sin\left(\frac{qa}{2}\right)\right| ,$$

$$\text{where} \quad q = -\frac{\pi}{a} + n\frac{2\pi}{Na} , \quad n = 1, \ldots, N \text{ (from the first Brillouin zone)} .$$

a) Determine the internal energy and the specific heat in the limit of high temperatures.

b) Show that the internal energy can be written in the following form by transition from the $q$-sum to the integral (in the thermodynamic limit):

$$E = \frac{Na}{\pi}\int_0^{\pi/a} dq\hbar\omega(q)\left(\frac{1}{e^{\beta\hbar\omega(q)} - 1} + \frac{1}{2}\right) .$$

c) Determine the internal energy (relative to the ground state energy) and the specific heat in the limit of low temperatures $T$, where $T$ should be so low that for $\hbar\omega(q) < k_B T$ the assumption $\hbar\omega(q) = \sqrt{\frac{k}{m}}\hbar a q = c_s q$ is justified. Specify the condition "low" temperature.

d) Show that in Debye approximation (i.e. the assumption $\hbar\omega(q) = c_s q$ for all $q$) one obtains for the internal energy

$$E(T) = \frac{Na}{c_s\pi}(k_B T)^2 D_1\left(\frac{c_s\pi}{ak_B T}\right) + \frac{N\pi c_s}{2a} ,$$

where the Debye functions are defined via

$$D_n(x) = \int_0^x dt\frac{t^n}{e^t - 1} .$$

These can be found tabulated, e.g. in Abramowitz-Stegun, Handbook of Mathematical Functions, Chap. 27, or they can be calculated relatively easily numerically. What results in Debye approximation for low and high temperatures?

e) Calculate the lowest non-vanishing corrections to Debye approximation. For this purpose make the substitution $x = \hbar\omega(q)\beta$ in the integral from b). Then expand an expression of the form

$$\sqrt{1 - \left(\frac{k_B T a}{2c_s}x\right)^2} .$$

in the integrand to the lowest non-vanishing order in $k_B T$. How well is this expansion justified?

f) Determine the temperature dependence of internal energy and specific heat exactly numerically (by numerical calculation of the integral in b), and in Debye approximation and with the first corrections from e) to Debye approximation and plot the 3 results for $E(T)/N$ and $c_V(T)/N$.

**Problem 4.6** ***Quantum corrections to the Dulong-Petit law***

Calculate the internal energy and specific heat of phonons in the high-temperature expansion up to contributions proportional to $1/T$ or $1/T^2$.

**Problem 4.7** ***Phonon densities of state***

The phonon density of states can be determined numerically by means of the definition (4.93). For this purpose, discretize a finite frequency interval $[0, \Omega_m]$, in which eigenfrequencies are to be expected, into $N_\omega$ pieces of length $\Delta\omega = \frac{\Omega_m}{N_\omega}$, choose representative $N_q$ different $\boldsymbol{q}$ values, calculate the corresponding eigenfrequencies $\omega_j(\boldsymbol{q})$ and determine the number $N(\omega_n)$ of eigenfrequencies $\omega_j(\boldsymbol{q})$ in the individual intervals $[\omega_{n-1}, \omega_n]$ (with $\omega_n = \frac{n}{N_\omega}\Omega_m$, $n = 1, \ldots, N_\omega$). The density of states at the discrete points $\omega_n$ is then simply

$$n(\omega_n) = \frac{N(\omega_n)}{N_q \Delta\omega} .$$

So that on average more than one state per frequency interval exists, it must hold $N_\omega \ll N_q$.

a) Determine the density of states of the 1-dimensional harmonic linear chain again numerically, that is, for the dispersion relation

$$\omega(q) = \omega_m \left|\sin\left(\frac{qa}{2}\right)\right| \quad \text{where} \quad \omega_m = 2\sqrt{\frac{K}{M}}$$

and compare the result with the exact analytical result (4.105).

b) Determine the density of states for the 2-dimensional phonon system from Problem 4.2, that is, for the phonon dispersion

$$\omega(\boldsymbol{q}) = 2\sqrt{\frac{\alpha}{M}}\sqrt{\sin^2\left(\frac{q_x a}{2}\right) + \sin^2\left(\frac{q_y a}{2}\right)} .$$

Note: For symmetry reasons, it is sufficient to choose the $\boldsymbol{q}$ values only from one simplex (triangle) of one quadrant of the Brillouin zone.

c) Determine the density of states for the 2-atom linear chain from Problem 4.3.

**Problem 4.8** ***Phonon spectrum and density of states for fcc lattice***

Consider a three-dimensional one-atom fcc lattice with harmonic nearest-neighbor coupling (atoms of mass $M$, coupled over "springs" with the spring constant $k$).

a) Show that the $q$-dependent dynamic matrix is given by

$$D_{ii}(\boldsymbol{q}) = \frac{2k}{M}\left[2 - \cos\left(q_i \frac{a}{2}\right)\sum_{j\neq i}\cos\left(q_j \frac{a}{2}\right)\right]$$
$$D_{ij}(\boldsymbol{q}) = \frac{2k}{M}\sin\left(\frac{q_i a}{2}\right)\sin\left(q_j \frac{a}{2}\right),$$

($i,j \in \{1,2,3\} = \{x,y,z\}$), where $a$ is the lattice constant of the conventional unit cell. Proceed as in Sec. 4.6.1in the derivation of (4.88).

b) Diagonalize the dynamic matrix numerically and plot the resulting eigenfrequencies $\omega_j(\boldsymbol{q})$ as functions of $q$, by varying $\boldsymbol{q}$ along selected directions in the $\boldsymbol{q}$-space. Represent $\omega(\boldsymbol{q})$ in particular for variation along the $(1,0,0)$-direction from the $\Gamma$-point $(0,0,0)$ to the X-point $\left(\frac{2\pi}{a},0,0\right)$, that is, for $\boldsymbol{q} = (q,0,0)\,, q \in [0,\frac{2\pi}{a}]$, for variation along the $(1,1,0)$-direction, that is, for $\boldsymbol{q} = (q,q,0)\,, q \in [0,\frac{2\pi}{a}]$, and along the $(1,1,1)$-direction from the $\Gamma$-point to the L-point, that is, for $\boldsymbol{q} = (q,q,q)\,, q \in \left[0,\frac{\pi}{a}\right]$.
Identify critical points and critical frequencies $\omega_c$ at which (Van Hove) singularities of the density of states are to be expected.

c) Determine the density of states of (acoustic) phonons in the fcc lattice using the method from Problem 4.7.
*Note* : As in Problem 4.7 b, it is sufficient to vary $\boldsymbol{q}$ only within a simplex in the first octant of the $\boldsymbol{q}$-space.

**Problem 4.9** ***Phonon modes for 2-dimensional 2-atom crystal***

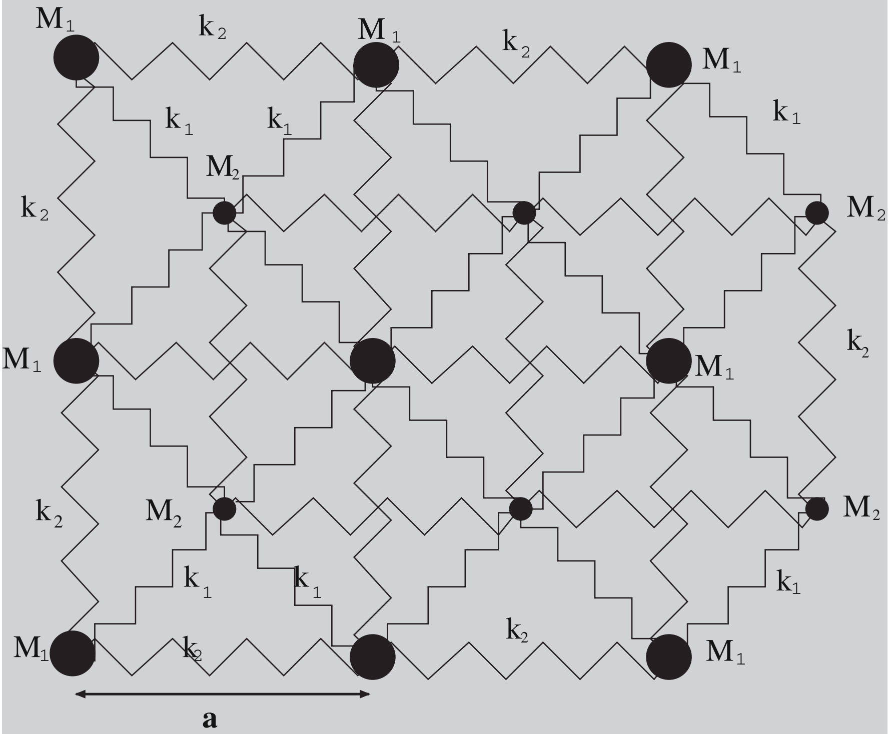

Given is a 2-dimensional square lattice with lattice constant $a$ and a basis of 2 atoms of mass $M_1$ and $M_2$ at $(0,0)$ and $(\frac{a}{2},\frac{a}{2})$ in the unit cell. Adjacent (different) atoms are coupled by springs of spring constant $k_1$, equal atoms (next-nearest-neighbor atoms, i.e. in adjacent unit cells) in $(1,0)$- or $(0,1)$-direction by springs of spring constant $k_2 < k_1$.

a) Show that the potential (in harmonic approximation) is given by:

$$\begin{aligned}
V = \sum_{\boldsymbol{R}} \Bigg\{ \frac{k_1}{4} \big[ &(u_{\boldsymbol{R}1x} - u_{\boldsymbol{R}2x} + u_{\boldsymbol{R}1y} - u_{\boldsymbol{R}2y})^2 \\
&+(-u_{\boldsymbol{R}+\boldsymbol{\Delta}_x 1x} + u_{\boldsymbol{R}2x} + u_{\boldsymbol{R}+\boldsymbol{\Delta}_x 1y} - u_{\boldsymbol{R}2y})^2 \\
&+(u_{\boldsymbol{R}+\boldsymbol{\Delta}_y 1x} - u_{\boldsymbol{R}2x} - u_{\boldsymbol{R}+\boldsymbol{\Delta}_y 1y} + u_{\boldsymbol{R}2y})^2 \\
&+(u_{\boldsymbol{R}+\boldsymbol{\Delta}_x+\boldsymbol{\Delta}_y 1x} - u_{\boldsymbol{R}2x} + u_{\boldsymbol{R}+\boldsymbol{\Delta}_x+\boldsymbol{\Delta}_y 1y} - u_{\boldsymbol{R}2y})^2 \big] \\
+\frac{k_2}{2} \big[ &(u_{\boldsymbol{R}+\boldsymbol{\Delta}_x 1x} - u_{\boldsymbol{R}1x})^2 + (u_{\boldsymbol{R}+\boldsymbol{\Delta}_x 2x} - u_{\boldsymbol{R}2x})^2 \\
&+(u_{\boldsymbol{R}+\boldsymbol{\Delta}_y 1y} - u_{\boldsymbol{R}1y})^2 + (u_{\boldsymbol{R}+\boldsymbol{\Delta}_y 2y} - u_{\boldsymbol{R}2y})^2 \big] \Bigg\}
\end{aligned}$$

where $\boldsymbol{R}$ runs through all lattice vectors, $\boldsymbol{\Delta}_x = (a, 0)$, $\boldsymbol{\Delta}_y = (0, a)$ are lattice vectors to nearest-neighbor lattice sites and (as usual according to the notation of Sect. 4.2) $u_{\boldsymbol{R}\mu\alpha}$ is the displacement of the atom $\mu \in \{1, 2\}$ in the unit cell $\boldsymbol{R}$ in α-direction ($\alpha \in \{x, y\}$).

b) Show that the following (classical) equations of motion result:

$$\begin{aligned}
M_1 \ddot{u}_{\boldsymbol{R}1x} = -\frac{k_1}{2}\big(&4u_{\boldsymbol{R}1x} - u_{\boldsymbol{R}2x} - u_{\boldsymbol{R}2y} - u_{\boldsymbol{R}-\boldsymbol{\Delta}_x 2x} + u_{\boldsymbol{R}-\boldsymbol{\Delta}_x 2y}\\
&-u_{\boldsymbol{R}-\boldsymbol{\Delta}_y 2x} + u_{\boldsymbol{R}-\boldsymbol{\Delta}_y 2y} - u_{\boldsymbol{R}-\boldsymbol{\Delta}_x-\boldsymbol{\Delta}_y 2x} - u_{\boldsymbol{R}-\boldsymbol{\Delta}_x-\boldsymbol{\Delta}_y 2y}\big)\\
&- k_2\big(2u_{\boldsymbol{R}1x} - u_{\boldsymbol{R}+\boldsymbol{\Delta}_x 1x} - u_{\boldsymbol{R}-\boldsymbol{\Delta}_x 1x}\big)\\
M_2 \ddot{u}_{\boldsymbol{R}2x} = -\frac{k_1}{2}\big(&4u_{\boldsymbol{R}2x} - u_{\boldsymbol{R}1x} - u_{\boldsymbol{R}1y} - u_{\boldsymbol{R}+\boldsymbol{\Delta}_x 1x} + u_{\boldsymbol{R}+\boldsymbol{\Delta}_x 1y}\\
&-u_{\boldsymbol{R}+\boldsymbol{\Delta}_y 1x} + u_{\boldsymbol{R}+\boldsymbol{\Delta}_y 1y} - u_{\boldsymbol{R}+\boldsymbol{\Delta}_x+\boldsymbol{\Delta}_y 1x} - u_{\boldsymbol{R}+\boldsymbol{\Delta}_x+\boldsymbol{\Delta}_y 1y}\big)\\
&- k_2\big(2u_{\boldsymbol{R}2x} - u_{\boldsymbol{R}+\boldsymbol{\Delta}_x 2x} - u_{\boldsymbol{R}-\boldsymbol{\Delta}_x 2x}\big)
\end{aligned}$$

and analogously for the $y$-components (*exchange* $x$ and $y$).

c) Show that the $\boldsymbol{q}$-dependent dynamical matrix is given by the following matrix elements:

$$\begin{aligned}
D_{1x,1x}(\boldsymbol{q}) &= \frac{2k_1}{M_1} + \frac{2k_2}{M_1}(1 - \cos(q_x a))\\
D_{1x,2x}(\boldsymbol{q}) &= -\frac{k_1}{2\sqrt{M_1 M_2}}\big(1 + e^{-i(q_x+q_y)a} + e^{-iq_y a} + e^{-iq_x a}\big)\\
D_{1x,1y}(\boldsymbol{q}) &= 0\\
D_{1x,2y}(\boldsymbol{q}) &= -\frac{k_1}{2\sqrt{M_1 M_2}}\big(1 + e^{-i(q_x+q_y)a} - e^{-iq_y a} - e^{-iq_x a}\big)\\
D_{2x,2x}(\boldsymbol{q}) &= \frac{2k_1}{M_2} + \frac{2k_2}{M_2}(1 - \cos(q_x a))\\
D_{2x,1x}(\boldsymbol{q}) &= -\frac{k_1}{2\sqrt{M_1 M_2}}\big(1 + e^{i(q_x+q_y)a} + e^{iq_y a} + e^{iq_x a}\big)\\
D_{2x,2y}(\boldsymbol{q}) &= 0\\
D_{2x,1y}(\boldsymbol{q}) &= -\frac{k_1}{2\sqrt{M_1 M_2}}\big(1 + e^{i(q_x+q_y)a} - e^{iq_y a} - e^{iq_x a}\big)
\end{aligned}$$

and analogously for the other 8 matrix elements (by exchanging $x$ and $y$).

d) Diagonalize the dynamic matrix numerically for different $\boldsymbol{q}$. Vary $\boldsymbol{q}$ along special paths in the Brillouin zone, for example from $(0, 0)$ to $(\frac{\pi}{a}, 0)$, from there to $(\frac{\pi}{a}, \frac{\pi}{a})$ and from there along the diagonal back to $(0, 0)$, and plot the 4 eigenfrequencies $\omega_i(\boldsymbol{q})$. Discuss the result. At which frequencies are Van Hove singularities to be expected?

e) Determine the phonon density of states $n(\omega)$ according to the definition. For this purpose, vary $\boldsymbol{q}$ over the entire Brillouin zone (or only over the range $0 < q_x < q_y < \frac{\pi}{a}$ due to symmetry) and "count" how many eigenvalues fall into a certain frequency interval. Plot and discuss $n(\omega)$.

**Problem 4.10** ***Van-Hove singularities in 2 dimensions***
Determine the type of singularities that occur in the (phonon) density of states of a 2-dimensional system in the vicinity of critical frequencies $\omega_c$. A critical frequency is present if there are $\boldsymbol{q}$ values with $\omega_c = \omega(\boldsymbol{q})$ and $\nabla_{\boldsymbol{q}}\omega(\boldsymbol{q}) = 0$.

*Note* : Proceed analogously to the discussion of 3-dimensional Van-Hove singularities in (4.114)–(4.118). Discuss extrema (maxima) and saddle points of the dispersion relation separately.

**Problem 4.11** ***Continuum limit of the linear harmonic chain***
Consider the model of the one-atom, linear harmonic chain (masses $M$, spring constants $k$, lattice constant $a$) again and carry out the continuum limit explicitly on the equations of motion for this model (cf. Sect. 4.7.1). What approximations are made and when are they valid? Solve the resulting partial differential equation with an appropriate exponential ansatz. What dispersion relation results and how does this compare to the exact relation for the linear chain?

**Problem 4.12** ***Phonon-polariton dispersion***

a) Explain that in an ionic crystal with 2 (oppositely charged) ions (masses $M_1$ and $M_2$, charges $\pm\, e$) per unit cell, which are coupled by springs of spring constant $k$, in an external electric field $\boldsymbol{E}$ in the long-wavelength limit, the equations of motion

$$\begin{aligned} M_1\ddot{\boldsymbol{u}}_+ &= -k(\boldsymbol{u}_+ - \boldsymbol{u}_-) + e\boldsymbol{E} \\ M_2\ddot{\boldsymbol{u}}_- &= -k(\boldsymbol{u}_- - \boldsymbol{u}_+) - e\boldsymbol{E}\ . \end{aligned}$$

apply. Derive from this (4.135) for $\boldsymbol{u} = \boldsymbol{u}_+ - \boldsymbol{u}_-$ and thus determine $\omega_0$ and $e^*$ from the given parameters $M_1, M_2, k, e$.

b) How do the equations and in particular the results (4.140), (4.142) for $\varepsilon(\omega)$ change if, in addition to (4.135), one also introduces a phenomenological damping term, i. e., if it is assumed that

$$\ddot{\boldsymbol{u}} + \alpha\dot{\boldsymbol{u}} = -\omega_0^2\boldsymbol{u} + e^*\boldsymbol{E}$$

applies. Plot $\varepsilon(\omega)$ for this case for different α.

c) How do the equations for the dielectric constant change if one omits the phenomenologically considered other contributions to polarization in the approach (4.136), that is, if the term $\gamma\boldsymbol{E}$ is neglected?

d) Plot $q^2(\omega)$, $q(\omega)$, and $\omega(q)$ starting from (4.146). What $q$-values result for frequencies from the interval $[\omega_0, \omega_l]$ ? Interpret this physically.

**Problem 4.13 *Mean square displacement***

Given is a $d$-dimensional crystal ($N$ lattice sites) with one atom (of mass $M$) per elementary cell; $\boldsymbol{R}_n$ is the lattice vector and $\boldsymbol{u}_n$ the displacement of the atom of the $n$-th elementary cell. In harmonic approximation, the phonon Hamiltonian operator is known to be

$$H = \sum_{\boldsymbol{q}j} \hbar\omega_j(\boldsymbol{q})\left(b^\dagger_{\boldsymbol{q}j}b_{\boldsymbol{q}j} + \frac{1}{2}\right) .$$

a) Show that for the $j$-th component of the displacement vector it holds:

$$u_{n,j} = \frac{1}{\sqrt{N}}\sum_{\boldsymbol{q}} e^{i\boldsymbol{q}\boldsymbol{R}_n}\sqrt{\frac{\hbar}{2M\omega_j(\boldsymbol{q})}}\left(b_{\boldsymbol{q}j} + b^\dagger_{-\boldsymbol{q}j}\right) ,$$

(where the Cartesian coordinate system was used, with respect to which the dynamic matrix is diagonal).

b) Calculate the mean thermal displacement $\langle \boldsymbol{u}_n \rangle$.

c) Show that for the mean square displacement it holds:

$$\langle \boldsymbol{u}_n^2 \rangle = \frac{1}{2M}\int d\omega n(\omega)\frac{1}{\omega}\coth(\beta\hbar\omega) ,$$

where $n(\omega)$ denotes the phonon density of states.

d) Explain why $\langle \boldsymbol{u}_n^2 \rangle$ diverges for $d = 1,2$ but not for $d = 3$. What are the consequences of this?

e) Show that for high temperatures it applies:

$$\langle \boldsymbol{u}_n^2 \rangle = k_B T\frac{1}{\hbar M}\int d\omega n(\omega)\frac{1}{\omega^2} .$$

f) Calculate $\langle \boldsymbol{u}_n^2 \rangle$ in the Debye model.

g) The crystal melts when the mean displacement reaches a certain fraction of the lattice constant (**Lindemann criterion**), that is, when

$$\langle \boldsymbol{u}_n^2 \rangle = x_s^2 a^2$$

applies. Derive from this and from e), f) a formula for the melting temperature.

**Problem 4.14** ***Particle scattering on phonons***

Use a simple dimensional analysis (of energy, momentum and wavelength) to explain why scattering experiments with thermal neutrons are suitable for measuring the entire phonon spectrum. Which part of the phonon spectrum can be measured by light scattering (scattering of photons with energies of the order of a few eV) (Brillouin scattering)? Why are X-rays (photons with energies of the order of keV) suitable for crystal structure analysis, but not for measuring the phonon spectrum?

**Problem 4.15** ***Anharmonic Corrections***

To investigate the influence of anharmonic corrections, we consider only a single oscillator under the influence of an anharmonic disturbance:

$$H = \frac{p^2}{2M} + \frac{k}{2}x^2 - \alpha x^3 \ , \quad (\alpha > 0) \ .$$

a) Calculate the quantum mechanical expectation value

$$\langle x \rangle_n$$

in the state $|n\rangle$ in first non-vanishing order perturbation theory in $\alpha$.
*Note* : Apply the quantum mechanical perturbation theory for the state $|n\rangle$ !
For which $n$ is this perturbation theory meaningful? (Sketch the potential curve for this!)

b) Then calculate the thermodynamic expectation value $\langle x \rangle$ in lowest order in $\alpha$. How can one interpret $\langle x \rangle$ and what temperature dependence do you obtain for this quantity?

# 5 Non-interacting Electrons in the Solid State

In this chapter we will make a number of simplifying and actually not realistic model assumptions, which are nevertheless very useful in order to understand the basics of the electronic structure of solids. In later chapters we will then see how to justify at least some of these assumptions. First, the lattice is to be considered as rigid, i.e. the lattice building blocks (the ions) are at fixed positions $\boldsymbol{R}_n$. This assumption is also reasonable in the sense of the Born-Oppenheimer approximation for the decoupling of lattice and electronic degrees of freedom. In addition, we want to assume that the positions of the atomic nuclei are the lattice vectors of a Bravais lattice. This is strictly only valid for very low temperatures; nevertheless, we will later calculate the thermodynamics for electrons in a strictly periodic potential, thus taking into account the influence of finite temperature, even though we know that there are also displacements of the ions from the equilibrium positions at any finite temperature. However, the strongest approximation of this chapter is the omission of any interaction of the electrons with each other. Since the Coulomb repulsion of the electrons is large (order of some eV), there is no obvious reason for this at first. In a later chapter we will then explicitly consider the electron-electron interaction and see that in many cases an interacting electron system can be mapped onto a non-interacting system with effective parameters; the interaction is then only contained in the parameters, which are usually to be determined self-consistently. If we therefore allow that the one-particle potential, which we will consider in this chapter, is not necessarily the potential generated by the bare atomic nuclei or ions, but an effective potential, in whose parameters also influences of the electron-electron interaction are included, then it becomes understandable that the presented treatment and the concepts to be introduced are relevant and useful despite the initially apparently unrealistic basic assumption.

© The Author(s), under exclusive license to Springer-Verlag GmbH, DE, part of Springer Nature 2023
G. Czycholl, *Solid State Theory, Volume 1*,
https://doi.org/10.1007/978-3-662-66135-2_5

So in the whole Chap. 5 we consider the Hamilton operator:

$$H = \sum_{i=1}^{N_\mathrm{e}} \frac{\boldsymbol{p}_i^2}{2m} + \sum_{i=1}^{N_\mathrm{e}} \sum_{n=1}^{N} v(\boldsymbol{r}_i - \boldsymbol{R}_n). \tag{5.1}$$

Here $N_\mathrm{e}$ is the number of electrons, $N$ the number of lattice points (unit cells), $m$ electron mass, $\boldsymbol{p}_i$ the momentum of the $i$-th electron, $v(\boldsymbol{r} - \boldsymbol{R}_n)$ is the potential that a single electron experiences through the $n$-th unit cell. Even in the presence of a basis, that is, more than one atom per unit cell, the potential can be represented in this way because of

$$v(\boldsymbol{r} - \boldsymbol{R}_n) = \sum_{\mu} \tilde{v}\big(\boldsymbol{r} - \boldsymbol{R}_n - \boldsymbol{R}_\mu\big). \tag{5.2}$$

A Hamilton operator of the type (5.1) is called a one-particle Hamiltonian, even if it is supposed to describe many electrons. With several electrons, it simply consists of additive one-particle terms, which is why the exact eigenfunctions can be represented as (antisymmetrized) products of one-particle eigenfunctions. Therefore, it is actually enough to solve a one-particle problem in order to also know the eigenvalues and eigenstates of the entire system of $N_\mathrm{e}$ electrons. The many-particle character only enters through the antisymmetrization, which is necessary to fulfill the Pauli principle and thus the Fermi statistics. A true **many-particle Hamiltonian** contains, on the other hand, interaction terms $u\big(\boldsymbol{r}_i - \boldsymbol{r}_j\big)$ and is therefore no longer representable as a sum of one-particle terms; the exact many-particle eigenfunction is then also not representable as a Slater determinant (that is, as a product of one-particle eigenfunctions).

In this chapter, therefore, only the problem of a single electron in the periodic potential is to be treated.

## 5.1 Electron in periodic potential, Bloch theorem

We first consider a single electron in a periodic potential, i.e. the time-independent Schrödinger [1]-equation:

$$H\psi(\boldsymbol{r}) = \left(-\frac{\hbar^2}{2m}\nabla^2 + V(\boldsymbol{r})\right)\psi(\boldsymbol{r}) = \varepsilon\psi(\boldsymbol{r}), \tag{5.3}$$

where $V(\boldsymbol{r})$ is invariant under translations with respect to lattice vectors, i.e.

---

[1] E. Schrödinger, *1887 in Vienna, †1961 ibid., Prof. in Stuttgart, Breslau, Zurich, Berlin, Oxford and Graz, 1938 emigrated and worked in Dublin, returned to Vienna in 1956, developed wave mechanics and Schrödinger equation in 1926, 1927 evidence of the equivalence to Heisenberg's matrix mechanics, rejected Copenhagen (statistical) interpretation of quantum mechanics, later works include gravitational theory, unified field theory and natural philosophical questions, Nobel Prize in 1933 (shared with P.A.M. Dirac).

$$V(\boldsymbol{r}) = V(\boldsymbol{r}+\boldsymbol{R}), \tag{5.4}$$

is fulfilled for every lattice vector $\boldsymbol{R}$. This translational invariance and, thus, the special symmetry of the system is linked with specific conserved quantities, which commute with the Hamiltonian operator. These are the translation operators $T_{\boldsymbol{R}}$ by lattice vectors. The translation operator is defined by

$$T_{\boldsymbol{R}} f(\boldsymbol{r}) = f(\boldsymbol{r}+\boldsymbol{R}), \tag{5.5}$$

for any arbitrary function $f(\boldsymbol{r})$. Every $T_{\boldsymbol{R}}$ commutes with the Hamiltonian operator:

$$[T_{\boldsymbol{R}}, H] = 0. \tag{5.6}$$

This is because:

$$\begin{aligned} T_{\boldsymbol{R}} H f(\boldsymbol{r}) &= T_{\boldsymbol{R}}\left(\frac{\boldsymbol{p}^2}{2m} + V(\boldsymbol{r})\right) f(\boldsymbol{r}) = \left(\frac{\boldsymbol{p}^2}{2m} + V(\boldsymbol{r}+\boldsymbol{R})\right) f(\boldsymbol{r}+\boldsymbol{R}) \\ &= \left(\frac{\boldsymbol{p}^2}{2m} + V(\boldsymbol{r})\right) f(\boldsymbol{r}+\boldsymbol{R}) = H T_{\boldsymbol{R}} f(\boldsymbol{r}). \end{aligned}$$

The translation operators also commute with each other:

$$[T_{\boldsymbol{R}}, T_{\boldsymbol{R}'}] = 0, \quad T_{\boldsymbol{R}} T_{\boldsymbol{R}'} = T_{\boldsymbol{R}'} T_{\boldsymbol{R}} = T_{\boldsymbol{R}+\boldsymbol{R}'}. \tag{5.7}$$

So the eigenfunctions of $H$ can be chosen as common eigenfunctions of $H$ and all $T_{\boldsymbol{R}}$:

$$H\psi(\boldsymbol{r}) = \varepsilon\psi(\boldsymbol{r}), T_{\boldsymbol{R}}\psi(\boldsymbol{r}) = c(\boldsymbol{R})\psi(\boldsymbol{r}), \tag{5.8}$$

where $\psi(\boldsymbol{r})$ denotes the common eigenfunctions and $c(\boldsymbol{R})$ the eigenvalues of $T_{\boldsymbol{R}}$. These fulfill the following relations:

$$c(\boldsymbol{R})c\big(\boldsymbol{R}'\big) = c\big(\boldsymbol{R}+\boldsymbol{R}'\big), \quad c(\boldsymbol{R})c(-\boldsymbol{R}) = 1, \quad c(\boldsymbol{R})^2 = c(2\boldsymbol{R}). \tag{5.9}$$

In addition, the following follows from the normalization:

$$\begin{aligned} 1 &= \int d^3r |\psi(\boldsymbol{r})|^2 = \int d^3r |\psi(\boldsymbol{r}+\boldsymbol{R})|^2 \\ &= \int d^3r |c(\boldsymbol{R})|^2 |\psi(\boldsymbol{r})|^2 = |c(\boldsymbol{R})|^2, \end{aligned}$$

from which it follows in total:

$$c(\boldsymbol{R}) = e^{i\boldsymbol{k}\boldsymbol{R}}. \tag{5.10}$$

The eigenfunctions of the periodic lattice Hamiltonian operator therefore fulfill

$$\boxed{\psi(\boldsymbol{r}+\boldsymbol{R}) = e^{i\boldsymbol{k}\boldsymbol{R}}\psi(\boldsymbol{r})}. \tag{5.11}$$

This property is also called the Bloch condition. The eigenfunctions are therefore not necessarily periodic in the lattice, but they can differ from one unit cell to the next by a phase factor. However, the electron density will again be periodic in the lattice due to

$$|\psi(\boldsymbol{r})|^2 = |\psi(\boldsymbol{r}+\boldsymbol{R})|^2. \tag{5.12}$$

To take into account the finiteness of the system, which is necessary in particular to be able to normalize the eigenfunctions, and still have the full translational symmetry, which is very important for the classification of the eigenfunctions, we again use periodic boundary conditions. The eigenfunctions then fulfill the boundary conditions

$$\psi(\boldsymbol{r}) = \psi(\boldsymbol{r}+N_\alpha \boldsymbol{a}_\alpha), \tag{5.13}$$

where $\boldsymbol{a}_\alpha, \alpha = 1, \ldots, d$ span the primitive unit cell and $N_\alpha$ is the system length in the α direction, i. e. the total number of unit cells is $N = N_1 \cdot \ldots \cdot N_d$. The $\boldsymbol{k}$ values, which can again be restricted to the first Brillouin zone, are then quantized and take (as with phonons) $N$ discrete values, i. e.

$$\boldsymbol{k} = \sum_{\alpha=1}^{d} \frac{n_\alpha}{N_\alpha} \boldsymbol{b}_\alpha \text{ where } n_\alpha \in \left\{-\frac{N_\alpha}{2}, \ldots, +\frac{N_\alpha}{2}\right\}. \tag{5.14}$$

The translation operator is also explicitly given by

$$T_{\boldsymbol{R}} = e^{i\boldsymbol{Rp}/\hbar}. \tag{5.15}$$

This follows from the Taylor expansion

$$\begin{aligned} T_{\boldsymbol{R}} f(\boldsymbol{r}) = f(\boldsymbol{r}+\boldsymbol{R}) &= \sum_{n=0}^{\infty} \frac{1}{n!} (\boldsymbol{R}\nabla)^n f(\boldsymbol{r}) = \sum_{n=0}^{\infty} \frac{1}{n!} \left(\frac{i}{\hbar}\boldsymbol{Rp}\right)^n f(\boldsymbol{r}) \\ &= \exp\left(\frac{i}{\hbar}\boldsymbol{Rp}\right) f(\boldsymbol{r}). \end{aligned} \tag{5.16}$$

For a common eigenfunction $\psi_{\boldsymbol{k}}(\boldsymbol{r})$ of the Hamiltonian operator and $e^{i\boldsymbol{kR}}$ eigenvalue of $T_{\boldsymbol{R}}$ we define a function

$$u_{\boldsymbol{k}}(\boldsymbol{r}) = e^{-i\boldsymbol{kr}} \psi_{\boldsymbol{k}}(\boldsymbol{r}). \tag{5.17}$$

These functions $u_{\boldsymbol{k}}(\boldsymbol{r})$ are then periodic with respect to the lattice, i.e. they fulfill:

$$u_{\boldsymbol{k}}(\boldsymbol{r}) = u_{\boldsymbol{k}}(\boldsymbol{r}+\boldsymbol{R}) \text{for each lattice vector} \boldsymbol{R}. \tag{5.18}$$

This is indeed the case as:

$$u_{\boldsymbol{k}}(\boldsymbol{r}+\boldsymbol{R}) = e^{-i\boldsymbol{k}(\boldsymbol{r}+\boldsymbol{R})} \psi_{\boldsymbol{k}}(\boldsymbol{r}+\boldsymbol{R}) = e^{-i\boldsymbol{kr}} e^{-i\boldsymbol{kR}} e^{i\boldsymbol{kR}} \psi_{\boldsymbol{k}}(\boldsymbol{r}) = u_{\boldsymbol{k}}(\boldsymbol{r}).$$

Thus, the normalized eigenfunctions of a one particle Hamiltonian with a lattice periodic potential can be represented as

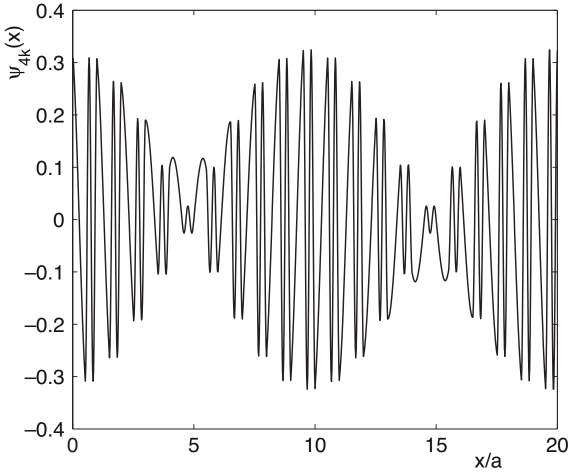

**Fig. 5.1** Bloch state for a 1-dimensional periodic potential (with $N = 20, k = \frac{\pi}{10a}$)

$$\boxed{\psi_{\boldsymbol{k}}(\boldsymbol{r}) = \frac{1}{\sqrt{V}} e^{i\boldsymbol{k}\,\boldsymbol{r}} u_{\boldsymbol{k}}(\boldsymbol{r})}, \tag{5.19}$$

with a lattice periodic **Bloch factor** $u_{\boldsymbol{k}}(\boldsymbol{r})$. This is the[2]

**Bloch-Theorem**$^2$**.**

Figure 5.1 shows such a Bloch function for a 1-dimensional crystal. The one-particle eigenfunctions of a lattice periodic Hamiltonian are given by the product of a plane wave with the lattice periodic Bloch factor. Thus, one can use extended eigenstates that can be represented as a plane wave with wave vector $\boldsymbol{k}$ from the first Brillouin zone, which is modulated by a lattice periodic function, namely the Bloch factor, over the whole crystal.

From the Schrödinger equation, one can derive a partial differential equation for the Bloch factors:

$$\begin{aligned} H\sqrt{V}\psi_{\boldsymbol{k}}(\boldsymbol{r}) &= \left(-\frac{\hbar^2\nabla^2}{2m} + V(\boldsymbol{r})\right) e^{i\boldsymbol{k}\boldsymbol{r}} u_{\boldsymbol{k}}(\boldsymbol{r}) = \varepsilon e^{i\boldsymbol{k}\boldsymbol{r}} u_{\boldsymbol{k}}\,(\boldsymbol{r}) \\ &= -\frac{\hbar^2}{2m} e^{i\boldsymbol{k}\,\boldsymbol{r}} \left(-k^2 + 2i\boldsymbol{k}\nabla + \nabla^2\right) u_{\boldsymbol{k}}\,(\boldsymbol{r}) + V(\boldsymbol{r}) e^{i\boldsymbol{k}\boldsymbol{r}} u_{\boldsymbol{k}}\,(\boldsymbol{r}). \end{aligned}$$

---

[2] F. Bloch, *1905 in Zürich, †1983 in Zürich, received his PhD in 1928 in Leipzig from Heisenberg on the quantum theory of electrons in a periodic potential, 1930 work on ferromagnetism and domain („Bloch") walls, emigrated in 1933 and from 1934 at Stanford University in California, work on magnetic moment of neutrons and development of nuclear magnetic resonance, for which he received the Nobel Prize in 1952.

Thus, for each $\boldsymbol{k}$ from the 1st Brillouin zone one has to solve a partial differential equation for $u_{\boldsymbol{k}}(\boldsymbol{r})$:

$$\boxed{h\,(\boldsymbol{k})u_{\boldsymbol{k}}\,(\boldsymbol{r}) = \left[\frac{\hbar^2}{2m}\left(\frac{1}{i}\nabla + \boldsymbol{k}\right)^2 + V(\boldsymbol{r})\right]u_{\boldsymbol{k}}\,(\boldsymbol{r}) = \varepsilon(\boldsymbol{k})u_{\boldsymbol{k}}\,(\boldsymbol{r})}. \tag{5.20}$$

The wave vector $\boldsymbol{k}$ acts here only as a parameter. Because $u_{\boldsymbol{k}}(\boldsymbol{r})$ is periodic with respect to lattice translations, it is a boundary value problem on the single unit cell, that is, on a finite, microscopic area. Therefore, for each fixed $\boldsymbol{k}$ there are discrete eigenvalues $\varepsilon_n(\boldsymbol{k})$ and corresponding eigenfunctions $u_{n\boldsymbol{k}}(\boldsymbol{r})$ to be expected. These can be orthonormalized on the unit cell, so that it holds:

$$\frac{1}{V_{pEZ}}\int_{V_{pEZ}} d^3r u^*_{n\boldsymbol{k}}(\boldsymbol{r})u_{n'\boldsymbol{k}}(\boldsymbol{r}) = \delta_{nn'}. \tag{5.21}$$

Thus, the Bloch functions $\psi_{n\boldsymbol{k}}(\boldsymbol{r}) = \frac{1}{\sqrt{V}}e^{i\boldsymbol{k}\boldsymbol{r}}u_{n\boldsymbol{k}}(\boldsymbol{r})$ satisfy:

$$\int_V d^3r\psi^*_{n\boldsymbol{k}}(\boldsymbol{r})\psi_{n'\boldsymbol{k}'}(\boldsymbol{r}) \tag{5.22}$$

$$= \frac{1}{V}\sum_{\boldsymbol{R}}\int_{V_{pEZ}(\boldsymbol{R})} d^3re^{-i\boldsymbol{k}(\boldsymbol{R}+\boldsymbol{r})}u^*_{n\boldsymbol{k}}(\boldsymbol{R}+\boldsymbol{r})e^{i\boldsymbol{k}'(\boldsymbol{R}+\boldsymbol{r})}u_{n'\boldsymbol{k}'}(\boldsymbol{R}+\boldsymbol{r})$$

$$= \frac{1}{N}\sum_{\boldsymbol{R}} e^{i(\boldsymbol{k}'-\boldsymbol{k})\boldsymbol{R}}\frac{1}{V_{pEZ}}\int_{V_{pEZ}} d^3ru^*_{n\boldsymbol{k}}(\boldsymbol{r})u_{n'\boldsymbol{k}'}(\boldsymbol{r}) = \delta_{\boldsymbol{k}\boldsymbol{k}'}\delta_{nn'}.$$

The eigenfunctions $\psi_{n\boldsymbol{k}}(\boldsymbol{r})$ and energy eigenvalues $\varepsilon_n(\boldsymbol{k})$ for the problem of an electron in the periodic potential are thus classified by two quantum numbers, namely the wave vector $\boldsymbol{k}$ from the first Brillouin zone and the index $n$, which numerates the discrete eigenvalues of the boundary value problem for the Bloch factors $u_{n\boldsymbol{k}}(\boldsymbol{r})$. This is analogous to the index $j$ in the phonon problem, which enumerated the different branches of the phonon spectrum. Here, the index $n$ is called the **band index**. In contrast to the phonons, where there are only a finite number of branches, there are infinitely many bands; because the effective Hamiltonian $h(\boldsymbol{k})$ is self-adjoint and its eigenfunctions $u_{n\boldsymbol{k}}(\boldsymbol{r})$ form a basis on the space of functions over the elementary cell $V_{pEZ}$ that are square integrable. Therefore, the completeness relation

$$\sum_n u^*_{n\boldsymbol{k}}\,(\boldsymbol{r})u_{n\boldsymbol{k}}\left(\boldsymbol{r}'\right) = V_{pEZ}\delta\left(\boldsymbol{r}-\boldsymbol{r}'\right). \tag{5.23}$$

must also be fulfilled. The $\boldsymbol{k}$ vectors in the first Brillouin zone are for a finite system with periodic (or even with realistic) boundary conditions strictly speaking also discrete; because the crystal is a macroscopic volume, the allowed $\boldsymbol{k}$ values are dense in the Brillouin zone and are often also considered as a continuous variable. As a function of $\boldsymbol{k}$, the dispersion relations $\varepsilon_n(\boldsymbol{k})$ are continuous functions. At special points or along lines or surfaces in the Brillouin zone, in particular also at the edge thereof, there can be **band degeneracies**, i.e. that for these special $\boldsymbol{k}$ and $n \neq n'$ $\varepsilon_n(\boldsymbol{k}) = \varepsilon_{n'}(\boldsymbol{k})$ is valid.

The Bloch theorem is so fundamentally important for the entire solid state physics, that here a second proof for it shall be presented, which does not require the translation operator. Since the potential is strictly periodic, we can expand it in a Fourier series, where the Fourier coefficients are determined by the reciprocal lattice vectors $\boldsymbol{G}$, as we have learned in Sec. 2.3 already:

$$V(\boldsymbol{r}) = \sum_{\boldsymbol{G}} V_{\boldsymbol{G}} e^{i\boldsymbol{G}\boldsymbol{r}} \tag{5.24}$$

with

$$V_{\boldsymbol{G}} = \frac{1}{V_{pEZ}} \int_{pEZ} d^3r V(\boldsymbol{r}) e^{-i\boldsymbol{G}\boldsymbol{r}}. \tag{5.25}$$

For the wave function we make also an ansatz as a Fourier series:

$$\psi(\boldsymbol{r}) = \sum_{\boldsymbol{q}} c_{\boldsymbol{q}} e^{i\boldsymbol{q}\boldsymbol{r}}. \tag{5.26}$$

The wave function $\psi(\boldsymbol{r})$ is **not** to be assumed periodic with respect to lattice translations, but it must fulfill the boundary conditions, here specifically periodic boundary conditions. Therefore

$$\boldsymbol{q} = \sum_{\alpha=1}^{3} \frac{n_\alpha}{N_\alpha} \boldsymbol{b}_\alpha \quad \text{with} \quad n_\alpha \text{ integer}, \tag{5.27}$$

applies, where the $\boldsymbol{b}_\alpha, \alpha = 1, \ldots, 3$ span the reciprocal lattice (and thus the $\boldsymbol{k}$ space) and $N_\alpha$ is the system length in α direction. The $\boldsymbol{q}$ are here not yet limited to the first Brillouin zone; any function that fulfills periodic boundary conditions can be represented in this way, even if it has nothing to do with the eigenfunctions for a periodic potential. If we now insert the Fourier expansion for the (periodic) potential and for the wave function into the Schrödinger equation, we get:

$$\left(-\frac{\hbar^2}{2m}\nabla^2 + V(\boldsymbol{r})\right)\psi(\boldsymbol{r}) = \left(-\frac{\hbar^2}{2m}\nabla^2 + \sum_{\boldsymbol{G}} V_{\boldsymbol{G}} e^{i\boldsymbol{G}\boldsymbol{r}}\right) \sum_{\boldsymbol{q}} c_{\boldsymbol{q}} e^{i\boldsymbol{q}\boldsymbol{r}}$$
$$= \sum_{\boldsymbol{q}} \left(\frac{\hbar^2 q^2}{2m} + \sum_{\boldsymbol{G}} V_{\boldsymbol{G}} e^{i\boldsymbol{G}\boldsymbol{r}}\right) c_{\boldsymbol{q}} e^{i\boldsymbol{q}\boldsymbol{r}} = \sum_{\boldsymbol{q}} \frac{\hbar^2 q^2}{2m} c_{\boldsymbol{q}} e^{i\boldsymbol{q}\boldsymbol{r}} + \sum_{\boldsymbol{q}\boldsymbol{G}} V_{\boldsymbol{G}} e^{i(\boldsymbol{G}+\boldsymbol{q})\boldsymbol{r}} c_{\boldsymbol{q}}$$
$$= \sum_{\boldsymbol{q}} \left(\frac{\hbar^2 q^2}{2m} c_{\boldsymbol{q}} + \sum_{\boldsymbol{G}} V_{\boldsymbol{G}} c_{\boldsymbol{q}-\boldsymbol{G}}\right) e^{i\boldsymbol{q}\boldsymbol{r}} = \varepsilon \sum_{\boldsymbol{q}} c_{\boldsymbol{q}} e^{i\boldsymbol{q}\boldsymbol{r}}.$$

So

$$\sum_{\boldsymbol{q}}\left[\left(\frac{\hbar^2 q^2}{2m}-\varepsilon\right)c_{\boldsymbol{q}}+\sum_{\boldsymbol{G}}V_{\boldsymbol{G}}c_{\boldsymbol{q}-\boldsymbol{G}}\right]e^{i\boldsymbol{q}\boldsymbol{r}}=0. \tag{5.28}$$

applies.

Since the functions $e^{i\boldsymbol{q}\boldsymbol{r}}$ form an orthonormal system, it follows:

$$\left(\frac{\hbar^2 q^2}{2m}-\varepsilon\right)c_{\boldsymbol{q}}+\sum_{\boldsymbol{G}}V_{\boldsymbol{G}}c_{\boldsymbol{q}-\boldsymbol{G}}=0. \tag{5.29}$$

As mentioned, $\boldsymbol{q}$ can still take on all values compatible with periodic boundary conditions and is not yet limited to the first Brillouin zone. For each $\boldsymbol{q}$, however, there is a unique $\boldsymbol{k} \in 1.\,\text{B. Z.}$ and a unique $\boldsymbol{G}$ reciprocal lattice vector, so that $\boldsymbol{q}=\boldsymbol{k}-\boldsymbol{G}$. This gives:

$$\left(\frac{\hbar^2}{2m}\left(\boldsymbol{k}-\boldsymbol{G}\right)^2-\varepsilon\right)c_{\boldsymbol{k}-\boldsymbol{G}}+\sum_{\boldsymbol{G}}V_{\boldsymbol{G}-\boldsymbol{G}}c_{\boldsymbol{k}-\boldsymbol{G}}=0. \tag{5.30}$$

This represents for each $\boldsymbol{k} \in 1.\,\text{B. Z.}$ a linear, homogeneous system of equations for the coefficients $c_{\boldsymbol{k}-\boldsymbol{G}}$. Apparently, only coefficients that differ by reciprocal lattice vectors are linked. For each $\boldsymbol{k}$ from the first Brillouin zone, one therefore has a separate equation system that is decoupled from those for other $\boldsymbol{k}'$. The possible solutions can therefore be classified according to $\boldsymbol{k}$ and one obtains:

$$\psi_{\boldsymbol{k}}(\boldsymbol{r})=\sum_{\boldsymbol{G}}c_{\boldsymbol{k}-\boldsymbol{G}}e^{i(\boldsymbol{k}-\boldsymbol{G})\boldsymbol{r}}=e^{i\boldsymbol{k}\boldsymbol{r}}\sum_{\boldsymbol{G}}c_{\boldsymbol{k}-\boldsymbol{G}}e^{-i\boldsymbol{G}\boldsymbol{r}}. \tag{5.31}$$

So the eigenfunctions of the Schrödinger equation can be represented as:

$$\psi_{\boldsymbol{k}}(\boldsymbol{r})=e^{i\boldsymbol{k}\boldsymbol{r}}u_{\boldsymbol{k}}(\boldsymbol{r}) \tag{5.32}$$

with $\boldsymbol{k}$ from the first Brillouin zone and

$$u_{\boldsymbol{k}}(\boldsymbol{r})=\sum_{\boldsymbol{G}}c_{\boldsymbol{k}-\boldsymbol{G}}e^{-i\boldsymbol{G}\boldsymbol{r}}=u_{\boldsymbol{k}}(\boldsymbol{r}+\boldsymbol{R}), \tag{5.33}$$

(because of $e^{-i\boldsymbol{G}\boldsymbol{R}}=1$). This statement just corresponds to the **Bloch theorem**.

## 5.2 Nearly Free Electron Approximation

In this section, we consider the model of free electrons and the periodic potential is considered as a perturbation to be treated in quantum mechanical, time-independent perturbation theory. We start from the Fourier-transformed Schrödinger equation (5.30):

$$\left(\frac{\hbar^2}{2m}(\boldsymbol{k}-\boldsymbol{G}_0)^2-\varepsilon\right)c_{\boldsymbol{k}-\boldsymbol{G}_0}+\sum_{\boldsymbol{G}}V_{\boldsymbol{G}-\boldsymbol{G}_0}c_{\boldsymbol{k}-\boldsymbol{G}}=0, \tag{5.34}$$

with $\boldsymbol{k}$ from the first Brillouin zone and $\boldsymbol{G},\boldsymbol{G_0}$ reciprocal lattice vectors. In 0th order in the potential, one can completely neglect this ($V\approx 0$) and immediately obtains

$$\varepsilon^{(0)}_{\boldsymbol{G}_0}(\boldsymbol{k})=\varepsilon^{(0)}_{\boldsymbol{k}-\boldsymbol{G}_0}=\frac{\hbar^2}{2m}(\boldsymbol{k}-\boldsymbol{G_0})^2. \tag{5.35}$$

Here, the lattice structure is already taken into account because a reciprocal lattice and a Brillouin zone have been introduced. However, the potential strength is still neglected, and strictly speaking, the lattice only becomes noticeable through a periodic potential. For really free (non-relativistic) electrons, one has the dispersion

$$\varepsilon^{(0)}(\boldsymbol{q})=\frac{\hbar^2q^2}{2m} \tag{5.36}$$

and as eigenfunctions plane waves

$$\psi_{\boldsymbol{q}}(\boldsymbol{r})=\frac{1}{\sqrt{Vol}}e^{i\,\boldsymbol{qr}}, \tag{5.37}$$

where $Vol$ is the volume of the system (crystal) and $\boldsymbol{q}$ runs over all wave vectors which are compatible with periodic boundary conditions (i.e. not limited to the first Brillouin zone). But every $\boldsymbol{q}$ can be uniquely represented as the sum of a $\boldsymbol{k}$ from the first Brillouin zone and a reciprocal lattice vector $\boldsymbol{G}_0$, if one chooses any lattice structure:

$$\boldsymbol{q}=\boldsymbol{k}-\boldsymbol{G}_0,\quad \varepsilon^{(0)}_{\boldsymbol{G}_0}(\boldsymbol{k})=\frac{\hbar^2}{2m}(\boldsymbol{k}-\boldsymbol{G}_0)^2,\quad \psi_{\boldsymbol{G}_0}(\boldsymbol{k})=\frac{1}{\sqrt{Vol}}e^{-i\boldsymbol{G}_0\boldsymbol{r}}e^{i\boldsymbol{kr}}. \tag{5.38}$$

Eigenenergies and -functions are then characterized by two quantum numbers, namely the wave vector $\boldsymbol{k}$ from the first Brillouin zone and the reciprocal lattice vector $\boldsymbol{G}_0$. The eigenfunctions can be represented as the product of the plane wave $e^{i\boldsymbol{kr}}$ and the function $e^{-i\boldsymbol{G}_0\boldsymbol{r}}$; the latter is a periodic function of the lattice and corresponds to the Bloch factor in the case of free electrons. We have thus confirmed the Bloch theorem for the trivial example of a lattice with vanishingly small (periodic) potential; the reciprocal lattice vectors play the role of the band indices $n$ here.

These properties are closely connected with the terms **reduced zone scheme** and **extended zone scheme**. This is illustrated in Fig. 5.2 for a one-dimensional system. The band structure of truly free electrons is a parabola; by shifting by reciprocal lattice vectors into the first Brillouin zone, one arrives at the **reduced zone scheme**; here, for each $k$ from the 1st zone, there are several (infinitely many) allowed energy eigenvalues, which differ in the reciprocal lattice vector (, by which they are shifted with respect to the free parabola,). If one now extends this band structure periodically from the first Brillouin zone into the other higher Brillouin zones, one arrives at the **extended zone scheme.**

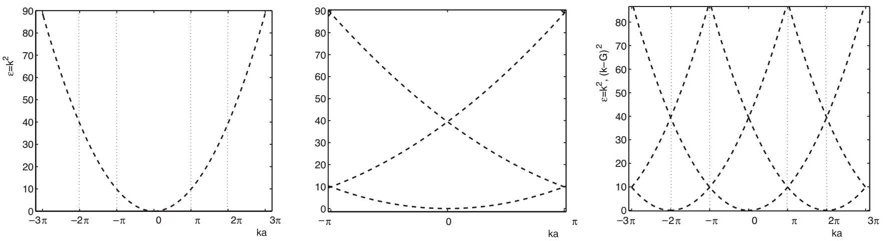

**Fig. 5.2** Dispersion of free electrons and their representation in the reduced and extended zone scheme for a one-dimensional system

If a finite periodic potential is switched on, the potential zero point can be chosen such that the 0th Fourier component, i.e. the potential mean value, vanishes:

$$V_{\mathbf{0}} = \frac{1}{V_{pEZ}} \int_{pEZ} d^3 r V(\boldsymbol{r}) = 0. \tag{5.39}$$

Then, from the Fourier-transformed Schrödinger equation, it follows that

$$\left(\varepsilon^{(0)}_{\boldsymbol{k}-\boldsymbol{G}_0} - \varepsilon\right) c_{\boldsymbol{k}-\boldsymbol{G}_0} = -\sum_{\boldsymbol{G}\neq\boldsymbol{G}_0} V_{\boldsymbol{G}-\boldsymbol{G}_0} c_{\boldsymbol{k}-\boldsymbol{G}}. \tag{5.40}$$

Here, $\varepsilon$ is the desired new energy in the band $\boldsymbol{G}_0$ in the presence of the potential, and according to the above considerations, it should not differ too much from $\varepsilon^{(0)}_{\boldsymbol{k}-\boldsymbol{G}_0}$. If the potential is weak, only small deviations from the behavior of free electrons are to be expected. Therefore, the classification of bands according to reciprocal lattice vectors $\boldsymbol{G}$ will continue to be possible and meaningful. Let us now consider the band to $\boldsymbol{G}_0$, then one can assume that the Fourier coefficients $c_{\boldsymbol{k}-\boldsymbol{G}}$ for $\boldsymbol{G} \neq \boldsymbol{G}_0$ are small, since they vanish for $V \to 0$. We write the corresponding equation of the linear equation system for the coefficients $\boldsymbol{G}$ but for the eigenenergy in the band $\boldsymbol{G}_0$ again:

$$\left(\varepsilon^{(0)}_{\boldsymbol{k}-\boldsymbol{G}} - \varepsilon\right) c_{\boldsymbol{k}-\boldsymbol{G}} = -\sum_{\boldsymbol{G}\neq\boldsymbol{G}} V_{\boldsymbol{G}-\boldsymbol{G}} c_{\boldsymbol{k}-\boldsymbol{G}} = -V_{\boldsymbol{G}_0-\boldsymbol{G}} c_{\boldsymbol{k}-\boldsymbol{G}_0} - \sum_{\boldsymbol{G}\neq\boldsymbol{G}_0,\boldsymbol{G}} V_{\boldsymbol{G}-\boldsymbol{G}} c_{\boldsymbol{k}-\boldsymbol{G}}. \tag{5.41}$$

Here we can now neglect the last term, since all summands are at least of order $V^2$while the first summand on the right hand side is at most linear in $V$, since $c_{\boldsymbol{k}-\boldsymbol{G}_0}$ is of order $O(1)$. It follows:

$$c_{\boldsymbol{k}-\boldsymbol{G}} = \frac{V_{\boldsymbol{G}_0-\boldsymbol{G}}}{\varepsilon - \varepsilon^{(0)}_{\boldsymbol{k}-\boldsymbol{G}}} c_{\boldsymbol{k}-\boldsymbol{G}_0}. \tag{5.42}$$

If one inserts this in (5.40), it follows:

$$\left(\varepsilon - \varepsilon^{(0)}_{\boldsymbol{k}-\boldsymbol{G}_0}\right) c_{\boldsymbol{k}-\boldsymbol{G}_0} = \sum_{\boldsymbol{G}} \frac{V_{\boldsymbol{G}-\boldsymbol{G}_0} V_{\boldsymbol{G}_0-\boldsymbol{G}}}{\varepsilon - \varepsilon^{(0)}_{\boldsymbol{k}-\boldsymbol{G}}} c_{\boldsymbol{k}-\boldsymbol{G}_0} \tag{5.43}$$

and thus:

$$\varepsilon = \varepsilon^{(0)}_{\boldsymbol{k}-\boldsymbol{G}_0} + \sum_{\boldsymbol{G}\neq\boldsymbol{G}_0} \frac{|V_{\boldsymbol{G}-\boldsymbol{G}_0}|^2}{\varepsilon - \varepsilon^{(0)}_{\boldsymbol{k}-\boldsymbol{G}}}. \tag{5.44}$$

This corresponds to the quantum mechanical Brillouin-Wigner-perturbation series up to the second order in the perturbation $V$; note that the eigenenergy to be determined $\varepsilon$ still occurs in the denominator on the right hand side. If there is no degeneracy and the perturbation term is really always small, the energy $\varepsilon$ can be replaced by its 0. approximation on the right hand side i.e. $\varepsilon^{(0)}_{\boldsymbol{k}-\boldsymbol{G}_0}$; one is then still exact up to the order $V^2$ in the periodic potential as a perturbation. Then one obtains:

$$\varepsilon = \varepsilon^{(0)}_{\boldsymbol{k}-\boldsymbol{G}_0} + \sum_{\boldsymbol{G}\neq\boldsymbol{G}_0} \frac{|V_{\boldsymbol{G}-\boldsymbol{G}_0}|^2}{\varepsilon^{(0)}_{\boldsymbol{k}-\boldsymbol{G}_0} - \varepsilon^{(0)}_{\boldsymbol{k}-\boldsymbol{G}}}. \tag{5.45}$$

This just corresponds to the Rayleigh-Schrödinger perturbation series up to 2nd order. In the range of the Brillouin zone, in which no band degeneracies of the undisturbed free electron energies occur, the eigenenergies calculated in 2nd order in the periodic potential are therefore modified by terms of the order of magnitude $\frac{V^2}{\Delta\varepsilon}$ compared to the energies for free electrons, where $\Delta\varepsilon$ is the energy distance between adjacent bands. As a rule, therefore, $|\Delta\varepsilon| = \left|\varepsilon^{(0)}_{\boldsymbol{k}-\boldsymbol{G}_0} - \varepsilon^{(0)}_{\boldsymbol{k}-\boldsymbol{G}}\right| \gg |V|$ applies, and then the approximation for the eigenenergies is justified. However, there are special $\boldsymbol{k}$ points in the Brillouin zone, at which degeneracy occurs, i.e. at which the undisturbed (free electron) eigenenergies for different reciprocal lattice vectors $\boldsymbol{G}_0 \neq \boldsymbol{G}_1$ are degenerate, i.e. $\varepsilon^{(0)}_{\boldsymbol{k}-\boldsymbol{G}_0} = \varepsilon^{(0)}_{\boldsymbol{k}-\boldsymbol{G}_1}$ is fulfilled. In the vicinity of these $\boldsymbol{k}$ points, the Rayleigh-Schrödinger perturbation theory is no longer possible due to the diverging denominator, a problem that one can often encounter in practice with (too naive application of) perturbation theory. In general, however, the degeneracy is only present for two reciprocal lattice vectors, then for $\boldsymbol{k}$ in the vicinity of this degeneracy point in the corresponding summand of (5.44) the desired eigenenergy in the denominator may not yet be replaced by the 0th order, since one would then divide by 0; for all other $\boldsymbol{G}$ the previous replacement is allowed, however. Therefore one obtains:

$$\varepsilon(\boldsymbol{k}) = \varepsilon^{(0)}_{\boldsymbol{k}-\boldsymbol{G}_0} + \frac{|V_{\boldsymbol{G}_1-\boldsymbol{G}_0}|^2}{\varepsilon(\boldsymbol{k}) - \varepsilon^{(0)}_{\boldsymbol{k}-\boldsymbol{G}_1}} + \sum_{\boldsymbol{G}\neq\boldsymbol{G}_0\boldsymbol{G}_1} \frac{|V_{\boldsymbol{G}-\boldsymbol{G}_0}|^2}{\varepsilon^{(0)}_{\boldsymbol{k}-\boldsymbol{G}_0} - \varepsilon^{(0)}_{\boldsymbol{k}-\boldsymbol{G}}}. \tag{5.46}$$

If one neglects the last term, which, as before may be considered to be small for the $\boldsymbol{k}$ values, which are not in the vicinity of degeneracy points, one obtains a quadratic equation for the desired eigenvalues with the solution:

$$\varepsilon(\boldsymbol{k}) = \frac{1}{2}\left[\varepsilon^{(0)}_{\boldsymbol{k}-\boldsymbol{G}_0} + \varepsilon^{(0)}_{\boldsymbol{k}-\boldsymbol{G}_1} \pm \sqrt{\left(\varepsilon^{(0)}_{\boldsymbol{k}-\boldsymbol{G}_0} - \varepsilon^{(0)}_{\boldsymbol{k}-\boldsymbol{G}_1}\right)^2 + 4|V_{\boldsymbol{G}_0-\boldsymbol{G}_1}|^2}\right]. \tag{5.47}$$

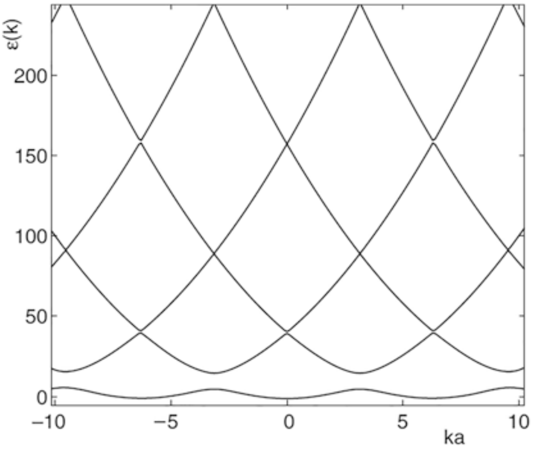

**Fig. 5.3** Band structure of free electrons for a simple-cubic lattice along selected symmetry directions in the 1st Brillouin zone.

At the degeneracy point $\boldsymbol{k}$, where $\varepsilon^{(0)}_{\boldsymbol{k}-\boldsymbol{G}_0} = \varepsilon^{(0)}_{\boldsymbol{k}-\boldsymbol{G}_1}$ holds, we now get two new eigenenergies

$$\boxed{\varepsilon^{\pm}(\boldsymbol{k}) = \varepsilon^{(0)}_{\boldsymbol{k}-\boldsymbol{G}_0} \pm |V_{\boldsymbol{G}_0-\boldsymbol{G}_1}|}\,. \tag{5.48}$$

The degeneracy is thus lifted in the presence of the periodic potential. The eigenenergies that coincide for free electron bands at $\boldsymbol{k}$ are split and separated by an **energy gap** $2|V_{\boldsymbol{G}_0-\boldsymbol{G}_1}|$. This is how energy bands, i.e. energy intervals in which eigenenergies lie, and energy gaps, i.e. intervals in which no allowed energy eigenvalues for the crystal occur, come about. The splitting and thus the size of the energy gap is directly determined by the strength of the potential. For nearly free electrons in one dimension the development of bands and band gaps according to (5.45, 47, 48) is demonstrated in Fig. 5.3.

As a simple 3-dimensional example of free electron bands in the presence of a crystal structure with an associated reciprocal lattice, the bands (in 0th order in the potential) for a simple cubic structure are shown in the following figure along the usual main symmetry directions of the Brillouin zone. Here, the band index is determined by reciprocal lattice vectors such as $\boldsymbol{G} = (0,0,0)$, $\frac{2\pi}{a}(1,0,0)$, $\frac{2\pi}{a}(0,1,0)$, $\frac{2\pi}{a}(0,0,1)$, $\frac{2\pi}{a}(1,1,0)$, $\frac{2\pi}{a}(1,0,1)$, $\frac{2\pi}{a}(0,1,1)$, $\frac{2\pi}{a}(1,1,1)$. However, along the main symmetry directions, some of the bands belonging to the above reciprocal lattice vectors are degenerate, so that a maximum of 7 different bands can be distinguished in the figure. The energy is measured in units of $\frac{\hbar^2}{2ma^2}$, which is of the order of $10^{-1}$eV if $a \sim 5$ Å. Along the (100) direction, the result is qualitatively similar to that of the 1-dimensional case. In the other directions, however, the situation becomes more complicated. In particular, this representation already allows a qualitative understanding of the fact that the band minimum of the higher lying band may be located at a different point in the $\boldsymbol{k}$-space than the band maximum of the lower lying band (Fig. 5.4).

**Fig. 5.4** Band structure of free electrons for a simple-cubic lattice along selected symmetry directions in the 1st Brillouin zone.

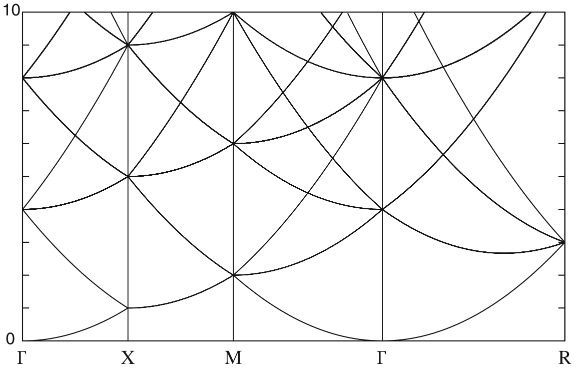

Thus, the occurrence of indirect band gaps can be qualitatively understood in the model of quasi-free electrons as a result of the crystal structure and the folding of the dispersion relation of free electrons into the first Brillouin zone. This is also evident from the second example shown in Fig. 5.5, where the free electron band structure (dashed lines) and the resulting band structure for nearly-free electrons (taking into account a few Fourier components of a periodic potential) are shown along special directions in the first Brillouin zone. Here too, there are indirect band gaps.

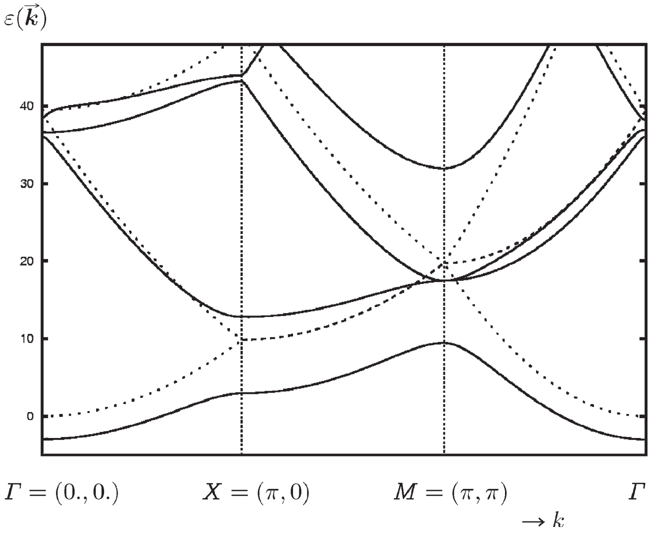

**Fig. 5.5** Band structure of free *(dashed)* and nearly-free *(solid lines)* electrons on a two-dimensional square lattice

## 5.3 Effective mass tensor, group velocity and $\boldsymbol{k}\cdot\boldsymbol{p}$-perturbation theory

In this section, some aspects of the $\boldsymbol{k}$-dependence in bands shall be studied in more detail. We start from the Schrödinger equation (5.20) for the Bloch factors. This can be rewritten as:

$$\left[\frac{\boldsymbol{p}^2}{2m}+V(\boldsymbol{r})+\frac{\hbar}{m}(\boldsymbol{k}\cdot\boldsymbol{p})\right]u_{n\boldsymbol{k}}(\boldsymbol{r})=\left[\varepsilon_n(\boldsymbol{k})-\frac{\hbar^2k^2}{2m}\right]u_{n\boldsymbol{k}}(\boldsymbol{r}), \qquad (5.49)$$

where $\boldsymbol{p}=\frac{\hbar}{i}\nabla$ denotes the momentum operator. Now the term $\sim\boldsymbol{kp}$ is to be considered as a perturbation; then the energy eigenvalues and -states can be approximately determined by means of quantum mechanical perturbation theory. In zeroth order in $\boldsymbol{k}$ one has to solve

$$\left[\frac{\boldsymbol{p}^2}{2m}+V(\boldsymbol{r})\right]u_{n\boldsymbol{0}}(\boldsymbol{r})=\varepsilon_n(\boldsymbol{0})u_{n\boldsymbol{0}}(\boldsymbol{r}) \qquad (5.50)$$

This corresponds again to a simple Schrödinger equation with periodic boundary conditions with respect to the unit cells. In second order quantum mechanical perturbation theory one now obtains:

$$\varepsilon_n(\boldsymbol{k})-\frac{\hbar^2k^2}{2m}=\varepsilon_n(0)+\frac{\hbar^2}{m^2}\sum_{n'\neq n}\frac{\langle n0|\boldsymbol{kp}|n'0\rangle\langle n'0|\boldsymbol{kp}|n0\rangle}{\varepsilon_n(0)-\varepsilon_{n'}(0)}. \qquad (5.51)$$

The following was used in the derivation of (5.51):

1. Quantum mechanical Rayleigh-Schrödinger perturbation theory, i.e.:
   Given Hamiltonian operator $H=H_0+H_1$, $|n^{(0)}\rangle$ denote eigenstates of $H_0$, i.e. $H_0|n^{(0)}\rangle=E_{n0}|n^{(0)}\rangle$. Then the energy eigenvalues $E_n$ of the full $H$ in second order in $H_1$ are approximately given by:

   $$E_n=E_{n0}+\langle n^{(0)}|H_1|n^{(0)}\rangle+\sum_{n'\neq n}\frac{\langle n^{(0)}|H_1|n'^{(0)}\rangle\langle n'^{(0)}|H_1|n^{(0)}\rangle}{E_{n0}-E_{n'0}}.$$

   This is an elementary and important relation from quantum mechanics, which is only applicable if there is no degeneracy. It was also used in (5.45) and derived for the specific problem there. The non-degeneracy requirement is often met for the present problem, since at the Γ point ($\boldsymbol{k}=0$) the bands to different band indices are usually not degenerate.
2. In (5.51) the ket notation for the Bloch factors was used, i.e. $u_{n\boldsymbol{k}}(\boldsymbol{r})=\langle\boldsymbol{r}|n\boldsymbol{k}\rangle$
3. If the periodic potential has inversion symmetry, i.e. $V(\boldsymbol{r})=V(-\boldsymbol{r})$ is fulfilled, the eigenfunction to $\boldsymbol{k}=0$ also has inversion symmetry, therefore the diagonal element of $\boldsymbol{kp}$ vanishes:

   $$\langle 0n|\boldsymbol{kp}|0n\rangle=0.$$

   Therefore, no term appears linearly in the perturbation.

Equation (5.51) can also be written as

$$\varepsilon_n(\boldsymbol{k}) - \frac{\hbar^2 k^2}{2m} = \varepsilon_n(0) + \frac{\hbar^2}{m^2}\sum_{\alpha\alpha'} k_\alpha k_{\alpha'} \sum_{n'\neq n} \frac{\langle n0|p_\alpha|n'0\rangle\langle n'0|p_{\alpha'}|n0\rangle}{\varepsilon_n(0)-\varepsilon_{n'}(0)}. \tag{5.52}$$

In the vicinity of the Γ point, a quadratic $k$-dependence is therefore to be expected in general in each band for small $k$, if the potential is inversion-symmetric. In all bands, even the higher ones, one therefore has at least for small $k$ the behavior as that for free electrons. However, already in order $k^2$, in general an anisotropy has to be expected, in addition the so-called **effective mass** can be drastically different from the free electron mass.

The **tensor of effective mass**in the band with band index $n$ is defined by

$$\left(\frac{1}{m^*(n)}\right)_{\alpha\alpha'} = \frac{1}{\hbar^2}\frac{\partial^2\varepsilon_n(\boldsymbol{k})}{\partial k_\alpha \partial k_{\alpha'}} = \frac{1}{m}\delta_{\alpha\alpha'} + \frac{2}{m^2}\sum_{n'\neq n}\frac{\langle n0|p_\alpha|n'0\rangle\langle n'0|p_{\alpha'}|n0\rangle}{\varepsilon_n(0)-\varepsilon_{n'}(0)} \tag{5.53}$$

where $m$ is the free electron mass. Then one has obviously

$$\varepsilon_n(\boldsymbol{k}) = \varepsilon_n(0) + \sum_{\alpha\alpha'}\left(\frac{1}{2m^*(n)}\right)_{\alpha\alpha'}\hbar^2 k_\alpha k_{\alpha'}. \tag{5.54}$$

If $m^*$ is diagonal and isotropic, one thus has the dispersion relation of free particles again, but with modified effective mass $m^*$. The effective mass can be drastically different from the value of free electrons, it can be smaller or much larger than $m$, it can even be negative. This is always the case when $\varepsilon_n(\boldsymbol{k})$ has a negative curvature, i.e. specifically at maxima of the dispersion relation. Then the main contribution in the $n'$-sum in the second-order term of the perturbation series is that of bands $n'$, which are energetically higher at $\boldsymbol{k} = 0$, so that the $n'$-sum is negative overall. Negative effective masses find their natural physical interpretation as holes (i.e. electron vacancies) in the almost filled energy band.

Also at $\boldsymbol{k}_0 \neq 0$ a perturbation calculation with respect to the $\boldsymbol{kp}$-term is possible and an effective mass can be defined. However, stronger deviations from free electron behavior are then to be expected. In particular, there is no longer any argument why the linear term in $\boldsymbol{k}$ in the perturbation calculation should disappear. If one takes into account that for the differential operator $h(\boldsymbol{k})$ in the boundary value problem (5.20) for the $u_{n\boldsymbol{k}}(\boldsymbol{r})$ it holds:

$$h(\boldsymbol{k}_0 + \boldsymbol{k}) = h(\boldsymbol{k}_0) + \frac{\hbar}{m}(\boldsymbol{p} + \hbar\boldsymbol{k}_0)\cdot\boldsymbol{k} + \frac{\hbar^2 k^2}{2m} \tag{5.55}$$

one finds in generalization of (5.51)

$$\varepsilon_n(\boldsymbol{k}_0 + \boldsymbol{k}) = \varepsilon_n(\boldsymbol{k}_0) + \frac{\hbar}{m}\boldsymbol{k}\cdot\langle\psi_{n\boldsymbol{k}_0}|\boldsymbol{p}|\psi_{n\boldsymbol{k}_0}\rangle \tag{5.56}$$

$$+\frac{\hbar^2 k^2}{2m} + \frac{\hbar^2}{m^2} \sum_{n' \neq n} \frac{\left\langle \psi_{n\boldsymbol{k}_0} | \boldsymbol{k}\boldsymbol{p} | \psi_{n'\boldsymbol{k}_0} \right\rangle \left\langle \psi_{n'\boldsymbol{k}_0} | \boldsymbol{k}\boldsymbol{p} | \psi_{n\boldsymbol{k}_0} \right\rangle}{\varepsilon_n\left(\boldsymbol{k}_0\right) - \varepsilon_{n'}\left(\boldsymbol{k}_0\right)}.$$

The following was used here:

$$\left\langle \psi_{n\boldsymbol{k}_0} | \boldsymbol{p} | \psi_{n'\boldsymbol{k}_0} \right\rangle = \left\langle n\boldsymbol{k}_0 | e^{-i\boldsymbol{k}_0\boldsymbol{r}} \boldsymbol{p} e^{i\boldsymbol{k}_0\boldsymbol{r}} | n'\boldsymbol{k}_0 \right\rangle = \left\langle n\boldsymbol{k}_0 | (\boldsymbol{p} + \hbar\boldsymbol{k}_0) | n'\boldsymbol{k}_0 \right\rangle. \tag{5.57}$$

So it holds

$$\nabla_{\boldsymbol{k}} \varepsilon_n(\boldsymbol{k}) = \frac{\hbar}{m} \langle \psi_{n\boldsymbol{k}} | \boldsymbol{p} | \psi_{n\boldsymbol{k}} \rangle. \tag{5.58}$$

This relation is the generalization of the known law for free electrons $\langle \boldsymbol{k} | \boldsymbol{p} | \boldsymbol{k} \rangle = \hbar\boldsymbol{k}$. However, the Bloch function $\psi_{n\boldsymbol{k}}(\boldsymbol{r})$ is no longer an eigenfunction of the momentum operator $\boldsymbol{p}$ like a plane wave.

One can also define an effective mass tensor for $\boldsymbol{k}_0 \neq 0$ by

$$\left(\frac{1}{m^*(n\boldsymbol{k}_0)}\right)_{\alpha\alpha'} = \frac{1}{\hbar^2} \frac{\partial^2 \varepsilon_n(\boldsymbol{k})}{\partial k_\alpha \partial k_{\alpha'}} |_{\boldsymbol{k}_0}. \tag{5.59}$$

The derivative of the energy dispersion of a band with respect to the wave vector has the physical meaning of a group velocity. This becomes clear through the following elementary consideration: Imagine a wave packet as a superposition of Bloch functions in the vicinity of a fixed $\boldsymbol{k}$, i. e.

$$\begin{aligned} \psi(\boldsymbol{r}, t) &= \sum_{\boldsymbol{\kappa}} a_{\boldsymbol{\kappa}} \psi_{n\boldsymbol{k}+\boldsymbol{\kappa}}(\boldsymbol{r}) e^{-i\varepsilon_n(\boldsymbol{k}+\boldsymbol{\kappa})t/\hbar} = \sum_{\boldsymbol{\kappa}} a_{\boldsymbol{\kappa}} u_{n\boldsymbol{k}+\boldsymbol{\kappa}}(\boldsymbol{r}) e^{i\left[(\boldsymbol{k}+\boldsymbol{\kappa})\boldsymbol{r} - \varepsilon_n(\boldsymbol{k}+\boldsymbol{\kappa})t/\hbar\right]} \\ &= e^{i(\boldsymbol{k}\boldsymbol{r} - \varepsilon_n(\boldsymbol{k})t/\hbar)} u_{n\boldsymbol{k}}(\boldsymbol{r}) \sum_{\boldsymbol{\kappa}} a_{\boldsymbol{\kappa}} e^{i\boldsymbol{\kappa}(\boldsymbol{r} - \nabla_{\boldsymbol{k}}\varepsilon_n(\boldsymbol{k})t/\hbar)}. \end{aligned} \tag{5.60}$$

The wave packet is thus composed of a Bloch wave multiplied by a spatial distribution that moves uniformly with the velocity $\frac{1}{\hbar}\nabla_{\boldsymbol{k}}\varepsilon_n(\boldsymbol{k})$. If you know the effective mass tensor and the group velocity, you can describe the band structure locally, i. e. in the vicinity of certain $\boldsymbol{k}$ points, quite well already in the first Brillouin zone. At the end of this section, some important but simple and self-evident symmetry relations of the electron dispersion should be mentioned. First of all, the

**Kramers – Theorem**[3]

$$\varepsilon_n(\boldsymbol{k}) = \varepsilon_n(-\boldsymbol{k}) \tag{5.61}$$

is valid. If the potential has inversion symmetry, the following proof of the Kramers theorem[3] is possible because the Hamiltonian operator then commutes with the parity operator $P$ $\big(\text{defined by } P\phi(\boldsymbol{r}) = \phi(-\boldsymbol{r})\big)^{*\dagger}$

---

[3] H.A.Kramers, 1894 in Rotterdam, †1952 in Oegstgeest (Netherlands), Dutch physicist, worked with Nils Bohr for his PhD (1919), derived with Heisenberg the Kramers–Heisenberg dispersion formula in 1925, which implicitly predicted the Raman effect, many other theorems, approximations, etc. bear his name (e.g. WKB approximation, Kramers-Kronig relations, etc.)

$$\begin{aligned} HP\psi_{nk}(\boldsymbol{r}) &= H\psi_{nk}(-\boldsymbol{r}) = PH\psi_{nk}(\boldsymbol{r}) = \varepsilon_n(\boldsymbol{k})P\psi_{nk}(\boldsymbol{r}) \\ T_{\boldsymbol{R}}P\psi_{nk}(\boldsymbol{r}) &= T_{\boldsymbol{R}}e^{-i\boldsymbol{k}\boldsymbol{r}}u_{nk}(-\boldsymbol{r}) = e^{-i\boldsymbol{k}\boldsymbol{R}}P\psi_{nk}(\boldsymbol{r}). \end{aligned} \tag{5.62}$$

So $P\psi_{nk}(\boldsymbol{r}) = e^{-i\boldsymbol{k}\boldsymbol{r}}u_{nk}(-\boldsymbol{r})$ is an eigenfunction of $H$ and the translation operator $T_{\boldsymbol{R}}$ to the wave vector $-\boldsymbol{k}$ and energy eigenvalue $\varepsilon_n(\boldsymbol{k})$.

But the Kramers theorem is even more general and also valid if the periodic potential does not have inversion symmetry. From the effective Schrödinger equation (5.20) it follows by forming the conjugate complex:

$$h^*(\boldsymbol{k})u_{\boldsymbol{k}}^*(\boldsymbol{r}) = \left[\frac{\hbar^2}{2m}\left(-\frac{1}{i}\nabla + \boldsymbol{k}\right)^2 + V(\boldsymbol{r})\right]u_{\boldsymbol{k}}^*(\boldsymbol{r}) = \varepsilon(\boldsymbol{k})u_{\boldsymbol{k}}^*(\boldsymbol{r})$$

$$= \left[\frac{\hbar^2}{2m}\left(\frac{1}{i}\nabla - \boldsymbol{k}\right)^2 + V(\boldsymbol{r})\right]u_{\boldsymbol{k}}^*(\boldsymbol{r}). \tag{5.63}$$

So $u_{\boldsymbol{k}}^*(\boldsymbol{r})$ solves the effective Schrödinger equation to $-\boldsymbol{k}$, so

$$u_{-\boldsymbol{k}}(\boldsymbol{r}) = u_{\boldsymbol{k}}^*(\boldsymbol{r}), \quad \varepsilon_n(-\boldsymbol{k}) = \varepsilon_n(\boldsymbol{k}) \tag{5.64}$$

and of course also for the Bloch functions:

$$\psi_{n\boldsymbol{k}}^*(\boldsymbol{r}) = \psi_{n-\boldsymbol{k}}(\boldsymbol{r}). \tag{5.65}$$

The Kramers theorem can ultimately also be traced back to the fundamental principle of time reversal invariance (and proved by it).

Analogously, one can infer that:

$$\varepsilon_n\left(\underline{\underline{D}}\boldsymbol{k}\right) = \varepsilon_n(\boldsymbol{k}), \tag{5.66}$$

if $\underline{\underline{D}}$ is a symmetry operation of the underlying lattice. Finally, we note the trivial relation

$$\varepsilon_n(\boldsymbol{k}) = \varepsilon_n(\boldsymbol{k} + \boldsymbol{G}) \tag{5.67}$$

for each reciprocal lattice vector $\boldsymbol{G}$, if one wants to continue the dispersion relations beyond the first Brillouin zone (i.e. in the extended zone scheme).

## 5.4 Tight binding model, Wannier states

Although the model of quasifree electrons already allows a qualitative understanding of the formation of energy bands and band gaps and of characteristic features in the band structure for certain Bravais lattices, it is usually not suitable for quantitative band structure calculations. The basic assumption of a weak periodic potential, with respect to which perturbation theory is possible, is usually not given. The potential is rather to be seen as strong. An alternative method for understanding the electronic energy band structure starts from the opposite limit of the strongly bound, localized electrons. It starts from the isolated atoms, assumes that the atomic eigenstates and energies are known and investigates the modification of these states when the atoms are brought close together, so that they interact with each other, enter into chemical bonds and form crystals. If we have an isolated atom at the position $\boldsymbol{R}$, then the atomic problem

$$H_{at,\boldsymbol{R}}\varphi_n(\boldsymbol{r}-\boldsymbol{R}) = E_n\varphi_n(\boldsymbol{r}-\boldsymbol{R}) \tag{5.68}$$

shall be assumed as solved. Here

$$H_{at,\boldsymbol{R}} = \frac{\boldsymbol{p}^2}{2m} + v(\boldsymbol{r}-\boldsymbol{R}). \tag{5.69}$$

$v(\boldsymbol{r}-\boldsymbol{R})$ is as always the (usually attractive) potential that an electron experiences from the atom (ion) at the location $\boldsymbol{R}$. The quantum numbers $n$ thus designate a complete set of atomic quantum numbers, so that, for example, $n = (\tilde{n}, l, m_l, \sigma)$ applies to hydrogen-like atoms, where $\tilde{n}$ is the principal quantum number, $(l, m_l)$ the quantum numbers of the orbital angular momentum, and $\sigma = \pm\frac{1}{2}$ the spin quantum number. As long as effects such as spin-orbit interaction are not taken into account, all states are degenerate with respect to the spin in a system without Coulomb interaction between the electrons. It is now to be examined how the atomic problem, which is assumed to be known, is modified if the atom is no longer isolated but is surrounded by other atoms of the same kind in a crystal. The full Hamiltonian operator for a single solid-state electron can then be represented as

$$\begin{aligned} H &= \frac{\boldsymbol{p}^2}{2m} + \sum_{\boldsymbol{R}} v(\boldsymbol{r}-\boldsymbol{R}) \\ &= H_{at,\boldsymbol{R}} + \Delta V_{\boldsymbol{R}}(\boldsymbol{r}) \end{aligned} \tag{5.70}$$

$$\text{with} \quad \Delta V_{\boldsymbol{R}}(\boldsymbol{r}) = \sum_{\boldsymbol{R}'\neq\boldsymbol{R}} v\left(\boldsymbol{r}-\boldsymbol{R}'\right). \tag{5.71}$$

The latter is thus the potential of all the other atoms except the one at the location $\boldsymbol{R}$, and this is to be considered as a perturbation when we want to examine the modification of the atomic states and energies by the presence of the other atoms. In Fig. 5.6 the atomic potential and the crystal potential are illustrated for a 1-d system.

The following basic idea lies behind this treatment: It is known from the elementary theory of chemical bonding that the (atomic) levels responsible for the binding split into two levels when two atoms are brought together, namely into a bonding and an antibonding state; if three atoms are brought together, a split into three levels is to be expected, etc. – if $N$ atoms are brought together, the $N$ levels degenerate for the separated atoms split into $N$ different energy levels, and if $N$ is very large, then these $N$ states lie close together and thus practically form a continuum of states in a certain energy interval, namely the **energy band**.

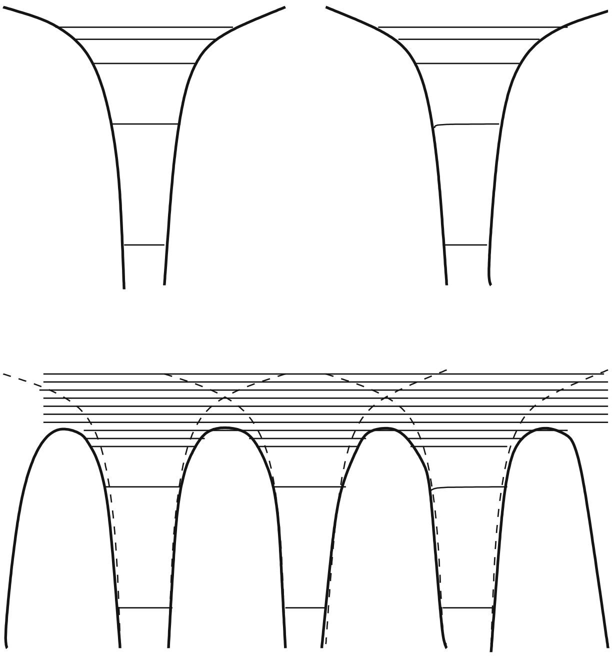

**Fig. 5.6** Schematic representation of the development of energy bands from the atomic levels due to the superposition of the atomic potentials

To construct a suitable ansatz for the wave function of the full solid-state Hamiltonian operator $H$ from the atomic wave functions of $H_{at,\boldsymbol{R}}$ we start from the following consideration: If the atomic wave functions $\varphi_n(\boldsymbol{r}-\boldsymbol{R})$ decrease so quickly that they already vanish in the region where $\Delta V_{\boldsymbol{R}}(\boldsymbol{r})$ is different from 0, then the states are not split, the atomic states are therefore also eigenstates of the full $H$:

$$H\varphi_n(\boldsymbol{r}-\boldsymbol{R}) = (H_{at,\boldsymbol{R}} + \Delta V_{\boldsymbol{R}}(\boldsymbol{r}))\varphi_n(\boldsymbol{r}-\boldsymbol{R}) = E_n\varphi_n(\boldsymbol{r}-\boldsymbol{R}). \tag{5.72}$$

However, they are not yet in the form of Bloch states, but a Bloch state can be constructed immediately by:

$$\psi_{n\boldsymbol{k}}(\boldsymbol{r}) = \frac{1}{\sqrt{N}}\sum_{\boldsymbol{R}} e^{i\boldsymbol{k}\boldsymbol{R}}\varphi_n(\boldsymbol{r}-\boldsymbol{R}). \tag{5.73}$$

Obviously, the $\psi_{n\boldsymbol{k}}(\boldsymbol{r})$ thus defined satisfies the periodicity condition

$$\psi_{n\boldsymbol{k}}(\boldsymbol{r}+\boldsymbol{R}) = e^{i\boldsymbol{k}\boldsymbol{R}}\psi_{n\boldsymbol{k}}(\boldsymbol{r}) \tag{5.74}$$

and thus has the elementary properties of a Bloch function. In addition,

$$H\psi_{n\boldsymbol{k}}(\boldsymbol{r}) = E_n\psi_{n\boldsymbol{k}}(\boldsymbol{r}). \tag{5.75}$$

The atomic levels therefore remain eigenenergies in the solid state, we get dispersionless (**k**-independent) bands, if the atomic states are localized so strongly that they have already fallen to 0 in the vicinity of the other atoms. But this can only be a reasonable assumption for inner core states. For crystals or even for molecules, the binding must occur precisely because the states overlap, so that the electrons can belong to all the atoms involved. For these states, i.e. at least for the outer atomic levels, the assumption $\Delta V_{\boldsymbol{R}}\varphi_n(\boldsymbol{r}-\boldsymbol{R}) = 0$ is no longer justified. Nevertheless, we can still use (5.73) as an ansatz for the sought-after Bloch function. The Bloch functions constructed in this way then fulfill the Bloch condition (5.11), but they are not exact eigenstates of the crystal. They are not orthonormal, but it holds:

$$\langle\psi_{n\boldsymbol{k}}|\psi_{n'\boldsymbol{k}}\rangle = \frac{1}{N}\sum_{\boldsymbol{R}_1,\boldsymbol{R}_2} e^{i\boldsymbol{k}(\boldsymbol{R}_1-\boldsymbol{R}_2)}\int d^3r\varphi_n^*(\boldsymbol{r}-\boldsymbol{R}_2)\varphi_{n'}(\boldsymbol{r}-\boldsymbol{R}_1) \tag{5.76}$$

$$= \sum_{\boldsymbol{R}} e^{-i\boldsymbol{k}\boldsymbol{R}}\int d^3r\varphi_n^*(\boldsymbol{r}-\boldsymbol{R})\varphi_{n'}(\boldsymbol{r}) = \delta_{nn'} + \sum_{\boldsymbol{R}\neq 0} e^{-i\boldsymbol{k}\boldsymbol{R}}\alpha_{nn'}(\boldsymbol{R}).$$

Here

$$\alpha_{nn'}(\boldsymbol{R}) = \int d^3r\varphi_n^*(\boldsymbol{r}-\boldsymbol{R})\varphi_{n'}(\boldsymbol{r}) \tag{5.77}$$

is the direct overlap of the atomic functions $\varphi_n, \varphi_{n'}$ localized at the lattice sites 0 and $\boldsymbol{R}$.

If we now use the functions (5.73) as an ansatz for the sought-after crystal eigenstates, even though they cannot be exact eigenstates, we obtain according to the Ritz method of quantum mechanics as the best approximation for the energy eigenvalues within the ansatz:

$$\varepsilon_n(\boldsymbol{k}) = \frac{\langle\psi_{n\boldsymbol{k}}|H|\psi_{n\boldsymbol{k}}\rangle}{\langle\psi_{n\boldsymbol{k}}|\psi_{n\boldsymbol{k}}\rangle}. \tag{5.78}$$

The normalization factor in the denominator was calculated above, so only the calculation of the matrix element of the Hamilton operator with respect to the assumed wave function remains.

$$\langle\psi_{n\boldsymbol{k}}|H|\psi_{n\boldsymbol{k}}\rangle = E_n\langle\psi_{n\boldsymbol{k}}|\psi_{n\boldsymbol{k}}\rangle \tag{5.79}$$

$$+\frac{1}{N}\sum_{\boldsymbol{R}_1,\boldsymbol{R}_2} e^{i\boldsymbol{k}(\boldsymbol{R}_1-\boldsymbol{R}_2)}\int d^3r\varphi_n^*(\boldsymbol{r}-\boldsymbol{R}_2)\sum_{\boldsymbol{R}_3\neq\boldsymbol{R}_1} v(\boldsymbol{r}-\boldsymbol{R}_3)\varphi_n(\boldsymbol{r}-\boldsymbol{R}_1).$$

It is to be integrated over a product of three functions $\varphi_n^*(\boldsymbol{r}-\boldsymbol{R}_2), v(\boldsymbol{r}-\boldsymbol{R}_3)$, $\varphi_n(\boldsymbol{r}-\boldsymbol{R}_1)$; each of these factors represents a function localized at $\boldsymbol{R}_i$, i.e. it is only clearly different from 0 in the vicinity of the relevant center $\boldsymbol{R}_i$. Therefore, if all three positions $\boldsymbol{R}_1, \boldsymbol{R}_2, \boldsymbol{R}_3$ are different, two of the three factors are small in all space regions, but if two $\boldsymbol{R}_i$ are equal and only the third is different, there is an integration area in which the integrand is not so small. There are therefore three cases to consider:

1. $\boldsymbol{R}_1 = \boldsymbol{R}_2 \neq \boldsymbol{R}_3$

$$\beta := \frac{1}{N}\sum_{\boldsymbol{R}_1}\int d^3r\varphi_n^*(\boldsymbol{r}-\boldsymbol{R}_1)\Delta V_{\boldsymbol{R}_1}(\boldsymbol{r})\varphi_n(\boldsymbol{r}-\boldsymbol{R}_1) \tag{5.80}$$

$$= \int d^3r\varphi_n^*(\boldsymbol{r})\Delta V_{\boldsymbol{0}}(\boldsymbol{r})\varphi_n(\boldsymbol{r}).$$

   This corresponds to the expectation value of the potential of all other atoms in the atomic state of the atom located at a fixed lattice position, which can be chosen to be 0 without loss of generality, and provides a constant energy shift relative to the atomic energy level.
2. $\boldsymbol{R}_2 = \boldsymbol{R}_3 \neq \boldsymbol{R}_1$. Then it applies:

$$\frac{1}{N}\sum_{\boldsymbol{R}_1\neq\boldsymbol{R}_2} e^{i\boldsymbol{k}(\boldsymbol{R}_1-\boldsymbol{R}_2)}\int d^3r\varphi_n^*(\boldsymbol{r}-\boldsymbol{R}_2)v(\boldsymbol{r}-\boldsymbol{R}_2)\,\varphi_n\,(\boldsymbol{r}-\boldsymbol{R}_1) \tag{5.81}$$

$$= \sum_{\boldsymbol{R}\neq 0} e^{-i\boldsymbol{k}\boldsymbol{R}}\int d^3r\varphi_n^*(\boldsymbol{r}-\boldsymbol{R})v(\boldsymbol{r}-\boldsymbol{R})\,\varphi_n\,(\boldsymbol{r}) = \sum_{\boldsymbol{R}\neq 0} e^{-i\boldsymbol{k}\boldsymbol{R}}\lambda(\boldsymbol{R}).$$

3. $\boldsymbol{R}_1 \neq \boldsymbol{R}_2 \neq \boldsymbol{R}_3 \neq \boldsymbol{R}_1$. Then the three-center integrals discussed above occur, in which in all integration areas at least two of the three factors are small. Therefore, these contributions (three-center integrals) can be neglected, i.e.

$$\int d^3r\varphi_n^*(\boldsymbol{r}-\boldsymbol{R}_2)v(\boldsymbol{r}-\boldsymbol{R}_3)\,\varphi_n\,(\boldsymbol{r}-\boldsymbol{R}_1) \approx 0. \tag{5.82}$$

In the (because of the non-orthonormality of the approximation for $\psi_{n\boldsymbol{k}}$ necessary) normalization factor in the denominator, one obtains according to (5.77) an analogous expression, namely

$$\int d^3r\psi_{n\boldsymbol{k}}^*(\boldsymbol{r})\psi_{n\boldsymbol{k}}(\boldsymbol{r}) = 1 + \sum_{\boldsymbol{R}\neq 0} e^{-i\boldsymbol{k}\boldsymbol{R}}\alpha(\boldsymbol{R}). \tag{5.83}$$

This gives us in total

$$\varepsilon_n(\boldsymbol{k}) = E_n + \frac{\beta + \sum_{\boldsymbol{R}\neq 0} e^{-i\boldsymbol{k}\boldsymbol{R}}\lambda(\boldsymbol{R})}{1 + \sum_{\boldsymbol{R}\neq 0} e^{-i\boldsymbol{k}\boldsymbol{R}}\alpha\,(\boldsymbol{R})}, \tag{5.84}$$

$$\text{with} \quad \beta = \int d^3r \varphi_n^*(\boldsymbol{r}) \sum_{\boldsymbol{R}\neq 0} v(\boldsymbol{r}-\boldsymbol{R})\, \varphi_n(\boldsymbol{r}) \tag{5.85}$$

$$\lambda(\boldsymbol{R}) = \int d^3r \varphi_n^*(\boldsymbol{r}-\boldsymbol{R}) v(\boldsymbol{r}-\boldsymbol{R})\, \varphi_n(\boldsymbol{r}) \tag{5.86}$$

$$\alpha(\boldsymbol{R}) = \int d^3r \varphi_n^*(\boldsymbol{r}-\boldsymbol{R})\, \varphi_n(\boldsymbol{r}). \tag{5.87}$$

In addition, the assumption is usually made that the occurring $\boldsymbol{R}$ sums can be limited to nearest or next-nearest neighbors; this can be justified physically because, due to the good localization of the atomic wave functions $\varphi_n(\boldsymbol{r}-\boldsymbol{R})$, the overlap should decrease quickly with increasing distance of the atoms.

**Wannier functions**[4]

The basic idea of the tight-binding method is to construct the Bloch functions from states localized at the atomic nuclei. The band structure, i.e. the dispersion relation $\varepsilon_n(\boldsymbol{k})$, then follows from matrix elements of the atomic potential with respect to such localized states. The simplest choice for these are atomic wave functions $\varphi_n(\boldsymbol{r})$. But these do not form an orthonormal basis of the solid-state Hilbert space. However, there exists a basis of localized states which form an orthonormal basis, and these are the **Wannier states**. These are defined by:

$$w_n(\boldsymbol{r}-\boldsymbol{R}) = \frac{1}{\sqrt{N}} \sum_{\boldsymbol{k}} e^{-i\boldsymbol{k}\boldsymbol{R}} \psi_{n\boldsymbol{k}}(\boldsymbol{r}). \tag{5.88}$$

We calculate easily:

$$\int d^3r w_n^*(\boldsymbol{r}-\boldsymbol{R}_1)\, w_l(\boldsymbol{r}-\boldsymbol{R}_2) = \frac{1}{N} \sum_{\boldsymbol{k},\boldsymbol{k}'} e^{i(\boldsymbol{k}\boldsymbol{R}_1 - \boldsymbol{k}'\boldsymbol{R}_2)} \int d^3r \psi_{n\boldsymbol{k}}^*(\boldsymbol{r}) \psi_{l\boldsymbol{k}'}(\boldsymbol{r})$$

$$= \frac{1}{N} \sum_{\boldsymbol{k}} e^{i\boldsymbol{k}(\boldsymbol{R}_1-\boldsymbol{R}_2)} \delta_{\boldsymbol{k}\boldsymbol{k}'} \delta_{nl} = \delta_{\boldsymbol{R}_1\boldsymbol{R}_2} \delta_{nl}\,. \tag{5.89}$$

The $\boldsymbol{k}$-sums are again restricted to the first Brillouin zone. Conversely, Bloch functions can also be represented as a linear combination of Wannier states:

---

[4] G.H. Wannier, *1911 in Basel, †1983 in Eugene (Oregon), Swiss physicist, PhD 1935 in Basel, from 1936/39 in the USA, 1949-60 at the Bell-Labs, from 1961 at the University of Oregon, introduced the Wannier excitons and Wannier functions, also contributions to the solution of the 2-d Ising model and to ion transport in gases, finally interested in the problem of electronic energy bands in the presence of electric and magnetic fields.

$$\psi_{nk}(\boldsymbol{r}) = \frac{1}{\sqrt{N}} \sum_{\boldsymbol{R}} e^{i\boldsymbol{kR}} w_n(\boldsymbol{r} - \boldsymbol{R}). \tag{5.90}$$

If we use the Wannier functions instead of the localized atomic functions in (5.73), the further calculation is basically exact; the matrix element of the direct overlap $\alpha(\boldsymbol{R})$ vanishes due to orthonormality and we get the dispersion relation:

$$\varepsilon_n(\boldsymbol{k}) = \tilde{E}_n + \sum_{\boldsymbol{R}\neq 0} e^{-i\boldsymbol{kR}} \tilde{\lambda}(\boldsymbol{R}) \tag{5.91}$$

$$\text{where} \quad \tilde{E}_n = \int d^3r w_n^*(\boldsymbol{r}) \left( \frac{\boldsymbol{p}^2}{2m} + \sum_{\boldsymbol{R}} v(\boldsymbol{r} - \boldsymbol{R}) \right) w_n(\boldsymbol{r}) \tag{5.92}$$

$$\text{and} \quad \tilde{\lambda}(\boldsymbol{R}) = \int d^3r w_n^*(\boldsymbol{r} - \boldsymbol{R}) v(\boldsymbol{r} - \boldsymbol{R}) w_n(\boldsymbol{r}). \tag{5.93}$$

Three-center contributions were neglected here as before, for which the product of two Wannier functions and the local potential would have to be integrated over three different lattice sites. Consistent with this neglect is the assumption that the $\tilde{\lambda}(\boldsymbol{R})$ are only significantly different from 0 for nearest or at most next-nearest neighbors. The simplest and often used tight-binding assumption is therefore:

$$\tilde{\lambda}(\boldsymbol{R}) = \begin{cases} t & \text{for } \boldsymbol{R} \text{ nearest neighbor lattice vector} \\ 0 & \text{else} \end{cases} . \tag{5.94}$$

The one parameter $t$ is also called hopping matrix element because it is related to the probability that an electron jumps from one lattice site to its nearest neighbor and thus becomes mobile and delocalized. For a 1-dimensional linear chain one then obtains the dispersion

$$\varepsilon(k) = \varepsilon_0 - 2t\cos(ka) \tag{5.95}$$

($a$ lattice constant). For a 3-dimensional simple cubic system the resulting dispersion relation is

$$\varepsilon(\boldsymbol{k}) = \varepsilon_0 - 2t(\cos(k_x a) + \cos(k_y a) + \cos(k_z a)). \tag{5.96}$$

Such cosine terms are characteristic for dispersion relations in tight binding approximation. In Fig. 5.7 this tight binding band structure for $6|t| = 1$ is plotted along the usual main symmetry directions of the simple cubic Brillouin zone. One thus obtains a band centered around $\varepsilon_0$, the expectation value of the Hamiltonian in a Wannier state, and of width $12|t|$. The hopping matrix element $t$ can in general be positive or negative. By assuming the same $t$ here for all three directions, we have assumed s-like (spatially isotropic) Wannier states. For small $|\boldsymbol{k}|$ one can expand the dispersion and obtains:

$$\varepsilon(\boldsymbol{k}) = \varepsilon_0 - 6t + a^2 t\boldsymbol{k}^2 \tag{5.97}$$

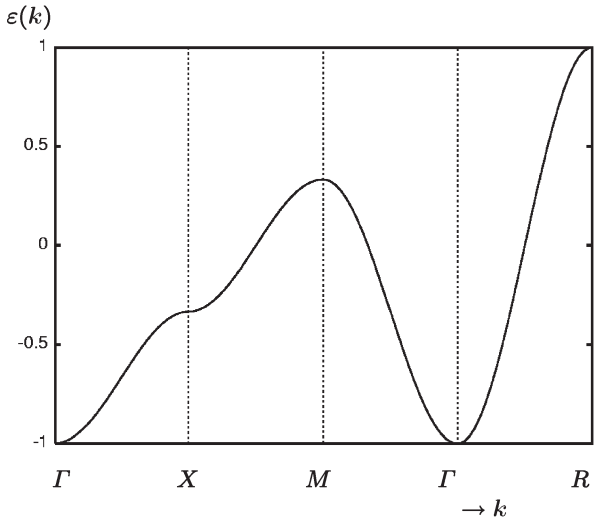

**Fig. 5.7** Course of the 3-dimensional simple cubic tight binding dispersion along the main symmetry directions

i.e. a behavior at the band edge like that of free electrons with isotropic effective mass

$$m^* = \frac{\hbar^2}{2a^2 t}. \tag{5.98}$$

The tight binding approximation seems physically quite reasonable, at least if one works with respect to the Wannier basis. Unfortunately, however, the Wannier functions are not known. If one wants to use the definition equation, one must know the Bloch functions and has already solved the problem.

For a one-dimensional periodic model potential in the form of potential wells of width $a/2$ and with lattice constants $a$, explicitly numerically calculated Wannier functions are shown in Fig. 5.8; they are localized in the area of one unit cell, but the higher the band index is, the more delocalized they become, and there are oscillations in the areas of the adjacent potential wells. Only under the assumption that the Bloch factor $u_{n\boldsymbol{k}}(\boldsymbol{r})$ hardly depends on $\boldsymbol{k}$, can the explicit form of the Wannier function be calculated analytically and, according to (5.88) one obtains for a simple cubic system

$$w_n(\boldsymbol{r}-\boldsymbol{R}) = \frac{1}{\sqrt{N}} u_{n\boldsymbol{0}}(\boldsymbol{r}) \sum_{\boldsymbol{k}} e^{i\boldsymbol{k}(\boldsymbol{r}-\boldsymbol{R})} \tag{5.99}$$

$$\sim u_{n\boldsymbol{0}}(\boldsymbol{r}) \frac{\sin(\pi(x-R_x)/a)\sin(\pi(y-R_y)/a)\sin(\pi(z-R_z)/a)}{\pi^3(x-R_x)(y-R_y)(z-R_z)},$$

i.e. a localized and rapidly decaying function around $\boldsymbol{R}$. On the other hand, there is also no justification for a $\boldsymbol{k}$-independence of the Bloch factors.

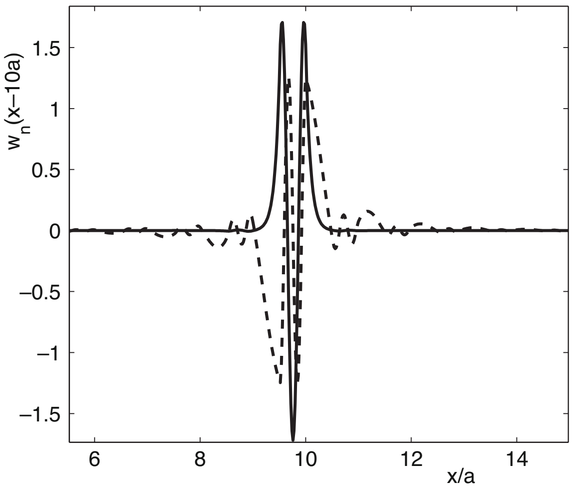

**Fig. 5.8** Wannier functions in one dimension (for band index $n = 3,4$)

One can also work without the knowledge of the explicit form of the Wannier function and use the hopping amplitude as an effective parameter that can be used as a fit parameter for fitting to experimental data. Often, however, one also tries to make suitable approaches and approximations for the Wannier functions.

If the hopping matrix elements are considered to be given parameters, then one works with a model Hamiltonian operator that has the following explicit form with respect to the Wannier basis in matrix representation:

$$H = \sum_{n\boldsymbol{R}} \tilde{E}_n |n\boldsymbol{R}\rangle \langle n\boldsymbol{R}| + \sum_{n,\boldsymbol{R},\boldsymbol{R}'} t_{\boldsymbol{R}\boldsymbol{R}'} |n\boldsymbol{R}\rangle \left\langle n\boldsymbol{R}' \right| \tag{5.100}$$

for example with

$$t_{\boldsymbol{R}\boldsymbol{R}'} = \begin{cases} t & \text{for } \boldsymbol{R},\, \boldsymbol{R}' \text{ nearest neighbors} \\ 0 & \text{else} \end{cases} . \tag{5.101}$$

Here, in position representation $w_n(\boldsymbol{r} - \boldsymbol{R}) = \langle \boldsymbol{r} | n\boldsymbol{R} \rangle$. The hopping matrix element is used as a parameter, then only the lattice symmetry enters into the band structure. If a good fit does not work with the nearest neighbor hopping, you may have to allow hopping to the next nearest neighbors, etc.

But if you want to calculate the parameters of the tight-binding Hamiltonian operator explicitly, then you also need to know the Wannier functions. One possible and after the previous discussions obvious possibility would be to approximate them by the atomic wave functions, i.e. to use the approximation

$$w_n(\boldsymbol{r} - \boldsymbol{R}) = \varphi_n(\boldsymbol{r} - \boldsymbol{R}) \tag{5.102}$$

Then one reobtains (5.73) and the subsequent results and the band index becomes identical with the atomic quantum numbers; one also speaks of 3s bands, 3d bands, etc., thus using the atomic classification for solid-state bands. As mentioned above, the main disadvantage of this approximation is that the atomic wave functions are not orthonormal at different lattice sites $\boldsymbol{R}$. An improvement is provided by the so-called

**LCAO-Method.**

The abbreviation “LCAO” stands for “linear combination of atomic orbitals”. As this name already indicates, the Wannier functions are not replaced by a single atomic orbital, but one uses a linear combination of atomic orbitals as an ansatz for the Wannier functions. This can be, for example, the five 3d states of copper or the four 2s and 2p states of carbon. So you make an ansatz for the Wannier functions in a subspace $U$ of the atomic states:

$$w(\boldsymbol{r}-\boldsymbol{R}) = \sum_{n\in U} a_n \varphi_n(\boldsymbol{r}-\boldsymbol{R}). \tag{5.103}$$

Then you can use the coefficients $a_n$ as variation parameters and determine optimal coefficients, so that, for example, at least within the subspace the states are orthonormal.

## 5.5 Basic ideas of numerical methods for calculating the electronic band structure

If one wants to go beyond the LCAO method and in principle determine the Wannier or Bloch functions exactly instead of working with (possibly optimized) approaches for this, nothing remains but to actually solve the Schrödinger equation. But this is not trivial in a 3-dimensional crystal potential and can only be done numerically, and even then certain approximations and assumptions are common and unavoidable. The basic ideas of these different numerical methods are briefly outlined below.

### 5.5.1 Cellular method

The basic problem is the solution of the Schrödinger equation:

$$\left(-\frac{\hbar^2}{2m}\nabla^2 + V(\boldsymbol{r})\right)\psi(\boldsymbol{r}) = \varepsilon\psi(\boldsymbol{r}). \tag{5.104}$$

In the so-called cellular method or **Wigner-Seitz method** one tries first to solve this equation only on a Wigner-Seitz cell and to use the Bloch condition

$$\psi_{\boldsymbol{k}}(\boldsymbol{r}+\boldsymbol{R}) = e^{i\boldsymbol{k}\boldsymbol{R}}\psi_{\boldsymbol{k}}(\boldsymbol{r}) \tag{5.105}$$

to obtain the full solution for the whole crystal. The problem is that the potential $V(\boldsymbol{r})$ is not rotationally symmetric within a cell. From quantum mechanics it is known that the 3-dimensional Schrödinger equation for rotationally symmetric potentials becomes relatively simple and can be reduced to an effective 1-dimensional problem. The potential of the Wigner-Seitz cell around the lattice vector $\boldsymbol{R} = 0$ is given by

$$V(\boldsymbol{r}) = v(\boldsymbol{r}) + \sum_{\boldsymbol{R} \neq 0} v(\boldsymbol{r} - \boldsymbol{R}) = v(|\boldsymbol{r}|) + \sum_{\boldsymbol{R} \neq 0} v(|\boldsymbol{r} - \boldsymbol{R}|). \tag{5.106}$$

In the last step, it was taken into account that the atomic potential $v$ may be assumed to be spherically symmetric in many cases, at least if only one atom is present in the elementary cell. However, the entire cell potential will not be spherically symmetric in general, since the atomic potentials of the other (in particular the adjacent) crystal cells will also be noticeable in the vicinity of the Wigner-Seitz cell at 0.

The qualitative course of a 2-dimensional periodic potential is shown in Fig. 5.9. From the 2-dimensional contour plot sketched at the bottom, it can be seen that the potential is only approximately spherically symmetric at the center of the cell, since here the potential of the atom at $\boldsymbol{R} = 0$ predominates over the potential contributions of the neighboring cells, but further out these neighboring atoms will be noticeable and the contour lines of equal potential will no longer be spheres (or circles in the 2-dimensional plot), but will adapt to the symmetry of the Wigner-Seitz cell (quadratic symmetry in the example of the drawing); in particular, potential maxima occur in the intermediate range between the Wigner-Seitz cells.

The basic idea of the Wigner-Seitz method is now to approximate the actual cell potential $V(\boldsymbol{r})$ by a rotationally symmetric potential. The simplest approach for this is the atomic potential $v(r)$ of the cell under consideration, i.e. that one simply neglects the influence of the neighboring cells in the area of the Wigner-Seitz cell around 0. In order to give the problem full spherical symmetry, the Wigner-Seitz cell is replaced by a sphere of the same volume. To solve the Schrödinger equation for the now spherically symmetric problem of a single Wigner-Seitz cell, one

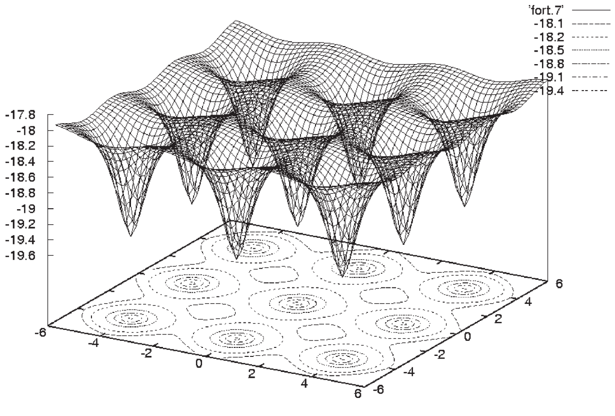

**Fig. 5.9** Qualitative course of a 2-dimensional periodic potential

can proceed as is known from quantum mechanics, i.e. one makes the separation ansatz

$$\psi(\boldsymbol{r}) = Y_{lm_l}(\vartheta, \varphi)\chi_l(r), \tag{5.107}$$

where $Y_{lm_l}(\vartheta, \varphi)$ denotes the spherical harmonics and the radial component $\chi_l(r)$ has to fulfill the ordinary differential equation

$$\chi_l''(r) + \frac{2}{r}\chi_l'(r) - \left(\frac{l(l+1)}{r^2} + \frac{2m}{\hbar^2}V(r)\right)\chi_l(r) = -\frac{2m}{\hbar^2}\varepsilon\chi_l(r). \tag{5.108}$$

As a differential equation, one can construct a solution for each $\varepsilon$, for example numerically by integration using the Runge-Kutta method and improvements thereof. An eigenvalue problem with possibly only discrete solutions arises from the differential equation by requiring special boundary conditions. In atomic physics, the appropriate boundary condition is the disappearance of the solution at infinity, but here in solid state physics another boundary condition has to be required, and this results essentially from the Bloch condition.

In practice one proceeds as follows: From the for fixed $\varepsilon$ and fixed angular momentum quantum numbers $l, m_l$ by integration obtained solutions of (5.108), one gets a general solution of the Schrödinger equation by linear combination:

$$\psi_\varepsilon(\boldsymbol{r}) = \sum_{lm_l} A_{lm_l} Y_{lm_l}(\vartheta, \varphi)\chi_{l\varepsilon}(r). \tag{5.109}$$

In practice, only finitely many coefficients $A_{lm}$will be considered here. As a boundary condition for the wave function and its first derivative, the Bloch condition

$$\psi_\varepsilon(\boldsymbol{r}) = e^{-i\boldsymbol{kR}}\psi_\varepsilon(\boldsymbol{r} + \boldsymbol{R}) \tag{5.110}$$

$$\hat{\boldsymbol{n}}(\boldsymbol{r})\nabla\psi_\varepsilon(\boldsymbol{r}) = -e^{-i\boldsymbol{kR}}\hat{\boldsymbol{n}}(\boldsymbol{r} + \boldsymbol{R})\nabla\psi_\varepsilon(\boldsymbol{r} + \boldsymbol{R}) \tag{5.111}$$

for $\boldsymbol{r}$ on the surface of the Wigner-Seitz cell results. This cannot be fulfilled for all $\boldsymbol{r}$ on the surface, already because of the not matching lattice symmetry of the actual Wigner-Seitz cell and the spherical symmetry assumed for the solution. Therefore, one will demand it for a finite number of selected $\boldsymbol{r}$, namely as many as one takes coefficients $A_{lm}$into account. Then the boundary conditions provide a homogeneous system of equations for the $A_{lm}$. Non-trivial solutions exist if the corresponding matrix is singular, that is, if the determinant vanishes. This then provides a relationship between $\varepsilon$ and $\boldsymbol{k}$, that is, the dispersion relation $\varepsilon(\boldsymbol{k})$.

The essential difference to the LCAO method discussed in the previous section is therefore that one forms the solid-state wave function here as a linear combination of local (obtained on the Wigner-Seitz cell ) solutions of the Schrödinger equation, which also already satisfy the boundary conditions adapted to the crystal situation, while one forms linear combinations of atomic wave functions in the LCAO, which satisfy atomic boundary conditions (disappearance at infinity).

## 5.5.2 Expansion in plane waves

In principle, as described in sections 5.1 and 5.2, one can also expand the periodic potential in a Fourier series (with reciprocal lattice vectors as Fourier components) and try to solve the Fourier transformed Schrödinger equation (5.30). In practice, however, one has to be satisfied with the inclusion of only a finite number of reciprocal lattice vectors in numerical solutions. Then one obtains the Bloch factor via the relation (5.33). This can be carried out explicitly for the example of a one-dimensional cosine potential as an exercise.

However, the method is not particularly useful for more realistic potentials. It turns out, for example, that for a quantitative satisfactory solution up to one hundred or more plane waves have to be included. The reason for this is that the Bloch factors oscillate rapidly in the vicinity of the atomic nuclei. These short-wavelength oscillations can only be represented by plane waves with a large reciprocal lattice vector $\boldsymbol{G}$. Therefore, many plane waves to be included ultimately only serve to describe the inner oscillations, which are automatically included in atomic wave functions.

## 5.5.3 APW-("Augmented Plane Waves")-Method

Slater proposed in 1937 a combination of the Wigner-Seitz method with the expansion in plane waves, namely the method of "augmented plane waves". For this purpose, the Wigner-Seitz cell is divided into two areas: an area around the centre of the Wigner-Seitz cell, in which a spherically symmetrical atomic potential is assumed, and an area in which a constant potential is assumed.

This takes into account that the real potential must indeed be relatively flat in the intermediate regions between the atoms, i.e. especially at the edge of the Wigner-Seitz cell.

This is also called a "muffin-tin potential"[5]. The ansatz for the potential is therefore of the form

$$V(\boldsymbol{r}) = \begin{cases} v(|\boldsymbol{r}-\boldsymbol{R}|) & \text{for } |\boldsymbol{r}-\boldsymbol{R}| < r_0 \\ v_0 = v(r_0) = 0 & \text{if } |\boldsymbol{r}-\boldsymbol{R}| > r_0 \text{ for all } \boldsymbol{R} \end{cases} . \tag{5.112}$$

A 2-dimensional "muffin-tin potential" (and a muffin baking sheet) are shown in Fig. 5.10; from the contour plot of the potential course it becomes clear that, in contrast to the real potential course from Fig. 5.9, now "spherical symmetry" around the center of each elementary cell exists.

Practically, one proceeds as follows: One solves the radial Schrödinger equation again within the sphere as in the cell method and thus obtains

$$\psi_\varepsilon(\boldsymbol{r}) = \sum_{lm} A_{lm} Y_{lm}(\vartheta, \varphi) \chi_{l\varepsilon}(r). \tag{5.113}$$

---

[5] "Muffin": round English or American tea pastry; "muffin tin" baking sheet for "muffins".

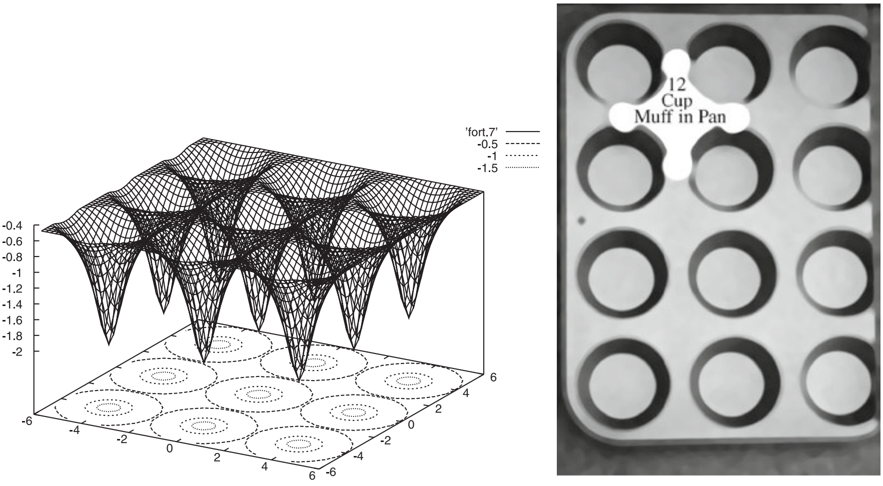

**Fig. 5.10** 2-dimensional muffin-tin potential with corresponding contour plot and photo of an American "muffin tin"

This solution must now be adapted to the solutions in the intermediate range at the edge of the muffin-tin sphere, which are plane waves

$$\Phi_{\boldsymbol{k}}(\boldsymbol{r}) = e^{i\boldsymbol{k}\boldsymbol{r}} \tag{5.114}$$

The boundary conditions provide a relationship between $\varepsilon$ and $\boldsymbol{k}$ and thus the dispersion relation $\varepsilon(\boldsymbol{k})$. For an exact adaptation, one would have to take into account an infinite number of coefficients, in practice one has to restrict oneself again to a finite number of angular momentum coefficients, specifically those of the atomic shell under consideration, from which the bands are formed.

The APW method and muffin-tin potentials are widespread in concrete band structure calculations and are seemingly very successful. The distinction between the core area and the intermediate area and the choice of the radius $r_0$ of the muffin-tin sphere seem to be somewhat arbitrary. Allegedly, however, the results are not sensitive to this choice; occasionally $r_0$ is chosen so large that the volume of the Wigner-Seitz cell is equal to that of the muffin-tin sphere ("Atomic Sphere Approximation, ASA"), at least in the currently widespread LMTO method ("linearized muffin tin orbitals").

### 5.5.4 Green function method by Korringa, Kohn and Rostoker, KKR method

A method closely related to the APW method, which usually also starts from the muffin-tin approach, is the Green function method, which was first proposed by Korringa, Kohn and Rostoker. For this purpose, one starts from the Green function for the Schrödinger equation, which is defined by:

$$\left(\varepsilon + \frac{\hbar^2}{2m}\nabla^2\right)G(\boldsymbol{r}-\boldsymbol{r}') = \delta(\boldsymbol{r}-\boldsymbol{r}'). \tag{5.115}$$

If one knows the solution $G_\varepsilon(\boldsymbol{r}-\boldsymbol{r}')$ of this equation, then the wave function $\psi(\boldsymbol{r})$ for a specific potential $V(\boldsymbol{r})$ is given by

$$\psi(\boldsymbol{r}) = \int d^3r' G_\varepsilon(\boldsymbol{r}-\boldsymbol{r}')V(\boldsymbol{r}')\psi(\boldsymbol{r}'). \tag{5.116}$$

Green functions were originally introduced for the construction of special solutions to inhomogeneous differential equations; in particular, Green functions can be determined for the given boundary conditions and then, for any inhomogeneity, a special solution for the given boundary condition can be constructed, as is done in particular in electrodynamics for boundary value problems of electrostatics and in the construction of the solution to the inhomogeneous wave equation for potentials (using the Lorenz gauge). Here one sees that Green functions can also be used for homogeneous differential equations by formally considering a part of the differential equation, here specifically the potential term, as inhomogeneity. With (5.116) one has then found not yet an explicit solution but only an equivalent integral equation to the Schrödinger equation. However, the boundary conditions are already built in when using the corresponding Green function. Specifically, for a crystal potential of the Muffin-Tin type

$$V(\boldsymbol{r}) = \sum_{\boldsymbol{R}} v(|\boldsymbol{r}-\boldsymbol{R}|) \tag{5.117}$$

one obtains

$$\begin{aligned}
\psi(\boldsymbol{r}) &= \sum_{\boldsymbol{R}} \int d^3r' G_\varepsilon(\boldsymbol{r}-\boldsymbol{r}')v(|\boldsymbol{r}'-\boldsymbol{R}|)\psi(\boldsymbol{r}') \\
&= \sum_{\boldsymbol{R}} \int d^3r'' G_\varepsilon(\boldsymbol{r}-\boldsymbol{r}''-\boldsymbol{R})v(r'')\psi(\boldsymbol{r}''+\boldsymbol{R}) \\
&= \sum_{\boldsymbol{R}} e^{i\boldsymbol{k}\boldsymbol{R}} \int d^3r' G_\varepsilon(\boldsymbol{r}-\boldsymbol{r}'-\boldsymbol{R})v(r')\psi(\boldsymbol{r}').
\end{aligned} \tag{5.118}$$

In the last step, the Bloch condition $\psi(\boldsymbol{r}+\boldsymbol{R}) = e^{i\boldsymbol{k}\boldsymbol{R}}\psi(\boldsymbol{r})$ was used. The $r'$-integral now only has to be extended over a single muffin-tin-sphere, so it only involves the Green function for a single spherically symmetric potential, which here even has only finite range. The Bloch function to be determined must therefore satisfy the integral equation

$$\psi_{\boldsymbol{k}}(\boldsymbol{r}) = \int d^3r' \tilde{G}_{\boldsymbol{k},\varepsilon}(\boldsymbol{r}-\boldsymbol{r}')v(r')\psi_{\boldsymbol{k}}(\boldsymbol{r}') \tag{5.119}$$

$$\text{where} \quad \tilde{G}_{\boldsymbol{k}\varepsilon}(\boldsymbol{r}-\boldsymbol{r}') = \sum_{\boldsymbol{R}} e^{i\boldsymbol{k}\boldsymbol{R}} G_\varepsilon(\boldsymbol{r}-\boldsymbol{r}'-\boldsymbol{R}) \tag{5.120}$$

$\boldsymbol{k}$-dependence and the crystal structure enter only via the Green function $\tilde{G}_{\boldsymbol{k}\varepsilon}$. But the Green function for the single muffin-tin sphere corresponds to the known Green function for a spherically symmetric problem:

$$G_\varepsilon\left(\boldsymbol{r}-\boldsymbol{r}'\right) = -\frac{e^{i\sqrt{2m\varepsilon/\hbar^2}|\boldsymbol{r}-\boldsymbol{r}'|}}{4\pi\left|\boldsymbol{r}-\boldsymbol{r}'\right|}. \tag{5.121}$$

So $\tilde{G}_{\boldsymbol{k}\varepsilon}$ is also explicitly known. The integral equation (5.116) is still not solved. One can define a functional from which the integral equation results as a functional derivative, namely

$$\Lambda[\psi] = \int d^3r\,\psi^*_{\boldsymbol{k}}(\boldsymbol{r})v(r)\psi_{\boldsymbol{k}}(\boldsymbol{r}) \tag{5.122}$$

$$+\int d^3r \int d^3r'\,\psi^*_{\boldsymbol{k}}(\boldsymbol{r})v(r)\tilde{G}_{\boldsymbol{k}\varepsilon}\left(\boldsymbol{r}-\boldsymbol{r}'\right)v(r')\psi_{\boldsymbol{k}}\left(\boldsymbol{r}'\right).$$

Variation according to $\psi^*$, thus $\frac{\delta\Lambda}{\delta\psi^*}$, reproduces the integral equation (5.119). If one then again uses as ansatz for the wave function a linear combination of products of spherical harmonics and radial wave functions, i.e.

$$\psi_{\boldsymbol{k}}(\boldsymbol{r}) = \sum_{lm} A_{lm}Y_{lm}(\vartheta,\varphi)\chi_l(r) \tag{5.123}$$

then $\Lambda[\psi]$ becomes a quadratic form in the $A_{lm}$ and the condition $\frac{\partial\Lambda}{\partial A_{lm}} = 0$, leads to a homogeneous linear equation system. Non-trivial solutions exist if

$$det\left(\frac{\partial\Lambda}{\partial A_{lm}}\right) = 0. \tag{5.124}$$

This provides a relationship between $\varepsilon$ and $\boldsymbol{k}$ and thus the dispersion relation $\varepsilon(\boldsymbol{k})$. Of course, in practice, only a finite number of coefficients $A_{lm}$ can be taken into account, because the determinant to be calculated should be finite.

### 5.5.5 OPW-("orthogonalized plane waves")-method

The Bloch factors show short-wavelength oscillations near the cores, as discussed. These are ultimately present because the wave functions must be orthogonal to the eigenstates of the inner core electrons. Instead of expanding the Bloch functions in terms of plane waves, they can be expanded in terms of orthogonalized plane waves that are already orthogonal to the states of the inner electrons from the outset. As a result, the oscillations that made the expansion in plane waves unsuitable are automatically taken into account.

We assume that the inner core states have practically no overlap between different elementary cells, so that the inner, low-lying "bands" of the solid are dispersionless. Let $\varphi_l(\boldsymbol{r}-\boldsymbol{R})$ be these inner atomic eigenfunctions with eigenenergies $E_l$, then one can construct core Bloch functions by

$$\psi_{l\boldsymbol{k}}^c(\boldsymbol{r}) = \left\langle \boldsymbol{r}|\psi_{l\boldsymbol{k}}^c \right\rangle = \frac{1}{\sqrt{N}}\sum_{\boldsymbol{R}} e^{i\boldsymbol{k}\boldsymbol{R}}\varphi_l(\boldsymbol{r}-\boldsymbol{R}) \tag{5.125}$$

(compare also (5.73); for the inner states this ansatz will be exact or at least a very good approximation). For the desired Bloch state of the outer (valence or conduction) bands one can now make the ansatz

$$\left|\psi_{n\boldsymbol{k}}^b\right\rangle = |\boldsymbol{k}\rangle - \sum_{l<n}\left|\psi_{l\boldsymbol{k}}^c\right\rangle\left\langle\psi_{l\boldsymbol{k}}^c|\boldsymbol{k}\right\rangle, \tag{5.126}$$

where $|\boldsymbol{k}\rangle$ is the free plane wave state, i.e. $\langle\boldsymbol{r}|\boldsymbol{k}\rangle = e^{i\boldsymbol{k}\boldsymbol{r}}$. This construction of the OPW is illustrated in Fig. 5.11. This state is automatically orthogonal to all inner core states, as can be seen immediately by simple calculation:

$$\left\langle\psi_{l\boldsymbol{k}}^c|\psi_{n\boldsymbol{k}}^b\right\rangle = 0. \tag{5.127}$$

From the construction, one thus takes a plane wave and modifies it in the region of the core states, and thus obtains a wave function that oscillates strongly in the region of the ion cores, but otherwise behaves like a plane wave. This ansatz

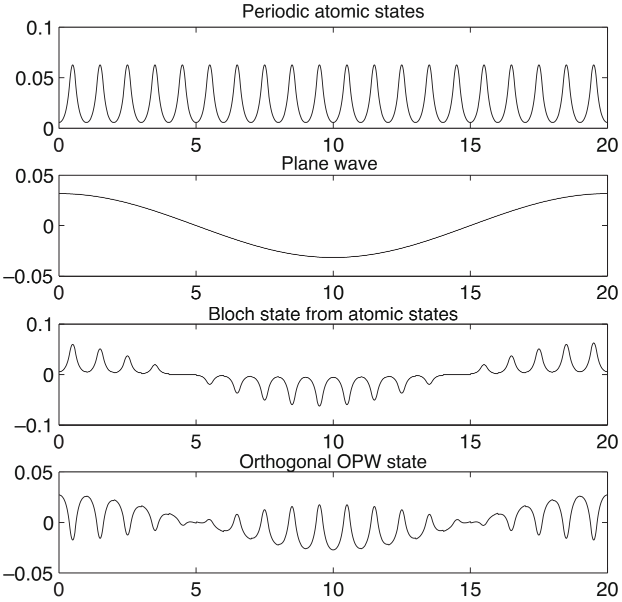

**Fig. 5.11** Schematic representation of periodic (restricted to the unit cell) ground states, a plane wave, a Bloch function constructed from the atomic ground states according to (5.125) and the orthogonalized plane wave (OPW) constructed according to (5.126)

appears to be physically very reasonable. Of course, it is not necessary to use the orthogonalized plane wave only for $\boldsymbol{k}$ from the first Brillouin zone. If one also allows shorter wavelengths, then for $\boldsymbol{k}$ from the first Brillouin zone the actual Bloch state can be a linear combination of OPWs

$$|\psi_{n\boldsymbol{k}}\rangle = \sum_{\boldsymbol{G}} a_{\boldsymbol{k}\boldsymbol{G}} \big|\psi^{b}_{n\boldsymbol{k}+\boldsymbol{G}}\big\rangle. \tag{5.128}$$

However, one then (in contrast to expansion in simple plane waves) usually only needs a few reciprocal lattice vectors $\boldsymbol{G}$. By varying the energy functional, one can determine the optimal coefficients $a_{\boldsymbol{k}\boldsymbol{G}}$ within the framework of the approach.

### 5.5.6 Pseudopotential method

The pseudopotential method is an extension of the OPW method and builds directly on this. The projection operator onto the core states can be defined by

$$P_{\boldsymbol{k}} = \sum_{l} \big|\psi^{c}_{l\boldsymbol{k}}\big\rangle\big\langle\psi^{c}_{l\boldsymbol{k}}\big| \tag{5.129}$$

Furthermore, define the linear combination of plane waves (with the same coefficients $a_{\boldsymbol{k}\boldsymbol{G}}$ as in (5.128))

$$|\phi_{\boldsymbol{k}}\rangle = \sum_{\boldsymbol{G}} a_{\boldsymbol{k}\boldsymbol{G}} |\boldsymbol{k}+\boldsymbol{G}\rangle. \tag{5.130}$$

Then the Bloch function to be determined is given by

$$|\psi_{n\boldsymbol{k}}\rangle = (1 - P_{\boldsymbol{k}})|\phi_{\boldsymbol{k}}\rangle. \tag{5.131}$$

From the Schrödinger equation for the $|\psi_{n\boldsymbol{k}}\rangle$

$$H|\psi_{n\boldsymbol{k}}\rangle = \varepsilon_n(\boldsymbol{k})|\psi_{n\boldsymbol{k}}\rangle \tag{5.132}$$

it follows that

$$\begin{aligned} H(1-P_{\boldsymbol{k}})|\phi_{\boldsymbol{k}}\rangle &= H|\phi_{\boldsymbol{k}}\rangle - \sum_{l<n} H\big|\psi^{c}_{l\boldsymbol{k}}\big\rangle\big\langle\,\psi^{c}_{l\boldsymbol{k}}\big|\phi_{\boldsymbol{k}}\big\rangle \\ &= H|\phi_{\boldsymbol{k}}\rangle - \sum_{l<n} E_l\big|\psi^{c}_{l\boldsymbol{k}}\big\rangle\big\langle\,\psi^{c}_{l\boldsymbol{k}}\big|\phi_{\boldsymbol{k}}\big\rangle \\ &= \varepsilon_n(\boldsymbol{k})\left(1 - \sum_{l<n}\big|\psi^{c}_{l\boldsymbol{k}}\big\rangle\big\langle\psi^{c}_{l\boldsymbol{k}}\big|\right)|\phi_{\boldsymbol{k}}\rangle. \end{aligned}$$

From this one obtains an effective Schrödinger equation for the linear combination of plane waves $|\phi_{\boldsymbol{k}}\rangle$:

$$\left[H + \sum_{l<n}(\varepsilon_n(\boldsymbol{k}) - E_l)\big|\psi^{c}_{l\boldsymbol{k}}\big\rangle\big\langle\psi^{c}_{l\boldsymbol{k}}\big|\right]|\phi_{\boldsymbol{k}}\rangle = \varepsilon_n(\boldsymbol{k})|\phi_{\boldsymbol{k}}\rangle. \tag{5.133}$$

The $|\phi_{\boldsymbol{k}}\rangle$, which can be represented as linear combinations of a few plane waves, are therefore eigenstates to the sought-after eigenenergies $\varepsilon_n(\boldsymbol{k})$ but not of the original crystal Hamiltonian operator but of an effective Hamiltonian operator that describes electrons in the **pseudopotential**

$$V_{ps} = V + \sum_{lcore} (\varepsilon_n(\boldsymbol{k}) - E_l) \big| \psi^c_{l\boldsymbol{k}} \big\rangle \big\langle \psi^c_{l\boldsymbol{k}} \big|. \tag{5.134}$$

The pseudopotential is not a real potential but formally an operator or a non-local potential that, in particular, contains the eigenenergy to be determined once again and that contains the influence of the inner shells. But for this one gets by with relatively few expansion coefficients. In the pseudopotential, the strong binding part of the actual potential is eliminated by subtracting the projection onto the inner core states, which come about precisely through this binding part. The pseudopotential can therefore actually be assumed to be weak, so that the perturbation calculation of Sec. 5.2, i.e. the method of nearly free electrons, can be used when the pseudopotential is used instead of the actual potential. This often turns out to be insensitive to further approximations to the pseudopotential, e.g. the replacement of the sought-after band energies by a constant energy of the right order of magnitude, such as the Fermi energy.

Finally, I would like to point out that the methods discussed here are useful and necessary in order to describe and understand the electronic band structure of certain materials in quantitative detail. In my opinion, simpler methods such as the tight-binding approximation are sufficient for a qualitative understanding. On the other hand, one cannot expect a quantitative description if one does not take into account the Coulomb interaction, which is never negligible because of its magnitude, as is the case here with the assumption of only a periodic one-particle potential. It was not until the end of the 1970s that a method was developed that allowed Coulomb interactions to be taken into account in band structure calculations, namely density functional theory in combination with the local density approximation. This method is discussed in Chap. 6 on the influence of the electron-electron interaction. However, it turns out that in the end one has to solve a one-particle Schrödinger equation for an electron in an effective, self-consistently determined periodic potential that implicitly contains the effects of the interaction. The methods discussed here for the calculation of electronic band structures are therefore of great practical importance together with the self-consistency problem of density functional theory.

## 5.6 Electronic classification of solids

The electronic one-particle states in a solid are characterized by three quantum numbers $(l, \boldsymbol{k}, \sigma)$ when taking into account the spin, where $l$ denotes the band index, $\boldsymbol{k}$ the wave vector from the first Brillouin zone and $\sigma$ the spin. Electrons are fermions because they have spin $\frac{1}{2}$ and are therefore subject to the Pauli principle, i.e. each one-particle state can be occupied at most once. If we neglect the interaction, as is still the case throughout this chapter, the eigenstate for $N_{\mathrm{e}}$ electrons can be described by specifying the occupation numbers of the one-particle states, i.e. by $|\{n_{lk\sigma}\}\rangle$ with $n_{lk\sigma} \in \{0,1\}$ and then it follows that

$$H|\{n_{lk\sigma}\}\rangle = \sum_{i=1}^{N_e}\left(\frac{\boldsymbol{p}_i^2}{2m} + \sum_{\boldsymbol{R}} v(\boldsymbol{r}_i - \boldsymbol{R})\right)|\{n_{lk\sigma}\}\rangle = \sum_{lk\sigma} n_{lk\sigma}\varepsilon_l(\boldsymbol{k})|\{n_{lk\sigma}\}\rangle. \quad (5.135)$$

In the ground state, the energetically lowest one-particle states are occupied until all $N_e$ electrons are accommodated. The energy between the highest occupied and the lowest unoccupied state is called the **Fermi energy** $E_F$. This is to be determined by

$$\sum_{\substack{lk\sigma \\ |\varepsilon_l(\boldsymbol{k})|<E_F}} 1 = 2 \sum_{\substack{lk \\ |\varepsilon_l(\boldsymbol{k})|<E_F}} 1 = N_e. \quad (5.136)$$

The ground state energy is given by

$$E_0 = 2 \sum_{\substack{lk \\ |\varepsilon_l(\boldsymbol{k})|<E_F}} \varepsilon_l(\boldsymbol{k}). \quad (5.137)$$

In each band $l$ there are exactly $N$ different $\boldsymbol{k}$ values and therefore (taking into account the spin) $2N$ different one-particle states if $N$ is the number of elementary cells. At $T = 0$ these states are filled from the bottom until all electrons are accommodated. There are now two possibilities:

- A band is completely filled, the band lying above it is completely empty. The Fermi energy then falls into the **band gap** or **energy gap** between the topmost filled band and the bottommost empty band. The topmost completely filled band is then called the **valence band**. Excitations from the ground state require at least this amount of energy corresponding to the band gap, which is usually between 1 and 7 eV. One deals with **semiconductors** or **insulators**.
- The Fermi energy is within a band that is not yet completely filled. Such a band that is not completely filled at $T = 0$ is also called a **conduction band**(even if it is still completely empty). The distance between the highest occupied level and the lowest unoccupied level is then practically 0 (of the order of $10^{-22}$ eV), so excitations with arbitrarily small energy expenditure are possible, it is a **metal**.

If $Z_e$ is the number of electrons per primitive unit cell (so that $Z_e$ is the atomic number for a one-atom basis due to charge neutrality), then the total number of electrons is $N_e = NZ_e$. If $Z_e$ is odd and no band overlap exists, then $\frac{Z_e-1}{2}$ bands are completely filled and the $\frac{Z_e+1}{2}$-th band is only half filled. According to this simple picture, a metal is always expected when $Z_e$ is odd, which is often the case. But if $Z_e$ is even and no band overlap exists, then the lowest $\frac{Z_e}{2}$bands are completely filled and therefore a semiconductor or insulator is expected. This is less well fulfilled, as the condition (no overlapping bands) is often not given.

In the discussion, one can disregard the fully closed shells (corresponding to a noble gas configuration with an even number of electrons) and only discuss the outer shells that are not yet completely filled. So let $Z_e'$ be the number of electrons in the outer atomic shell.

- $Z_e' = 1$
  This is the case with: Li, K, Na, Rb, Cs (alkali metals) and with Cu, Ag, Au (noble metals). One expects a half-filled s-band as a conduction band and therefore good metals.
- $Z_e' = 3$
  This is the case with: Al, Ga, In, Tl. The Fermi energy should be within the p-bands, there are metals to be expected.
- $Z_e' = 2$
  This is the case with the alcaline earth metals Be, Mg, Ca, Sr, Ba, Ra. These are metals despite an even number of electrons, because p- and s-bands overlap and there is no energy gap between p- and s-bands. In the free atom, s- and p-states are often almost degenerate.
- Transition metals
  The elements Sc, Ti, V, Cr, Mn, Fe, Co, Ni, Cu, Zn all have an atomic electron configuration $3\,\mathrm{d}^{n(+1)}4\mathrm{s}^{2(1)}$. The 3d and 4s levels are energetically adjacent; the resulting 3d and 4s bands overlap. The 4s states are less well localized at the atomic cores than the atomic 3d states. The 3d bands are therefore much narrower than the 4s band. s-band and 3d-bands therefore cross and hybridize with each other.
  As an example, the band structure for copper is shown in Fig. 5.12. Five relatively flat (and therefore narrow) 3d bands and the wide 4s band are clearly visible. For copper, the Fermi energy is outside the range of the d-bands, so the conduction electrons at the Fermi edge have pure s-character. For Fe, Co, Ni etc., however, the Fermi energy lies in the range of the d-bands. Because of the overlap of the bands, the Fermi energy does not lie in a gap for even and odd $Z_e'$, so metallic behavior is observed.
- Elements of the 4th group of the periodic system
  These systems often crystallize in the diamond structure, that is, with 2 atoms per elementary cell, so that the number of electrons per elementary cell is $\mathrm{Z}'_{\mathrm{e}} = 8$. From the atomic s and p orbitals, per atom 4 hybridized $\mathrm{sp}^3$ -orbitals are formed, which can be represented by linear combinations of the atomic s- and p-wave functions according to

  $$s + p_x + p_y + p_z, \quad s + p_x - p_y - p_z, \quad s - p_x + p_y - p_z, \quad s - p_x - p_y + p.$$

  These form four tetrahedrally oriented orbitals. This results in the tetrahedral structure of the diamond. In total, there are 8 orbitals per elementary cell and therefore 8 bands that are spin-degenerate, at least as long as the spin-orbit

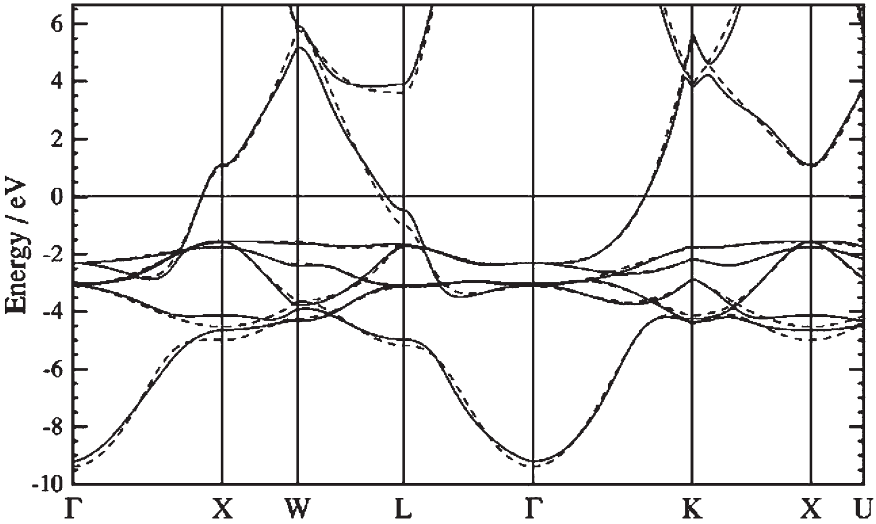

**Fig. 5.12** Band structure of copper along the main symmetry directions of the fcc Brillouin zone [6]

coupling is still neglected. There are 4 valence bands and 4 conduction bands that are formed, the valence bands are completely filled with the 8 electrons and the Fermi energy falls into a band gap, which is so large in C (diamond) that an insulator is present. In the technically most important semiconductor silicon there is an indirect band gap, see Fig. 5.13.

**Fig. 5.13** Band structure of silicon

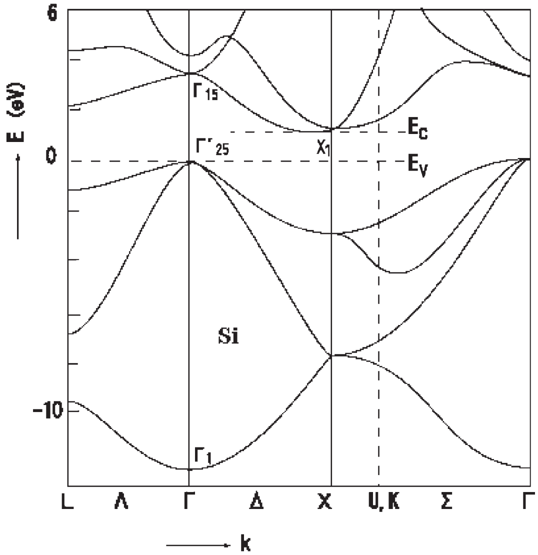

---

[6] calculated by Ilan Schnell, PhD thesis Bremen (2002)

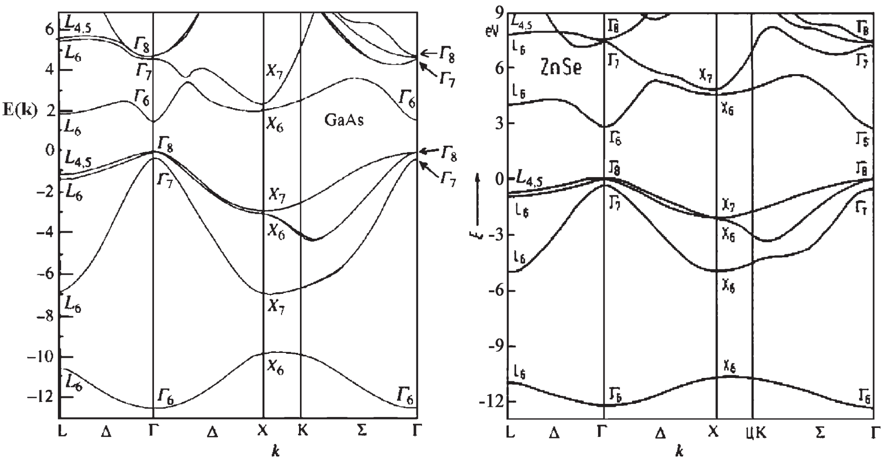

**Fig. 5.14** Band structures of the III–V semiconductor GaAs and the II–VI semiconductor ZnSe

- III–V and II–VI semiconductors[7]
  In these technically important systems like *GaAs*, *InSb*, *ZnSe*, *ZnS*, the situation is qualitatively similar to that of Si, except that there are two different atoms per unit cell. In total, there are $Z_e' = 8$ valence electrons per unit cell, which completely fill the 4 valence bands at $T = 0$, while the 4 conduction bands remain empty. The Fermi energy lies in the energy gap, which is usually a direct gap. Typical band structures are shown in Fig. 5.14.
  Since the mid-1990s, interest in the III-nitride semiconductors *GaN*, *AlN*, *InN* has increased enormously due to their potential applications. In principle, the nitride semiconductors belong to the III-V semiconductors, but they usually do not crystallize in the zinc blende structure, but in the wurtzite structure.[9] (cf. exercise 2.4), therefore have an anisotropic (hexagonal) lattice, in which the z-(c-) direction is not equivalent to the xy-plane (or the $a, b$-directions). The band structure of GaN is shown in Fig. 5.15.
  Again, there is a direct band gap with an energy gap of about 3.3 eV. Therefore, blue light-emitting diodes (LEDs) can be realized on the basis of nitride semiconductors, while arsenide semiconductors (with a band gap of about 1.5 eV for GaAs) are basic components for red LEDs.
- Elements of the 5th group of the periodic system
  Elements such as Sb, As, Bi have 5 valence electrons in the outer atomic shell, but crystallize in structures with 2 atoms per elementary cell, so that $Z_e' = 10$ applies. Nevertheless, they are usually not semiconductors but **semimetals**,

---

[7] The band structure diagrams for the semiconductors Si, GaAs and ZnSe are taken from: M.L. Cohen, J.R. Chelikowsky: Electronic Structure and Optical Properties of Semiconductors, Springer Series in Solid-State Sciences 75 (1989). The band structure of GaN is taken from: https://www.ioffe.ru/SVA/NSM/Semicond/GaN/bandstr.html

[8] Named after C.A.Wurtz, ∗ 1817, † 1884, French chemist.

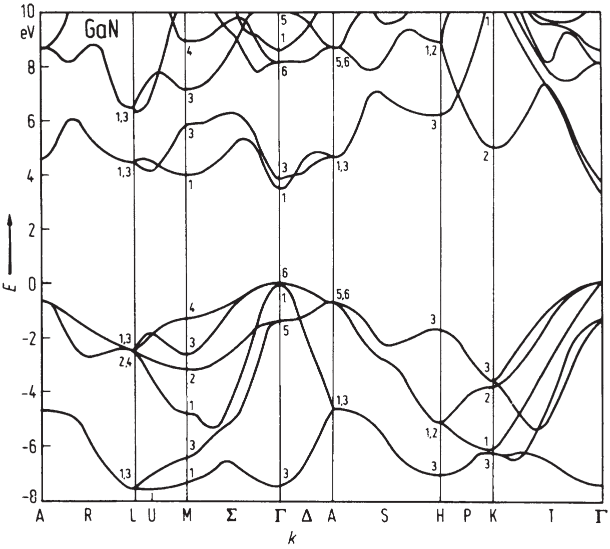

**Fig. 5.15** Band structure of the III-nitride semiconductor GaN (with wurtzite structure)

since band overlap is present, so that the fifth band is not completely filled and the sixth band is already partially filled.

- Ionic crystals from elements of the 1st and 7th groups
  These are systems such as NaCl, KBr, NaJ, etc., which crystallize in the NaCl structure or the CsCl structure, that is, again with 2 atoms per elementary cell. So you have $Z_e' = 8$ again and therefore expect a semiconductor or insulator, as is actually the case.
- Solid hydrogen
  Single atomic solid hydrogen should actually be an ideal metal with the Fermi energy in the middle of the 1s band. However, atomic hydrogen (H) does not exist under normal circumstances in the solid state, but only molecular hydrogen $H_2$. With solid $H_2$ you have 2 electrons per elementary cell and therefore an insulator. You can also imagine it this way: the 1s states of atomic hydrogen split up during molecule formation into the bonding and antibonding molecule orbitals; the bonding state is doubly occupied (by one spin-up and one spin-down electron). If the $H_2$ molecules form a crystal, the molecule orbitals split into bands, the band generated by the bonding orbitals is completely filled, the Fermi energy is in the gap between the bonding and the antibonding band.
  There have always been speculations about metallic atomic hydrogen. This is said to be not only a good metal but even a superconductor. If it exists at all, it only exists under extremely high pressures and has not been realized on Earth yet. There are (hard to refute) theories that the pressure for metallic, atomic, superconducting hydrogen is sufficient in the interior of Saturn or Jupiter and that this is the cause of the planet's magnetic field.

## 5.7 Electronic density of states and Fermi surface

The band structure $\varepsilon_n(\boldsymbol{k})$ discussed in the previous section provides the full dispersion relation for the electrons in the solid state. However, in many cases, one is not interested in this full information, but it is enough to know in which energy range states are possible at all and how many states there are in a certain energy range and where energy gaps exist. For this purpose, one defines an

**electronic density of states**

as for the phonons by

$$\rho(E) = \frac{1}{N}\sum_{nk\sigma}\delta(E - \varepsilon_n(\boldsymbol{k})) \tag{5.138}$$

$\rho(E)\cdot\Delta E$ is the number of electronic one-particle states with energy between $E$ and $E + \Delta E$ per unit cell. The Fermi energy is determined by the relationship:

$$\int_{-\infty}^{E_F} dE\rho(E) = Z_e. \tag{5.139}$$

Sometimes one only considers the density of states for individual bands, usually conduction or valence bands. There are quite similar relationships as they already occurred in the discussion of the phonon density of states in Sec. 4.6, namely, inter alia,

$$\rho(E) = -\frac{1}{\pi}\mathrm{Im}G(E + i0) = -\frac{1}{\pi}\frac{1}{N}\mathrm{Im}\sum_{nk\sigma}\frac{1}{E + i0 - \varepsilon_n(\boldsymbol{k})} \tag{5.140}$$

and one can again express the density of states by a surface integral over an area of constant energy

$$\rho(E) = \frac{V}{N}\frac{1}{4\pi^3\hbar}\sum_n\int_{S(E)}\frac{ds}{|\boldsymbol{v}_{n\boldsymbol{k}}|}. \tag{5.141}$$

Here $S(E)$ is an area of constant energy in the $k$-space and according to (5.58)

$$\boldsymbol{v}_{n\boldsymbol{k}} = \frac{1}{\hbar}\nabla_{\boldsymbol{k}}\varepsilon_n(\boldsymbol{k})$$

is the group velocity of the $n$-th band. The density of states of free electrons, that is, of electrons with the dispersion relation $\varepsilon(\boldsymbol{k}) = \frac{\hbar^2\boldsymbol{k}^2}{2m}$, is particularly simple. Then $\boldsymbol{v}_{\boldsymbol{k}} = \frac{\hbar k}{m}$ and with $k = \sqrt{\frac{2mE}{\hbar^2}}$ it follows from (5.141)

$$\rho(E) = \frac{V}{N}\frac{1}{4\pi^3\hbar}\int_{S(E)}\frac{ds}{\hbar k/m} = \frac{V}{N}\frac{4\pi k^2 m}{4\pi^3\hbar^2 k} = \frac{Vmk}{N\pi^2\hbar^2} = \frac{V}{N}\frac{\sqrt{2m^3}}{\pi^2\hbar^3}\sqrt{E}. \tag{5.142}$$

This follows not only from the surface integral over an area of constant energy according to (5.141) but also from the definition (5.138)

$$\rho(E) = \frac{1}{N}\sum_{\boldsymbol{k}\sigma}\delta\left(E - \frac{\hbar^2k^2}{2m}\right) = \frac{2V}{N(2\pi)^3}\int d^3k\delta\left(E - \frac{\hbar^2k^2}{2m}\right)$$

$$= \frac{V}{4\pi^3N}4\pi\int dkk^2\delta\left(E - \frac{\hbar^2k^2}{2m}\right) = \frac{V}{\pi^2N}\frac{m}{\hbar^2}\sqrt{\frac{2m}{\hbar^2}E}. \tag{5.143}$$

A root singularity at the band edge, i.e. $\rho(E) \sim \sqrt{E}$ is characteristic for the electronic densities of states of 3-dimensional systems. Accordingly, it can be shown that for 2-dimensional systems the density of states has a jump at the band edge and for a 1-dimensional electronic density of states a $1/\sqrt{E}$ singularity at the band edge is characteristic. With regard to Van-Hove singularities, the statements already discussed for phonon densities of states apply again. In particular, in addition to the singularities at the band edge (root singularities $\sim \sqrt{E - E_c}$ in dimension $d = 3$, jump for $d = 2$) there are also inner singularities at critical points where $\nabla_{\boldsymbol{k}}\varepsilon_n(\boldsymbol{k}) = 0$. The behavior of the density of states at these critical points is completely analogous to that in the phonon case.

As an example, the density of states $\rho_3(E)$ for the simple cubic tight-binding band

$$\varepsilon(\boldsymbol{k}) = 2t(\cos(k_xa) + \cos(k_ya) + \cos(k_za)) \tag{5.144}$$

is shown in Fig. 5.16, again for $6|t| = 1$ (cf. the band structure in Fig. 5.7). The root singularities are seen at the band edges and singularities of the type

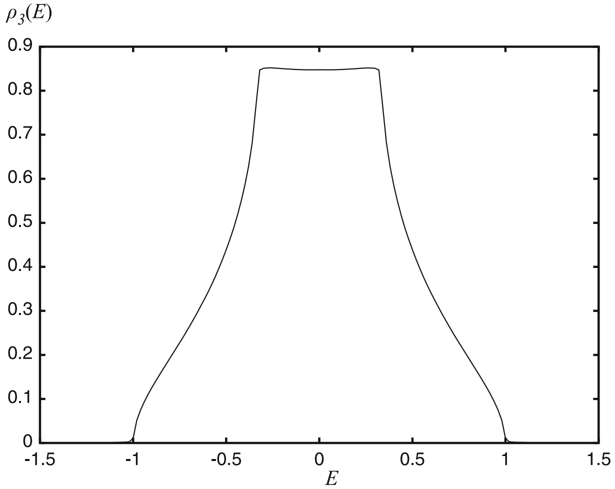

**Fig. 5.16** Electronic density of states for the 3-dimensional simple cubic tight-binding band

$C - \sqrt{|E - E_c|}$ at the critical points, where there are saddle points of the dispersion relation.

This density of states can also be calculated using

$$G(z) = \frac{1}{N}\sum_{\boldsymbol{k}} \frac{1}{z - 2t(\cos(k_x a) + \cos(k_y a) + \cos(k_z a))}$$

$$= \frac{V}{(2\pi)^3 N}\int d^3k \frac{1}{z - 2t(\cos(k_x a) + \cos(k_y a) + \cos(k_z a))}$$

$$= -i\left(\frac{a}{2\pi}\right)^3 \int_0^\infty d\lambda e^{i\lambda z} J_0^3(2t\lambda), \tag{5.145}$$

where

$$J_0(y) = \frac{1}{2\pi}\int_{-\pi}^{\pi} dx e^{-iy\cos(x)} = \frac{1}{\pi}\int_0^{\pi} dx e^{-iy\cos(x)} \tag{5.146}$$

is the Bessel function of 0th order, which is tabulated or can be found in program libraries for numerical calculations.

The tight-binding densities of states for the linear chain and the 2-dimensional square lattice are shown in Fig. 5.17 for $2|t| = 1$ and $4|t| = 1$, respectively.

The 1-dimensional tight-binding density of states is explicitly analytically given by

$$\rho_1(E) = \begin{cases} \frac{1}{\pi}\frac{1}{\sqrt{4t^2 - E^2}} & \text{for } -2|t| < E < 2|t| \\ 0 & \text{else} \end{cases} . \tag{5.147}$$

The two-dimensional tight-binding density of states can be calculated using the following relation

$$\rho_2(E) = -\frac{1}{\pi}\Im G_2(E + i0) \quad \text{with} \quad G_2(z) = \frac{1}{\pi}\int_0^{\pi} dx \frac{1}{\sqrt{(z - 2t\cos(x))^2 - 1}}; \tag{5.148}$$

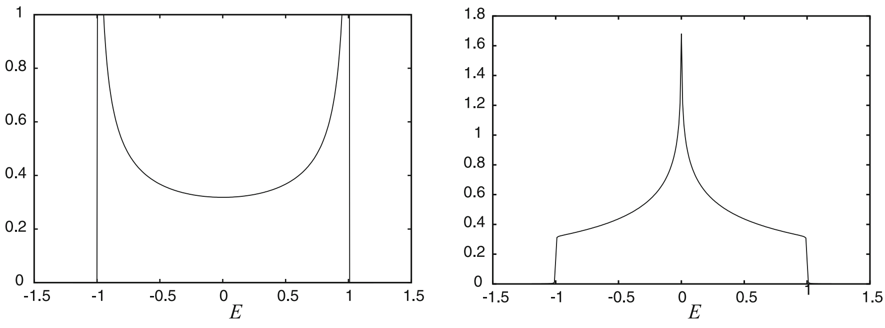

**Fig. 5.17** Densities of states for the 1- and 2-dimensional simple cubic tight-binding band

it can also be expressed in terms of the complete elliptic integral of the first kind

$$K(\lambda) = \int_0^{\pi} \frac{d\phi}{\sqrt{1 - \lambda^2 \cos^2 \phi}} \tag{5.149}$$

as

$$\rho_2(E) = \begin{cases} \frac{1}{2\pi^2|t|} K\left(\sqrt{1 - \frac{E^2}{16t^2}}\right) & \text{for } |E| < 4|t| \\ 0 & \text{else} \end{cases} . \tag{5.150}$$

A more realistic density of states for copper, i. e. for the band structure shown in Fig. 5.12, is shown in Fig. 5.18; the total number of electrons in the outer (3d and 4s) shells is here $Z'_e = 11$ and defines the Fermi energy (chosen to be 0 here). The d-bands have a relatively high density of states and a narrow bandwidth; the 4s density of states is much smaller, but the s-band is wider. The 4s electrons behave like quasi-free electrons.

**Fermi surface**

The surfaces of constant energy $S(E)$ in $\boldsymbol{k}$ space are defined by

$$\varepsilon_n(\boldsymbol{k}) = E. \tag{5.151}$$

Particularly important is the **Fermi surface**[9] $S(E_F)$, which separates the occupied part of the$\boldsymbol{k}$-space from the unoccupied part. The Fermi surface is also characteristic for certain materials and certain crystal structures. Only for free electrons is the

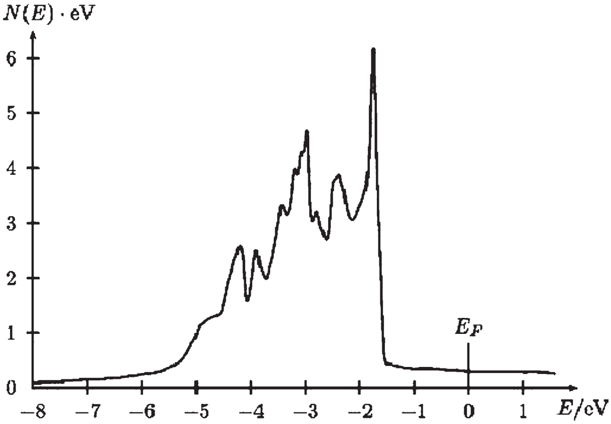

**Fig. 5.18** Density of states of Cu in the range of the 3d and 4s bands[6] (See Footnote Text 6)

---

[9] E. Fermi, *1904 in Rome, †1954 in Chicago, studied in Pisa and received his doctorate aged 21, then went to Göttingen to M. Born, from 1926 professor in Rome and work on the electron gas taking into account the Pauli principle, from 1934 interested in artificial radioactivity, Physics Nobel Prize 1938, emigrated from Stockholm to the USA because of his aversion to fascism, worked in Chicago on the realization of nuclear chain reactions.

Fermi surface simply a sphere. Even in the model of free electrons or nearly free electrons on the basis of a special crystal structure, the Fermi surface can be relatively complicated if the "Fermi sphere" intersects the boundary of the Brillouin zone. The Fermi surface is then no longer a closed, simply connected surface. With consideration of realistic band structures, highly complex Fermi surfaces with interesting topological structure can arise.

For the 2-dimensional square tight-binding band, the "surfaces" (lines) of constant energy $S(E)$ are shown in Fig. 5.19; depending on the given number of electrons (filling) these will be the Fermi "surfaces". For small filling one apparently has approximately a Fermi "sphere", but at half filling the Fermi surface becomes flat and the Fermi body a square and at more than half filling the Fermi lines intersect the boundaries of the Brillouin zone. The Fermi surface is then not simply connected within the 1st Brillouin zone. In the extended zone scheme one recognizes (see Fig. 5.20), that in this situation in two dimensions there is again a closed "surface" which encloses an empty, unoccupied area of the $\boldsymbol{k}$-space. The Fermi surface thus becomes gradually a sphere again, which does not enclose electron states but hole states.

Possible 3-dimensional Fermi surfaces are shown in Figs. 5.21, 5.22, once for the 3-dimensional simple cubic tight-binding band at half filling (i.e. the dispersion from Fig. 5.7 or the density of states from Fig. 5.16 for $E_F = 0.$) and for copper (i.e. the dispersion from Fig. 5.12). In both cases, the "necks" of the Fermi surfaces can be seen, which form towards the edge of the Brillouin zone.

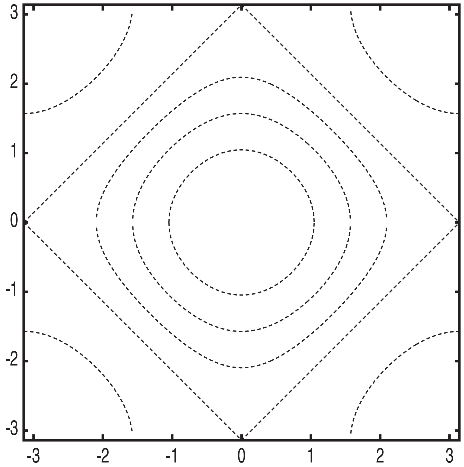

**Fig. 5.19** Fermi "surface" for the 2-dimensional square tight-binding band for different Fermi energies $E_F/(2|t|) = -1.5, -1., -0.5, 0., 1$

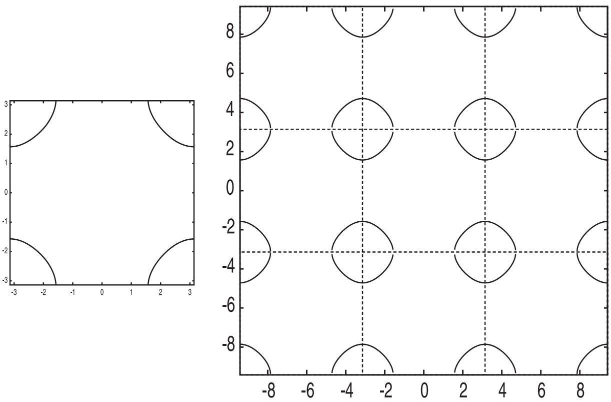

**Fig. 5.20** 2-dimensional Fermi surfaces of the square lattice at $E_F/(2|t|) = 1$ in the 1st Brillouin zone and in the extended zone scheme

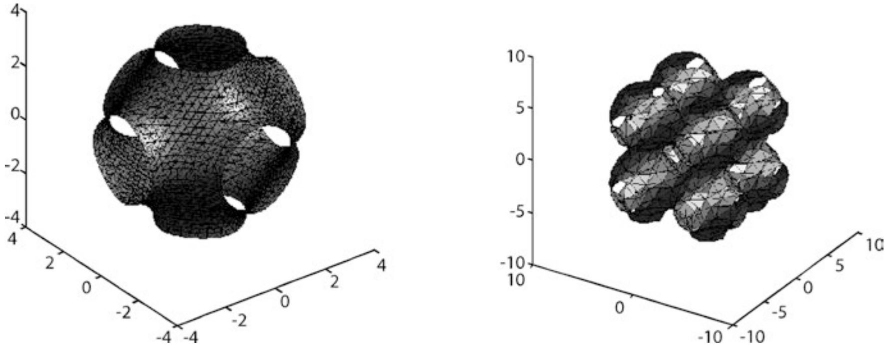

**Fig. 5.21** Fermi surface for the simple cubic tight-binding band at half filling in the 1st Brillouin zone *(left)* and over several Brillouin zones *(extended zone scheme)*

**Fig. 5.22** Fermi surface (and 1st Brillouin zone) of copper (See Footnote 6)

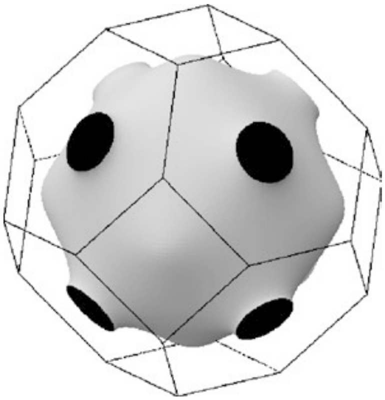

## 5.8 Quantum statistics and thermodynamics of solid-state electrons

As is known from the lecture on Statistical Physics, the occupation number representation is particularly suitable for describing the many-particle states of an electron system. An electronic many-particle state in the solid state is therefore described by $|\{n_{lk\sigma}\}\rangle$, where for fermions the occupation number for the one-particle state $\boldsymbol{lk\sigma} n_{lk\sigma}$ can only take the values 0 or 1 because of the Pauli principle.[10] In particular, for the non-interacting system, these states are already eigenstates of the Hamiltonian operator in the occupation number representation with respect to the one-particle Bloch states, i.e.

$$H|\{n_{lk\sigma}\}\rangle = \sum_{lk\sigma} n_{lk\sigma}\varepsilon_l(\boldsymbol{k})|\{n_{lk\sigma}\}\rangle, \tag{5.152}$$

where, because of the particle number conservation

$$N_\mathrm{e} = \sum_{lk\sigma} n_{lk\sigma} = 2\sum_{lk} n_{lk\sigma} \tag{5.153}$$

must be fulfilled. At finite temperatures, excited states can also be occupied, and according to Statistical Physics, the problem is conveniently treated using the grand canonical ensemble. A central quantity is the **grand canonical partition function**:

$$\begin{aligned} Z_{GK} &= \sum_{\{n_{lk\sigma}\}} \exp\left(-\beta\sum_{lk\sigma}(\varepsilon_l(\boldsymbol{k})-\mu)n_{lk\sigma}\right) \\ &= \sum_{\{n_{lk\sigma}\}}\prod_{lk\sigma}\exp\left(-\beta(\varepsilon_l(\boldsymbol{k})-\mu)n_{lk\sigma}\right) \\ &= \prod_{lk\sigma}\left(1+\exp\left(-\beta(\varepsilon_l(\boldsymbol{k})-\mu)\right)\right), \end{aligned} \tag{5.154}$$

where, as always, $\beta = \frac{1}{k_B T}$is set. The chemical potential μ is to be determined from the requirement that the mean particle number is equal to the given particle number $N_\mathrm{e}$:

$$\langle N_\mathrm{e}\rangle = \sum_{lk\sigma}\langle n_{lk\sigma}\rangle = N_\mathrm{e} \tag{5.155}$$

---

[10] W. Pauli, *1900 in Wien, †1958 in Zürich, Austrian theoretical physicist, recieved his PhD in 1921 under the supervision of A. Sommerfeld in Munich, afterwards one year in Göttingen as assistant to M. Born, 1923-1928 Professor in Hamburg, since 1928 at ETH Zürich, 1940-1946 in the USA at the Institute for Advanced Studies in Princeton, returned to Zürich in 1946, postulated in 1924 a new quantum number with two possible values, which turned out to be the spin (in which he had refused to believe when it was proposed by Kronig), formulated the Pauli exclusion principle in 1925, postulated the existence of the neutrino in 1931, Physics Nobel Prize 1945

and the mean occupation number for a one-particle state $\boldsymbol{lk}\sigma$ can be calculated easily similar as the partition function as

$$\begin{aligned}\langle n_{l\boldsymbol{k}\sigma}\rangle &= \frac{1}{Z_{GK}} \sum_{\{n_{l'\boldsymbol{k}'\sigma'}\}} \exp\left(-\beta \sum_{l'\boldsymbol{k}'\sigma'} \left(\varepsilon_{l'}\left(\boldsymbol{k}'\right) - \mu\right) n_{l'\boldsymbol{k}'\sigma'}\right) n_{l\boldsymbol{k}\sigma} \\ &= \frac{1}{Z_{GK}} \prod_{(l'\boldsymbol{k}'\sigma')\neq(l\boldsymbol{k}\sigma)} \left(1 + \exp\left(-\beta\left(\varepsilon_{l'}\left(\boldsymbol{k}'\right) - \mu\right)\right)\right) \\ &\qquad \times \exp\left(-\beta(\varepsilon_l(\boldsymbol{k}) - \mu)\right) \\ &= \frac{\exp\left(-\beta(\varepsilon_l(\boldsymbol{k}) - \mu)\right)}{1 + \exp\left(-\beta(\varepsilon_l(\boldsymbol{k}) - \mu)\right)} = \frac{1}{\exp\left(\beta(\varepsilon_l(\boldsymbol{k}) - \mu)\right) + 1}. \end{aligned} \tag{5.156}$$

The mean occupation number is therefore given by the Fermi distribution:

$$\langle n_{l\boldsymbol{k}\sigma}\rangle = f(\varepsilon_l(\boldsymbol{k})) \tag{5.157}$$

with the Fermi function

$$f(E) = \frac{1}{\exp\left(\beta(E - \mu)\right) + 1}. \tag{5.158}$$

shown in Fig. 5.23. For $T \to 0$,

$$\exp((E - \mu)/k_B T) = \begin{cases} \infty & \text{für} \quad E > \mu \\ 0 & \text{für} \quad E < \mu \end{cases} \tag{5.159}$$

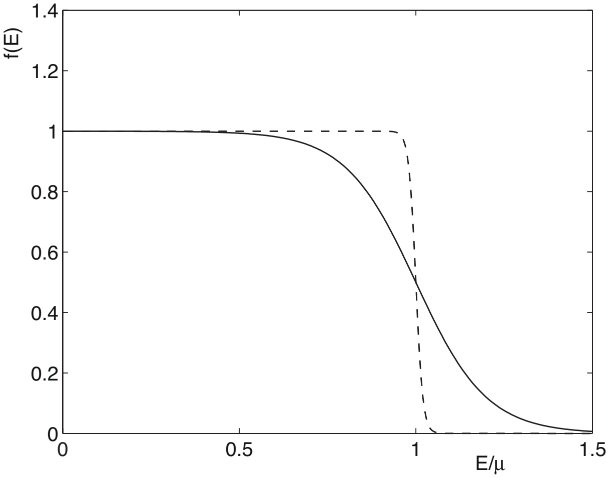

**Fig. 5.23** Fermi function for temperature $k_B T = 0.01\mu$ *(dashed)* and $k_B T = 0.1\mu$ *(solid)*

and therefore

$$f(E) = \begin{cases} 1 \text{ für} & E < \mu \\ 0 \text{ für} & E > \mu \end{cases} . \tag{5.160}$$

The Fermi function is thus a step function for $T = 0$. The chemical potential $\mu(T)$, which is generally temperature-dependent, therefore goes over to the Fermi energy for $T \to 0$:

$$\mu(T = 0) = E_F . \tag{5.161}$$

This corresponds to the interpretation of the chemical potential in thermodynamics as the energy that has to be expended to bring another particle into the system.

Of interest are quantities such as the internal energy of the electron system; this is given by

$$U = \sum_{lk\sigma} \langle n_{lk\sigma} \rangle \varepsilon_l(\boldsymbol{k}) = N \int dEf(E)\rho(E)E \tag{5.162}$$

where the total electronicdensity of states (per unit cell), $\rho(E)$, is defined in (5.138). This also allows the particle number condition, which determines the chemical potential, to be expressed according to

$$N_\mathrm{e} = \sum_{lk\sigma} \langle n_{lk\sigma} \rangle = N \int dE\rho(E)f(E). \tag{5.163}$$

If one uses the normalized quantities energy per unit cell $u = U/N$ and electron number per unit cell $Z_e = N_\mathrm{e}/N$, the corresponding relations are

$$u(T) = \int dE\rho(E)f(E)E, \quad Z_e = \int dE\rho(E)f(E). \tag{5.164}$$

For the evaluation of integrals of the type

$$\int dEH(E)f(E)$$

we use here in particular the so-called[11]

**Sommerfeld-expansion.**[11]

Assuming that $H(E)$ is a "reasonable" function (in particular, it is differentiable several times and also integrable and vanishes for $E \to -\infty$), it follows that

---

[11] A. Sommerfeld, *1868 in Königsberg (then East-Prussia, Germany, now Kaliningrad, Russia), †1951 in Munich, Professor of Theoretical Physics in Munich 1906–1935, Contributions to all areas and author of a well-known textbook of theoretical physics, in particular work on atomic physics, extension of the Bohr model, introduction of the azimuth and magnetic quantum number, work on wave mechanics and the theory of electrons in metals, doctoral advisor of Pauli and Heisenberg.

$$\int_{-\infty}^{+\infty} dEH(E)f(E) = \int_{-\infty}^{+\infty} dEK(E)\left(-\frac{df}{dE}\right) \tag{5.165}$$

which follows from partial integration, where $K(E)$ is the primitive (antiderivative) of $H(E)$, that is,

$$K(E) = \int_{-\infty}^{E} dE' H(E'). \tag{5.166}$$

The negative derivative of the Fermi function is explicitly given by

$$-\frac{df}{dE} = \frac{1}{k_B T}\frac{1}{\left(e^{\beta(E-\mu)}+1\right)\left(e^{-\beta(E-\mu)}+1\right)}. \tag{5.167}$$

It is symmetrical around the chemical potential μ and falls off exponentially on both sides of the chemical potential. For $T \rightarrow 0$ the derivative goes over into a Delta function (of course, since the Fermi function becomes a step function). For finite temperature, the derivative of the Fermi function is only noticeably different from 0 in a relatively small interval around μ, which becomes larger approximately proportional to the temperature; in practice (for example, in numerical calculations), it turns out that only a finite interval $[\mu - 10.k_B T, \mu + 10.k_B T]$ has to be considered, so that the density of states integrals actually have to be extended only over a finite interval. Therefore, it does not matter in practice if densities of states do not fulfill some of the aforementioned requirements (for example, no differentiability at the band edges due to van Hove singularities). Since the energy integral only has to extend over a small interval around μ, one now expands the function $K(E)$ into a Taylor series around μ, i.e.

$$K(E) = K(\mu) + \sum_{n=1}^{\infty}\frac{1}{n!}(E-\mu)^n \frac{d^n K(E)}{dE^n}|_{E=\mu}. \tag{5.168}$$

If one inserts this into the integral to be calculated, one obtains

$$\int_{-\infty}^{+\infty} dEH(E)f(E) = \int_{-\infty}^{\mu} dEH(E) \tag{5.169}$$

$$+\sum_{n=1}^{\infty}\left.\frac{d^{n-1}H(E)}{dE^{n-1}}\right|_{E=\mu}\int_{-\infty}^{+\infty} dE\frac{(E-\mu)^n}{n!}\left(-\frac{df}{dE}\right).$$

In the series, only derivatives of the function $H(E)$ to be integrated at the chemical potential μ occur and integrals (independent on $H(E)$ ) of $(E-\mu)^n$ multiplied by the derivative of the Fermi function have to be calculated. But since $-\frac{df}{dE}$ is symmetrical around μ, only even powers $n$ occur here. Finally, after substitution $x = \beta(E-\mu)$ one obtains:

$$\int_{-\infty}^{+\infty} dEH(E)f(E) = \int_{-\infty}^{\mu} dEH(E) + \sum_{n=1}^{\infty} a_n (k_B T)^{2n}\left.\frac{d^{2n-1}H(E)}{dE^{2n-1}}\right|_{E=\mu} \tag{5.170}$$

$$\text{where} \quad a_n = \int_{-\infty}^{+\infty} dx \frac{x^{2n}}{(2n)!} \frac{1}{(e^x + 1)(e^{-x} + 1)}. \tag{5.171}$$

The $a_n$ can be calculated analytically to

$$a_n = \left(2 - \frac{1}{2^{2(n-1)}}\right)\zeta(2n), \tag{5.172}$$

where the **Riemann zeta function** $\zeta(x)$ is defined by

$$\zeta(x) = \sum_{m=1}^{\infty} \frac{1}{m^x} = 1 + \frac{1}{2^x} + \frac{1}{3^x} + \ldots \tag{5.173}$$

In particular,

$$a_1 = \zeta(2) = \frac{\pi^2}{6}, \quad a_2 = \frac{7}{4}\zeta(4) = \frac{7}{4}\frac{\pi^4}{90} = \frac{7\pi^4}{360}. \tag{5.174}$$

If we now evaluate the integrals in (5.164) using the Sommerfeld expansion, we get

$$Z_e = \int_{-\infty}^{\mu} dE \rho(E) + \frac{\pi^2}{6}(k_B T)^2 \rho'(\mu) + O\big(T^4\big) \tag{5.175}$$

$$u = \int_{-\infty}^{\mu} E\rho(E) dE + \frac{\pi^2}{6}(k_B T)^2 \big(\mu\rho'(\mu) + \rho(\mu)\big) + O\big(T^4\big). \tag{5.176}$$

For low temperatures ($k_B T \ll E_F$, which is well fulfilled even at room temperature at least for metals), $\mu(T)$ only deviates from the Fermi energy $E_F$ by relatively small values of the order of $(k_B T)^2$. Therefore,

$$\int_{-\infty}^{\mu(T)} dE \rho(E) = \int_{-\infty}^{E_F} dE \rho(E) + (\mu - E_F)\rho(E_F) = Z_e + (\mu - E_F)\rho(E_F).$$

It follows:

$$Z_e = Z_e + (\mu - E_F)\rho(E_F) + \frac{\pi^2}{6}(k_B T)^2 \rho'(E_F). \tag{5.177}$$

Thus, one obtains the temperature dependence of the chemical potential of the electrons for low temperatures to

$$\boxed{\mu = E_F - \frac{\pi^2}{6}\frac{\rho'(E_F)}{\rho(E_F)}(k_B T)^2}. \tag{5.178}$$

For the internal energy per unit cell, one obtains

$$\begin{aligned} u &= \int_{-\infty}^{E_F} dE E \rho(E) + (\mu - E_F) E_F \rho(E_F) + \frac{\pi^2}{6}(k_B T)^2 (E_F \rho'(E_F) + \rho(E_F)) \\ &= \int_{-\infty}^{E_F} dE E \rho(E) - \frac{\pi^2}{6} E_F \rho'(E_F)(k_B T)^2 + \frac{\pi^2}{6}(k_B T)^2 E_F \rho'(E_F) \\ &\quad + \frac{\pi^2}{6}(k_B T)^2 \rho(E_F). \end{aligned}$$

**Fig. 5.24** Experimentally determined values of the specific heat of copper and sodium, plotted in the form $\frac{c_V}{T}$ as a function of $T^2$

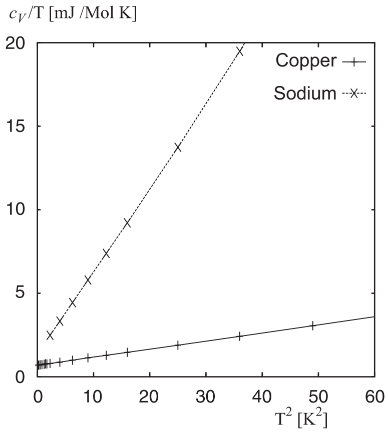

Thus, the temperature dependence of the internal energy per unit cell for low temperatures results in

$$\boxed{u(T) = u_0 + \frac{\pi^2}{6}\rho(E_f)(k_B T)^2}. \tag{5.179}$$

This gives the specific heat per elementary cell

$$\boxed{c_V = \frac{\pi^2}{3}\rho(E_F)k_B^2 T}. \tag{5.180}$$

If the density of states does not vanish at the Fermi energy, as is always the case for metals, there is therefore a linear temperature law of the specific heat due to the electronic contribution.

Including the contribution of the acoustic phonons discussed in Sec. 4.5, one therefore expects for the specific heat of metals at low temperatures

$$c_V(T) = \gamma T + AT^3, \tag{5.181}$$

where

$$\gamma = \frac{\pi^2}{3}\rho(E_F)k_B^2 \quad \text{and} \quad A = \frac{12\pi^4}{5}k_B\frac{1}{\Theta_D^3}.$$

This is the specific heat per unit cell; the phonon contribution therefore differs by the factor $\frac{N}{V}$ from the specific heat per volume calculated in (4.74); $\Theta_D$ is the Debye temperature. This law is well confirmed by experiment. It is customary to plot $c_V/T$ as a function of $T^2$, then the abscissa intercept directly gives the linear, electronic specific heat coefficient $\gamma$ (and thus the density of states at the Fermi energy) and the slope gives the phonon coefficient $A$ (and thus the Debye temperature). Such a plot of experimental results for Cu and Na is shown in Fig. 5.24.

Experimentally, it is customary, as in Fig. 5.24[12], to measure the specific heat per mole (and not per unit cell); then the Avogadro number $N_A = 6 \cdot 10^{23}\text{mol}^{-1}$ has to be multiplied, because one mole of a substance contains $N_A$ molecules. With $N_A k_B = R = 8.3\,\frac{\text{Joule}}{\text{Mol}\cdot\text{K}} = 1.99\,\frac{\text{cal}}{\text{Mol}\cdot\text{K}}$ one therefore obtains for the electronic part of the specific heat per mole:

$$C = \frac{\pi^2}{3}\rho(E_F)Rk_BT. \tag{5.182}$$

In particular, for free electrons or for the model of nearly free electrons with effective mass $m^*$, which is applicable to many metals, the density of states is given by [13] (according to (5.142, 5.143))

$$\rho(E) = \frac{2^{1/2}Vm^{*3/2}}{N\pi^2\hbar^3}\sqrt{E}. \tag{5.183}$$

If then $Z_e$ is the number of electrons in this topmost conduction band of (quasi-)free electrons, the Fermi energy is to be determined from

$$Z_e = \int_0^{E_F} dE\,\rho(E) = \frac{2^{3/2}Vm^{*3/2}}{3N\pi^2\hbar^3}E_F^{3/2}. \tag{5.184}$$

So the Fermi energy for free electrons is explicitly given by

$$E_F = \left(3Z_e\frac{N}{V}\pi^2\right)^{\frac{2}{3}}\frac{\hbar^2}{2m^*} = \frac{3}{2}\frac{Z_e}{\rho(E_F)}. \tag{5.185}$$

Thus

$$\rho(E_F) = \frac{3Z_e}{2E_F} = 3\frac{Z_e}{\hbar^2\left(3Z_e\frac{N}{V}\pi^2\right)^{\frac{2}{3}}}m^* \sim m^*. \tag{5.186}$$

In the model of (quasi-) free electrons, the density of states at the Fermi energy and thus the linear temperature coefficient $\gamma$ of the specific heat is therefore directly proportional to the effective mass $m^*$. The measurement of this coefficient $\gamma$ thus allows a – in principle simple – determination of the effective mass. It is found that in many simple metals (such as Na, K, Cu, Ag, Mg, Ca, Ba, Al, Zn) the effective mass is actually of the same order of magnitude as the mass of free electrons, so that the model of free electrons seems to be surprisingly good. But there are also drastic deviations. In half-metals (e.g. Bi) one finds a much smaller effective mass ($m^* \sim 0.1\,m$), in transition metals one finds much larger effective masses ($m^* \approx 10$–$30\,m$ e.g. in Nb, Mn, Pd, Ni). The reason for this is on the one hand that the density of states in the narrow d-bands, in which the Fermi energy lies in the transition metals, is higher in comparison to the density of states in the s-and p-bands, on the other hand, however, correlation effects (i.e. influences of the electron-electron interaction) are important and contribute significantly to the $\gamma$-coefficient and thus to the effective mass$m^*$.Even larger $\gamma$-coefficients of the specific heat and effective masses $m^*$ up to$100$–$1000\,m$can be found in the so-called**heavy-fermion systems**(e.g. $CeCu_2Si_2$, $CeAl_3$, etc.); here, correlation effects are dominant, and the investigation of heavy-fermion systems is an active research topic in solid-state physics both experimentally and theoretically.

---

[12] Experimental data taken from: Y.S. Touloukian, E.H. Buyco, "Thermophysical Properties of Matter", Vol. 4 (Plenum 1970).

[13] At least if the Fermi energy is not too far from the band edge.

## 5.9 Statistics of electrons and holes in semiconductors

The specific calculations and results of the previous chapter relate to metallic solids; in particular, only for metals the Sommerfeld expansion is meaningful. Therefore, in this section, the thermal electronic properties of semiconductors are to be considered separately. The simplest conceivable semiconductor model is a two-band model consisting of a valence band and a conduction band separated by an energy gap of size $\Delta$. Then one has a valence band density of states $\rho_v(E)$, the lower band edge of which can be chosen to be 0 eV and the upper band edge of which is denoted by $E_v$, and a conduction band density of states $\rho_c(E)$ with the lower band edge $E_c > E_v$ and $E_c - E_v = \Delta$ applies. This is illustrated in Fig. 5.25.

The bands should not overlap and the total density of states is $\rho(E) = \rho_v(E) + \rho_c(E)$. The Fermi energy is in the band gap, and for the usual semiconductors, $\Delta$ is of the order of a few eV, so that for all achievable temperatures $k_B T \ll \Delta$ is fulfilled. For $T = 0$ only the valence band is filled, i.e.

$$Z_e = \int_0^{E_v} dE \rho_v(E) = \int_0^{E_F} dE \rho(E). \tag{5.187}$$

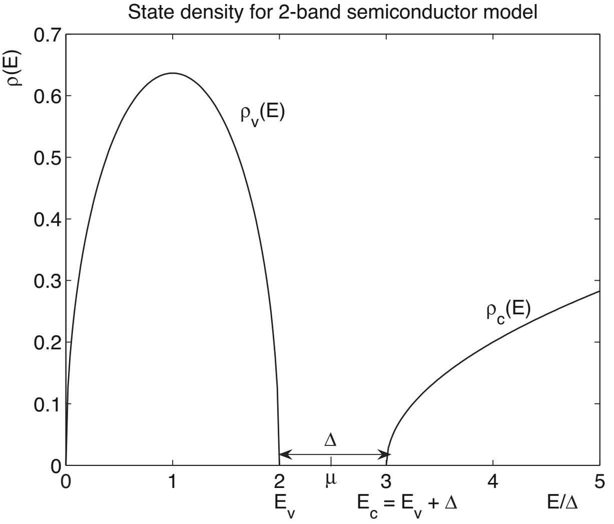

**Fig. 5.25** Density of states of a 2-band semiconductor model

For finite temperatures $T$ it applies

$$Z_e = \int_0^\infty dEf(E)\rho(E) = \int_0^{E_v} dEf(E)\rho_v(E) + \int_{E_c}^\infty dEf(E)\rho_c(E). \quad (5.188)$$

Thus we get:

$$\int_0^{E_v} dE(1-f(E))\rho_v(E) = \int_{E_c}^\infty dEf(E)\rho_c(E). \quad (5.189)$$

This just says that the number of (thermally excited) electrons in the conduction band

$$n_e(T) = \int_{E_c}^\infty dEf(E)\rho_c(E) \quad (5.190)$$

must be equal to the number of unoccupied states in the valence band

$$n_h(T) = \int_0^{E_v} dE(1-f(E))\rho_v(E), \quad (5.191)$$

and these unoccupied states, i.e. electron vacancies in the valence band, are also interpreted as (positively charged) **holes**(index "h"). For undoped, **intrinsic** semiconductors, therefore,

$$n_e(T) = n_h(T). \quad (5.192)$$

applies. The chemical potential $\mu$ lies within the band gap, but not necessarily in the center, but this depends on the effective masses and thus the densities of states $\rho_{c,v}(E)$ of the conduction band and valence band and on the temperature. Obviously the relation

$$1-f(E) = 1 - \frac{1}{e^{(E-\mu)/k_BT}+1} = \frac{1}{e^{-(E-\mu)/k_BT}+1}. \quad (5.193)$$

is valid. This is also a Fermi distribution, but for negative energies. The probability of finding a hole in the valence band at an energy $-|E-\mu|$ is therefore also determined by a Fermi distribution. Holes are therefore also subject to Fermi statistics, but with energy measured from the Fermi energy downwards.

It applies

$$E_v < \mu < E_c \text{ and } E_c - \mu \gg k_BT \text{ and } \mu - E_v \gg k_BT. \quad (5.194)$$

Therefore, for energies $E > E_c$ within the conduction band:

$$f(E) = \frac{1}{e^{(E-\mu)/k_BT}+1} \approx e^{-(E-\mu)/k_BT} \quad (5.195)$$

and for energies $E < E_v$ within the valence band

$$1-f(E) = \frac{1}{e^{(\mu-E)/k_BT}+1} \approx e^{-(\mu-E)/k_BT}. \quad (5.196)$$

Because the energy gap is large compared to thermal energies, the Fermi distributions can be replaced by a classical Boltzmann distribution in the energy regimes of non-vanishing density of states.

Thus one has:

$$n_e(T) = e^{-(E_c-\mu)/k_BT} \int_{E_c}^{\infty} dE \rho_c(E) e^{-(E-E_c)/k_BT} \tag{5.197}$$

and accordingly

$$n_h(T) = e^{-(\mu-E_v)/k_BT} \int_{0}^{E_v} dE \rho_v(E) e^{-(E_v-E)/k_BT}. \tag{5.198}$$

In the vicinity of the band edges, the valence and conduction electron densities of states usually behave like those of free electrons with an effective mass. Therefore, the following assumptions are plausible:

$$\begin{aligned} \rho_c(E) &= \frac{V}{2\pi^2\hbar^3 N}(2m_e)^{3/2}(E-E_c)^{1/2} \\ \rho_v(E) &= \frac{V}{2\pi^2\hbar^3 N}(2m_h)^{3/2}(E_v-E)^{1/2} \end{aligned} \tag{5.199}$$

(compare equations (5.142, 5.143)). This results in

$$\begin{aligned} n_e(T) &= \frac{V}{2\pi^2\hbar^3 N}(2m_e)^{3/2} e^{-(E_c-\mu)/k_BT}(k_BT)^{3/2}\, 2\int_0^{\infty} dx x^2 e^{-x^2} \\ &= 2\frac{V}{N}\left(\frac{m_e k_B T}{2\pi\hbar^2}\right)^{3/2} e^{-(E_c-\mu)/k_BT} \\ n_v(T) &= \frac{V}{2\pi^2\hbar^3 N}(2m_h)^{3/2} e^{-(\mu-E_v)/k_BT}(k_BT)^{3/2}\, 2\int_0^{\infty} dx x^2 e^{-x^2} \\ &= 2\frac{V}{N}\left(\frac{m_h k_B T}{2\pi\hbar^2}\right)^{3/2} e^{-(\mu-E_v)/k_BT}. \end{aligned} \tag{5.200}$$

Here, the substitution $x^2 = (E-E_c)/(k_BT)$ or $x^2 = (E_v-E)/(k_BT)$ was made, $\int_0^{\infty} dx x^2 e^{-x^2} = \sqrt{\pi}/4$ was used and $\sqrt{E_v/k_BT} \approx \infty$ was approximated, which is plausible because the valence band width $E_v$ is also large compared to typical temperatures.

From the condition $n_e = n_h$, one then obtains for the chemical potential:

$$\mu(T) = \frac{1}{2}(E_c+E_v) + \frac{3}{4}k_BT \ln\left(\frac{m_h}{m_e}\right). \tag{5.201}$$

For $T = 0$ the chemical potential $\mu(0) = E_F$ therefore lies exactly in the center of the band gap, but at finite temperatures it does not anymore, but the deviation from the Fermi energy varies in general linear with the temperature[14] if $\mu(T)$ moves upwards with the temperature (towards the conduction band) or downwards (towards the valence band) depends on the ratio of the effective masses of electrons and holes. However, by doping with differently valent impurities, the position of the Fermi energy can be easily changed compared to the position exactly in the middle of the band. In order to give an order of magnitude for the carrier concentration at room temperature in intrinsic semiconductors, we assume$\Delta = 1\,\mathrm{eV}, T = 300\,\mathrm{K}$; The carrier density is essentially determined by the factor$e^{-\Delta/2k_BT} \approx e^{-15} \sim 10^{-7} - 10^{-6}$, so that of the $10^{23}$electrons of the solid about $10^{17}$are in the conduction band.

The specific heat of semiconductors can be calculated analogously to the hole and electron numbers. Here, the calculation will be briefly sketched only and an approximate result will be given; more detailed calculations are left as an exercise for the reader. We start from the definition equation for the specific heat per unit cell:

$$c_V = \frac{\partial u}{\partial T} = \int dEE\rho(E)\frac{\partial f}{\partial T} = \int_0^{E_v} dEE\rho_v(E)\frac{\partial f}{\partial T} + \int_{E_c}^{\infty} dEE\rho_c(E)\frac{\partial f}{\partial T}. \tag{5.202}$$

Because of

$$\frac{\partial f}{\partial T} = \frac{\partial}{\partial T}\frac{1}{e^{\beta(E-\mu)}+1} = \left(-\frac{e^{\beta(E-\mu)}}{(e^{\beta(E-\mu)}+1)^2}\right)\left(-\frac{E-\mu}{k_BT^2} - \beta\frac{\partial\mu}{\partial T}\right) \tag{5.203}$$

and as one has to integrate only over energies far away from the chemical potential one obtains

$$\begin{aligned} c_V = {} & e^{\beta(E_v-\mu)}\int_0^{E_v} dEE\left(\frac{E-\mu}{k_BT^2} + \frac{1}{k_BT}\frac{\partial\mu}{\partial T}\right)\rho_v(E)e^{\beta(E-E_v)} \\ & + e^{-\beta(E_c-\mu)}\int_{E_c}^{\infty} dEE\left(\frac{E-\mu}{k_BT^2} + \frac{1}{k_BT}\frac{\partial\mu}{\partial T}\right)\rho_c(E)e^{-\beta(E-E_c)}. \end{aligned} \tag{5.204}$$

For low temperatures, the terms with prefactor $\frac{1}{k_BT^2}$ are the leading ones and the temperature dependence of the chemical potential can be neglected, i.e. approximately $\mu = E_F = \frac{1}{2}(E_v + E_c)$. This results in

$$\begin{aligned} c_V = \frac{e^{-\frac{\Delta}{2k_BT}}}{k_BT^2}\Bigg(&\int_0^{E_v} dEE(E-E_F)\rho_v(E)e^{-\beta(E_v-E)} \\ & + \int_{E_c}^{\infty} dEE(E-E_F)\rho_c(E)e^{-\beta(E-E_c)}\Bigg). \end{aligned} \tag{5.205}$$

If one substitutes analogously as above for the calculation of the integrals for $n_e, n_h$, then in leading order in the temperature these integrals with prefactors $E_{v,c}$, $(E_{v,c} - E_F)$ are reproduced. Finally, this results in

---

[14] In contrast to the square $T$-dependence according to (5.178) in metals.

$$c_V = 2\frac{V}{N}\frac{k_B}{(2\pi\hbar^2)^{3/2}}\frac{\Delta}{2}\left(m_e^{3/2}E_c - m_h^{3/2}E_v\right)\frac{e^{-\Delta/2k_BT}}{\sqrt{k_BT}} \tag{5.206}$$

or especially for equal effective mass in the valence and conduction band:

$$c_V = 2\frac{V}{N}k_B\left(\frac{m}{2\pi\hbar^2}\right)^{3/2}\frac{\Delta^2}{2}\frac{e^{-\Delta/2k_BT}}{\sqrt{k_BT}}. \tag{5.207}$$

The specific heat therefore goes to 0 exponentially for $T \to 0$. Such an exponential law, more precisely a behavior $c_V \sim e^{-\Delta/k_BT}/(k_BT)^{\alpha}$, is characteristic of systems with a gap in the excitation spectrum. We had already found such a behavior for the Einstein model for phonons. However, the exponent α is dependent on details of the spectrum (dimension, density of states, etc.); here, for the semiconductor model with squareroot-shaped densities of states, one obtains $\alpha = \frac{1}{2}$, for Einstein phonons $\alpha = 2$, for one- or two-dimensional electronic densities of states other values for this α result.

## 5.10 Problems for Chapter 5

**Problem 5.1** ***Electron in the superposition potential of several "nuclei"***
Consider the 1-dimensional potential

$$V(x) = \sum_{n=1}^{N} v(x - X_n)$$

with the 1-dimensional attractive box potential

$$v(x) = \begin{cases} -v_0 & \text{for} \quad |x| < b \\ 0 & \quad\text{else} \end{cases}.$$

Determine the energy eigenvalues and eigenstates numerically for different potential strengths $v_0$, different atomic numbers $N$ and different atomic positions $X_n$(in particular also different atomic distances and also for the case of a periodic arrangement of the $X_n$ with lattice constants $a = X_{n+1} - X_n > b$ and with periodic boundary conditions) and present the results in an appropriate way graphically, i. e. plot the energy eigenvalues and the eigenstates.

**Problem 5.2** ***Attractive Kronig-Penney model***
Consider the 1-dimensional periodic potential

$$V(x) = -v_0\sum_n \delta(x - na) \; (v_0 > 0)$$

i.e. attractive Delta-peaks at the lattice sites $na$.

Solve the Schrödinger equation for bound states (i.e. with eigenenergies $E < 0$).

*Instruction*: Make the ansatz

$$\psi(x) = C_n e^{\kappa(x-na)} + D_n e^{-\kappa(x-na)} \text{ for } na < x < (n+1)a.$$

How is κ related to the sought eigenenergies E? Show that the first derivative at $x = na$ (or $x = (n+1)a$) makes a jump of size

$$-\frac{2mv_0}{\hbar^2}\psi(na).$$

Furthermore, use the Bloch theorem

$$\psi(x+a) = e^{ika}\psi(x),$$

to get a relation between the coefficients $C_{n+1}, D_{n+1}$ and $C_n, D_n$ and derive a homogeneous system of equations for $C_n, D_n$. When does this have non-trivial solutions?

Show that between κ (and thus possible eigenenergies) and $k$ the relation

$$\kappa\cosh(\kappa a) - \frac{mv_0}{\hbar^2}\sinh(\kappa a) = \kappa\cos(ka)$$

must be fulfilled in order for eigenvalues to exist. Discuss this relation graphically and determine the energy range in which energy eigenvalues can occur. Plot $\kappa(k)$ or $E(k)$.

**Problem 5.3 *Kronig-Penney model with potential wells of finite width***
In the original work by Kronig and Penney[15] no Delta-potentials but potential wells of finite width $b$ and depth $v_0$ were treated, which is analytically somewhat more involved than in Exercise 5.2, but numerically more convenient.

We now consider the periodic potential

$$V(x) = \begin{cases} -v_0 & \text{für} \quad na < x < na + b \\ 0 & \text{für} \quad na + b < x < (n+1)\,a \end{cases} \quad (b < a).$$

Solve the one-dimensional Schrödinger equation

$$-\frac{\hbar^2}{2m}\frac{d^2\psi}{dx^2} + V(x)\psi(x) = E\psi(x)$$

by discretization (analogously as in Problem 3.2).

---

[15] R. de L. Kronig, W.G. Penney, Proc. Roy. Soc. (London) A130, 499 (1931), reprinted in "Mathematical Physics in One Dimension", p. 243 (Academic Press New York 1966).

*Note*: Choose $N = 20$ lattice points (unit cells) with periodic boundary conditions, $a = 1$ and energy units so that $\hbar^2/2m = 1$, consider the finite interval $[0, 20]$ and choose the discretization step $h = 0.1$. Then the discretized Schrödinger equation has the form:

$$-\psi_{i+1} - \psi_{i-1} + 2 * \psi_i + V(x_i) * h * h * \psi_i = E * h * h * \psi_i$$
$$\text{with} \quad x_i = i * h, \quad i = 1, \ldots, 200.$$

To realize periodic boundary conditions, the grid point $i = 0$ has to be identified with $i = N = 200$ and $i = N + 1 = 201$ with $i = 1$, i. e. the Hamiltonian matrix must have corresponding non-vanishing matrix elements $h(1, 200) = h(200, 1)$.

Plot the potential curve, some selected eigenstates and the lowest 40 or 60 energy eigenvalues.

### Problem 5.4 *Bloch factors for the Kronig-Penney model*

Consider the same problem as in Problem 5.3. According to (5.20), the Bloch factor in one dimension must satisfy the boundary value (eigenvalue) equation

$$-\frac{\hbar^2}{2m}\frac{d^2u_k}{dx^2} - \frac{\hbar^2 ik}{m}\frac{du_k}{dx} + \frac{\hbar^2k^2}{2m}u_k + V(x)u_k(x) = E_k u_k(x)$$

with periodic boundary conditions on the unit cell, e.g. $[0, 1]$. Also solve this boundary value problem by discretization and plot the lowest 3 energy eigenvalues $E_n$(k) as a function of $k$ in the range $[-\pi, \pi]$ (1st Brillouin zone for $a = 1$) and also in the range $[-2\pi, 2\pi]$ ("extended zone scheme") and also vary the potential strength $v_0$(e.g. $v_0 = 0, 10, 20, 50, 100$). Also plot some selected Bloch states.

### Problem 5.5 *Cosine potential*

Consider the 1-dimensional periodic potential

$$V(x) = v_0 \cos\left(2\pi\frac{x}{a}\right).$$

Determine the energy bands approximately by means of the method of nearly free electrons.

**Problem 5.6** ***Symmetry of the band structure***

If $\underline{\underline{D}}$ denotes a symmetry operation (rotation or reflection, element of the point group) which maps the lattice onto itself, one can define an associated operator $\hat{D}$ on the Hilbert space by:

$$\hat{D}f(\boldsymbol{r}) = f(\underline{\underline{D}}\boldsymbol{r}).$$

Then $\hat{D}$ commutes with the Hamiltonian operator (for non-interacting electrons in the lattice potential).

Show that the band structure (eigenenergies) fulfill

$$\varepsilon(\boldsymbol{k}) = \varepsilon(\underline{\underline{D}}\boldsymbol{k})$$

*Hint:* First show that

$$\hat{D}\psi_{\boldsymbol{k}}(\boldsymbol{r}) = \psi_{\boldsymbol{k}}(\underline{\underline{D}}\boldsymbol{r})$$

is an eigenstate of the Hamiltonian operator $H$ to the eigenenergy $\varepsilon(\boldsymbol{k})$. Then show

$$\psi_{\boldsymbol{k}}(\underline{\underline{D}}\boldsymbol{r}) = \psi_{\underline{\underline{D}}^{-1}\boldsymbol{k}}(\boldsymbol{r}).$$

For this purpose, investigate how an arbitrary translation operator $T_{\boldsymbol{R}}$ acts on $\psi_{\boldsymbol{k}}(\underline{\underline{D}}\boldsymbol{r})$.

**Problem 5.7** ***Kronig-Penney model with Delta potentials in Tight-Binding approximation***

Treat the Kronig-Penney model from problem 5.2 in Tight-Binding approximation by first solving the "atomic problem" (only a single attractive Delta potential) exactly and calculating the overlap matrix elements of the "atomic" wave functions explicitly. Compare the result for the band structure with the exact result from problem 5.2.

**Problem 5.8** ***Kronig-Penney model with finite potential wells in tight-binding approximation***

Treat the Kronig-Penney model from problem 5.3 in tight-binding approximation, by first solving the "atomic problem" (only a single attractive potential well of depth $-v_0$ and width $b$) and then calculating the overlap matrix elements of the "atomic" wave functions (from nearest-neighbor "atoms" separated by the lattice constant $a > b$). Compare the result for the tight-binding band structure according to (5.81) with the exact result from problem 5.3.

**Problem 5.9** ***Wannier functions and tight-binding band structure***

a) Show that the Wannier states defined by

$$|n\boldsymbol{R}\rangle = \frac{1}{\sqrt{N}} \sum_{\mathbf{k}} e^{-i\boldsymbol{k}\boldsymbol{R}} |\psi_{n\boldsymbol{k}}\rangle$$

($w_n(\boldsymbol{r}-\boldsymbol{R}) = \langle \boldsymbol{r}|n\boldsymbol{R}\rangle$) form a complete orthonormal basis (if the Bloch states $|\psi_{n\mathbf{k}}\rangle$ are such a basis).

b) Show that the band structure is given by

$$\varepsilon_n(\boldsymbol{k}) = \sum_{\boldsymbol{R}} e^{i\boldsymbol{k}\boldsymbol{R}} \langle n\mathbf{0}|H|n\boldsymbol{R}\rangle .$$

**Problem 5.10** ***Tight-Binding Band Structures***

Determine, using the tight-binding approximation (5.91) only for nearest-neighbor vectors, the energy dispersion of a tight-binding band for an fcc lattice and a bcc lattice and plot the band structure along selected directions of the Brillouin zone.

**Problem 5.11** ***Tight-Binding Model for the 2-dimensional triangular lattice***

Determine the tight-binding dispersion for electrons on a triangular lattice taking into account only nearest-neighbor hopping.

**Problem 5.12** ***Tight-Binding model for graphene:***

A 2-dimensional hexagonal lattice consists of a triangular lattice with a 2-atom basis. The triangular lattice is spanned by the basis vectors $\boldsymbol{a}_1 = a(\frac{3}{2}, -\frac{\sqrt{3}}{2})$, $\boldsymbol{a}_2 = a(\frac{3}{2}, \frac{\sqrt{3}}{2})$ (with respect to an orthonormal coordinate system), the basis consists of 2 carbon atoms at $(0,0)$ and at $\boldsymbol{a} = (a,0)$ in the primitive unit cell. Each atom contributes with one state (and one electron) to the band formation. We only consider nearest-neighbor coupling, i. e. only between the localized (orthogonalized) atomic states at adjacent atoms should a non-vanishing matrix element $t$exist.

Determine the 2-dimensional band structure $\varepsilon(k_x, k_y)$ and represent it in a 3D plot.

*Instruction*: The Tight-Binding Hamiltonian operator can be represented as follows:

$$H = \sum_{\boldsymbol{R}} t(|\boldsymbol{R}\rangle\langle\boldsymbol{R}+\boldsymbol{a}| + |\boldsymbol{R}+\boldsymbol{a}\rangle\langle\boldsymbol{R}| + |\boldsymbol{R}+\boldsymbol{a}\rangle\langle\boldsymbol{R}+\boldsymbol{a}_1|$$
$$+|\boldsymbol{R}+\boldsymbol{a}_1\rangle\langle\boldsymbol{R}+\boldsymbol{a}| + |\boldsymbol{R}+\boldsymbol{a}\rangle\langle\boldsymbol{R}+\boldsymbol{a}_2| + |\boldsymbol{R}+\boldsymbol{a}_2\rangle\langle\boldsymbol{R}+\boldsymbol{a}|).$$

The transition to the $\boldsymbol{k}$ representation is made by the unitary transformations

$$|\boldsymbol{R}\rangle = \frac{1}{\sqrt{N}}\sum_{\boldsymbol{k}} e^{i\boldsymbol{k}\boldsymbol{R}}|A\boldsymbol{k}\rangle,\ |\boldsymbol{R}+\boldsymbol{a}\rangle = \frac{1}{\sqrt{N}}\sum_{\boldsymbol{k}} e^{i\boldsymbol{k}(\boldsymbol{R}+\boldsymbol{a})}|B\boldsymbol{k}\rangle.$$

So you have two states $|A\boldsymbol{k}\rangle$, $|B\boldsymbol{k}\rangle$per $\boldsymbol{k}$ $\in$1. BZ, because there are 2 atoms per elementary cell, and therefore also 2 bands, whose dispersion is obtained by diagonalizing a $2 * 2$ matrix.

**Problem 5.13** ***Wannier Functions***

Determine the Wannier functions $w_l(x-na)$ according to the definition (5.85) for the Kronig-Penney model from problem 5.3 from the Bloch functions calculated there, and compare them with corresponding "atomic" states $\varphi_l(x-na)$ (eigenstates of the individual potential wells of the same width and depth). Vary the potential strength (depth of the wells) and the lattice constant if necessary.

**Problem 5.14** ***OPW Method***

Given a one-dimensional finite-depth potential well, i.e. the potential

$$V(x) = \begin{cases} -V_0 & \text{for } -a < x < a \\ 0 & \text{else} \end{cases}.$$

a) Determine the energy eigenvalue $E_0 < 0$ and the corresponding eigenfunction $\varphi_0(x)$ for the bound state; choose $V_0$ so that there is only one bound state.

b) According to the OPW prescription, one can construct orthogonal plane waves from the usual plane waves $e^{ikx}$ (orthogonal to $|\varphi_0\rangle$) by

$$|\psi_k\rangle = |k\rangle - |\varphi_0\rangle\langle\varphi_0|k\rangle.$$

Determine this $\psi_k(x)$ explicitly and plot these wave functions.

c) Compare the OPWs thus constructed with the exact eigenfunctions (scattering states) that result for the full problem for $E > 0$. Solve the problem numerically if necessary (also) by discretizing the 1-dimensional

Schrödinger equation on a (large) interval $[-b, b]$ (with periodic boundary conditions and $b \gg a$) and comparing the (unbound) eigenstates with the (then also numerically determined) $\psi_k(x)$ (for $k = \frac{n\pi}{b}$, why?)

**Problem 5.15** ***Density of states of (quasi-)free electrons***
Determine the density of states of free electrons (with dispersion $\varepsilon(\boldsymbol{k}) = \frac{\hbar^2 k^2}{2m}$) in dimension $d = 1, d = 2$ and $d = 4$ analytically. Proceed as in the derivation of (5.142) resp. (5.143). Draw the densities of states.

**Problem 5.16** ***Tight-Binding density of states for fcc and bcc Lattices***
Consider the nearest-neighbor tight-binding model on an fcc or bcc lattice, i.e. the dispersion relations derived in problem 5.10.

a) At which energies are Van Hove singularities to be expected and what is their nature?
b) Determine the densities of states $\rho(E)$ numerically. Use the methods developed for the numerical determination of phonon densities of states in Problem 4.7.

**Problem 5.17** ***Tight-Binding Density of States for Triangular Lattices and for Graphene***
Consider the nearest-neighbor tight-binding model on a 2-dimensional triangular lattice with a one-atom basis (cf. Problem 5.11) and with a 2-atom basis ("honeycomb lattice", i.e. graphene, cf. Problem 5.12), i.e. for the dispersion relations derived in Problems 5.11 and 5.12.

Determine the densities of states $\rho(E)$ numerically. Use the method developed for the numerical determination of phonon densities of states in Problem 4.7

**Problem 5.18** ***Fermi Surface for Tight-Binding Bands***
Determine and plot the Fermi surface for nearest-neighbor tight-binding dispersions for different filling factors, i.e. total electron numbers, or positions of the Fermi energy $E_F$ for a cubic lattice of your choice (sc, fcc or bcc), possibly first only for a two-dimensional lattice.

**Problem 5.19** ***Free Electrons in 2 Dimensions***

Consider free electrons with dispersion

$$\varepsilon(\boldsymbol{k}) = \frac{\hbar^2 k^2}{2m} = \frac{\hbar^2}{2m}\left(k_x^2 + k_y^2\right)$$

in 2 dimensions.

a) Determine the relationship between the Fermi wave vector $k_F$ and the Fermi energy $E_F$ with the particle density $n = N/F$ ($N$ total electron number, $F$ area or "volume" of the 2-dimensional system).

b) Determine the density of states $\rho(E)$.

c) Determine the chemical potential $\mu(T)$, in particular its temperature dependence, i.e. the first corrections to $E_F$.

d) Determine the internal energy $U(T)$ and the specific heat $c_V(T)$ up to the first corrections to the linear $T$-law.

**Problem 5.20** ***Temperature dependence of chemical potential and internal energy***

Determine the temperature dependence of the chemical potential and the internal energy of free non-relativistic fermions numerically also for higher temperatures $T \sim T_F$. In suitably chosen dimensionless units one can assume

$$\rho(E) = \sqrt{E}$$

$$1 = \int_0^\infty dE \rho(E) f(E),$$

with the Fermi function

$$f(E) = \frac{1}{e^{(E-\mu)/T} + 1}.$$

Discuss the high-temperature limit ($T > T_F$) also analytically.

**Problem 5.21** ***Specific heat of semiconductors***

a) Confirm the result (5.206) or (5.207) for the specific heat of the semiconductor model (5.199) with a squareroot-shaped (and thus 3-dimensional) valence and conduction band density of states by explicit recalculation, i.e. carry out the (only briefly sketched) intermediate steps between the equations (5.204)–(5.207).

b) Consider the following semiconductor model with constant valence and conduction band densities of states:

$$\rho(E) = \begin{cases} \frac{1}{E_0} & \text{für} \quad 0 < E < E_0 \quad \text{und} \quad E_0 + \Delta < E < 2E_0 + \Delta \\ 0 & \text{sonst} \end{cases} .$$

Then there is obviously a gap of size $\Delta$ and for 1 electron per elementary cell the Fermi energy falls into this gap.
Determine the temperature dependence of the specific heat in the limit of low temperatures for this model.

# Electron–Electron Interaction

# 6

In the last chapter we neglected the interaction of electrons with each other, which is ultimately not justified quantitatively. Quantum mechanically, one then has to solve only a one-particle problem, namely that of an electron in a periodic potential, which at least already explains the formation of energy bands and band gaps. A many-particle problem was only considered in the form of the ideal Fermi gas known from the basic lecture on statistical physics, but in this case many-particle effects are only taken into account via the Pauli principle. Real interactions and correlations between the electrons have not been considered so far.

In this chapter we want to investigate the influence of the electron–electron interaction. We consider $N_\mathrm{e}$ electrons in an external (usually again periodic) potential and with a repulsive interaction with each other. The Hamiltonian operator can then be written as:

$$H = H_0 + H_1 \tag{6.1}$$

$$\text{with} \quad H_0 = \sum_{i=1}^{N_\mathrm{e}} h_i = \sum_{i=1}^{N_\mathrm{e}} \frac{\boldsymbol{p}_i^2}{2m} + \sum_{i=1}^{N_\mathrm{e}} V(\boldsymbol{r}_i) \tag{6.2}$$

$$H_1 = \sum_{i<j} u\left(\boldsymbol{r}_i - \boldsymbol{r}_j\right). \tag{6.3}$$

Here, strictly speaking, the interaction $u\left(\boldsymbol{r} - \boldsymbol{r}'\right)$ is the Coulomb repulsion, that is

$$u\left(\boldsymbol{r} - \boldsymbol{r}'\right) = \frac{e^2}{|\boldsymbol{r} - \boldsymbol{r}'|}. \tag{6.4}$$

Sometimes, however, other, effective interactions are used here, for example a screened Coulomb interaction, then one no longer considers all electrons and charges of the system microscopically, but imagines certain influences, for

© The Author(s), under exclusive license to Springer-Verlag GmbH, DE, part of Springer Nature 2023

G. Czycholl, *Solid State Theory, Volume 1*,
https://doi.org/10.1007/978-3-662-66135-2_6

example those of the inner shells, already contained in an effective one-particle potential $V(\boldsymbol{r})$. On the other hand, if a fully microscopic treatment and thus the use of the bare Coulomb potential for $u\left(\boldsymbol{r}-\boldsymbol{r}'\right)$ is possible, it should be possible to derive effects such as screening, dielectric constant, screened Coulomb potential, effective one-particle potential microscopically. But that only works approximately. Almost no exact statements and results can be achieved taking into account the interaction.

## 6.1 Occupation Number Representation ("Second Quantization") for Fermions

The Form ((6.1)–(6.3)) of the Hamiltonian operator $H$ we will refer to as "1. Quantization". In this section we will give a representation of the Hamiltonian operator in **occupation number representation** or **"Second Quantization"** which is particularly suitable for the systematic treatment of interaction effects. To this end, we assume that we can solve the one-particle problem exactly. Let us consider the $i$ -th electron in particular, then it should hold:

$$h_i|k_\alpha\rangle^{(i)} = \varepsilon_{k_\alpha}|k_\alpha\rangle^{(i)} \tag{6.5}$$

or in position representation

$$h_i\varphi_{k_\alpha}(\boldsymbol{r}_i) = \left(\frac{\boldsymbol{p}_i^2}{2m} + V(\boldsymbol{r}_i)\right)\varphi_{k_\alpha}(\boldsymbol{r}_i) = \varepsilon_{k_\alpha}\varphi_{k_\alpha}(\boldsymbol{r}_i). \tag{6.6}$$

Here, $\{k_\alpha\}$ is a complete set of one-particle quantum numbers, in solid state physics, for example, $k_\alpha \equiv (l\boldsymbol{k}\sigma)$ ($l$ band index, $\boldsymbol{k} \in 1.BZ$ wave vector, σ spin), if one uses the Bloch states as a one-particle basis. The Pauli principle, which one can regard as another basic axiom of quantum mechanics for fermions, i.e. systems of identical particles with half-integer spin, states that only the subspace of the product space of the $N_\mathrm{e}$ particle Hilbert space is realized, which consists of the many-particle wave functions which are totally antisymmetric in the particle indices. A basis of this total antisymmetric $N_\mathrm{e}$-particle Hilbert space $\mathcal{H}_A(N_\mathrm{e})$ is given by the so-called **Slater determinants**[1], which can be constructed from the one-particle basis states according to:

$$\begin{aligned} |\Psi_{k_1\ldots k_{N_\mathrm{e}}}(1\ldots N_\mathrm{e})\rangle &= \frac{1}{\sqrt{N_\mathrm{e}!}}\sum_{P\varepsilon S_{N_\mathrm{e}}}(-1)^{\chi_P}|k_{P(1)}\rangle^{(1)}\ldots|k_{P(N_\mathrm{e})}\rangle^{(N_\mathrm{e})} \\ &= \frac{1}{\sqrt{N_\mathrm{e}!}}\det\begin{pmatrix} |k_1\rangle^{(1)} & \ldots & |k_1\rangle^{(N_\mathrm{e})} \\ \vdots & \ddots & \vdots \\ |k_{N_\mathrm{e}}\rangle^{(1)} & \ldots & |k_{N_\mathrm{e}}\rangle^{(N_\mathrm{e})} \end{pmatrix} = \frac{1}{\sqrt{N_\mathrm{e}!}}\det(|k_\alpha\rangle^{(i)}). \end{aligned} \tag{6.7}$$

---

[1] J.C. Slater, *1900 in Oak Park (Illinois, USA), †1976 in Florida, American physicist, professor at Harvard, MIT and the University of Florida (Gainesville), work on quantum theory, especially on atomic and molecular structure and solid state theory.

Here $P$ denotes the elements of the permutation group $S_{N_e}$ of $N_e$ elements, $\chi_P$ is the character of the permutation (i.e. the number of transpositions that lead to the permutation). The product state $|k_1\rangle^{(1)}|k_2\rangle^{(2)}\ldots|k_{N_e}\rangle^{(N_e)}$ would mean that particle 1 is in state $k_1$, particle 2 in state $k_2$, etc., particle $N_e$ in state $k_{N_e}$; since the particles are indistinguishable, it must be irrelevant whether particle 1 or particle 2 or particle $N_e$ is in state $k_1$ etc., therefore one has to sum over all possible permutations, the prefactor $1/\sqrt{N_e!}$ just ensures that the state is normalized again. However, it should be emphasized that not all states of the antisymmetrized $N_e$-particle Hilbert space $\mathcal{H}_A(N_e)$ can be represented as a Slater determinant of one-particle states; but the Slater determinants form a basis of $\mathcal{H}_A(N_e)$. The general quantum mechanical postulate corresponding to the Pauli principle refers to the antisymmetry of the total wave function, the common form of the Pauli principle.

> "Two fermions of a many-particle system cannot be in the same single-particle state" only applies specifically to Slater determinants, because if two single-particle quantum numbers $k_\alpha$ were equal, two rows of the determinant would be equal and the determinant vanishes.

The basis described by the Slater determinants can also be given in occupation number representation, as it was already used in the (grand canonical) treatment of the ideal Fermi gas in statistical physics (and in the previous chapter). If it is anyway irrelevant whether particle 1, particle 2, etc., or particle $N_e$ is in the single-particle state $k_\alpha$, one does not need to specify these possibilities and sum over all permutations, but can simply specify how many of the indistinguishable $N_e$ particles are in the state $k_\alpha$. So for a countable single-particle basis $\{k_\alpha|\alpha \in N\}$ one specifies the basis state in the form $|\{n_{k_\alpha}\}\rangle = |n_{k_1}, n_{k_2}, \ldots, n_{k_\alpha}, \ldots\rangle$, where $n_{k_\alpha}$ is the occupation number of the state $k_\alpha$. If the total particle number is $N_e$ and they are fermions, the following must be fulfilled:

$$n_{k_\alpha} \in \{0, 1\} \quad \text{and} \quad \sum_{\alpha=1}^{\infty} n_{k_\alpha} = N_e. \tag{6.8}$$

The last summation restriction is still a bit annoying for practical work in occupation number representation. But you can simply omit it. However, this means that you may be considering different total particle numbers, so you are no longer working exactly in the $N_e$-particle Hilbert space but in the so-called **Fock space**[2]

$$\mathcal{H}_{A,\text{Fock}} = \mathcal{H}_A(0) \oplus \mathcal{H}_A(1) \oplus \ldots \oplus \mathcal{H}_A(N_e) \oplus \ldots \tag{6.9}$$

---

[2] W.A. Fock, *1898 in St. Petersburg, †1974 ibid, Soviet physicist, professor in Leningrad from 1932, fundamental work on quantum theory and relativity, developed approximation methods for the wave equation of many-particle systems ("Hartree-Fock approximation") in 1930 and, in general, quantum theory for systems with variable numbers of particles (quantum mechanics in the "Fock-Space").

which is defined as the direct sum over all possible particle numbers $N_e$ of the antisymmetric $N_e$ -Particle-Hilbert-spaces . This corresponds to the procedure of statistical physics in the grand-canonical treatment, in which it is only required via the chemical potential that the mean particle number corresponds to the given particle number.

On the Fock-space defined above, one can now define new operators that change the particle number by just 1, and are therefore called **creation operators** (creators) or **annihilation-operators** (annihilators). For fermions, these operators can be defined as follows:

$$\begin{aligned} c_{k_\alpha}|n_{k_1},\ldots,n_{k_\alpha},\ldots\rangle &= (-1)^{S_\alpha} n_{k_\alpha}|n_{k_1},\ldots,n_{k_\alpha}-1,\ldots\rangle \\ c^\dagger_{k_\alpha}|n_{k_1},\ldots,n_{k_\alpha},\ldots\rangle &= (-1)^{S_\alpha}(1-n_{k_\alpha})|n_{k_1},\ldots,n_{k_\alpha}+1,\ldots\rangle \\ \text{with} \quad S_\alpha &= \sum_{\delta=1}^{\alpha-1} n_{k_\delta}. \end{aligned} \tag{6.10}$$

Obviously it is valid:

$$\begin{aligned} c_{k_\alpha}|\ldots 1..0\ldots \overbrace{0}^{\alpha} \ldots 1\ldots\rangle &= 0 \\ c_{k_\alpha}|\ldots 1..0\ldots \overbrace{1}^{\alpha} \ldots 1\ldots\rangle &= \pm|\ldots 1..0\ldots \overbrace{0}^{\alpha} \ldots 1\ldots\rangle \\ c^\dagger_{k_\alpha}|\ldots 1..0\ldots \overbrace{0}^{\alpha} \ldots 1\ldots\rangle &= \pm|\ldots 1..0\ldots \overbrace{1}^{\alpha} \ldots 1\ldots\rangle \\ c^\dagger_{k_\alpha}|\ldots 1..0\ldots \overbrace{1}^{\alpha} \ldots 1\ldots\rangle &= 0. \end{aligned} \tag{6.11}$$

The sign depends on the occupation of the other states due to the prefactor $(-1)^{S_\alpha}$; this is precisely because of the antisymmetry of the state. It applies

$$\begin{aligned} c^\dagger_{k_\alpha}c_{k_\alpha}|n_{k_1},\ldots,n_{k_\alpha},\ldots\rangle &= (-1)^{S_\alpha} n_{k_\alpha} c^\dagger_{k_\alpha}|n_{k_1},\ldots,n_{k_\alpha}-1,\ldots\rangle \\ &= (-1)^{S_\alpha} n_{k_\alpha}(-1)^{S_\alpha}(1-(n_{k_\alpha}-1))|n_{k_1},\ldots,n_{k_\alpha},\ldots\rangle \\ &= (-1)^{2S_\alpha} n_{k_\alpha}(2-n_{k_\alpha})|n_{k_1},\ldots,n_{k_\alpha},\ldots\rangle \\ &= n_{k_\alpha}|n_{k_1},\ldots,n_{k_\alpha},\ldots\rangle \end{aligned}$$

because for $n_{k_\alpha} \in \{0,1\}$ it applies: $n_{k_\alpha}(2-n_{k_\alpha}) = n_{k_\alpha}$.

$$\begin{aligned} c_{k_\alpha}c^\dagger_{k_\alpha}|n_{k_1},\ldots,n_{k_\alpha},\ldots\rangle &= (-1)^{2S_\alpha}(n_{k_\alpha}+1)(1-n_{k_\alpha})|n_{k_1},\ldots,n_{k_\alpha},\ldots\rangle \\ &= (1-n_{k_\alpha})|n_{k_1},\ldots,n_{k_\alpha},\ldots\rangle. \end{aligned} \tag{6.12}$$

The operator $c^\dagger_{k_\alpha}c_{k_\alpha}$ has as eigenvalue precisely the occupation number $n_{k_\alpha}$. The particle number operator is therefore given by:

$$\hat{N}_e = \sum_{\alpha=1}^{\infty} c_{k_\alpha}^\dagger c_{k_\alpha}. \tag{6.13}$$

The fermion creators and annihilators satisfy the **anti-commutation relations**

$$\boxed{\{c_{k_\alpha}, c_{k_\beta}\} = 0 = \left\{c_{k_\alpha}^\dagger, c_{k_\beta}^\dagger\right\}, \left\{c_{k_\alpha}, c_{k_\beta}^\dagger\right\} = \delta_{\alpha\beta}}. \tag{6.14}$$

The anti-commutator of two operators $A, B$ is defined by:

$$\{A, B\} = [A, B]_+ = AB + BA. \tag{6.15}$$

Of the anti-commutation relations (6.14) the proof for equal α has been given already with (6.12) , since from this $c_{k_\alpha} c_{k_\alpha}^\dagger = 1 - c_{k_\alpha}^\dagger c_{k_\alpha}$ follows; it must therefore only be shown for different quantum numbers $k_\alpha \neq k_\beta$ that the fermion creators and annihilators anti-commute. For this purpose, without restriction $\alpha < \beta$:

$$\begin{aligned}
&c_{k_\alpha} c_{k_\beta} |n_{k_1}, \ldots, n_{k_\alpha}, \ldots, n_{k_\beta}, \ldots\rangle \\
&\quad = (-1)^{S_\alpha} (-1)^{S_\beta} |n_{k_1}, \ldots, n_{k_\alpha} - 1, \ldots, n_{k_\beta} - 1, \ldots\rangle \\
&c_{k_\beta} c_{k_\alpha} |n_{k_1}, \ldots, n_{k_\alpha}, \ldots, n_{k_\beta}, \ldots\rangle \\
&\quad = (-1)^{S_\alpha} (-1)^{S_\beta - 1} |n_{k_1}, \ldots, n_{k_\alpha} - 1, \ldots, n_{k_\beta} - 1, \ldots\rangle \\
&\quad = -c_{k_\alpha} c_{k_\beta} |n_{k_1}, \ldots, n_{k_\alpha}, \ldots, n_{k_\beta}, \ldots\rangle.
\end{aligned} \tag{6.16}$$

Completely analogously, for $\alpha < \beta$:

$$c_{k_\alpha} c_{k_\beta}^\dagger = -c_{k_\beta}^\dagger c_{k_\alpha} \qquad c_{k_\alpha}^\dagger c_{k_\beta}^\dagger = -c_{k_\beta}^\dagger c_{k_\alpha}^\dagger. \tag{6.17}$$

In particular, these anti-commutation relations imply:

$$c_{k_\alpha}^2 = c_{k_\alpha}^{\dagger 2} = 0, \tag{6.18}$$

i.e. it is not possible to create two particles with the same one-particle quantum number $k_\alpha$, i.e. the Pauli principle is automatically taken into account if the creators and annihilators fulfill the above anti-commutation relations.

### Field Operators

With the particle wave functions $\varphi_{k_\alpha}(\boldsymbol{r}) = \langle \boldsymbol{r} | k_\alpha \rangle$, which belong to the chosen one-particle basis, and the creation and annihilation operators, so-called **field operators** can be defined by:

$$\hat{\Phi}(\boldsymbol{r}) = \sum_\alpha \varphi_{k_\alpha}(\boldsymbol{r}) c_{k_\alpha}, \quad \hat{\Phi}^\dagger(\boldsymbol{r}) = \sum_\alpha \varphi_{k_\alpha}^*(\boldsymbol{r}) c_{k_\alpha}^\dagger. \tag{6.19}$$

The field operators $\hat{\Phi}(\boldsymbol{r})$ ($\hat{\Phi}^\dagger(\boldsymbol{r})$) destroy (create) a particle at the location $\boldsymbol{r}$ (while the creators and annihilators do the same for a particle in a certain one-particle state). The field operators fulfill the commutation relation

$$\left\{\hat{\Phi}^{(\dagger)}(\boldsymbol{r}),\hat{\Phi}^{(\dagger)}\left(\boldsymbol{r}'\right)\right\}=0,\quad \left\{\hat{\Phi}(\boldsymbol{r}),\hat{\Phi}^{\dagger}\left(\boldsymbol{r}'\right)\right\}=\delta\left(\boldsymbol{r}-\boldsymbol{r}'\right).\tag{6.20}$$

This can be directly derived from the (anti-)commutation relation (6.14) and the completeness relation for the basis wave functions

$$\sum_{\alpha}\varphi_{k_\alpha}^{*}(\boldsymbol{r})\varphi_{k_\alpha}\left(\boldsymbol{r}'\right)=\delta\left(\boldsymbol{r}-\boldsymbol{r}'\right).$$

The field operators are representation-free and can be expanded in different one-particle-basis systems (with corresponding one-particle-wave functions and creation and annihilation operators). Formally, the annihilators (creators) replace the expansion coefficients in the expansion of any wave function with respect to the one-particle basis wave functions.

**Operators in Occupation Number Representation**

There are so-called one-particle operators and two-particle operators in the description of many-particle systems in practice. In “1. Quantization” a **one-particle operator** for a $N_\mathrm{e}$-particle system can be written as

$$A^{(1)}=\sum_{i=1}^{N_\mathrm{e}}A^{(1)}(\boldsymbol{r}_i).\tag{6.21}$$

A one-particle operator thus consists of additive contributions, each of which is only effective for one of the $N_\mathrm{e}$ particles. Examples of one-particle operators are therefore the part $H_0$ of the Hamilton operator in (6.2) or its parts kinetic energy and external potential, but also many other operators such as current operator, particle density operator are one-particle operators.

A **two-particle operator** is, on the other hand, in “1. Quantization” of the form

$$A^{(2)}=\frac{1}{2}\sum_{i\neq j}A^{(2)}\left(\boldsymbol{r}_i,\boldsymbol{r}_j\right).\tag{6.22}$$

A two-particle operator can therefore not be decomposed into the sum of only those contributions that only act on a single particle, but all summands act simultaneously on two different particles. An example of a two-particle operator is the Coulomb interaction, i.e. the part $H_1$ (6.3) of the Hamilton operator (6.1).

A one particle operator can be expressed as follows by the creators and annihilators introduced above. We again consider a complete, orthonormal one-particle basis and add for each $i$ twice a unit operator in the form $\sum_\alpha |k_\alpha \overset{(i)}{\rangle}\overset{(i)}{\langle} k_\alpha|=1$. Then it follows:

$$\begin{aligned}A^{(1)}&=\sum_{i=1}^{N_\mathrm{e}}\sum_{\alpha=1}^{\infty}|k_\alpha \overset{(i)}{\rangle}\overset{(i)}{\langle} k_\alpha|A^{(1)}(\boldsymbol{r}_i)\sum_{\beta=1}^{\infty}|k_\beta \overset{(i)}{\rangle}\overset{(i)}{\langle} k_\beta|\\&=\sum_{\alpha,\beta=1}^{\infty}\langle k_\alpha|A^{(1)}(\boldsymbol{r})|k_\beta\rangle\sum_{i=1}^{N_\mathrm{e}}|k_\alpha \overset{(i)}{\rangle}\overset{(i)}{\langle} k_\beta|.\end{aligned}\tag{6.23}$$

Here it has already been taken into account that the matrix element of $A^{(1)}$ with respect to the one-particle states no longer depends on the particle index $i$:

$$\overset{(i)}{\langle}\, k_\alpha|A^{(1)}(\boldsymbol{r}_i)|k_\beta\, \overset{(i)}{\rangle} = \int d^3r_i\varphi^*_{k_\alpha}(\boldsymbol{r}_i)A^{(1)}(\boldsymbol{r}_i)\varphi_{k_\beta}(\boldsymbol{r}_i) = \langle k_\alpha|A^{(1)}(\boldsymbol{r})|k_\beta\rangle. \tag{6.24}$$

Now it holds:

$$\sum_{i=1}^{N_\mathrm{e}} |k_\alpha\, \overset{(i)}{\rangle}\overset{(i)}{\langle}\, k_\beta| = c^\dagger_{k_\alpha}c_{k_\beta}. \tag{6.25}$$

Because if you apply the operator $\sum_{i=1}^{N_\mathrm{e}} |k_\alpha\, \overset{(i)}{\rangle}\overset{(i)}{\langle}\, k_\beta|$ to a $N_\mathrm{e}$-particle state, only a non-vanishing term results if the particle state $k_\beta$ is occupied in this many-particle state, then, because of the orthonormality, a factor 1 results and the one-particle state $|k_\beta\rangle$ within this many-particle state is replaced by $|k_\alpha\rangle$. So the occupation of the one-particle state $k_\beta$ is replaced by the occupation of the one-particle state $k_\alpha$, that is, a particle in the state $k_\beta$ is destroyed and replaced by one in the state $k_\alpha$.

Thus, a one-particle operator can be written in occupation-number representation as:

$$A^{(1)} = \sum_{\alpha,\beta=1}^{\infty} A^{(1)}_{k_\alpha,k_\beta}c^\dagger_{k_\alpha}c_{k_\beta} \tag{6.26}$$

with:

$$A^{(1)}_{k_\alpha,k_\beta} = \langle k_\alpha|A^{(1)}(\boldsymbol{r})|k_\beta\rangle. \tag{6.27}$$

Every one-particle operator can therefore uniquely be represented as a linear combination of all possible pairs of creators and annihilators in occupation-number representation, where the coefficients are exactly the matrix elements of the one-particle operator with respect to the one-particle basis states.

The corresponding consideration can be made for a two-particle operator. If you insert 4 "ones" to be formed from the complete one-particle basis system here, you get:

$$\begin{aligned} A^{(2)} &= \frac{1}{2}\sum_{i\neq j}\sum_{\alpha,\beta,\gamma,\delta} |k_\alpha\, \overset{(i)}{\rangle}\; |k_\beta\, \overset{(j)}{\rangle}\overset{(i)}{\langle}\, k_\alpha|\; \overset{(j)}{\langle}\, k_\beta|A^{(2)}\big(\boldsymbol{r}_i,\boldsymbol{r}_j\big)|k_\gamma\, \overset{(j)}{\rangle}\; |k_\delta\, \overset{(i)}{\rangle}\overset{(j)}{\langle}\, k_\gamma|\; \overset{(i)}{\langle}\, k_\delta| \\ &= \frac{1}{2}\sum_{\alpha,\beta,\gamma,\delta} A^{(2)}_{k_\alpha k_\beta,k_\gamma k_\delta}\sum_{i\neq j}|k_\alpha\, \overset{(i)}{\rangle}\; |k_\beta\, \overset{(j)}{\rangle}\overset{(j)}{\langle}\, k_\gamma|\; \overset{(i)}{\langle}\, k_\delta| \end{aligned} \tag{6.28}$$

with the two-particle matrix element

$$\begin{aligned} A^{(2)}_{k_\alpha k_\beta,k_\gamma k_\delta} &= \overset{(i)}{\langle}\, k_\alpha|\; \overset{(j)}{\langle}\, k_\beta|A^{(2)}\big(\boldsymbol{r}_i,\boldsymbol{r}_j\big)|k_\gamma\, \overset{(j)}{\rangle}\; |k_\delta\, \overset{(i)}{\rangle} \\ &= \int d^3r\int d^3r'\varphi^*_{k_\alpha}(\boldsymbol{r})\varphi^*_{k_\beta}\big(\boldsymbol{r}'\big)A^{(2)}\big(\boldsymbol{r},\boldsymbol{r}'\big)\varphi_{k_\gamma}\big(\boldsymbol{r}'\big)\varphi_{k_\delta}(\boldsymbol{r}), \end{aligned} \tag{6.29}$$

which is again independent of the particle indices $i, j$, since it is integrated over when forming the matrix element in position representation.

If you apply the operator $\sum_{i\neq j} |k_\alpha \overset{(i)}{\rangle}\, |k_\beta \overset{(j)}{\rangle} \overset{(j)}{\langle}\, k_\gamma|\, \overset{(i)}{\langle}\, k_\delta|$ to a $N_\mathrm{e}$-particle state, you only get something different from zero if the one-particle state $k_\gamma$ and the one-particle state $k_\delta$ were contained in the many-particle state (occupied), and the application of the above-mentioned operator replaces these one-particle states by the one-particle states $k_\alpha, k_\beta$. When this operator is applied, the previously occupied one-particle states $k_\gamma, k_\delta$ become unoccupied and the states $k_\alpha, k_\beta$ become occupied, that is, particles are destroyed in $k_\gamma, k_\delta$ and created again in $k_\alpha, k_\beta$. Therefore, it applies:

$$\sum_{i\neq j} |k_\alpha \overset{(i)}{\rangle}\, |k_\beta \overset{(j)}{\rangle} \overset{(j)}{\langle}\, k_\gamma|\, \overset{(i)}{\langle}\, k_\delta| = c^\dagger_{k_\alpha} c^\dagger_{k_\beta} c_{k_\gamma} c_{k_\delta}. \tag{6.30}$$

This makes it possible to represent the two-particle operator $A^{(2)}$ in occupation number representation with the help of fermion creators and annihilators as:

$$A^{(2)} = \frac{1}{2} \sum_{\alpha,\beta,\gamma,\delta} A^{(2)}_{k_\alpha k_\beta, k_\gamma k_\delta} c^\dagger_{k_\alpha} c^\dagger_{k_\beta} c_{k_\gamma} c_{k_\delta} \tag{6.31}$$

$$A^{(2)}_{k_\alpha k_\beta, k_\gamma k_\delta} = \int d^3r \int d^3r' \varphi^*_{k_\alpha}(\boldsymbol{r}) \varphi^*_{k_\beta}(\boldsymbol{r}') A^{(2)}(\boldsymbol{r}, \boldsymbol{r}') \varphi_{k_\gamma}(\boldsymbol{r}') \varphi_{k_\delta}(\boldsymbol{r}). \tag{6.32}$$

So all operators can be represented as linear combinations of products of creators and annihilators with coefficients that are just the one-particle matrix elements of the one-particle or two-particle operator in the one-particle states.

The operators can also be expressed using the representation-free field operators according to

$$A^{(1)} = \int d^3r \hat{\Phi}^\dagger(\boldsymbol{r}) A^{(1)}(\boldsymbol{r}) \hat{\Phi}(\boldsymbol{r}) \tag{6.33}$$

$$A^{(2)} = \frac{1}{2} \int d^3r \int d^3r' \hat{\Phi}^\dagger(\boldsymbol{r}) \hat{\Phi}^\dagger(\boldsymbol{r}') A^{(2)}(\boldsymbol{r}, \boldsymbol{r}') \hat{\Phi}(\boldsymbol{r}') \hat{\Phi}(\boldsymbol{r}). \tag{6.34}$$

If one inserts here the expansion (6.19) of the field operators with respect to a certain one-particle basis, the relations (6.26), (6.31) are reproduced exactly.

One therefore has the following "recipe" for the construction of one-particle and two-particle operators in occupation number representation:

> Form the expectation values of the one- and two-particle operators with respect to one-particle wave functions $\phi(\boldsymbol{r})$ and then replace the wave functions with field operators $\hat{\Phi}(\boldsymbol{r})$, which fulfill the permutation relations (6.20).

The wave functions of elementary quantum mechanics are therefore replaced by operators, that is, "quantized" by demanding certain commutation relations. Therefore, the somewhat misleading and strange, but common name **"2. Quantization"** for the occupation number representation.

In particular, the Hamilton operator (6.1)–(6.3) can now be written in occupation number representation (2. Quantization) as:

$$H = H_0 + H_1 = \sum_{\alpha} \varepsilon_{k_\alpha} c^\dagger_{k_\alpha} c_{k_\alpha} + \frac{1}{2} \sum_{\alpha\beta,\gamma\delta} u_{k_\alpha k_\beta, k_\gamma k_\delta} c^\dagger_{k_\alpha} c^\dagger_{k_\beta} c_{k_\gamma} c_{k_\delta}, \tag{6.35}$$

where the one-particle eigenbasis of the one-particle Hamilton operator $H_0$ was used and

$$u_{k_\alpha k_\beta, k_\gamma k_\delta} = \int d^3r \int d^3r' \varphi^*_{k_\alpha}(\boldsymbol{r}) \varphi^*_{k_\beta}(\boldsymbol{r}') u(\boldsymbol{r} - \boldsymbol{r}') \varphi_{k_\gamma}(\boldsymbol{r}') \varphi_{k_\delta}(\boldsymbol{r}) \tag{6.36}$$

applies. However, the underlying one-particle basis does not have to be an eigenbasis of $H_0$ or $h_i$; any other basis of the one-particle Hilbert space can be used, then $H_0$ also has non-diagonal elements.

The Hamiltonian operator and other observables in the occupation number representation are defined on the entire Fock space. However, the particle number is conserved, i.e. it commutes with the particle number operator. This simply follows from the fact that in each summand of the expansion with respect to creators and annihilators, as many creators as annihilators occur.

## 6.2 Models of Interacting Electron Systems in Solid State Physics

According to the rules set out in the previous section, a general Hamiltonian operator can be given which describes electrons interacting with each other in a crystal. In first quantization, this purely electronic Hamiltonian operator has the form

$$H = \sum_{i=1}^{N_e} \frac{\boldsymbol{p}_i^2}{2m} + \sum_{i=1}^{N_e} V(\boldsymbol{r}_i) + \frac{1}{2} \sum_{i \neq j} \frac{e^2}{|\boldsymbol{r}_i - \boldsymbol{r}_j|}, \tag{6.37}$$

with periodic (external one-particle) potential

$$V(\boldsymbol{r}) = V(\boldsymbol{r} + \boldsymbol{R}) \tag{6.38}$$

for each lattice vector $\boldsymbol{R}$. According to Chap. 5, the Bloch basis $|n\boldsymbol{k}\sigma\rangle$ is a possible one-particle basis with respect to which we give the Hamiltonian operator in occupation number representation, and according to the rules of the previous section, the Hamiltonian operator in 2. Quantization has the explicit form:

$$\begin{aligned} H = & \sum_{n\boldsymbol{k}\sigma} \varepsilon_n(\boldsymbol{k}) c^\dagger_{n\boldsymbol{k}\sigma} c_{n\boldsymbol{k}\sigma} \\ & + \frac{1}{2} \sum_{(n_1\boldsymbol{k}_1\sigma_1)\ldots(n_4\boldsymbol{k}_4\sigma_4)} u_{(n_1\boldsymbol{k}_1\sigma_1)(n_2\boldsymbol{k}_2\sigma_2),(n_3\boldsymbol{k}_3\sigma_3)(n_4\boldsymbol{k}_4\sigma_4)} c^\dagger_{n_1\boldsymbol{k}_1\sigma_1} c^\dagger_{n_2\boldsymbol{k}_2\sigma_2} c_{n_3\boldsymbol{k}_3\sigma_3} c_{n_4\boldsymbol{k}_4\sigma_4}. \end{aligned} \tag{6.39}$$

Here $n, n_j$ denotes the band indices, $\boldsymbol{k}, \boldsymbol{k}_j$ the wave vectors from the first Brillouin zone and $\sigma, \sigma_j$ the spin of the crystal electrons. The interaction matrix element is explicitly given by

$$\begin{aligned} & u_{(n_1\boldsymbol{k}_1\sigma_1)(n_2\boldsymbol{k}_2\sigma_2),(n_3\boldsymbol{k}_3\sigma_3)(n_4\boldsymbol{k}_4\sigma_4)} \\ & \quad = \int d^3r \int d^3r'\, \psi^*_{n_1\boldsymbol{k}_1}(\boldsymbol{r})\, \psi^*_{n_2\boldsymbol{k}_2}\left(\boldsymbol{r}'\right) \frac{e^2}{|\boldsymbol{r}-\boldsymbol{r}'|}\, \psi_{n_3\boldsymbol{k}_3}\left(\boldsymbol{r}'\right) \psi_{n_4\boldsymbol{k}_4}(\boldsymbol{r})\, \delta_{\sigma_1\sigma_4}\delta_{\sigma_2\sigma_3}, \end{aligned} \tag{6.40}$$

where $\psi_{n\boldsymbol{k}}(\boldsymbol{r})$ denotes the Bloch functions. Since the interaction does not depend on the spin, the spin parts simply give Delta relations when forming the matrix elements, this means physically that the spin is not changed by the Coulomb interaction.

One will almost never consider the above electronic solid-state Hamiltonian operator in full generality, but rather one only takes into account certain parts of this operator explicitly. To neglect certain parts of the full Hamiltonian is characteristic for formulating physical models; here it flows in, which parts are considered to be particularly important for explaining a certain effect. Model-building is also necessary for practical reasons, since one cannot even approximately deal with the Hamiltonian operator in full generality. But even if one could numerically treat the full Hamiltonian operator one day and confirm or predict all experimental results computationally, model-building would still be justified and necessary in order to identify which parts and interactions of the full Hamiltonian operator are responsible for which effects.

One way of modeling is to only consider the outer (valence and conduction) bands and not to take into account the inner, filled bands or to treat the inner electrons as core electrons and thus ions with partially filled inner shells instead of naked atomic nuclei. In the simplest case, only one band, namely the conduction band, is taken into account. Such a **single-band model** is certainly justified for certain metals and has the explicit form:

$$H = \sum_{\boldsymbol{k}\sigma} \varepsilon(\boldsymbol{k})\, c^\dagger_{\boldsymbol{k}\sigma} c_{\boldsymbol{k}\sigma} + \frac{1}{2} \sum_{\sigma,\sigma'} \sum_{\boldsymbol{k}_1\boldsymbol{k}_2,\boldsymbol{k}_3\boldsymbol{k}_4} u_{\boldsymbol{k}_1\boldsymbol{k}_2,\boldsymbol{k}_3\boldsymbol{k}_4}\, c^\dagger_{\boldsymbol{k}_1\sigma} c^\dagger_{\boldsymbol{k}_2\sigma'} c_{\boldsymbol{k}_3\sigma'} c_{\boldsymbol{k}_4\sigma}. \tag{6.41}$$

If one further assumes that the non-interacting (uncorrelated) electrons can be described by (quasi-)free electrons, then:

$$\varepsilon(\boldsymbol{k}) = \frac{\hbar^2 k^2}{2m} \text{ and } \psi_{\boldsymbol{k}}(\boldsymbol{r}) = \frac{1}{\sqrt{V}} e^{i\boldsymbol{k}\boldsymbol{r}} \tag{6.42}$$

(V volume of the system), and the interaction matrix element can be explicitly calculated to

$$\begin{aligned} u_{\boldsymbol{k}_1\boldsymbol{k}_2,\boldsymbol{k}_3\boldsymbol{k}_4} &= \frac{1}{V^2} \int d^3r \int d^3r'\, e^{-i\boldsymbol{k}_1\boldsymbol{r}} e^{-i\boldsymbol{k}_2\boldsymbol{r}'} \frac{e^2}{|\boldsymbol{r}-\boldsymbol{r}'|} e^{i\boldsymbol{k}_3\boldsymbol{r}'} e^{i\boldsymbol{k}_4\boldsymbol{r}} \\ &= \frac{1}{V} \int d^3r \frac{1}{V} \int d^3r''\, e^{i(\boldsymbol{k}_2-\boldsymbol{k}_3)\boldsymbol{r}''} \frac{e^2}{r''} e^{i(\boldsymbol{k}_4-\boldsymbol{k}_1-\boldsymbol{k}_2+\boldsymbol{k}_3)\boldsymbol{r}} \\ &= \frac{4\pi e^2}{V|\boldsymbol{k}_2-\boldsymbol{k}_3|^2} \delta_{\boldsymbol{k}_2-\boldsymbol{k}_3,\boldsymbol{k}_4-\boldsymbol{k}_1}. \end{aligned} \tag{6.43}$$

In the last step, the substitution $\boldsymbol{r}'' = \boldsymbol{r} - \boldsymbol{r}'$ was made and the Fourier transformation of the Coulomb potential was used:

$$\begin{aligned}\int d^3r \frac{e^{i\boldsymbol{qr}}}{r} &= \lim_{\alpha\to 0} \int d^3r \frac{e^{i\boldsymbol{qr}} e^{-\alpha r}}{r} = \lim_{\alpha\to 0} \int_0^\infty drr^2 2\pi \int_{-1}^{+1} due^{iqru} \frac{e^{-\alpha r}}{r} \\ &= \lim_{\alpha\to 0} \int_0^\infty dr \frac{2\pi}{iq} \left(e^{(iq-\alpha)r} - e^{-(iq+\alpha)r}\right) = \lim_{\alpha\to 0} \frac{2\pi}{iq} \left(-\frac{1}{iq-\alpha} - \frac{1}{iq+\alpha}\right) \\ &= \lim_{\alpha\to 0} \frac{2\pi 2iq}{iq(q^2+\alpha^2)} = \frac{4\pi}{q^2}.\end{aligned} \tag{6.44}$$

Here, the integration volume $V$ was pushed to infinity and a convergence-generating factor $e^{-\alpha r}$ was introduced, otherwise the Fourier integral would diverge; at the end of the calculation, the limiting case $\alpha \to 0$ was carried out. The $1/q^2$ -divergence of the Fourier transform of the Coulomb potential is directly related to the slow fall-off $1/r$ of the Coulomb potential in space. From the above calculation of the Fourier transform of the Coulomb potential, it follows that a screened Coulomb potential, e.g. a Yukawa potential $\frac{e^{-\alpha r}}{r}$, has the Fourier transform $\sim \frac{1}{q^2+\alpha^2}$, which no longer diverges for $q \to 0$.

The Hamiltonian operator for free electrons with Coulomb repulsion between them thus has the explicit form:

$$H = \sum_{\boldsymbol{k}\sigma} \frac{\hbar^2 k^2}{2m} c^\dagger_{\boldsymbol{k}\sigma} c_{\boldsymbol{k}\sigma} + \frac{1}{2V} \sum_{\sigma,\sigma'} \sum_{\boldsymbol{kk}'\boldsymbol{q}} \frac{4\pi e^2}{q^2} c^\dagger_{\boldsymbol{k}-\boldsymbol{q}\sigma} c^\dagger_{\boldsymbol{k}'+\boldsymbol{q}\sigma'} c_{\boldsymbol{k}'\sigma'} c_{\boldsymbol{k}\sigma}. \tag{6.45}$$

This model is usually called

**Homogeneous Electron Gas.**

The interaction term has a simple, physically intuitive interpretation, which is also frequently represented diagrammatically as in Fig. 6.1:

An electron with spin σ is scattered from the state $\boldsymbol{k}$ into the state $\boldsymbol{k} - \boldsymbol{q}$ by the interaction, the second electron interacting with the first with spin $\sigma'$ is scattered from the state $\boldsymbol{k}'$ into the state $\boldsymbol{k}' + \boldsymbol{q}$; thus, the momentum $\boldsymbol{q}$ is transferred from the first to the second electron by the interaction, while the spin remains unchanged. Diagrammatically, one draws incoming lines for annihilators, outgoing lines for creators, and usually represents the interaction by a dashed or wavy line; on the

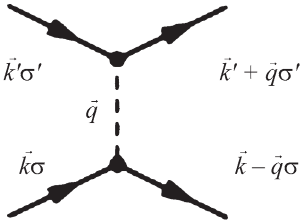

**Fig. 6.1** Diagrammatic representation of the electron–electron interaction (scattering)

lines one usually writes the quantum numbers, the interaction line gets here the transferred momentum as "quantum number".

Another possible one-particle basis is formed by the. Wannier functions $w_n(\boldsymbol{r}-\boldsymbol{R}) = \langle \boldsymbol{r}|n\boldsymbol{R}\rangle$ introduced in Sect.5.4. However, with respect to these, the one-particle part of the Hamiltonian is no longer diagonal. The most general electronic Hamiltonian operator in Wannier representation is given by:

$$\begin{aligned} H = &\sum_{n\boldsymbol{R},n'\boldsymbol{R}',\sigma} t_{n\boldsymbol{R},n'\boldsymbol{R}'} c^\dagger_{n\boldsymbol{R}\sigma} c_{n'\boldsymbol{R}'\sigma} \\ &+ \frac{1}{2}\sum_{\sigma\sigma'} \sum_{(n_1\boldsymbol{R}_1)\dots(n_4\boldsymbol{R}_4)} u_{(n_1\boldsymbol{R}_1)(n_2\boldsymbol{R}_2),(n_3\boldsymbol{R}_3)(n_4\boldsymbol{R}_4)} c^\dagger_{n_1\boldsymbol{R}_1\sigma} c^\dagger_{n_2\boldsymbol{R}_2\sigma'} c_{n_3\boldsymbol{R}_3\sigma'} c_{n_4\boldsymbol{R}_4\sigma} \end{aligned} \tag{6.46}$$

with:

$$\begin{aligned} t_{n\boldsymbol{R},n'\boldsymbol{R}'} &= \langle n\boldsymbol{R}|\left(\frac{\boldsymbol{p}^2}{2m} + V(\boldsymbol{r})\right)|n'\boldsymbol{R}'\rangle \\ &= \int d^3r w_n^*(\boldsymbol{r}-\boldsymbol{R})\left(\frac{\boldsymbol{p}^2}{2m} + V(\boldsymbol{r})\right) w_{n'}\left(\boldsymbol{r}-\boldsymbol{R}'\right) \end{aligned} \tag{6.47}$$

$$\begin{aligned} u_{(n_1\boldsymbol{R}_1)(n_2\boldsymbol{R}_2),(n_3\boldsymbol{R}_3)(n_4\boldsymbol{R}_4)} &= \langle n_1\boldsymbol{R}_1|\langle n_2\boldsymbol{R}_2|\frac{e^2}{|\boldsymbol{r}-\boldsymbol{r}'|}|n_3\boldsymbol{R}_3\rangle|n_4\boldsymbol{R}_4\rangle \\ &= \int d^3r \int d^3r' w^*_{n_1}(\boldsymbol{r}-\boldsymbol{R}_1) w^*_{n_2}\left(\boldsymbol{r}'-\boldsymbol{R}_2\right) \frac{e^2}{|\boldsymbol{r}-\boldsymbol{r}'|} w_{n_3} \\ &\quad \left(\boldsymbol{r}'-\boldsymbol{R}_3\right) w_{n_4}(\boldsymbol{r}-\boldsymbol{R}_4). \end{aligned} \tag{6.48}$$

So far, the Hamiltonian operator of the solid-state electrons is formally exact in Wannier representation again. The modeling now consists again in simplifying assumptions and neglects of individual components of this operator. First, one will again disregard the inner bands, that is, the inner core states and only consider conduction bands or valence and conduction bands. In addition, it is usually assumed that, because of the good localization of the Wannier functions, only a few matrix elements of the one-particle Hamiltonian operator, namely only the diagonal elements as well as the nearest-neighbor and possibly the next-nearest-neighbor matrix elements, can be of importance. And finally, one makes similar simplifying assumptions for the interaction matrix elements. With respect to the one-particle matrix elements, this is quite in line with the tight-binding approximation discussed in Sect. 5.4. In the simplest case, only one band is considered (for metals) and only the matrix elements

$$\begin{aligned} E_0 = t_{\boldsymbol{R},\boldsymbol{R}} &= \langle \boldsymbol{R}|\left(\frac{\boldsymbol{p}^2}{2m} + V(\boldsymbol{r})\right)|\boldsymbol{R}\rangle \quad \text{and} \\ t = t_{\boldsymbol{R},\boldsymbol{R}+\boldsymbol{\Delta}} &= \langle \boldsymbol{R}|\left(\frac{\boldsymbol{p}^2}{2m} + V(\boldsymbol{r})\right)|\boldsymbol{R}+\boldsymbol{\Delta}\rangle. \end{aligned} \tag{6.49}$$

Here, $\boldsymbol{\Delta}$ denotes lattice vectors to nearest neighbors. If one makes analogous assumptions for the interaction matrix element, one is also limited here to diagonal elements and contributions of nearest and at most next-nearest neighbors. Specifically, the following can be taken into account:

$$U = u_{\boldsymbol{RR},\boldsymbol{RR}} = \int d^3r \int d^3r' |w(\boldsymbol{r})|^2 |w(\boldsymbol{r}')|^2 \frac{e^2}{|\boldsymbol{r}-\boldsymbol{r}'|}, \tag{6.50}$$

$$V = u_{\boldsymbol{RR}+\boldsymbol{\Delta},\boldsymbol{R}+\boldsymbol{\Delta}\boldsymbol{R}} = \int d^3r \int d^3r' |w(\boldsymbol{r})|^2 |w(\boldsymbol{r}'-\boldsymbol{\Delta})|^2 \frac{e^2}{|\boldsymbol{r}-\boldsymbol{r}'|} \tag{6.51}$$

$$X = u_{\boldsymbol{RR},\boldsymbol{RR}+\boldsymbol{\Delta}} = \int d^3r \int d^3r' w^*(\boldsymbol{r}) w(\boldsymbol{r}-\boldsymbol{\Delta}) |w(\boldsymbol{r}')|^2 \frac{e^2}{|\boldsymbol{r}-\boldsymbol{r}'|}, \tag{6.52}$$

$$u_{\boldsymbol{RR}+\boldsymbol{\Delta},\boldsymbol{RR}+\boldsymbol{\Delta}} = \int d^3r \int d^3r' w^*(\boldsymbol{r}) w^*(\boldsymbol{r}'-\boldsymbol{\Delta}) \frac{e^2}{|\boldsymbol{r}-\boldsymbol{r}'|} w(\boldsymbol{r}') w(\boldsymbol{r}-\boldsymbol{\Delta}), \tag{6.53}$$

$$u_{\boldsymbol{RR}+\boldsymbol{\Delta},\boldsymbol{RR}+\boldsymbol{\Delta}'} = \int d^3r \int d^3r' w^*(\boldsymbol{r}) w^*(\boldsymbol{r}'-\boldsymbol{\Delta}) \frac{e^2}{|\boldsymbol{r}-\boldsymbol{r}'|} w(\boldsymbol{r}') w(\boldsymbol{r}-\boldsymbol{\Delta}') \tag{6.54}$$

and other contributions in which only Wannier functions localized in neighboring elementary cells occur in the $\boldsymbol{r}$ or $\boldsymbol{r}'$ integration. It should be noted here that it may no longer be justified to form the interaction matrix elements with the bare Coulomb interaction if one makes the one-band approximation. Because the ions can be polarized by the occupied inner shells and thus screening is possible, a screened (and thus short-ranged) Coulomb interaction is probably more realistic than the naked one. An estimate of the order of magnitude of the individual contributions in the case of 3d bands is due to Hubbard[3]; this estimate is probably based on the use of atomic 3d wave functions as an ansatz for the corresponding Wannier functions. According to this, the following orders of magnitude are realistic:

- for the lattice-site diagonal "Hubbard-U": $U = u_{\boldsymbol{RR},\boldsymbol{RR}} = 20\,\text{eV}$,
- for the nearest-neighbor (density-density) interaction $V = u_{\boldsymbol{RR}+\boldsymbol{\Delta},\boldsymbol{R}+\boldsymbol{\Delta}\boldsymbol{R}} = 6\,\text{eV}$,
- for the "conditional hopping" interaction $X = u_{\boldsymbol{RR},\boldsymbol{RR}+\boldsymbol{\Delta}} = 0.5\,\text{eV}$,
- and $u_{\boldsymbol{RR}+\boldsymbol{\Delta},\boldsymbol{RR}+\boldsymbol{\Delta}} = \frac{1}{40}\,\text{eV}$,

where all other contributions are considered to be even smaller; the one-particle "hopping" matrix element is usually estimated to be of the order of $t \approx 1\,\text{eV}$. Therefore, Hubbard proposed to only take into account the dominant interaction contribution, which is the lattice-site diagonal **Hubbard interaction** $U$, which, due to the Pauli principle, can only act between electrons with different spins, but which are in the same atomic state. This[4]

---

[3] J. Hubbard, *1931, †1980, English solid state theorist, works on electron correlation in the homogeneous electron gas and in systems with narrow energy bands, on the application of the functional integral method and on the ferromagnetism of iron, initially at Harwell (England) and from 1976 at the IBM research center in San Jose (California).

**Hubbard Model**

is therefore given by

$$\begin{aligned} H &= \sum_{\boldsymbol{R}\sigma} \sum_{\boldsymbol{\Delta} n.N.} t\, c^{\dagger}_{\boldsymbol{R}\sigma} c_{\boldsymbol{R}+\boldsymbol{\Delta}\sigma} + \frac{U}{2} \sum_{\boldsymbol{R}\sigma\sigma'} c^{\dagger}_{\boldsymbol{R}\sigma} c^{\dagger}_{\boldsymbol{R}\sigma'} c_{\boldsymbol{R}\sigma'} c_{\boldsymbol{R}\sigma} \\ &= \sum_{\boldsymbol{R}\sigma} \sum_{\boldsymbol{\Delta} n.N.} t\, c^{\dagger}_{\boldsymbol{R}\sigma} c_{\boldsymbol{R}+\boldsymbol{\Delta}\sigma} + U \sum_{\boldsymbol{R}} c^{\dagger}_{\boldsymbol{R}\uparrow} c_{\boldsymbol{R}\uparrow} c^{\dagger}_{\boldsymbol{R}\downarrow} c_{\boldsymbol{R}\downarrow}, \end{aligned} \tag{6.55}$$

where the diagonal element $E_0$ was chosen to be 0. The Hubbard model therefore has only two parameters, namely the hopping matrix element $t$, which determines the bandwidth and delocalization of the electrons in the band under consideration if there is no interaction, and the lattice-diagonal Coulomb correlation $U$. It is therefore the simplest possible model for an interacting electron system. An interaction is only taken into account for two electrons at the same lattice site, which then have to have different spin due to the Pauli principle. The actually very long-range Coulomb interaction is therefore replaced by an extremely short-ranged, lattice-diagonal interaction. Despite its simplicity and the existence of two exactly solvable boundary cases $t = 0$ and $U = 0$ and research work over a period of more than 50 years, the Hubbard model is still not satisfactorily treatable today and is still the subject of current research. It contains such interesting properties as metallic behavior, insulator behavior, a metal-insulator transition, antiferromagnetism, possibly also ferromagnetism and superconductivity, depending on the choice of parameters ($t$, $U$, band filling, i.e. number of electrons $Z_e$, lattice type and spatial dimension).

Even when using the above simple estimates of the orders of magnitude of the parameters, one is not quite consistent when taking into account the hopping matrix element $t$ and neglecting the nearest-neighbor interaction $V$. A more realistic approach is therefore the

**extended Hubbard Model**

$$\begin{aligned} H = &\sum_{\boldsymbol{R}\sigma} \sum_{\boldsymbol{\Delta} n.n.} t\, c^{\dagger}_{\boldsymbol{R}\sigma} c_{\boldsymbol{R}+\boldsymbol{\Delta}\sigma} + U \sum_{\boldsymbol{R}} c^{\dagger}_{\boldsymbol{R}\uparrow} c_{\boldsymbol{R}\uparrow} c^{\dagger}_{\boldsymbol{R}\downarrow} c_{\boldsymbol{R}\downarrow} \\ &+ \frac{1}{2} V \sum_{\boldsymbol{R}\boldsymbol{\Delta}} \sum_{\sigma\sigma'} c^{\dagger}_{\boldsymbol{R}\sigma} c_{\boldsymbol{R}\sigma} c^{\dagger}_{\boldsymbol{R}+\boldsymbol{\Delta}\sigma'} c_{\boldsymbol{R}+\boldsymbol{\Delta}\sigma'}. \end{aligned} \tag{6.56}$$

---

[4] In fact, this model was first (work submitted in 1962) proposed by the Swiss physicist Martin Gutzwiller (*1925, †2014), who developed a—still very popular—variation approach for it (Gutzwiller wave function), the first work by Hubbard was only submitted in 1963 and independently and almost simultaneously a work by the Japanese Junjiro Kanamori.

Sometimes one only wants to investigate the effect of the nearest-neighbor interaction; then the spin does not need to be taken into account, because between electrons in Wannier states or atomic states at nearest-neighbor lattice sites the Coulomb interaction is independent of the spin. This leads to the

**spinless Fermion Model**

$$H = \sum_{\boldsymbol{R}} \sum_{\boldsymbol{\Delta} n.N.} t\, c^{\dagger}_{\boldsymbol{R}} c_{\boldsymbol{R}+\boldsymbol{\Delta}} + \frac{1}{2} V \sum_{\boldsymbol{R}\boldsymbol{\Delta}} c^{\dagger}_{\boldsymbol{R}} c_{\boldsymbol{R}} c^{\dagger}_{\boldsymbol{R}+\boldsymbol{\Delta}} c_{\boldsymbol{R}+\boldsymbol{\Delta}} . \tag{6.57}$$

Although the model may not be very realistic because there are no "spinless" fermions, it is interesting because it can describe a phase transition; at least at half-filling, in addition to the homogeneous phase, a phase with spatial super-structure can occur, so that the lattice sites alternately have a larger and smaller mean occupation number for the electrons.

The Hubbard model was proposed by Hubbard to describe the band magnetism in transition metals, where the 3d bands are decisive. Therefore, Hubbard estimated the parameters for 3d states; in narrow bands like the d-bands, the tendency to localization at a single lattice site is more pronounced and therefore the local interaction is particularly important. On the other hand, it is not justified to consider only a single band for 3d-bands, as is the case with the original Hubbard model. In the form (6.55), the model rather describes a narrow s-band, since on the one hand it is only twofold(spin-) degenerate, and on the other hand the hopping matrix elements for all neighboring vectors have been assumed to be the same, which can only be true for an s-like symmetry (spherically symmetric around the lattice site). In addition, one should consider the fivefold degenerate 3d-bands, which are still energetically close and overlapping even after the degeneracy is lifted and in the solid state. More realistic for transition metals is therefore a

**Multiband Hubbard Model**

$$\begin{aligned} H = & \sum_{\boldsymbol{R}\boldsymbol{\Delta}\sigma} \sum_{n,n'} t_{n\boldsymbol{R},n'\boldsymbol{R}+\boldsymbol{\Delta}} d^{\dagger}_{n\boldsymbol{R}\sigma} d_{n'\boldsymbol{R}+\boldsymbol{\Delta}\sigma} \\ & + \frac{1}{2} \sum_{\boldsymbol{R},n,n',\sigma,\sigma'} \left( U_{nn'} d^{\dagger}_{n\boldsymbol{R}\sigma} d_{n\boldsymbol{R}\sigma} d^{\dagger}_{n'\boldsymbol{R}\sigma'} d_{n'\boldsymbol{R}\sigma'} + I d^{\dagger}_{n\boldsymbol{R}\sigma} d_{n'\boldsymbol{R}\sigma} d^{\dagger}_{n'\boldsymbol{R}\sigma'} d_{n\boldsymbol{R}\sigma'} \right) \end{aligned} \tag{6.58}$$

Here, the assumption of a purely lattice-diagonal interaction was retained, but also inter-band interaction (between electrons at the same lattice site, but in different d-states) was taken into account. It has been shown that, precisely because of the explicitly considered exchange term $I$ in the multi-band Hubbard model, magnetic order occurs more easily than in the original single-band Hubbard model.

On the other hand, one can at least argue from a mathematical-theoretical point of view that one should first understand the simple single-band Hubbard model before trusting treatments of the more realistic models.

## 6.3 Hartree-Fock Approximation

A fundamental approximation for the treatment of interacting electron systems not only in solids, but also e.g. in atoms and molecules is the Hartree[5]-Fock approximation (HFA). The basic idea should be familiar to every physicist. The Hartree-Fock approximation can be derived in various ways, namely from the Ritz variation principle of quantum mechanics with a suitable ansatz for the ground state, from a variation principle for the free energy (or the grand canonical potential) and with special, diagrammatic methods of many-body theory. The first method comes from 1st quantization and should also be familiar to experimental physicists; but if one knows the formalism of "2nd quantization", the derivation is even shorter and more intuitive and allows the approximation to be carried out directly on the Hamiltonian operator; this formulation of the Hartree-Fock approximation should therefore be familiar to all theoretically interested and working physicists. The mentioned, special methods of many-body theory for deriving the Hartree-Fock approximation are of particular interest because they immediately reveal how the approximation can be systematically improved. Since the special methods of many-body theory are not to be presupposed or discussed here, only the two other derivations of the Hartree-Fock approximation are given below.

### 6.3.1 Derivation from the Ritz Variation Principle

It is known from quantum mechanics that, for a given Hamiltonian operator $H$, the energy functional

$$E\{\psi\} = \frac{\langle\psi|H|\psi\rangle}{\langle\psi|\psi\rangle} \tag{6.59}$$

assumes its absolute minimum for the ground state $|\psi_0\rangle$ of $H$ (Ritz's[6] variational method for the ground state). If one does not know the ground state, one can make Ansätze for it, which may still depend on certain parameters, and the best approximation for the ground state within the Ansatz is obtained for the $|\psi\rangle$, for which the above energy functional assumes its minimum. If one were to minimize with respect to all states and find the absolute minimum, one would also find the exact ground state. But in practice one cannot vary with respect to all states, but must restrict oneself to a certain subclass of states, and if one has found the state in this class that minimizes the energy functional, one has come closest to the ground state in this class, that is, one has found the best approximation for the ground state within the Ansatz.

---

[5] D.R. Hartree, *1897 in Cambridge (England), †1958 ebd., Prof. for mathematical physics in Manchester and Cambridge, developed quantum mechanical approximation methods and numerical methods for the solution of ballistic and hydrodynamic problems.

[6] Named after W. Ritz, *1878 in Sitten (Switzerland), †1909 in Göttingen, Swiss mathematician and physicist, who in 1907 developed a variational method for solving eigenvalue problems and boundary value problems.

Here we consider the Hamiltonian operator ((6.1)–(6.3)) for interacting electrons in 1st quantization and choose as ansatz for the ground state a Slater determinant of one-particle states, i.e.:

$$|\psi\rangle = \frac{1}{\sqrt{N_\mathrm{e}!}} \sum_{P\in S_{N_\mathrm{e}}} (-1)^{\chi_P} |k_{P(1)} \overset{(1)}{\rangle} \dots |k_{P(N_\mathrm{e})} \overset{(N_\mathrm{e})}{\rangle} \tag{6.60}$$

with initially arbitrary (but orthonormal) one-particle states $|k_\alpha\rangle$. It should be emphasized once again that the eigenstates and, thus, the ground state of the interacting problem can in general, **not** be represented as a Slater determinant of one-particle states. The approximation consists precisely in choosing the ground state as being a Slater determinant and then deriving from the Ritz variation principle a differential equation for the states $|k_\alpha\rangle$, so that the best possible approximation for the ground state results within this ansatz.

If the one-particle states are assumed to be orthonormal, the total state $|\psi\rangle$ is already normalized; therefore, only the matrix element of the Hamilton operator in this state has to be calculated. It holds:

$$\begin{aligned}\langle\psi|H|\psi\rangle &= \frac{1}{N_\mathrm{e}!} \sum_{P\tilde{P}\in S_{N_\mathrm{e}}} (-1)^{\chi_P+\chi_{\tilde{P}}} \\ &\quad \overset{(N_\mathrm{e})}{\langle} k_{\tilde{P}(N_\mathrm{e})}| \dots \overset{(1)}{\langle} k_{\tilde{P}(1)}|H|k_{P(1)} \overset{(1)}{\rangle} \dots |k_{P(N_\mathrm{e})} \overset{(N_\mathrm{e})}{\rangle} \\ &= \langle\psi|H_0|\psi\rangle + \langle\psi|H_1|\psi\rangle\end{aligned} \tag{6.61}$$

Here,

$$\begin{aligned}\langle\psi|H_0|\psi\rangle &= \langle\psi|\sum_{i=1}^{N_\mathrm{e}} h_i|\psi\rangle \\ &= \sum_{i=1}^{N_\mathrm{e}} \frac{1}{N_\mathrm{e}!} \times \sum_{P,\tilde{P}\in S_{N_\mathrm{e}}} (-1)^{\chi_P}(-1)^{\chi_{\tilde{P}}} \\ &\quad \overset{(N_\mathrm{e})}{\langle} k_{\tilde{P}(N_\mathrm{e})}| \dots \overset{(1)}{\langle} k_{\tilde{P}(1)}|h_i|k_{P(1)} \overset{(1)}{\rangle} \dots |k_{P(N_\mathrm{e})} \overset{(N_\mathrm{e})}{\rangle} \\ &= \sum_{i=1}^{N_\mathrm{e}} \frac{1}{N_\mathrm{e}!} \sum_{P,\tilde{P}\in S_{N_\mathrm{e}}} (-1)^{\chi_P+\chi_{\tilde{P}}} \prod_{j=1, j\neq i}^{N_\mathrm{e}} \delta_{P(j),\tilde{P}(j)} \overset{(i)}{\langle} k_{\tilde{P}(i)}|h_i|k_{P(i)} \overset{(i)}{\rangle} .\end{aligned} \tag{6.62}$$

For each fixed particle index $i$, the permutations $P$ and $\tilde{P}$ must therefore agree with each other for all $j \neq i$ because of the orthonormality of the one-particle wave functions, then they must also agree for the last value, i.e. $P(i) = \tilde{P}(i)$, thus $P = \tilde{P}$ and thus:

$$\langle\psi|H_0|\psi\rangle = \sum_{i=1}^{N_\mathrm{e}}\frac{1}{N_\mathrm{e}!}\sum_{P\in S_{N_\mathrm{e}}} \overset{(i)}{\langle}\ k_{P(i)}|h_i|k_{P(i)}\ \overset{(i)}{\rangle}\ . \tag{6.63}$$

If $P$ runs over all $N_\mathrm{e}!$ permutations, $P(i)$ runs over all numbers from 1 to $N_\mathrm{e}$, namely exactly $(N_\mathrm{e}-1)!$ times; because for each fixed $P(i)$, the other $N_\mathrm{e}-1$ indices can still be permuted arbitrarily, for which there are $(N_\mathrm{e}-1)!$ possibilities. Thus it follows:

$$\langle\psi|H_0|\psi\rangle = \sum_{i=1}^{N_\mathrm{e}}\frac{(N_\mathrm{e}-1)!}{N_\mathrm{e}!}\sum_{\alpha=1}^{N_\mathrm{e}} \overset{(i)}{\langle}\ k_\alpha|h_i|k_\alpha\ \overset{(i)}{\rangle} = \sum_{\alpha=1}^{N_\mathrm{e}}\langle k_\alpha|h|k_\alpha\rangle. \tag{6.64}$$

In the last step, it was used again that the matrix element $\overset{(i)}{\langle}\ k_\alpha|h_i|k_\alpha\ \overset{(i)}{\rangle}$ is independent of the particle index $i$, since, for example, in position representation, one simply integrates over the particle coordinate $\boldsymbol{r}_i$. The total energy of the $N_\mathrm{e}$-particle system belonging to the one-particle part of the Hamilton operator $H_0$ is therefore simply additive in the one-particle energies.

The expectation value of $H_1 = \frac{1}{2}\sum_{i\neq j} u_{ij} = \frac{1}{2}\sum_{i<j} u(\boldsymbol{r}_i - \boldsymbol{r}_j)$ is now calculated in the many-particle state assumed to be a Slater determinant of one-particle states:

$$\begin{aligned}
\langle\psi|H_1|\psi\rangle &= \frac{1}{2}\sum_{i\neq j}\frac{1}{N_\mathrm{e}!} \\
&\quad\times \sum_{P,\tilde{P}\in S_{N_\mathrm{e}}} (-1)^{\chi_P}(-1)^{\chi_{\tilde{P}}} \\
&\quad\quad \overset{(N_\mathrm{e})}{\Big\langle}\ k_{\tilde{P}(N_\mathrm{e})}|\ldots \overset{(1)}{\Big\langle}\ k_{\tilde{P}(1)}|u_{ij}|k_{P(1)}\ \overset{(1)}{\Big\rangle}\ \ldots|k_{P(N_\mathrm{e})}\ \overset{(N_\mathrm{e})}{\Big\rangle} \\
&= \frac{1}{2}\sum_{i\neq j}\frac{1}{N_\mathrm{e}!}\sum_{P,\tilde{P}\in S_{N_\mathrm{e}}} (-1)^{\chi_P+\chi_{\tilde{P}}} \\
&\quad\times \prod_{l=1,l\neq i,j}^{N_\mathrm{e}} \delta_{P(l),\tilde{P}(l)}\ \overset{(i)}{\Big\langle}\ k_{\tilde{P}(i)}|\ \overset{(j)}{\Big\langle}\ k_{\tilde{P}(j)}|u_{i,j}|k_{P(j)}\ \overset{(j)}{\Big\rangle}\ |k_{P(i)}\ \overset{(i)}{\Big\rangle}\ .
\end{aligned}$$

The permutations $P, \tilde{P}$ must match for $N_\mathrm{e}-2$ terms ($l\neq i, l\neq j$) because of the orthonormality of the one-particle states. But this time two possibilities remain, namely $P(i)=\tilde{P}(i)$ and $P(j)=\tilde{P}(j)$ or $P(i)=\tilde{P}(j)$ and $P(j)=\tilde{P}(i)$. In the first case, $P, \tilde{P}$ are identical again, in the second they differ just by a permutation (transposition) of the particles $i,j$, which is why $(-1)^{\chi_P}(-1)^{\chi_{\tilde{P}}} = -1$ follows. Therefore:

$$\begin{aligned}
\langle\psi|H_1|\psi\rangle = \frac{1}{2}\sum_{i\neq j}\frac{1}{N_\mathrm{e}!}\sum_{P\in S_{N_\mathrm{e}}} \Bigg[ &\overset{(i)}{\Big\langle}\ k_{P(i)}|\ \overset{(j)}{\Big\langle}\ k_{P(j)}|u_{ij}|k_{P(j)}\ \overset{(j)}{\Big\rangle}\ |k_{P(i)}\ \overset{(i)}{\Big\rangle} \\
- &\overset{(i)}{\Big\langle}\ k_{P(j)}|\ \overset{(j)}{\Big\langle}\ k_{P(i)}|u_{ij}|k_{P(j)}\ \overset{(j)}{\Big\rangle}\ |k_{P(i)}\ \overset{(i)}{\Big\rangle} \Bigg].
\end{aligned} \tag{6.65}$$

If $i \neq j$ is true and $P$ runs over all permutations, $P(i)$ runs over all numbers from $1 \ldots N_\mathrm{e}$ and $P(j)$ over all of these numbers except $P(i)$; all other values of $P(l)$ for $l \neq i, l \neq j$ can be permuted again at will, so that there are $(N_\mathrm{e} - 2)!$ different possibilities. Therefore:

$$\begin{aligned}\langle\psi|H_1|\psi\rangle &= \frac{1}{2}\sum_{i\neq j}\frac{(N_\mathrm{e}-2)!}{N_\mathrm{e}!}\sum_{\alpha\neq\gamma}\\ &\left[ \overset{(i)}{\langle}\, k_\alpha|\, \overset{(j)}{\langle}\, k_\gamma|u_{ij}|k_\gamma \,\overset{(j)}{\rangle}\, |k_\alpha \,\overset{(i)}{\rangle} - \overset{(i)}{\langle}\, k_\gamma|\, \overset{(j)}{\langle}\, k_\alpha|u_{ij}|k_\gamma \,\overset{(j)}{\rangle}\, |k_\alpha \,\overset{(i)}{\rangle}\right].\end{aligned} \tag{6.66}$$

The matrix elements are again independent of $i,j$ (because it has to be integrated over the corresponding coordinates). Therefore, the $i,j$ double sum just results in the factor $N_\mathrm{e}(N_\mathrm{e} - 1)$ and it remains:

$$\begin{aligned}&\langle\psi|H_1|\psi\rangle\\ &= \frac{1}{2}\sum_{\alpha\neq\gamma}\left[ \overset{(i)}{\langle}\, k_\alpha|\, \overset{(j)}{\langle}\, k_\gamma|u_{ij}|k_\gamma \,\overset{(j)}{\rangle}\, |k_\alpha \,\overset{(i)}{\rangle} - \overset{(i)}{\langle}\, k_\gamma|\, \overset{(j)}{\langle}\, k_\alpha|u_{ij}|k_\gamma \,\overset{(j)}{\rangle}\, |k_\alpha \,\overset{(i)}{\rangle}\right]\end{aligned} \tag{6.67}$$

The summation restriction $\gamma \neq \alpha$ can be dropped because for $\gamma = \alpha$ both terms cancel each other.

In general, the quantum numbers and the states consist of an orbital and a spin part, and the interaction potential is the Coulomb potential, i.e.

$$|k_\alpha\rangle = |\tilde{k}_\alpha\sigma\rangle = |\tilde{k}_\alpha\rangle|\sigma\rangle, u_{ij} = \frac{e^2}{|\boldsymbol{r}_i - \boldsymbol{r}_j|}.$$

This gives:

$$\begin{aligned}\langle\psi|H_1|\psi\rangle = \frac{1}{2}\sum_{\alpha,\gamma}\sum_{\sigma,\sigma'}\Bigg[ &\overset{(i)}{\langle}\, \tilde{k}_\alpha\sigma|\, \overset{(j)}{\langle}\, \tilde{k}_\gamma\sigma'|u_{ij}|\tilde{k}_\gamma\sigma' \,\overset{(j)}{\rangle}\, |\tilde{k}_\alpha\sigma \,\overset{(i)}{\rangle}\\ &- \overset{(i)}{\langle}\, \tilde{k}_\gamma\sigma'|\, \overset{(j)}{\langle}\, \tilde{k}_\alpha\sigma|u_{ij}|\tilde{k}_\gamma\sigma' \,\overset{(j)}{\rangle}\, |\tilde{k}_\alpha\sigma \,\overset{(i)}{\rangle}\Bigg].\end{aligned} \tag{6.68}$$

Apparently, in the second summand in the scalar product formation in spin space, Delta relations $\delta_{\sigma\sigma'}$ arise, so that the second summand occurs only for the same spin direction. In particular, in position representation, the entire energy functional now has the form:

$$\begin{aligned}E\{\psi\} = E\{\varphi_{k_\alpha}(\boldsymbol{r})\} &= \sum_\sigma\sum_\alpha\int d^3r\varphi^*_{\tilde{k}_\alpha}(\boldsymbol{r})h(\boldsymbol{r})\varphi_{\tilde{k}_\alpha}(\boldsymbol{r}) + \frac{1}{2}\sum_{\alpha,\gamma,\sigma}\int d^3r\int d^3r'\\ &\frac{e^2}{|\boldsymbol{r}-\boldsymbol{r}'|}\left[\sum_{\sigma'}|\varphi_{\tilde{k}_\alpha}(\boldsymbol{r})|^2|\varphi_{\tilde{k}_\gamma}(\boldsymbol{r}')|^2 - \varphi^*_{\tilde{k}_\alpha}(\boldsymbol{r})\varphi^*_{\tilde{k}_\gamma}(\boldsymbol{r}')\varphi_{\tilde{k}_\alpha}(\boldsymbol{r}')\varphi_{\tilde{k}_\gamma}(\boldsymbol{r})\right].\end{aligned} \tag{6.69}$$

This result (6.69) for the energy functional within the Hartree-Fock approximation can also be derived more quickly and compactly (without permutations, etc.), if one is familiar with the formalism of the occupation number representation (2nd quantization) and the working with (fermion) creation and annihilation operators. Then the Hartree-Fock approximation for the many-particle state simply reads as

$$|\psi\rangle = \prod_{\lambda\in I} c^{\dagger}_{k_\lambda}|0\rangle, \tag{6.70}$$

where $I$ is a $N_{\mathrm{e}}$ -element subset of the quantum numbers (or quantum number indices) and $|0\rangle$ is the vacuum state. Then it follows:

$$\begin{aligned}\langle\psi|H_0|\psi\rangle &= \sum_{\alpha,\beta} h_{k_\alpha k_\beta}\langle 0|\prod_{\lambda\in I} c_{k_\lambda} c^{\dagger}_{k_\alpha} c_{k_\beta}\prod_{\mu\in I} c^{\dagger}_{k_\mu}|0\rangle = \sum_{\alpha\in I} h_{k_\alpha k_\alpha}\\ &= \sum_{\alpha\in I}\langle k_\alpha|h|k_\alpha\rangle,\end{aligned} \tag{6.71}$$

which obviously agrees with (6.64). In the last step it was used that the annihilation operator $c_{k_\beta}$ can only give something different from 0 if the corresponding state $|k_\beta\rangle$ was occupied, i.e. if $k_\beta \in I$ holds. Subsequently, all states from $I$ are annihilated from the left, i.e. they must be occupied, then $k_\alpha = k_\beta$ must also be true. Analogously, it follows for the interaction term:

$$\langle\psi|H_1|\psi\rangle = \frac{1}{2}\sum_{\alpha\beta\gamma\delta\in I} u_{k_\alpha k_\beta, k_\gamma k_\delta}\langle 0|\prod_{\lambda\in I} c_{k_\lambda} c^{\dagger}_{k_\alpha} c^{\dagger}_{k_\beta} c_{k_\gamma} c_{k_\delta}\prod_{\mu\in I} c^{\dagger}_{k_\mu}|0\rangle. \tag{6.72}$$

Now the two annihilation operators $c_{k_\gamma} c_{k_\delta}$ act on a product state and only give something non-vanishing if $\gamma, \delta \in I$ holds, then these two states from $I$ are unoccupied and must be occupied again first (by the action of $c^{\dagger}_{k_\alpha} c^{\dagger}_{k_\beta}$), so that after the action of all annihilation operators from $I$ (in the "bra" state) a finite value remains. But now there are two possibilities $\alpha = \delta$ and $\beta = \gamma$ or $\alpha = \gamma$ and $\beta = \delta$. In the second case, a permutation must be carried out once, so that the annihilation operator and the creation operator are directly next to each other (and thus compensate each other). As a result, finally:

$$\langle\psi|H_1|\psi\rangle = \frac{1}{2}\sum_{\alpha,\gamma\in I}\left(u_{k_\alpha k_\gamma, k_\gamma k_\alpha} - u_{k_\alpha k_\gamma, k_\alpha k_\gamma}\right) \tag{6.73}$$

which agrees with (6.67).

The energy functional depends on all particle wave functions of the approach. The goal is to find the optimal wave functions that minimize the functional. For this, the variation of the energy functional must disappear. We vary for fixed $k_\beta = (\tilde{k}_\beta\sigma)$ with respect to the state $\langle k_\beta|$ or according to the wave function $\varphi^{*}_{\tilde{k}_\beta}(\boldsymbol{r})$ under the condition of the normality of the states, which we add to the energy functional with Lagrange multipliers $\varepsilon_\beta$, i.e.

$$\delta\left(E\{\varphi_{\tilde{k}_\gamma}\} - \varepsilon_\beta\left(\int d^3r|\varphi_{\tilde{k}_\beta}(\boldsymbol{r})|^2 - 1\right)\right) = 0 \tag{6.74}$$

is determined by variation with respect to a wave function for fixed $(\tilde{k}_\beta\sigma)$. In the second interaction contribution, this wave function occurs twice, namely in the γ- and in the α-summation. The variation then results in:

$$\begin{aligned} h(\boldsymbol{r})\varphi_{\tilde{k}_\beta}(\boldsymbol{r}) + \sum_{\gamma,\sigma'}\int d^3r'\frac{e^2|\varphi_{\tilde{k}_\gamma}(\boldsymbol{r}')|^2}{|\boldsymbol{r}'-\boldsymbol{r}|}\varphi_{\tilde{k}_\beta}(\boldsymbol{r}) \\ -\sum_{\gamma}\int d^3r'\varphi^*_{\tilde{k}_\gamma}(\boldsymbol{r}')\frac{e^2}{|\boldsymbol{r}-\boldsymbol{r}'|}\varphi_{\tilde{k}_\beta}(\boldsymbol{r}')\varphi_{\tilde{k}_\gamma}(\boldsymbol{r}) = \varepsilon_\beta\varphi_{\tilde{k}_\beta}(\boldsymbol{r}). \end{aligned} \tag{6.75}$$

These are the **Hartree-Fock equations** for determining the one-particle wave functions, with which the Slater determinant gives the best approximation for the true ground state. Without interaction, the Schrödinger equation for the one-particle wave functions results. From the interaction there are two contributions, which one also calls **Hartree contribution** and **Fock-** or **exchange contribution**, and if only the first summand is taken into account, the approximation is also called **Hartree approximation** and the above equations without the last term on the left hand side are called **Hartree equations**. The Hartree and the Hartree-Fock equations represent $N_e$ nonlinear equations for the one-particle wave functions, which can only be solved by iteration in practice. The Hartree contribution has a simple, physically intuitive interpretation: The electrons that occupy the quantum mechanical one-particle wave functions with quantum numbers $k_\gamma$, cause a charge density

$$\rho(\boldsymbol{r}') = e\sum_{\gamma,\sigma'}|\varphi_{\tilde{k}_\gamma}(\boldsymbol{r}')|^2 \tag{6.76}$$

and this charge density creates at the location $\boldsymbol{r}$ an electrostatic potential

$$\Phi(\boldsymbol{r}) = \int d^3r'\frac{\rho(\boldsymbol{r}')}{|\boldsymbol{r}-\boldsymbol{r}'|} = \int d^3r'\sum_{\gamma,\sigma'}|\varphi_{\tilde{k}_\gamma}(\boldsymbol{r}')|^2\frac{e}{|\boldsymbol{r}-\boldsymbol{r}'|}. \tag{6.77}$$

The electron in the state $k_\beta$ at the location $\boldsymbol{r}$ experiences this effective potential created by all other electrons, this enters the Schrödinger equation like an external potential. The difference to a simple one-particle problem lies in the fact that the exact strength of this potential, which depends on the distribution of the electrons in the system and thus on the wave functions to be determined, can only be calculated by solving the Hartree equations themselves. Such equations form a so called **self-consistency problem**. Approximations of the type of the Hartree and the Hartree-Fock approximation, in which a single particle is considered in an effective field created by all other particles, are also referred to as **"Mean-Field Approximation"** or **Molecular Field Approximation**.

The Fock term is even more complicated than the Hartree contribution, because the wave function to be determined $\varphi_{\tilde{k}_\beta}$ is in the integrand. The exchange potential is therefore a non-local potential, the wave function to be determined $\varphi_{\tilde{k}_\beta}(\boldsymbol{r})$ enters the equations not only at the point $\boldsymbol{r}$, but also at all other locations $\boldsymbol{r}'$. This is therefore a complicated, nonlinear integro-differential equation. The exchange (Fock) term has no classical, physically intuitive analogue (like the Hartree contribution), but it is a quantum effect and a direct consequence of the indistinguishability of the particles. It arises in the quantum mechanical treatment automatically if one starts from correctly antisymmetrized wave functions. If one were to work with a simple product ansatz of one-particle wave functions, the Hartree term would also arise, but not the Fock term.

The energies $\varepsilon_\beta$ were originally introduced as Lagrange parameters. If one interprets the Hartree-Fock equations as a one-electron Schrödinger equation in the effective potential, the $\varepsilon_\beta$ take on the meaning of energy eigenvalues. However, they are not one-particle energies in the usual sense, as is particularly evident from the fact that the total energy does not correspond to the sum of the effective one-particle energies:

$$E_{HF} \neq \sum_{\alpha \in I} \varepsilon_\alpha . \tag{6.78}$$

If one multiplies the Hartree-Fock equations (6.75) on both sides by $\varphi^*_{\tilde{k}_\beta}(\boldsymbol{r})$, integrates over $\boldsymbol{r}$ and sums over $\beta$ and spin, one obtains:

$$\begin{aligned}\sum_{\beta\sigma} \varepsilon_\beta = \sum_{\sigma}\sum_{\beta} \int d^3r |\varphi_{\tilde{k}_\beta}(\boldsymbol{r})|^2 h(\boldsymbol{r}) + \sum_{\beta,\gamma,\sigma} \int d^3r \int d^3r' \frac{e^2}{|\boldsymbol{r}-\boldsymbol{r}'|} \\ \left[ \sum_{\sigma'} |\varphi_{\tilde{k}_\beta}(\boldsymbol{r})|^2 |\varphi_{\tilde{k}_\gamma}(\boldsymbol{r}')|^2 - \varphi^*_{\tilde{k}_\beta}(\boldsymbol{r}) \varphi^*_{\tilde{k}_\gamma}(\boldsymbol{r}') \varphi_{\tilde{k}_\beta}(\boldsymbol{r}') \varphi_{\tilde{k}_\gamma}(\boldsymbol{r}) \right].\end{aligned} \tag{6.79}$$

A comparison with the Eq. (6.69) for the energy functional, which, when the wave function is correctly determined, gives the energy in the Hartree-Fock state, shows that the interaction energy is counted twice when summing the Hartree-Fock one-particle energies. The reason for this is that, for a given state $\beta$, the interaction with the electrons in all other occupied states $\gamma$ has been taken into account within the approximation. But if one sums over all $\beta$, one also takes into account, from the point of view of the other electron with quantum number $\gamma$, the interaction with the electron in state $\beta$, i.e. one counts all interaction energies twice. It therefore follows that

$$\sum_{\beta\sigma} \varepsilon_\beta = E\{\psi\} + E_{WW} = E\{\psi\} + \langle\psi|H_1|\psi\rangle = \langle\psi|H_0|\psi\rangle + 2\langle\psi|H_1|\psi\rangle. \tag{6.80}$$

The following consideration, however, shows which physical meaning we can still attribute to the Hartree-Fock one-particle energies. Given an interacting $N_\mathrm{e}$-particle system, into which another particle $N_\mathrm{e}+1$ is brought. Under the assumption that the states of the first $N_\mathrm{e}$ particles remain unchanged, it follows:

$$\begin{aligned}
E_{HF}^{(N_e+1)} &= \sum_{\alpha=1}^{N_e+1} \langle k_\alpha | h(\boldsymbol{r}) | k_\alpha \rangle \\
&\quad + \frac{1}{2} \sum_{\alpha \neq \gamma} \left[ \langle k_\alpha | \langle k_\gamma | \frac{e^2}{|\boldsymbol{r}-\boldsymbol{r}'|} | k_\gamma \rangle | k_\alpha \rangle - \langle k_\alpha | \langle k_\gamma | \frac{e^2}{|\boldsymbol{r}-\boldsymbol{r}'|} | k_\alpha \rangle | k_\gamma \rangle \right] \\
&= E_{HF}^{(N_e)} + \langle k_{N_e+1} | h(\boldsymbol{r}) | k_{N_e+1} \rangle \\
&\quad + \frac{1}{2} \sum_{\gamma \leq N_e} \left[ \langle k_{N_e+1} | \langle k_\gamma | \frac{e^2}{|\boldsymbol{r}-\boldsymbol{r}'|} | k_\gamma \rangle | k_{N_e+1} \rangle - \langle k_{N_e+1} | \langle k_\gamma | \frac{e^2}{|\boldsymbol{r}-\boldsymbol{r}'|} | k_{N_e+1} \rangle | k_\gamma \rangle \right] \\
&\quad + \frac{1}{2} \sum_{\alpha \leq N_e} \left[ \langle k_\alpha | \langle k_{N_e+1} | \frac{e^2}{|\boldsymbol{r}-\boldsymbol{r}'|} | k_{N_e+1} \rangle | k_\alpha \rangle - \langle k_\alpha | \langle k_{N_e+1} | \frac{e^2}{|\boldsymbol{r}-\boldsymbol{r}'|} | k_\alpha \rangle | k_{N_e+1} \rangle \right] \\
&= E_{HF}^{(N_e)} + \varepsilon_{k_{N_e+1}} .
\end{aligned} \tag{6.81}$$

The Hartree-Fock one-particle energy $\varepsilon_{k_{Ne+1}}$ is therefore just the energy that has to be expended to add this $(N_e+1)$th-particle to the $N_e$-particle system. This statement is also referred to as the **Koopmans theorem**[7].

### 6.3.2 Derivation from a Variational Principle for the Grand Canonical Potential

The fundamental quantity that one has to calculate for a given Hamiltonian operator $H$ is the partition function or the grand canonical potential

$$\Phi_{GK} = -k_B T \ln Z_{GK} = -k_B T \ln \mathrm{Tr}(e^{-\beta(H-\mu N)}). \tag{6.82}$$

However, for a Hamiltonian operator with interaction, the partition function cannot be calculated rigorously in general, but very easily without interaction, as is known from the lectures on Statistical Physics and from Sect. 5.8. Therefore, one tries to approximate the actual Hamiltonian operator of the interacting electron system

$$H = \sum_k \varepsilon_k c_k^\dagger c_k + \frac{1}{2} \sum_{k_1 k_2, k_3 k_4} u_{k_1 k_2, k_3 k_4} c_{k_1}^\dagger c_{k_2}^\dagger c_{k_3} c_{k_4} \tag{6.83}$$

---

[7] T. Koopmans, *1910 in the Netherlands, †1985 in New Haven (Connecticut), Dutch physicist and economist, studied mathematics and physics in Utrecht from 1927 to 1932, 1933 publication on the "Koopmans theorem", then studied economics in Amsterdam and obtained his doctorate in 1936 in Leiden, worked as an economist on optimization problems, 1940 emigrated to the USA and worked in Princeton, later in Chicago and at Yale University, from 1946 US citizen, Nobel Prize in Economics 1975 (for contributions to the optimal use of resources).

by the best possible effective single-particle Hamiltonian operator

$$H_{\text{eff}} = \sum_k x_k c_k^\dagger c_k \tag{6.84}$$

with still to be determined effective single-particle energies $x_k$. One still needs a criterion for what one understands by "as good as possible". This one gets from a

**Variational principal for the grand cananonical potential**

Consider on the set of all ( statistical operators ρ (on the given Fock space) the functional

$$\Phi[\rho] = \text{Tr}(\rho(H - \mu N + k_B T \ln \rho)). \tag{6.85}$$

In particular, for the grand canonical statistical operator

$$\rho_{GK} = \frac{1}{Z_{GK}} e^{-\beta(H-\mu N)}$$

this functional fulfills

$$\begin{aligned} \Phi[\rho_{GK}] &= \text{Tr}\{\rho_{GK}[H - \mu N + k_B T(-\beta(H - \mu N)) - k_B T \ln Z_{GK}]\} \\ &= -k_B T \ln Z_{GK} = \Phi. \end{aligned} \tag{6.86}$$

, i.e. the functional $\Phi[\rho]$ takes the value of the grand canonical potential just for the grand canonical statistical operator. Now the following inequality is valid for any statistical operator *ρ:*

$$\Phi[\rho_{GK}] \leq \Phi[\rho]. \tag{6.87}$$

The functional $\Phi[\rho]$ therefore takes its absolute minimum for the grand canonical statistical operator and the value of the functional then corresponds to the grand canonical potential. For the proof of the above inequality, we first note that for any two statistical operators $\rho$, $\rho'$ it applies:

$$\text{Tr}(\rho \ln \rho) \geq \text{Tr}(\rho \ln \rho'). \tag{6.88}$$

Namely let $\{|\nu\rangle\}$ be eigenbasis of $\rho'$, $\{|\alpha\rangle\}$ eigenbasis of ρ, then it is valid:

$$\begin{aligned} \text{Tr}\big[\rho(\ln \rho' - \ln \rho)\big] &= \sum_\alpha \big[\rho_\alpha(\langle\alpha|\ln \rho'|\alpha\rangle - \ln \rho_\alpha)\big] = \\ \sum_{\alpha,\nu} \rho_\alpha |\langle\alpha|\nu\rangle|^2 (\ln \rho'_\nu - \ln \rho_\alpha) &= \sum_{\alpha,\nu} \rho_\alpha |\langle\alpha|\nu\rangle|^2 \ln \frac{\rho'_\nu}{\rho_\alpha} \leq \sum_{\alpha,\nu} \rho_\alpha |\langle\alpha|\nu\rangle|^2 \left(\frac{\rho'_\nu}{\rho_\alpha} - 1\right) \\ &= \sum_{\alpha,\nu} (\rho'_\nu |\langle\alpha|\nu\rangle|^2 - \rho_\alpha |\langle\alpha|\nu\rangle|^2) = \text{Tr}\rho' - \text{Tr}\rho = 0, \end{aligned} \tag{6.89}$$

where the fundamental (trivial) inequality $\ln x \leq x - 1$ has been used. Therefore, it follows:

$$\begin{aligned}\Phi[\rho] &= \mathrm{Tr}(\rho(H-\mu N)) + k_B T \mathrm{Tr}(\rho \ln \rho) \\ &\geq \mathrm{Tr}(\rho(H-\mu N)) + k_B T \mathrm{Tr}(\rho \ln \rho_{GK}) \\ &= \mathrm{Tr}(\rho(H-\mu N)) - k_B T \beta \mathrm{Tr}(\rho(H-\mu N)) - k_B T \mathrm{Tr}(\rho \ln Z_{GK}) \\ &= -k_B T \ln Z_{GK} = \Phi = \Phi[\rho_{GK}].\end{aligned} \tag{6.90}$$

Consider now $\rho_{GK}$ the grand-canonical statistical operator to the Hamiltonian $H$ with interaction and with grand canonical potential $\Phi = \Phi[\rho_{GK}] = \Phi_H$ and the grand-canonical statistical operator

$$\rho_{\text{eff}} = \frac{1}{Z_{\text{eff}}} e^{-\beta(H_{\text{eff}}-\mu N)} \tag{6.91}$$

of the effective Hamiltonian (6.84) with grand canonical potential $\Phi_{\text{eff}} = -k_B T \ln Z_{\text{eff}}$. Then it is valid:

$$\begin{aligned}\Phi[\rho_{\text{eff}}] &= \mathrm{Tr}(\rho_{\text{eff}}(H - \mu N + k_B T \ln \rho_{\text{eff}})) \\ &= \mathrm{Tr}(\rho_{\text{eff}}[H - \mu N + k_B T(-\beta(H_{\text{eff}} - \mu N) - \ln Z_{\text{eff}})]).\end{aligned} \tag{6.92}$$

This results in:

$$\boxed{\Phi[\rho_{\text{eff}}] = \langle H - H_{\text{eff}} \rangle_{\text{eff}} + \Phi_{\text{eff}} \geq \Phi_H}. \tag{6.93}$$

Here the thermal averages have to be calculated with the effective Hamiltonian-, i. e.:

$$\langle A \rangle_{\text{eff}} = \frac{1}{Z_{\text{eff}}} \mathrm{Tr}\left(A e^{-\beta(H_{\text{eff}}-\mu N)}\right). \tag{6.94}$$

We now have to determine the effective one-particle Hamiltonian operator $H_{\text{eff}}$ for which $\Phi[\rho_{\text{eff}}]$ is minimal, then this functional comes closest to the actual interaction Hamiltonian operator and thus to the desired grand canonical potential. To do this, we use the Hamiltonian operator $H$ and $H_{\text{eff}}$ from (6.83), (6.84) for the calculation of the above functional and minimize with respect to the still unknown single-particle parameters of $H_{\text{eff}}$ and obtain:

$$\Phi[\rho_{\text{eff}}] = \Phi_{\text{eff}} + \sum_k (\varepsilon_k - x_k) \left\langle c_k^\dagger c_k \right\rangle_{\text{eff}} + \frac{1}{2} \sum_{k_1 k_2, k_3 k_4} u_{k_1 k_2, k_3 k_4} \left\langle c_{k_1}^\dagger c_{k_2}^\dagger c_{k_3} c_{k_4} \right\rangle_{\text{eff}} \tag{6.95}$$

Now for quartic expectation values of fermion creators and annihilators with respect to a non-interacting (one-particle) Hamiltonian operator it is valid:

$$\begin{aligned}\left\langle c_{k_1}^\dagger c_{k_2}^\dagger c_{k_3} c_{k_4} \right\rangle_{\text{eff}} &= \left\langle c_{k_2}^\dagger c_{k_3} \right\rangle_{\text{eff}} \delta_{k_2 k_3} \left\langle c_{k_1}^\dagger c_{k_4} \right\rangle_{\text{eff}} \delta_{k_1 k_4} \\ &\quad - \left\langle c_{k_2}^\dagger c_{k_4} \right\rangle_{\text{eff}} \delta_{k_2 k_4} \left\langle c_{k_1}^\dagger c_{k_3} \right\rangle_{\text{eff}} \delta_{k_1 k_3},\end{aligned} \tag{6.96}$$

as can be easily shown as an exercise. Then minimizing $\Phi[\rho_{\text{eff}}]$ with respect to the still unknown effective one-particle parameters $x_k$ of the effective Hamiltonian yields:

$$\begin{aligned}\frac{\partial \Phi[\rho_{\text{eff}}]}{\partial x_k} &= \frac{\partial \Phi_{\text{eff}}}{\partial x_k} - \left\langle c_k^\dagger c_k \right\rangle_{\text{eff}} + \sum_{k'} (\varepsilon_{k'} - x_{k'}) \frac{\partial}{\partial x_k} \left\langle c_{k'}^\dagger c_{k'} \right\rangle_{\text{eff}} \\ &+ \frac{1}{2} \sum_{k_1,k_2} u_{k_1k_2,k_2k_1} \left( \left\langle c_{k_2}^\dagger c_{k_2} \right\rangle_{\text{eff}} \frac{\partial}{\partial x_k} \left\langle c_{k_1}^\dagger c_{k_1} \right\rangle_{\text{eff}} + \left\langle c_{k_1}^\dagger c_{k_1} \right\rangle_{\text{eff}} \frac{\partial}{\partial x_k} \left\langle c_{k_2}^\dagger c_{k_2} \right\rangle_{\text{eff}} \right) \\ &- \frac{1}{2} \sum_{k_1,k_2} u_{k_1k_2,k_1k_2} \left( \left\langle c_{k_2}^\dagger c_{k_2} \right\rangle_{\text{eff}} \frac{\partial}{\partial x_k} \left\langle c_{k_1}^\dagger c_{k_1} \right\rangle_{\text{eff}} + \left\langle c_{k_1}^\dagger c_{k_1} \right\rangle_{\text{eff}} \frac{\partial}{\partial x_k} \left\langle c_{k_2}^\dagger c_{k_2} \right\rangle_{\text{eff}} \right).\end{aligned} \tag{6.97}$$

Now because of

$$\frac{\partial}{\partial x_k} \Phi_{\text{eff}} = \frac{\partial}{\partial x_k} \left( -k_B T \ln Sp e^{-\beta \sum_{k'} (x_{k'} - \mu) c_{k'}^\dagger c_{k'}} \right) = \left\langle c_k^\dagger c_k \right\rangle_{\text{eff}}. \tag{6.98}$$

and the symmetry of the interaction matrix elements

$$u_{k_1k_2,k_3k_4} = u_{k_2k_1,k_4k_3} \neq u_{k_2k_1,k_3k_4} \tag{6.99}$$

one obtains, after renaming the summation indices

$$0 = \sum_{k_1} \frac{\partial \left\langle c_{k_1}^\dagger c_{k_1} \right\rangle_{\text{eff}}}{\partial x_k} \left( \varepsilon_{k_1} - x_{k_1} + \sum_{k_2} (u_{k_1k_2,k_2k_1} - u_{k_1k_2,k_1k_2}) \left\langle c_{k_2}^\dagger c_{k_2} \right\rangle_{\text{eff}} \right). \tag{6.100}$$

One possible solution of this minimization condition is apparently:

$$x_k = \varepsilon_k + \sum_{k_2} (u_{kk_2,k_2k} - u_{kk_2,kk_2}) \left\langle c_{k_2}^\dagger c_{k_2} \right\rangle_{\text{eff}} \tag{6.101}$$

The best effective single-particle Hamiltonian operator is therefore given by:

$$H_{\text{eff}} = \sum_k \left( \varepsilon_k + \sum_{k_2} (u_{kk_2,k_2k} - u_{kk_2,kk_2}) \left\langle c_{k_2}^\dagger c_{k_2} \right\rangle_{\text{eff}} \right) c_k^\dagger c_k. \tag{6.102}$$

This Hamiltonian operator comes as close as possible to the actually interesting interacting Hamiltonian operator in that the value of the functional $\Phi[\rho]$ for the to $H_{\text{eff}}$ corresponding $\rho_{\text{eff}}$ is minimal and thus comes closest to the grand canonical potential of $H$, at least on the set of all possible **single-particle Hamiltonian operators**. The parameters $x_k$ still have to be determined self-consistently; they depend in particular on the thermodynamic occupation numbers of the states $k_2$, which in turn have to be determined from $H_{\text{eff}}$.

For the ground state, the result (6.101) for the diagonal elements of the effective Hamiltonian operator is equivalent to the effective Hartree-Fock Schrödinger equation (6.75) derived in the previous subsection; this can be written in a representation-free way as

$$\hat{h}|k\rangle + \sum_{k_2 \in I} (\langle k_2|u|k_2\rangle|k\rangle - \langle k_2|u|k\rangle|k_2\rangle) = \tilde{\varepsilon}_k|k\rangle, \tag{6.103}$$

where only over all occupied (occurring in the Slater determinant or the index set $I$) states $|k_2\rangle$ is summed, i. e. for $T = 0$ over all states with $\tilde{\varepsilon}_k \leq E_F$. This summation restriction can also be expressed by the Fermi factor $\langle c^\dagger_{k_2} c_{k_2}\rangle$. With (6.102) one also has the generalization of the Hartee-Fock approximation, which originally (and as described in Sect. 6.3.1) was only an approximation for the ground state, to finite temperatures.

You can construct the Hartree-Fock approximation (HFA) according to the above result simply from the original Hamiltonian operator in 2nd quantization according to the rule that you replace the product of the four fermion operators (2 creators and 2 annihilators) in the interaction term in all possible ways by the product of one creator and one annihilator multiplied with the thermodynamic expectation value of the two remaining fermion operators. The decoupling rule, which leads to the Hartree-Fock approximation, is therefore easy to remember and reads:

$$\begin{aligned} c^\dagger_{k_1} c^\dagger_{k_2} c_{k_3} c_{k_4} \rightarrow & \left\langle c^\dagger_{k_2} c_{k_3} \right\rangle c^\dagger_{k_1} c_{k_4} + \left\langle c^\dagger_{k_1} c_{k_4} \right\rangle c^\dagger_{k_2} c_{k_3} \\ & - \left\langle c^\dagger_{k_1} c_{k_3} \right\rangle c^\dagger_{k_2} c_{k_4} - \left\langle c^\dagger_{k_2} c_{k_4} \right\rangle c^\dagger_{k_1} c_{k_3} . \end{aligned} \tag{6.104}$$

If one assumes that the effective Hamiltonian operator is to be diagonal in $k$ like the one-particle term, one obtains Delta relations $\delta_{k_1 k_4}\delta_{k_2 k_3}$ for the first two and $\delta_{k_1 k_3}\delta_{k_2 k_4}$ for the second two summands and it follows:

$$\begin{aligned} H \rightarrow H_{\text{eff}} = & \sum_k \varepsilon_k c^\dagger_k c_k \\ & + \frac{1}{2} \sum_{k_1 k_2} \Big( u_{k_1 k_2, k_2 k_1} \left\langle c^\dagger_{k_1} c_{k_1} \right\rangle c^\dagger_{k_2} c_{k_2} + u_{k_1 k_2, k_2 k_1} \left\langle c^\dagger_{k_2} c_{k_2} \right\rangle c^\dagger_{k_1} c_{k_1} \\ & - u_{k_1 k_2, k_1 k_2} \left\langle c^\dagger_{k_1} c_{k_1} \right\rangle c^\dagger_{k_2} c_{k_2} - u_{k_1 k_2, k_1 k_2} \left\langle c^\dagger_{k_2} c_{k_2} \right\rangle c^\dagger_{k_1} c_{k_1} \Big) . \end{aligned} \tag{6.105}$$

Simple renumbering leads back to the same effective Hamiltonian operator as before. In later applications of the Hartree-Fock approximation we will always simply make this decoupling of the Hamiltonian operator in 2nd quantization (and no longer minimize the functional $\Phi[\rho]$).

Finally, it should be noted that the approximation for the grand canonical potential **is not** the grand canonical potential of the effective Hamiltonian operator, but the value of the functional $\Phi[\rho_{\text{eff}}]$; this came closest to the actual grand canonical potential . The difference to $\Phi_{\text{eff}}$ is given by t:

$$\begin{aligned}\Phi[\rho] &= \langle H - H_{\mathrm{eff}}\rangle_{\mathrm{eff}} + \Phi_{\mathrm{eff}} \\ &= \Phi_{\mathrm{eff}} + \frac{1}{2}\sum_{k_1k_2k_3k_4} u_{k_1k_2,k_3k_4}\left\langle c^{\dagger}_{k_1}c^{\dagger}_{k_2}c_{k_3}c_{k_4}\right\rangle_{\mathrm{eff}} \\ &\quad - \sum_{k_1k_2} u_{k_1k_2,k_2k_1}\left\langle c^{\dagger}_{k_1}c_{k_1}\right\rangle_{\mathrm{eff}}\left\langle c^{\dagger}_{k_2}c_{k_2}\right\rangle_{\mathrm{eff}} + \sum_{k_1k_2} u_{k_1k_2,k_1k_2}\left\langle c^{\dagger}_{k_1}c_{k_1}\right\rangle_{\mathrm{eff}}\left\langle c^{\dagger}_{k_2}c_{k_2}\right\rangle_{\mathrm{eff}} \\ &= \Phi_{\mathrm{eff}} + \frac{1}{2}\sum_{k_1k_2}(u_{k_1k_2,k_2k_1} - u_{k_1k_2,k_1k_2})\left\langle c^{\dagger}_{k_1}c_{k_1}\right\rangle_{\mathrm{eff}}\left\langle c^{\dagger}_{k_2}c_{k_2}\right\rangle_{\mathrm{eff}} \\ &\quad - \sum_{k_1k_2}(u_{k_1k_2,k_2k_1} - u_{k_1k_2,k_1k_2})\left\langle c^{\dagger}_{k_1}c_{k_1}\right\rangle_{\mathrm{eff}}\left\langle c^{\dagger}_{k_2}c_{k_2}\right\rangle_{\mathrm{eff}} \\ &= \Phi_{\mathrm{eff}} - \frac{1}{2}\sum_{k_1k_2}(u_{k_1k_2,k_2k_1} - u_{k_1k_2,k_1k_2})\left\langle c^{\dagger}_{k_1}c_{k_1}\right\rangle_{\mathrm{eff}}\left\langle c^{\dagger}_{k_2}c_{k_2}\right\rangle_{\mathrm{eff}}.\end{aligned} \tag{6.106}$$

By subtracting the last term, the double counting of the interaction term is corrected when forming thermodynamic expectation values with respect to $H_{\mathrm{eff}}$.

The interaction term would also be counted twice if one were to determine the internal energy from $H_{\mathrm{eff}}$. Namely, it is valid

$$\langle H_{\mathrm{eff}}\rangle_{\mathrm{eff}} = \sum_{k}\varepsilon_k\left\langle c^{\dagger}_{k}c_{k}\right\rangle_{\mathrm{eff}} + \sum_{k_1k_2}(u_{k_1k_2,k_2k_1} - u_{k_1k_2,k_2k_1})\left\langle c^{\dagger}_{k_1}c_{k_1}\right\rangle_{\mathrm{eff}}\left\langle c^{\dagger}_{k_2}c_{k_2}\right\rangle_{\mathrm{eff}} \tag{6.107}$$

but

$$\begin{aligned}\langle H\rangle_{\mathrm{eff}} &= \sum_{k}\varepsilon_k\left\langle c^{\dagger}_{k}c_{k}\right\rangle_{\mathrm{eff}} + \frac{1}{2}\sum_{k_1k_2k_3k_4} u_{k_1k_2,k_3k_4}\left\langle c^{\dagger}_{k_1}c^{\dagger}_{k_2}c_{k_3}c_{k_4}\right\rangle_{\mathrm{eff}} \\ &= \sum_{k}\varepsilon_k\left\langle c^{\dagger}_{k}c_{k}\right\rangle_{\mathrm{eff}} + \frac{1}{2}\sum_{k_1k_2}(u_{k_1k_2,k_2k_1} - u_{k_1k_2,k_1k_2})\left\langle c^{\dagger}_{k_1}c_{k_1}\right\rangle_{\mathrm{eff}}\left\langle c^{\dagger}_{k_2}c_{k_2}\right\rangle_{\mathrm{eff}},\end{aligned} \tag{6.108}$$

where the (for expectation values with respect to non-interacting, one-particle Hamiltonian operators valid) decoupling (6.96) of the four-fermion-operator expectation value was applied. Apparently, the interaction term occurs in the expectation value of the actual Hamiltonian operator $H$ with a factor $\frac{1}{2}$, while this factor is missing when calculating the expectation value of the effective one-particle Hamiltonian. With this, the interaction energy would be counted twice.

In the derivation of the HFA from a minimal principle for the grand canonical potential, which ultimately leads to a simple decoupling rule for the Hamiltonian operator in 2nd quantization (occupation number representation), the factorization of four-fermion-operator expectation values into the sum of all possible products of two-fermion-operator expectation values was decisive. This rule (6.96) can also be interpreted as a special case of the more general **Wick theorem**[8] which is only valid for thermodynamic expectation values with respect to (effective) one-particle Hamiltonian operators. This rule automatically led to two summands, which can again be interpreted as Hartree and Fock (exchange) terms.

## 6.4 Homogeneous Electron Gas in Hartree-Fock Approximation

In this chapter, the model of a free electron gas with $N_\mathrm{e}$ electrons with Coulomb repulsion between each other shall be considered, that is, essentially the model Hamiltonian operator (6.45). But in order to simulate a solid, charge neutrality must be ensured, i.e. there must be as much positive charge as negative charge. It would be realistic to model this by arranging positive point charges on a Bravais lattice, but then one would no longer have to deal with free electrons but with lattice electrons, the eigenfunctions would not be simple plane waves but Bloch functions, and even the simple $k^2$-dispersion would not be strictly valid but only near the band edges. Therefore, in the model considered here, the positive ions are replaced by a constant, evenly smeared positive background charge density $e\rho_0 = e\frac{N_\mathrm{e}}{V}$. This model is also called **"Jellium"**[9].

In first quantization, the Hamiltonian operator for this model is given by

$$H = \sum_{i=1}^{N_\mathrm{e}} \frac{\boldsymbol{p}_i^2}{2m} - \sum_{i=1}^{N_\mathrm{e}} \int_V d^3r' \frac{\rho_0 e^2}{|\boldsymbol{r}_i - \boldsymbol{r}'|} + \frac{1}{2} \sum_{i=1}^{N_\mathrm{e}} \sum_{j=1, j\neq i}^{N_\mathrm{e}} \frac{e^2}{|\boldsymbol{r}_i - \boldsymbol{r}_j|}. \tag{6.109}$$

Due to charge neutrality, the positive and negative charge densities are equal, so it follows:

$$\rho_0 = \int_V d^3r' \sum_{\boldsymbol{k}\sigma} |\psi_{\boldsymbol{k}}(\boldsymbol{r}')|^2 \tag{6.110}$$

where $\psi_{\boldsymbol{k}}(\boldsymbol{r})$ are the (still unknown) one-particle wave functions, which have to be determined by solving the Hartree-Fock equation (6.75), in general. However, it is apparent that plane waves

$$\psi_{\boldsymbol{k}}(\boldsymbol{r}) = \frac{1}{\sqrt{V}} e^{i\boldsymbol{k}\boldsymbol{r}} \tag{6.111}$$

---

[8] G.C. Wick, *1909 in Turin, †1992 ibid, Italian theoretical physicist, 1940 successor to Fermi in Rome, from 1946 active in the USA (including Berkeley, California), 1951 Wick's theorem for relativistic quantum field theory, which later found applications in solid state and nuclear theory, 1977 returned to Italy (initially Pisa).

[9] From English jelly: jelly, evenly solidified mass.

as one-particle wave functions result in a homogeneous charge density. Thus, according to ((6.75)–(6.77)) the Hartree component of the electron–electron interaction cancels out against the potential of the homogeneous positive background charge in the Jellium model. Therefore, only the Fock component remains for this model and the Hartree-Fock equation (6.75) has the explicit form:

$$-\frac{\hbar^2}{2m}\nabla^2\psi_{\boldsymbol{k}}(\boldsymbol{r}) - \sum_{\boldsymbol{k}'}\int d^3r'\psi^*_{\boldsymbol{k}'}(\boldsymbol{r}')\frac{e^2}{|\boldsymbol{r}-\boldsymbol{r}'|}\psi_{\boldsymbol{k}}(\boldsymbol{r}')\psi_{\boldsymbol{k}'}(\boldsymbol{r}) = \varepsilon_{HF}(\boldsymbol{k})\psi_{\boldsymbol{k}}(\boldsymbol{r}). \tag{6.112}$$

This equation is now satisfied with the above plane waves as one-particle wave functions and one obtains:

$$\varepsilon_{HF}(\boldsymbol{k}) = \frac{\hbar^2k^2}{2m} - \frac{1}{V}\sum_{\boldsymbol{k}'}\frac{4\pi e^2}{|\boldsymbol{k}-\boldsymbol{k}'|^2}. \tag{6.113}$$

Here, it was used

$$\begin{gathered}\frac{1}{V}\int d^3r' e^{-i\boldsymbol{k}'\boldsymbol{r}'}\frac{e^2}{|\boldsymbol{r}-\boldsymbol{r}'|}e^{i\boldsymbol{k}\boldsymbol{r}'}\frac{1}{\sqrt{V}}e^{i\boldsymbol{k}'\boldsymbol{r}} = \\ \frac{1}{V}\int d^3r' e^{-i(\boldsymbol{k}'-\boldsymbol{k})(\boldsymbol{r}'-\boldsymbol{r})}\frac{e^2}{|\boldsymbol{r}-\boldsymbol{r}'|}\frac{1}{\sqrt{V}}e^{i\boldsymbol{k}\boldsymbol{r}} = \frac{4\pi e^2}{V|\boldsymbol{k}-\boldsymbol{k}'|^2}\frac{1}{\sqrt{V}}e^{i\boldsymbol{k}\boldsymbol{r}},\end{gathered} \tag{6.114}$$

which follows from (6.44) (Fourier transformation of the Coulomb potential). For the ground state, the $\boldsymbol{k}'$-sum over the lowest lying, occupied states has to be extended up to the Fermi edge. This $k'$-sum can be calculated explicitly by a transition to the integral according to:

$$\begin{aligned}\frac{1}{V}\sum_{\boldsymbol{k}',k'<k_F}\frac{1}{|\boldsymbol{k}-\boldsymbol{k}'|^2} &= \int\frac{d^3k'}{(2\pi)^3}\frac{1}{|\boldsymbol{k}-\boldsymbol{k}'|^2} \\ &= \frac{1}{(2\pi)^2}\int_0^{k_F}dk'k'^2\int_{-1}^{+1}\frac{du}{k^2+k'^2-2kk'u} \\ &= \frac{1}{2\pi^2}k_F\left[\frac{1}{2}+\frac{1-(k/k_F)^2}{4(k/k_F)}\ln\left|\frac{1+k/k_F}{1-k/k_F}\right|\right].\end{aligned} \tag{6.115}$$

The effective one-particle energies in the Hartree-Fock approximation are therefore explicitly given by:

$$\boxed{\varepsilon_{HF}(\boldsymbol{k}) = \frac{\hbar^2k^2}{2m} - \frac{e^2k_F}{2\pi}\left[2+\frac{k_F^2-k^2}{kk_F}\ln\left|\frac{k+k_F}{k-k_F}\right|\right]}. \tag{6.116}$$

In particular, for $k = 0$ (band minimum) one obtains

$$\varepsilon_{HF}(\boldsymbol{k}=0) = -2\frac{e^2k_F}{\pi}, \tag{6.117}$$

**Fig. 6.2** Hartree-Fock dispersion of the homogeneous electron gas (*dashed*) and (quadratic) dispersion of free electrons

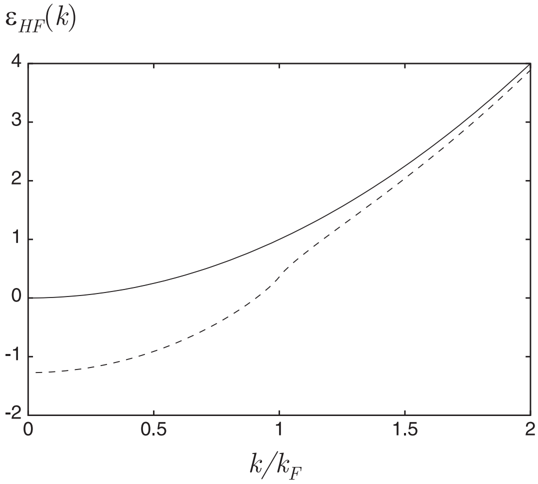

where $\frac{1}{x}\ln(1+x) \approx 1$ was used for $|x| \ll 1$. For $k = k_F$ one obtains:

$$\varepsilon_{HF}(k_F) = \frac{\hbar^2 k_F^2}{2m} - \frac{e^2 k_F}{\pi}. \tag{6.118}$$

The course of $\varepsilon_{HF}(k)$ is shown in Fig. 6.2; the dashed curve shows the Hartree-Fock dispersion, the solid curve the dispersion of free electrons $\frac{\hbar^2 k^2}{2m}$. Here $k_F = (3\pi^2\rho_0)^{1/3}$ is used (cf. (5.185)) and energies are measured in units of $\frac{\hbar^2}{2ma_0^2} = \frac{e^2}{2a_0} = 13.6\,\text{eV} = 1\,\text{Ryd}$ ($a_0$ Bohr radius).

It is common to characterize the electron density $\rho_0$ by a dimensionless parameter $r_s$ which is also called "electron gas parameter" and which is defined by

$$\frac{4\pi}{3} r_s^3 a_0^3 = \frac{1}{\rho_0}, \tag{6.119}$$

with $a_0$ Bohr radius; $r_s a_0$ is thus the radius of a sphere containing one electron on average, $r_s$ is a measure of the average distance between two electrons (measured in Bohr radii). This gives $k_F^3 = \frac{9\pi}{4}\frac{1}{r_s^3 a_0^3}$ and it follows:

$$\frac{\hbar^2 k^2}{2m} = \frac{\hbar^2}{2ma_0^2}\left(\frac{1.92}{r_s}\right)^2\left(\frac{k}{k_F}\right)^2, \quad e^2 k_F = \frac{e^2}{a_0}\frac{1.92}{r_s} \tag{6.120}$$

(because of $(\frac{9\pi}{4})^{1/3} = 1.92$). The plot of $\varepsilon_{HF}(k)$ has been done for $\frac{1.92}{r_s} = 1$. The logarithmic singularity at the Fermi edge can be regarded to be an artifact of the approximation, as will be discussed later.

The total energy of the homogeneous electron gas in Hartree-Fock approximation can also be calculated elementarily, but as emphasized in the previous section, one must be careful not to count the interaction energy twice. Therefore, the total energy is

$$E_{HF} = 2\sum_{k<k_F} \frac{\hbar^2 k^2}{2m} - \frac{e^2 k_F}{2\pi} \sum_{k<k_F} \left[ 2 + \frac{k_F^2 - k^2}{kk_F} \ln \left| \frac{k+k_F}{k-k_F} \right| \right]. \tag{6.121}$$

Here, the first factor 2 results from the sum over the two spin directions. All $k$-sums can be calculated explicitly by transition to the three-dimensional $k$-integral. This results in:

$$2\sum_{k<k_F} \frac{\hbar^2 k^2}{2m} = \frac{\hbar^2 V}{2m\pi^2} \int_0^{k_F} k^4 dk = \frac{\hbar^2 V}{10m\pi^2} k_F^5 \tag{6.122}$$

$$\begin{aligned} \sum_{k<k_F} \frac{k_F^2 - k^2}{kk_F} \ln \left| \frac{k+k_F}{k-k_F} \right| &= \frac{V}{2\pi^2 k_F} \int_{-k_F}^{+k_F} dk \left( k_F^2 k - k^3 \right) \ln(k_F + k) \\ &= \frac{V}{6\pi^2} k_F^3. \end{aligned} \tag{6.123}$$

Because of $N_\mathrm{e} = \frac{V}{3\pi^2} k_F^3$,

$$E_{HF} = N_\mathrm{e} \left( \frac{3\hbar^2}{10m} k_F^2 - \frac{3e^2}{4\pi} k_F \right). \tag{6.124}$$

If one expresses $k_F$ again by the dimensionless parameter $r_s$ according to $k_F = \frac{1.92}{r_s a_0}$, one obtains:

$$E_{HF} = \frac{N_\mathrm{e} \hbar^2}{2ma_0^2} \left( \frac{2.21}{r_s^2} - \frac{0.916}{r_s} \right) = E_\mathrm{kin} + E_{ex} \tag{6.125}$$

where the two summands are referred to as the total kinetic energy and exchange energy of the system, respectively. The total energy is extensive (proportional to the particle number $N_\mathrm{e}$). The single-particle contribution, i.e. the ground state energy of the non-interacting electrons, is also proportional to the Fermi energy of the non-correlated system or to the square of the Fermi momentum. This is the total kinetic energy of the electron system, so

$$E_\mathrm{kin} \sim N_\mathrm{e} k_F^2 \sim N_\mathrm{e} \rho_0^{2/3}. \tag{6.126}$$

The exchange contribution to the energy is, on the other hand, proportional to $k_F$, i.e.

$$E_{ex} \sim N_\mathrm{e} k_F \sim N_\mathrm{e} \rho_0^{1/3}. \tag{6.127}$$

It should be made clear once more that the same results can be derived from the treatment of the Hartree-Fock approximation in the formalism of 2nd quantization discussed in Sect. 6.3.2. The Hamilton operator for the jellium is in 2nd quantization given by

$$\begin{aligned} H = &\sum_{\boldsymbol{k},\sigma} \frac{\hbar^2 k^2}{2m} c_{\boldsymbol{k}\sigma}^\dagger c_{\boldsymbol{k}\sigma} - \sum_{\boldsymbol{kq}\sigma} \frac{4\pi e^2}{q^2} \rho(\boldsymbol{q}) c_{\boldsymbol{k}-\boldsymbol{q}\sigma}^\dagger c_{\boldsymbol{k}\sigma} \\ &+ \frac{1}{2V} \sum_{\boldsymbol{kk}'\boldsymbol{q}\sigma\sigma'} \frac{4\pi e^2}{q^2} c_{\boldsymbol{k}-\boldsymbol{q}\sigma}^\dagger c_{\boldsymbol{k}'+\boldsymbol{q}\sigma'}^\dagger c_{\boldsymbol{k}'\sigma'} c_{\boldsymbol{k}\sigma}, \end{aligned} \tag{6.128}$$

(compare also the model of the homogeneous electron gas in (6.45)). Here, $\rho(\boldsymbol{q})$ is the Fourier transform of the particle density, which, due to charge neutrality, should be the same for the positive background charge as for the electrons. The 2nd term therefore describes the attractive single-particle potential caused by this positive background charge. In order to avoid problems caused by the divergence ($\frac{1}{q^2}$ -behavior) of the Coulomb matrix element, one still works here with position-dependent charge densities and a Fourier transform that is therefore $q$ -dependent. The Hartree decoupling according to the rules of Sect. 6.3.2 leads to the effective Hamilton operator:

$$\begin{aligned} H_{\text{eff}} &= \sum_{\boldsymbol{k},\sigma} \frac{\hbar^2 k^2}{2m} c^\dagger_{\boldsymbol{k}\sigma} c_{\boldsymbol{k}\sigma} - \sum_{\boldsymbol{kq}\sigma} \frac{4\pi e^2}{q^2} \rho(\boldsymbol{q}) c^\dagger_{\boldsymbol{k}-\boldsymbol{q}\sigma} c_{\boldsymbol{k}\sigma} \\ &+ \frac{1}{V} \sum_{\boldsymbol{kk}'\boldsymbol{q}\sigma\sigma'} \frac{4\pi e^2}{q^2} \left( \left\langle c^\dagger_{\boldsymbol{k}'+\boldsymbol{q}\sigma'} c_{\boldsymbol{k}'\sigma'} \right\rangle c^\dagger_{\boldsymbol{k}-\boldsymbol{q}\sigma} c_{\boldsymbol{k}\sigma} - \left\langle c^\dagger_{\boldsymbol{k}-\boldsymbol{q}\sigma} c_{\boldsymbol{k}'\sigma'} \right\rangle c^\dagger_{\boldsymbol{k}'+\boldsymbol{q}\sigma'} c_{\boldsymbol{k}\sigma} \right). \end{aligned} \tag{6.129}$$

With the (Fourier-transformed) particle density operator

$$\hat{\rho}(\boldsymbol{q}) = \frac{1}{V} \sum_{\boldsymbol{k}'\sigma'} c^\dagger_{\boldsymbol{k}'+\boldsymbol{q}\sigma'} c_{\boldsymbol{k}'\sigma'} \tag{6.130}$$

(and $\rho(\boldsymbol{q}) = \langle \hat{\rho}(\boldsymbol{q}) \rangle$), one recognizes again that the Hartree contribution and the attractive single-particle interaction of the positive background charge cancel each other and it remains:

$$\begin{aligned} H_{\text{eff}} &= \sum_{\boldsymbol{k},\sigma} \frac{\hbar^2 k^2}{2m} c^\dagger_{\boldsymbol{k}\sigma} c_{\boldsymbol{k}\sigma} - \frac{1}{V} \sum_{\boldsymbol{kk}'\boldsymbol{q}\sigma\sigma'} \frac{4\pi e^2}{q^2} \underbrace{\left\langle c^\dagger_{\boldsymbol{k}-\boldsymbol{q}\sigma} c_{\boldsymbol{k}'\sigma'} \right\rangle}_{\delta_{\sigma\sigma'}\delta_{\boldsymbol{k}-\boldsymbol{q},\boldsymbol{k}'}} c^\dagger_{\boldsymbol{k}'+\boldsymbol{q}\sigma'} c_{\boldsymbol{k}\sigma} \\ &= \sum_{\boldsymbol{k},\sigma} \frac{\hbar^2 k^2}{2m} c^\dagger_{\boldsymbol{k}\sigma} c_{\boldsymbol{k}\sigma} - \frac{1}{V} \sum_{\boldsymbol{kk}'\sigma} \frac{4\pi e^2}{|\boldsymbol{k}-\boldsymbol{k}'|^2} \left\langle c^\dagger_{\boldsymbol{k}'\sigma} c_{\boldsymbol{k}'\sigma} \right\rangle c^\dagger_{\boldsymbol{k}\sigma} c_{\boldsymbol{k}\sigma} . \end{aligned} \tag{6.131}$$

The effective single-particle energies for electrons in the state $\boldsymbol{k}\sigma$ in Hartree-Fock approximation can now be read off directly to

$$\varepsilon_{HF}(k) = \frac{\hbar^2 k^2}{2m} - \frac{1}{V} \sum_{\boldsymbol{k}'} \frac{4\pi e^2}{|\boldsymbol{k}-\boldsymbol{k}'|^2} \left\langle c^\dagger_{\boldsymbol{k}'\sigma} c_{\boldsymbol{k}'\sigma} \right\rangle . \tag{6.132}$$

In general, the Hartree-Fock single-particle energies are therefore temperature-dependent, which can not be seen in the Hartree-Fock treatment for the ground state.

The effective Hamilton operator (6.131) describes formally non-interacting electrons in an effective one-particle potential. The spatial dependence of this **exchange potential** $V_{ex}(\boldsymbol{r})$ can be calculated explicitly; according to the rules for the representation of a Hamilton operator in occupation number representation, it must hold:

$$\langle \psi_{\boldsymbol{k}} | V_{ex}(\boldsymbol{r}) | \psi_{\boldsymbol{k}} \rangle = \frac{1}{V} \int d^3 r V_{ex}(\boldsymbol{r}) = -\sum_{\boldsymbol{k}'} \left\langle c^\dagger_{\boldsymbol{k}'} c_{\boldsymbol{k}'} \right\rangle \frac{4\pi e^2}{V|\boldsymbol{k} - \boldsymbol{k}'|^2}. \tag{6.133}$$

This is fulfilled by

$$V_{ex}(\boldsymbol{r}) = -\sum_{\boldsymbol{k}'} \left\langle c^\dagger_{\boldsymbol{k}'} c_{\boldsymbol{k}'} \right\rangle \frac{e^{i(\boldsymbol{k}-\boldsymbol{k}')\boldsymbol{r}} e^2}{r}, \tag{6.134}$$

because the Fourier transform of the Coulomb potential is just $\frac{4\pi e^2}{q^2}$. For $T = 0$ the $\boldsymbol{k}'$-sum can be calculated explicitly by transition to the $k'$-integral:

$$\begin{aligned} \sum_{\boldsymbol{k}'} \left\langle c^\dagger_{\boldsymbol{k}'} c_{\boldsymbol{k}'} \right\rangle e^{-i\boldsymbol{k}'\boldsymbol{r}} &= \frac{V}{(2\pi)^3} 2\pi \int_0^{k_F} dk' k'^2 \int_{-1}^{+1} du e^{-ik'ru} \\ &= \frac{V}{2\pi^2 r} \underbrace{\int_0^{k_F} dk' k' \sin(k'r)}_{-\frac{d}{dr}\int_0^{k_F} dk' \cos(k'r)} = \frac{-V}{2\pi^2 r} \frac{d}{dr} \frac{\sin(k_F r)}{r} \\ &= \frac{-V}{2\pi^2} \left( \frac{k_F \cos(k_F r)}{r^2} - \frac{\sin(k_F r)}{r^3} \right). \end{aligned} \tag{6.135}$$

Because of $V = 3\pi^2 \frac{N_e}{k_F^3}$ one obtains for the exchange potential

$$\begin{aligned} V_{ex}(\boldsymbol{r}) &= \frac{V}{2\pi^2} e^{i\boldsymbol{k}\boldsymbol{r}} e^2 \left( \frac{k_F \cos(k_F r)}{r^3} - \frac{\sin(k_F r)}{r^4} \right) \\ &= \frac{3}{2} N_e e^{i\boldsymbol{k}\boldsymbol{r}} \frac{e^2}{r} g(k_F r), \end{aligned} \tag{6.136}$$

with a function g(x), which is defined in (6.137) and shown in Fig. 6.3

$$g(x) = \frac{x\cos(x) - \sin(x)}{x^3}. \tag{6.137}$$

The exchange potential and the associated exchange charge density therefore oscillate with the wave number $k_F$ around 0. Overall, the one-particle energies are lowered by the exchange contribution. However, at $k = k_F$ there is an anomaly in the form of a logarithmic singularity. There the derivative of the dispersion relation diverges, which would also lead to a vanishing density of states at the Fermi edge. This is unrealistic and ultimately a consequence of the $\frac{1}{q^2}$ divergence in the interaction term, and this is due to the fact that the Coulomb potential is so long-ranged. All problems are eliminated if one works with a screened Coulomb interaction instead of a naked Coulomb interaction. On the other hand, the mobile charges of the system themselves must be able to provide the screening. This is

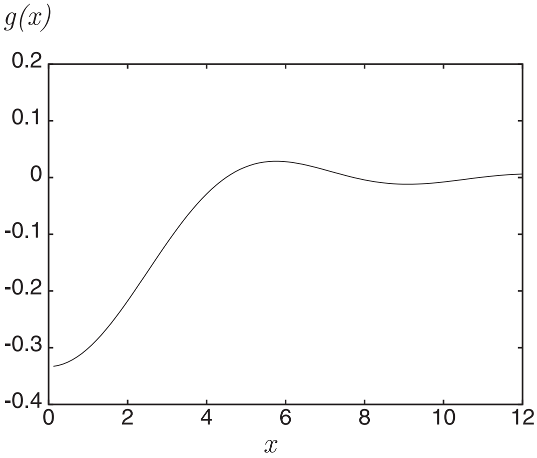

**Fig. 6.3** Behavior of the function $g(x)$ in the exchange potential

actually the case with the homogeneous electron gas model discussed here, but not in Hartree-Fock approximation. To take into account screening, one has to go beyond Hartree-Fock approximation; but this is only possible with the use of special methods of many-body theory, which cannot be discussed here. We will, however, get to know elementary theories of dielectric screening in one of the following sections.

## 6.5 Basic Ideas of Density Functional Theory

In the numerical calculations of the electronic properties of concrete materials, for solids therefore in band structure calculations, the Coulomb interaction of the electrons with each other must also be taken into account. In principle, one could (or should) use the Hartree-Fock approximation discussed in the previous sections as the simplest method to explicitly consider Coulomb interaction. In fact, however, over the past few decades, the density functional theory (DFT) and within it the so-called local density approximation have prevailed and are used routinely. Specifically, numerical calculations within DFT are usually less expensive than corresponding HFA calculations, and problems such as the—in Sect. 6.4 discussed—occurrence of logarithmic divergences in the effective one-particle energies are avoided. The basic idea of the density functional theory and the local density approximation shall therefore be discussed in this section.

We continue to consider $N_e$ electrons with Coulomb repulsion with each other in an external potential that can be assumed to be periodic for solids. The Hamiltonian in first quantization is therefore again given by

$$H = \sum_{i=1}^{N_e} \frac{\boldsymbol{p}_i^2}{2m} + \sum_{i=1}^{N_e} V(\boldsymbol{r}_i) + \sum_{i<j} \frac{e^2}{|\boldsymbol{r}_i - \boldsymbol{r}_j|}. \tag{6.138}$$

A quantity of interest for this Hamiltonian is the ground state and in particular the ground state energy $E_0$. In principle, one has to solve the full Schrödinger equation, and the (many-body) eigenstate with the lowest eigenenergy is the ground state. The basic idea of the density functional theory is then not to consider the complicated, antisymmetric ground state wave function $\psi_0(\underline{x}_1, \ldots, \underline{x}_{N_e})$ but instead the particle density

$$n_0(\boldsymbol{r}) = \int d^3r_1 \ldots \int d^3r_{N_e} \psi_0^*(\underline{x}_1, \ldots, \underline{x}_{N_e}) \sum_{i=1}^{N_e} \delta(\boldsymbol{r} - \boldsymbol{r}_i) \psi_0(\underline{x}_1, \ldots, \underline{x}_{N_e}) \tag{6.139}$$

in the ground state. For the following theorem is valid:[10, 11]

**Theorem of Hohenberg and Kohn:**

The ground state energy is a unique functional of the ground state density $n_0(\boldsymbol{r})$: $E_0 = E\{n_0(\boldsymbol{r})\}$. Each (many-particle) state $|\psi\rangle$ (or each many-particle wave function) can be assigned an energy via

$$E\{|\psi\rangle\} = \frac{\langle\psi|H|\psi\rangle}{\langle\psi|\psi\rangle}, \tag{6.140}$$

the energy is therefore a functional of the wave function, on the other hand, according to $n(\boldsymbol{r}) = \langle\psi| \sum_i \delta(\boldsymbol{r} - \boldsymbol{r}_i)|\psi\rangle$, each wave function also belongs to a certain particle density. The statement of the Hohenberg-Kohn theorem is now that for the ground state of $H$ these relationships must be unique. The ground state $|\psi_0\rangle$ also belongs to a certain ground state particle density $n_0(\boldsymbol{r})$. It remains to be proven that this relationship is also unique, that is, that two different ground states cannot have the same particle density. The proof is indirect, i. e. we assume that there are two different ground states $|\psi\rangle \neq |\psi'\rangle$ with the same particle density $n(\boldsymbol{r}) = \langle\psi| \sum_i \delta(\boldsymbol{r} - \boldsymbol{r}_i)|\psi\rangle = \langle\psi'| \sum_i \delta(\boldsymbol{r} - \boldsymbol{r}_i)|\psi'\rangle = n'(\boldsymbol{r})$. But if $|\psi\rangle$ and $|\psi'\rangle$ are both supposed to be ground states and if the ground state is non-degenerate, then they must be ground states of different Hamilton operators $H, H'$. But given a fixed electron number $N_e$, the kinetic energy and the interaction energy must be equal in the Hamilton operator, so that $H, H'$ can differ only in the öne-particle potential $V(\boldsymbol{r}) \neq V'(\boldsymbol{r})$ . Then it applies:

$$\begin{aligned} E = \langle\psi|H|\psi\rangle < \langle\psi'|H|\psi'\rangle &= \langle\psi'|H' + V - V'|\psi'\rangle = E' + \langle\psi'|V - V'|\psi'\rangle \\ &= E' + \int d^3r \big(V(\boldsymbol{r}) - V'(\boldsymbol{r})\big) n'(\boldsymbol{r}). \end{aligned} \tag{6.141}$$

---

[10] P.C. Hohenberg, *1934 in Neuilly-sur-Seine (France), died 2017, Ph. D. 1962 at Harvard University, from 1964 at Bell Labs, from 1975 briefly Professor in Munich, work on the theory of superconductivity and superfluidity, electron theory of solids and on phase transitions and critical phenomena.

[11] S. footnote 6.12.

If you exchange $H, H'$, the following follows accordingly:

$$E' < E + \int d^3r \big(V'(\boldsymbol{r}) - V(\boldsymbol{r})\big) n(\boldsymbol{r}). \tag{6.142}$$

The addition of the two equations leads to a contradiction because of the assumption $n(\boldsymbol{r}) = n'(\boldsymbol{r})$. So the specification of a certain particle density $n(\boldsymbol{r})$ as the ground state particle density uniquely determines the one-particle potential $V$ and thus the Hamilton operator $H$ and thus the ground state energy $E_0$.

For any anti-symmetric $N_\mathrm{e}$ -particle state $\psi(\underline{x}_1, \ldots, \underline{x}_{N_\mathrm{e}})$, the Ritz variation principle applies:

$$E_0 = E\{n_0(\boldsymbol{r})\} \leq \langle\psi|H|\psi\rangle. \tag{6.143}$$

To $|\psi\rangle$ belongs the particle density $n(\boldsymbol{r}) = \langle\psi| \sum_i \delta(\boldsymbol{r} - \boldsymbol{r}_i)|\psi\rangle$, which can be associated with an energy according to

$$E\{n(\boldsymbol{r})\} = \langle\psi|H|\psi\rangle, \tag{6.144}$$

so the following statement applies:

The particle density $n_0(\boldsymbol{r})$ for which the energy density functional $E\{n(\boldsymbol{r})\}$ assumes its absolute minimum is the ground state particle density and the corresponding value of the functional $E_0 = E\{n_0(\boldsymbol{r})\}$ is the ground state energy of $H$. So one has a variational principle:

$$\delta E\{n(\boldsymbol{r})\} = 0 \tag{6.145}$$

under the constraint

$$\int d^3r n(\boldsymbol{r}) = N_\mathrm{e}. \tag{6.146}$$

If one takes into account the constraint as usual by means of a Lagrange parameter $\mu$, it follows that

$$\delta \left[ E\{n(\boldsymbol{r})\} - \mu \left( \int d^3r n(\boldsymbol{r}) - N_\mathrm{e} \right) \right] = 0. \tag{6.147}$$

One has to vary on the set of all possible particle densities $n(\boldsymbol{r})$ which are determined by

$$n(\boldsymbol{r}) = \langle\psi| \sum_{i=1}^{N_\mathrm{e}} \delta(\boldsymbol{r} - \boldsymbol{r}_i)|\psi\rangle \tag{6.148}$$

from an $N_\mathrm{e}$-particle state $|\psi\rangle$.

The problem is that the functional dependence $E\{n(\boldsymbol{r})\}$ is not known. One can decompose the energy density functional according to

$$E\{n(\boldsymbol{r})\} = T\{n(\boldsymbol{r})\} + V\{n(\boldsymbol{r})\} + U\{n(\boldsymbol{r})\} \tag{6.149}$$

with the density functional of the kinetic energy:

$$T\{n(\boldsymbol{r})\} = \langle\psi|\sum_{i=1}^{N_{\mathrm{e}}}\frac{\boldsymbol{p}_i^2}{2m}|\psi\rangle. \tag{6.150}$$

the density functional of the potential energy:

$$V\{n(\boldsymbol{r})\} = \langle\psi|\sum_{i=1}^{N_{\mathrm{e}}}V(\boldsymbol{r}_i)|\psi\rangle = \int d^3rV(\boldsymbol{r})n(\boldsymbol{r}). \tag{6.151}$$

and the density functional of the interaction energy:

$$U\{n(\boldsymbol{r})\} = \langle\psi|\frac{e^2}{2}\sum_{i\neq j}\frac{1}{|\boldsymbol{r}_i-\boldsymbol{r}_j|}|\psi\rangle. \tag{6.152}$$

Apparently, only the relatively trivial functional dependence of the functional for the one-particle potential $V\{n(\boldsymbol{r})\}$ is known explicitly. In contrast, the functionals for the kinetic energy and the interaction energy are not known explicitly. A natural approach to the density functional of the interaction energy is given by

$$U\{n(\boldsymbol{r})\} = \frac{e^2}{2}\int d^3r\int d^3r'\frac{n(\boldsymbol{r})n(\boldsymbol{r}')}{|\boldsymbol{r}-\boldsymbol{r}'|}. \tag{6.153}$$

This corresponds to the classical electrostatic interaction energy of a charge distribution $\rho(\boldsymbol{r}) = -en(\boldsymbol{r})$. Quantum mechanically, however, this is only the Hartree contribution, as a comparison with (6.69) shows, and already in the still very simple Hartree-Fock approximation there are corrections to it. In general, one therefore assumes:

$$U\{n(\boldsymbol{r})\} = \frac{e^2}{2}\int d^3r\int d^3r'\frac{n(\boldsymbol{r})n(\boldsymbol{r}')}{|\boldsymbol{r}-\boldsymbol{r}'|} + E_{xc}\{n(\boldsymbol{r})\} \tag{6.154}$$

where $E_{xc}\{n(\boldsymbol{r})\}$ is the **exchange-correlation energy** (the index $x$ stands for **"exchange"**, $c$ for **"correlation"**), whose functional dependence on the density $n(\boldsymbol{r})$ is still unknown, just as the density functional of the kinetic energy is still unknown.

In order to be able to work out an explicit example of the application of the density functional method, we make a simple ansatz for the functional of the kinetic energy and neglect the exchange correlation contribution. In Sect. 6.4 for the homogeneous electron gas we found for the kinetic energy (see (6.122)):

$$E_{\mathrm{kin}} = \frac{\hbar^2}{10m\pi^2}Vk_F^5 = \frac{3\hbar^2}{10m}\left(3\pi^2\right)^{2/3}Vn_0^{5/3} \tag{6.155}$$

where $N_{\mathrm{e}} = \frac{V}{3\pi^2}k_F^3$ was used and $n_0 = \frac{N_{\mathrm{e}}}{V}$ denotes the particle density, which is constant for the homogeneoius electron gas. In generalization of this relation one can make the following ansatz for the density functional of the kinetic energy

$$T\{n(\boldsymbol{r})\} = \frac{3}{10}\left(3\pi^2\right)^{2/3}\frac{\hbar^2}{m}\int d^3r(n(\boldsymbol{r}))^{5/3}. \tag{6.156}$$

The only justification for the use of this ansatz is that it is correct for the homogeneous electron gas. The entire energy density functional in this approximation is given by:

$$
\begin{aligned}
E\{n(\boldsymbol{r})\} = {} & \frac{3(3\pi^2)^{2/3}\hbar^2}{10m} \int d^3r (n(\boldsymbol{r}))^{5/3} + \int d^3r V(\boldsymbol{r}) n(\boldsymbol{r}) \\
& + \frac{e^2}{2} \int d^3r \int d^3r' \frac{n(\boldsymbol{r}) n(\boldsymbol{r}')}{|\boldsymbol{r} - \boldsymbol{r}'|} .
\end{aligned}
\tag{6.157}
$$

Variation (according to (6.147) with the constraint (6.146) added with a Lagrange parameter) leads to:

$$
\begin{aligned}
& \frac{\hbar^2}{2m}(3\pi^2 n(\boldsymbol{r}))^{2/3} + V(\boldsymbol{r}) + \int d^3r' \frac{e^2}{|\boldsymbol{r} - \boldsymbol{r}'|} n(\boldsymbol{r}') \\
& = \frac{\hbar^2}{2m}\left(3\pi^2\right)^{2/3} (n(\boldsymbol{r}))^{2/3} + V_{\text{eff}}(\boldsymbol{r}) = \mu
\end{aligned}
\tag{6.158}
$$

with

$$
V_{\text{eff}}(\boldsymbol{r}) = V(\boldsymbol{r}) + \int d^3r' \frac{e^2}{|\boldsymbol{r} - \boldsymbol{r}'|} n(\boldsymbol{r}') \tag{6.159}
$$

(external particle potential plus self-consistently to be determined Hartree potential). This leads to

$$
n(\boldsymbol{r}) = \frac{1}{3\pi^2} \left[ \frac{2m}{\hbar^2} (\mu - V_{\text{eff}}(\boldsymbol{r})) \right]^{3/2} . \tag{6.160}
$$

This provides for $T = 0$ just the **Thomas-Fermi approximation**, which is known from atomic physics and will be briefly discussed in one of the following sections on simple approximations for screening. Since in this ansatz the relation valid for free electrons between kinetic energy and density is also used for position (r-) dependent problems and densities, the electrons are locally treated like free electrons. This is consistent with the assumption of a slow spatial variation underlying the Thomas-Fermi theory, so that in the vicinity of $\boldsymbol{r}$ the system can be assumed to be homogeneous (i. e. the potential approximately constant). With the above equation one has not yet found the final solution, since $V_{\text{eff}}(\boldsymbol{r})$ itself still depends on $n(\boldsymbol{r})$. So one still has a self-consistency problem or an integral equation to be solved, which can be converted into a differential equation (Poisson equation). This will not be further elaborated here, because the Thomas-Fermi approximation is much too coarse for realistic quantitative calculations; here it should only serve as the simplest example for the method.

In particular, one needs a better approach to the density functional of the kinetic energy. The general considerations on the existence of an energy density functional as above also apply to a hypothetical non-interacting electron system. For a non-interacting $N_{\text{e}}$-particle Hamiltonian operator

$$H_0 = \sum_{i=1}^{N_e} \frac{\boldsymbol{p}_i^2}{2m} + \sum_{i=1}^{N_e} \tilde{V}(\boldsymbol{r}_i) \tag{6.161}$$

the wave functions are known to be Slater determinants of one-particle wave functions $\psi_i(\boldsymbol{r})$:

$$\psi(\underline{x}_1, \ldots, \underline{x}_{N_e}) = \frac{1}{\sqrt{N_e!}} \det(\psi_i(\underline{x}_j)). \tag{6.162}$$

The particle density for the non-interacting system is simply:

$$n(\boldsymbol{r}) = \sum_{i=1}^{N_e} |\psi_i(\boldsymbol{r})|^2 \tag{6.163}$$

and the energy in this state $|\psi\rangle$ and thus for this particle density $n(\boldsymbol{r})$ is simply

$$E\{n(\boldsymbol{r})\} = \sum_{i=1}^{N_e} -\frac{\hbar^2}{2m} \int d^3r \psi_i^*(\boldsymbol{r}) \nabla^2 \psi_i(\boldsymbol{r}) + \sum_{i=1}^{N_e} \int d^3r \tilde{V}(\boldsymbol{r}) |\psi_i(\boldsymbol{r})|^2 . \tag{6.164}$$

Even in this simple case of the non-interacting system, the functional dependence of the kinetic energy on the particle density is only known implicitly. This now suggests to use the same implicit representation for the density functional of the kinetic energy for the actual interacting electron system. The approximation or ansatz is therefore:

$$T\{n(\boldsymbol{r})\} = \sum_{i=1}^{N_e} -\frac{\hbar^2}{2m} \int d^3r \psi_i^*(\boldsymbol{r}) \nabla^2 \psi_i(\boldsymbol{r}) \tag{6.165}$$

if the particle density can be represented as

$$n(\boldsymbol{r}) = \sum_{i=1}^{N_e} |\psi_i(\boldsymbol{r})|^2, \tag{6.166}$$

with still unknown one-particle wave functions $\psi_i(\boldsymbol{r})$. This implies that the still unknown ground state particle density of the interacting Hamiltonian operator can also be the particle density to an as yet unknown effective single-particle Hamiltonian operator. However, this is not certain, for wave functions at least it does not apply. Even if it is possible to represent the exact ground state density by single-particle wave functions, it is not certain that the kinetic energy can be represented in the same way as for the non-interacting system by these single-particle wave functions. Nevertheless, the above approach for the functional of the kinetic energy shall be used, then with optimized single-particle wave functions, and corrections to the kinetic energy, which must ultimately also be consequences of the electron–electron interaction, can be incorporated into the still undefined exchange correlation potential. With this approach, our entire energy density functional now looks as follows:

$$\begin{aligned} E\{n(\boldsymbol{r})\} = \sum_{i=1}^{N_e} -\frac{\hbar^2}{2m} \int d^3r \psi_i^*(\boldsymbol{r}) \nabla^2 \psi_i(\boldsymbol{r}) + \int d^3r V(\boldsymbol{r}) n(\boldsymbol{r}) \\ + \frac{e^2}{2} \int d^3r \int d^3r' \frac{n(\boldsymbol{r}) n(\boldsymbol{r}')}{|\boldsymbol{r} - \boldsymbol{r}'|} + E_{xc}\{n(\boldsymbol{r})\}. \end{aligned} \tag{6.167}$$

$E_{xc}\{n(\boldsymbol{r})\}$ now contains all exchange correlation contributions from the interaction energy and possibly still interaction corrections to the kinetic energy. For the ground state, this functional is to be minimal. But then it is also possible to vary the still unknown single-particle wave functions $\psi_i^*(\boldsymbol{r})$ under the condition that they are normalized. This leads to the variational problem

$$\delta_{\psi_i^*} \left\{ E\{n(\boldsymbol{r})\} - \sum_{j=1}^{N_e} \varepsilon_j \left( \int d^3r |\psi_j(\boldsymbol{r})|^2 - 1 \right) \right\} = 0. \tag{6.168}$$

This results in the differential equation:

$$\left\{ -\frac{\hbar^2}{2m} \nabla^2 + V(\boldsymbol{r}) + \int d^3r' \frac{e^2}{|\boldsymbol{r} - \boldsymbol{r}'|} n(\boldsymbol{r}') + \frac{\delta E_{xc}\{n(\boldsymbol{r})\}}{\delta n(\boldsymbol{r})} \right\} \psi_i(\boldsymbol{r}) = \varepsilon_i \psi_i(\boldsymbol{r}) \tag{6.169}$$

These are the[12, 13]

### Kohn-Sham Equations

for the effective one-particle wave functions $\psi_i(\boldsymbol{r})$. They are obviously of the form of a one-particle Schrödinger equation in the presence of the effective one-particle potential:

$$V_{\text{eff}}(\boldsymbol{r}) = V(\boldsymbol{r}) + \int d^3r' \frac{e^2 n(\boldsymbol{r}')}{|\boldsymbol{r} - \boldsymbol{r}'|} + \frac{\delta E_{xc}\{n(\boldsymbol{r})\}}{\delta n(\boldsymbol{r})}. \tag{6.170}$$

As long as all influences of exchange-correlation energy and interaction contributions to the kinetic energy are contained in the still unknown functional $E_{xc}\{n(\boldsymbol{r})\}$, the Kohn-Sham equations are formally exact at least under the assumption that the density can be represented according to (6.166) by one-particle wave functions. The one-particle wave functions $\psi_i$ and -energies $\varepsilon_i$ have no direct physical meaning themselves; they are only auxiliary quantities for determining the density via (6.166). There is still a self-consistency problem because the density to be

---

[12] W. Kohn, *1923 in Vienna, died 2016 in Santa Barbara, since 1947 US citizen, promotion 1948 at Harvard University, since 1960 professor at the University of California San Diego (UCSD), numerous important contributions to solid state theory, in particular the density functional theory, for which he received the Nobel Prize in Chemistry in 1998, since 1984 at University of California Santa Barbara.

[13] L.J. Sham, *1938 in Hong Kong, studied in England, PhD 1963 in Cambridge, developed 1964 as PostDoc of W. Kohn the Kohn-Sham-Equations and the foundations of LDA, since 1968 Professor at UCSD and works on semiconductors, superconductors et al.

determined enters into the effective one-particle potential. This is usually solved numerically by iteration. The essential steps of such an iteration procedure are the following:

1. Start with a suitably chosen particle density $n(\boldsymbol{r})$
2. Determination of the effective one-particle potential $V_{\text{eff}}(\boldsymbol{r})$
3. Solution of the Kohn-Sham equations, i.e. an effective one-particle Schrödinger equation for the one-particle wave functions $\psi_i(\boldsymbol{r})$; since in solids the effective potential is also periodic in the lattice (if the bare potential has lattice periodicity), the band structure calculation methods from Sect. 5.5 are used here
4. Determination of the new particle density $\tilde{n}(\boldsymbol{r})$ from the $\psi_i$ via (6.166)
5. Comparison of $n(\boldsymbol{r}), \tilde{n}(\boldsymbol{r})$; if they do not agree, set $n(\boldsymbol{r}) = \tilde{n}(\boldsymbol{r})$ and let the iteration loop run from 2. again, otherwise you are finished and know the ground state density and energy.

In principle, therefore, a similar self-consistency problem arises as with the Hartree-Fock equations (6.75), but the Kohn-Sham equations are simpler in that the effective potential becomes a local potential. With the Kohn-Sham equations, it has become possible in particular to treat the density functional of the kinetic energy essentially exactly (at least if all corrections are included in the exchange-correlation functional $E_{xc}\{n(\boldsymbol{r})\}$). At least this represents a significant advance over the Thomas-Fermi approximation.

However, the problem remains that the density functional of the exchange-correlation contribution is not known, and for this one still depends on approximations, assumptions and approaches. The simplest approach uses the same argumentation as for the Thomas-Fermi approximation for the kinetic energy: For the homogeneous electron gas, we know from Sect. 6.4 the dependence of the correlation energy on the (in this case homogeneous, $\boldsymbol{r}$-independent) particle density $n_0$ at least in Hartree-Fock approximation. According to (6.124), the correlation energy for the homogeneous electron gas is:

$$E_x = -\frac{3e^2}{4\pi} N_{\text{e}} k_F = -\frac{3e^2}{4\pi} V n_0 (3\pi^2 n_0)^{1/3} \tag{6.171}$$

(because of $n_0 = \frac{N_{\text{e}}}{V} = \frac{k_F^3}{3\pi^2}$). Therefore, a possible approximation or ansatz for the density dependence of the exchange-correlation energy (or here only the exchange energy, because no correlations beyond HFA are considered) is

$$E_x\{n(\boldsymbol{r})\} = -\frac{3e^2}{4\pi} \left(3\pi^2\right)^{1/3} \int d^3r (n(\boldsymbol{r}))^{4/3}. \tag{6.172}$$

The only justification for this ("Hartree-Fock-Slater") approach is that for the homogeneous electron gas the Hartree-Fock result is reproduced. One thus makes a kind of Thomas-Fermi approximation, but for the exchange-correlation functional, and for this an approximation of this kind seems to be much less problematic than for the kinetic energy. The resulting exchange potential, that is, the contribution to the effective single-particle potential arising from the exchange-correlation energy functional, is simply

$$V_x(\boldsymbol{r}) = \frac{\delta E_x\{n(\boldsymbol{r})\}}{\delta n(\boldsymbol{r})} = -e^2 \left(\frac{3}{\pi}\right)^{1/3} (n(\boldsymbol{r}))^{1/3}. \tag{6.173}$$

In this approximation the exchange potential (or exchange-correlation potential) at the location $\boldsymbol{r}$ thus depends only on the density at the same location $\boldsymbol{r}$. Such an approximation is therefore also called a **local density approximation** ("LDA"). In general, one can imagine and it will be the case in reality that the exchange potential also depends on the particle densities at all other locations, as it is already the case for the simple Hartree potential. Then probably also more complicated functional dependencies between exchange-correlation energy and particle density will exist.

In practice, current band structure calculations usually use heuristically determined, improved approaches to the exchange-correlation functional compared to (6.172), but remain within the framework of the local density approximation. In many cases, effective parameters are introduced, with respect to which further optimization is possible. A common approach to the exchange potential is, for example,

$$V_x(\boldsymbol{r}) = \beta(n(\boldsymbol{r}))(n(\boldsymbol{r}))^{1/3} \tag{6.174}$$

with an empirically determined function $\beta(x)$. For the homogeneous electron gas, it is possible to systematically improve the Hartree-Fock approximation by means of special diagrammatic methods of many-body theory, and the corresponding corrections to the total energy can be expressed in terms of the Fermi momentum or the dimensionless electron gas parameter $r_s$ or the (constant) density $n_0$ as in the Hartree-Fock result (6.124). If $n_0$ is then replaced by $n(\boldsymbol{r})$, one obtains a new approach to the density functional of the exchange-correlation energy in the local density approximation. In the limit of the homogeneous electron gas, this approach then reproduces the improvement of the Hartree-Fock approximation. Nowadays, an approach for the exchange-correlation potential is often used in LDA applications, so that for constant density the (numerically) exact (quantum Monte Carlo) solution for the ground state energy of the homogeneous electron gas is reproduced.

The current "first-principles ab initio" numerical methods "without adjustable parameters" for calculating the electronic structure of solids taking into account interaction effects within the framework of density functional theory and LDA are therefore not yet completely free of assumptions, approaches and approximations, even if it sometimes sounds different. On the other hand, these methods are usually very successful, and it is often possible to achieve excellent agreement with experimental results, and the success justifies the means (and approximations).

The density functional theory can be extended by introducing the particle density $n(\boldsymbol{r})$ as well as the magnetization density $m(\boldsymbol{r})$ as two fundamental variables, or by considering the energy as a functional of the particle densities $n_\sigma(\boldsymbol{r})$ for the two spin directions $\sigma = \uparrow, \downarrow$, where the total particle density is given by $n(\boldsymbol{r}) = n_\uparrow(\boldsymbol{r}) + n_\downarrow(\boldsymbol{r})$ and the magnetization density by $m(\boldsymbol{r}) = n_\uparrow(\boldsymbol{r}) - n_\downarrow(\boldsymbol{r})$ . This is always necessary when describing magnetic substances, that is, materials in which a finite magnetization exists in the ground state. This is important in the context of band structure calculations when predicting whether the solid has a ferromagnetic or antiferromagnetic ground state, or when applying an external magnetic field. The resulting generalizations of the Kohn-Sham equations discussed above and the **Local Spin Density Approximation** (LSDA) are elementary and are therefore not discussed here in more detail. It should be emphasized once again, however, that the density functional theory and, with it, the methods for calculating electronic band structures are limited to the description of the ground state. So one can calculate and predict whether a substance has a magnetic ground state at $T = 0$, but one cannot calculate the temperature dependence of the magnetization or the Curie temperature.

In general, it is problematic (or not so easy) to describe excited states by means of density functional theory. Among other things, for this reason, the energy gaps of semiconductors could not be correctly calculated by means of DFT-LDA. Currently, attempts are being made to find improved approaches to the density functional of the exchange correlation energy. These attempts go in different directions; with the "generalized gradient approximation" (GGA), one tries to take into account that the exchange correlation functional or potential not only depends locally on the particle density at the location $\boldsymbol{r}$ but also on the density at other locations $\boldsymbol{r}'$, by making the functional also dependent on the gradient $\nabla n(\boldsymbol{r})$. The "exact exchange (XX) functionals" are constructed in such a way that the Hartree-Fock approximation (and thus the exact compensation of unphysical self-interaction terms) is contained in the exchange correlation functional. Very current is finally the so-called "GW approximation", which, going beyond the HFA, takes into account many-body contributions to be described by means of so-called Feynman diagrams (and then also screening). And often one uses pragmatically (more or less heuristically motivated) hybrid methods between the mentioned LDA improvements.

## 6.6 Elementary Theory of Static Screening

As is known, an electric field in a medium with mobile charges causes a displacement of these charges, i.e. a polarization of the medium and thus a change of the field, so that the original external field is screened. As is known from electrodynamics, this is how the difference between $D$- and E-field arises. The material constant characteristic for the medium is the (static) dielectric constant, which is generally a tensorial quantity. While in electrodynamics this dielectric constant is introduced phenomenologically, in a microscopic theory of the medium it must also be possible to calculate it microscopically. But this is possible only approximately, and the simplest approximation methods for treating static screening and for calculating the static dielectric constant are to be discussed here. As a model for the medium, we will again consider a kind of jellium with freely movable electrons.

First, a few simple relationships between external and induced charge and external and induced electrostatic potential or field, known from electrodynamics, are to be compiled. For this purpose, we use the spatial Fourier transforms of the corresponding quantities. Between external potential $\Phi^{\text{ext}}(\boldsymbol{q})$ and total potential

$\Phi(\boldsymbol{q})$ and the external charge density $\rho^{\text{ext}}(\boldsymbol{q})$, induced $\rho^{\text{ind}}(\boldsymbol{q})$ and total charge density $\rho(\boldsymbol{q})$, the relationships are:

$$\begin{aligned} &\Phi^{\text{ext}}(\boldsymbol{q}) = \varepsilon(\boldsymbol{q})\Phi(\boldsymbol{q}), \quad q^2\Phi^{\text{ext}}(\boldsymbol{q}) = 4\pi\rho^{\text{ext}}(\boldsymbol{q}), \quad q^2\Phi(\boldsymbol{q}) = 4\pi\rho(\boldsymbol{q}) \\ &\rho^{\text{ind}}(\boldsymbol{q}) = \rho(\boldsymbol{q}) - \rho^{\text{ext}}(\boldsymbol{q}) = \chi(\boldsymbol{q})\Phi(\boldsymbol{q}) \end{aligned} \tag{6.175}$$

where $\varepsilon(\boldsymbol{q})$ is the (static) dielectric constant and $\chi(\boldsymbol{q})$ is the (electric) susceptibility. It follows:

$$\Phi^{\text{ext}}(\boldsymbol{q}) = \left(1 - \frac{4\pi}{q^2}\chi(\boldsymbol{q})\right)\Phi(\boldsymbol{q})$$

and thus:

$$\boxed{\varepsilon(\boldsymbol{q}) = 1 - \frac{4\pi}{q^2}\chi(\boldsymbol{q}) = 1 - \frac{4\pi}{q^2}\frac{\rho^{\text{ind}}(\boldsymbol{q})}{\Phi(\boldsymbol{q})}}\,. \tag{6.176}$$

### 6.6.1 Thomas-Fermi Theory of Screening

One has to calculate the induced charge density or the change in charge density in the presence of an electrostatic potential $\Phi(\boldsymbol{r})$. Here, $\Phi(\boldsymbol{r})$ is generally the full electrostatic potential including the modification due to the charge redistribution itself. Then you have to deal with a self-consistency problem. As mentioned, we assume that there are mobile, quasi-free electrons in the system. The electrons interact with each other and cause their own contribution to the electrostatic potential; but this shall only be taken into account within the framework of a Hartree approximation. Therefore, one starts with the one-particle Schrödinger equation

$$-\frac{\hbar^2}{2m}\nabla^2\psi_i(\boldsymbol{r}) - e\Phi(\boldsymbol{r})\psi_i(\boldsymbol{r}) = \varepsilon_i\psi_i(\boldsymbol{r}). \tag{6.177}$$

We now assume that the potential $\Phi(\boldsymbol{r})$ is only slowly varying in space and that we can divide the overall system into subsystems so that the potential is nearly constant in each subsystem; the $\Phi(\boldsymbol{r})$ should therefore vary on a macroscopic length scale. On the other hand, the subsystems should be large enough that the laws of equilibrium thermodynamics are applicable. Then one has in each subsystem a free electron gas present but with different constant potentials and thus varying mean particle numbers from subsystem to subsystem. The particle density is thus dependent on the position, and is determined in each subsystem by the Fermi distribution:

$$n(\boldsymbol{r}) = \int \frac{d^3k}{4\pi^3}\frac{1}{\exp\left[\beta\left(\frac{\hbar^2k^2}{2m} - e\Phi(\boldsymbol{r}) - \mu\right)\right] + 1}. \tag{6.178}$$

Here, the $\boldsymbol{k}$-sum was replaced in the usual way by a $k$-integral, the spin was taken into account by a factor of 2, and divided by the volume of the subvolume to obtain the particle density in the subvolume at $\boldsymbol{r}$. Without an electrostatic potential, the particle density is as usual independent of location and given by

$$n_0(\mu) = \int \frac{d^3k}{4\pi^3} \frac{1}{\exp\left[\beta\left(\frac{\hbar^2k^2}{2m} - \mu\right)\right] + 1} \tag{6.179}$$

and the position-dependent particle density can also be written as

$$n(\boldsymbol{r}) = n_0(\mu + e\Phi(\boldsymbol{r})). \tag{6.180}$$

The difference between the position-dependent particle density in the presence of an electrostatic field or potential and the constant particle density in the absence of the field just determines the change in particle and thus charge density caused by the field. The induced charge density is therefore given by:

$$\rho^{\text{ind}}(\boldsymbol{r}) = -e(n_0(\mu + e\Phi(\boldsymbol{r})) - n_0(\mu)). \tag{6.181}$$

In the case of a weak potential, one obtains by expanding a constant ($\boldsymbol{q}$-independent) susceptibility

$$\chi(\boldsymbol{q}) = -e^2\frac{\partial n_0}{\partial\mu}. \tag{6.182}$$

Therefore we obtain for the static dielectric constant in Thomas-Fermi approximation[14]:

$$\varepsilon(\boldsymbol{q}) = 1 + \frac{4\pi e^2}{q^2}\frac{\partial n_0}{\partial\mu} = 1 + \frac{k_{TF}^2}{q^2} \tag{6.183}$$

with the **Thomas-Fermi wave number**

$$k_{TF}^2 = 4\pi e^2\frac{\partial n_0}{\partial\mu}. \tag{6.184}$$

To illustrate the meaning of $k_{TF}$ consider the simple example of the screening of the potential of an external point charge:

$$\Phi^{\text{ext}}(\boldsymbol{r}) = \frac{Q}{r}, \Phi^{\text{ext}}(\boldsymbol{q}) = \frac{4\pi Q}{q^2} \tag{6.185}$$

The total potential is then given in Thomas-Fermi approximation by

$$\Phi(\boldsymbol{q}) = \frac{1}{\varepsilon(\boldsymbol{q})}\Phi^{\text{ext}}(\boldsymbol{q}) = \frac{4\pi Q}{q^2 + k_{TF}^2}. \tag{6.186}$$

As it is known from the calculation of the Fourier transform of the Coulomb potential, we get by back-transformation in the position space

$$\Phi(\boldsymbol{r}) = \frac{Q}{r}e^{-k_{TF}r}. \tag{6.187}$$

---

[14] Named after L.H. Thomas (American physicist of British origin, professor in Columbus, Ohio, and at Columbia University in New York, works on atomic physics and spin-orbit interaction) and E. Fermi, see footnote 5.8.

The total potential is therefore a screened Coulomb potential which behaves like a normal Coulomb potential for small distances but goes to zero exponentially for large distances. $1/k_{TF}$ is the characteristic length scale on which the transition between the two behaviors occurs; $1/k_{TF}$ is therefore a measure of the range of the potential. For the Fourier transform of such a screened Coulomb potential, there are apparently no problems with divergences for $q \to 0$; this is already clear because of the general principle "short-range in position space → long-range in $q$-space". Such a Coulomb potential modified by an exponential decay factor is also called a **Yukawa potential.**[15]

The Thomas-Fermi theory is very simple; the weak point is the use of the equilibrium distribution for free particles in a constant potential also in the case of a spatially varying potential. However, this is a possible standard procedure for the treatment of non-equilibrium processes by spatial inhomogeneities. In statistical physics, we actually only know the statistical operators (density operators) for thermal equilibrium. One way to deal with non-equilibrium phenomena is to assume a slow spatial variation and to decompose the system into subsystems, so that in each subsystem thermal equilibrium prevails. This is how one treats, in particular, temperature gradients and phenomena such as heat conduction. On the other hand, one can also try to improve this treatment. Since one has already linearized in the position-dependent potential in the Thomas-Fermi approximation, one can also take this into account in a perturbative way. This leads to

### 6.6.2 Lindhard Theory of Screening

Within quantum mechanical perturbation theory one can calculate the change in energy eigenvalues and eigenstates due to a time-independent perturbation. In lowest (linear) order in the perturbation $H_1 = -e\Phi(\boldsymbol{r})$ it holds according to quantum mechanics:

$$|\psi_{\boldsymbol{k}}\rangle = |\psi_{\boldsymbol{k}}^0\rangle + \sum_{\boldsymbol{k}' \neq \boldsymbol{k}} \frac{|\psi_{\boldsymbol{k}'}^0\rangle\langle\psi_{\boldsymbol{k}'}^0|H_1|\psi_{\boldsymbol{k}}^0\rangle}{\varepsilon_{\boldsymbol{k}} - \varepsilon_{\boldsymbol{k}'}}. \tag{6.188}$$

Especially here in the treatment of screening by a homogeneous electron gas, the unperturbed eigenstates $|\psi_{\boldsymbol{k}}^0\rangle$ are plane waves and therefore

$$\left\langle \psi_{\boldsymbol{k}'}^0|H_1|\psi_{\boldsymbol{k}}^0\right\rangle = -\frac{e}{V}\int d^3r e^{i(\boldsymbol{k}-\boldsymbol{k}')\boldsymbol{r}}\Phi(\boldsymbol{r}) = -e\Phi(\boldsymbol{q}) \tag{6.189}$$

with $\boldsymbol{q} = \boldsymbol{k} - \boldsymbol{k}'$. This results in the particle density at the location $\boldsymbol{r}$:

---

[15] H. Yukawa, 1907–1981, Japanese physicist, postulated 1935 such an interaction potential between nucleons mediated by bosons with finite rest mass; these turned out to be the pi-mesons found in 1937 in cosmic rays; Nobel Prize 1949.

$$\begin{aligned} n(\boldsymbol{r}) &= 2\sum_{\boldsymbol{k}} f_{\boldsymbol{k}} |\psi_{\boldsymbol{k}}(\boldsymbol{r})|^2 \\ &= 2\sum_{\boldsymbol{k}} f_{\boldsymbol{k}} |\psi^0_{\boldsymbol{k}}(\boldsymbol{r})|^2 + 2\frac{e}{V}\sum_{\boldsymbol{kq}} f_{\boldsymbol{k}} \Phi(\boldsymbol{q}) \frac{e^{i\boldsymbol{kr}} e^{-i(\boldsymbol{k}-\boldsymbol{q})\boldsymbol{r}} + e^{-i\boldsymbol{kr}} e^{i(\boldsymbol{k}-\boldsymbol{q})\boldsymbol{r}}}{\hbar^2\left(\frac{\boldsymbol{kq}}{m} - \frac{q^2}{2m}\right)} . \end{aligned} \tag{6.190}$$

For the induced charge density, one obtains

$$\begin{aligned} \rho^{\text{ind}}(\boldsymbol{r}) &= \frac{2e^2}{V}\sum_{\boldsymbol{q}} e^{i\boldsymbol{qr}} \sum_{\boldsymbol{k}} f_{\boldsymbol{k}} \left( \frac{1}{\hbar^2\left(\boldsymbol{kq}/m - q^2/2m\right)} - \frac{1}{\hbar^2\left(\boldsymbol{kq}/m + q^2/2m\right)} \right) \Phi(\boldsymbol{q}) \\ &= \frac{2e^2}{V}\sum_{\boldsymbol{q}} e^{i\boldsymbol{qr}} \Phi(\boldsymbol{q}) \sum_{\boldsymbol{k}} \frac{f_{\boldsymbol{k}+\boldsymbol{q}/2} - f_{\boldsymbol{k}-\boldsymbol{q}/2}}{\hbar^2 \boldsymbol{kq}/m} . \end{aligned} \tag{6.191}$$

Obviously

$$\rho^{\text{ind}}(\boldsymbol{q}) = \frac{2e^2}{V}\sum_{\boldsymbol{k}} \frac{f_{\boldsymbol{k}+\boldsymbol{q}/2} - f_{\boldsymbol{k}-\boldsymbol{q}/2}}{\hbar^2 \boldsymbol{kq}/m} \Phi(\boldsymbol{q}) \tag{6.192}$$

and therefore

$$\chi(\boldsymbol{q}) = \frac{2e^2}{V}\sum_{\boldsymbol{k}} \frac{f_{\boldsymbol{k}+\boldsymbol{q}/2} - f_{\boldsymbol{k}-\boldsymbol{q}/2}}{\hbar^2 \boldsymbol{kq}/m} = e^2 \int \frac{d^3k}{4\pi^3} \frac{f_{\boldsymbol{k}+\boldsymbol{q}/2} - f_{\boldsymbol{k}-\boldsymbol{q}/2}}{\hbar^2 \boldsymbol{kq}/m} . \tag{6.193}$$

This is the (static) **Lindhard-susceptibility**.[16] In particular, for small $q$, one obtains by expanding the Fermi functions:

$$f_{\boldsymbol{k}\pm\boldsymbol{q}/2} = \frac{1}{\exp\left[\beta\left(\frac{\hbar^2(\boldsymbol{k}\pm\boldsymbol{q}/2)^2}{2m} - \mu\right)\right] + 1} = f_{\boldsymbol{k}} \mp \frac{\hbar^2 \boldsymbol{kq}}{2m} \frac{\partial f_{\boldsymbol{k}}}{\partial \mu} . \tag{6.194}$$

This shortens the denominator in (6.193), the susceptibility becomes $q$ -independent and only the derivative at the Fermi edge remains. The Lindhard susceptibility therefore goes over to the Thomas-Fermi susceptibility for $q \to 0$. So you can reproduce the above Thomas-Fermi result from the perturbation theoretical treatment carried out here. This is consistent with the assumption of a slowly varying potential made in the Thomas-Fermi approximation: If something varies slowly in space and thus has a long range, its Fourier transform is short-ranged and thus only significantly different from 0 for small $q$.

---

[16] J. Lindhard, *1922, †1997 in Aarhus (Denmark), Danish theoretical physicist, student of Niels Bohr, worked in the 1950s on the dielectric response of the electron gas and on the penetration of ion beams into solids (ion implantation etc.), since 1957 professor in Aarhus.

For any $\boldsymbol{q}$, the Lindhard dielectric constant is given by

$$\varepsilon(\boldsymbol{q}) = 1 - \frac{4\pi}{q^2}\chi(\boldsymbol{q}) = 1 - \frac{e^2 m}{\hbar^2\pi^2 q^2}\int d^3k \frac{f_{\boldsymbol{k}+\boldsymbol{q}/2} - f_{\boldsymbol{k}-\boldsymbol{q}/2}}{\boldsymbol{kq}}. \tag{6.195}$$

Obviously, $\varepsilon(\boldsymbol{q}) = \varepsilon(-\boldsymbol{q})$ and it follows:

$$\begin{aligned} \varepsilon(\boldsymbol{q}) &= 1 + \frac{4e^2 m}{\pi^2\hbar^2 q^2}\int d^3k \frac{f(\varepsilon_{\boldsymbol{k}})}{q^2 + 2\boldsymbol{kq}} \\ &= 1 + \frac{4e^2 m}{\pi^2\hbar^2 q^2} 2\pi \int_0^{k_F} dk k^2 \int_{-1}^{+1} \frac{du}{q^2 + 2kqu}. \end{aligned} \tag{6.196}$$

The remaining integrals are elementary analytically calculable for $T = 0$ and one obtains as a result for the static Lindhard dielectric constant:

$$\varepsilon(\boldsymbol{q}) = 1 + \frac{4mk_F e^2}{\pi\hbar^2 q^2} F\left(\frac{q}{2k_F}\right) \tag{6.197}$$

with the **Lindhard function**

$$F(x) = \frac{1}{2} + \frac{1-x^2}{4x}\ln\left|\frac{1+x}{1-x}\right|, \tag{6.198}$$

which was already introduced in (6.115) and is graphically represented in Fig. 6.4. Since $F(x) \to 1$ for $x \to 0$, it follows in the limit $\frac{q}{2k_F} \ll 1$

$$\varepsilon(q) \to 1 + \frac{4mk_F e^2}{\pi\hbar^2 q^2} = 1 + \frac{k_{TF}^2}{q^2}, \tag{6.199}$$

which corresponds to the Thomas-Fermi result. For $q \to 0$, the dielectric constant diverges, therefore a long-wavelength potential is completely screened, since $V_{\boldsymbol{q}}/\varepsilon(\boldsymbol{q})$ vanishes.

The Lindhard function disappears asymptotically for large $x$ proportional to $\frac{1}{x^2}$, the susceptibility is therefore proportional $1/q^2$ and the deviation of the dielectric constant from 1 goes like $1/q^4$. Short-wavelength perturbations with $q \gg 2k_F$ are therefore only weakly screened. For $q \approx 2k_F$, the dielectric constant behaves like

$$\varepsilon(q) \approx 1 + \left(\frac{k_{TF}}{2k_F}\right)^2 \left[\frac{1}{2} + \frac{1}{2}\left(1 - \frac{q}{2k_F}\right)\ln\frac{2}{|1 - \frac{q}{2k_F}|}\right]. \tag{6.200}$$

It therefore has a logarithmic singularity at $q = 2k_F$, the "**$2k_F$-singularity**".

It can also be estimated analytically—as in the Thomas-Fermi approximation—how the screened Coulomb potential of a point charge looks explicitly in the Lindhard approximation. If one sets $\varepsilon(q) = 1 + \frac{g^2(q)}{q^2}$ with $g^2(q) = k_{TF}^2 F(\frac{q}{2k_F})$, then the screened potential fulfills

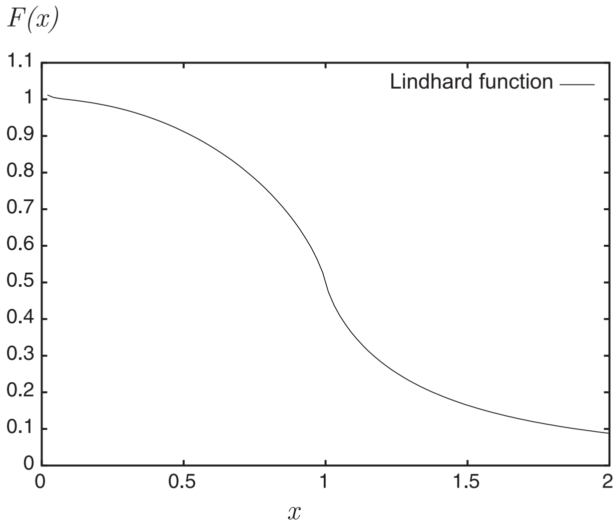

**Fig. 6.4** Lindhard function

$$\begin{aligned}\Phi(\boldsymbol{r}) &= \int \frac{d^3q}{(2\pi)^3}\Phi(q)e^{i\boldsymbol{qr}} = \int \frac{d^3q}{(2\pi)^3}\frac{4\pi Q}{q^2+g^2(q)}e^{i\boldsymbol{qr}} \\ &= \frac{1}{(2\pi)^2}\int_0^\infty dqq^2\Phi(q)\int_{-1}^{+1} due^{iqru} = \frac{1}{r}\frac{1}{2\pi^2}\int_0^\infty dqq\Phi(q)\sin(qr) \\ &= \frac{Q}{r}\frac{2}{\pi}\int_0^\infty dq\frac{q\sin(qr)}{q^2+g^2(q)}. \end{aligned} \tag{6.201}$$

For the analytical calculation of the last $q$-integral, one can convince oneself that a contribution due to the $2k_F$-singularity is dominant. After some conversion using residue techniques, the screened Coulomb potential in Lindhard approximation finally follows as:

$$\Phi(r) = CQ\frac{\cos(2k_F r)}{r^3} \text{ with } C = \left(\frac{k_{TF}}{4k_F\varepsilon(2k_F)}\right)^2. \tag{6.202}$$

Instead of the short-range Yukawa potential in Thomas-Fermi approximation, one thus obtains a long-range, oscillating potential which falls off for large $r$ like $1/r^3$. These oscillations are also called “**Friedel oscillations**”.

### 6.6.3 Static Screening in Semiconductors

In semiconductors, excitations due to an external electrostatic potential $\Phi(\boldsymbol{r})$ are only possible via transitions from the valence band to the conduction band. Therefore, one can no longer work with the model of free electrons as in metals to describe screening effects, but must explicitly consider several bands. Analogous to (6.188), for the states modified by the presence of $\Phi(\boldsymbol{r})$, first-order perturbation theory yields

$$\psi_{\boldsymbol{k}n}(\boldsymbol{r}) = \psi^0_{\boldsymbol{k}n}(\boldsymbol{r}) + \sum_{n'\boldsymbol{k}'} \psi^0_{\boldsymbol{k}'n'}(\boldsymbol{r}) \frac{\int d^3r' \psi^{0*}_{\boldsymbol{k}'n'}(\boldsymbol{r}')(-e\Phi(\boldsymbol{r}'))\psi^0_{\boldsymbol{k}n}(\boldsymbol{r}')}{E_n(\boldsymbol{k}) - E_{n'}(\boldsymbol{k}')}. \tag{6.203}$$

The change in charge density due to the action of the electrostatic potential is therefore

$$\begin{aligned}
\rho^{\text{ind}}(\boldsymbol{r}) &= 2e^2 \sum_{nkn'k'} f(E_n(\boldsymbol{k})) \Bigg( \psi^{0*}_{\boldsymbol{k}n}(\boldsymbol{r})\psi^0_{\boldsymbol{k}'n'}(\boldsymbol{r}) \frac{\int d^3r' \psi^{0*}_{\boldsymbol{k}'n'}(\boldsymbol{r}')\Phi(\boldsymbol{r}')\psi^0_{\boldsymbol{k}n}(\boldsymbol{r}')}{E_n(\boldsymbol{k}) - E_{n'}(\boldsymbol{k}')} \\
&\quad + \psi^{0*}_{\boldsymbol{k}'n'}(\boldsymbol{r})\psi^0_{\boldsymbol{k}n}(\boldsymbol{r}) \frac{\int d^3r' \psi^{0*}_{\boldsymbol{k}n}(\boldsymbol{r}')\Phi(\boldsymbol{r}')\psi^0_{\boldsymbol{k}'n'}(\boldsymbol{r}')}{E_n(\boldsymbol{k}) - E_{n'}(\boldsymbol{k}')} \Bigg) \\
&= 2e^2 \sum_{nkn'k'} \frac{f(E_n(\boldsymbol{k})) - f(E_{n'}(\boldsymbol{k}'))}{E_n(\boldsymbol{k}) - E_{n'}(\boldsymbol{k}')} \psi^{0*}_{\boldsymbol{k}'n'}(\boldsymbol{r})\psi^0_{\boldsymbol{k}n}(\boldsymbol{r}) \\
&\quad \times \int d^3r' \psi^{0*}_{\boldsymbol{k}'n'}(\boldsymbol{r}')\Phi(\boldsymbol{r}')\psi^0_{\boldsymbol{k}n}(\boldsymbol{r}').
\end{aligned} \tag{6.204}$$

We now use the Fourier transformation and its inverse for $\rho^{\text{ind}}(\boldsymbol{r})$, $\Phi(\boldsymbol{r})$:

$$\rho^{\text{ind}}(\boldsymbol{q}) = \frac{1}{V}\int d^3r e^{-i\boldsymbol{q}\boldsymbol{r}} \rho^{\text{ind}}(\boldsymbol{r}), \quad \Phi(\boldsymbol{r}) = \sum_{\boldsymbol{q}} e^{i\boldsymbol{q}\boldsymbol{r}}\Phi(\boldsymbol{q}). \tag{6.205}$$

It follows as the unperturbed eigenfunctions $\psi^0_{\boldsymbol{k}n}(\boldsymbol{r})$ are Bloch functions:

$$\begin{aligned}
\int d^3r \psi^{0*}_{\boldsymbol{k}'n'}(\boldsymbol{r}) e^{i\boldsymbol{q}\boldsymbol{r}} \psi^0_{\boldsymbol{k}n}(\boldsymbol{r}) &= \frac{1}{V}\int d^3r u^*_{\boldsymbol{k}'n'}(\boldsymbol{r}) e^{i(\boldsymbol{k}+\boldsymbol{q}-\boldsymbol{k}')\boldsymbol{r}} u_{\boldsymbol{k}n}(\boldsymbol{r}) \\
&= \underbrace{\frac{1}{N}\sum_{\boldsymbol{R}} e^{i(\boldsymbol{k}+\boldsymbol{q}-\boldsymbol{k}')\boldsymbol{R}}}_{\delta_{\boldsymbol{k}+\boldsymbol{q},\boldsymbol{k}'}} \frac{1}{V_{EZ}} \int_{EZ} d^3r u^*_{\boldsymbol{k}'n'}(\boldsymbol{r}) e^{i(\boldsymbol{k}+\boldsymbol{q}-\boldsymbol{k}')\boldsymbol{r}} u_{\boldsymbol{k}n}(\boldsymbol{r}).
\end{aligned} \tag{6.206}$$

This gives the Fourier transform of the induced charge density as

$$\rho^{\text{ind}}(\boldsymbol{q}) = \frac{2e^2}{V} \sum_{\boldsymbol{k},n,n'} \frac{f(E_n(\boldsymbol{k})) - f(E_{n'}(\boldsymbol{k}+\boldsymbol{q}))}{E_n(\boldsymbol{k}) - E_{n'}(\boldsymbol{k}+\boldsymbol{q})} \left|M_{n,n'}(\boldsymbol{k},\boldsymbol{q})\right|^2 \Phi(\boldsymbol{q}), \tag{6.207}$$

with

$$\begin{aligned}M_{nn'}(\boldsymbol{k},\boldsymbol{q}) &= \frac{1}{V_{EZ}}\int_{EZ} d^3r u^*_{\boldsymbol{k}+\boldsymbol{q}n'}(\boldsymbol{r})u_{\boldsymbol{k}n}(\boldsymbol{r}) = \frac{1}{V}\int d^3r \psi^{0*}_{\boldsymbol{k}+\boldsymbol{q}n'}(\boldsymbol{r})e^{i\boldsymbol{q}\boldsymbol{r}}\psi^{0}_{\boldsymbol{k}n}(\boldsymbol{r}) \\ &= \langle \boldsymbol{k}+\boldsymbol{q}n'|e^{i\boldsymbol{q}\boldsymbol{r}}|\boldsymbol{k}n\rangle.\end{aligned} \tag{6.208}$$

So far, it has not yet been used that we want to consider semiconductors. It has only been a generalization of the Lindhard treatment to the case where the unperturbed eigenfunctions are no longer described as plane waves but as Bloch functions. If, conversely, one replaces $|\boldsymbol{k}n\rangle$ by plane waves again, one obtains $M_{nn'}(\boldsymbol{k},\boldsymbol{q}) = 1$ and the Lindhard result is reproduced. For semiconductors, the following assumptions are made:

- For $T = 0$ only the valence band $n \equiv v$ is occupied, the unperturbed conduction band states $c \equiv n'$ are unoccupied
- The energy difference between valence and conduction band energies is approximated by the constant band gap:

$$E_c(\boldsymbol{k}+\boldsymbol{q}) - E_v(\boldsymbol{k}) \approx \Delta. \tag{6.209}$$

For $n \neq n'$ the matrix elements $M_{nn'}(\boldsymbol{k},\boldsymbol{q})$ vanish for $q \to 0$ due to the orthonormality of the Bloch states for different band indices. Therefore, for small $q$:

$$M_{nn'}(\boldsymbol{k},\boldsymbol{q}) \sim \alpha q. \tag{6.210}$$

It follows for the susceptibility

$$\chi(\boldsymbol{q}) = -e^2 n_0 \frac{\alpha^2 q^2}{\Delta} \tag{6.211}$$

with $n_0 = N_e/V$ the electron density. For semiconductors and insulators, the susceptibility for $q \to 0$ is thus proportional to $q^2$, and the physical reason for this is ultimately that only excitations between different bands (valence and conduction band) are possible, which is why the matrix elements are at least linear in $q$ and the energy denominator is constantly equal to the energy gap. Consequently, for the dielectric constant one obtains for small $q$:

$$\varepsilon(\boldsymbol{q}) = 1 + \frac{4\pi e^2 \alpha^2 n_0}{\Delta}. \tag{6.212}$$

The static dielectric constant therefore has a finite value for $q = 0$. So it is not possible to screen as well as in metals. The potential of a point charge $Q$ is therefore modified in semiconductors in

$$\Phi(\boldsymbol{r}) = \frac{Q}{\varepsilon(0)r}. \tag{6.213}$$

So there remains a long-range $1/r$-potential but with a strength modified (decreased) by the dielectric constant. In a metal, the conduction electrons can arrange themselves by their good mobility so that at a sufficiently large distance the point charge is no longer felt, since the total potential falls off much faster than the bare Coulomb potential. In semiconductors, the screening (by the electrons at least) is much weaker.

A rough estimate of the order of magnitude of α can be found using the generally valid commutation relation $[[H, e^{i\boldsymbol{qr}}], e^{-i\boldsymbol{qr}}] = -\frac{\hbar^2 q^2}{m}$ from which follows

$$\langle\nu|\big[\big[H, e^{i\boldsymbol{qr}}\big], e^{-i\boldsymbol{qr}}\big]|\nu\rangle = \sum_{\nu'}(E_\nu - E_{\nu'})|\langle\nu|e^{i\boldsymbol{qr}}|\nu'\rangle|^2 = -\frac{\hbar^2 q^2}{m}. \tag{6.214}$$

This allows us to estimate

$$\alpha^2 \sim \frac{\hbar^2}{m\Delta}. \tag{6.215}$$

Since in (6.214) in contrast to (6.207) a complete system of eigenstates $|\nu'\rangle$ of the Hamiltonian operator is summed up, this result cannot be exact but only an estimate; a real dielectric constant of semiconductors has in particular a (weak) $q$ -dependence.

## 6.7 Excitations in the Homogeneous Electron Gas, Plasmons

In this section the homogeneous electron gas is considered again, that is, the Hamiltonian operator in 2nd quantization

$$H = H_0 + H_1 = \sum_{\boldsymbol{k},\sigma} E(\boldsymbol{k}) c^\dagger_{\boldsymbol{k}\sigma} c_{\boldsymbol{k}\sigma} + \frac{1}{2}\sum_{\boldsymbol{q}} v_{\boldsymbol{q}} \rho^\dagger(\boldsymbol{q})\rho(\boldsymbol{q}) \tag{6.216}$$

with

$$E(\boldsymbol{k}) = \frac{\hbar^2 k^2}{2m}, \quad v_{\boldsymbol{q}} = \frac{4\pi e^2}{Vq^2} \tag{6.217}$$

$$\rho(\boldsymbol{q}) = \sum_{\boldsymbol{k},\sigma} c^\dagger_{\boldsymbol{k}\sigma} c_{\boldsymbol{k}+\boldsymbol{q}\sigma}, \quad \rho^\dagger(\boldsymbol{q}) = \sum_{\boldsymbol{k}\sigma} c^\dagger_{\boldsymbol{k}+\boldsymbol{q}\sigma} c_{\boldsymbol{k}\sigma}, \tag{6.218}$$

which are the Fourier transforms of the particle density operator and its adjoint operator.

Without interaction term, in the ground state all particle states $\boldsymbol{k}$ are occupied with $|k| \leq k_F$, and that also applies to the system with interaction at least in Hartree-Fock approximation. The simplest conceivable excitations of the system are therefore the annihilation of an electron in a state $\boldsymbol{k}$ below the Fermi edge and the creation of the electron in another previously unoccupied state $\boldsymbol{k} + \boldsymbol{q}$, which must therefore be above the Fermi edge. There is thus an electron vacancy, that is, a "hole" in the Fermi sphere and at the same time a particle with momentum (wave vector) outside the Fermi sphere. Therefore, one also speaks of

**particle-hole excitations**. Associated with such a particle-hole excitation, which can be generated thermally or optically (i.e. by photons) or by the interaction with other particles at $T = 0$, is an energy and momentum transfer. The particle-hole pair generated can therefore be assigned the energy and momentum:

$$E_{TL}(\boldsymbol{q}) = \frac{\hbar^2(\boldsymbol{k}+\boldsymbol{q})^2}{2m} - \frac{\hbar^2 k^2}{2m} \quad \text{and} \quad \hbar\boldsymbol{q}. \tag{6.219}$$

Here $|\boldsymbol{k}| \leq k_F$ and $|\boldsymbol{k}+\boldsymbol{q}| \geq k_F$ apply. Therefore, it follows:

$$E_{TL}(\boldsymbol{q}) \geq 0, \quad E_{TL}(\boldsymbol{q}) = \frac{\hbar^2}{m}\left(kq\cos\vartheta + \frac{q^2}{2}\right)\begin{cases} \leq \frac{\hbar^2}{m}\left(k_F q + \frac{q^2}{2}\right) \\ \geq \frac{\hbar^2}{m}\left(-k_F q + \frac{q^2}{2}\right) \end{cases}. \tag{6.220}$$

In the energy-momentum diagram of Fig. 6.5 the energies of the particle-hole excitations are therefore in the shaded area, bounded by the two parabolas and the $q$-axis. For these excitation energies, there is therefore no longer a clear assignment between energy and momentum, but for a given momentum $q$ there can be several possible particle-hole excitations with corresponding energies. In addition to these individual particle-hole excitations, which already exist in a non-interacting system or in a system of uncharged fermions, there are also collective excitations of the homogeneous electron gas. This can already be seen by the following simple consideration: If one deflects the electron gas as a whole by a distance $\boldsymbol{u}$ with respect to the positive background charge in a Jellium system, a polarization per unit volume of

$$\boldsymbol{P} = -ne\boldsymbol{u} \tag{6.221}$$

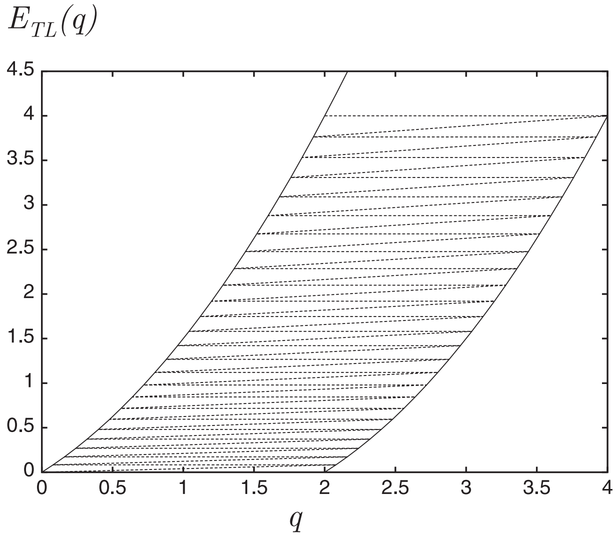

**Fig. 6.5** Energy range of particle-hole excitations in the electron gas

is created, where $n$ is the electron density. This in turn causes an electric field per unit volume

$$\boldsymbol{E} = 4\pi \boldsymbol{P} = -4\pi ne\boldsymbol{u}. \tag{6.222}$$

This in turn causes a restoring force on the electrons; per unit volume ,therefore, the following equation of motion applies

$$nm\ddot{\boldsymbol{u}} = -4\pi n^2 e^2 \boldsymbol{u}. \tag{6.223}$$

This is apparently the equation of motion of a harmonic oscillator. So harmonic oscillations of the electron system as a whole are to be expected around the equilibrium position. The characteristic frequency for this collective oscillation is given by the

**Plasma Frequency**

$$\omega_P = \sqrt{\frac{4\pi ne^2}{m}}. \tag{6.224}$$

Already according to this simple, classical consideration, collective excitations of the electron system as a whole are to be expected in addition to the elementary particle-hole excitations. The quantized plasma oscillations are also called

**Plasmons**

The following consideration from classical electrodynamics also shows once again that a special reaction of the electron system is to be expected at the plasma frequency given above. From the Maxwell equations for a conducting medium

$$\nabla \boldsymbol{E} = 0, \nabla \times \boldsymbol{E} = -\frac{1}{c}\frac{\partial \boldsymbol{B}}{\partial t}, \nabla \times \boldsymbol{H} = \frac{4\pi}{c}\boldsymbol{j} + \frac{1}{c}\frac{\partial \boldsymbol{E}}{\partial t} \tag{6.225}$$

it follows with $\boldsymbol{j} = \sigma \boldsymbol{E}$ (Ohm's law)

$$\nabla^2 \boldsymbol{E} - \frac{1}{c^2}\left(\frac{\partial^2 \boldsymbol{E}}{\partial t^2} + 4\pi\sigma \frac{\partial \boldsymbol{E}}{\partial t}\right) = 0. \tag{6.226}$$

With the ansatz of a plane wave $\boldsymbol{E} = \boldsymbol{E}_0 e^{i(\boldsymbol{kr}-\omega t)}$ one obtains

$$k^2 = \frac{\omega^2}{c^2}\left(1 + i\frac{4\pi\sigma}{\omega}\right), \tag{6.227}$$

thus a complex wave number. The imaginary part leads to an exponential decay of an electromagnetic wave in the conductive medium, which is physically due to the energy absorption from the wave by conversion into kinetic energy of the electron system. However, the conductivity σ is also frequency-dependent. The simplest phenomenological theory of conductivity, namely the Drude theory (see also Sect. 1.1 in Volume 2), will be briefly outlined here. In the alternating electric field, the equation of motion for electrons is

$$m\dot{\boldsymbol{v}} + \frac{m}{\tau}\boldsymbol{v} = e\boldsymbol{E}_0 e^{-i\omega t}, \tag{6.228}$$

where $\frac{m}{\tau}\boldsymbol{v}$ is a phenomenological friction force and τ can be interpreted as the collision time or lifetime of the electrons. With the ansatz $\boldsymbol{v} = \boldsymbol{v}_0 e^{-i\omega t}$ one obtains

$$m\left(-i\omega + \frac{1}{\tau}\right)\boldsymbol{v}_0 = e\boldsymbol{E}_0. \tag{6.229}$$

From this follows for the current density

$$\boldsymbol{j} = ne\boldsymbol{v} = \frac{ne^2\tau}{m(1 - i\omega\tau)}\boldsymbol{E}. \tag{6.230}$$

The complex, frequency-dependent conductivity is therefore

$$\sigma(\omega) = \frac{ne^2\tau}{m}\frac{1}{1 - i\omega\tau}. \tag{6.231}$$

In the limit $\omega\tau \gg 1$ the "conductivity" becomes purely imaginary

$$\sigma_P \approx i\frac{ne^2}{m\omega} \tag{6.232}$$

and the relationship between wave number and frequency goes over into

$$k^2 = \frac{\omega^2}{c^2}\left(1 - \frac{\omega_P^2}{\omega^2}\right) \tag{6.233}$$

with the **plasma frequency**$\omega_P = \sqrt{\frac{4\pi ne^2}{m}}$. The (complex) refractive index is therefore given by

$$\tilde{n}^2 = 1 - \frac{\omega_P^2}{\omega^2}. \tag{6.234}$$

For frequencies $\omega < \omega_P$ and $\tau\omega \gg 1$, the refractive index is therefore purely imaginary and the wave cannot propagate in the metal, but is reflected. For frequencies $\omega > \omega_P$, the refractive index is real and the wave can penetrate into the metal (the "plasma" of free electrons and positive charges). If you solve the above equation for ω, you get the dispersion relation

$$\omega^2 = \omega_P^2 + c^2k^2. \tag{6.235}$$

After we have convinced ourselves of the importance of the characteristic frequency $\omega_P$ for the respective plasma (metal) by means of two different classical considerations, a microscopically quantum-mechanical derivation of the existence of a collective excitation mode shall follow.

If one considers the time dependence of the operators $c^\dagger_{\boldsymbol{k}+\boldsymbol{q}\sigma}c_{\boldsymbol{k}\sigma}$, which describe the elementary excitations and whose $\boldsymbol{k}$-sum is the Fourier transform of the particle density, then in the Heisenberg picture the following equation of motion is valid

$$\frac{d}{dt} c^\dagger_{\boldsymbol{k}+\boldsymbol{q}\sigma} c_{\boldsymbol{k}\sigma} = \frac{i}{\hbar}\left[H, c^\dagger_{\boldsymbol{k}+\boldsymbol{q}\sigma} c_{\boldsymbol{k}\sigma}\right]. \tag{6.236}$$

Using the commutation rules

$$\left[c^\dagger_{\boldsymbol{k}'\sigma'} c_{\boldsymbol{k}'\sigma'}, c^\dagger_{\boldsymbol{k}+\boldsymbol{q}\sigma} c_{\boldsymbol{k}\sigma}\right] = \delta_{\boldsymbol{k}+\boldsymbol{q}\boldsymbol{k}'}\delta_{\sigma\sigma'} c^\dagger_{\boldsymbol{k}'\sigma'} c_{\boldsymbol{k}\sigma} - \delta_{\boldsymbol{k}\boldsymbol{k}'}\delta_{\sigma\sigma'} c^\dagger_{\boldsymbol{k}+\boldsymbol{q}\sigma} c_{\boldsymbol{k}'\sigma'} \tag{6.237}$$

and

$$\begin{aligned}
&\left[c^\dagger_{\boldsymbol{k}'+\boldsymbol{q}'\sigma'} c_{\boldsymbol{k}'\sigma'} c^\dagger_{\boldsymbol{k}''-\boldsymbol{q}'\sigma''} c_{\boldsymbol{k}''\sigma''}, c^\dagger_{\boldsymbol{k}+\boldsymbol{q}\sigma} c_{\boldsymbol{k}\sigma}\right] \\
&\quad = \delta_{\boldsymbol{k}+\boldsymbol{q}\boldsymbol{k}''}\delta_{\sigma\sigma''} c^\dagger_{\boldsymbol{k}'+\boldsymbol{q}'\sigma'} c_{\boldsymbol{k}'\sigma'} c^\dagger_{\boldsymbol{k}''-\boldsymbol{q}'\sigma''} c_{\boldsymbol{k}\sigma} + \delta_{\boldsymbol{k}+\boldsymbol{q}\boldsymbol{k}'}\delta_{\sigma\sigma'} c^\dagger_{\boldsymbol{k}'+\boldsymbol{q}'\sigma'} c_{\boldsymbol{k}\sigma} c^\dagger_{\boldsymbol{k}''-\boldsymbol{q}'\sigma''} c_{\boldsymbol{k}''\sigma''} \\
&\quad - \delta_{\boldsymbol{k}''-\boldsymbol{q}'\boldsymbol{k}}\delta_{\sigma\sigma''} c^\dagger_{\boldsymbol{k}'+\boldsymbol{q}'\sigma'} c_{\boldsymbol{k}'\sigma'} c^\dagger_{\boldsymbol{k}+\boldsymbol{q}\sigma} c_{\boldsymbol{k}''\sigma''} - \delta_{\boldsymbol{k}'+\boldsymbol{q}'\boldsymbol{k}}\delta_{\sigma\sigma'} c^\dagger_{\boldsymbol{k}+\boldsymbol{q}\sigma} c_{\boldsymbol{k}'\sigma'} c^\dagger_{\boldsymbol{k}''-\boldsymbol{q}'\sigma''} c_{\boldsymbol{k}''\sigma''}
\end{aligned} \tag{6.238}$$

results in

$$\begin{aligned}
\frac{\hbar}{i}\frac{d}{dt}\left(c^\dagger_{\boldsymbol{k}+\boldsymbol{q}\sigma} c_{\boldsymbol{k}\sigma}\right) &= (E(\boldsymbol{k}+\boldsymbol{q}) - E(\boldsymbol{k}))c^\dagger_{\boldsymbol{k}+\boldsymbol{q}\sigma} c_{\boldsymbol{k}\sigma} \\
&+ \sum_{\boldsymbol{q}'\boldsymbol{k}'\sigma'} v_{\boldsymbol{q}'}\left(c^\dagger_{\boldsymbol{k}'+\boldsymbol{q}'\sigma'} c_{\boldsymbol{k}'\sigma'} c^\dagger_{\boldsymbol{k}+\boldsymbol{q}-\boldsymbol{q}'\sigma} c_{\boldsymbol{k}\sigma} - c^\dagger_{\boldsymbol{k}'+\boldsymbol{q}'\sigma'} c_{\boldsymbol{k}'\sigma'} c^\dagger_{\boldsymbol{k}+\boldsymbol{q}\sigma} c_{\boldsymbol{k}+\boldsymbol{q}'\sigma}\right).
\end{aligned} \tag{6.239}$$

Since on the right hand side of this equation of motion apparently products of four fermion creation and annihilation operators occur, the equation of motion does not close, but one obtains an infinite hierarchy of equations. This is characteristic for the application of equation of motion methods to systems of interacting electron systems. Approximations are necessary to close the equations, and the approximation that is closest to the Hartree-Fock treatment is to replace the product of four Fermi operators in an appropriate way by the product of an expectation value of two Fermi operators times a product of a creator and annihilator. This leads to the approximation

$$\begin{aligned}
\frac{\hbar}{i}\frac{d}{dt}\left(c^\dagger_{\boldsymbol{k}+\boldsymbol{q}\sigma} c_{\boldsymbol{k}\sigma}\right) &= (E(\boldsymbol{k}+\boldsymbol{q}) - E(\boldsymbol{k}))c^\dagger_{\boldsymbol{k}+\boldsymbol{q}\sigma} c_{\boldsymbol{k}\sigma} \\
&+ \sum_{\boldsymbol{q}'\boldsymbol{k}'\sigma'} v_{\boldsymbol{q}'}\left(\left\langle c^\dagger_{\boldsymbol{k}+\boldsymbol{q}-\boldsymbol{q}'\sigma} c_{\boldsymbol{k}\sigma}\right\rangle c^\dagger_{\boldsymbol{k}'+\boldsymbol{q}'\sigma'} c_{\boldsymbol{k}'\sigma'} - \left\langle c^\dagger_{\boldsymbol{k}+\boldsymbol{q}\sigma} c_{\boldsymbol{k}+\boldsymbol{q}'\sigma}\right\rangle c^\dagger_{\boldsymbol{k}'+\boldsymbol{q}'\sigma'} c_{\boldsymbol{k}'\sigma'}\right).
\end{aligned} \tag{6.240}$$

It is easy to calculate that for the second obvious decoupling the two summands compensate each other. One can now further convince oneself that only for $\boldsymbol{q}' = \boldsymbol{q}$ a non-vanishing contribution remains. Because at least when the expectation values are calculated with respect to the Hartree-Fock Hamiltonian operator, these must be diagonal in $\boldsymbol{k}$. In addition, one can argue that for any $\boldsymbol{q}'$ the matrix elements of $c^\dagger_{\boldsymbol{k}+\boldsymbol{q}\sigma} c_{\boldsymbol{k}+\boldsymbol{q}'\sigma}$ and the corresponding operator in the second summand are complex numbers with phase factors that are not correlated with each other. If one therefore sums over $\boldsymbol{q}'$, the contributions of the two summands should cancel each other out with the exception of the contribution of $\boldsymbol{q}' = \boldsymbol{q}$. Because of this justification with the uncorrelated phase factors for $\boldsymbol{q}' \neq \boldsymbol{q}$, this approximation is also called

**Random Phase Approximation (RPA).**

The RPA is ultimately an approximation for two-particle excitations which is consistent with the Hartree-Fock approximation. One now obtains in RPA the equation of motion

$$\begin{aligned}\frac{\hbar}{i}\frac{d}{dt}\left(c^{\dagger}_{\boldsymbol{k}+\boldsymbol{q}\sigma}c_{\boldsymbol{k}\sigma}\right) &= (E(\boldsymbol{k}+\boldsymbol{q}) - E(\boldsymbol{k}))c^{\dagger}_{\boldsymbol{k}+\boldsymbol{q}\sigma}c_{\boldsymbol{k}\sigma} \\ &\quad + (f(E(\boldsymbol{k})) - f(E(\boldsymbol{k}+\boldsymbol{q})))v_{\boldsymbol{q}}\sum_{\boldsymbol{k}'\sigma'} c^{\dagger}_{\boldsymbol{k}'+\boldsymbol{q}\sigma'}c_{\boldsymbol{k}'\sigma'}.\end{aligned} \tag{6.241}$$

For eigenstates, a time dependence of the form $e^{i\omega t}$ must result, from which, after summation over $\boldsymbol{k}, \sigma$, it follows:

$$\sum_{\boldsymbol{k}\sigma} c^{\dagger}_{\boldsymbol{k}+\boldsymbol{q}\sigma}c_{\boldsymbol{k}\sigma} = \rho^{\dagger}(\boldsymbol{q}) = \sum_{\boldsymbol{k}\sigma} v_{\boldsymbol{q}}\frac{f(E(\boldsymbol{k})) - f(E(\boldsymbol{k}+\boldsymbol{q}))}{\hbar\omega - E(\boldsymbol{k}+\boldsymbol{q}) + E(\boldsymbol{k})}\rho^{\dagger}(\boldsymbol{q}). \tag{6.242}$$

So one obtains for the possible eigenfrequencies ω the implicit equation

$$F_{\boldsymbol{q}}(\omega) := \sum_{\boldsymbol{k}\sigma} v_{\boldsymbol{q}}\frac{f(E(\boldsymbol{k})) - f(E(\boldsymbol{k}+\boldsymbol{q}))}{\hbar\omega + E(\boldsymbol{k}) - E(\boldsymbol{k}+\boldsymbol{q})} = 1. \tag{6.243}$$

The function $F_{\boldsymbol{q}}(\omega)$ is qualitatively represented in Fig. 6.6; it evidently has simple poles at the particle-hole excitation energies $E(\boldsymbol{k}+\boldsymbol{q}) - E(\boldsymbol{k})$. Between each two poles, it must also take on the value 1 once.

So there is also a continuum of particle-hole excitations in the interacting system, but the excitation energies are slightly shifted compared to those of the non-interacting system. Since the function $F_{\boldsymbol{q}}(\omega)$ falls off for $\omega \to \infty$ proportional $\frac{1}{\omega}$ asymptotically, it must also take the value 1 again for frequencies ω outside the particle-hole continuum. There is therefore for each $\boldsymbol{q}$ an excitation energy $E_p(\boldsymbol{q}) = \hbar\omega_p(\boldsymbol{q})$, which does not arise from a particle-hole excitation of the non-interacting system, and this is precisely the collective plasma oscillation. For small $|\boldsymbol{q}|$, the frequency of this collective excitation can be estimated analytically. Because $v_{\boldsymbol{q}} = v_{-\boldsymbol{q}}$ one also has $F_{\boldsymbol{q}}(\omega) = F_{-\boldsymbol{q}}(\omega)$. Then, by renaming the summation indices

$$F_{\boldsymbol{q}}(\omega) = \sum_{\boldsymbol{k}\sigma} f(E(\boldsymbol{k}))v_{\boldsymbol{q}}\frac{2(E(\boldsymbol{k}+\boldsymbol{q}) - E(\boldsymbol{k}))}{\hbar^2\omega^2 - (E(\boldsymbol{k}) - E(\boldsymbol{k}+\boldsymbol{q}))^2}. \tag{6.244}$$

In the region of the collective mode, $\hbar\omega \gg E(\boldsymbol{k}+\boldsymbol{q}) - E(\boldsymbol{k}) = \frac{\hbar^2}{m}\left(\boldsymbol{k}\boldsymbol{q} + \frac{q^2}{2}\right)$ applies. This results in a n expansion in lowest order:

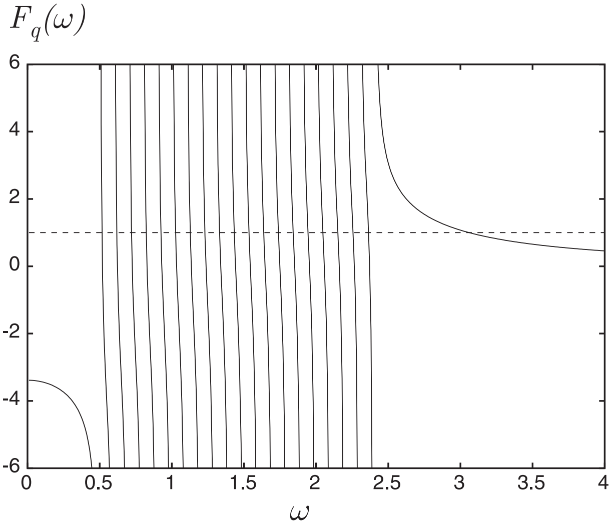

**Fig. 6.6** Graphical determination of the excitation energies

$$1 = \frac{4\pi e^2}{Vq^2\hbar^2\omega^2} \sum_{\boldsymbol{k}\sigma} f(E(\boldsymbol{k})) \frac{2\hbar^2}{m} \left( \frac{q^2}{2} + \boldsymbol{kq} \right). \tag{6.245}$$

For symmetry reasons ($E(\boldsymbol{k}) = E(-\boldsymbol{k})$ etc.) it applies

$$\sum_{\boldsymbol{k}} f(E(\boldsymbol{k}))(\boldsymbol{kq}) = 0.$$

So because of $N = \sum_{\boldsymbol{k}\sigma} f(E(\boldsymbol{k}))$ one finds for the frequency of the collective excitation mode in lowest order:

$$\omega_P^2 = \frac{4\pi e^2 N}{mV}. \tag{6.246}$$

This is precisely the plasma frequency introduced above; if one drives the development one order further, one can also calculate the $q$-dependence of the frequency of the collective plasma excitation for small $q$ and finds

$$\omega_p(q) = \omega_P \left( 1 + \frac{3}{10} \frac{\hbar^2 k_F^2}{m^2 \omega_P^2} q^2 \right). \tag{6.247}$$

## 6.8 Excitons in Semiconductors

This section discusses an important and experimentally observable consequence of the Coulomb interaction of electrons in semiconductors, namely the bound states between an electron in the conduction band and the hole left behind in the valence band, known as excitons. For a qualitative understanding, only a simple, rudimentary model is used from the outset, which, however, contains the most important components for the effect to be described. The starting point is in principle the general electronic solid-state Hamiltonian operator (6.39) in 2nd quantization taking into account the Coulomb interaction. For simplicity, the following model assumptions are made:

1. Only two bands are considered, namely a valence band and a conduction band. The interaction-free part of the Hamiltonian operator therefore has the form

$$H_0 = \sum_{\boldsymbol{k}} \left( E_v(\boldsymbol{k}) c^\dagger_{v\boldsymbol{k}} c_{v\boldsymbol{k}} + E_l(\boldsymbol{k}) c^\dagger_{l\boldsymbol{k}} c_{l\boldsymbol{k}} \right), \tag{6.248}$$

   where the indices $v, l$ stand for valence and conduction band.
2. Only the Coulomb interaction between electrons in the conduction band and in the valence band is taken into account . So only the following part of the general interaction Hamiltonian operator is considered:

$$H_1 = \sum_{\boldsymbol{k}_1\boldsymbol{k}_2\boldsymbol{k}_3\boldsymbol{k}_4} u_{\boldsymbol{k}_1\boldsymbol{k}_2,\boldsymbol{k}_3\boldsymbol{k}_4} c^\dagger_{v\boldsymbol{k}_1} c^\dagger_{l\boldsymbol{k}_2} c_{l\boldsymbol{k}_3} c_{v\boldsymbol{k}_4}. \tag{6.249}$$

   In particular, the interactions of the conduction and valence electrons with each other are not taken into account. This is based on the assumption that in the valence and conduction band structure $E_{v,l}(\boldsymbol{k})$ these interactions are already effectively (at least, for example, in a Hartree-Fock treatment) taken into account.
3. It is assumed that the excited states to be determined are independent of spin, so the spin index is omitted. In reality, any differences between singlet and triplet excitations that may be conceivable cannot be described with these model assumptions.
4. Of the interaction matrix elements, only those of the direct interaction should be considered, i.e. exchange terms are neglected. There is no quantitative justification for this, but it turns out that the effect to be described is already contained in the greatly simplified model, so that only quantitative corrections are to be expected from exchange terms, etc. The interaction matrix element is therefore given by

$$u_{\boldsymbol{k}_1\boldsymbol{k}_2,\boldsymbol{k}_3\boldsymbol{k}_4} = \int d^3r \int d^3r' \varphi^*_{v\boldsymbol{k}_1}(\boldsymbol{r}) \varphi^*_{l\boldsymbol{k}_2}(\boldsymbol{r}') \frac{e^2}{\varepsilon|\boldsymbol{r}-\boldsymbol{r}'|} \varphi_{l\boldsymbol{k}_3}(\boldsymbol{r}') \varphi_{v\boldsymbol{k}_4}(\boldsymbol{r}). \tag{6.250}$$

   Here, the $\varphi_{l,v\boldsymbol{k}}(\boldsymbol{r})$ are the valence or conduction band Bloch functions. In addition, a finite static dielectric constant $\varepsilon$ was taken into account in the Coulomb interaction between valence and conduction electrons; this should arise from the screening due to all other charges (electrons and ions) not explicitly considered here.
5. The further simplifying model assumption used later is that a direct gap exists at the $\Gamma$ point and the band structures in the vicinity of the upper valence band

edge or lower conduction band edge can be described in an effective mass picture. This means concretely for the band structures the assumptions:

$$E_v(\boldsymbol{k}) = -\frac{\hbar^2 k^2}{2m_v}, \quad E_l(\boldsymbol{k}) = \Delta + \frac{\hbar^2 k^2}{2m_l}, \tag{6.251}$$

as schematically shown in Fig. 6.7.

Here, $\Delta$ is the (direct) band gap, $m_l$ is the effective mass of the conduction electrons and $-m_v$ is the effective mass of the valence electrons, which is negative at the upper valence band edge. A missing electron with negative effective mass can also be interpreted as a hole (electron vacancy) with positive effective mass. A positively charged hole is then generated when an electron is destroyed. Therefore, creators and annihilators for holes can be defined by

$$h_{\boldsymbol{k}}^\dagger = c_{v\boldsymbol{k}}, \; h_{\boldsymbol{k}} = c_{v\boldsymbol{k}}^\dagger. \tag{6.252}$$

The hole operators then also fulfill the usual fermion commutation rules. Holes are therefore quasiparticles with fermion character, positive mass $m_v$ and positive charge. In the electron-hole picture, the entire model Hamiltonian operator takes the form

$$\begin{aligned} H = H_0 + H_1 = E_0 + \Delta + \sum_{\boldsymbol{k}} \frac{\hbar^2 k^2}{2m_v} h_{\boldsymbol{k}}^\dagger h_{\boldsymbol{k}} + \sum_{\boldsymbol{k}} \frac{\hbar^2 k^2}{2m_l} c_{l\boldsymbol{k}}^\dagger c_{l\boldsymbol{k}} \\ - \sum_{\boldsymbol{k}_1\boldsymbol{k}_2\boldsymbol{k}_3\boldsymbol{k}_4} u_{\boldsymbol{k}_1\boldsymbol{k}_2,\boldsymbol{k}_3\boldsymbol{k}_4} h_{\boldsymbol{k}_4}^\dagger h_{\boldsymbol{k}_1} c_{l\boldsymbol{k}_2}^\dagger c_{l\boldsymbol{k}_3}, \end{aligned} \tag{6.253}$$

as can be seen by simple application of the fermion commutation rules. From the repulsive Coulomb interaction between two electrons, an attractive interaction between the electron in the conduction band and the positive hole in the valence band is automatically generated in the hole picture.

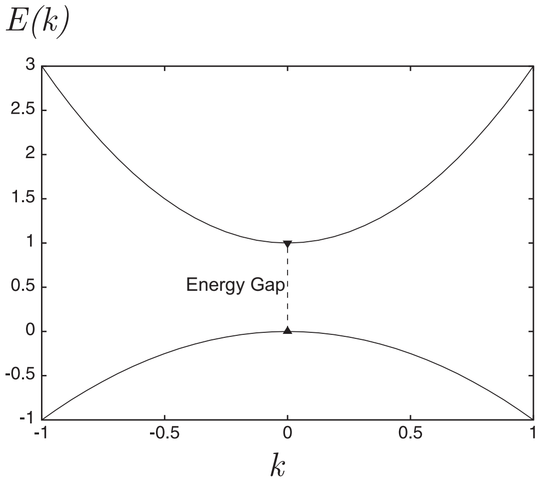

**Fig. 6.7** Valence and conduction band dispersion in semiconductors

In the ground state, all valence band states are occupied and all conduction band states are unoccupied. The many-particle ground state is therefore given by

$$|\Phi_0\rangle = \prod_{\boldsymbol{k}} c^{\dagger}_{v\boldsymbol{k}}|0\rangle, \tag{6.254}$$

where $|0\rangle$ describes the vacuum state. The ground state energy is simply:

$$E_0 = \sum_{\boldsymbol{k}} E_v(\boldsymbol{k}). \tag{6.255}$$

The application of both the conduction band term and the interaction term of the Hamiltonian operator to the ground state results in 0 because the conduction electron annihilation operator applied to the vacuum gives 0. Now the simplest excited state is to be constructed for the described model; Excitations can only arise from transitions of electrons from the valence band to the conduction band. A physically plausible ansatz for the simplest excited state is therefore

$$|\phi\rangle = \sum_{\boldsymbol{k},\boldsymbol{k}'} a_{\boldsymbol{k}\boldsymbol{k}'} c^{\dagger}_{l\boldsymbol{k}} c_{v\boldsymbol{k}'}|\Phi_0\rangle = \sum_{\boldsymbol{k},\boldsymbol{k}'} a_{\boldsymbol{k}\boldsymbol{k}'} c^{\dagger}_{l\boldsymbol{k}} h^{\dagger}_{\boldsymbol{k}'}|\Phi_0\rangle. \tag{6.256}$$

The excited state is therefore assumed to be a linear combination over all possibilities to create an electron-hole pair. The coefficients $a_{\boldsymbol{k}\boldsymbol{k}'}$ are now to be determined such that $|\Phi\rangle$ is an eigenstate of $H$. The application of the Hamiltonian operator to $|\Phi\rangle$ yields

$$\begin{aligned}
&\sum_{\boldsymbol{k}\boldsymbol{k}'} a_{\boldsymbol{k}\boldsymbol{k}'} \Bigg( \left[ \sum_{\boldsymbol{k}_1} E_v(\boldsymbol{k}_1) - E_v\big(\boldsymbol{k}'\big) + E_l(\boldsymbol{k}) \right] c^{\dagger}_{l\boldsymbol{k}} c_{v\boldsymbol{k}'}|\Phi_0\rangle \\
&\qquad + \sum_{\boldsymbol{k}_1\boldsymbol{k}_2\boldsymbol{k}_3\boldsymbol{k}_4} u_{\boldsymbol{k}_1\boldsymbol{k}_2,\boldsymbol{k}_3\boldsymbol{k}_4} c^{\dagger}_{v\boldsymbol{k}_1} c^{\dagger}_{l\boldsymbol{k}_2} c_{l\boldsymbol{k}_3} c_{v\boldsymbol{k}_4} c^{\dagger}_{l\boldsymbol{k}} c_{v\boldsymbol{k}'}|\Phi_0\rangle \Bigg) \\
&\quad = E_0|\Phi\rangle + \sum_{\boldsymbol{k}\boldsymbol{k}'} \big(E_l(\boldsymbol{k}) - E_v\big(\boldsymbol{k}'\big)\big) a_{\boldsymbol{k}\boldsymbol{k}'} c^{\dagger}_{l\boldsymbol{k}} c_{v\boldsymbol{k}'}|\Phi_0\rangle \\
&\qquad - \sum_{\boldsymbol{k}_1\boldsymbol{k}_2\boldsymbol{k}_3\boldsymbol{k}_4} u_{\boldsymbol{k}_1\boldsymbol{k}_2,\boldsymbol{k}_3\boldsymbol{k}_4} a_{\boldsymbol{k}_3\boldsymbol{k}_1} c^{\dagger}_{l\boldsymbol{k}_2} c_{v\boldsymbol{k}_4}|\Phi_0\rangle,
\end{aligned} \tag{6.257}$$

as can be seen immediately from the anti-commutation relations for the fermion creators and annihilators. By relabeling the summation indices it follows:

$$\sum_{\boldsymbol{k}\boldsymbol{k}'} \Big[ a_{\boldsymbol{k}\boldsymbol{k}'} \big(E_0 - E + E_l(\boldsymbol{k}) - E_v\big(\boldsymbol{k}'\big)\big) - \sum_{\boldsymbol{k}_1\boldsymbol{k}_3} u_{\boldsymbol{k}_1\boldsymbol{k},\boldsymbol{k}_3\boldsymbol{k}'} a_{\boldsymbol{k}_1\boldsymbol{k}_3} \right] c^{\dagger}_{l\boldsymbol{k}} c_{v\boldsymbol{k}'}|\Phi_0\rangle = 0. \tag{6.258}$$

Since the states $c^{\dagger}_{l\boldsymbol{k}} c_{v\boldsymbol{k}'}|\Phi_0 >$ form an orthonormal system, a homogeneous system of equations for the coefficients follows:

$$a_{\boldsymbol{k}\boldsymbol{k}'} \big(E_0 - E + E_l(\boldsymbol{k}) - E_v\big(\boldsymbol{k}'\big)\big) - \sum_{\boldsymbol{k}_1\boldsymbol{k}_3} u_{\boldsymbol{k}_1\boldsymbol{k},\boldsymbol{k}_3\boldsymbol{k}'} a_{\boldsymbol{k}_1\boldsymbol{k}_3} = 0. \tag{6.259}$$

Without interaction, the naively expected result for the excitation energies is obtained:

$$\Delta E = E - E_0 = E_l(\boldsymbol{k}) - E_v\left(\boldsymbol{k}'\right) = \Delta + \frac{\hbar^2 k^2}{2m_l} + \frac{\hbar^2 k'^2}{2m_v}. \tag{6.260}$$

The lowest excited state then lies just above the energy gap Δ from the ground state energy, as one would expect from the one-particle picture of semiconductors. As can be seen from the Eqs. (6.258), (6.259), however, the states $c^\dagger_{l\boldsymbol{k}} c_{v\boldsymbol{k}'} |\Phi_0\rangle$ are not eigenstates of the Hamiltonian operator themselves, but only by suitable linear combinations of these states can eigenstates be constructed, and the excitation energies are lowered compared to those of non-interacting particles and holes.

For further simplification, it is assumed that the interaction matrix elements $u_{\boldsymbol{k}_1\boldsymbol{k}_2,\boldsymbol{k}_3\boldsymbol{k}_4}$ can be approximately expressed by those of free particles. In other words, this means that the Bloch factors are neglected when calculating these Coulomb matrix elements and the Bloch functions are replaced by plane waves. Since screening in semiconductors only manifests itself in a constant dielectric constant, the Fourier transform of the screened Coulomb potential results again, that is:

$$\begin{aligned} u_{\boldsymbol{k}_1\boldsymbol{k}_2,\boldsymbol{k}_3\boldsymbol{k}_4} &= \frac{1}{V^2}\int d^3r \int d^3r' e^{-i\boldsymbol{k}_1\boldsymbol{r}} e^{-i\boldsymbol{k}_2\boldsymbol{r}'} \frac{e^2}{\varepsilon|\boldsymbol{r}-\boldsymbol{r}'|} e^{i\boldsymbol{k}_3\boldsymbol{r}'} e^{i\boldsymbol{k}_4\boldsymbol{r}} \\ &= \frac{4\pi e^2}{\varepsilon V}\frac{1}{|\boldsymbol{k}_3-\boldsymbol{k}_2|^2}\delta_{\boldsymbol{k}_3-\boldsymbol{k}_2,\boldsymbol{k}_1-\boldsymbol{k}_4}. \end{aligned} \tag{6.261}$$

Then it follows from (6.259)

$$(\Delta E - \Delta) a_{\boldsymbol{k}\boldsymbol{k}'} = \left(\frac{\hbar^2 k^2}{2m_l} + \frac{\hbar^2 k'^2}{2m_v}\right) a_{\boldsymbol{k}\boldsymbol{k}'} - \sum_{\boldsymbol{q}} \frac{4\pi e^2}{\varepsilon V q^2} a_{\boldsymbol{k}'+\boldsymbol{q}\boldsymbol{k}+\boldsymbol{q}}. \tag{6.262}$$

This eigenvalue equation for the coefficient matrix $(a_{\boldsymbol{k}\boldsymbol{k}'})$ is equivalent to the two-particle Schrödinger equation

$$\left(-\frac{\hbar^2}{2m_l}\nabla^2_{\boldsymbol{r}_1} - \frac{\hbar^2}{2m_v}\nabla^2_{\boldsymbol{r}_2} - \frac{e^2}{\varepsilon|\boldsymbol{r}_1-\boldsymbol{r}_2|}\right)\psi(\boldsymbol{r}_1,\boldsymbol{r}_2) = \tilde{E}\psi(\boldsymbol{r}_1,\boldsymbol{r}_2). \tag{6.263}$$

If the two-particle wave function here is expanded in plane waves

$$\psi(\boldsymbol{r}_1,\boldsymbol{r}_2) = \frac{1}{V}\sum_{\boldsymbol{k}_1\boldsymbol{k}_2} a_{\boldsymbol{k}_1\boldsymbol{k}_2} e^{i(\boldsymbol{k}_1\boldsymbol{r}_1 - \boldsymbol{k}_2\boldsymbol{r}_2)} \tag{6.264}$$

and for the Coulomb interaction the Fourier transformation is used

$$\frac{1}{|\boldsymbol{r}_1-\boldsymbol{r}_2|} = \sum_{\boldsymbol{q}} \frac{4\pi}{Vq^2} e^{i\boldsymbol{q}(\boldsymbol{r}_1-\boldsymbol{r}_2)}, \tag{6.265}$$

then it follows

$$\begin{aligned} 0 &= \sum_{\boldsymbol{k}_1\boldsymbol{k}_2}\left(\frac{\hbar^2k_1^2}{2m_l}+\frac{\hbar^2k_2^2}{2m_v}-\tilde{E}-\sum_{\boldsymbol{q}}\frac{4\pi e^2}{V\varepsilon q^2}e^{i\boldsymbol{q}(\boldsymbol{r}_1-\boldsymbol{r}_2)}\right)a_{\boldsymbol{k}_1\boldsymbol{k}_2}e^{i(\boldsymbol{k}_1\boldsymbol{r}_1-\boldsymbol{k}_2\boldsymbol{r}_2)} \\ &= \sum_{\boldsymbol{k}_1\boldsymbol{k}_2}\left[\left(\frac{\hbar^2k_1^2}{2m_l}+\frac{\hbar^2k_2^2}{2m_v}-\tilde{E}\right)a_{\boldsymbol{k}_1\boldsymbol{k}_2}-\sum_{\boldsymbol{q}}\frac{4\pi e^2}{V\varepsilon q^2}a_{\boldsymbol{k}_1-\boldsymbol{q}\boldsymbol{k}_2-\boldsymbol{q}}\right]e^{i(\boldsymbol{k}_1\boldsymbol{r}_1-\boldsymbol{k}_2\boldsymbol{r}_2)}. \end{aligned} \tag{6.266}$$

Obviously (6.262) is reproduced from the two-particle Schrödinger equation (6.263). Because of the orthogonality of the plane waves, the electron and the defect electron (hole) behave just like two free particles with masses $m_l, m_v$ and opposite elementary charges. So we have an effective hydrogen problem, only that instead of the heavy proton here the positive particle is the hole in the valence band, which has the mass $m_v$, and this effective mass is much smaller than the proton mass. Therefore, it is not justified to treat the positive particle as approximately at rest, as in the quantum mechanical hydrogen problem, but one must treat the quantum mechanical two-particle problem. For this purpose, the center-of-mass and relative coordinates are introduced by

$$\boldsymbol{X} = \frac{m_l\boldsymbol{r}_1+m_v\boldsymbol{r}_2}{m_l+m_v}, \boldsymbol{r} = \boldsymbol{r}_1-\boldsymbol{r}_2. \tag{6.267}$$

The Schrödinger equation (6.263) then becomes

$$\left(-\frac{\hbar^2}{2(m_v+m_l)}\nabla_{\boldsymbol{X}}^2-\frac{\hbar^2}{2\mu}\nabla_{\boldsymbol{r}}^2-\frac{e^2}{\varepsilon r}\right)\psi = \tilde{E}\psi, \tag{6.268}$$

with $\mu = \frac{m_l m_v}{m_l+m_v}$ the effective mass. This equation can be solved by separation. For the center-of-mass coordinate, the behavior of a free particle results and for the relative coordinate a simple effective hydrogen problem remains. For the eigenfunctions and eigenvalues we therefore find:

$$\psi_{\boldsymbol{\kappa},n}(\boldsymbol{X},\boldsymbol{r}) = e^{i\boldsymbol{\kappa}\boldsymbol{X}}F_n(\boldsymbol{r}), \quad \tilde{E}_{\boldsymbol{\kappa},n} = \frac{\hbar^2\kappa^2}{2(m_l+m_v)}-\frac{E_B}{n^2}. \tag{6.269}$$

Here, the binding energy

$$E_B = \frac{\mu e^4}{2\varepsilon^2\hbar^2} \tag{6.270}$$

is the analogue of the Rydberg energy in the usual hydrogen problem and differs from this by the occurrence of the reduced mass $\mu$ instead of the free electron mass and by the occurrence of the factor $1/\varepsilon^2$. Because of the static screening, the effective charge is $e/\sqrt{\varepsilon}$; $F_n(\boldsymbol{r})$ denotes the hydrogen eigenfunctions known from quantum mechanics.

The physical interpretation of this result is the following: The electron in the conduction band and the hole in the valence band bind to each other because of the (screened) Coulomb attraction and thus form a new quasiparticle, the **exciton**. The bound states of the exciton are hydrogen-like, an exciton thus has certain analogies to a hydrogen atom. The exciton as a whole can move like a free particle

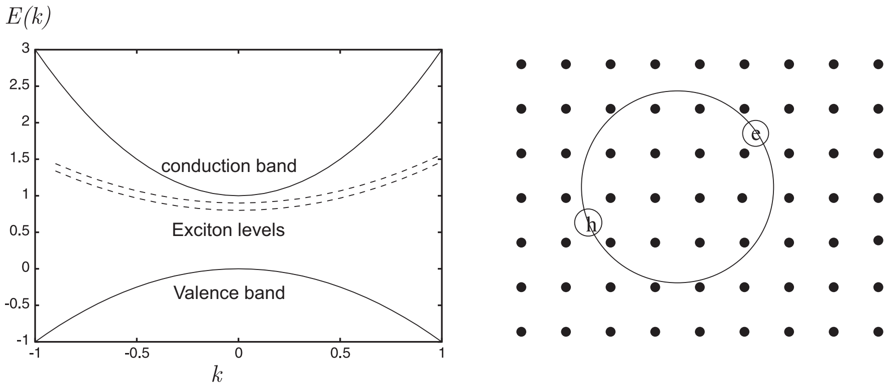

**Fig. 6.8** Schematic representation of the energetic position of the exciton levels and a Wannier exciton in the lattice

with momentum $\hbar\boldsymbol{\kappa}$. The lowest excited states therefore do not consist of a quasi-free electron in the conduction band and a quasi-free hole in the valence band, but there are energetically lower lying bound exciton states due to the Coulomb interaction. The energy difference between the excited (exciton) states and the semiconductor ground state is

$$\Delta E = \varDelta + \frac{\hbar^2\kappa^2}{2(m_l + m_v)} - \frac{E_B}{n^2} \quad \text{with integer n.} \tag{6.271}$$

Excitons and exciton levels are schematically sketched in Fig. 6.8. For the lowest excited state one has,

$$\Delta E_1 = \varDelta - E_B = \varDelta - \frac{\mu e^4}{2\varepsilon^2\hbar^2}. \tag{6.272}$$

The “Bohr radius” and thus the spatial size of an exciton differs by a factor $\varepsilon\frac{m}{\mu}$ from the actual Bohr radius $a_0 = 0.5$ Å. This can be of the order of 100 and more in some semiconductors; then the exciton is also extended (compared to lattice constants). In the derivation of the above result, in particular, it was used that a non-interacting electron and hole can be described as quasi-free particles with plane waves as eigenfunctions. These excitons built from free particles and relatively delocalized, that is, spatially extended excitons with large orbital radius are also referred to as[17]

**Wannier- or Mott-Excitons.**

There are also well-localized excitons with a small orbit radius; in the extreme case, the hole and the conduction electron bound to it by electrostatic means are always located at the same atom. In this case, it is also convenient to use the localized Wannier basis instead of the delocalized Bloch basis (or the plane waves)[18] to describe the problem in occupation number representation. The interaction Hamiltonian operator can be written quite generally, this time taking into account exchange terms, in Wannier representation as:

---

[17] G.H. Wannier, see footnote 5.4.

$$H_1 = \sum_{\boldsymbol{R}_1\boldsymbol{R}_2\boldsymbol{R}_3\boldsymbol{R}_4} \left( u^{vl,lv}_{\boldsymbol{R}_1\boldsymbol{R}_2,\boldsymbol{R}_3\boldsymbol{R}_4} c^\dagger_{v\boldsymbol{R}_1} c^\dagger_{l\boldsymbol{R}_2} c_{l\boldsymbol{R}_3} c_{v\boldsymbol{R}_4} + u^{vl,vl}_{\boldsymbol{R}_1\boldsymbol{R}_2,\boldsymbol{R}_3\boldsymbol{R}_4} c^\dagger_{v\boldsymbol{R}_1} c^\dagger_{l\boldsymbol{R}_2} c_{v\boldsymbol{R}_3} c_{l\boldsymbol{R}_4} \right) \quad (6.273)$$

with

$$\begin{aligned} u^{vl,lv}_{\boldsymbol{R}_1\boldsymbol{R}_2,\boldsymbol{R}_3\boldsymbol{R}_4} &= \int d^3r \int d^3r' w^*_v(\boldsymbol{r}-\boldsymbol{R}_1) w^*_l(\boldsymbol{r}'-\boldsymbol{R}_2) \frac{e^2}{\varepsilon|\boldsymbol{r}-\boldsymbol{r}'|} \\ &\quad \times w_l(\boldsymbol{r}'-\boldsymbol{R}_3) w_v(\boldsymbol{r}-\boldsymbol{R}_4), \\ u^{vl,vl}_{\boldsymbol{R}_1\boldsymbol{R}_2,\boldsymbol{R}_3\boldsymbol{R}_4} &= \int d^3r \int d^3r' w^*_v(\boldsymbol{r}-\boldsymbol{R}_1) w^*_l(\boldsymbol{r}'-\boldsymbol{R}_2) \frac{e^2}{\varepsilon|\boldsymbol{r}-\boldsymbol{r}'|} \\ &\quad \times w_v(\boldsymbol{r}'-\boldsymbol{R}_3) w_l(\boldsymbol{r}-\boldsymbol{R}_4). \end{aligned} \quad (6.274)$$

If the Wannier functions are well localized, one can, with analogous arguments as in Sect. 5.4 on the tight-binding approximation and in Sect. 6.2 on the justification of the Hubbard model and related models, argue that the Wannier functions localized at different lattice sites have only little overlap. Therefore, the matrix elements with $\boldsymbol{R}_1 = \boldsymbol{R}_4$ and $\boldsymbol{R}_2 = \boldsymbol{R}_3$ should at least be significantly larger than the others. Taking into account only these dominant terms, one obtains:

$$H_1 = \sum_{\boldsymbol{R}\boldsymbol{R}'} \left( u^{vl,lv}_{\boldsymbol{R}\boldsymbol{R}',\boldsymbol{R}'\boldsymbol{R}} c^\dagger_{v\boldsymbol{R}} c^\dagger_{l\boldsymbol{R}'} c_{l\boldsymbol{R}'} c_{v\boldsymbol{R}} - u^{vl,vl}_{\boldsymbol{R}\boldsymbol{R}',\boldsymbol{R}'\boldsymbol{R}} c^\dagger_{v\boldsymbol{R}} c^\dagger_{l\boldsymbol{R}'} c_{l\boldsymbol{R}} c_{v\boldsymbol{R}'} \right). \quad (6.275)$$

The first interaction contribution describes the interaction of a hole at the position $\boldsymbol{R}$ with an electron at the position $\boldsymbol{R}'$, the second describes a hopping of both the electron and the hole from the same lattice site $\boldsymbol{R}$ to another lattice site $\boldsymbol{R}'$. It is plausible and consistent with the already made assumptions to allow only nearest or next-nearest neighbors for $\boldsymbol{R}, \boldsymbol{R}'$. The second interaction term then allows for the propagation of a bound electron-hole pair as a whole through the crystal.

In this approximation, the valence band hole and the conduction band electron thus always remain at the same lattice site; the excitation, i.e. the exciton, is therefore well localized. This is also referred to as the[19]

**Frenkel-Exciton.**

---

[18] Sir Neville Mott, 1905 in Leeds, 1996 in Milton Keynes (England), English theoretical physicist, works on the scattering of atomic particles and the electrical and mechanical properties of metals and semiconductors, in particular amorphous (disordered) systems, Nobel Prize 1977.

[19] J.I. Frenkel, *1894 in Rostow (Russia), †1952 in Leningrad, Soviet solid-state physicist, professor in Leningrad since 1921, investigations of the conductivity of metals and of defects in crystal lattices (Frenkel defects), introduced the concept of the exciton.

Such well-localized excitons are found in particular in ionic crystals with a large gap, e.g. the alkali halides, and in molecular crystals with larger (organic) molecules, e.g. in anthracenes.

You can also introduce exciton creation operators by

$$B^{\dagger}_{\boldsymbol{R}} = c^{\dagger}_{l\boldsymbol{R}} c_{v\boldsymbol{R}} = c^{\dagger}_{l\boldsymbol{R}} h^{\dagger}_{\boldsymbol{R}} \tag{6.276}$$

and the corresponding annihilators. However, these are not simple one-particle operators, i.e. they do not exactly obey Bose commutation rules, as one could assume for a pair of fermions.

Overall, the transition between Frenkel and Wannier excitons is gradual. As long as you use the exact Bloch or Wannier functions, both representations are equivalent. To distinguish between Wannier and Frenkel excitons, it has come about through the different approximations. When using the Wannier functions as a basis, their good localization was assumed, which then also leads to localized excitations at a lattice point. In Bloch representation, however, one worked with the approximation of plane waves for the Bloch states from the conduction and valence band, which leads to the effective hydrogen spectrum and thus to the Mott-Wannier exciton. Although this idea is widespread and the experimentally observed exciton states can often be classified well according to an effective hydrogen spectrum, the associated approximation is strictly speaking doubtful, as the following simple consideration shows: If one considers, for example, the excitation of a valence electron from the state $\boldsymbol{k}$ into the conduction band with the same $\boldsymbol{k}$ from the first Brillouin zone, then the corresponding eigenstates, from which the Coulomb matrix element is calculated, must be orthogonal, since they have the same $\boldsymbol{k}$ but different band index as a quantum number. If you approximate the eigenstates by plane waves, they are no longer orthogonal for the same $\boldsymbol{k}$. The— in the derivation of the spectrum of the Mott-Wannier exciton—neglected Bloch factor can therefore have decisive importance.

## 6.9 Quasiparticles and Landau Theory of the Fermi Liquid

Many of the methods for treating interacting electron systems discussed in this chapter try to map the many-particle problem onto an effective one-particle problem. Thus, in Hartree, Hartree-Fock, and density functional theory, an effective one-particle potential is introduced, the parameters of which are then to be determined self-consistently, since they depend on the occupation of the states or the density of the electrons. That a description by or mapping onto an effective one-particle problem is possible in many cases and apparently works well justifies the successful use of the model of non-interacting electrons treated in detail in Chap. 5 only in retrospect. After all, interaction effects are never small and never to be neglected or considered as a weak perturbation. Therefore, there are actually no free electrons in a solid, but in many solids and especially in metals, the electronic excitations still behave like those of free particles with—in comparison to free electrons usually more or less strongly—changed, effective parameters. The picture of free electrons with a quadratic dispersion remains applicable in many cases, but then one has to attribute to it an effective mass that is—compared to really free electrons—often strongly changed. All interaction effects are then contained in this effective and actually self-consistently to be determined parameter effective mass, which is to be distinguished from the in Chap. 5 introduced, effective electron mass based only on band structure effects. Free electrons in the solid are therefore strictly speaking quasiparticles, that is, excitations that can be described formally as free particles.

Landau[20] formulated in the 1950s a phenomenological theory for interacting electron systems , which starts from the following postulates: The ground state of the system of interacting fermions, which is also called **Fermi liquid**, develops from the ground state of the non-interacting "Fermi gas"—as if there were an adiabatic switching on of the interaction, the wave numbers $\boldsymbol{k}$ remain good quantum numbers, there is still a dispersion relation $\varepsilon(\boldsymbol{k})$ and the total energy is a functional of the occupation numbers $\{n_{\boldsymbol{k}\sigma}\}$, and since the **quasiparticles** should still have fermion character, the $n_{\boldsymbol{k}\sigma}$ at $T = 0$ have a jump at the Fermi surface (as the Fermi function, i.e. the occupation function of non-interacting electrons has), so a sharp Fermi surface is retained, in particular. The approach of regarding the total energy as a functional of the occupation numbers is analogous to the basic approach of density functional theory, which regards the energy as a functional of the particle density. However, this functional is unknown here as well, and it is certainly more complicated than the simple relationship

$$E = \sum_{\boldsymbol{k}\sigma} n_{\boldsymbol{k}\sigma} \varepsilon^0_{\boldsymbol{k}}.$$

that is valid for free electrons. However, one can also assign a dispersion to the quasiparticles via

$$\varepsilon_{\boldsymbol{k}\sigma} = \frac{\delta E\{n_{\boldsymbol{k}'\sigma'}\}}{\delta n_{\boldsymbol{k}\sigma}}, \tag{6.277}$$

where $\delta E$ is the change in total energy due to an excitation, i.e. the change in all occupation numbers by $\delta n_{\boldsymbol{k}\sigma}$. In the presence of interaction, however, this quasiparticle dispersion depends in a complicated and unknown manner on all the other occupation numbers $n_{\boldsymbol{k}'\sigma'}$. Formally, one can write these occupation numbers again as Fermi functions as in the case of free fermions:

---

[20] L.D. Landau, *1908 in Baku (Azerbaijan), †1968 in Moscow, one of the most important Russian physicists, groundbreaking contributions to all areas of theoretical physics, from the theory of metals to stellar matter, cosmic radiation, plasma physics, nuclear physics to hydrodynamics, numerous effects and theories bear his name (Landau diamagnetism, Landau damping in plasma physics, Landau cut in high-energy physics), founder of a famous school for theoretical physics in Moscow and editor of the comprehensive textbook series, Nobel Prize in Physics 1962, also known for that after a serious car accident in 1962 he was several times revived from a clinically dead state, but then did not regain his productivity.

$$n_{\boldsymbol{k}\sigma} = \frac{1}{e^{(\varepsilon_{\boldsymbol{k}\sigma}-\mu)/k_B T} + 1}. \tag{6.278}$$

However, because of the mentioned dependence of $\varepsilon_{\boldsymbol{k}\sigma}$ on all occupation numbers, this is only an implicit equation for $n_{\boldsymbol{k}\sigma}$, whose actual $\boldsymbol{k}$ dependence—even at $T = 0$—**is not** of the familiar form of the Fermi function. The change in total energy due to excitations can be written as

$$\delta E\{n_{\boldsymbol{k}'\sigma'}\} = \sum_{\boldsymbol{k}\sigma} \varepsilon^0_{\boldsymbol{k}\sigma} \delta n_{\boldsymbol{k}\sigma} + \frac{1}{2} \sum_{\boldsymbol{k}\sigma,\boldsymbol{k}'\sigma'} f_{\boldsymbol{k}\sigma,\boldsymbol{k}'\sigma'} \delta n_{\boldsymbol{k}\sigma} \delta n_{\boldsymbol{k}'\sigma'}. \tag{6.279}$$

The last term is precisely the interaction contribution to the total energy, because this contribution only exists if both the $\boldsymbol{k}\sigma$ and the $\boldsymbol{k}'\sigma'$ occupation numbers change. The quasiparticle dispersion can then be written as

$$\begin{aligned} \varepsilon_{\boldsymbol{k}\sigma} &= \varepsilon^0_{\boldsymbol{k}\sigma} + \sum_{\boldsymbol{k}'\sigma'} f_{\boldsymbol{k}\sigma,\boldsymbol{k}'\sigma'} \delta n_{\boldsymbol{k}'\sigma'} \\ &= \varepsilon_F + \frac{\hbar^2 k_F (k - k_F)}{m} + \sum_{\boldsymbol{k}'\sigma'} f_{\boldsymbol{k}\sigma,\boldsymbol{k}'\sigma'} \delta n_{\boldsymbol{k}'\sigma'}, \end{aligned} \tag{6.280}$$

where, in the last step, linearization was carried out around the Fermi surface because, at low temperatures, only excitations in the vicinity of the Fermi surface are possible.

The sense and success of the Landau theory of Fermi liquids lies in the fact that it manages, with only a few phenomenological parameters, to derive relations between quantities such as specific heat, magnetic susceptibility, compressibility, etc., which are experimentally verifiable, and the phenomenological parameters of the Fermi liquid theory are therefore the **effective mass** $m^*$ and the $f_{\boldsymbol{k}\sigma,\boldsymbol{k}'\sigma'}$ for the quasiparticle interaction.

In contrast to the free fermions, however, the quasiparticles have a finite lifetime in a state $\boldsymbol{k}$. But the concept of elementary excitation with momentum $\boldsymbol{k}$ only makes sense if the damping is small compared to the excitation energy. But it can be shown that for fermions the lifetime τ due to the scattering of electrons on each other fulfills $\tau \sim \frac{1}{T^2}$, so that at sufficiently low temperatures $T$ the inverse lifetime can always be considered to be small compared to the excitation energy.

It is possible to microsopically justify the phenomenological Fermi liquid theory of Landau. Starting from a general, microscopic Hamiltonian operator for interacting electron systems of the type (6.35) or (6.39), it can be shown by perturbation theory with respect to the interaction term that the essential assumptions or statements of the Landau theory are fulfilled to any order in the perturbation series, i.e. up to any order in the interaction and therefore also after—in practice mostly not possible—summation of the perturbation series, which should correspond to the exact result if the perturbation series converges. But to prove this statement, one needs the mathematical apparatus of many-body theory with Green functions, Feynman diagrams, etc., which is why this cannot be discussed here. The above statement is at least true for three-dimensional systems, but certainly not for one-dimensional systems.

Most metals and also the Fermi system $^3$He can be described very well as a Fermi liquid, at least as long as they remain in the normal state, that is, no phase transition to a superconducting (or superfluid for $^3$He) or magnetic phase occurs. Only recently, an increasing number of metallic systems are being found and studied in which apparently no Fermi liquid property is present. This is a current research topic and can be due to reduced dimensionality (e.g. quasi-two-dimensional systems), proximity to a (magnetic) phase transition, or disorder.

## 6.10 Problems for Chap. 6

**Problem 6.1 One-*Particle Operators in Occupation Number Representation***
Determine for free electrons in a box of volume $V$ with periodic boundary conditions the momentum operator, current density operator and the particle density operator in 2nd quantization with respect to the eigenstates.

**Problem 6.2 *Fermionic 2-Level System and Occupation Number Representation***
Given a Fermi system with 2 one-particle states $|\varphi_1\rangle, |\varphi_2\rangle$, which span the (2-dimensional) one-particle Hilbert space.

a) What is the dimension of the two-particle Hilbert space, what is the dimension of the Fock space? Give the basis of the Fock space in the form of Slater determinants and in the occupation number representation explicitly.

b) Determine with respect to this basis the matrix representation of the fermion creators and annihilators $c_i, c_i^\dagger$ $(i = 1, 2)$ as well as the occupation number operators $n_i = c_i^\dagger c_i$.

c) Calculate the anti-commutation relations

$$\left\{c_i, c_j\right\} = \left\{c_i^\dagger, c_j^\dagger\right\} = 0\ ;\ \left\{c_i, c_j^\dagger\right\} = \delta_{ij}$$

explicitly by matrix multiplication of the matrices determined in b).

d) A Hamiltonian operator

$$H = H_0 + H_1$$

with one-particle-component $H_0$ and interaction-(two-particle-)component $H_1$ has with respect to the $|\varphi_i\rangle$ the matrix elements

$$\langle\varphi_i|H_0|\varphi_i\rangle = \varepsilon;\ \langle\varphi_i|H_0|\varphi_j\rangle = t$$

$${}^{(1)}\langle\varphi_1|^{(2)}\langle\varphi_2|H_1|\varphi_2\rangle^{(2)}|\varphi_1\rangle^{(1)} = U;\ {}^{(1)}\langle\varphi_1|^{(2)}\langle\varphi_2|H_1|\varphi_1\rangle^{(2)}|\varphi_2\rangle^{(1)} = J.$$

Give $H$ in 2nd quantization and in matrix representation (with respect to the original one-particle basis) . Determine the eigenvalues and eigenstates of $H$.

e) Give $H$ in 2nd quantization with respect to the eigenstates of $H_0$. What is the relationship between these creators and annihilators and the original (in a)–d) considered)?

**Problem 6.3** ***Wick's Theorem***

a) Show that for non-interacting fermions, which can be described in eigen-representation by a Hamiltonian operator of the form

$$H = \sum_\alpha \varepsilon_\alpha c_\alpha^\dagger c_\alpha,$$

it holds for (grand canonical) expectation values:

$$\begin{aligned}\langle c_{\alpha_1}^\dagger c_{\alpha_2}^\dagger c_{\alpha_3} c_{\alpha_4}\rangle &= \langle c_{\alpha_1}^\dagger c_{\alpha_4}\rangle\langle c_{\alpha_2}^\dagger c_{\alpha_3}\rangle \delta_{\alpha_1\alpha_4}\delta_{\alpha_2\alpha_3} \\ &\quad - \langle c_{\alpha_1}^\dagger c_{\alpha_3}\rangle\langle c_{\alpha_2}^\dagger c_{\alpha_4}\rangle \delta_{\alpha_1\alpha_3}\delta_{\alpha_2\alpha_4}.\end{aligned}$$

b) Conclude from a) that also with respect to any other one-particle basis $\{|n\rangle\}$ it holds for non-interacting fermions:

$$\left\langle c_{n_1}^\dagger c_{n_2}^\dagger c_{n_3} c_{n_4}\right\rangle = \left\langle c_{n_1}^\dagger c_{n_4}\right\rangle\left\langle c_{n_2}^\dagger c_{n_3}\right\rangle - \left\langle c_{n_1}^\dagger c_{n_3}\right\rangle\left\langle c_{n_2}^\dagger c_{n_4}\right\rangle.$$

With respect to this basis, the Hamiltonian operator is not diagonal, thus of the form

$$H = \sum_{n,m} t_{nm} c_n^\dagger c_m.$$

*Note*: By a unitary transformation $c_n = \sum_\alpha u_{n\alpha} c_\alpha$, $H$ must be diagonalizable, so that a) can be applied and then the canonical transformation can be redone.

**Problem 6.4** ***Interacting 2-Particle Model in One Dimension***

We consider the following two-particle model for a helium atom in one dimension in appropriate dimensionless coordinates:

$$H = -\frac{d^2}{dx_1^2} - 2V(|x_1|) - \frac{d^2}{dx_2^2} - 2V(|x_2|) + V(|x_1 - x_2|)$$

$$\text{with} \quad V(x) = \frac{2}{x+\delta},$$

("truncated" one-dimensional Coulomb potential, see Problem 3.4, factor 2 in front of single-particle potential because of two-fold charged atomic nucleus).

a) Determine the Hamilton operator in 2nd quantization in the form

$$H = \sum_{i,\sigma} \varepsilon_i c^\dagger_{i\sigma} c_{i\sigma} + \frac{1}{2} \sum_{i_1 i_2, i_3 i_4 \sigma\sigma'} u_{i_1 i_2, i_3 i_4} c^\dagger_{i_1\sigma} c^\dagger_{i_2\sigma'} c_{i_3\sigma'} c_{i_4\sigma}$$

with respect to the eigenstates $|i\rangle$ of the one-particle Hamilton operator, i. e. the $\varphi_i(x) = \langle x|i\rangle$ should fulfill:

$$\left(-\frac{d^2}{dx^2} - 2V(|x|)\right)\varphi_i(x) = \varepsilon_i \varphi_i(x).$$

Determine the $\varepsilon_i$ and the Coulomb matrix elements for $i, i_l \in \{1, 2\}$ numerically using the method developed in Problem 3.4 for solving the one-dimensional one-particle Schrödinger equation.

b) Determine the lowest energy 2-particle states exactly and in Hartree-Fock approximation under the assumption that one can restrict oneself to the lowest two quantum numbers (i. e. again $i, i_l \in \{1, 2\}$). Treat the singlet case (antiparallel spins, "para-helium") and the triplet case (total spin 1, "ortho-helium") separately.

**Problem 6.5** ***1-Dimensional Helium Atom Model***

Consider the 2-particle model from Problem 6.4 for a helium atom in one dimension:

$$H = -\frac{d^2}{dx_1^2} - 2V(|x_1|) - \frac{d^2}{dx_2^2} - 2V(|x_2|) + V(|x_1 - x_2|)$$

$$\text{with} \quad V(x) = \frac{2}{x + \delta},$$

("truncated" one-dimensional Coulomb potential, see Exercise 3.4, factor 2 in front of particle potential because of two-fold charged atomic nucleus).

a) Determine the ground state energy in Hartree-(Fock-)approximation in 1st quantization by solving the Hartree-Fock equation (6.75).
Show first that the Hartree-Fock equation for this case is explicitly given by

$$\left(-\frac{d^2}{dx^2} - 2V(|x|) + V_{HF}(x)\right)\phi_{HF1}(x) = \varepsilon_{HF1}\phi_{HF1}(x)$$

$$\text{with:} \quad V_{HF}(x) = \int dx' \frac{2|\phi_{HF1}(x')|^2}{|x-x'|+\delta}.$$

Solve this effective Schrödinger equation with the known discretization method iteratively starting from the solution of the simple one-particle problem. The Hartree-Fock ground state energy of this 2-electron problem is then given by

$$E_{HF0} = 2\varepsilon_{HF1} - \int dx \int dx' \frac{2|\phi_{HF1}(x)|^2|\phi_{HF1}(x')|^2}{|x-x'|+\delta},$$

where the last double integral is to be subtracted in order to avoid the double counting of the interaction contribution.
Determine $E_{HF0}$ and compare the result with the result determined in Problem 6.4 for the ground state energy.

b) Determine $H$ in 2. Quantization with respect to the one-particle basis of the Hartree-Fock eigenfunctions $\phi_{HFi}(x)$ and determine the (lowest) 2-particle energy eigenvalues in it and compare with the result of Problem 6.4.

c) Based on the physical idea that a single electron does not "see" the doubly charged nucleus, but a nucleus screened by the 2nd electron with effective charge $1 < Z < 2$, one can—analogous to the procedure for the actual helium problem[21]—use the following as a variation ansatz for the 2-particle ground state wave function:

$$\psi(x_1, x_2) = \varphi_Z(x_1)\varphi_Z(x_2)$$

where $\varphi_Z(x)$ is the 1-particle ground state wave function for the Z-fold charged nucleus. $\varphi_Z(x)$ therefore satisfies:

$$\left(-\frac{d^2}{dx^2} - ZV(|x|)\right)\varphi_Z(x) = \varepsilon_{Z0}\varphi_Z(x)$$

The symmetric product ansatz for the 2-particle wave function in position space is possible here, since a spin singlet (i.e. an antisymmetric spin state) can be assumed for the ground state.
Determine $\varphi_Z(x)$ for different $Z \in [1, 2]$ numerically and from this an approximation for the ground state energy $E_0(Z)$ within the framework of the ansatz. Plot $E_0(Z)$ as a function of $Z$ and determine the optimal $Z_0$; compare $E_0(Z_0)$ with the other approximations for the ground state energy of this model obtained in Problems 6.4 and 6.5.

---

[21] See, for example, F. Schwabl, Quantum Mechanics, Section 13.2.3 (Springer 2007).

**Problem 6.6** ***Two-Site Hubbard Model***

The Hubbard model (6.55) for the case that only 2 lattice sites 1 and 2 are present, is given explicitly by:

$$\begin{aligned} H = \varepsilon_0\Big(&c_{1\uparrow}^\dagger c_{1\uparrow} + c_{1\downarrow}^\dagger c_{1\downarrow} + c_{2\uparrow}^\dagger c_{2\uparrow} + c_{2\downarrow}^\dagger c_{2\downarrow}\Big) \\ &+ t\Big(c_{1\uparrow}^\dagger c_{2\uparrow} + c_{1\downarrow}^\dagger c_{2\downarrow} + c_{2\uparrow}^\dagger c_{1\uparrow} + c_{2\downarrow}^\dagger c_{1\downarrow}\Big) \\ &+ U\Big(c_{1\uparrow}^\dagger c_{1\uparrow} c_{1\downarrow}^\dagger c_{1\downarrow} + c_{2\uparrow}^\dagger c_{2\uparrow} c_{2\downarrow}^\dagger c_{2\downarrow}\Big) \end{aligned}$$

a) Determine the two-particle eigenenergies analytically exact. Again, treat the case of parallel and antiparallel spins separately. Plot the results as a function of $U/t$.

*Hint*: For antiparallel spins, a basis of the 2-particle Hilbert space is given by:

$$c_{1\uparrow}^\dagger c_{1\downarrow}^\dagger|0\rangle, \quad c_{2\uparrow}^\dagger c_{2\downarrow}^\dagger|0\rangle, \quad c_{1\uparrow}^\dagger c_{2\downarrow}^\dagger|0\rangle, \quad c_{2\uparrow}^\dagger c_{1\downarrow}^\dagger|0\rangle.$$

Determine the matrix representation of the Hamilton operator with respect to this basis and diagonalize the resulting $4 * 4$-matrix.

b) Determine the ground state in Hartree-Fock approximation and compare the result with the exact result from a).

**Problem 6.7** ***Hartree-Fock Approximation for Two-Particle System***

Repeat the derivation of the Hartree-Fock approximation from the Ritz variation method shown in the text (Sect. 6.3.1) once more explicitly for a 2-particle system.

So consider a concrete 2-particle Hamiltonian operator that can be written in 1st quantization in the form

$$H = h(r_1) + h(r_2) + v(r_1 - r_2),$$

and make for the 2-particle wave function the (antisymmetrized) product ansatz

$$\psi(r_1, r_2) = \frac{1}{\sqrt{2}}(\phi_n(r_1)\phi_m(r_2) - \phi_m(r_1)\phi_n(r_2)),$$

where $n, m$ are one-particle quantum numbers. Calculate $\langle\psi|H|\psi\rangle$ for this and determine the Hartree-Fock equations by variation with respect to the $\phi_n^*(r)$ under the condition of normalization of the one-particle wave functions.

**Problem 6.8 *Hartree Approximation***

Consider again the $N$-particle Hamiltonian operator in 1st quantization

$$H = \sum_{i=1}^{N} h(r_i) + \frac{1}{2}\sum_{i\neq j} v(r_i - r_j)$$

and make the ansatz for the $N$-particle wave function simply as (unsymmetrized) product of 1-particle wave functions (instead of the correctly antisymmetrized Slater determinant), i.e.

$$\psi(r_1, \ldots, r_N) = \prod_{i=1}^{N} \phi_{n_i}(r_i) = \phi_{n_1}(r_1)\ldots\phi_{n_N}(r_n).$$

a) Show that then one obtains for the expectation value of H:

$$\begin{aligned}\langle\psi|H|\psi\rangle &= \sum_i \int dr \phi^*_{n_i}(r) h(r)\phi_{n_i}(r)\\ &+ \frac{1}{2}\sum_{i\neq j}\int dr \int dr' \phi^*_{n_i}(r)\phi^*_{n_j}(r') v(r - r')\phi_{n_j}(r')\phi_{n_i}(r).\end{aligned}$$

b) Show that by variation with respect to a fixed $\phi^*_n(r)$ under the constraint of normalization the Hartree equations

$$h(r)\phi_n(r) + \sum_j \int dr' |\phi_{n_j}(r')|^2 v(r - r')\phi_n(r) = \varepsilon_n \phi_n(r)$$

result.

**Problem 6.9 *homogeneous Electron Gas***

Confirm the Eqs. (6.115) and (6.123) by explicit recalculation of the $\boldsymbol{k}, \boldsymbol{k}'$-integrals, i.e. show:

a) $$\frac{1}{V}\sum_{\boldsymbol{k}', k' < k_F} \frac{1}{|\boldsymbol{k} - \boldsymbol{k}'|^2} = \frac{1}{2\pi^2} k_F \left[\frac{1}{2} + \frac{1 - (k/k_F)^2}{4(k/k_F)} \ln\left|\frac{1 + k/k_F}{1 - k/k_F}\right|\right]$$

b) $$\sum_{k < k_F} \frac{k_F^2 - k^2}{k k_F} \ln\left|\frac{k + k_F}{k - k_F}\right| = \frac{V}{6\pi^2} k_F^3.$$

**Problem 6.10** ***1-Dimensional Homogeneous Electron Gas***[22]

The homogeneous electron gas in one dimension is given by the Hamiltonian operator in 1. Quantization

$$H = \sum_{i=1}^{N_e} \left( \frac{p_i^2}{2m} + V(x_i) \right) + \frac{1}{2} \sum_{i \neq j} v(x_i - x_j)$$

$$\text{with} \quad V(x) = -\int dx' \frac{\rho(x')e^2}{|x - x'| + \delta}$$

(attractive potential of positive background charge $e\rho(x')$)

$$v(x_i - x_j) = \frac{e^2}{|x_i - x_j| + \delta}$$

(Model for Coulomb interaction in one dimension)

or in 2. Quantization by

$$H = \sum_{k\sigma} \varepsilon_k c_{k\sigma}^\dagger c_{k\sigma} - \frac{1}{L} \sum_{kq\sigma} \tilde{v}(q)\tilde{\rho}(q) c_{k+q\sigma}^\dagger c_{k\sigma} + \frac{1}{2L} \sum_{kk'q,\sigma\sigma'} \tilde{v}(q) c_{k+q\sigma}^\dagger c_{k'-q\sigma'}^\dagger c_{k'\sigma'} c_{k\sigma}$$

$$\text{with} \quad \tilde{v}(q) = \int dx e^{iqx} v(x)$$

the Fourier transform of the Coulomb interaction

$$\tilde{\rho}(q) = \int dx e^{iqx} \rho(x).$$

Fourier transform of the particle density of the positive background charge.

Treat this model analogously to the treatment of the three-dimensional homogeneous electron gas in Hartree-Fock approximation in Sect. 6.4. In particular, determine and plot $\varepsilon_{HF}(k)$.

*Note*: The Fourier transform of the one-dimensional model Coulomb potential can be reduced to the so-called integral cosine or -sinus, which can be found in tables.[23] Since of course only one-dimensional integrals occur, these can be calculated purely numerically from the outset (introducing an effective "cut-off" as an upper limit of integration).

---

[22] S. Ilan Schnell, Study Paper Univ. Bremen 1997, http://ilan.schnell-web.net/physics/studienarbeit.ps.gz.

[23] E.g. in Bronstein, Semendjajew, Handbook of Mathematics, pp. 14 ff.

**Problem 6.11** ***Thomas-Fermi approximation in atomic physics***
An atom consists of a $Z$-fold positively charged atomic nucleus and the electron shell surrounding it. In the Hartree approximation, the potential for a single electron at the position $\boldsymbol{r}$ is therefore given by:

$$V(\boldsymbol{r}) = \int d^3r' \frac{e^2}{|\boldsymbol{r} - \boldsymbol{r}'|} n(\boldsymbol{r}') - \frac{Ze^2}{r} \tag{6.281}$$

where $n(\boldsymbol{r})$ is the electron density.

In the Thomas-Fermi approximation, it is assumed that the potential $V(\boldsymbol{r})$ varies so slowly that it is practically constant in a region around $\boldsymbol{r}$. Then at $\boldsymbol{r}$ there is a local, homogeneous electron gas present.

a) Derive that from these assumptions it follows:

$$n(\boldsymbol{r}) = \frac{[2m(\varepsilon_F - V(\boldsymbol{r}))]^{3/2}}{3\pi^2} \tag{6.282}$$

where $\varepsilon_F$ is the energy of the highest occupied level.

b) Derive that for a neutral atom $\varepsilon_F = 0$ applies.

c) Show that the Poisson equation results from (6.281) and deduce from this and from b) under the assumption of spherical symmetry for $r > 0$ the *Thomas-Fermi equations*

$$-\frac{3\pi}{r^2}\frac{\partial}{\partial r}\left(r^2 \frac{\partial V(r)}{\partial r}\right) = 4e^2[-2mV(r)]^{3/2} \tag{6.283}$$

.

d) Show that with the substitutions

$$V(r) = -\frac{Ze^2}{r}\Phi(x), \quad r = Z^{-1/3}bx, \quad b = \frac{1}{2}\left(\frac{3\pi}{4}\right)^{2/3} a_0, \quad a_0 = \frac{1}{me^2}$$

the differential equation

$$\frac{d^2}{dx^2}\Phi(x) = x^{-1/2}\Phi^{3/2}(x) \tag{6.284}$$

results with the boundary conditions

$$\Phi(0) = 1, \quad \Phi(x \to \infty) \to 0$$

($\hbar = 1$ in this problem!)

e) Solve the differential Eq. (6.284) numerically and plot $\Phi(x)$ or $V(r)$ and $4\pi r^2 n(r)$.

**Problem 6.12** ***Screening in 1-Dimensional Electron Systems***

a) Determine for a 1-dimensional free electron gas with quadratic dispersion $\varepsilon(k) = k^2$ the Lindhard susceptibility $\chi(q)$ analytically.

b) In order to get a feeling for the required accuracy of numerical $k$-integrals, solve the same problem numerically and compare the analytical and numerical results for $\chi(q)$.

c) Now determine $\chi(q)$ numerically for a one-dimensional Tight-Binding band $\varepsilon(k) = -\cos(k)$ with Fermi energy in the band center.

**Problem 6.13** ***Generalized Lindhard Susceptibility for Semiconductors and Metals***

Consider the Kronig-Penney model from Problems 5.3 and 5.4 again for $v_0 = 50$. As in Problem 5.4 the Bloch factors $u_{nk}(x)$ and the energy eigenvalues $\varepsilon_n(k)$ can be calculated explicitly numerically. Calculate the $q$-dependent susceptibility from this, which (in generalized Lindhard approximation) is given in suitable dimensionless units according to Eq. (6.207) by:

$$\chi(q) = \sum_{n,n',k} \frac{f(\varepsilon_n(k)) - f(\varepsilon_{n'}(k+q))}{\varepsilon_n(k) - \varepsilon_{n'}(k+q)} |M_{n,n'}(k,q)|^2$$

$$\text{with} \quad M_{n,n'}(k,q) = \langle u_{n',k+q} | u_{nk} \rangle,$$

a) for semiconductors, if the Fermi energy is in the band gap between 2nd and 3rd energy band,

b) for metals, if the Fermi energy is in the middle of the 2nd energy band.

Plot the $q$-dependence of $\chi(q)$ and discuss the result.

**Problem 6.14** ***Excitons in One Dimension***

Consider the following spinless two-band model, where the Coulomb interaction is considered only between the conduction and valence bands from the outset:

$$H = \sum_k \varepsilon_v(k) v_k^\dagger v_k + \sum_k \varepsilon_c(k) c_k^\dagger c_k + \sum_{k,k',q} u_q v_{k+q}^\dagger c_{k'-q}^\dagger c_{k'} v_k .$$

The ground state consists of the filled valence band:

$$|\Phi_0\rangle = \prod_k v_k^\dagger |0\rangle, \; E_0 = \sum_k \varepsilon_v(k).$$

a) Make the ansatz

$$|\Phi_1\rangle = \sum_k a_k c_k^\dagger v_k |\Phi_0\rangle$$

for excitons (i.e. an excited particle-hole state) without momentum transfer and derive the following eigenvalue equation from it analogously to the derivation in the text by applying the Hamilton operator:

$$a_k(E_0 + \varepsilon_c(k) - \varepsilon_v(k) - E) - \sum_q u_q a_{k-q} = 0.$$

b) Take a finite-range box potential as a simple model for the interaction between two electrons:

$$u(x-x') = \begin{cases} u_0 & \text{for} \quad |x-x'| < a \\ 0 & \text{otherwise} \end{cases} .$$

Determine $u_q$ for this interaction under the assumption that one can describe conduction and valence band in the vicinity of $k = 0$ by quasi-free particles.

c) Solve the resulting effective single-particle Schrödinger equation (numerically) both in momentum space and in position space.

**Problem 6.15** ***Excitons in a Spatially Confined System***

Consider a one-dimensional box potential

$$V(x) = \begin{cases} -V_0 & \text{for} \quad |x| < L \\ 0 & \text{otherwise} \end{cases} .$$

a) Determine $V_0$ so that there are four bound one-particle states $1, \ldots, 4$.

b) Calculate the matrix elements $u_{ij,kl}$ of the Coulomb interaction ($i, j, k, l \in \{1, 2, 3, 4\}$) between these, for example using the already frequently used model potential

$$u(x-x') = \frac{e^2}{|x-x'| + \delta}.$$

c) Determine the ground state and the ground state energy for a total particle number $N = 4$, taking spin into account.

d) Determine the first excited state and the excitation energy and compare this with the excitation energy (“energy gap”) that would result without Coulomb interaction.

**Problem 6.16** ***Commutators with Fermi Operators***

Show that for fermion creation and annihilation operators it holds that:

$$\begin{aligned}\left[c^\dagger_{k_1}c_{k_2}c^\dagger_{k_3}c_{k_4}, c^\dagger_{k_5}c_{k_6}\right] &= \delta_{k_4k_5}c^\dagger_{k_1}c_{k_2}c^\dagger_{k_3}c_{k_6} + \delta_{k_2k_5}c^\dagger_{k_1}c_{k_6}c^\dagger_{k_3}c_{k_4}\\ &\quad - \delta_{k_3k_6}c^\dagger_{k_1}c_{k_2}c^\dagger_{k_5}c_{k_4} - \delta_{k_1k_6}c^\dagger_{k_5}c_{k_2}c^\dagger_{k_3}c_{k_4}.\end{aligned}$$

# Electron-phonon Interaction

# 7

## 7.1 Hamiltonian of the Electron-Phonon Interaction

At the very beginning in Chap. 3 when discussing the Born-Oppenheimer approximation, we convinced ourselves that one can consider the electronic degrees of freedom, i.e. the dynamics of the electrons, and the lattice degrees of freedom, i.e. the dynamics of the ions, decoupled from each other to a good approximation. Accordingly, in Chap. 4 we only considered the lattice vibrations (phonons) and in Chaps. 5 and 6 only the electrons. But we already know from the treatment of the Born-Oppenheimer approximation that there are corrections to this decoupling, which can be classified by powers of $\sqrt{m/M}$. In this chapter, these corrections are to be taken into account in lowest non-vanishing order.

In Chaps. 5 and 6 we generally assumed that the particle potential $V(\boldsymbol{r})$ is periodic in the lattice, i.e. $V(\boldsymbol{r}+\boldsymbol{R}) = V(\boldsymbol{r})$ is fulfilled. This means that the ions (or atomic nuclei) occupy their equilibrium positions and do not move. But this can actually only be the case at $T= 0$, at any finite temperature the ions will be deflected from their equilibrium positions and at a given time $t$there will be no periodic potential anymore. In this chapter we want to investigate the consequences of this.

We first consider again the electronic part of the total Hamiltonian operator, which is given in first quantization (as has often been the case) by

$$H = \sum_{i=1}^{N_e} \frac{\boldsymbol{p}_i^2}{2m} + \sum_{i=1}^{N_e} V(\boldsymbol{r}_i) + \sum_{i<j} u\left(\boldsymbol{r}_i - \boldsymbol{r}_j\right). \tag{7.1}$$

The particle potential can be written as a linear combination of the contributions of the individual unit cells, i.e.

$$V(\boldsymbol{r}) = \sum_{n=1}^{N} v(\boldsymbol{r} - \boldsymbol{R}_n). \tag{7.2}$$

© The Author(s), under exclusive license to Springer-Verlag GmbH, DE, part of Springer Nature 2023
G. Czycholl, *Solid State Theory, Volume 1*,
https://doi.org/10.1007/978-3-662-66135-2_7

In contrast to the Chaps. 5 and 6 however, now deviations from the equilibrium positions are to be allowed, i.e. the $\boldsymbol{R}_n$ are no longer themselves vectors of a Bravais lattice but it applies

$$\boldsymbol{R}_n = \boldsymbol{R}_{n0} + \boldsymbol{u}_n, \tag{7.3}$$

where $\boldsymbol{R}_{n0}$ is a lattice vector and $\boldsymbol{u}_n$ the deviation of the $n$-th ion from the equilibrium position. For simplicity, only a one-atom lattice will be considered here, the generalization to the treatment of several atoms per elementary cell is elementary simple. For small deviations $\boldsymbol{u}_n$ the potential of the individual unit cell can be developed:

$$\begin{aligned} v(\boldsymbol{r} - \boldsymbol{R}_n) &= v(\boldsymbol{r} - \boldsymbol{R}_{n0} - \boldsymbol{u}_n) \\ &= v(\boldsymbol{r} - \boldsymbol{R}_{n0}) - \nabla v(\boldsymbol{r} - \boldsymbol{R}_{n0}) \cdot \boldsymbol{u}_n. \end{aligned} \tag{7.4}$$

If one writes the particle contribution of the electron Hamiltonian operator as

$$H_0 = \sum_{i=1}^{N_e} h(\boldsymbol{r}_i) \tag{7.5}$$

then it follows that

$$h(\boldsymbol{r}_i) = \frac{\boldsymbol{p}_i^2}{2m} + \underbrace{\sum_{n=1}^{N} v(\boldsymbol{r}_i - \boldsymbol{R}_{n0})}_{V_{\text{per}}(\boldsymbol{r}_i)} - \underbrace{\sum_{n=1}^{N} \nabla v(\boldsymbol{r}_i - \boldsymbol{R}_{n0}) \boldsymbol{u}_n}_{V_{el-ph}(\boldsymbol{r}_i)}. \tag{7.6}$$

In 2. Quantization with respect to the Bloch representation, the first translationally invariant (periodic) part of the potential, $V_{\text{per}}(\boldsymbol{r})$ together with the kinetic energy, is diagonal, but the 2. part $V_{el-ph}(\boldsymbol{r})$ has non-diagonal elements in Bloch representation. $V_{el-ph}(\boldsymbol{r})$ is not translationally invariant with respect to lattice vectors $\boldsymbol{R}_{m0}$ , since the displacements $\boldsymbol{u}_n$ from lattice site to lattice site are different. If one restricts oneself to a single band for the sake of simplicity, the particle contribution to the Hamiltonian operator takes the form:

$$H_0 = \sum_{\boldsymbol{k}\sigma} \varepsilon(\boldsymbol{k}) c_{\boldsymbol{k}\sigma}^\dagger c_{\boldsymbol{k}\sigma} - \sum_{\boldsymbol{k}\boldsymbol{k}'\sigma} \langle \boldsymbol{k} | V_{el-ph}(\boldsymbol{r}) | \boldsymbol{k}' \rangle c_{\boldsymbol{k}'\sigma}^\dagger c_{\boldsymbol{k}\sigma}. \tag{7.7}$$

Here it has already been used that the matrix elements of $V_{el-ph}$ must be spin-diagonal; the potential change due to the displacement of an ion has no effect whatsoever on the spin. This matrix element can now be further transformed according to

$$\left\langle \boldsymbol{k} | V_{el-ph} | \boldsymbol{k}' \right\rangle = \int d^3 r \psi_{\boldsymbol{k}}^*(\boldsymbol{r}) \sum_{l=1}^{N} \nabla v(\boldsymbol{r} - \boldsymbol{R}_{l0}) \boldsymbol{u}_l \psi_{\boldsymbol{k}'}(\boldsymbol{r}). \tag{7.8}$$

The potential $v(\boldsymbol{r})$ of a single ion (or a single unit cell) can be expanded in a Fourier series according to

$$\begin{aligned} v(\boldsymbol{r}) &= \sum_{\boldsymbol{\kappa}} v_{\boldsymbol{\kappa}} e^{i\boldsymbol{\kappa r}} \quad \text{mit} \quad v_{\boldsymbol{\kappa}} = \frac{1}{V}\int d^3r e^{-i\boldsymbol{\kappa r}} v(\boldsymbol{r}) \\ \rightarrow \nabla v(\boldsymbol{r}) &= \sum_{\boldsymbol{\kappa}} i\boldsymbol{\kappa} v_{\boldsymbol{\kappa}} e^{i\boldsymbol{\kappa r}}. \end{aligned} \tag{7.9}$$

This results in:

$$\left\langle \boldsymbol{k}|V_{el-ph}|\boldsymbol{k}'\right\rangle = \sum_{\boldsymbol{\kappa}} i\boldsymbol{\kappa} v_{\boldsymbol{\kappa}} \int d^3r \psi^*_{\boldsymbol{k}}(\boldsymbol{r}) \sum_{l=1}^{N} e^{i\boldsymbol{\kappa}(\boldsymbol{r}-\boldsymbol{R}_{l0})} \boldsymbol{u}_l \psi_{\boldsymbol{k}'}(\boldsymbol{r}). \tag{7.10}$$

The displacements $\boldsymbol{u}_l$ can be represented as a linear combination of phonon generators and destroyers according to (cf. (4.173)):

$$\boldsymbol{u}_l = \frac{1}{\sqrt{N}} \sum_{\boldsymbol{q}j} \sqrt{\frac{\hbar}{2M\omega_j(\boldsymbol{q})}} \left(b_{\boldsymbol{q}j} + b^\dagger_{-\boldsymbol{q}j}\right) \boldsymbol{e}_j(\boldsymbol{q}) e^{i\boldsymbol{qR}_{l0}}. \tag{7.11}$$

This gives:

$$\begin{aligned} \langle \boldsymbol{k}\,|V_{el-ph}|\boldsymbol{k}'\rangle &= \frac{1}{\sqrt{N}} \sum_{\boldsymbol{q\kappa}j} i\boldsymbol{\kappa}\cdot \boldsymbol{e}_j(\boldsymbol{q}) v_{\boldsymbol{\kappa}} \overbrace{\sum_{l=1}^{N} e^{i(\boldsymbol{q}-\boldsymbol{\kappa})\boldsymbol{R}_{l0}}}^{N\cdot\sum_{\boldsymbol{G}} \delta_{\boldsymbol{\kappa q}+\boldsymbol{G}}} \\ \times \; & \overbrace{\frac{1}{V}\int d^3r e^{i(\boldsymbol{k}'-\boldsymbol{k})\boldsymbol{r}} u^*_{\boldsymbol{k}}(\boldsymbol{r}) e^{i\boldsymbol{\kappa r}} u_{\boldsymbol{k}'}(\boldsymbol{r})}^{\frac{1}{N}\sum_{\boldsymbol{R}} e^{i(\boldsymbol{k}'+\boldsymbol{\kappa}-\boldsymbol{k})\boldsymbol{R}} \frac{1}{V_{EZ}}\int_{EZ} d^3r e^{i(\boldsymbol{k}'+\boldsymbol{\kappa}-\boldsymbol{k})\boldsymbol{r}} u^*_{\boldsymbol{k}}(\boldsymbol{r}) u_{\boldsymbol{k}'}(\boldsymbol{r})} \sqrt{\frac{\hbar}{2M\omega_j(\boldsymbol{q})}} \left(b_{\boldsymbol{q}j} + b^\dagger_{-\boldsymbol{q}j}\right) \\ &= \sqrt{N} \sum_{\boldsymbol{Gq}j} i(\boldsymbol{q}+\boldsymbol{G})\cdot \boldsymbol{e}_j(\boldsymbol{q}) v_{\boldsymbol{q}+\boldsymbol{G}} \sqrt{\frac{\hbar}{2M\omega_j(\boldsymbol{q})}} \left(b_{\boldsymbol{q}j} + b^\dagger_{-\boldsymbol{q}j}\right) \\ & \quad \times \frac{1}{V_{EZ}} \int_{EZ} d^3r u^*_{\boldsymbol{k}}(\boldsymbol{r}) u_{\boldsymbol{k}-\boldsymbol{q}-\boldsymbol{G}}(\boldsymbol{r}) \delta_{\boldsymbol{k}'\boldsymbol{k}-\boldsymbol{q}-\boldsymbol{G}}. \end{aligned} \tag{7.12}$$

The electronic particle Hamiltonian operator is therefore given by

$$\begin{aligned} H_0 &= \sum_{\boldsymbol{k}\sigma} \varepsilon(\boldsymbol{k}) c^\dagger_{\boldsymbol{k}\sigma} c_{\boldsymbol{k}\sigma} + \sum_{\boldsymbol{kqG}j\sigma} M^j_{\boldsymbol{k},\boldsymbol{q}+\boldsymbol{G}} \left(b_{\boldsymbol{q}j} + b^\dagger_{-\boldsymbol{q}j}\right) c^\dagger_{\boldsymbol{k}\sigma} c_{\boldsymbol{k}-\boldsymbol{q}-\boldsymbol{G}\sigma} \\ &= \sum_{\boldsymbol{k}\sigma} \varepsilon(\boldsymbol{k}) c^\dagger_{\boldsymbol{k}\sigma} c_{\boldsymbol{k}\sigma} + \sum_{\boldsymbol{kqG}j\sigma} M^j_{\boldsymbol{k},\boldsymbol{q}+\boldsymbol{G}} \left(b_{\boldsymbol{q}j} + b^\dagger_{-\boldsymbol{q}j}\right) c^\dagger_{\boldsymbol{k}+\boldsymbol{q}+\boldsymbol{G}\sigma} c_{\boldsymbol{k}\sigma} \end{aligned} \tag{7.13}$$

with the **matrix element of the electron-phonon coupling**

$$M^j_{\boldsymbol{k},\boldsymbol{q}+\boldsymbol{G}} = -\sqrt{\frac{\hbar N}{2M\omega_j(\boldsymbol{q})}} i(\boldsymbol{q}+\boldsymbol{G})\cdot \boldsymbol{e}_j(\boldsymbol{q}) v_{\boldsymbol{q}+\boldsymbol{G}} \frac{1}{V_{EZ}} \int_{EZ} d^3r u^*_{\boldsymbol{k}+\boldsymbol{q}+\boldsymbol{G}}(\boldsymbol{r}) u_{\boldsymbol{k}}(\boldsymbol{r}). \tag{7.14}$$

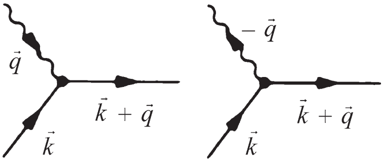

**Fig. 7.1** Elementary electron-phonon vertex with phonon absorption or emission

This Hamiltonian operator (or sometimes a slightly more specialized, version of it) is also referred to as

**Fröhlich-Model**[1]

of electron-phonon interaction. The term has a simple, physically intuitive interpretation:

The displacements lead to transitions or scattering of the electrons from Bloch states with wave vector $\boldsymbol{k}$ to states with wave vector $\boldsymbol{k}' = \boldsymbol{k} + \boldsymbol{q}$ under absorption (destruction) of a phonon with wave number $\boldsymbol{q}$ or under emission of a phonon with wave number $-\boldsymbol{q}$. It is customary to represent these processes by diagrams like in Fig. 7.1.

At the **"interaction vertex"** of such a diagram, momentum is conserved. Here, $\boldsymbol{k}$ can be restricted to the first Brillouin zone; if $\boldsymbol{k} + \boldsymbol{q}$ is outside the 1st Brillouin zone, then a reciprocal lattice vector $\boldsymbol{G}$ can be added so that $\boldsymbol{k} + \boldsymbol{q} + \boldsymbol{G}$ is again in the first Brillouin zone. Such processes are also called **Umklapp processes**, because adding the reciprocal lattice vector can transform the momentum almost in the opposite direction. If, on the other hand, $\boldsymbol{k} + \boldsymbol{q}$ remains with $\boldsymbol{k}$ in the first Brillouin zone, then no reciprocal lattice vector can be added. These processes are called **Normal processes**. For Normal processes at least, there apparently is only coupling of the electrons to the longitudinal phonons, as can be seen from the scalar product $\boldsymbol{q} \cdot \boldsymbol{e}_j(\boldsymbol{q})$; transverse phonons with an oscillation direction $\sim \boldsymbol{e}_j$ perpendicular to the phonon wave vector $\boldsymbol{q}$ apparently do not contribute to effective electron scattering, since the matrix element vanishes.

In the above derivation of the Hamilton operator of the electron-phonon interaction in 2nd quantization, actually only one approximation was made, namely the linearization in the displacements, i.e. the Taylor expansion of the electron-ion potential with truncation after the first term. The electron-ion potential and its gradient were then expanded into a Fourier series, which is in principle exact. The displacements were expanded into phonon creators and annihilators, which is always possible and exact, even if one goes beyond the simple harmonic approximation. The calculation of the electronic matrix elements in Bloch representation and special lattice sums from the Fourier expansion and the expansion according to phonon operators provide Delta relations, which can be interpreted as momentum conservation. The electron-phonon coupling matrix element is therefore essentially determined by the gradient of the electron-ion potential . We have explicitly written the Hamilton operator for a single band model and for only one atom per elementary cell, so that only acoustic phonons can occur. A generalization to several electronic bands is certainly unproblematic and would only increase the number of indices. In a multi-band model, interband scattering is also possible under phonon absorption or emission. If one has to deal with multi-atomic unit cells, the coupling of optical phonons to the electrons is also possible.

---

[1] H. Fröhlich, *1905 in Rexingen (Neckar), †1991 in Liverpool, 1932/33 Professor in Freiburg, emigrated to England and Professor in Bristol and Liverpool, works on solid state theory, in particular on the theory of dielectrics and superconductivity, 1950 famous work on electron-phonon interaction.

The entire solid-state Hamiltonian operator can be written according to the above considerations as follows:

$$\begin{aligned} H = &\sum_{\boldsymbol{k}\nu\sigma} \varepsilon_\nu(\boldsymbol{k}) c^\dagger_{\boldsymbol{k}\nu\sigma} c_{\boldsymbol{k}\nu\sigma} + \sum_{\boldsymbol{k}\nu\boldsymbol{q}\boldsymbol{G}j\sigma} M^{j\nu\nu'}_{\boldsymbol{k},\boldsymbol{q}+\boldsymbol{G}} \left( b_{\boldsymbol{q}j} + b^\dagger_{-\boldsymbol{q}j} \right) c^\dagger_{\boldsymbol{k}+\boldsymbol{q}+\boldsymbol{G}\nu\sigma} c_{\boldsymbol{k}\nu'\sigma} \\ &+ \frac{1}{2} \sum_{\boldsymbol{k}_1\boldsymbol{k}_2\boldsymbol{q}} \sum_{\sigma\sigma'\nu\nu'} u_{\boldsymbol{k}_1+\boldsymbol{q}\nu\boldsymbol{k}_2-\boldsymbol{q}\nu',\boldsymbol{k}_2\nu'\boldsymbol{k}_1\nu} c^\dagger_{\boldsymbol{k}_1+\boldsymbol{q}\nu\sigma} c^\dagger_{\boldsymbol{k}_2-\boldsymbol{q}\nu'\sigma'} c_{\boldsymbol{k}_2\nu'\sigma'} c_{\boldsymbol{k}_1\nu\sigma} \\ &+ \sum_{\boldsymbol{q}j} \hbar\omega_j(\boldsymbol{q}) \left( b^\dagger_{\boldsymbol{q}j} b_{\boldsymbol{q}j} + \frac{1}{2} \right) \end{aligned} \tag{7.15}$$

where ν is to denote the band index.

Finally, the most important consequences of the electron-phonon interaction shall be listed:

1. The wave vector $\boldsymbol{k}$ is apparently no longer a good quantum number for the electrons, they are scattered from $\boldsymbol{k}$ to $\boldsymbol{k}'$. The electrons therefore have a finite lifetime in the Bloch state $\boldsymbol{k}$. This results in particular in a significant contribution to the electrical resistance.

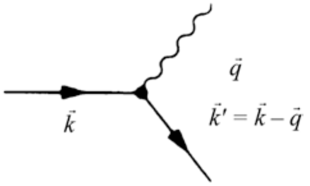

2. The electronic eigenstates and eigenvalues are modified. In particular, there may be a co-movement of a lattice polarization with the electron through the lattice. Under certain circumstances, one speaks of a new quasiparticle, the

**polaron,** which consists of an electron plus the polarization cloud surrounding it. The polaron has a larger effective mass than a normal conduction electron.

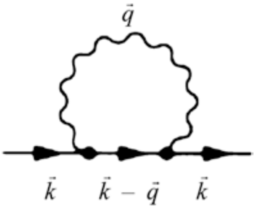

3. The phonon emitted by an electron can be absorbed by another electron, so that this phonon effectively transfers an electron-electron interaction . This can be attractive, which is the mechanism of (conventional) superconductivity. This can also be understood intuitively, that the polarization of the lattice induced by one electron is still attractive to a 2. electron at a later time due to the accumulation (displacement) of positive ion charges.

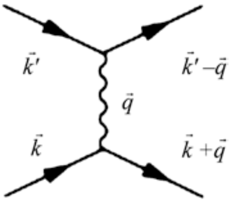

4. The phonon properties and effective frequencies are also renormalized by the electron-phonon interaction. In particular, there are processes in which a propagating phonon can be absorbed by electrons or a hole-electron pair can be generated.

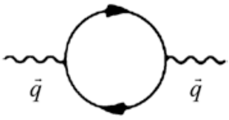

In general, there is a wide analogy to processes and concepts that are important in quantum electrodynamics. Electrons couple to electromagnetic fields, which can be quantized as linear combinations of photon creattors and annihilators. The phenomena and consequences discussed above correspond, for example, in quantum electrodynamics to the renormalization of electron mass and charge by the surrounding photon cloud, the transfer of the electromagnetic interaction by the exchange of a photon, the generation of an  electron-positron pair ("pair generation").

## 7.2 Renormalization of the Effective Electron Mass

In this section, the influence of the electron-phonon interaction on the electronic properties of solids is to be estimated. For this purpose, the change in the ground state energy is to be calculated perturbatively. According to quantum mechanical perturbation theory one gets in second order in the perturbation:

$$E_n^{(2)} = E_n^{(0)} + \langle n|V|n\rangle + \sum_{m \neq n} \frac{|\langle n|V|m\rangle|^2}{E_n^{(0)} - E_m^{(0)}} \tag{7.16}$$

if $V$ is a perturbation term in the Hamiltonian operator and $|n\rangle, |m\rangle$ are the unperturbed eigenstates with eigenvalues $E_n^{(0)}, E_m^{(0)}$. We now start from the electronic ground state $|0\rangle$ with ground state energy

$$E_0 = \sum_{\boldsymbol{k},(k<k_F)} \varepsilon_{\boldsymbol{k}}.$$

$\varepsilon_{\boldsymbol{k}}$ unperturbed electronic one-particle energies (i.e. band structure) where $\boldsymbol{k}$ should generally stand for a set of one-particle quantum numbers. In the unperturbed ground state, no phonons are excited. Then, for the ground state energy in 2nd order perturbation theory with respect to electron-phonon coupling, we get:

$$E^{(2)} = E_0 + \sum_{\boldsymbol{kq}} \frac{\left\langle 0|b_{-\boldsymbol{q}} c_{\boldsymbol{k}}^{\dagger} c_{\boldsymbol{k}+\boldsymbol{q}} b_{-\boldsymbol{q}}^{\dagger} c_{\boldsymbol{k}+\boldsymbol{q}}^{\dagger} c_{\boldsymbol{k}}|0\right\rangle \left|M_{\boldsymbol{k},\boldsymbol{q}}\right|^2}{\varepsilon_{\boldsymbol{k}} - \varepsilon_{\boldsymbol{k}+\boldsymbol{q}} - \hbar\omega_{-\boldsymbol{q}}}. \tag{7.17}$$

Here, we disregard Umklapp processes, also only the one relevant (longitudinal acoustic) phonon branch is considered, and we sum over intermediate states in which a phonon with momentum $-\boldsymbol{q}$ is present and an electron with momentum $\boldsymbol{k}$ is scattered into a state with momentum $\boldsymbol{k} + \boldsymbol{q}$. Therefore,

$$E_0 - E_n = \varepsilon_{\boldsymbol{k}} - \varepsilon_{\boldsymbol{k}+\boldsymbol{q}} - \hbar\omega_{-\boldsymbol{q}}.$$

The electron creators and annihilators in the matrix elements automatically ensure that only those $\boldsymbol{k}, \boldsymbol{q}$ occur for which $|\boldsymbol{k}| < k_F$ and $|\boldsymbol{k} + \boldsymbol{q}| > k_F$ hold. This can (also for $T = 0$) be expressed by Fermi factors $f(\varepsilon_{\boldsymbol{k}})$ or $(1 - f(\varepsilon_{\boldsymbol{k}+\boldsymbol{q}}))$. The modified ground state energy is therefore given by:

$$E^{(2)} = E_0 + \sum_{\boldsymbol{k},\boldsymbol{q}} \frac{\left|M_{\boldsymbol{k},\boldsymbol{q}}\right|^2 f(\varepsilon_{\boldsymbol{k}})\left(1 - f\left(\varepsilon_{\boldsymbol{k}+\boldsymbol{q}}\right)\right)}{\varepsilon_{\boldsymbol{k}} - \varepsilon_{\boldsymbol{k}+\boldsymbol{q}} - \hbar\omega_{-\boldsymbol{q}}}. \tag{7.18}$$

This is the total ground state energy of the $N_e$-electron system taking into account electron-phonon interaction up to 2nd order. But how does the energy eigenvalue of a single electron change, what modification does the band structure experience? It is physically clear from the outset that modifications are to be expected in particular in the vicinity of the Fermi edge. At least for metallic systems, the activation of the electron-phonon coupling allows for a continuous scattering of the electrons from the occupied one-particle state $\boldsymbol{k}$ into unoccupied states $\boldsymbol{k}+\boldsymbol{q}$ , and that should be particularly easy for electrons at the Fermi edge. The energy that is to be assigned to a single electron at the Fermi edge as a result of the electron-phonon interaction can be estimated by the following simple consideration. We imagine that an additional electron is added to a given $N_e$-electron system, whose ground state energy is given by the above expression. This additional electron must occupy a state $\boldsymbol{k}_0$ directly above the Fermi edge and would therefore have the energy $\varepsilon_{\boldsymbol{k}_0} = \frac{\hbar^2 k_0^2}{2m}$ in the undisturbed case. In the disturbed case, that is, taking into account the electron-phonon coupling in 2. order perturbation theory, one must assign the energy $E_{\boldsymbol{k}_0}$ to this additional electron, by which the ground state energy changes when this electron is added. The additional electron can once again make transitions into all unoccupied states by phonon emission, but on the other hand, the state $\boldsymbol{k}_0$ is no longer accessible to the other electrons in the Fermi sea, since $\boldsymbol{k}_0$ is now occupied. Therefore,

$$E_{\boldsymbol{k}_0} = \frac{\hbar^2 k_0^2}{2m} + \sum_{\boldsymbol{q}} \frac{|M_{\boldsymbol{k}_0,\boldsymbol{q}}|^2 \left(1 - f\left(\varepsilon_{\boldsymbol{k}_0+\boldsymbol{q}}\right)\right)}{\varepsilon_{\boldsymbol{k}_0} - \varepsilon_{\boldsymbol{k}_0+\boldsymbol{q}} - \hbar\omega_{-\boldsymbol{q}}} - \sum_{\boldsymbol{q}} \frac{|M_{\boldsymbol{k}_0-\boldsymbol{q},\boldsymbol{q}}|^2 f\left(\varepsilon_{\boldsymbol{k}_0-\boldsymbol{q}}\right)}{\varepsilon_{\boldsymbol{k}_0-\boldsymbol{q}} - \varepsilon_{\boldsymbol{k}_0} - \hbar\omega_{-\boldsymbol{q}}} \cdot \tag{7.19}$$

If the $k$-dependence of $M_{\boldsymbol{q},\boldsymbol{k}}$ is neglected, which is at least then correct if the Bloch factors can be replaced by 1 and therefore should be justified for metals in the case of the validity of the model of free electrons, and if $|M_{\boldsymbol{q}}|^2 = |M_{-\boldsymbol{q}}|^2$ is taken into account, then the last two summands can be combined and one obtains

$$E_{\boldsymbol{k}_0} = \frac{\hbar^2 k_0^2}{2m} + \sum_{\boldsymbol{q}} \frac{|M_{\boldsymbol{q}}|^2}{\varepsilon_{\boldsymbol{k}_0} - \varepsilon_{\boldsymbol{k}_0+\boldsymbol{q}} - \hbar\omega_{-\boldsymbol{q}}} - \sum_{\boldsymbol{q}} \frac{2|M_{\boldsymbol{q}}|^2 f\left(\varepsilon_{\boldsymbol{k}_0+\boldsymbol{q}}\right)\hbar\omega_{-\boldsymbol{q}}}{\left(\varepsilon_{\boldsymbol{k}_0+\boldsymbol{q}} - \varepsilon_{\boldsymbol{k}_0}\right)^2 - \hbar^2\omega_{-\boldsymbol{q}}^2} \cdot \tag{7.20}$$

This is therefore the modification of the electronic band structure in the vicinity of the Fermi edge due to the electron-phonon interaction, if this is taken into account in second-order perturbation theory. The first summand gives a smooth function of $\boldsymbol{k}_0$ and therefore usually only causes a shift of $\varepsilon_{\boldsymbol{k}}$. But the second summand has a sharp structure right at the Fermi edge due to the Fermi factor. If one calculates the gradient of $E_{\boldsymbol{k}}$, the correction, i.e. the deviation from the simple free electron behaviour, is dominated by this part due to the Fermi function, since the derivative of the Fermi function at low temperatures is a delta function. Therefore:

$$\nabla_{\boldsymbol{k}} E_{\boldsymbol{k}}|_{\boldsymbol{k}=\boldsymbol{k}_0} \approx \nabla_{\boldsymbol{k}} \varepsilon_{\boldsymbol{k}_0} - \sum_{\boldsymbol{q}} \frac{2|M_{\boldsymbol{q}}|^2 \nabla_{\boldsymbol{k}} f\left(\varepsilon_{\boldsymbol{k}_0+\boldsymbol{q}}\right)\hbar\omega_{-\boldsymbol{q}}}{\left(\varepsilon_{\boldsymbol{k}_0+\boldsymbol{q}} - \varepsilon_{\boldsymbol{k}_0}\right)^2 - \hbar^2\omega_{-\boldsymbol{q}}^2} = \nabla_{\boldsymbol{k}} \varepsilon_{\boldsymbol{k}}(1 - \alpha_{\boldsymbol{k}})|_{\boldsymbol{k}=\boldsymbol{k}_0} \cdot \tag{7.21}$$

with

$$\alpha_{\boldsymbol{k}_0} = -\sum_{\boldsymbol{q}} \frac{2|M_{\boldsymbol{q}}|^2 \hbar\omega_{-\boldsymbol{q}} \delta\left(\varepsilon_{\boldsymbol{k}_0+\boldsymbol{q}} - E_F\right)}{\left(\varepsilon_{\boldsymbol{k}_0+\boldsymbol{q}} - \varepsilon_{\boldsymbol{k}_0}\right)^2 - \hbar^2\omega_{-\boldsymbol{q}}^2} . \tag{7.22}$$

If $\boldsymbol{k}_0$ and $\boldsymbol{k}_0 + \boldsymbol{q}$ are both at the Fermi edge, this will become a surface integral over the Fermi surface. $\alpha_{\boldsymbol{k}_0}$ is then positive and given by

$$\alpha_{\boldsymbol{k}_0} \sim \int dS_{\boldsymbol{k}} \frac{2\left|M_{\boldsymbol{q}}\right|^2}{\hbar\omega_{\boldsymbol{q}}}. \tag{7.23}$$

The increase in the electronic dispersion is therefore reduced at the Fermi edge by the electron-phonon coupling, the effective electron mass therefore increases due to this factor α:

$$m^* = \frac{m}{1-\alpha} \approx m(1+\alpha). \tag{7.24}$$

## 7.3 Screening Effects on Phonon Dispersion and Electron-Phonon Interaction

The electron-phonon interaction is caused by the attractive potential that electrons experience through the ions or atomic nuclei, and this is ultimately the electrostatic Coulomb potential. However, this is usually not a bare Coulomb potential, but this ionic potential is screened by the other electrons and in particular by the electrons in the inner shells. After learning about elementary theories of screening in the previous chapter, we can discuss the influence of screening on ionic potentials and thus on phonons and the electron-phonon interaction qualitatively and phenomenologically.

In the discussion of acoustic phonons it has already been pointed out that there is a long-wavelength vibration mode for all crystals in which all ions are deflected from the rest position to a nearly uniform extent. However, the ions are also charged particles of the positive charge $Ze$, and if all ions are deflected to a uniform extent, the ionic charge density is shifted with respect to its rest position. If the electrons remain in their equilibrium position, one expects a collective plasma oscillation of the ion system around its equilibrium position. The ionic plasma frequency is given by:

$$\Omega_P^2 = 4\pi \frac{Z^2 e^2 n_i}{M} \tag{7.25}$$

where $n_i$ is the ion density and $M$ is the ion mass. This apparent result of a collective, uniform oscillation of all ions with the constant ionic plasma frequency contradicts the results of Chap. 4, according to which the eigenfrequency should vanish linearly with $q$ in the long-wavelength limit. The physical reason why the ionic plasma frequency is not decisive for phonons is that when the ions are deflected, the electrons do not remain in their rest positions but follow the ionic motion and thus immediately screen any polarization that might arise.

For metals, the screening can be described in Thomas-Fermi approximation for large wavelengths (small $q$). According to this, the dielectric constant  is given by

$$\varepsilon(\boldsymbol{q}) = 1 + \frac{k_{TF}^2}{q^2}, \tag{7.26}$$

with the Thomas-Fermi wave number

$$k_{TF}^2 = 4\pi e^2 \frac{\partial n_0}{\partial \mu}.$$

The restoring electric field caused by the deflection of the ions is thus screened by the well-mobile electrons and is smaller by a factor $1/\varepsilon(q)$ than the bare field without screening. Accordingly, the expected oscillation frequency changes in

$$\omega^2 = \frac{\Omega_p^2}{\varepsilon(\boldsymbol{q})} = \frac{4\pi Z^2 e^2 n_i}{M\left(q^2 + k_{TF}^2\right)} q^2. \tag{7.27}$$

For small $q$ one obtains

$$\omega(q) = \sqrt{\frac{4\pi Z^2 e^2 n_i}{M k_{TF}^2}}\, q. \tag{7.28}$$

As expected for acoustic phonons, a linear dispersion relation between frequency $\omega(q)$ and wave number $q$ results. The sound velocity of metals is according to these considerations approximately given by

$$c = \sqrt{\frac{4\pi Z^2 e^2 n_i}{M k_{TF}^2}}. \tag{7.29}$$

This can be converted further by using the relationship between ion and electron density $n_i = n_e/Z$ (because of charge neutrality) and by using $n_e = k_F^3/3\pi^2$ and $k_{TF}^2 = 4me^2 k_F/\pi\hbar^2$ (cf. (6.199)):

$$c^2 = \frac{4\pi Z^2 e^2 n_i}{M k_{TF}^2} = \frac{4\pi Z e^2 k_F^3 \pi \hbar^2}{M 4 m e^2 k_F 3\pi^2} = \frac{1}{3} Z \frac{m}{M} v_F^2 \tag{7.30}$$

where $v_F$is the Fermi velocity of the electrons ($mv_F^2 = \hbar^2 k_F^2/m$). The ratio between sound velocity and electronic Fermi velocity is thus determined by the square root of the ratio of electron and ion mass

$$\frac{c}{v_F} \sim \sqrt{\frac{m}{M}}, \tag{7.31}$$

which agrees with earlier estimates of the relevant orders of magnitude. The above result for the sound velocity in metals is also called

**Bohm-Staver-Relation.**[2]

---

[2] Named after D. Bohm (*1917, †1992, American physicist, working in London from 1961, work on plasma physics, on plasma oscillations of metal electrons and particularly known for the Aharonov-Bohm effect) and his collaborator Tor Staver.

The ions themselves also cause a screening of (external) potentials. However, since the ionic movement takes place on a different time scale than the electron movement, the dynamic screening must be taken into account for the ionic screening, i.e. one has to work with a frequency-dependent ionic dielectric constant, while the electronic shielding can still be treated statically. The "naked", not screened by electrons, ion-induced contribution to the dielectric constant would then be given by

$$\varepsilon_{\text{ion}}^{(0)} = 1 - \frac{\Omega_p^2}{\omega^2}$$

Since the ions are themselves screened, the "naked" plasma frequency $\Omega_p^2$ has to be replaced by $\Omega_p^2/\varepsilon_{el}(q) = \omega^2(q)$, as it was already used in (7.27). The ionic part of the dielectric constant is therefore

$$\varepsilon_{\text{ion}} = 1 - \frac{\omega^2(q)}{\omega^2}. \tag{7.32}$$

The total dielectric constant caused by electronic and ionic screening is then given by

$$\frac{1}{\varepsilon} = \frac{1}{\varepsilon_{el}(q)}\frac{1}{\varepsilon_{\text{ion}}} = \frac{1}{1+\frac{k_{TF}^2}{q^2}}\frac{1}{1-\frac{\omega^2(q)}{\omega^2}}. \tag{7.33}$$

A bare ("naked") Coulomb potential $\frac{4\pi e^2}{q^2}$ goes over into a screened one of the type

$$\frac{4\pi e^2}{q^2+k_{TF}^2}\left(1+\frac{\omega(q)^2}{\omega^2-\omega^2(q)}\right). \tag{7.34}$$

Two different electrons with momenta $\boldsymbol{k},\boldsymbol{k}'$ in the system (metal) therefore do not feel the bare Coulomb repulsion but the screened interaction

$$v_{\boldsymbol{k},\boldsymbol{k}'} = \frac{1}{V}\frac{4\pi e^2}{\left(\boldsymbol{k}-\boldsymbol{k}'\right)^2+k_{TF}^2}\left(1+\frac{\omega^2\left(\boldsymbol{k}-\boldsymbol{k}'\right)}{\omega^2-\omega^2\left(\boldsymbol{k}-\boldsymbol{k}'\right)}\right). \tag{7.35}$$

In the interaction of two electrons, the relevant energy or frequency scale is the energy difference $\hbar\omega = \varepsilon_{\boldsymbol{k}} - \varepsilon_{\boldsymbol{k}'}$ between the electrons. If the energy difference between the electrons is significantly greater than the phonon energies (of the order of the Debye energy), the phonon contribution or ionic contribution to the screening of the Coulomb interaction is therefore to be neglected, one obtains the electronically screened Coulomb interaction according to the Thomas-Fermi approximation again. But if the energy difference is smaller than the Debye energy, the second, phonon-related contribution is negative, and the total effective electron-electron interaction can become negative, i.e. attractive. This is a first indication that phonons can mediate an effective attractive interaction between electrons in a shell of thickness Debye energy $\hbar\omega_D$around the Fermi surface, which is the microscopic origin of (conventional) superconductivity. This will be discussed in more detail in the chapter on superconductivity in Volume 2.

The additional contribution to the interaction between two electrons in the states $\boldsymbol{k}$ and $\boldsymbol{k}'$ caused by ionic screening is therefore given by

$$v^{ep}_{\boldsymbol{k}\boldsymbol{k}'} = \frac{1}{V} \frac{4\pi e^2}{\left(\boldsymbol{k}-\boldsymbol{k}'\right)^2 + k_{TF}^2} \frac{\hbar^2\omega^2\left(\boldsymbol{k}-\boldsymbol{k}'\right)}{\left(\varepsilon_{\boldsymbol{k}}-\varepsilon_{\boldsymbol{k}'}\right)^2 - \hbar^2\omega^2\left(\boldsymbol{k}-\boldsymbol{k}'\right)}. \tag{7.36}$$

On the other hand, the effective interaction between two electrons transmitted by the ions can also be estimated from the Hamiltonian operator of the electron-phonon coupling using perturbation theory. The states

$$|\Phi_0\rangle = \prod_{k\leq k_F} c^\dagger_{\boldsymbol{k}}|0\rangle \qquad |\Phi_1\rangle = c^\dagger_{\boldsymbol{k}'+\boldsymbol{q}} c^\dagger_{\boldsymbol{k}-\boldsymbol{q}} c_{\boldsymbol{k}} c_{\boldsymbol{k}'}|\Phi_0\rangle \tag{7.37}$$

are both eigenstates of the unperturbed, non-interacting electronic Hamiltonian operator, $|\Phi_0\rangle$ is the ground state (filled Fermi sea) and $|\Phi_1\rangle$ a special excited state (with energy $E_1 = E_0 + \varepsilon_{\boldsymbol{k}'+\boldsymbol{q}} + \varepsilon_{\boldsymbol{k}-\boldsymbol{q}} - \varepsilon_{\boldsymbol{k}} - \varepsilon_{\boldsymbol{k}'}$), in which two electrons from the states $\boldsymbol{k},\boldsymbol{k}'$ below the Fermi energy are excited into previously unoccupied states $\boldsymbol{k}-\boldsymbol{q},\boldsymbol{k}'+\boldsymbol{q}$ . Without taking into account the electron-electron and the electron-phonon interaction, there are no matrix elements of the Hamilton operator between these two states $|\Phi_0\rangle, |\Phi_1\rangle$. However, taking into account the electron-phonon coupling, there is a non-vanishing matrix element between the (modified) ground state $|\tilde{\Phi}_0\rangle$ and the state $|\tilde{\Phi}_1\rangle$. According to quantum mechanical perturbation theory, in lowest order in the perturbation $H_1$:

$$\left|\tilde{\Phi}_0\right\rangle = |\Phi_0\rangle + \sum_{l\neq 0} \frac{|l\rangle\langle l|H_1|\Phi_0\rangle}{E_0 - E_l}. \tag{7.38}$$

Analogously, it follows:

$$\langle\tilde{\Phi}_1| = \langle\Phi_1| + \sum_{l\neq 0} \frac{\langle\Phi_1|H_1|l\rangle\langle l|}{E_1 - E_l}. \tag{7.39}$$

Thus:

$$\langle\tilde{\Phi}_1|H_1|\tilde{\Phi}_0\rangle = \sum_{l\neq 0}\left(\frac{\langle\Phi_1|H_1|l\rangle\langle l|H_1|\Phi_0\rangle}{E_0 - E_l} + \frac{\langle\Phi_1|H_1|l\rangle\langle l|H_1|\Phi_0\rangle}{E_1 - E_l}\right). \tag{7.40}$$

If $H_1$is the Hamilton operator of the electron-phonon interaction, then for fixed $\boldsymbol{k},\boldsymbol{k}',\boldsymbol{q}$ only one intermediate state $|l\rangle$ is possible, in which a phonon with momentum $\boldsymbol{q}$ is excited, namely

$$|l\rangle = b^\dagger_{\boldsymbol{q}} c^\dagger_{\boldsymbol{k}-\boldsymbol{q}} c_{\boldsymbol{k}}|\Phi_0\rangle. \tag{7.41}$$

The corresponding energy denominators are:

$$E_0 - E_l = \varepsilon_{\boldsymbol{k}} - \varepsilon_{\boldsymbol{k}-\boldsymbol{q}} - \hbar\omega_{\boldsymbol{q}} \quad \text{und} \quad E_1 - E_l = \varepsilon_{\boldsymbol{k}'+\boldsymbol{q}} - \varepsilon_{\boldsymbol{k}'} - \hbar\omega_{\boldsymbol{q}}. \tag{7.42}$$

In total, one thus obtains for the matrix element $\langle\tilde{\Phi}_1|H_1|\tilde{\Phi}_0\rangle$, which precisely describes the effective interaction of the electrons $\boldsymbol{k},\boldsymbol{k}'$:

$$v^{ep}_{\boldsymbol{k}\boldsymbol{k}'\boldsymbol{q}} = \langle\tilde{\Phi}_1|H_1|\tilde{\Phi}_0\rangle = \frac{|M_{\boldsymbol{q}}|^2}{\varepsilon_{\boldsymbol{k}} - \varepsilon_{\boldsymbol{k}-\boldsymbol{q}} - \hbar\omega_{\boldsymbol{q}}} + \frac{|M_{\boldsymbol{q}}|^2}{\varepsilon_{\boldsymbol{k}'+\boldsymbol{q}} - \varepsilon_{\boldsymbol{k}'} - \hbar\omega_{\boldsymbol{q}}}. \tag{7.43}$$

Here, an eventual $\boldsymbol{k}$-dependence of the electron-phonon matrix element has already been neglected. There results an effective electron-electron interaction, which, after summation over all $\boldsymbol{k},\boldsymbol{k}',\boldsymbol{q}$, can be written as

$$\begin{aligned} V &= \frac{1}{2}\sum_{\boldsymbol{k},\boldsymbol{k}',\boldsymbol{q}} v^{ep}_{\boldsymbol{k}\boldsymbol{k}'\boldsymbol{q}} c^\dagger_{\boldsymbol{k}'+\boldsymbol{q}} c^\dagger_{\boldsymbol{k}-\boldsymbol{q}} c_{\boldsymbol{k}} c_{\boldsymbol{k}'} \\ &= \frac{1}{2}\sum_{\boldsymbol{k},\boldsymbol{k}',\boldsymbol{q}} |M_{\boldsymbol{q}}|^2 \left(\frac{1}{\varepsilon_{\boldsymbol{k}} - \varepsilon_{\boldsymbol{k}-\boldsymbol{q}} - \hbar\omega_{\boldsymbol{q}}} + \frac{1}{\varepsilon_{\boldsymbol{k}\ +\boldsymbol{q}} - \varepsilon_{\boldsymbol{k}}\ - \hbar\omega_{\boldsymbol{q}}}\right) c^\dagger_{\boldsymbol{k}'+\boldsymbol{q}} c^\dagger_{\boldsymbol{k}-\boldsymbol{q}} c_{\boldsymbol{k}} c_{\boldsymbol{k}'} \\ &= \frac{1}{2}\sum_{\boldsymbol{k},\boldsymbol{k}',\boldsymbol{q}} \frac{2|M_{\boldsymbol{q}}|^2\hbar\omega_{\boldsymbol{q}}}{(\varepsilon_{\boldsymbol{k}} - \varepsilon_{\boldsymbol{k}-\boldsymbol{q}})^2 - \hbar^2\omega^2_{\boldsymbol{q}}} c^\dagger_{\boldsymbol{k}'+\boldsymbol{q}} c^\dagger_{\boldsymbol{k}-\boldsymbol{q}} c_{\boldsymbol{k}} c_{\boldsymbol{k}'}, \end{aligned} \tag{7.44}$$

where, in the last step, the summation indices were once renumbered: $\boldsymbol{k}' \to \boldsymbol{k}, \boldsymbol{q} \to -\boldsymbol{q}$. Furthermore, $\omega_{\boldsymbol{q}} = \omega_{-\boldsymbol{q}}$ was used. Thus:

$$v^{ep}_{\boldsymbol{k}\boldsymbol{k}'\boldsymbol{q}} \equiv v^{ep}_{\boldsymbol{k}\boldsymbol{q}} = \frac{2\hbar\omega_{\boldsymbol{q}}\left|M_{\boldsymbol{q}}\right|^2}{(\varepsilon_{\boldsymbol{k}} - \varepsilon_{\boldsymbol{k}-\boldsymbol{q}})^2 - \hbar^2\omega^2_{\boldsymbol{q}}}. \tag{7.45}$$

From this one recognizes again that the effective electron-electron interaction mediated by phonon exchange is negative, i.e. attractive, if $|\varepsilon_{\boldsymbol{k}} - \varepsilon_{\boldsymbol{k}-\boldsymbol{q}}| < \hbar\omega_{\boldsymbol{q}}$ what is of decisive importance for the explanation of superconductivity. If one compares this result with the result obtained from the phenomenological consideration with respect to the ionic and electronic screening (7.36), one obtains for the matrix element of the electron-phonon coupling:

$$|M_{\boldsymbol{q}}|^2 = \frac{4\pi e^2}{V\left(q^2 + k^2_{TF}\right)}\frac{1}{2}\hbar\omega_{\boldsymbol{q}}. \tag{7.46}$$

For small $|q|$ the matrix element of the electron-phonon coupling should therefore be proportional $\sqrt{q}$ due to the above qualitative and heuristic considerations. But this is quite in line with the result

$$M_{\boldsymbol{q}} \sim \sqrt{\frac{\hbar}{2M\omega_{\boldsymbol{q}}}}\boldsymbol{e}\boldsymbol{q}v_{\boldsymbol{q}}$$

for a $q$-independent Fourier transform $v_{\boldsymbol{q}} = v_0$ of the electron-ion potential, and this is in turn fulfilled for very short-range potentials (exactly for Delta potentials) in real space, which can only be true for sufficiently strong screening.

If one uses the estimate obtained for free electrons for the Thomas-Fermi wave number

$$\frac{4\pi e^2}{k_{TF}^2} = \frac{2E_F}{3n_e},$$

where $E_F$ is the Fermi energy and $n_e$ the electron density, one obtains for small $q \ll k_{TF}$ for the electron-phonon coupling in metals the estimate

$$|M_{\boldsymbol{q}}|^2 \approx \frac{\hbar\omega_{\boldsymbol{q}} E_F}{3n_e V} = \frac{\hbar\omega_{\boldsymbol{q}} E_F}{3N_e}. \tag{7.47}$$

This form of $|M_{\boldsymbol{q}}|^2$ and in particular the proportionality to $q$ for small $q$ (or the behavior proportional to the dispersion of acoustic phonons) also has important and experimentally verifiable consequences for the part of the electrical resistance of metals caused by electron-phonon scattering, which will also be discussed later (in the chapter on electronic transport in solids in Volume 2).

## 7.4 Electron-Phonon Interaction in Ionic Crystals

While in metals the screening is so strong that the electrons feel a short-range effective ion potential instead of the original attractive, long-range Coulomb potential, in ionic crystals the Coulomb potential remains decisive and noticeable. It is screened, but only by a constant factor and thus remains long-range, in particular. In ionic crystals, opposite displacements of the differently charged ions are possible, that is, optical phonons, and these vibrations generate long-range dipole fields to which electrons can couple.

The starting point should be the general electron-phonon Hamiltonian operator from Sect. 7.1, slightly generalized to the case of several ions per elementary cell:

$$H_{el-ph} = \sum_{\boldsymbol{k},\alpha} \sum_{\boldsymbol{q},j,\boldsymbol{G}} M^{j,\alpha}_{\boldsymbol{k},\boldsymbol{q}+\boldsymbol{G}} \left( b_{\boldsymbol{q}j} + b^\dagger_{-\boldsymbol{q},j} \right) c^\dagger_{\boldsymbol{k}+\boldsymbol{q}+\boldsymbol{G}} c_{\boldsymbol{k}} \tag{7.48}$$

with

$$\begin{aligned} M^{j,\alpha}_{\boldsymbol{k},\boldsymbol{q}+\boldsymbol{G}} = & -i\sqrt{\frac{\hbar N}{2M_\alpha \omega_j(\boldsymbol{q})}} (\boldsymbol{q}+\boldsymbol{G}) \boldsymbol{e}^{(j)}_\alpha(\boldsymbol{q}) v_{\alpha,\boldsymbol{q}+\boldsymbol{G}} \times \\ & \times \int d^3r u^*_{\boldsymbol{k}+\boldsymbol{q}+\boldsymbol{G}}(\boldsymbol{r}) u_{\boldsymbol{k}}(\boldsymbol{r}). \end{aligned} \tag{7.49}$$

For further simplification, the following assumptions are made:

- The Bloch factors are approximated by constants, as is strictly justified only for a free electron system.
- Umklapp processes are neglected, i.e. $\boldsymbol{G} = 0$.
- Only two ions per elementary cell, one positively charged and one negatively charged, are considered, i.e. $\alpha = 1, 2$.

The electron-ion potentials are thus an attractive and a repulsive, constantly screened Coulomb potential:

$$v_1(\boldsymbol{r}-\boldsymbol{R}_1)=F\frac{Ze^2}{|\boldsymbol{r}-\boldsymbol{R}_1|},\quad v_2(\boldsymbol{r}-\boldsymbol{R}_2)=-F\frac{Ze^2}{|\boldsymbol{r}-\boldsymbol{R}_2|}. \tag{7.50}$$

Their Fourier transforms are:

$$v_{1,\boldsymbol{q}}=\frac{4\pi FZe^2}{Vq^2},\quad v_{2,\boldsymbol{q}}=-\frac{4\pi FZe^2}{Vq^2}, \tag{7.51}$$

where $Z$ is the charge number of the ions and $V$ is the system volume and $F$ is a static screening factor.

For optical phonons, the ions are deflected in opposite directions, i.e. $\boldsymbol{e}_1=-\boldsymbol{e}_2$; in addition, because of the scalar product $\boldsymbol{e}_\alpha\boldsymbol{q}$ only the interaction of electrons with longitudinal phonons exists. If only this longitudinal component is considered and the matrix elements of the electron-phonon coupling for both atoms in the elementary cell are combined, one obtains

$$\begin{aligned} M_{\boldsymbol{q}}=M_{\boldsymbol{q}}^1+M_{\boldsymbol{q}}^2&=-i\sqrt{\frac{\hbar N}{2\tilde{M}\omega_{LO}(q)}}\,q(v_{1\boldsymbol{q}}-v_{2\boldsymbol{q}})\\ &=-i\sqrt{\frac{\hbar}{2N\tilde{M}\omega_{LO}}}\,F\frac{8\pi Ze^2}{V_{EZ}q}. \end{aligned} \tag{7.52}$$

Here, a kind of reduced mass of the two ions was introduced via

$$\frac{1}{\sqrt{\tilde{M}}}=\frac{1}{\sqrt{M_1}}+\frac{1}{\sqrt{M_2}}. \tag{7.53}$$

In addition, in the last step, the $q$-dependence of the optical dispersion relation was neglected. This results in a $1/q$-dependence of the electron-phonon matrix element, which is typical for the coupling of electrons to optical phonons in ionic crystals. Often, the Hamiltonian operator of the electron-phonon interaction is referred to as the **Fröhlich model** only with this coupling to optical phonons in ionic crystals. In the following, the effective screening factor $F$ is to be determined more precisely. The effective interaction that two electrons experience in the crystal consists of the Coulomb repulsion (screened by all other charges except those of the two charges considered) and the effective interaction mediated by the ions, i.e. by the optical phonons. Therefore, one obtains for the total dielectric constant $\varepsilon_0$

$$\frac{4\pi e^2}{\varepsilon_0 Vq^2}=\frac{4\pi e^2}{\varepsilon_\infty Vq^2}-\frac{2\left|M_{\boldsymbol{q}}\right|^2}{\hbar\omega_{LO}}=\frac{4\pi e^2}{Vq^2}\left(\frac{1}{\varepsilon_\infty}-\frac{16\pi Z^2e^2}{\tilde{M}\omega_{LO}^2V_{EZ}}F^2\right). \tag{7.54}$$

Here, $\varepsilon_\infty$ is the dielectric constant, which results from the screening caused by all other charges (electrons, e.g. in inner shells). For the effective interaction mediated by the phonons, the result of the previous section was used, assuming the same energy for the electrons. From this one obtains for the (heuristically introduced) screening factor $F$, which determines the strength of the Coulomb interaction between the ion and the electron

$$F = \sqrt{\frac{\tilde{M} V_{EZ} \omega_{LO}^2}{16\pi Z^2 e^2}} \sqrt{\frac{1}{\varepsilon_\infty} - \frac{1}{\varepsilon_0}}. \tag{7.55}$$

It follows for the electron-phonon matrix element of the coupling to longitudinal optical phonons in ionic crystals

$$M_{\boldsymbol{q}} = -i\sqrt{2\pi\hbar\omega_{LO}} \frac{e}{\sqrt{V} q} \sqrt{\frac{1}{\varepsilon_\infty} - \frac{1}{\varepsilon_0}}. \tag{7.56}$$

As the symbols already suggest, the screening constants are the static dielectric constant $\varepsilon_0$ and the high-frequency dielectric constant $\varepsilon_\infty$. At low frequencies or in the static case, the screening is caused by all other charges in the crystal, that is, by the ions and all the electrons (in the inner and outer shells). But at high frequencies, the ions can no longer follow the vibration of the field, so only the electronic part of the screening remains. The contribution to the screening of all other charges with the exception of the oscillating ions is therefore described by the high-frequency dielectric constant, the entire screening including the ionic contribution is described at low frequencies by the static dielectric constant. It was already pointed out once before (in the discussion of the Lyddane-Sachs-Teller relation) that

$$\varepsilon_\infty < \varepsilon_0.$$

The advantage of the representation found here is that the electron-phonon matrix element can be expressed by independently measurable quantities. The high-frequency dielectric constant can be determined from optical measurements (refractive index), the static dielectric constant by introducing the crystal into a static electric field (plate capacitor), and the frequency of the longitudinal optical phonon can be determined independently of this.

## 7.5 The Polaron

When a single electron moves in an ionic crystal, it will not behave like a free or a simple band electron, but it will experience a change in its energy due to the coupling to optical phonons. Intuitively, the negatively charged electron at each point of the lattice causes a lattice polarization, thus deflecting the ions from their rest positions, namely the differently charged ions in opposite directions. Thus, the electron generates an optical phonon. On the other hand, a sufficiently slow electron is always influenced by the lattice polarization itself, or in other words, it absorbs the phonon again. So the electron moves with the polarization cloud induced by itself through the ionic crystal, and this elementary excitation electron plus polarization cloud is also called **Polaron**. It is physically intuitive that such a polaron has a significantly increased effective mass compared to the free electron.

In this section, an estimate for the effective mass of the polaron shall be given in the relatively simple case of weak coupling, in which a perturbative treatment is sufficient. The physically more interesting case of strong or moderate coupling requires the application of more specialized methods that go beyond the scope of this textbook. We only consider a single electron with undisturbed eigenenergy $E_0(\boldsymbol{k}) = \frac{\hbar^2 k^2}{2m}$. In the unperturbed ground state, no phonon is excited. The eigenenergy of the electron taking into account the coupling to the optical phonons is then given in 2nd order perturbation theory by:

$$E(\boldsymbol{k}) = E_0(\boldsymbol{k}) + \sum_{\boldsymbol{q}} \frac{|M_{\boldsymbol{q}}|^2}{E_0(\boldsymbol{k}) - E_0(\boldsymbol{k}-\boldsymbol{q}) - \hbar\omega_{LO}}. \tag{7.57}$$

Here, the $q$-dependence of the frequency of the longitudinal optical phonon is neglected again (the optical phonon is therefore treated in Einstein approximation). Therefore it applies:

$$\begin{aligned}\Delta E(\boldsymbol{k}) &= E(\boldsymbol{k}) - E_0(\boldsymbol{k}) \\ &= \sum_{\boldsymbol{q}} \frac{|M_{\boldsymbol{q}}|^2}{E_0(\boldsymbol{k}) - E_0(\boldsymbol{k}-\boldsymbol{q}) - \hbar\omega_{LO}} \\ &= \frac{a^2}{(2\pi)^3} \int \frac{d^3q}{q^2} \frac{1}{-\frac{\hbar^2}{2m}q^2 + \frac{\hbar^2}{2m}2\boldsymbol{kq} - \hbar\omega_{LO}},\end{aligned} \tag{7.58}$$

with

$$a^2 = 2\pi\hbar\omega_{LO}e^2\left(\frac{1}{\varepsilon_\infty} - \frac{1}{\varepsilon_0}\right). \tag{7.59}$$

The further calculation then results in:

$$\begin{aligned}\Delta E(\boldsymbol{k}) &= -\frac{a^2}{4\pi^2}\int dq \int_{-1}^{+1} du \frac{1}{\hbar\omega_{LO} + \frac{\hbar^2}{2m}q^2 - \frac{\hbar^2}{2m}2kqu} \\ &= -\frac{ma^2}{2\pi^2\hbar^2}\int_0^\infty dq \frac{1}{2kq} \ln \frac{\frac{2m}{\hbar}\omega_{LO} + q^2 + 2kq}{\frac{2m}{\hbar}\omega_{LO} + q^2 - 2kq}.\end{aligned} \tag{7.60}$$

Actually, the three-dimensional $q$-integral is to be extended over the first Brillouin zone; in order to be able to evaluate the integral explicitly, however, isotropy was assumed here and the integral was evaluated in spherical coordinates, then the upper integration limit for the $q$-integral is to be shifted to infinity. Furthermore, it is consistent with the assumptions already made to only evaluate the integral for small $k$; the use of a quadratic dispersion for the electron corresponds to the effective mass approximation, which is only valid for small $k$ anyway. Then the integrand can also be expanded according to

$$\ln \frac{1+x}{1-x} = 2\left(x + \frac{1}{3}x^3\right)$$

and one obtains

$$\Delta E(\boldsymbol{k}) = -\frac{ma^2}{2\pi^2\hbar^2}\int_0^\infty dq \frac{1}{2kq} 2\left(\frac{2kq}{\frac{2m}{\hbar}\omega_{LO} + q^2} + \frac{1}{3}\frac{(2kq)^3}{\left(\frac{2m}{\hbar}\omega_{LO} + q^2\right)^3}\right). \tag{7.61}$$

Using the elementary integrals

$$\int_0^\infty \frac{dx}{x^2+\gamma} = \frac{\pi}{2\sqrt{\gamma}}, \quad \int_0^\infty \frac{x^2 dx}{(x^2+\gamma)^3} = \frac{\pi}{16\gamma^{3/2}} \tag{7.62}$$

one obtains

$$\Delta E(\boldsymbol{k}) = -\frac{ma^2}{\pi^2\hbar^2}\frac{\pi}{2\sqrt{\frac{2m}{\hbar}\omega_{LO}}} - \frac{4}{3}k^2 \frac{\pi}{16\left(\frac{2m}{\hbar}\omega_{LO}\right)^{3/2}}\frac{ma^2}{\pi^2\hbar^2}. \tag{7.63}$$

Inserting the constants $a^2$ from (7.59) finally leads to

$$E(\boldsymbol{k}) = -\hbar\omega_{LO}\alpha + \frac{\hbar^2 k^2}{2m}\left(1 - \frac{\alpha}{6}\right) \tag{7.64}$$

with the dimensionless constant

$$\alpha = \frac{e^2}{2\hbar\omega_{LO}}\sqrt{\frac{2m\omega_{LO}}{\hbar}}\left(\frac{1}{\varepsilon_\infty} - \frac{1}{\varepsilon_0}\right). \tag{7.65}$$

$\alpha$ is essentially the appropriately dimensionless electron-phonon coupling matrix element and plays the role of a coupling constant. The perturbation calculation carried out here is only valid in the range $|\alpha| \ll 1$(case of weak coupling). Corrections to the above result can be classified according to powers of $\alpha$. In the case of strong coupling ($|\alpha| \gg 1$), which, for example, is the case for most alkali halide crystals, perturbation calculations with respect to $\alpha$ are no longer applicable and other theoretical methods (functional integrals, variational approaches, etc.) must be used.

From the above result of the perturbation theory, one can see the influence of the coupling to the longitudinal optical phonon in two ways. On the one hand, there is a constant energy shift $-\hbar\omega_{LO}\alpha$, i.e. the eigenvalue spectrum is shifted downwards compared to the free electrons without coupling to phonons. Around this minimum, one again has to deal with an excitation spectrum of quasi-free particles, as can be seen from the $k^2$-dispersion, but the excitations have a different effective mass

$$m^* = \frac{m}{1 - \frac{\alpha}{6}} \sim m\left(1 + \frac{\alpha}{6}\right), \tag{7.66}$$

compared to the quasi-free electrons, which is consistent with the results obtained previously, which are all only valid in linear order in α in perturbation theory. The electron plus the polarization cloud surrounding it thus form a new type of elementary excitation, namely the polaron, which can move as a quasi-free particle in an ionic crystal, and the electron plus polarization must have a different (larger) effective mass than the free electron. There are formal analogies to quantum electrodynamics here, where electrons are to be considered with the photon "cloud" surrounding it.

To better understand the meaning of the parameter α, one can also calculate the average number of phonons involved in a polaron. In the ground state, no phonon should be excited, so without electron-phonon coupling, the average number of phonons would be 0. Now one can also determine the eigenstate approximately according to the relation known from quantum mechanics

$$\left|\tilde{\Phi}_0\right\rangle = |\Phi_0\rangle + \sum_{l \neq 0} \frac{|\Phi_l\rangle\langle\Phi_l|H_{ep}|\Phi_0\rangle}{E_0 - E_l}. \tag{7.67}$$

Here $|\Phi_0\rangle = |\boldsymbol{k}\rangle_{el}|0\rangle_{ph}$ is the unperturbed state with an electron in the state $\boldsymbol{k}$ and phonon vacuum and it is to be summed over all states $|\Phi_l\rangle = |\boldsymbol{k} - \boldsymbol{q}\rangle_{el}|\boldsymbol{q}\rangle_{ph}$ with electron in the state $\boldsymbol{k} - \boldsymbol{q}$ and a phonon in the state $\boldsymbol{q}$ excited. Therefore

$$E_0 - E_l = E_0(\boldsymbol{k}) - E_0(\boldsymbol{k} - \boldsymbol{q}) - \hbar\omega_{LO}. \tag{7.68}$$

The mean number of phonons is given by

$$\langle N_{ph}\rangle = \left\langle \tilde{\Phi}_0 \middle| \sum_{\boldsymbol{q}} b^\dagger_{\boldsymbol{q}} b_{\boldsymbol{q}} \middle| \tilde{\Phi}_0 \right\rangle. \tag{7.69}$$

With respect to the unperturbed state $|\Phi_0\rangle$, the expectation value of the phonon occupation numbers is 0. Therefore

$$\langle N_{ph}\rangle = \sum_{\boldsymbol{q}} \frac{\left|M_{\boldsymbol{q}}\right|^2}{\left[E_0(\boldsymbol{k}) - E_0(\boldsymbol{k} - \boldsymbol{q}) - \hbar\omega_0\right]^2}. \tag{7.70}$$

This results in $q$-integrals of similar type as in the calculation of the energy eigenvalue in 2nd order perturbation theory. The result is quite simple, namely

$$\langle N_{ph}\rangle = \frac{\alpha}{2}. \tag{7.71}$$

The mean number of phonons accompanying a slow electron in an ionic crystal and thus belonging to the composite quasiparticle "polaron" is therefore just $\alpha/2$ . This derivation, like the above calculation of the polaron dispersion, only applies in the limit of weak coupling, that is, small α.

## 7.6 Problems for Chap. 7

**Problem 7.1** ***Fermion-Boson-Model***

The simplest model containing a coupling between a fermion (electron) and a boson (phonon) of the type (7.13) is given by:

$$H = \varepsilon c^\dagger c + M\big(b^\dagger + b\big)c^\dagger c + \omega b^\dagger b$$

where $c(^\dagger)$ are Fermion and $b(^\dagger)$ Boson-creator or -annihilator . The Hilbert space (Fock space) is in occupation number representation spanned by the states $|n_f, n_b\rangle$ , with $n_f \in \{0,1\}$ the fermion occupation number and $n_b \in \{0,1,2,\ldots\}$ the boson occupation number. The Fock space apparently decomposes into a subspace to $n_f = 0$ and one to $n_f = 1$.

a) Give the matrix representation of $H$ with respect to $|n_f, n_b\rangle$ in the two subspaces to $n_f = 0, 1$ explicitly.

b) Diagonalize $H$ analytically by "quadratic complement", i.e. bring $H$ into the form

$$H = \tilde{\varepsilon} c^\dagger c + \omega \tilde{b}^\dagger \tilde{b}.$$

Determine $\tilde{\varepsilon}$ and $\tilde{b}$, show that $\tilde{b}(^\dagger)$ still fulfill Bose commutation rules and give the energy eigenvalues explicitly.

c) Diagonalize the Hamilton matrix from a) on the subspace to $n_f = 1$ numerically by introducing an artificial cut-off Bose occupation number $n_{bmax}$. Compare the numerical and the analytical result for different $n_{bmax}$.

d) Determine the fermionic one – particle Green function numerically

$$G_c(z) = \frac{1}{\mathcal{Z}} \sum_{n,m} \frac{\langle n|c|m\rangle \langle m|c^\dagger|n\rangle}{z + E_n - E_m} \left(e^{-\beta(E_n - N(n)\mu)} + e^{-\beta(E_m - N(m)\mu)}\right)$$

where $\mathcal{Z} = \sum_n e^{-\beta(E_n - N(n)\mu)}$

is the grand canonical partition function, $|n\rangle$ the (many-particle) eigenstates, $\beta = 1/k_B T$ the inverse temperature and $z = E + i\delta$ a (complex) energy (frequency) . Plot the fermionic spectral function

$$\rho_c(E) = -\frac{1}{\pi} \mathrm{Im} G_c(E + i0)$$

as a function of energy $E$.

**Problem 7.2** ***Jaynes-Cummings model***
Consider the following model containing a fermion-boson coupling

$$H = \varepsilon_1 c_1^\dagger c_1 + \varepsilon_2 c_2^\dagger c_2 + \omega b^\dagger b + M\left(b^\dagger c_1^\dagger c_2 + b c_2^\dagger c_1\right).$$

The model contains 2 fermionic states 1,2 and one bosonic degree of freedom and ( for example for $\varepsilon_1 < \varepsilon_2$ ) describes transitions from 2 to 1 under emission of a boson (for example, a photon) and vice versa transitions from 1 to 2 under absorption of a boson . It thus only contains resonant contributions with respect to the fermionic transitions and no coupling of the bosons to the fermion density (diagonal terms $c_i^\dagger c_i$).

a) Determine the energy eigenvalues and -eigenstates exactly.
*Note*: A suitable basis is of course again given in occupation number representation through $|n_1, n_2, n\rangle$ with $n_i \in \{0, 1\}, n \in N$. Convince yourself that only the states $|1, 0, n+1\rangle$ and $|0, 1, n\rangle$ couple to each other, so that only a $2 * 2$-matrix has to be diagonalized.

b) Determine (as in the previous problem 7.1) the fermionic one – particle Green function $G_{c_1}(z)$ and the resulting spectral function $\rho_{c_1}(E) = -\frac{1}{\pi}\mathrm{Im}G_{c_1}(E + i0)$ analytically and numerically.

**Problem 7.3** ***2-fermion-boson model***
In a slight generalization of the problems 7.1 and 7.2 we now consider the following 2-fermion model coupled to a boson (optical phonon, etc.), i.e. the model

$$H = \sum_{i=1}^{2} \varepsilon_i c_i^\dagger c_i + \omega b^\dagger b + M_1\left(b + b^\dagger\right) \sum_i c_i^\dagger c_i$$
$$+ M_2\left(c_1^\dagger c_2 + c_2^\dagger c_1\right)\left(b + b^\dagger\right).$$

Calculate the fermionic spectral function $\rho_{c_1}(E) = -\frac{1}{\pi}\mathrm{Im}G_{c_1}(E + i0)$ for different temperatures, phonon frequencies ω and electron-phonon coupling matrix elements $M_{1,2}$ numerically and plot it.

# Solutions to the Exercise Problems

# 8

## 8.1 Solution of the Problems for Chap. 2

**Problem 2.1, Sphere Packing in Crystal Structures**

- **simple cubic (sc)**
  Distance to the nearest neighbor sites: $a$, maximum sphere radius $\frac{a}{2}$
  Volume of the atomic sphere: $V_A = \frac{4\pi}{3}\left(\frac{a}{2}\right)^3 = \frac{\pi a^3}{6}$
  1 atom per conventional unit cell
  $\rightarrow$ packing ratio $p_{\text{sc}} = \frac{V_A}{V_E} = \frac{\pi}{6} = 0.524$
- **face-centered cubic (fcc)**
  Distance to nearest neighbor sites: $\frac{a}{\sqrt{2}}$, maximum sphere radius $\frac{a}{2\sqrt{2}}$
  Volume of atomic sphere: $V_A = \frac{4\pi}{3}\left(\frac{a}{2\sqrt{2}}\right)^3 = \frac{\pi a^3}{12\sqrt{2}}$
  4 atoms per conventional unit cell have volume $4V_A = \frac{\pi a^3}{3\sqrt{2}}$
  $\rightarrow$ packing ratio $p_{\text{fcc}} = \frac{\pi}{3\sqrt{2}} = 0.740$
- **body-centered cubic (bcc)**
  Distance to nearest neighbor sites: $\frac{a\sqrt{3}}{2}$, maximum sphere radius $\frac{a\sqrt{3}}{4}$
  Volume of atomic sphere: $V_A = \frac{4\pi}{3}\left(\frac{a\sqrt{3}}{4}\right)^3 = \frac{\pi\sqrt{3}}{16}a^3$
  2 atoms per conventional unit cell have volume $2V_A = \frac{\pi\sqrt{3}a^3}{8}$
  $\rightarrow$ packing ratio $p_{\text{bcc}} = \frac{\pi\sqrt{3}}{8} = 0.680$
- **hexagonal closest packed (hcp)**
  Distance to next nearest neighbors: $a$, maximum sphere radius $\frac{a}{2}$,
  Volume of atomic sphere: $V_A = \frac{4\pi}{3}\left(\frac{a}{2}\right)^3 = \frac{\pi a^3}{6}$

© The Author(s), under exclusive license to Springer-Verlag GmbH, DE, part of Springer Nature 2023

G. Czycholl, *Solid State Theory, Volume 1*,
https://doi.org/10.1007/978-3-662-66135-2_8

2 atoms per conventional unit cell have volume $2V_A = \frac{\pi a^3}{3}$

Volume of conventional unit cell $V_{EZ} = a\frac{\sqrt{3}}{2}a\sqrt{\frac{8}{3}}a = \sqrt{2}a^3$

$\rightarrow$ packing ratio $p_{\text{hcp}} = \frac{2V_A}{V_{EZ}} = \frac{\pi}{3\sqrt{2}} = 0.740$

## Problem 2.2, Direct and Reciprocal Lattice

a) According to (2.1), (2.2) it holds:

$$\boldsymbol{b}_1 = \frac{2\pi}{V_{pEZ}}(\boldsymbol{a}_2 \times \boldsymbol{a_3}), \boldsymbol{b}_2 = \frac{2\pi}{V_{pEZ}}(\boldsymbol{a}_3 \times \boldsymbol{a_1}), \boldsymbol{b}_3 = \frac{2\pi}{V_{pEZ}}(\boldsymbol{a}_1 \times \boldsymbol{a_2})$$

$$\text{where} \quad V_{pEZ} = |\boldsymbol{a}_1 \cdot (\boldsymbol{a}_2 \times \boldsymbol{a}_3)|,$$

and for the volume of the unit cell of the reciprocal lattice it holds according to (2.6):

$$V_{rEZ} = |\boldsymbol{b}_1 \cdot (\boldsymbol{b}_2 \times \boldsymbol{b}_3)| = \frac{(2\pi)^3}{V_{pEZ}}.$$

Then it holds for the reciprocal lattice of the reciprocal lattice:

$$\boldsymbol{c}_3 = \frac{2\pi}{V_{rEZ}}(\boldsymbol{b}_1 \times \boldsymbol{b}_2) = \frac{V_{pEZ}}{(2\pi)^2}\frac{(2\pi)^2}{V_{pEZ}^2}((\boldsymbol{a}_2 \times \boldsymbol{a_3}) \times (\boldsymbol{a}_3 \times \boldsymbol{a}_1))$$

$$\frac{1}{V_{pEZ}}\left[\boldsymbol{a}_3((\boldsymbol{a}_2 \times \boldsymbol{a}_3)\boldsymbol{a}_1) - \boldsymbol{a}_1 \underbrace{((\boldsymbol{a}_2 \times \boldsymbol{a}_3)\boldsymbol{a}_3)}_{=0}\right]$$

$$= \frac{1}{V_{pEZ}} \underbrace{(\boldsymbol{a}_1(\boldsymbol{a}_2 \times \boldsymbol{a}_3))}_{=V_{pEZ}} \boldsymbol{a}_3 = \boldsymbol{a}_3.$$

So the reciprocal lattice vector $\boldsymbol{c}_3$ of the reciprocal lattice coincides with the original lattice vector $\boldsymbol{a}_3$ of the real lattice, analogously it follows $\boldsymbol{c}_1 = \boldsymbol{a}_1$, $\boldsymbol{c}_2 = \boldsymbol{a}_2$.

b) Choose the vectors

$$\boldsymbol{a}_1 = \frac{a}{2}\begin{pmatrix}1\\1\\0\end{pmatrix} \quad \boldsymbol{a}_2 = \frac{a}{2}\begin{pmatrix}0\\1\\1\end{pmatrix} \quad \boldsymbol{a}_3 = \frac{a}{2}\begin{pmatrix}1\\0\\1\end{pmatrix}.$$

that span the primitive unit cell of the fcc lattice. Note: The numbering is different from that in Sect. 2.1.4, namely chosen so that

$$\boldsymbol{a}_1 \cdot (\boldsymbol{a}_2 \times \boldsymbol{a}_3) = \frac{a^3}{8}\det\begin{pmatrix}1&0&1\\1&1&0\\0&1&1\end{pmatrix} = \frac{a^3}{4}$$

is positive. Then

$$\boldsymbol{b}_1 = \frac{2\pi}{V_{pEZ}}(\boldsymbol{a}_2 \times \boldsymbol{a}_3) = \frac{8\pi}{a^3}\frac{a^2}{4}\begin{pmatrix} 0 \\ 1 \\ 1 \end{pmatrix} \times \begin{pmatrix} 1 \\ 0 \\ 1 \end{pmatrix} = \frac{2\pi}{a}\begin{pmatrix} 1 \\ 1 \\ -1 \end{pmatrix}$$

$$\boldsymbol{b}_2 = \frac{2\pi}{V_{pEZ}}(\boldsymbol{a}_3 \times \boldsymbol{a}_1) = \frac{8\pi}{a^3}\frac{a^2}{4}\begin{pmatrix} 1 \\ 0 \\ 1 \end{pmatrix} \times \begin{pmatrix} 1 \\ 1 \\ 0 \end{pmatrix} = \frac{2\pi}{a}\begin{pmatrix} -1 \\ 1 \\ 1 \end{pmatrix}$$

$$\boldsymbol{b}_3 = \frac{2\pi}{V_{pEZ}}(\boldsymbol{a}_1 \times \boldsymbol{a}_2) = \frac{8\pi}{a^3}\frac{a^2}{4}\begin{pmatrix} 1 \\ 1 \\ 0 \end{pmatrix} \times \begin{pmatrix} 0 \\ 1 \\ 1 \end{pmatrix} = \frac{2\pi}{a}\begin{pmatrix} 1 \\ -1 \\ 1 \end{pmatrix}.$$

The vectors $\boldsymbol{b}_1, \boldsymbol{b}_2, \boldsymbol{b}_3$ just span a possible primitive unit cell of a bcc lattice with volume

$$V_{rEZ} = \boldsymbol{b}_1(\boldsymbol{b}_2 \times \boldsymbol{b}_3) = \frac{(2\pi)^3}{a^3}\det\begin{pmatrix} 1 & -1 & 1 \\ 1 & 1 & -1 \\ -1 & 1 & 1 \end{pmatrix} = 4\frac{(2\pi)^3}{a^3} = \frac{(2\pi)^3}{V_{pEZ}}.$$

So the reciprocal lattice of the fcc lattice is a bcc lattice. The converse follows from a).

### Problem 2.3, Centered Rectangular Lattice

If the conventional unit cell is a rectangle with edge lengths $a$ and $b$, the primitive unit cell of the centered rectangular lattice is spanned by

$$\boldsymbol{a}_1 = \begin{pmatrix} a \\ 0 \end{pmatrix} \quad \boldsymbol{a}_2 = \begin{pmatrix} \frac{a}{2} \\ \frac{b}{2} \end{pmatrix}.$$

The "volume" of the primitive unit cell is

$$V_{pEZ} = |\boldsymbol{a}_1 \times \boldsymbol{a}_2| = \frac{ab}{2}.$$

The associated reciprocal lattice is spanned by

$$\boldsymbol{b}_1 = \frac{2\pi}{V_{pEZ}}\begin{pmatrix} -\frac{b}{2} \\ \frac{a}{2} \end{pmatrix} = 2\pi\begin{pmatrix} -\frac{1}{a} \\ \frac{1}{b} \end{pmatrix}$$

$$\boldsymbol{b}_2 = \frac{2\pi}{V_{pEZ}}\begin{pmatrix} 0 \\ a \end{pmatrix} = 4\pi\begin{pmatrix} 0 \\ \frac{1}{b} \end{pmatrix}$$

because it is obviously fulfilled:

$$\boldsymbol{a}_1 \cdot \boldsymbol{b}_1 = \boldsymbol{a}_2 \cdot \boldsymbol{b}_2 = 2\pi, \quad \boldsymbol{a}_1 \cdot \boldsymbol{b}_2 = \boldsymbol{a}_2 \cdot \boldsymbol{b}_1 = 0.$$

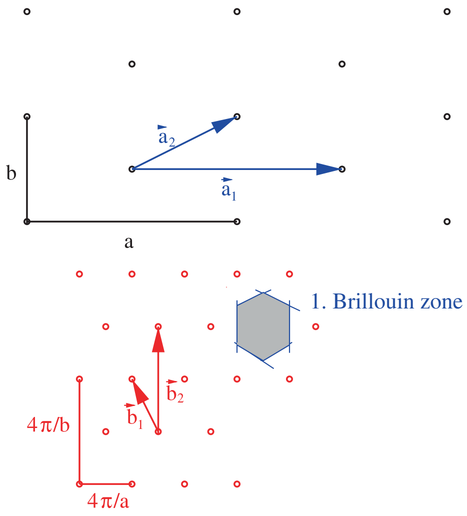

## Problem 2.4, Crystal Structure of $La_2CuO_4$

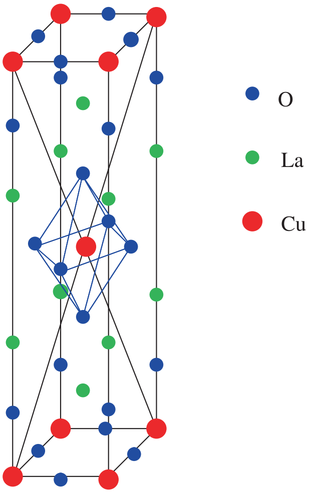

As can be seen from the formulation of the problem you have 4 lanthanum, 8 oxygen and 2 copper ions, so 2 formula units of $La_2CuO_4$ per conventional elementary cell. This is also evident from the plot: The 8 Cu ions in the corners of the tetrahedron each belong to 8 unit cells and therefore contribute with the factor $\frac{1}{8}$ to the elementary cell under consideration, the one Cu ion in the center, however, belongs only to this cell, so there are $1 + 8 * \frac{1}{8} = 2$ Cu ions, of the 22 oxygen ions shown, 16 are on edges and therefore contribute with the factor $\frac{1}{4}$, 4 on faces and therefore contribute with the factor $\frac{1}{2}$, and 2 belong only to the elementary cell shown, so $16 * \frac{1}{4} + 4 * \frac{1}{2} + 2 = 8$ oxygen ions per elementary cell, and there are 8 La ions on edges and 2 completely within the cell, so $8 * \frac{1}{4} + 2 = 4$ La ions. This gives 1 formula unit per primitive elementary cell.

The octahedron ("cage") of 6 oxygen ions around each Cu is evident from the sketch, as is the formation of $CuO_2$ layers. These form a square lattice with lattice constant $a = 3.8$ Å and a basis consisting of a Cu ion at (0,0) and 2 oxygen ions at $\left(\frac{1}{2}, 0\right)$ and $\left(0, \frac{1}{2}\right)$.

**Problem 2.5, Wurtzite Structure**
In the Wurtzite structure both the A atoms and the B atoms form an hcp structure.

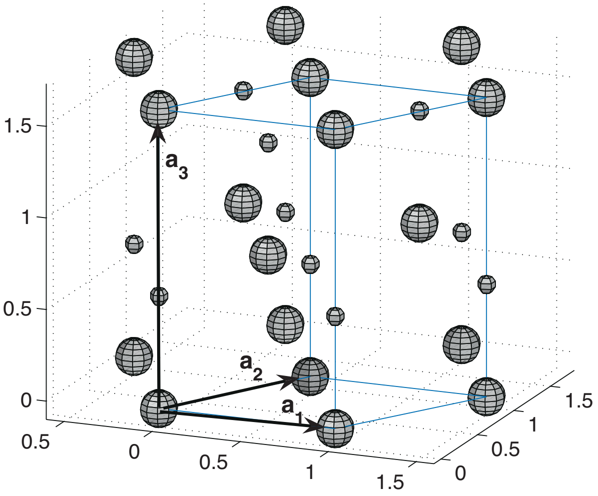

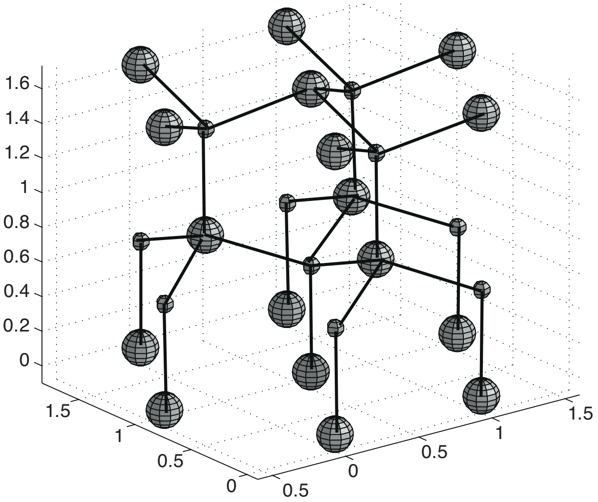

So there is a hexagonal lattice. If you choose the unit vectors spanning the conventional unit cell $\boldsymbol{a}_1, \boldsymbol{a}_2, \boldsymbol{a}_3$ as in the sketch above (note: unlike in the figure in the text in Sect. 2.1.5), then the basis consists of 2 A atoms at $\boldsymbol{R}_1 = 0$ and $\boldsymbol{R}_2 = \frac{1}{3}\boldsymbol{a}_1 + \frac{1}{3}\boldsymbol{a}_2 + \frac{1}{2}\boldsymbol{a}_3$ and 2 B atoms at $\boldsymbol{R}_3 = b\boldsymbol{a}_3$ and $\boldsymbol{R}_4 = \frac{1}{3}\boldsymbol{a}_1 + \frac{1}{3}\boldsymbol{a}_2 + \left(b + \frac{1}{2}\right)\boldsymbol{a}_3$. If $|\boldsymbol{a}_1| = |\boldsymbol{a}_2| = a$, then for the hcp structure $|\boldsymbol{a}_3| = \sqrt{\frac{8}{3}}a$ and $b = \frac{3}{8}$. Then both the A atoms and the B atoms each form an hcp structure, which are shifted from each other by $b\boldsymbol{a}_3$. The distances between an A atom and the 4 neighboring B atoms are always exactly $b|\boldsymbol{a}_3| = \frac{3}{8}\sqrt{\frac{8}{3}}a = \sqrt{\frac{3}{8}}a$, so tetrahedral structures are formed. This is easily calculated, for example, by using a Cartesian coordinate system and setting $a = 1$. Then you have

$$\boldsymbol{a}_1 = (1,0,0),\ \boldsymbol{a}_2 = \left(\frac{1}{2}, \frac{\sqrt{3}}{2}, 0\right),\ \boldsymbol{a}_3 = \left(0, 0, \sqrt{\frac{8}{3}}\right)$$

$$\boldsymbol{R}_1 = (0,0,0),\ \boldsymbol{R}_2 = \left(\frac{1}{2}, \frac{\sqrt{3}}{6}, \frac{1}{2}\sqrt{\frac{8}{3}}\right),\ \boldsymbol{R}_3 = \left(0, 0, \sqrt{\frac{3}{8}}\right),$$

$$\boldsymbol{R}_4 = \left(\frac{1}{2}, \frac{\sqrt{3}}{6}, \sqrt{\frac{2}{3}} + \sqrt{\frac{3}{8}}\right).$$

Then it follows: $|\boldsymbol{R}_3| = |\boldsymbol{R}_2 - \boldsymbol{R}_3| = |\boldsymbol{R}_3 + \boldsymbol{a}_2 - \boldsymbol{R}_2| = |\boldsymbol{R}_3 + \boldsymbol{a}_1 - \boldsymbol{R}_2| = \sqrt{\frac{3}{8}}$ etc.

## 8.2 Solution to Exercise Problems for Chap. 3

**Problem 3.1, Born-Oppenheimer Approximation**

a) With $x_1 = \frac{\tilde{x}_1}{\sqrt{M}}, p_1 = \sqrt{M}\tilde{p}_1, x_2 = \frac{\tilde{x}_2}{\sqrt{m}}, p_2 = \sqrt{m}\tilde{p}_2,\ \tilde{x}_i, \tilde{p}_i$ are still canonically conjugate to each other and it holds:

$$\begin{aligned} H &= \frac{p_1^2}{2M} + \frac{p_2^2}{2m} + \frac{K}{2}x_1^2 + \frac{k}{2}(x_1 - x_2)^2 \\ &= \frac{1}{2}\left(\tilde{p}_1^2 + \tilde{p}_2^2 + \frac{K}{M}\tilde{x}_1^2 + \frac{k}{M}\tilde{x}_1^2 - 2\frac{k}{\sqrt{Mm}}\tilde{x}_1\tilde{x}_2 + \frac{k}{m}\tilde{x}_2^2\right) \\ &= \frac{1}{2}\left(\underline{\boldsymbol{p}}^t\ \underline{\underline{\mathbf{1}}}\ \underline{\boldsymbol{p}} + \underline{\boldsymbol{x}}^t\ \underline{\underline{\Omega}}\ \underline{\boldsymbol{x}}\right) \end{aligned}$$

with

$$\underline{\boldsymbol{x}} = \begin{pmatrix} \tilde{x}_2 \\ \tilde{x}_2 \end{pmatrix},\ \underline{\boldsymbol{p}} = \begin{pmatrix} \tilde{p}_1 \\ \tilde{p}_2 \end{pmatrix},\ \underline{\underline{\Omega}} = \begin{pmatrix} \frac{K+k}{M} & -\frac{k}{\sqrt{Mm}} \\ -\frac{k}{\sqrt{mM}} & \frac{k}{m} \end{pmatrix}.$$

Diagonalization of $\underline{\underline{\Omega}}$ yields the eigenfrequencies of these coupled harmonic oscillators:

$$\det\left(\underline{\underline{\Omega}} \;-\; \omega^2\,\underline{\underline{\mathbf{1}}}\right) = \det\begin{pmatrix} \frac{K+k}{M} - \omega^2 & -\frac{k}{\sqrt{Mm}} \\ -\frac{k}{\sqrt{mM}} & \frac{k}{m} - \omega^2 \end{pmatrix} = 0.$$

This results in

$$\omega_{1,2}^2 = \frac{1}{2}\left(\frac{K+k}{M} + \frac{k}{m}\right) \pm \sqrt{\frac{1}{4}\left(\frac{K+k}{M} - \frac{k}{m}\right)^2 + \frac{k^2}{Mm}}.$$

After diagonalization, these are decoupled harmonic oscillators. The eigenenergies are therefore

$$E_{n_1 n_2} = \hbar\omega_1\left(n_1 + \frac{1}{2}\right) + \hbar\omega_2\left(n_2 + \frac{1}{2}\right)$$

with integer $n_1, n_2$.

b) In the Born-Oppenheimer approximation, one first solves the “electronic” problem

$$\frac{p_2^2}{2m} + \frac{K}{2}x_1^2 + \frac{k}{2}(x_1 - x_2)^2 = \frac{p_2^2}{2m} + \frac{k}{2}\bar{x}_2^2 + \frac{K}{2}x_1^2$$

with $\bar{x}_2 = x_2 - x_1$, which is also conjugate to $p_2$ for fixed “atomic” (or nucleus) position $x_1$. This is obviously a single harmonic oscillator with (for fixed $x_1$) constant additional potential $\frac{K}{2}x_1^2$. The eigenenergies therefore result in:

$$\varepsilon_{n_1}(x_1) = \hbar\sqrt{\frac{k}{m}}\left(n_1 + \frac{1}{2}\right) + \frac{K}{2}x_1^2.$$

These “electronic” eigenenergies form the effective potential for the “nucleus” dynamics. So one has to determine the eigenvalues of the effective Hamiltonian operator

$$\frac{p_1^2}{2M} + \varepsilon_{n_1}(x_1) = \frac{p_1^2}{2M} + \frac{K}{2}x_1^2 + \hbar\sqrt{\frac{k}{m}}\left(n_1 + \frac{1}{2}\right)$$

This is again a single harmonic oscillator with a constant additional term for each “electronic” quantum number $n_1$. The eigenvalues therefore result in:

$$E_{n_1 n_2} = \hbar\sqrt{\frac{K}{M}}\left(n_2 + \frac{1}{2}\right) + \hbar\sqrt{\frac{k}{m}}\left(n_1 + \frac{1}{2}\right)$$

with integer $n_1, n_2$.

c) Expansion of the exact eigenfrequencies from a) with respect to the small parameter $\frac{m}{M}$ yields

$$\begin{aligned}\omega_{1,2}^2 &= \frac{1}{2}\left(\frac{K+k}{M}+\frac{k}{m}\right) \pm \sqrt{\frac{1}{4}\left(\frac{K+k}{M}-\frac{k}{m}\right)^2+\frac{k^2}{Mm}} \\ &= \frac{1}{2}\left(\frac{K+k}{M}+\frac{k}{m}\right) \pm \frac{1}{2}\frac{k}{m}\sqrt{\left(1-\frac{k+K}{k}\frac{m}{M}\right)^2+4\frac{m}{M}} \\ &= \frac{1}{2}\left(\frac{K+k}{M}+\frac{k}{m} \pm \frac{k}{m}\left(1-\frac{K+k}{k}\frac{m}{M}+2\frac{m}{M}\right)\right).\end{aligned}$$

This yields in lowest order:

$$\omega_1^2 = \frac{k}{m}+\frac{k}{M} = \frac{k}{m}\left(1+\frac{m}{M}\right),\ \omega_2^2 = \frac{K}{M}$$

and thus for the eigenenergies

$$E_{n_1 n_2} = \hbar\sqrt{\frac{k}{m}}\left(n_1+\frac{1}{2}\right)+\hbar\sqrt{\frac{K}{M}}\left(n_2+\frac{1}{2}\right).$$

Physical interpretation: "thick" oscillator oscillates for itself without feeling small oscillator, small oscillator oscillates relatively to "thick" as if this were at rest, i.e. decoupled harmonic oscillators.

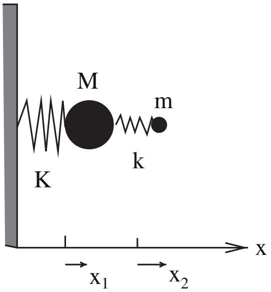

### Problem 3.2, 1-Dimensional "Hydrogen Molecule Ion"

a) If you multiply the equation

$$-\frac{1}{2}\psi''(\tilde{x}) - \left(\frac{1}{|\tilde{x}-\tilde{a}|+\tilde{\delta}}+\frac{1}{|\tilde{x}+\tilde{a}|+\tilde{\delta}}\right)\psi(\tilde{x}) = \tilde{E}\psi(\tilde{x})$$

with $e^2/a_0 = me^4/\hbar^2 = \hbar^2/(ma_0^2)$, the equation

$$-\frac{\hbar^2}{2m}\frac{d^2}{dx^2}\psi(x) - \left(\frac{e^2}{|x-a|+\delta}+\frac{e^2}{|x+a|+\delta}\right)\psi(x) = E\psi(x).$$

apparently results again.

b) After discretization $x_i = a + (i-1) * h$, the 2nd derivative has to be replaced by

$$\psi''(x_i) \to \frac{\psi(x_{i+1}) + \psi(x_{i-1}) - 2\psi(x_i)}{h^2}.$$

Then the given difference equation results after multiplication with $2h^2$ for $h = 0.1$.

c) The eigenvalue problem for the given matrix $\underline{\underline{A}}$

$$\underline{\underline{A}}\,\underline{a} = E_w \underline{a}$$

results in the $i$-th line $(1 < i < 201)$:

$$-a_{i-1} + h_i * a_i - a_{i+1} = E_w a_i,$$

which, with the given $h_i$ and $a_i = \psi(x_i)$, apparently corresponds to the difference equation from b). So that the matrix $\underline{\underline{A}}$ is tridiagonal, the boundary condition $\psi(x_0) = \psi(-10.1) = \psi(x_{202}) = \psi(10.1) = 0$ must apparently be assumed.

d) A Matlab source code for numerical diagonalization is given below:

```
clear all;delta=0.1;
for ia=1:70
     af(ia)=ia*0.1;
     a=af(ia);
     x=[-10:.1:10];
     for i=1:201
          v(i)=1/(abs(x(i)-a)+delta)+1/(abs(x(i)+a)+delta);
     end
     h=zeros(201,201);
     for i=1:201
          h(i,i)=2*(1-v(i)*0.01);
          if i <201 h(i,i+1)=-1;h(i+1,i)=-1;end
     end
     [ev,ew]=eig(h);
     for i=1:4
          en(i)=ew(i,i)/0.02;
     end
     energ(1,ia)=en(1);energ(2,ia)=en(2);
     veff(1,ia)=energ(1,ia)+1/(2*a+delta);
     veff(2,ia)=energ(2,ia)+1/(2*a+delta);
end
figure(1); plot(2*af,energ(1,:),2*af,energ(2,:))
figure(2); plot(2*af,veff(1,:),2*af,veff(2,:))
```

For $a = 1$ (i.e. nucleus distance 2) the 4 lowest eigenvalues result:
$E_1 = -3.5422$, $E_2 = -3.3142$, $E_3 = -0.7186$, $E_4 = -0.5186$. The potential curve and the eigenstates are shown in the following two figures:

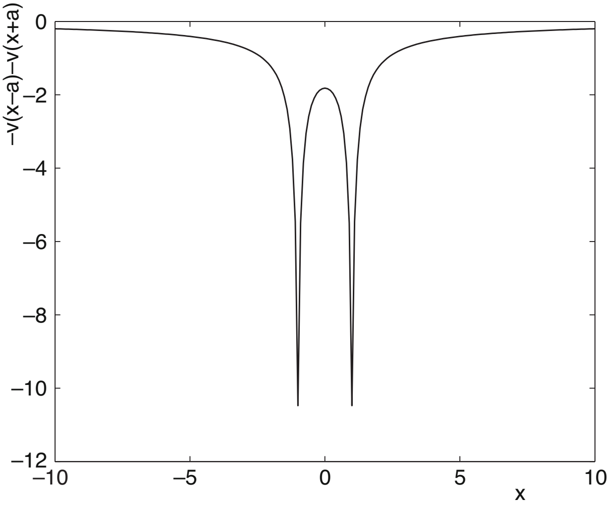

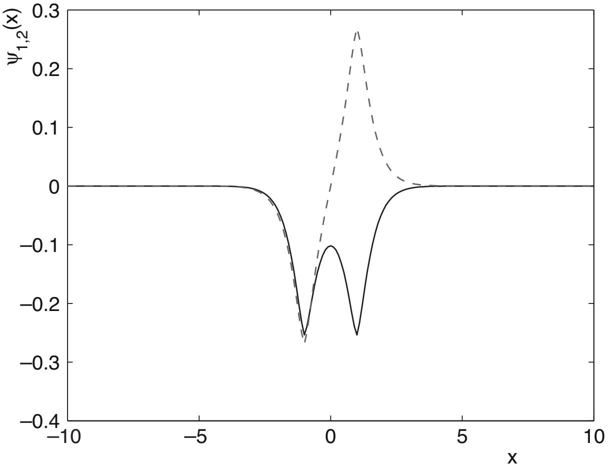

The lowest ("bonding") state is symmetrical, which results in a high probability of electrons in this state in the middle between the two atomic nuclei. The 2nd ("antibonding") state is antisymmetrical, the probability of residence therefore has a zero point exactly between the atomic nuclei.

For $a = 7$ (i.e. atomic distance 14) the lowest 4 eigenvalues result:
$E_1 = -3.0101$, $E_2 = -3.0101$, $E_3 = -0.4354$, $E_4 = -0.4328$.

The 1st and 2nd eigenvalues are therefore degenerate (within the numerical accuracy), the 3rd and 4th are almost degenerate.
The following two figures show the potential course and the lowest eigenstates again.

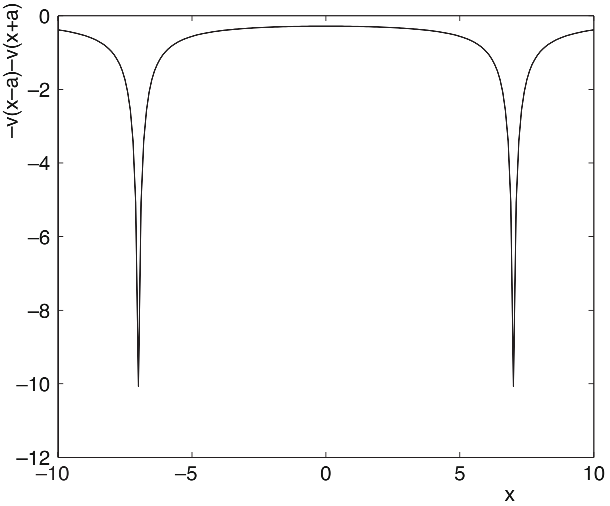

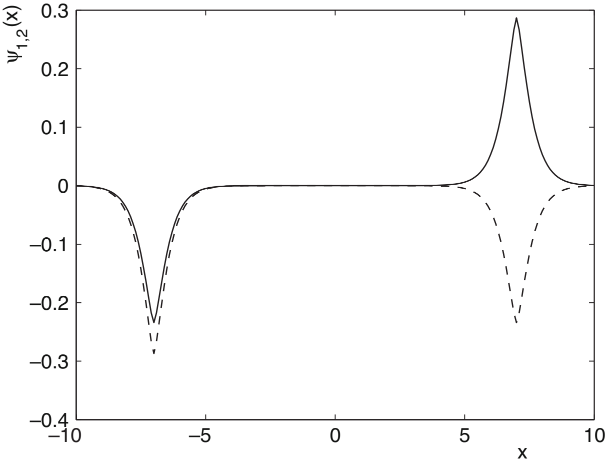

The two lowest (degenerate) states now correspond to the eigenstates of the separated atoms; of course, any linear combination of these two states is again an eigenstate.

e) The following figure shows the dependence of the lowest 2 eigenvalues on the distance of the two atoms.

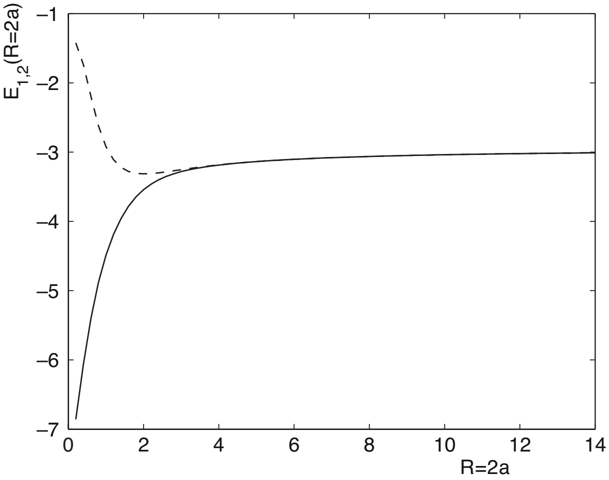

Obviously, the two eigenvalues are identical for large $a$; then one has two separated identical atoms with the same eigenvalue, that is, 2 degenerate states. With decreasing $a$, these states split into a “bonding” (binding) state, whose energy is lower than the eigenenergy of the single atom, and an “antibonding” state with increased energy compared to the free atom. The splitting becomes larger with decreasing $a$.

f) If one now adds the Coulomb repulsion of the nuclei (which in the present one-electron problem is the only contribution that counteracts a too close approaching of the two ions), then the course of the binding energy, which according to the Born-Oppenheimer approximation represents the effective interaction potential between the two nuclei, results in the following figure:

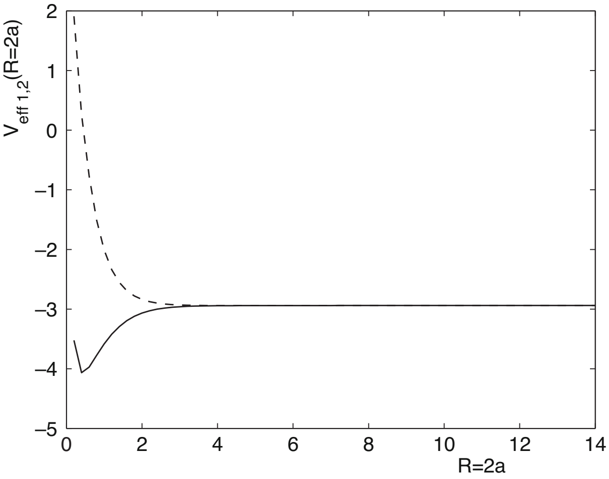

Only for the lowest binding state does a minimum occur at relatively small distances (probably because the "Coulomb interaction" is effectively relatively small due to the cutoff parameter $\delta = 0.1$). The dependence of this result on this cutoff parameter could be investigated.

## 8.3 Solution of the Exercise Problems for Chap. 4

**Problem 4.1, Vibration Modes of a (1-Dimensional) Molecule**

a)

$$\begin{aligned} m\ddot{u}_1 &= -k(u_1 - u_2) = -ku_1 + ku_2 \\ M\ddot{u}_2 &= -k(u_2 - u_1) - k(u_3 - u_2) = ku_1 - 2ku_2 + ku_3 \\ m\ddot{u}_3 &= -k(u_3 - u_2) = ku_2 - ku_3. \end{aligned}$$

b)

$$\underline{\underline{\Phi}} = \begin{pmatrix} k & -k & 0 \\ -k & 2k & -k \\ 0 & -k & k \end{pmatrix}$$

$$\underline{\underline{D}} = \begin{pmatrix} \frac{k}{m} & -\frac{k}{\sqrt{mM}} & 0 \\ -\frac{k}{\sqrt{mM}} & \frac{2k}{M} & -\frac{k}{\sqrt{mM}} \\ 0 & -\frac{k}{\sqrt{mM}} & \frac{k}{m} \end{pmatrix}.$$

c) Eigenfrequencies $\omega^2$ result from the condition:

$$\det(\underline{\underline{D}} - \omega^2 \underline{\underline{1}}) = 0 = \left(\frac{k}{m} - \omega^2\right)^2 \left(\frac{2k}{M} - \omega^2\right) - 2\left(\frac{k}{m} - \omega^2\right)\frac{k^2}{mM}.$$

This cubic equation obviously has the 3 solutions

$$\omega_1^2 = 0, \quad \omega_2^2 = \frac{k}{m}, \quad \omega_3^2 = 2\frac{k}{M} + \frac{k}{m}$$

with associated (non-normalised) eigenvectors

$$\underline{v}_1 = \begin{pmatrix} \sqrt{m} \\ \sqrt{M} \\ \sqrt{m} \end{pmatrix}, \quad \underline{v}_2 = \begin{pmatrix} 1 \\ 0 \\ -1 \end{pmatrix}, \quad \underline{v}_3 = \begin{pmatrix} 1 \\ -2\sqrt{\frac{m}{M}} \\ 1 \end{pmatrix}.$$

d) If one considers that according to the approach (4.23), the true amplitudes of the eigenvibrations still have a factor $1/\sqrt{\text{Mass}}$ with respect to the eigenvectors, the 3 eigenvibrations result as special solutions:

$$\underline{u}_1 = \begin{pmatrix} 1 \\ 1 \\ 1 \end{pmatrix} e^{-i\omega_1 t}, \quad \underline{u}_2 = \begin{pmatrix} 1 \\ 0 \\ -1 \end{pmatrix} e^{-i\omega_2 t}, \quad \underline{u}_3 = \begin{pmatrix} 1 \\ -2\frac{m}{M} \\ 1 \end{pmatrix} e^{-i\omega_2 t}.$$

The 3 components of the 3 vectors $\underline{u}_i$ correspond to the displacements of the mass point $j \in \{1, 2, 3\}$. Then, the first eigen-"vibration" corresponds to a displacement of all 3 mass points by the same distance, the springs therefore remain relaxed and no vibration is excited. The whole system is only translated, therefore the "vibration frequency" is 0. In the 2nd vibration mode, the middle mass $M$ remains at rest (not displaced), and the other two masses $m$ oscillate relative to this resting mass $M$ in opposite directions with the frequency of a single oscillator. In the 3rd eigenvibration, the two outer masses $m$ oscillate in the same direction and thus also excite the middle mass $M$ to vibrations.

e) A numerical treatment of this analytically exactly solvable problem can be carried out at different levels. On the one hand, the dynamic matrix from b) can be diagonalized. If one measures frequencies (or frequency squares) in units of the frequency square of the simple pendulum $\frac{k}{m}$ and chooses $M = 2m$, then the following matrix is to be diagonalized:

$$\underline{\underline{D}} = \begin{pmatrix} 1 & -\frac{1}{\sqrt{2}} & 0 \\ -\frac{1}{\sqrt{2}} & 1 & -\frac{1}{\sqrt{2}} \\ 0 & -\frac{1}{\sqrt{2}} & 1 \end{pmatrix}.$$

The diagonalization is carried out in the following Matlab code:

```
clear;
d=zeros(3,3);
>> d = [1 , -1/sqrt(2) , 0;
-1/sqrt(2), 1, -1/sqrt(2);
0 ,-1/sqrt(2), 1]

d =

1.0000   -0.7071     0
-0.7071   1.0000   -0.7071
0   -0.7071   1.0000
>> [ev,ew]=eig(d)

ev =

-0.5000   -0.7071   0.5000
-0.7071   -0.0000   -0.7071
-0.5000   0.7071   0.5000

ew =

0.0000     0   0
0   1.0000   0
0   0   2.0000
```

So the eigenvalues $\omega_i^2 = 0, 1, 2$ result, which agrees with c) for the chosen units and mass ratios, as well as the (now normalized to 1) eigenvectors.
Alternatively, however, one can also directly solve the equations of motion from a) numerically by integration using one of the Runge-Kutta procedures available in Matlab. The 3 coupled (time-dependent) differential equations of 2nd order can be easily transformed into a system of 6 coupled differential equations of 1st order. The Matlab function to be called for this is given by:

```
function dy = ystrich1(t,y)
dy=zeros(6,1);
dy(1)=y(4); dy(2)=y(5);  dy(3)=y(6);
dy(4)=-y(1)+y(2);
dy(5)=0.5*(y(1)+y(3))-y(2);
dy(6)=-y(3)+y(2);
```

This is, for example, called by:

```
clear all;
y=zeros(6,1);y0=zeros(6,1);
y0(1)=1;y0(2)=0;y0(3)=-1;
tspan=[0:0.1:12];
[t,y]= ode45(@ystrich1,tspan,y0);
plot(t,y(:,1),t,y(:,2),t,y(:,3))
```

The above initial condition directs the two outer mass points $m$ in opposite directions and leaves the middle mass at rest. Then the solutions shown in the figure below left result; the mass points 1 and 3 therefore oscillate exactly opposite with a period $T = 2\pi$, which corresponds to the frequency $\omega = 1$, while the middle mass 2 remains at rest. If, on the other hand, the initial conditions are: y0(1)=1;y0(2)=1;y0(3)=1, the result is shown on the right below, all 3 mass points therefore remain constantly deflected (and do not oscillate, i.e. $\omega = 0$).

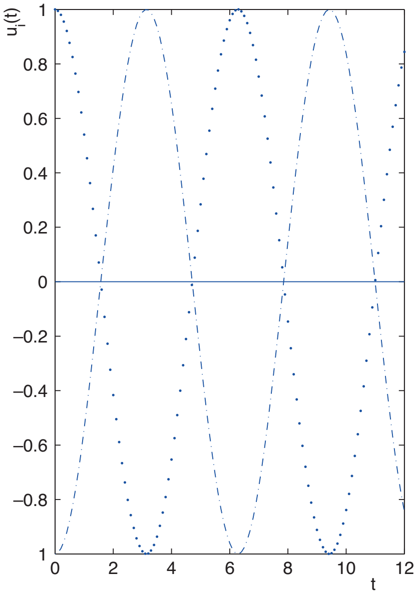

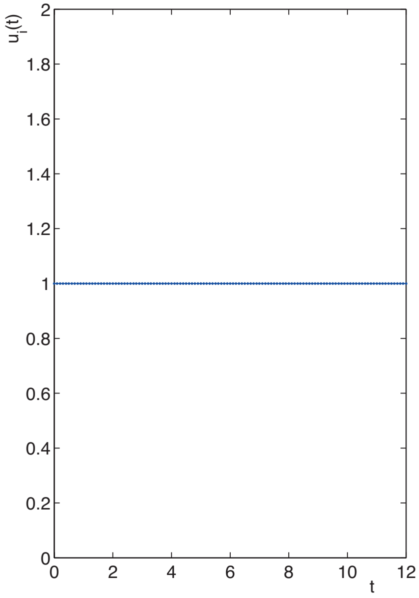

For the initial condition y0(1)=1;y0(2)=sqrt(2);y0(3)=1, on the other hand, the result shown on the left below is obtained; all 3 mass points oscillate with a vibration period of $T \approx 4.44$ corresponding to a frequency $\omega = \sqrt{2}$. With a different initial condition, e.g. y0(1)=1;y0(2)=0;y0(3)=0, however, superpositions of vibrations of different frequencies result, as shown on the right below.

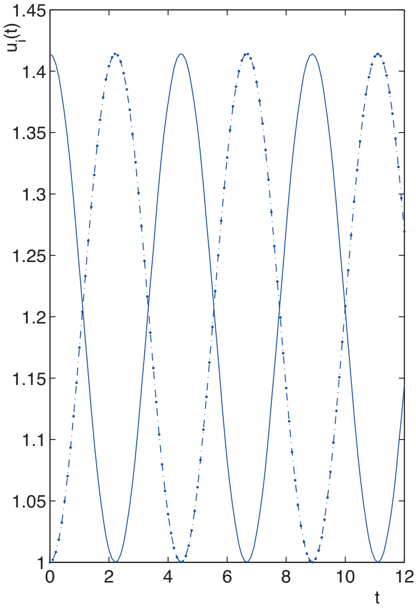

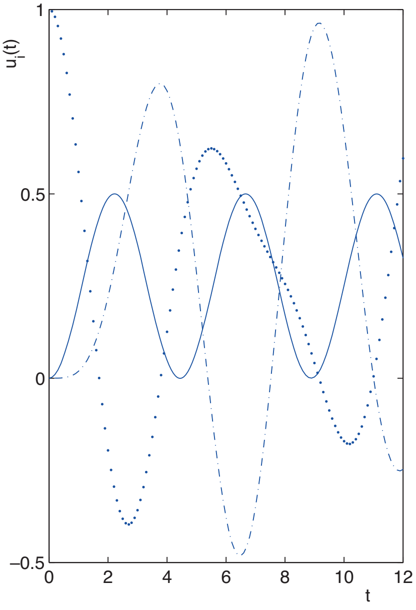

### Problem 4.2, Lattice Waves on the Square Lattice

$$\begin{aligned}
V &= \frac{\alpha}{2}\sum_{\boldsymbol{R}}\left[\boldsymbol{u}^2_{\boldsymbol{R}+\boldsymbol{a}_1} + \boldsymbol{u}^2_{\boldsymbol{R}} + \boldsymbol{u}^2_{\boldsymbol{R}+\boldsymbol{a}_2} + \boldsymbol{u}^2_{\boldsymbol{R}} - 2\boldsymbol{u}_{\boldsymbol{R}+\boldsymbol{a}_1}\boldsymbol{u}_{\boldsymbol{R}} - 2\boldsymbol{u}_{\boldsymbol{R}+\boldsymbol{a}_2}\boldsymbol{u}_{\boldsymbol{R}}\right] \\
&= \frac{\alpha}{2}\sum_{\boldsymbol{R}i}\left[4u^2_{\boldsymbol{R}i} - 2u_{\boldsymbol{R}+\boldsymbol{a}_1 i}u_{\boldsymbol{R}i} - 2u_{\boldsymbol{R}+\boldsymbol{a}_2 i}u_{\boldsymbol{R}i}\right] \\
&= \frac{1}{2}\sum_{\boldsymbol{R}i,\boldsymbol{R}'i'}\Phi_{\boldsymbol{R}i,\boldsymbol{R}'i'}u_{\boldsymbol{R}i}u_{\boldsymbol{R}'i'}
\end{aligned}$$

$$\begin{aligned}
\text{where}\quad \Phi_{\boldsymbol{R}i,\boldsymbol{R}i'} &= 4\alpha\delta_{ii'} \\
\Phi_{\boldsymbol{R}i,\boldsymbol{R}'i'} &= \Phi_{ii'}(\boldsymbol{R}'-\boldsymbol{R}) = \begin{cases} -\alpha\delta_{ii'} & \text{for} \quad \boldsymbol{R}' = \boldsymbol{R}\pm\boldsymbol{a}_l (l=1,2) \\ 0 & \qquad\text{else} \end{cases}.
\end{aligned}$$

*Note*: The double sum over all $\boldsymbol{R},\boldsymbol{R}'$ can be written (with numbering of the places) as:

$$\begin{aligned}
\sum_{nm}\Phi_{nm}u_n u_m &= \sum_n \Phi_{nn}u_n^2 + \sum_n\sum_{m\neq n}\Phi_{nm}u_n u_m \\
&= \sum_n \Phi_{nn}u_n^2 + \sum_n\sum_{m>n}2\Phi_{nm}u_n u_m
\end{aligned}$$

therefore, the non-diagonal elements of $\underline{\underline{\Phi}}$ are only given by $-\alpha$ if $\boldsymbol{R},\boldsymbol{R}'$ are next neighbors.

Then the Fourier-transformed dynamic matrix is

$$\begin{aligned}
D_i(\boldsymbol{q}) &= \sum_{\boldsymbol{R}}\frac{1}{M}\Phi_{ii}(\boldsymbol{R})e^{i\boldsymbol{q}\boldsymbol{R}} = 4\alpha - \alpha e^{iq_x a} - \alpha e^{-iq_x a} - \alpha e^{iq_y a} - \alpha e^{-iq_y a} \\
&= 2\frac{\alpha}{M}\left(2 - \cos(q_x a) - \cos\left(q_y a\right)\right) = 4\frac{\alpha}{M}\left(\sin^2\left(\frac{q_x a}{2}\right) + \sin^2\left(\frac{q_y a}{2}\right)\right).
\end{aligned}$$

These are already the squares of the eigenfrequencies $\omega_i^2(\boldsymbol{q})$, which are therefore degenerate with respect to the cartesian component $i$ here.

Along special lines (from $(0,0)$ to $(1,0)$, from $(1,0)$ to $(1,1)$ and back along the diagonal of $(1,1)$ to $(0,0)$ in units of $\pi/a$) in the Brillouin zone, the dispersion relation is shown in the following figure.

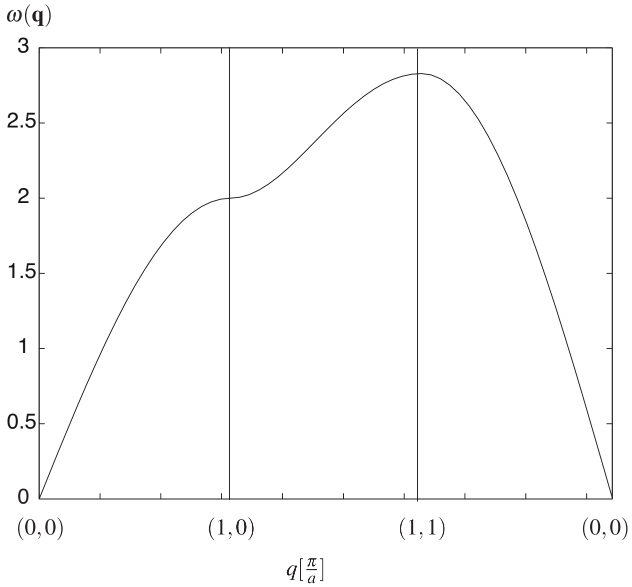

**Problem 4.3, Linear Chain with 2 Atom Types per Unit Cell**

a) The procedure of Sect. 4.2 can be applied to this example. We consider a one-dimensional lattice with lattice constants $2a$, periodic boundary conditions and 2 atoms in the elementary cell, namely one of mass $M$ at 0 and one of mass $m$ at $a$. The position vectors of the $i$-th atom in the $n$-th elementary cell are therefore $R_i = n * 2a + (i-1) * a + u_{n,i}(i{=}1,2)$. The equation of motion is

$$M\ddot{u}_{n,1} = K(u_{n,2} - u_{n,1} + u_{n-1,2} - u_{n,1}) = K(u_{n,2} + u_{n-1,2} - 2u_{n,1})$$
$$m\ddot{u}_{n,2} = K(u_{n+1,1} - u_{n,2} + u_{n,1} - u_{n,2}) = K(u_{n+1,1} + u_{n,1} - 2u_{n,2}).$$

$$\text{Ansatz:}\quad u_{n,1} = \frac{v_{n,1}}{\sqrt{M}}e^{i\omega t}, \quad u_{n,2} = \frac{v_{n,2}}{\sqrt{m}}e^{i\omega t}$$

$$\sqrt{M}\omega^2 v_{n,1} = \frac{2K}{\sqrt{M}}v_{n,1} - K\left(\frac{1}{\sqrt{m}}v_{n,2} + \frac{1}{\sqrt{m}}v_{n-1,2}\right)$$
$$\sqrt{m}\omega^2 v_{n,2} = K\left(\frac{2}{\sqrt{m}}v_{n,2} - \frac{1}{\sqrt{M}}v_{n+1,1} - \frac{1}{\sqrt{M}}v_{n,1}\right).$$

$$\text{Ansatz:}\quad v_{n,i} = e^{iq2na}w_i$$

$$\omega^2 e^{iq2na}w_1 = 2\frac{K}{M}e^{iq2na}w_1 - \frac{K}{\sqrt{Mm}}e^{iq2na}w_2 - \frac{K}{\sqrt{Mm}}e^{iq(n-1)2a}w_2$$
$$\omega^2 e^{iq2na}w_2 = 2\frac{K}{M}e^{iq2na}w_2 - \frac{K}{\sqrt{Mm}}e^{iq2(n+1)a}w_1 - \frac{K}{\sqrt{Mm}}e^{iqn2a}w_1$$
$$\omega^2 w_1 = 2\frac{K}{M}w_1 - \frac{K}{\sqrt{Mm}}w_2 - \frac{K}{\sqrt{Mm}}e^{-iq2a}w_2$$
$$\omega^2 w_2 = 2\frac{K}{m}w_2 - \frac{K}{\sqrt{Mm}}e^{iq2a}w_1 - \frac{K}{\sqrt{Mm}}w_1.$$

This is just an eigenvalue problem for the dynamical matrix

$$\underline{\underline{D}}(q) = \begin{pmatrix} 2\frac{K}{M} & -\frac{K}{\sqrt{Mm}} - \frac{K}{\sqrt{Mm}}e^{-iq2a} \\ -\frac{K}{\sqrt{Mm}}e^{iq2a} - \frac{K}{\sqrt{Mm}} & 2\frac{K}{m} \end{pmatrix}.$$

The eigenvalues result from the condition

$$\begin{aligned} 0 &= \det \begin{pmatrix} 2\frac{K}{M} - \omega^2 & -\left(\frac{K}{\sqrt{Mm}} + \frac{K}{\sqrt{Mm}}e^{-iq2a}\right) \\ -\left(\frac{K}{\sqrt{Mm}}e^{iq2a} + \frac{K}{\sqrt{Mm}}\right) & 2\frac{K}{m} - \omega^2 \end{pmatrix} \\ &= \left(2\frac{K}{M} - \omega^2\right)^2 \left(2\frac{K}{m} - \omega\right)^2 \\ &\quad - \left(\frac{K}{\sqrt{Mm}} + \frac{K}{\sqrt{Mm}}e^{-iq2a}\right)\left(\frac{K}{\sqrt{Mm}}e^{iq2a} + \frac{K}{\sqrt{Mm}}\right). \end{aligned}$$

The solution of this quadratic equation yields

$$\begin{aligned} \omega^2 &= \frac{K}{M} + \frac{K}{m} \pm \sqrt{2\frac{K^2}{Mm}\cos(2qa) - 2\frac{K^2}{Mm} + \left(\frac{K}{M} + \frac{K}{m}\right)^2} \\ &= \frac{K}{Mm}\left(m + M \pm \sqrt{M^2 + m^2 + 2Mm\cos(2qa)}\right). \end{aligned}$$

For each $q$ there are therefore 2 eigenvibrations and there are 2 branches (an acoustic and an optical) of the phonon dispersion relation.

b) For $q \to 0$ $\cos(2qa) \to 1$ and we obtain

$$\omega^2 \to \begin{cases} \frac{2K(M+m)}{Mm} \\ 0 \end{cases}.$$

For $q \to \frac{\pi}{2a}$ $\cos(2qa) \to \cos(\pi) = -1$ and we obtain

$$\omega^2 \to \begin{cases} \frac{2K}{m} \\ \frac{2K}{M} \end{cases}.$$

For $K = 1$ and a mass ratio $M/m = 2$ the dispersion relations $\omega_i(q)$ look as follows:

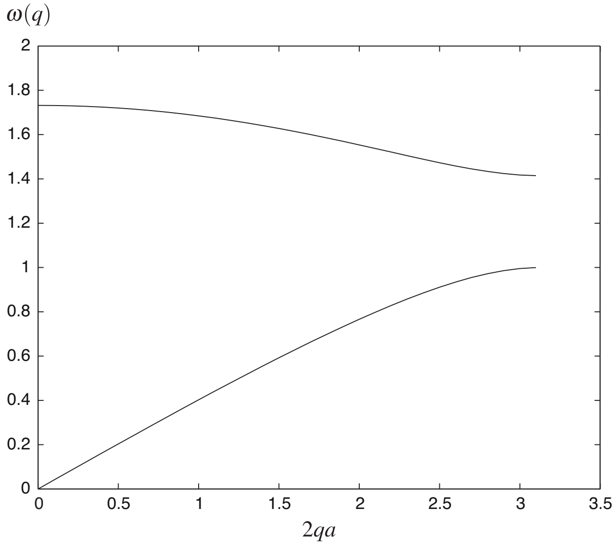

c) For $m = M$ one obtains

$$\omega^2 = \frac{K}{M}\left(2 \pm \sqrt{2 + 2\cos(2qa)}\right) = \frac{K}{M}(2 \pm 2\cos(qa)).$$

This results in:

$$\omega_1(q) = 2\sqrt{\frac{K}{M}}\left|\sin\left(\frac{qa}{2}\right)\right|$$
$$\omega_2(q) = 2\sqrt{\frac{K}{M}}\left|\cos\left(\frac{qa}{2}\right)\right|.$$

The 1st branch corresponds to the usual dispersion relation for a one-atom chain. The 2nd branch results from the first by adding a reciprocal lattice vector of the superlattice due to

$$\omega_1\left(\frac{\pi}{a} - q\right) = 2\sqrt{\frac{K}{M}}\left|\sin\left(-\frac{qa}{2} + \frac{\pi}{2}\right)\right| = 2\sqrt{\frac{K}{M}}\cos\left(\frac{qa}{2}\right).$$

Since the masses are the same translational invariance prevails with respect to $a$, and one can consider instead of 2 dispersion relations over the Brillouin zone of the superlattice with lattice constant $2a$ also a dispersion relation over the (twice as large) Brillouin zone of the actual lattice with lattice constant $a$.

**Problem 4.4, Linear Chain with Rigid Boundary Conditions**

The equation of motion is the same as for the chain with periodic boundary conditions:

$$M\ddot{u}_n = K(u_{n+1} + u_{n-1} - 2u_n)$$

with the boundary conditions $u_0 = u_N = 0$. The ansatz

$$u_n = A\sin(nqa)e^{i\omega t}$$

satisfies these boundary conditions if $Nqa = l\pi$ with integer $l$ applies. Substitution into the equation of motion leads to

$$\omega^2 A\sin(nqa) = \frac{K}{M}(2\sin(nqa) - \sin((n+1)qa) - \sin((n-1)qa))A.$$

Application of the addition theorem $\sin(x+y) = \sin(x)\cos(y) + \cos(x)\sin(y)$ leads to

$$\begin{aligned}\omega^2\sin(nqa) &= \frac{K}{M}(2\sin(nqa) - \sin(nqa)\cos(qa) - \cos(nqa)\sin(qa)\\ &\quad - \sin(nqa)\cos(-qa) - \cos(nqa)\sin(-qa))\\ &= \frac{K}{M}(2\sin(nqa) - \sin(nqa)\cos(qa) - \cos(nqa)\sin(qa)\\ &\quad - \sin(nqa)\cos(qa) + \cos(nqa)\sin(qa))\\ &= \frac{K}{M}(2 - 2\cos(qa))\sin(nqa).\end{aligned}$$

So one finds

$$\omega^2(q) = \frac{K}{M}(2 - 2\cos(qa)) = 4\frac{K}{M}\sin^2(qa/2),$$

i.e. the same dispersion relation as with periodic boundary conditions. Only the allowed $q$ values are different, namely $q = \frac{l\pi}{Na}$ for rigid and $q = \frac{l2\pi}{Na}$ for periodic boundary conditions. In both cases $N$ $q$ values are allowed, but a larger $q$ range is allowed for periodic boundary conditions (from 0 to $\frac{2\pi}{a}$ or $-\frac{\pi}{a}$ to $+\frac{\pi}{a}$; 1st Brillouin zone), for rigid boundary conditions only from 0 to $\frac{\pi}{a}$, reason: for periodic boundary conditions there are running waves to the left and to the right, but for rigid boundary conditions $-q$ does not provide anything new compared to +$q$ ( it does not matter whether the mass point oscillates first up or down).

In other words: For rigid boundary conditions, integer multiples of half the wavelength must fit the system length , i.e. $l\frac{\lambda}{2} = Na = l\frac{\pi}{q} \rightarrow q = \frac{l\pi}{Na}$, for periodic boundary conditions, integer multiples of the full wavelength must fit into the system: $q = \frac{l2\pi}{Na}$. The argument with the wavelengths can also be used to explain why a restriction to the 1st Brillouin zone or unit cell of the reciprocal lattice is sufficient: Wavelengths smaller than the lattice constant do not need to be considered in a discrete system.

### Problem 4.5, Internal Energy of the Linear Harmonic Chain

$$\begin{aligned}\hbar\omega(q) &= 2\sqrt{\frac{k}{m}}\left|\sin\left(\frac{qa}{2}\right)\right|\\ E(T) &= \sum_q \hbar\omega(q)\left(\frac{1}{e^{\beta\hbar\omega(q)}-1}+\frac{1}{2}\right), \quad c_V(T)=\frac{\partial E(T)}{\partial T}.\end{aligned}$$

a) High temperatures $T$ means: $\hbar\omega(q) \ll k_BT$ for all $q$, i. e. $\beta\hbar\omega(q) \ll 1$. Then the exponential function can be expanded according to $e^{\beta\hbar\omega(q)} \approx 1+\beta\hbar\omega(q)$ and it follows:

$$E(T) \approx \sum_q \left(\frac{\hbar\omega(q)}{1+\beta\hbar\omega(q)-1}+\frac{\hbar\omega(q)}{2}\right) \approx \sum_q k_BT = Nk_BT$$

$$c_V(T) = Nk_B.$$

b)

$$\begin{aligned}E &= \frac{L}{2\pi}\int_{-\frac{\pi}{a}}^{+\frac{\pi}{a}} dq\hbar\omega(q)\left(\frac{1}{e^{\beta\hbar\omega(q)}-1}+\frac{1}{2}\right)\\ &= \frac{Na}{\pi}\int_0^{+\frac{\pi}{a}} dq\hbar\omega(q)\left(\frac{1}{e^{\beta\hbar\omega(q)}-1}+\frac{1}{2}\right).\end{aligned}$$

c) For low temperatures $T$ contributions with $\beta\hbar\omega(q) \gg 1$ can be neglected because the factor $\left(e^{\beta\hbar\omega(q)}-1\right)^{-1} \approx e^{-\beta\hbar\omega(q)}$ is exponentially small. We assume that $T$ is so low that the expansion

$$\begin{aligned}\hbar\omega(q) = 2\hbar\sqrt{\frac{k}{m}}\sin\left(\frac{qa}{2}\right) &\approx \hbar\sqrt{\frac{k}{m}}aq = c_sq\\ \text{with:}\quad c_s = \hbar\sqrt{\frac{k}{m}}a\end{aligned}$$

is valid for $\hbar\omega(q) \le k_BT$. Then

$$E(T) = \frac{Na}{\pi}\int_0^{\frac{\pi}{a}} dqc_sq\left(\frac{1}{e^{\beta c_sq}-1}+\frac{1}{2}\right).$$

results. With the substitution

$$x = \frac{c_sq}{k_BT}, \quad dx = \frac{c_s}{k_BT}dq$$

it follows

$$\begin{aligned}E(T)-E_0 &= \frac{Na}{\pi}\frac{(k_BT)^2}{c_s}\int_0^{c_s\pi/ak_BT} dx\frac{x}{e^x-1} = \frac{Na}{\pi}\frac{(k_BT)^2}{c_s}D_1(\frac{c_s\pi}{ak_BT})\\ &\approx \frac{Na}{\pi}\frac{(k_BT)^2}{c_s}D_1(\infty) = \frac{Na\pi}{6c_s}(k_BT)^2.\end{aligned}$$

Here

$$D_1(\infty) = \zeta(2) = \frac{\pi^2}{6} \quad , D_n(x) = \int_0^x dy \frac{y^n}{e^y - 1} \text{ n-th Debye function}$$

was used with the Riemann zeta function

$$\zeta(s) = \sum_{k=0}^{\infty} k^{-s}.$$

The more precise condition for “low” temperature is therefore:

$$k_B T \ll \frac{c_s \pi}{a}.$$

For the specific heat, in the limit of low $T$ results:

$$c_V(T) = \frac{Na\pi}{3c_s} k_B^2 T.$$

The specific heat therefore disappears linearly with the temperature for $T \to 0$, which is generally true for acoustic phonons in one dimension.

d)

$$\begin{aligned} E(T) &= \frac{Na}{\pi} \left( \int_0^{\pi/a} dq \frac{c_s q}{e^{\beta c_s q} - 1} + \frac{c_s q}{2} \right) \\ &= \frac{Na}{\pi} \frac{(k_B T)^2}{c_s} \int_0^{\Theta_D/T} dx \frac{x}{e^x - 1} + \frac{Nac_s}{4\pi} \left( \frac{\pi}{a} \right)^2 \\ &= \frac{Na}{c_s \pi} (k_B T)^2 D_1 \left( \frac{\Theta_D}{T} \right) + \frac{N\pi c_s}{4a} \end{aligned}$$

with the Debye temperature $\Theta_D = \frac{c_s \pi}{a k_B}$

$$D_n(x) = \int_0^x dt \frac{t^n}{e^t - 1}.$$

For low $T$ one can set $\Theta_D/T \approx \infty$ and obtains

$$E(T) - E_0 = N \frac{a}{c_s \pi} (k_B T)^2 D_1(\infty) = \frac{N\pi a}{6c_s} (k_B T)^2$$

because of $D_1(\infty) = \frac{\pi^2}{6}$, for high temperatures

$$E(T) \to \frac{Na}{c_s \pi} (k_B T)^2 \frac{\Theta_D}{T} = Nk_B T$$

follows so the exact high and low temperature behavior is reproduced.

e) The substitution

$$\begin{aligned}
x &= \hbar\omega(q)\beta = 2\hbar\sqrt{\frac{k}{m}}\sin\left(\frac{qa}{2}\right)\beta = \frac{2c_s}{ak_BT}\sin\left(\frac{qa}{2}\right)\\
dx &= \hbar a\sqrt{\frac{k}{m}}\cos\left(\frac{qa}{2}\right)\beta dq = c_s\beta\sqrt{1-\sin^2\left(\frac{qa}{2}\right)}dq\\
&= c_s\beta\sqrt{1-\left(\frac{k_BTa}{2c_s}x\right)^2}\,dq
\end{aligned}$$

leads to

$$\begin{aligned}
E-E_0 &= \frac{Na}{\pi}\frac{(k_BT)^2}{c_s}\int_0^{2c_s/ak_BT}\frac{dx}{\sqrt{1-\left(\frac{ak_BT}{2c_s}x\right)^2}}\frac{x}{e^x-1}\\
&= \frac{Na}{\pi c_s}(k_BT)^2\left[\int dx\frac{x}{e^x-1}+\frac{1}{8}\left(\frac{ak_BT}{c_s}\right)^2\int dx\frac{x^3}{e^x-1}\right]\\
&= \frac{Na}{\pi c_s}(k_BT)^2\left[\frac{\pi^2}{6}+\frac{1}{8}\left(\frac{ak_BT}{c_s}\right)^2\frac{\pi^4}{15}\right].
\end{aligned}$$

The expansion of the root under the integral is only an asymptotic expansion, which is not valid throughout the integration area because of the divergence of the integrand at the upper integration limit. For low $T$ one can still make the expansion approximately, because for larger $x$ the (no longer correct) contributions no longer play a role because of the exponentially small second factor.

f) For numerical calculation one can go to dimensionless units by setting $a=1$, $2\hbar\sqrt{k/m}=1$ and $k_B=1$ (thus $c_s=0.5$) and discretizing the integral from b):

$$\begin{aligned}
(E-E_0)/N &= \frac{1}{\pi}\sum_{n=1}^{N}\frac{\pi}{N}\sin\left(\frac{n}{2N}\pi\right)\frac{1}{e^{\sin(n\pi/2N)/T}-1} = \frac{1}{N}\sum_{n=1}^{N}\frac{a_n}{e^{a_n/T}-1}\\
\text{with:}\quad a_n &= \sin\left(\frac{n\pi}{2N}\right).
\end{aligned}$$

The Debye functions can be calculated according to the definition, see d), and then the result of the Debye approximation can be calculated according to the formula given in d). In the following figures, the exact results (solid curves) for the internal energy and specific heat are compared with those of the Debye approximation (dashed curves).

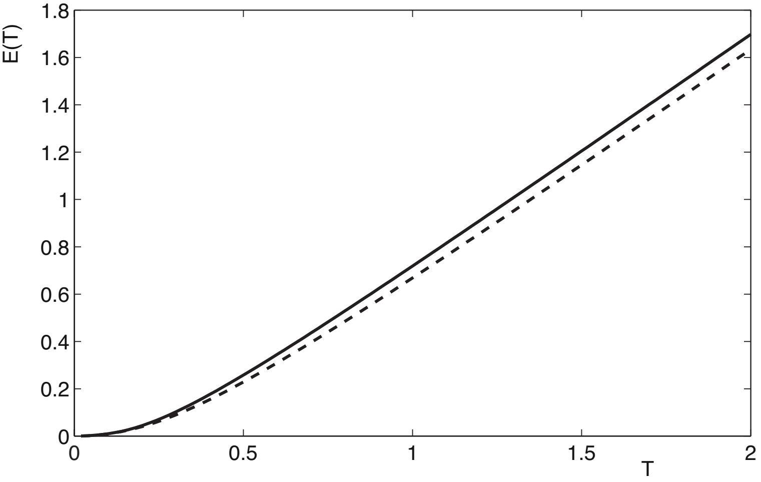

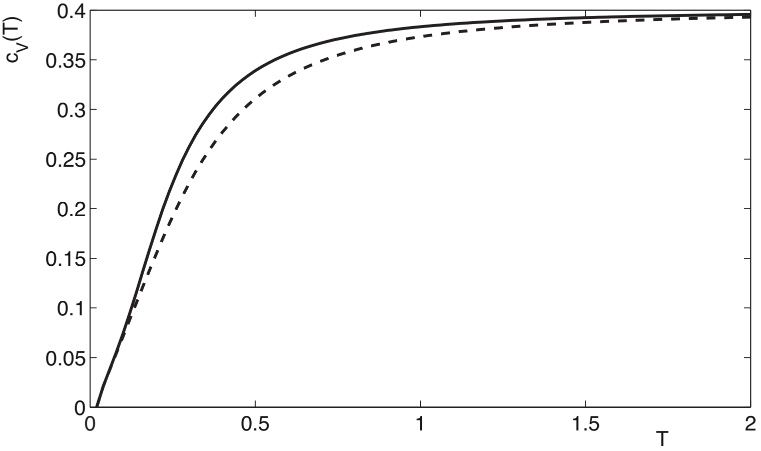

It is clearly visible that for low and high $T$ the Debye approximation is correct, but that there are corrections in the range of intermediate temperatures. For low temperatures, the internal energy has also been calculated with the correction formula from e); the corresponding result (dotted curve) is—with the exact (solid) and the Debye result (dashed)—also plotted. It can be seen that for very low $T$ all 3 curves agree, but the result with the correction is almost identical to the exact result up to higher $T$, but of course "runs away" for even higher $T$ (due to contributions proportional to $T^2$ or $T^4$).

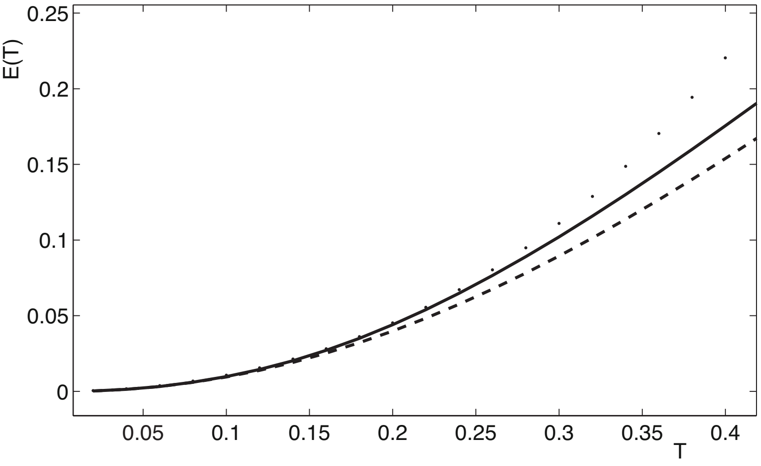

### Problem 4.6, Quantum Corrections to the Dulong-Petit Law

If for high temperatures, i.e. $\beta\hbar\omega_j(q) \ll 1$, one takes into account the 3rd order in the expansion of the exponential term in the denominator of the Bose function, one obtains

$$\begin{aligned}
&E(T) = \\
&= \sum_{\boldsymbol{q}j} \hbar\omega_j(\boldsymbol{q}) \left( \frac{1}{e^{\beta\hbar\omega_j(\boldsymbol{q})} - 1} + \frac{1}{2} \right) \\
&= \sum_{\boldsymbol{q}j} \hbar\omega_j(\boldsymbol{q}) \left( \frac{1}{1 + \beta\hbar\omega_j(\boldsymbol{q}) + \frac{1}{2}(\beta\hbar\omega(\boldsymbol{q}))^2 + \frac{1}{6}(\beta\hbar\omega(\boldsymbol{q}))^3 + \ldots - 1} + \frac{1}{2} \right) \\
&= \sum_{\boldsymbol{q}j} \hbar\omega_j(\boldsymbol{q}) \left( \frac{k_B T}{\hbar\omega_j(\boldsymbol{q})} \frac{1}{1 + \frac{1}{2}\beta\hbar\omega(\boldsymbol{q}) + \frac{1}{6}(\beta\hbar\omega(\boldsymbol{q}))^2} + \frac{1}{2} \right) \\
&= \sum_{\boldsymbol{q}j} \hbar\omega_j(\boldsymbol{q}) \left[ \frac{k_B T}{\hbar\omega_j(\boldsymbol{q})} \left( 1 - \frac{1}{2}\beta\hbar\omega_j(\boldsymbol{q}) + \frac{1}{4}(\beta\hbar\omega_j(\boldsymbol{q}))^2 - \frac{1}{6}(\beta\hbar\omega_j(\boldsymbol{q}))^2 \right) + \frac{1}{2} \right] \\
&= \sum_{\boldsymbol{q}j} \left[ k_B T - \frac{1}{2}\hbar\omega_j(\boldsymbol{q}) + \frac{1}{12} \frac{(\hbar\omega_j(\boldsymbol{q}))^2}{k_B T} + \frac{\hbar\omega_j(\boldsymbol{q})}{2} \right] \\
&= 3Nk_B T + \frac{1}{12} \frac{A}{k_B T},
\end{aligned}$$

with

$$A = \sum_{\boldsymbol{q}j} (\hbar\omega_j(\boldsymbol{q}))^2.$$

*Note*: The zero point energy is thus exactly compensated by the 2nd term in the high temperature expansion (and does not remain as an additive constant to the Dulong-Petit result), the first corrections to the Dulong-Petit result are proportional $1/T$.

**Problem 4.7, Phonon Densities of State**

The statement is clear according to the definition of the density of states.

a) For 1 dimension, $N_\omega = 200$, $\Omega_m = 2$, $\omega_m = 1$ and $N_q = 20.000$ were chosen numerically and the $q$ values were discretized as $q = i\frac{\pi}{2a}$ $(i = 1, \ldots, N_q)$. Below is the Matlab program and the figure with the result for the one-dimensional phonon density of states:

```
clear all;
nm=200;de=2/nm;nq=20000;
rho=zeros(nm);
rhoex=zeros(nm);
e=zeros(nm);
for ie=1:nm
     e(ie)=ie*de;
end
for ix=1:nq
     qx=ix*pi/(2*nq);
     om=sin(qx);
     ee=om;
     ie=ceil(ee/de);
     rho(ie)=rho(ie)+1;
end
for ie=1:100
     rho(ie)=rho(ie)/(nq*de);
     if e(ie) < 1 rhoex(ie)=2/(pi*sqrt(1-e(ie)*e(ie)));end
end
plot(e,rho,'k-',e,rhoex,'k-.')
axis([0 1.4 0 4])
set(gca,'FontSize',16)
text(1.4,-0.3,'\omega','FontSize',16)
text(-0.2,4.2,'n_{1d}(\omega)','FontSize',16)
```

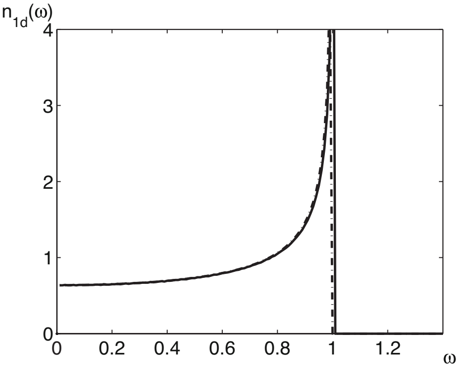

b) Because of the symmetry of the square lattice, it is sufficient to restrict $\boldsymbol{q}$ to the area $0 \le q_x \le \frac{\pi}{a}$, $0 \le q_y \le q_x$ of the 1st Brillouin zone, since the 4 quadrants of the Brillouin zone lead to equivalent $\omega(\boldsymbol{q})$ values and within each quadrant a restriction to a simplex (triangle) is sufficient because the dispersion is symmetrical when $q_x$ and $q_y$ are interchanged. For the specific numerical calculation, $N_\omega = 200$, $\Omega_m = 2$ were chosen again and 500 discretization points for $q_x$ and 250 discretization points for $q_y$.

```
clear all;
nm=200;de=2/nm;nqx=500;
rho=zeros(nm);
e=zeros(nm);
for ie=1:nm
     e(ie)=ie*de;
end
for ix=1:nqx
     qx=ix*pi/(2*nqx);
     for iy=1:ix
          qy=iy*pi/(2*nqx);
          om=sqrt(sin(qx)*sin(qx)+sin(qy)*sin(qy));
          ee=om;
          ie=ceil(ee/de);
          rho(ie)=rho(ie)+1;
     end
end
for ie=1:nm
     rho(ie)=rho(ie)/(nqx*nqx/2*de);
end
plot(e,rho,'k-','Linewidth',2)
axis([0 1.8 0 3]);
set(gca,'FontSize',16)
```

```
text(1.8,-0.3,'\omega','FontSize',16);
text(-0.2,3.2,'n_{2d}(\omega)','FontSize',16)
```

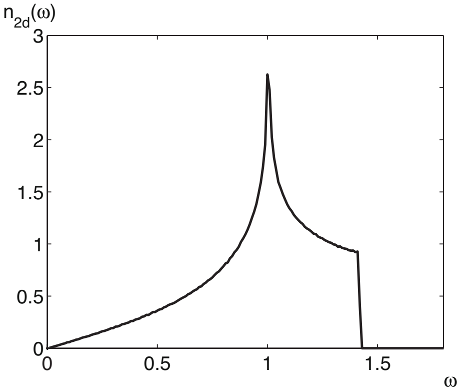

One clearly recognizes a linear behavior of the density of states for small ω (as in the Debye model), a logarithmic Van Hove singularity at $\omega = 1$ and a jump to 0 at the upper edge of the spectrum at $\omega \approx 1.41 = \sqrt{2}$; here ω was measured in units of $2\sqrt{\alpha/M}$.

c) An analogous program as in a) with the dispersion calculated in problem 4.3 (and shown in the figure in the solution of problem 4.3b) yields the following result for the density of states:

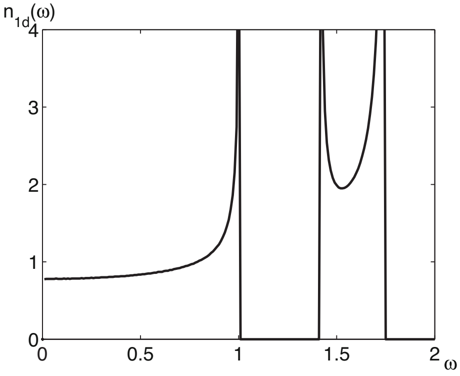

The typical 1-dimensional Van Hove singularities are also visible at the top and bottom of the spectrum of optical phonons.

### Problem 4.8, Phonon Spectrum and Density of States for fcc Lattice

a) If $a$ denotes the edge length of the cube of the conventional unit cell, the 12 nearest-neighbor vectors for the fcc lattice are given by $\boldsymbol{\Delta} = (\pm a/2, \pm a/2, 0)$, $(\pm a/2, 0, \pm a/2)$, $(0, \pm a/2, \pm a/2)$. Then, for example, from (4.86) by comparison with (4.18) it can be seen that the matrix elements of the force constant matrix are given by:

$$\Phi_{ii}(0) = \frac{k}{\mathbf{\Delta}^2} \sum_{\mathbf{\Delta}} \Delta_i^2 = 4k$$

because for fixed $i$ for 8 of the 12 $\mathbf{\Delta}0 \neq \Delta_i = a/2$ and $\mathbf{\Delta}^2 = a^2/2$ applies. For $i \neq j$ it is valid

$$\Phi_{ij}(0) = -\frac{k}{a^2/2} \sum_{\mathbf{\Delta}} \Delta_i \Delta_j = 0$$

because of the 4 $\mathbf{\Delta}$ with $\Delta_i \neq 0$ and $\Delta_j \neq 0$ two $\Delta_i \Delta_j = +a^2/4$ and two $\Delta_i \Delta_j = -a^2/4$ result, which cancels out when summed over all $\mathbf{\Delta}$. Similarly, for fixed $\mathbf{\Delta}$:

$$\Phi_{ii}(\mathbf{\Delta}) = -\frac{k}{2}$$

because of $\Delta_i^2 = a^2/4$ and $\mathbf{\Delta}^2 = a^2/2$ and

$$\Phi_{ij}(\mathbf{\Delta}) = \pm\frac{k}{2}$$

because $\Delta_i \Delta_j = \pm a^2/4$ applies (for 2 of the 4 $\mathbf{\Delta}$ with $\Delta_i \neq 0$ and $\Delta_j \neq 0$ positive, for 2 negative). The (Fourier-transformed, $\boldsymbol{q}$-dependent) dynamic matrix thus results from the general relation (4.27)

$$D_{ij}(\boldsymbol{q}) = \frac{1}{M} \sum_{\boldsymbol{R}} \Phi_{ij}(\boldsymbol{R}) e^{-i\boldsymbol{q}\boldsymbol{R}} = \frac{1}{M} \left( \Phi_{ij}(0) + \sum_{\mathbf{\Delta}} \Phi_{ij}(\mathbf{\Delta}) e^{-i\boldsymbol{q}\mathbf{\Delta}} \right).$$

b) For the following figure, $\boldsymbol{q}$ was varied in 30 discretization steps from the $\Gamma$ point to the X point according to $\boldsymbol{q} = (q, 0, 0)$, $q = 0, \ldots, \frac{2\pi}{a}$, then according to $\boldsymbol{q} = \left(\frac{2\pi}{a}, q, 0\right)$ from the X point to the point $\left(\frac{2\pi}{a}, \frac{2\pi}{a}, 0\right)$, from this back to the $\Gamma$ point according to $\boldsymbol{q} = \left(\frac{2\pi}{a} - q, \frac{2\pi}{a} - q, 0\right)$ $q = 0, \ldots, \frac{2\pi}{a}$ and finally again from the $\Gamma$ point to the L point according to $\boldsymbol{q} = (q, q, q)$ $q = 0, \ldots, \frac{\pi}{a}$. For each of the (a total of 120) $\boldsymbol{q}$ values, the dynamic matrix is set up according to a) and diagonalized. The roots of the three eigenvalues are the eigenfrequencies.

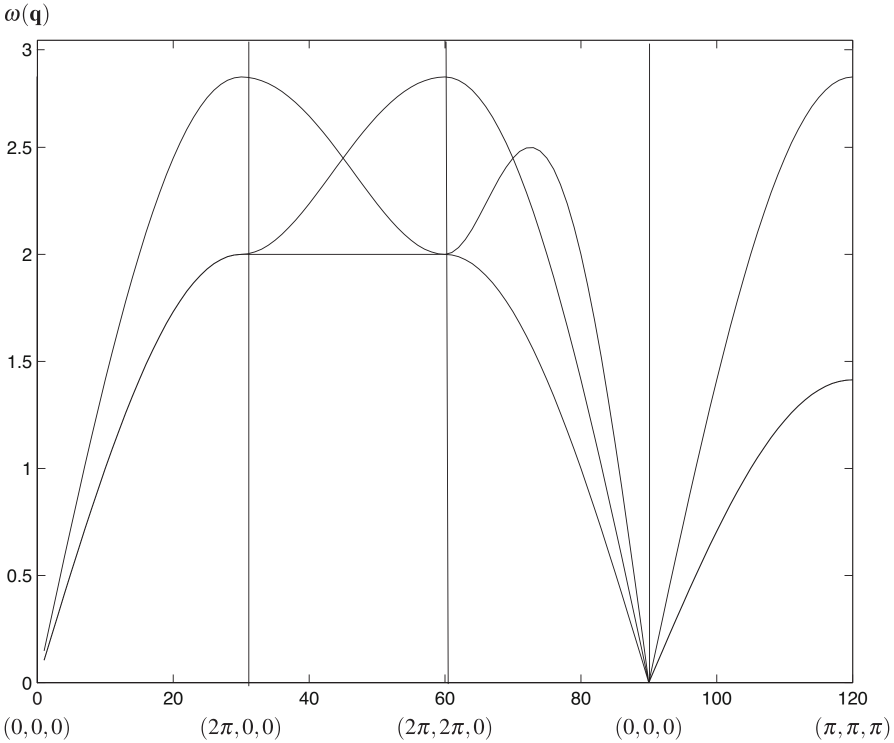

Critical points are therefore to be expected at $\omega_c \approx 2.8,\ 2.4,\ 2,\ 1.4 = \sqrt{2}$. The Matlab code for calculating these dispersion curves is printed below.

```
clear;
d=zeros(3,3);
qx=zeros(120);qy=zeros(120);qz=zeros(120);
x=zeros(120);
for j=1:120
x(j)=j;
if j <=30
qx(j)=2.*pi*j/30;
qy(j)=0;qz(j)=0;
end
if j>30 & j <=60
qx(j)=2*pi;
qy(j)=2*pi*(j-30)/30;qz(j)=0;end
if 60 < j & j<=90
```

```
qx(j)=2*pi-(j-60)*2*pi/30;
qy(j)=2*pi-(j-60)*2*pi/30;
qz(j)=0;end
if j>90 & j<=120
qx(j)=(j-90)*pi/30;qy(j)=qx(j);qz(j)=qx(j);
end
d(1,1)=2*(2-cos(0.5*qx(j))*cos(0.5*qy(j))-cos(0.5*qx(j))*
        cos(0.5*qz(j)));
d(1,2)=2*sin(0.5*qx(j))*sin(0.5*qy(j));
d(1,3)=2*sin(0.5*qx(j))*sin(0.5*qz(j));
d(2,1)=d(1,2);
d(2,2)=2*(2-cos(0.5*qy(j))*cos(0.5*qx(j))-cos(0.5*qy(j))*
        cos(0.5*qz(j)));
d(2,3)=2*sin(0.5*qy(j))*sin(0.5*qz(j));
d(3,1)=d(1,3);d(3,2)=d(2,3);
d(3,3)=2*(2-cos(0.5*qz(j))*cos(0.5*qx(j))-cos(0.5*qz(j))*
        cos(0.5*qy(j)));
[ev,ew]=eig(d);
for i=1:3
omega(j,i)=sqrt(ew(i,i));
end
end
plot(x,omega(:,1),x,omega(:,2),x,omega(:,3))
```

c) Because of the cubic symmetry, it is sufficient to consider $\boldsymbol{q}$ only on a simplex $\left(\frac{2\pi}{a} \geq q_x \geq q_y \geq q_z \geq 0\right)$ of an octahedron of the $\boldsymbol{q}$-space.
The calculation of the density of states is otherwise carried out analogously to the solution of Problem 4.7, for each $\boldsymbol{q}$ the dynamical matrix is to be diagonalized as in a). The result for the density of states is shown below, ω is of course measured in units of $\sqrt{\frac{k}{M}}$:

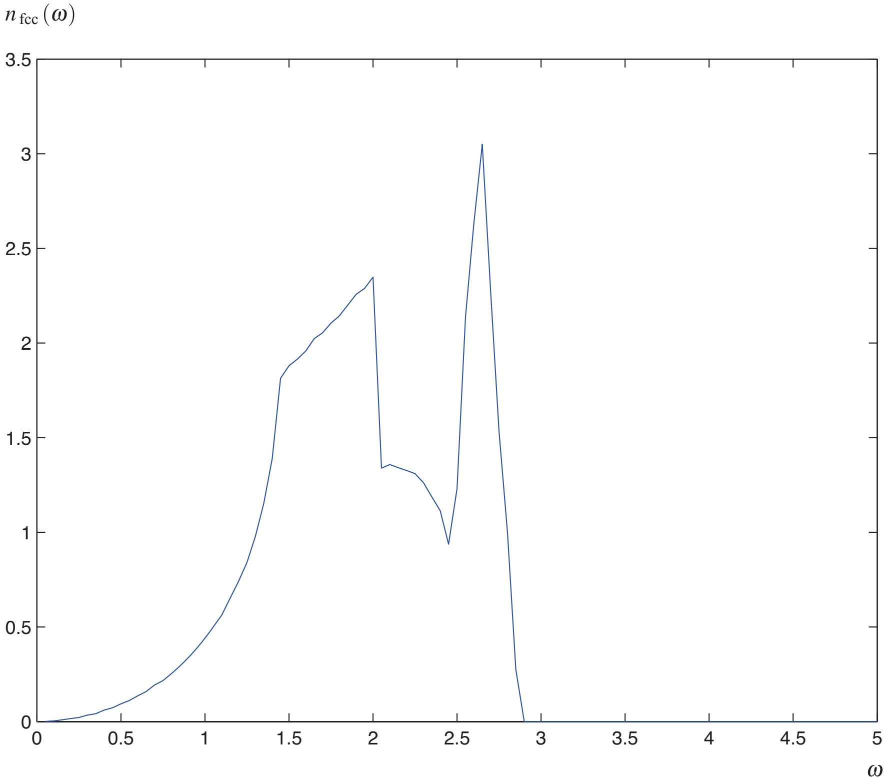

Here, 80 discretization points were chosen for $q_x \in [0, 2\pi]$. The $\omega^2$-behavior for small ω and the Van-Hove singularities at $\omega_c \approx 1.4,\ 2,\ 2.4,\ 2.8$ can be seen.

**Problem 4.9, Phonon Modes for 2-Atom 2-Dimensional Crystal**

a) For each unit cell there are apparently 8 springs, 4 in the direction of the diagonals, which couple the central mass $M_2$ with the 4 mass points $M_1$ at the corners of the square, and 4 springs, which couple the masses $M_2$ and $M_1$ each with the next similar atoms in $(1, 0)$- and $(0, 1)$-direction, respectively. According to (4.82) a single spring contributes with

$$V = \frac{k}{2}\left(\frac{\boldsymbol{\Delta R} \cdot \boldsymbol{\Delta u}}{|\boldsymbol{\Delta R}|}\right)^2$$

to the potential in harmonic approximation, where $\boldsymbol{\Delta R}$ is the connecting vector between the rest positions of the initial and final point of the relaxed spring and $\boldsymbol{\Delta u}$ is the difference vector between the displacements of the initial and final point. Therefore, $\boldsymbol{\Delta R} = (\pm\frac{a}{2}, \pm\frac{a}{2})$ applies to the 4 springs $k_1$ and $\boldsymbol{\Delta R} = (a, 0)$

or $(0, a)$ for the 4 springs $k_2$. Summation over all 8 springs then just delivers the result given in the problem formulation.

b) The claim follows from

$$M_i \ddot{u}_{\boldsymbol{R}ix} = -\frac{\partial V}{\partial u_{\boldsymbol{R}ix}}$$

taking into account the fact that each fixed $\boldsymbol{R}$ under the $\boldsymbol{R}$-sum also occurs once as $\boldsymbol{R} + \boldsymbol{\Delta}_x$ etc. In the equation of motion for $u_{\boldsymbol{R}ix}$ the 4 $u_{\boldsymbol{R}iy}$ containing summands compensate for each other.

c) The ansatz according to (4.23)–(4.25)

$$u_{\boldsymbol{R}ix} = \frac{1}{\sqrt{M_i}} w_{ix} e^{i(\boldsymbol{qR}-\omega t)}$$

yields inserted in the equations of motion

$$\begin{aligned}
\omega^2 w_{1x} = {} & \frac{2k_1}{M_1} w_{1x} - \frac{k_1}{2\sqrt{M_1 M_2}} w_{2x} \left(1 + e^{-i\boldsymbol{q\Delta}_x} + e^{-i\boldsymbol{q\Delta}_y} + e^{-i\boldsymbol{q}(\boldsymbol{\Delta}_x+\boldsymbol{\Delta}_y)}\right) \\
& - \frac{k_1}{2\sqrt{M_1 M_2}} w_{2y} \left(1 - e^{-i\boldsymbol{q\Delta}_x} - e^{-i\boldsymbol{q\Delta}_y} + e^{-i\boldsymbol{q}(\boldsymbol{\Delta}_x+\boldsymbol{\Delta}_y)}\right) \\
& + \frac{2k_2}{M_1} w_{1x} (1 - \cos(q_x a)) \\
\omega^2 w_{2x} = {} & \frac{2k_1}{M_2} w_{2x} - \frac{k_1}{2\sqrt{M_1 M_2}} w_{1x} \left(1 + e^{+i\boldsymbol{q\Delta}_x} + e^{+i\boldsymbol{q\Delta}_y} + e^{+i\boldsymbol{q}(\boldsymbol{\Delta}_x+\boldsymbol{\Delta}_y)}\right) \\
& - \frac{k_1}{2\sqrt{M_1 M_2}} w_{1y} \left(1 - e^{+i\boldsymbol{q\Delta}_x} - e^{+i\boldsymbol{q\Delta}_y} + e^{+i\boldsymbol{q}(\boldsymbol{\Delta}_x+\boldsymbol{\Delta}_y)}\right) \\
& + \frac{2k_2}{M_2} w_{2x} (1 - \cos(q_x a)),
\end{aligned}$$

from which the given representation for the $q$-dependent dynamic matrix follows.

d) A Matlab source code for the diagonalization of the dynamic matrix is given below:

```
clear;
k1=1;M1=3;k3=0.2;M2=1;im=1i;
for ix=1:120
q(ix)=ix*pi/40;
if ix<=40 qx=q(ix);qy=0;end
if ix>40&ix<=80 qx=pi;qy=(ix-40)*pi/40;end
if ix>80&ix<=120 qx=pi-(ix-80)*pi/40;qy=qx;end
d=zeros(4,4);k11=k1/M1;k12=k1/sqrt(M1*M2);k22=k1/M2;
k31=k3/M1;k32=k3/M2;
d(1,1)=2*k11;d(2,2)=2*k22;d(3,3)=2*k11;d(4,4)=2*k22;
```

```
d(1,2)=-0.5*k12*(1+exp(-im*(qx+qy))+exp(-im*qx)+exp(-im*qy));
d(1,3)=0;d(1,4)=-0.5*k12*(1+exp(-im*(qx+qy))-exp(-im*qx)-
       exp(-im*qy));
d(2,1)=-0.5*k12*(1+exp(im*(qx+qy))+exp(im*qx)+exp(im*qy));
d(2,3)=-0.5*k12*(1+exp(im*(qx+qy))-exp(im*qx)-exp(im*qy));
d(2,4)=0;
d(3,1)=conj(d(1,3));d(3,2)=conj(d(2,3));d(3,4)=d(1,2);
d(4,1)=conj(d(1,4));d(4,2)=conj(d(2,4));d(4,3)=conj(d(3,4));
d(1,1)=d(1,1)+2*k31*(1-cos(qx));d(2,2)=d(2,2)+2*k32*
       (1-cos(qx));
d(3,3)=d(3,3)+2*k31*(1-cos(qy));
d(4,4)=d(4,4)+2*k32*(1-cos(qy));
     [ev,ew] = eig(d);
eigw1(ix)=sqrt(ew(1,1));eigw2(ix)=sqrt(ew(2,2));
eigw3(ix)=sqrt(ew(3,3));eigw4(ix)=sqrt(ew(4,4));
end
plot(q,eigw1,'.',q,eigw2,'.',q,eigw3,'.',q,eigw4,'.')
```

The result is (specifically for a choice of parameters of $k_1 = 1$, $k_2 = 0.2$, $M_1 = 3$, $M_2 = 1$, $a = 1$) plotted below:

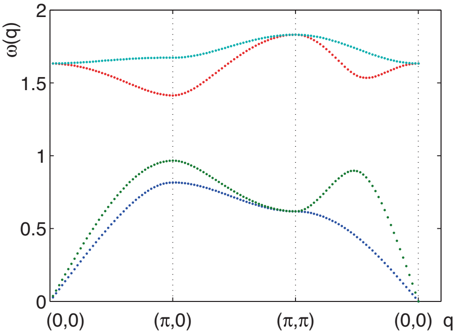

You can see the appearance of 4 phonon modes, one longitudinal acoustic (LA), one transverse acoustic (TA), one longitudinal optical (LO), and one transverse optical (TO) branch. The acoustic branches go linearly with $q$ towards 0 for $q \to 0$, the optical branches go towards a constant value for $q \to 0$. LO and TO branch are degenerate for $q \to 0$, the effect, which is mentioned in Sect. 4.7.2 (or (4.134)), that $\omega_{LO} > \omega_{TO}$ should hold for $q \to 0$ is thus not included in the simple model, because no additional restoring force was considered due to a macroscopic electric field. There are several $q$-points with $\frac{d\omega}{dq} = 0$, in particular at $\boldsymbol{q} = (\pi, 0), (\pi, \pi)$, but also at an inner $\boldsymbol{q}$-point along the diagonal. There are Van-Hove singularities to be expected there, for the chosen parameters thus at the frequencies $\omega \approx 0.6, 0.8, 0.9, 1.55, 1.65$ as well as at the edges of the spectrum, thus at $\omega = 0.95$ (upper edge of the spectrum of the acoustic branches) as well as at about $\omega = 1.4, 1.8$ (upper and lower edge of the optical phonon spectrum).

e) The Matlab code for calculating the phonon density of states:

```
clear;nmax=200;nom=400;
k1=1;M1=3;k3=0.2;M2=1;im=1i;
for iom=1:nom
om(iom)=iom*2.5/nom;rho(iom)=0;
end
for ix=1:nmax
q(ix)=ix*pi/nmax;
qx=q(ix);
for iy=1:ix
q(iy)=iy*pi/nmax;
qy=q(iy);
d=zeros(4,4);k11=k1/M1;k12=k1/sqrt(M1*M2);k22=k1/M2;
k31=k3/M1;k32=k3/M2;
d(1,1)=2*k11;d(2,2)=2*k22;d(3,3)=2*k11;d(4,4)=2*k22;
d(1,2)=-0.5*k12*(1+exp(-im*(qx+qy))+exp(-im*qx)+exp(-im*qy));
d(1,3)=0;d(1,4)=-0.5*k12*(1+exp(-im*(qx+qy))-exp(-im*qx)-
        exp(-im*qy));
d(2,1)=-0.5*k12*(1+exp(im*(qx+qy))+exp(im*qx)+exp(im*qy));
d(2,3)=-0.5*k12*(1+exp(im*(qx+qy))-exp(im*qx)-exp(im*qy));
d(2,4)=0;
d(3,1)=conj(d(1,3));d(3,2)=conj(d(2,3));d(3,4)=d(1,2);
d(4,1)=conj(d(1,4));d(4,2)=conj(d(2,4));d(4,3)=conj(d(3,4));
d(1,1)=d(1,1)+2*k31*(1-cos(qx));d(2,2)=d(2,2)+2*k32*
        (1-cos(qx));
d(3,3)=d(3,3)+2*k31*(1-cos(qy));
d(4,4)=d(4,4)+2*k32*(1-cos(qy));
[ev,ew]=eig(d);
for   iew=1:4   eigw(iew)=sqrt(ew(iew,iew));ie=ceil(eigw(iew)*
nom/2.5);
rho(ie)=rho(ie)+1;
end
end
end
s=0;
for ie=1:nom
rho(ie)=2*rho(ie)*nom/(2.5*nmax*nmax);
s=s+rho(ie)*2.5/nom;
end
s
plot(om,rho);
```

The result is—for the same parameters as in d)—shown in the following figure.

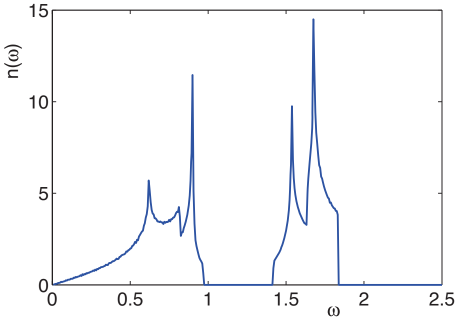

The Van-Hove singularities are clearly visible at $\omega = 0.6, 0.8, 0.9, 0.95,\ 1.4,$ $1.55,\ 1.65,\ 1.8$. At the edges of the spectrum ($\omega = 0.95, 1.4, 1.8$) there are jumps in the density of states (from 0 to a finite value), the inner Van-Hove singularities (especially at $\omega = 0.6, 0.9, 1.55, 1.65$) are logarithmic singularities. This type of Van-Hove singularity is characteristic of 2-dimensional systems.

**Problem 4.10, Van-Hove Singularities in 2 Dimensions**

Analogously to (4.113), (4.114) one has in the vicinity of a maximum of the dispersion $\omega_c$ in 2 dimensions (with $C_1,\ C_2 > 0$)

$$\omega = \omega_c - C_1\kappa_1^2 - C_2\kappa_2^2$$

For the density of states one therefore obtains:

$$n(\omega) \sim \int d^2\kappa\,\delta(\omega - \omega_c + C_1\kappa_1^2 + C_2\kappa_2^2) = \frac{1}{C_1 C_2}\int dxdy\,\delta(\omega - \omega_c + x^2 + y^2)$$
$$\sim \int drr\delta(\omega - \omega_c + r^2) \sim \int du\delta(\omega - \omega_c + u) = \begin{cases} \text{const.} & \text{für } \omega < \omega_c \\ 0 & \text{für } \omega > \omega_c \end{cases}.$$

At maxima of the dispersion, in particular at the upper edge of the spectrum, a jump in the density of states is therefore to be expected in 2-dimensional systems from a finite value to 0.

At a saddle point of the dispersion $\omega(\boldsymbol{q})$ one has

$$\omega = \omega_c - C_1\kappa_1^2 + C_2\kappa_2^2.$$

Then one obtains

$$\begin{aligned}n(\omega) &\sim \int dxdy\delta(\omega-\omega_c+x^2-y^2) \sim \int dx\frac{du}{\sqrt{u}}\delta(\omega-\omega_c+x^2-u)\\ &= \int dx\sqrt{\omega-\omega_c+x^2}\\ &= \ln(2\sqrt{\omega-\omega_c+x^2}+2x)|_0^{x_0} \sim \ln\frac{\sqrt{\omega-\omega_c+x_0^2}+2x_0}{\sqrt{\omega-\omega_c}}\\ &\sim -\frac{1}{2}\ln(\omega-\omega_c).\end{aligned}$$

So one has a logarithmic singularity at inner critical points at which a saddle point of the dispersion is present.

### Problem 4.11, Continuum Limit of the Linear Harmonic Chain

$$\begin{aligned}M\ddot{u}_n &= k(u_{n+1}+u_{n-1}-2u_n)\\ u_{n'} &= u(R_{n'}) = u(R_n) + \left.\frac{du}{dx}\right|_{R_n}(R_{n'}-R_n) + \frac{1}{2}\left.\frac{d^2}{dx^2}\right|_{R_n}(R_{n'}-R_n)^2\\ M\ddot{u}(R_n) &= k\left(u(R_n)+\frac{du}{dx}a+\frac{1}{2}\frac{d^2u}{dx^2}a^2+u(R_n)-\frac{du}{dx}a+\frac{1}{2}\frac{d^2u}{dx^2}a^2-2u(R_n)\right)\\ &= ka^2\left.\frac{d^2u}{dx^2}\right|_{R_n}.\end{aligned}$$

Assumption: slow variation of $u(R_n)$ over lengths of the order of the lattice constant. Let $R_n$ be a continuous variable $x$ and divide by $a$:

$$\rho\frac{\partial^2u(x,t)}{\partial t^2} = ka\frac{\partial^2u(x,t)}{\partial x^2}$$

with $\rho = M/a$ as linear mass density.
Continuum limit: Limit $M \to 0, a \to 0, N \to \infty, k \to \infty$ with $\rho = M/a = \text{const.}$, $f = ka = \text{const.}$, $L = Na = \text{const.}$

$$\frac{\partial^2u}{\partial x^2} - \frac{\rho}{f}\frac{\partial^2u}{\partial t^2} = 0.$$

This is the one-dimensional wave equation.
Ansatz for special solution:

$$u(x,t) = u_0e^{i(qx-\omega t)}$$

yields

$$-q^2 + \frac{\rho}{f}\omega^2 = 0, \quad \text{therefore} \quad \omega = \sqrt{\frac{f}{\rho}}q = c_s q$$

with $c_s = \sqrt{f/\rho}$ as sound velocity.
The exact dispersion relation for the linear harmonic chain

$$\omega(q) = 2\sqrt{\frac{k}{M}}\sin\left(\frac{qa}{2}\right) \approx \sqrt{\frac{ka^2}{M}}q = \sqrt{\frac{f}{\rho}}q$$

yields the same in the continuum limit.

**Problem 4.12, Phonon-Polariton Dispersion**

a)

$$\begin{aligned}
M_+\ddot{\boldsymbol{u}}_+ &= -k(\boldsymbol{u}_+ - \boldsymbol{u}_-) + e\boldsymbol{E} \\
M_-\ddot{\boldsymbol{u}}_- &= -k(\boldsymbol{u}_- - \boldsymbol{u}_+) - e\boldsymbol{E} \\
\ddot{\boldsymbol{u}} = \ddot{\boldsymbol{u}}_+ - \ddot{\boldsymbol{u}}_- &= -\left(\frac{k}{M_+} + \frac{k}{M_-}\right)(\boldsymbol{u}_+ - \boldsymbol{u}_-) + \left(\frac{e}{M_+} + \frac{e}{M_-}\right)\boldsymbol{E} \\
\rightarrow\ \ddot{\boldsymbol{u}} &= -\omega_0^2\boldsymbol{u} + e^*\boldsymbol{E} \\
\text{where} \quad \omega_0^2 &= k\frac{M_+ + M_-}{M_+M_-}, e^* = e\frac{M_+ + M_-}{M_+M_-}.
\end{aligned}$$

b)

$$\begin{aligned}
\ddot{\boldsymbol{u}} + \alpha\dot{\boldsymbol{u}} + \omega_0^2\boldsymbol{u} &= e^*\boldsymbol{E} \\
\rightarrow\ \boldsymbol{u} &= \frac{e^*}{\omega_0^2 - \omega^2 - i\alpha\omega}\boldsymbol{E}
\end{aligned}$$

as in the case of the driven damped oscillator in classical mechanics. For the frequency-dependent dielectric constant, we obtain analogously to the derivation of (4.140):

$$\varepsilon(\omega) = 1 + 4\pi\left(\gamma + \frac{\beta e^*}{\omega_0^2 - \omega^2 - i\omega\alpha}\right).$$

The dielectric constant thus becomes complex, has a real and an imaginary part, which (for $\alpha = 0.1$, $4\pi\gamma = 0.5$, $4\pi\beta e^* = 1$) are shown in the following figure.

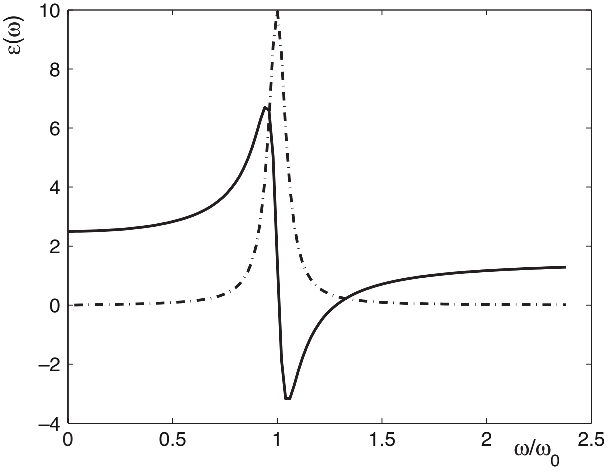

c) For $\gamma = 0$, $\varepsilon_\infty = 1$, there is no contribution to polarization for high frequencies.
d) The real and imaginary parts of $q^2(\omega)$ according to (4.146) are shown in the following figure (for the same parameters as in b)).

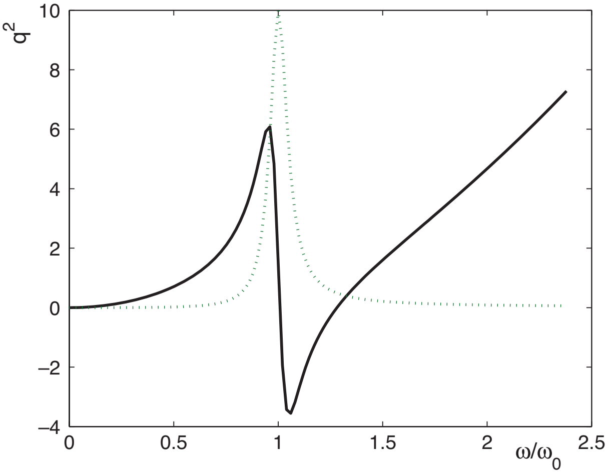

$q^2$ can therefore become negative (and has an imaginary part); this means physically exponentially decaying solutions. The resulting real part of $\omega(q)$ is shown in the following figure. There is now a third branch of ω values in the range $\omega_0 = 1 < \omega < \omega_l$; For these frequencies, $q$ has a finite imaginary part, i.e. there are no solutions propagating through the system but damped solutions (with finite penetration depth, etc.).

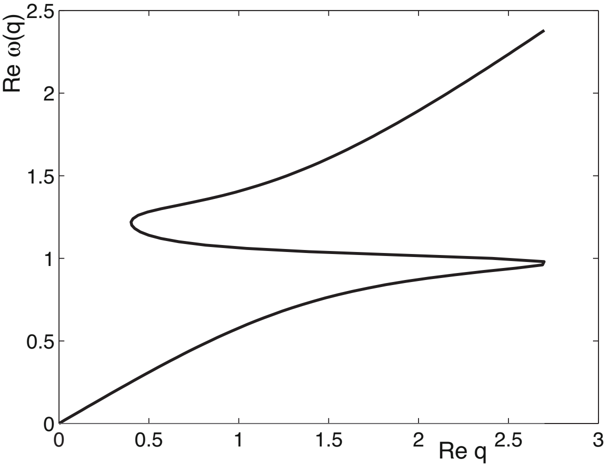

### Problem 4.13, Mean Square Displacement

$$H = \sum_{\boldsymbol{q}j} \hbar\omega_j(\boldsymbol{q}) \left( b^\dagger_{\boldsymbol{q}j} b_{\boldsymbol{q}j} + \frac{1}{2} \right).$$

a)

$$u_{n,j} = \frac{1}{\sqrt{N}} \sum_{\boldsymbol{q}} e^{i\boldsymbol{q}\boldsymbol{R}_n} \sqrt{\frac{\hbar}{2M\omega_j(\boldsymbol{q})}} \left( b_{\boldsymbol{q}j} + b^\dagger_{-\boldsymbol{q}j} \right)$$

follows from the inversion of the definition of phonon creators and annihilators:

$$\begin{aligned} b_{qj} &= \frac{1}{\sqrt{N}} \sum_{\boldsymbol{R}} e^{-i\boldsymbol{q}\boldsymbol{R}} \left( \sqrt{\frac{M\omega_j(q)}{2\hbar}} u_{Rj} + i \sqrt{\frac{1}{2M\hbar\omega_j(q)}} p_{Rj} \right) \\ b^\dagger_{qj} &= \frac{1}{\sqrt{N}} \sum_{\boldsymbol{R}} e^{i\boldsymbol{q}\boldsymbol{R}} \left( \sqrt{\frac{M\omega_j(q)}{2\hbar}} u_{Rj} - i \sqrt{\frac{1}{2M\hbar\omega_j(q)}} p_{Rj} \right). \end{aligned}$$

b)

$$\langle \boldsymbol{u}_n \rangle = \frac{1}{\sqrt{N}} \sum_{q} e^{i\boldsymbol{q}\boldsymbol{R}_n} \sqrt{\frac{\hbar}{2M\omega_j(\boldsymbol{q})}} \left( \langle b_{\boldsymbol{q}j} \rangle + \langle b^\dagger_{-\boldsymbol{q}j} \rangle \right) = 0$$

since the equilibrium expectation values have to be taken with respect to H and all diagonal elements of creation and annihilation operators alone vanish in the eigen representation, since the application of these operators always yields a state with an increased or decreased occupation number, thus another eigenstate.

c)

$$\begin{aligned}
\langle \boldsymbol{u}_n^2 \rangle &= \sum_j \langle u_{nj}^2 \rangle \\
&= \frac{1}{N} \sum_{\boldsymbol{q}\boldsymbol{q}'j} e^{i\boldsymbol{q}\boldsymbol{R}_n + i\boldsymbol{q}'\boldsymbol{R}_n} \frac{\hbar}{2M} \frac{1}{\sqrt{\omega_j(\boldsymbol{q})\omega_j(\boldsymbol{q}')}} \Big( \langle b_{\boldsymbol{q}j} b_{\boldsymbol{q}'j} \rangle + \langle b^\dagger_{-\boldsymbol{q}j} b^\dagger_{-\boldsymbol{q}'j} \rangle \\
&\quad + \langle b_{\boldsymbol{q}j} b^\dagger_{-\boldsymbol{q}'j} \rangle + \langle b^\dagger_{-\boldsymbol{q}j} b_{\boldsymbol{q}'j} \rangle \Big) \\
&= \frac{1}{N} \sum_{\boldsymbol{q}j} \frac{1}{2M\omega_j(\boldsymbol{q})} \Big( 2 \langle b^\dagger_{\boldsymbol{q}j} b_{\boldsymbol{q}j} \rangle + 1 \Big) \\
&= \frac{1}{2M} \int d\omega n(\omega) \left( 2 \frac{1}{e^{\beta\hbar\omega} - 1} + 1 \right) \frac{1}{\omega} \\
&= \frac{1}{2M} \int d\omega n(\omega) \frac{1}{\omega} \coth\left( \frac{\beta\hbar\omega}{2} \right)
\end{aligned}$$

with the phonon density of states] (cf. (4.92))

$$n(\omega) = \frac{1}{N} \sum_{\boldsymbol{q}j} \delta(\omega - \omega_j(\boldsymbol{q})).$$

d) According to Sect. 4.6.2 the phonon density of states fulfills for small ω in dimension $d$, (see (4.106–4.108))

$$n(\omega) \sim \omega^{d-1}.$$

Because of $\coth(x) \sim \frac{1}{x}$ for small $x$ it follows that

$$\langle \boldsymbol{u}_n^2 \rangle \sim \int_0^{\cdots} d\omega \omega^{d-1} \frac{2}{\omega^2}$$

therefore this integral diverges for $d=1,2$ and thus also $\langle \boldsymbol{u}_n^2 \rangle$, while for $d=3$ it remains finite. But a divergence of the displacement square means an instability of the crystal against such displacements. Real 1- and 2-dimensional crystals are therefore not stable. There are strictly speaking no (thermodynamically stable) crystalline orders in dimension $d=1$ and $d=2$. This can be shown in general (special case of the so-called Mermin-Wagner theorem).[1]

e) For high temperatures the asymptotics $\coth(\beta\hbar\omega/2) \approx \frac{2k_BT}{\hbar\omega}$ applies throughout the frequency range (non-vanishing density of states). Then it follows

$$\langle \boldsymbol{u}_n^2 \rangle = \frac{k_B T}{\hbar M} \int d\omega \frac{n(\omega)}{\omega^2}.$$

---

[1] That there are nevertheless now real 2-dimensional crystals like graphene and these are apparently stable can be understood by anharmonic corrections and possible displacements of the atoms into the 3rd dimension, with which also the rippling (deviations from the exactly planar structure) can be explained.

f) In the Debye model,

$$n_D(\omega) = \frac{3a^3}{2\pi^2 c^3}\omega^2 \quad \text{für} \quad \omega \le \omega_D = c\left(6\pi^2\frac{N}{V}\right)^{1/3}$$

applies (cf. (4.69), (4.109)). This gives:

$$\langle \boldsymbol{u}_n^2\rangle = \frac{k_B T}{\hbar M}\int_0^{\omega_D} d\omega n_D(\omega)\frac{1}{\omega^2} = \frac{k_B T}{\hbar M}\frac{3a^3}{2\pi^2 c^3}\omega_D = \frac{9k_B T}{\hbar M}\frac{1}{\omega_D^2}.$$

g)

$$k_B T_s = M\hbar x_s^2 a^2 \frac{\omega_D^2}{9}.$$

This predicts a dependence of the melting temperature on ion mass, lattice constant and Debye frequency.

**Problem 4.14, Particle Scattering on Phonons**
For thermal neutrons it applies:

$$\langle E_{\text{kin}}\rangle = \left\langle \frac{M}{2}v^2\right\rangle = \frac{3}{2}k_B T \approx 0.04\,\text{eV}$$

at room temperature. So the energies are in the correct order of magnitude of phonon energies. For the velocity, the order of magnitude results in

$$v \approx \sqrt{\frac{E_{\text{kin}}}{M}} \approx 2\times 10^3\,\frac{\text{m}}{\text{s}}\,,$$

(using $M = 1.6\times 10^{-27}$ kg). This results in an impulse in the order of magnitude of $p \approx 3\times 10^{-24}\,\text{kg}\,\frac{\text{m}}{\text{s}} = \hbar q$ (according to the de Broglie relation), from which the wave number follows $q \approx 3\times 10^{10}\,\text{m}^{-1} = 3\,\text{Å}^{-1}$. So for thermal neutrons, both energy and impulse (wave vector) have just the right order of magnitude of phonon energies and impulses. For visible light, photons have an energy of the order of a few eV, but wave numbers of the order of $10^{-4}\,\text{Å}^{-1}$. Therefore, phonons can only be excited in the limit of small $q$ by light scattering. X-ray quanta of the energy of a few keV have $q$ values of the correct order of magnitude, but the relative energy transfer by a phonon is of the order of $10^{-5}$–$10^{-6}$ and therefore usually not resolvable.

**Problem 4.15, Anharmonic Corrections**

$$H = \frac{p^2}{2M} + \frac{k}{2}x^2 - \alpha x^3 = \hbar\omega\left(b^\dagger b + \frac{1}{2}\right) - \alpha x^3 \quad \text{with} \quad \omega = \sqrt{\frac{k}{M}},\ (\alpha > 0).$$

a) Perturbation theory of quantum mechanics yields:

$$|n\rangle = |n\rangle^0 + \sum_{m\neq n}|m\rangle^0 \frac{{}^0\langle m| - \alpha x^3|n\rangle^0}{E_n^0 - E_m^0}.$$

Then it follows (since all matrix elements are real for the oscillator)

$$\begin{aligned}\langle n|x|n\rangle &= -\frac{2\alpha}{\hbar\omega}\sum_{m\neq n}\frac{{}^0\langle n|x|m\rangle^0\;{}^0\langle m|x^3|n\rangle^0}{n-m}\\ &= \frac{2\alpha}{\hbar\omega}\left(\frac{\hbar}{2M\omega}\right)^2\sum_{m\neq n}\frac{{}^0\langle n|(b+b^\dagger)|m\rangle^0\;{}^0\langle m|(b+b^\dagger)^3|n\rangle^0}{n-m}\\ &= -\frac{\alpha\hbar}{2M^2\omega^3}\Big[\sqrt{n}\;{}^0\langle n-1|(b+b^\dagger)^3|n\rangle^0\\ &\qquad -\sqrt{n+1}\;{}^0\langle n+1|(b+b^\dagger)^3|n\rangle^0\Big].\end{aligned}$$

The factor 2 arises here because the perturbed state $|n\rangle$ occurs once as a ket and once as a bra in the expectation value formation. Now it holds

$$C := (b+b^\dagger)^3 = b^3 + b^{\dagger 3} + b^\dagger b^2 + bb^\dagger b + b^2 b^\dagger + b^{\dagger 2} b + b^\dagger b b^\dagger + b b^{\dagger 2}.$$

For the matrix elements between the unperturbed oscillator states $|n \pm 1\rangle$ and $|n\rangle$ it follows

$$\begin{aligned}{}^0\langle n-1|C|n\rangle^0 &= \sqrt{n}(n-1) + n\sqrt{n} + (n+1)\sqrt{n} = 3n\sqrt{n}\\ {}^0\langle n+1|C|n\rangle^0 &= \sqrt{n+1}n + (n+1)\sqrt{n+1}(n+2)\sqrt{n+1}\\ &= 3(n+1)\sqrt{n+1}.\end{aligned}$$

As a result, finally:

$$\begin{aligned}\langle n|x|n\rangle &= -\frac{\alpha\hbar}{2M^2\omega^3}\left[3n^2 - 3(n+1)^2\right] = \frac{3\alpha\hbar}{2M^2\omega^3}(2n+1)\\ &= \frac{3\alpha}{M^2\omega^4}\left(n+\frac{1}{2}\right)\hbar\omega = \frac{3\alpha}{M^2\omega^4}E_n.\end{aligned}$$

b) For the thermodynamic expectation value, one obtains

$$\langle x\rangle = \frac{3\alpha}{M^2\omega^4}\frac{1}{\mathcal{Z}}\sum_n E_n e^{-\beta E_n} = \frac{3\alpha}{M^2\omega^4}\langle H_0\rangle.$$

Here, it was taken into account that non-vanishing expectation values are already linear in the perturbation, so that the thermal average can be formed with the unperturbed Hamilton operator. As a result, one obtains

$$\langle x\rangle = \frac{3\alpha}{M^2\omega^4}\hbar\omega\left(\frac{1}{e^{\beta\hbar\omega}-1}+\frac{1}{2}\right).$$

For high temperatures, one obtains

$$\langle x\rangle = \frac{3\alpha}{M^2\omega^4}(k_B T).$$

This can be interpreted as the simplest model for thermal expansion. However, the expansion of the perturbation is only meaningful for states $|n\rangle$ whose eigenenergies are below the potential maximum; an $x^3$-potential in the area "behind" the maximum is physically not meaningful.

## 8.4 Solution of the Problems for Chap. 5

**Problem 5.1, Electron in the Superposition Potential of Several "Nuclei"**
Below is a Matlab source code that sets an attractive box potential $v(x) = -v_0$ for $na < x < na + b$) for $b = 0.6$ at 4 randomly selected sites $n$ of a system of 20 sites.

```
clear all;
v0=50;
for ix=1:6
     vv(ix)=-v0;
end
for i=1:200
     for j=1:200
          h(i,j)=0;
     end
     v(i)=0;
end
for nzuf=1:4
     n(nzuf)=ceil(20*rand)-1;
     for ix=1:6
          v(10*n(nzuf)+ix)=vv(ix);
     end
end
for i=1:200
     x(i)=i*0.1;
     h(i,i)=2+v(i)*0.01;
     ip1=i+1;if ip1>200 ip1=ip1-200;end
     h(i,ip1)=-1;
     h(ip1,i)=-1;
end
     [ev,ew]=eig(h);
for iw=1:40
     en(iw)=ew(iw,iw)/0.01;
end
figure(1);plot(x,v)
figure(2);plot(x,ev(:,1),x,ev(:,2),x,ev(:,3))
figure(3);plot(en,'.')
```

If you have only one potential well with, you get two bound states with energies $E_1$ = -38.17, $E_2$ = -8.42. With 4 potential wells, you get 4 bound states each with energies in the vicinity of $E_1$ and 4 with energies from an interval around $E_2$. The lowest eigenenergies and eigenstates are shown below. The number of potential wells, their distance, etc. can still be varied.

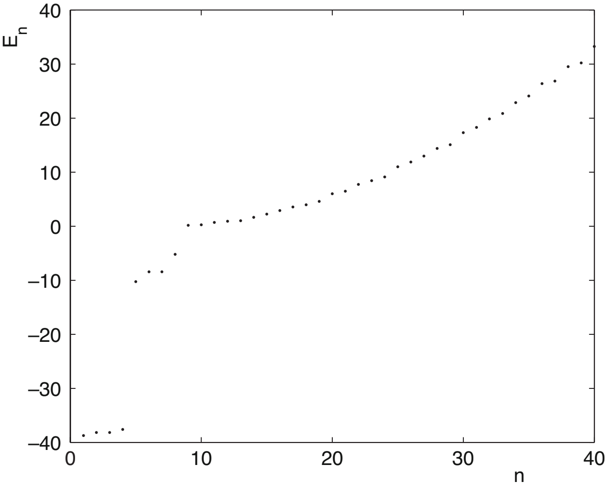

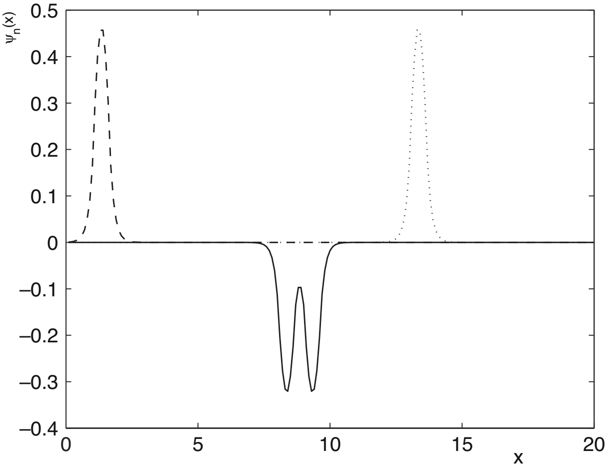

## Problem 5.2, Attractive Kronig-Penney Model

$$-\frac{\hbar^2}{2m}\frac{d^2\psi}{dx^2} + V(x)\psi(x) = \varepsilon\psi(x)$$

$$\text{with} \quad V(x) = -v_0 \sum_n \delta(x - na) \ (v_0 > 0)$$

is solved by the given approach with

$$\varepsilon = -\frac{\hbar^2\kappa^2}{2m} < 0,$$

since the potential in the intermediate area $na < x < (n+1)a$ between 2 "atoms" disappears.
Jump condition at $na$:

$$\begin{aligned}\psi'(na+0) - \psi'(na-0) &= -\frac{2mv_0}{\hbar^2}\psi(na)\\ \kappa C_n - \kappa D_n - C_{n-1}\kappa e^{\kappa a} + D_{n-1}e^{-\kappa a} &= -\frac{2mv_0}{\hbar^2}(C_n + D_n).\end{aligned}$$

From the continuity at $na$ it follows:

$$C_n + D_n = C_{n-1}e^{\kappa a} + D_{n-1}e^{-\kappa a}.$$

From the Bloch theorem it follows:

$$\psi(x+a) = e^{ika}\psi(x) \;\rightarrow\; \psi'(x+a) = e^{ika}\psi'(x)$$
$$e^{ika}(C_{n-1} + D_{n-1}) = C_n + D_n, \quad e^{ika}(C_{n-1} - D_{n-1}) = C_n - D_n.$$

Thus,

$$\begin{aligned}e^{ika}C_{n-1} - e^{ika}D_{n-1} - e^{\kappa a}C_{n-1} + e^{-\kappa a}D_{n-1} &= -\frac{2mv_0}{\hbar^2\kappa}\left(e^{ika}C_{n-1} + e^{ika}D_{n-1}\right)\\ e^{ika}C_{n-1} + e^{ika}D_{n-1} &= e^{\kappa a}C_{n-1} + e^{-\kappa a}D_{n-1}\end{aligned}$$

is a homogeneous system of equations for the coefficients $C_{n-1}, D_{n-1}$:

$$\begin{aligned}\left(e^{ika} - e^{\kappa a} + \frac{2mv_0}{\hbar^2\kappa}e^{ika}\right)C_{n-1} + \left(e^{-\kappa a} - e^{ika} + \frac{2mv_0}{\hbar^2\kappa}e^{ika}\right)D_{n-1} &= 0\\ \left(e^{ika} - e^{\kappa a}\right)C_{n-1} + \left(e^{ika} - e^{-\kappa a}\right)D_{n-1} &= 0.\end{aligned}$$

Non-trivial solutions exist if the determinant vanishes:

$$\begin{aligned}&e^{2ika} - e^{ika}e^{\kappa a} - e^{ika}e^{-\kappa a} + 1 + \frac{2mv_0}{\hbar^2\kappa}(e^{2ika} - e^{ika}e^{-\kappa a})\\ &- e^{ika}e^{-\kappa a} + 1 + e^{2ika} - e^{ika}e^{\kappa a} - \frac{2mv_0}{\hbar^2\kappa}(e^{2ika} - e^{ika}e^{\kappa a}) = 0.\end{aligned}$$

This leads—after excluding and shortening of $4e^{ika}$—to

$$\cos(ka) - \cosh(\kappa a) + \frac{mv_0}{\hbar^2\kappa}\sinh(\kappa a) = 0,$$

which is equivalent to the given relation

$$\kappa\cosh(\kappa a) - \frac{mv_0}{\hbar^2}\sinh(\kappa a) = \kappa\cos(ka).$$

Obviously, there can only be bound solutions (to negative energy eigenvalues) if the following inequality is valid:

$$|f(\kappa a)| = \left|\cosh(\kappa a) - \frac{\tilde{v_0}}{\kappa a}\sinh(\kappa a)\right| < 1$$

with $\tilde{v_0} = mv_0 a/\hbar^2$. In the area of $0 < x = \kappa a < 4$ the function $f(x)$ is plotted for 3 different values of $\tilde{v_0}$ (2,2.5,3) below. It can be seen that there is a finite range of κ values and thus energies, for which $-1 < f(x) < 1$ applies, so that the condition equation is satisfiable for certain $k$. There is therefore exactly one energy band of bound eigenenergies, which becomes narrower with increasing potential strength and moves to larger κ and thus lower energies.

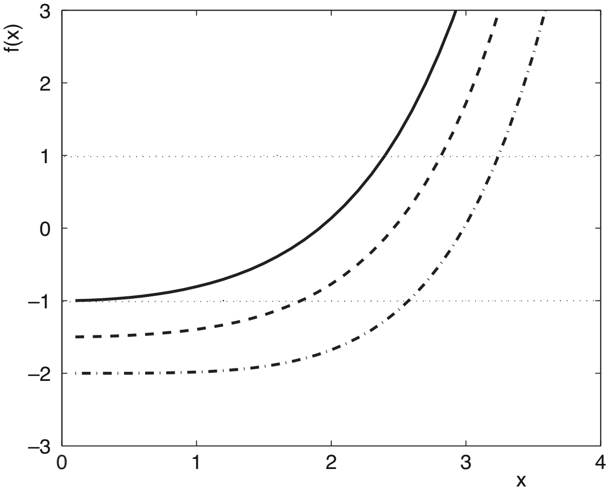

By (graphical or numerical) solving the condition equation, one obtains $\kappa(k)$ and from this $\varepsilon(k)$, which is shown in the two following plots for $\tilde{v_0} = 3$.

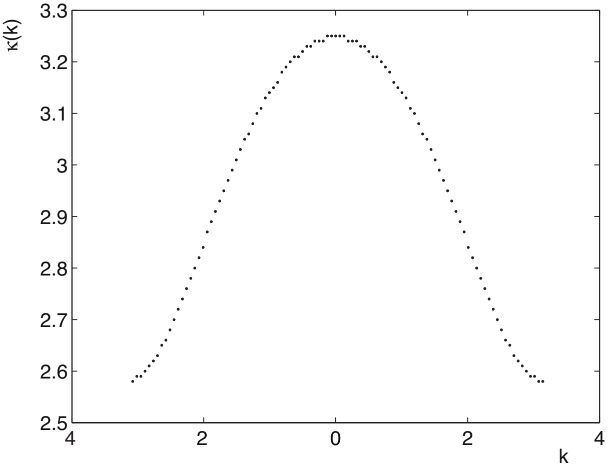

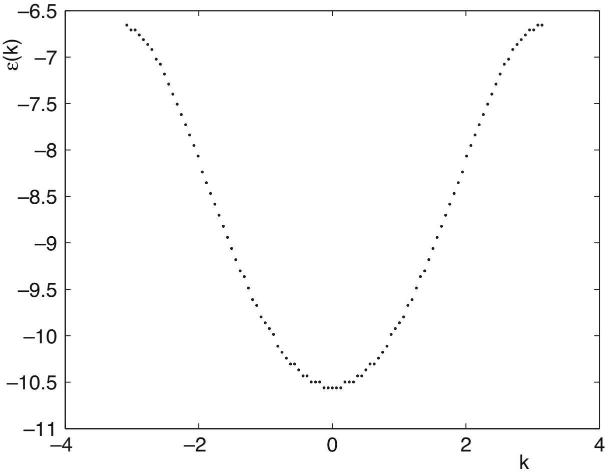

### Problem 5.3, Kronig-Penney Model with Potential Wells of Finite Width

$$V(x) = \begin{cases} -v_0 & \text{for } na < x < na + b \\ 0 & \text{for } na + b < x < (n+1)a \end{cases} \quad (b < a),$$

$$-\frac{\hbar^2}{2m}\frac{d^2\psi}{dx^2} + V(x)\psi(x) = E\psi(x).$$

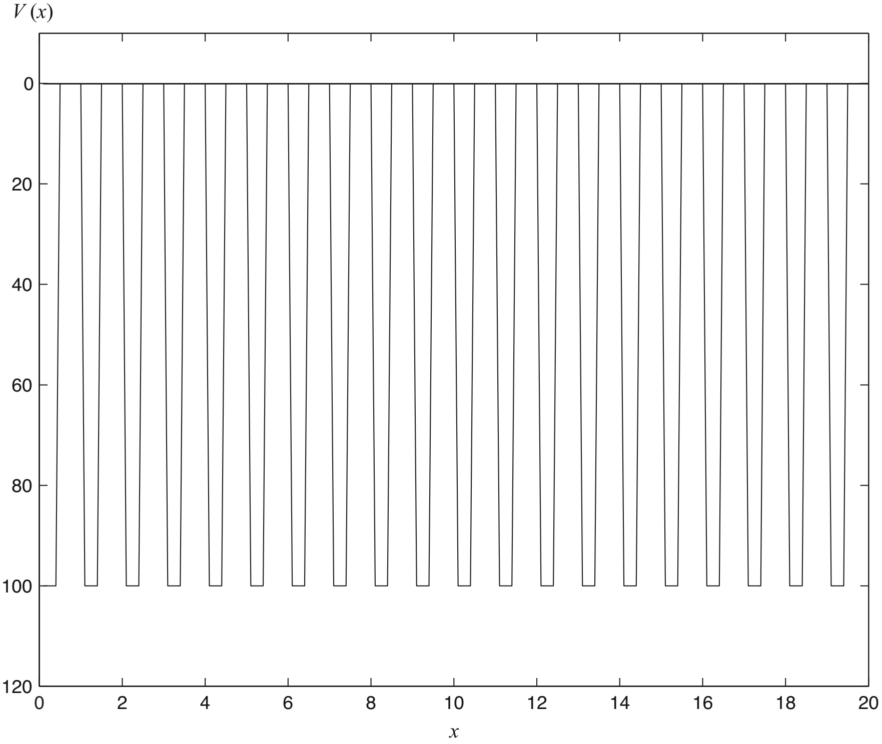

Discrete Schrödinger equation:

$$-\psi_{i+1} - \psi_{i-1} + 2 * \psi_i + V(x_i) * h * h * \psi_i = E * h * h * \psi_i$$

with $x_i = i * h, i = 1, \ldots, 200.$

Matlab source code:

```
clear;
h=zeros(200,200);
v=zeros(200);
for i=1:200
x(i)=i*0.1;
end
for n=0:19
for i=1:4
v(10*n+i)=-100;
end
end
for i=1:200
```

```
h(i,i)=2*1+v(i)*0.01;
if i<=199 h(i,i+1)=-1; end
if i>=2 h(i,i-1)=-1; end
end
h(1,200)=-1;
h(200,1)=-1;
[ev,ew]=eig(h);
for j=1:40
k(j)=j;
eps(j)=ew(j,j)/0.02;
end
figure(1); plot(x,ev(:,5))
figure(2); plot(eps,'x')
figure(3); plot(x,v)
```

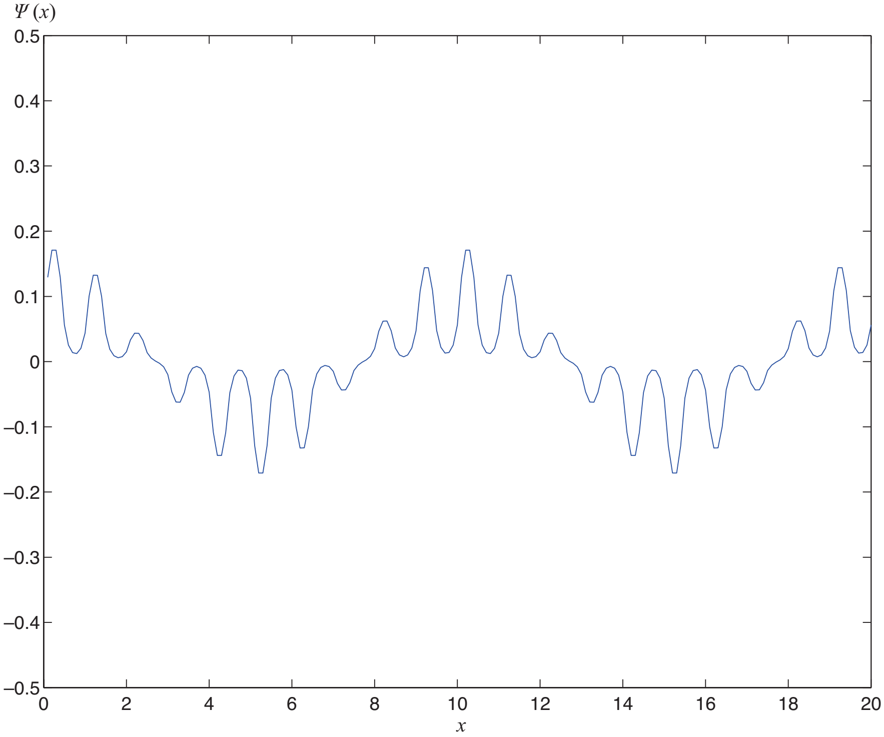

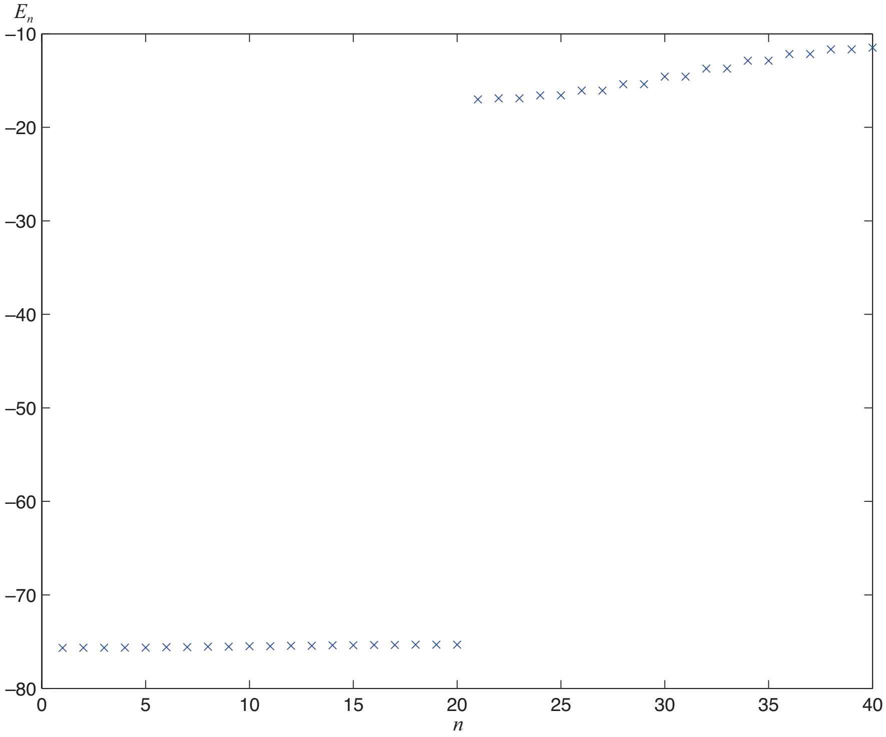

The 5th Bloch function and the lowest 40 energy eigenvalues are plotted for $v_0 = 100$ in the above plots. The Bloch function is clearly seen to be composed of a plane wave with wavelength of about 10 *a* multiplied by a periodic component localized on the unit cell (Bloch factor). In the eigenvalues, the formation of 2 bands with negative energy, a low lying and almost dispersionless one and one with stronger dispersion is seen.

### Problem 5.4, Bloch Factors for the Kronig-Penney Model

Boundary value (eigenvalue) equation:

$$-\frac{\hbar^2}{2m}\frac{d^2u_k}{dx^2} - \frac{\hbar^2 ik}{m}\frac{du_k}{dx} + \frac{\hbar^2k^2}{2m}u_k + V(x)u_k(x) = E_k u_k(x)$$

discrete version:

$$-u_{n+1} - u_{n-1} + 2u_n - ik(u_{n+1} - u_{n-1})h + (k^2 + V(x_n))u_n h^2 = Eu_n h^2.$$

Matlab source code for dispersions:

```
clear;
xx=zeros(400);
im=1.0i;
h=zeros(10,10);
v=zeros(10);
for i=1:10
x(i)=i*0.1;
end
for i=1:4
v(i)=-100;
end
%ik=110
for ik=1:200
k(ik)=-pi+(ik-1)*2*pi/200;
kim=k(ik)*im;
for i=1:10
h(i,i)=-2-(v(i)+k(ik)*k(ik))*0.01;
if i<=9 h(i,i+1)=1+kim*0.1; end
if i>=2 h(i,i-1)=1-kim*0.1; end
end
h(1,10)=1-kim*0.1;
h(10,1)=1+kim*0.1;
[ev,ew]=eig(h);
eps(ik,1)=-ew(10,10)/0.01;
eps(ik,2)=-ew(9,9)/0.01;
eps(ik,3)=-ew(8,8)/0.01;
end
figure(1); plot(k,eps(:,1),k,eps(:,2),k,eps(:,3))
figure(2); plot(x,ev(:,9))
```

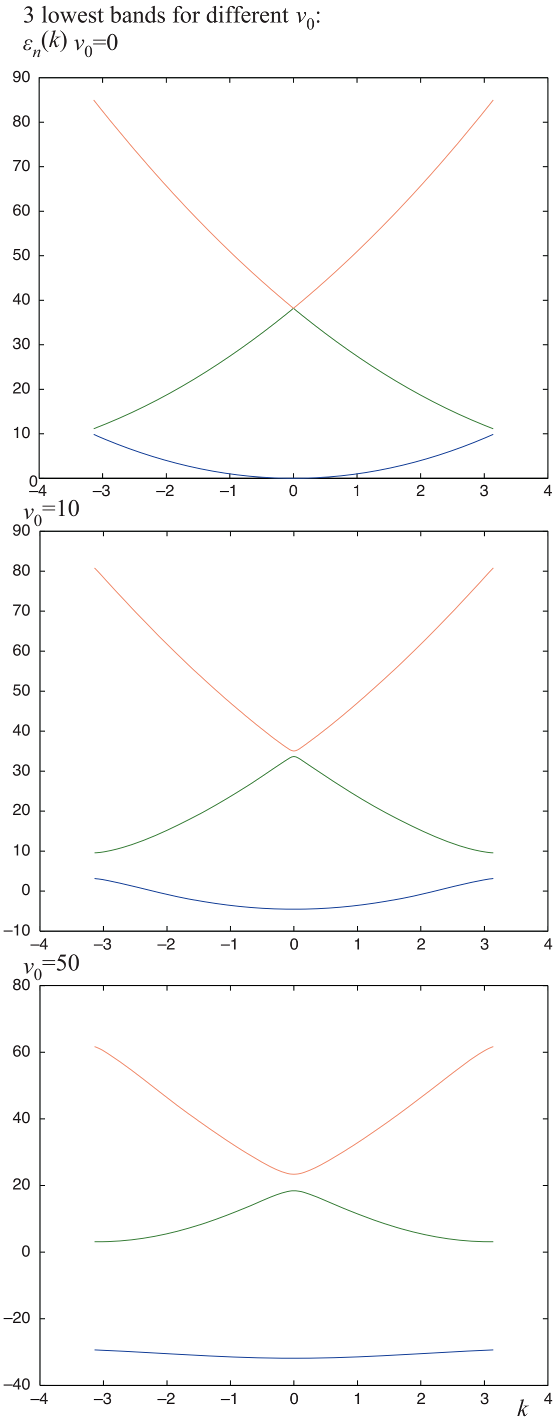
3 lowest bands for different $v_0$:
$\varepsilon_n(k)$ $v_0$=0
90
80
70
60
50
40
30
20
10
0
−4
−3
−2
−1
0
1
2
3
4
$v_0$=10
90
80
70
60
50
40
30
20
10
0
−10
−4
−3
−2
−1
0
1
2
3
4
$v_0$=50
80
60
40
20
0
−20
−40
−4
−3
−2
−1
0
1
2
3
4
$k$

Bands for $v_0$=100 (cf. Task 5.3):

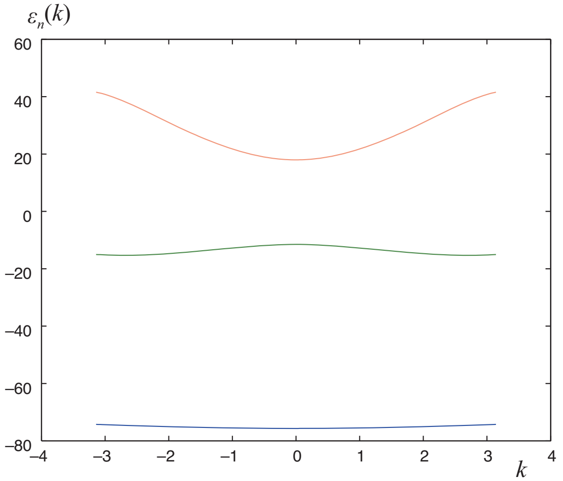

Bloch function for $v_0 = 30$:

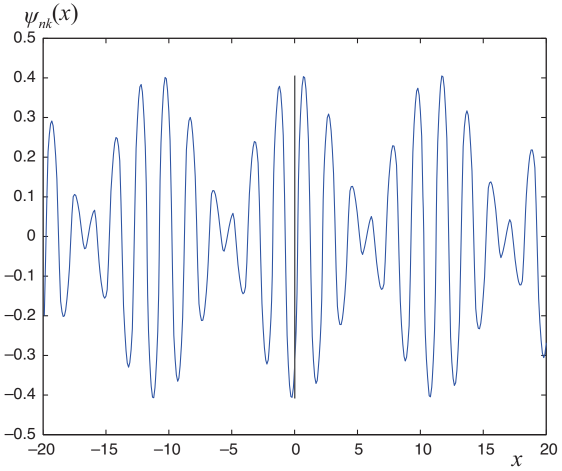

## Problem 5.5, Cosine Potential

$$V(x) = \frac{v_0}{2}\left(e^{iG_a x} + e^{-iG_a x}\right) \quad \text{where} \quad G_a = \frac{2\pi}{a}.$$

The potential has exactly two non-vanishing Fourier coefficients. From (5.34) it follows in this special case:

$$\left(\frac{\hbar^2}{2m}(k - G_0)^2 - \varepsilon\right)c_{k-G_0} + \frac{v_0}{2}c_{k-G_0+G_a} + \frac{v_0}{2}c_{k-G_0-G_a} = 0.$$

Explicitly written out for $G_0 = 0, \pm G_a$ this gives:

$$\left(\frac{\hbar^2}{2m}(k-G_a)^2-\varepsilon\right)c_{k-G_a}+\frac{v_0}{2}c_k+\frac{v_0}{2}c_{k-2G_a}=0$$
$$\left(\frac{\hbar^2}{2m}k^2-\varepsilon\right)c_k+\frac{v_0}{2}c_{k-G_a}+\frac{v_0}{2}c_{k+G_a}=0$$
$$\left(\frac{\hbar^2}{2m}(k+G_a)^2-\varepsilon\right)c_{k+G_a}+\frac{v_0}{2}c_k+\frac{v_0}{2}c_{k+2G_a}=0.$$

If one neglects the coefficients $c_{k\pm 2G_a}$ to "higher" bands, one obtains:

$$c_{k\pm G_a}=-\frac{v_0}{2\left(\frac{\hbar^2}{2m}(k\pm G_a)^2-\varepsilon\right)}c_k$$

and thus

$$\varepsilon=\frac{\hbar^2k^2}{2m}-\frac{v_0^2}{4}\frac{1}{\frac{\hbar^2(k+G_a)^2}{2m}-\varepsilon}-\frac{v_0^2}{4}\frac{1}{\frac{\hbar^2(k-G_a)^2}{2m}-\varepsilon}.$$

In the range $k<0$ ($k>0$) one can replace $k+G_a$ ($k-G_a$) in the denominator $\varepsilon$ by the zeroth approximation $\hbar^2k^2/2m$ and it remains a quadratic equation with solution:

$$\varepsilon=\frac{1}{2}\left(a_{kG_a}\pm\sqrt{a_{kG_a}^2+4b_{kG_a}}\right)$$
$$\text{with}\quad a_{kG_a}=\frac{\hbar^2k^2}{2m}+\frac{\hbar^2(k+G_a)^2}{2m}-\frac{mv_0^2}{\hbar^2(2G_a^2-4kG_a)}$$
$$\text{and}\quad b_{kG_a}=\frac{v_0^2}{4}\frac{2G_a^2+k^2}{G_a^2-2kG_a}-\frac{\hbar^4}{4m^2}k^2(k+G_a)^2.$$

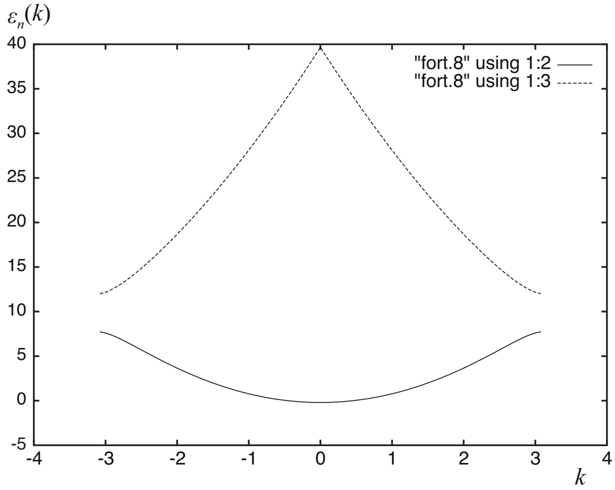

The figure shows the two lowest bands of the cosine potential for potential strength $v_0 = 2$.

### Problem 5.6, Symmetry of the Band Structure

First of all:

$$\hat{D}Hf(\boldsymbol{r}) = \hat{D}\left( (\frac{\boldsymbol{p}^2}{2m} + V(\boldsymbol{r}))f(\boldsymbol{r}) \right) = \left( \frac{\boldsymbol{p}^2}{2m} + V(\underline{\underline{D}}\boldsymbol{r}) \right) f(\underline{\underline{D}}\boldsymbol{r}) = H\hat{D}f(\boldsymbol{r})$$

Here it was used that the orthogonal transformation (rotation, etc.) $\underline{\underline{D}}$ leaves scalars and therefore scalar products invariant, so that:

$$\begin{aligned} V(\underline{\underline{D}}\boldsymbol{r}) &= \sum_{\boldsymbol{R}} v(|\underline{\underline{D}}\boldsymbol{r} - \boldsymbol{R}|) = \sum_{\boldsymbol{R}} v(|\underline{\underline{D}}(\boldsymbol{r} - \underline{\underline{D}}^{-1}\boldsymbol{R})|) \\ &= \sum_{\boldsymbol{R}'} v(|\underline{\underline{D}}(\boldsymbol{r} - \boldsymbol{R}')|) = \sum_{\boldsymbol{R}'} v(|\boldsymbol{r} - \boldsymbol{R}'|) = V(\boldsymbol{r}). \end{aligned}$$

Here it was used that for each lattice vector $\boldsymbol{R}$ also $\boldsymbol{R}' = \underline{\underline{D}}\boldsymbol{R}$ is a lattice vector according to the assumption. So:

$$H\psi_{\boldsymbol{k}}(\underline{\underline{D}}\boldsymbol{r}) = H\hat{D}\psi_{\boldsymbol{k}}(\boldsymbol{r}) = \hat{D}H\psi_{\boldsymbol{k}}(\boldsymbol{r}) = \varepsilon(\boldsymbol{k})\hat{D}\psi_{\boldsymbol{k}}(\boldsymbol{r}) = \varepsilon(\boldsymbol{k})\psi_{\boldsymbol{k}}(\underline{\underline{D}}\boldsymbol{r}).$$

Therefore, $\psi_{\boldsymbol{k}}(\underline{\underline{D}}\boldsymbol{r})$ is an eigenstate of $H$ which has the same eigenvalue as $\psi_{\boldsymbol{k}}(\boldsymbol{r})$.

However, the Bloch function is supposed to be a common eigenstate of $H$ and the translation operator $T_{\boldsymbol{R}}$. Application of this operator yields:

$$T_{\boldsymbol{R}}\psi_{\boldsymbol{k}}(\underline{\underline{D}}\boldsymbol{r}) = \psi_{\boldsymbol{k}}(\underline{\underline{D}}(\boldsymbol{r} + \boldsymbol{R})) = \psi_{\boldsymbol{k}}(\underline{\underline{D}}\boldsymbol{r} + \boldsymbol{R}') = e^{i\boldsymbol{k}\boldsymbol{R}'}\psi_{\boldsymbol{k}}(\underline{\underline{D}}\boldsymbol{r})$$

with $\boldsymbol{R}' = \underline{\underline{D}}\boldsymbol{R}$ another (rotated) lattice vector. But now:

$$\boldsymbol{k}\boldsymbol{R}' = \boldsymbol{k}\underline{\underline{D}}\boldsymbol{R} = \underline{\underline{D}}\boldsymbol{k}'\underline{\underline{D}}\boldsymbol{R} = \boldsymbol{k}'\boldsymbol{R} = \underline{\underline{D}}^{-1}\boldsymbol{k}\boldsymbol{R},$$

where $\boldsymbol{k} = \underline{\underline{D}}\boldsymbol{k}'$ is to apply. So:

$$T_{\boldsymbol{R}}\psi_{\boldsymbol{k}}(\underline{\underline{D}}\boldsymbol{r}) = e^{i\underline{\underline{D}}^{-1}\boldsymbol{k}\boldsymbol{R}}\psi_{\boldsymbol{k}}(\underline{\underline{D}}\boldsymbol{r}).$$

Therefore,

$$\psi_{\boldsymbol{k}}(\underline{\underline{D}}\boldsymbol{r})$$

is a common eigenfunction of $H$ and $T_{\boldsymbol{R}}$ to the wave vector $\underline{\underline{D}}^{-1}\boldsymbol{k}$, so

$$\psi_{\boldsymbol{k}}(\underline{\underline{D}}\boldsymbol{r}) = \psi_{\underline{\underline{D}}^{-1}\boldsymbol{k}}(\boldsymbol{r}) \quad \varepsilon(\boldsymbol{k}) = \varepsilon(\underline{\underline{D}}^{-1}\boldsymbol{k}).$$

**Problem 5.7, Kronig-Penney Model in Tight-Binding Approximation**
Atomic problem:

$$-\frac{\hbar^2}{2m}\phi''(x) - v_0\delta(x)\phi(x) = E\phi(x).$$

Ansatz:

$$\phi(x) = Ae^{-\kappa|x|}$$

solves the Schrödinger equation with:

$$E = -\frac{\hbar^2\kappa^2}{2m},$$

if the boundary condition

$$\phi'(0+\delta) - \phi'(0-\delta) = -\frac{2mv_0}{\hbar^2}\phi(0)$$

is fulfilled, i.e. for

$$\kappa = \frac{mv_0}{\hbar^2} \quad \text{and} \quad E = -\frac{m}{2\hbar^2}v_0^2.$$

From the normalization it follows

$$A = \sqrt{\kappa}.$$

So atomic wave function of the (one) bound state:

$$\phi(x) = \sqrt{\kappa}e^{-\kappa|x|}.$$

In a periodic arrangement of atomic potentials, the overlap matrix elements between atomic wave functions at 0 and at $a$ are to be calculated in the tight binding approximation according to (5.85–5.87).

In leading order in $e^{-\kappa a}$, the energy band is:

$$E(k) = -\frac{\hbar^2\kappa^2}{2m} - 2v_0\kappa e^{-\kappa a}\cos(ka) = -\frac{mv_0^2}{\hbar^2}\left(\frac{1}{2} + 2e^{-\kappa a}\cos(ka)\right).$$

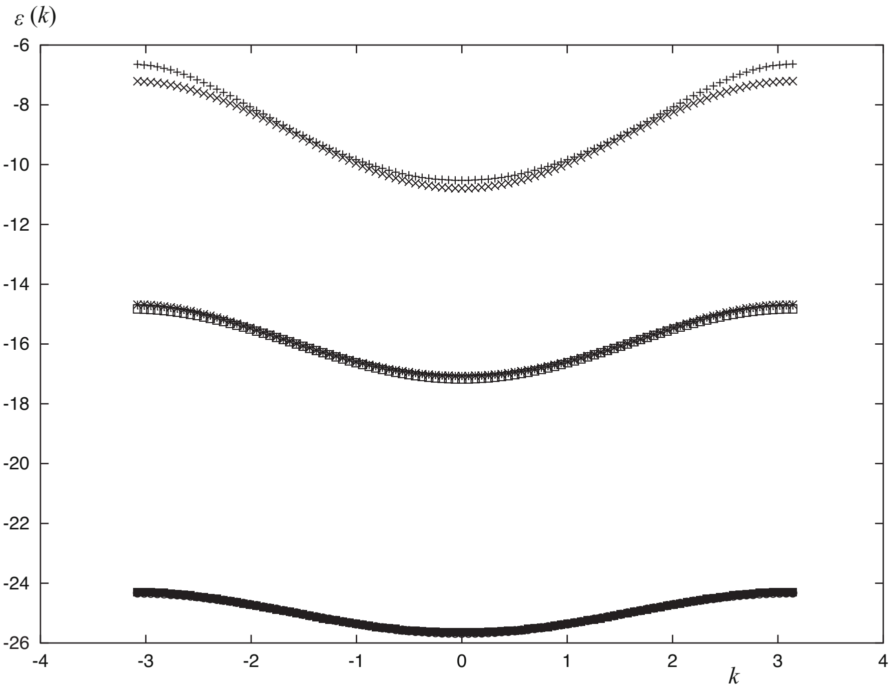

The figure shows the exact bands (solution of the implicit equation from Problem 5.2) and the tight binding bands for 3 different values of $\frac{mv_0}{\hbar^2} = 3, 4, 5$. It can be seen that the bands are lower (i.e. the electrons are more strongly bound) and narrower with increasing strength (depth) of the attractive potentials $v_0$ and that the agreement between exact and tight binding band structure also improves as $v_0$ increases.

### Problem 5.8, Kronig-Penney Model with Finite Potential Wells in Tight-Binding Approximation

The following is a Matlab program that calculates the overlap matrix elements $\beta, \lambda(\boldsymbol{R}), \alpha(\boldsymbol{R})$ according to (5.85)–(5.87) from the "atomic" states for a single attractive square potential (atomic potential) and from these the tight-binding band structures according to (5.84).

```
clear;
v0=120;na=80;b=0.5;
nb=b*na;
dx=1/na;
N=10;
```

```
nges=N*na;
for i=1:nges
   x(i)=i*dx;
   v(i)=0;
end
for i=(nges-nb)/2+1:(nges+nb)/2
   v(i)=-v0;
end
figure(1);plot(x,v)
for i=1:nges   for j=1:nges
      h(i,j)=0;
   end
end
for i=1:nges
   h(i,i)=v(i)+2/(dx*dx);
   if i <nges h(i,i+1)= -1 (dx*dx);end
```

Results for the Tight-Binding band structures:

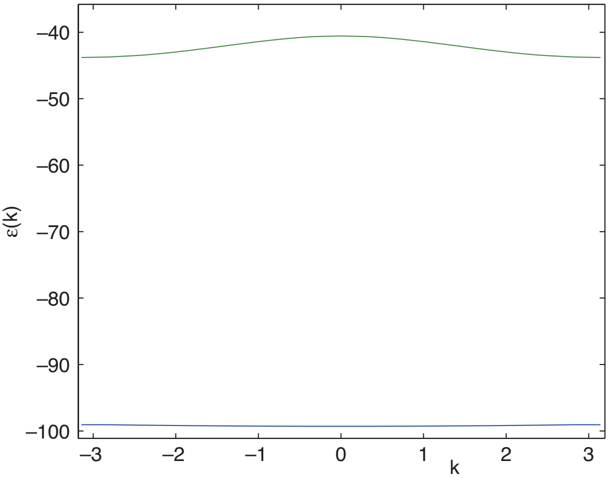

For the low-lying bands that develop from the bound atomic states (here at negative energies), the tight-binding approximation already provides almost the exact band structure (if, for example, it is compared with numerically exact results from problem 5.4[2]).

---

[2] Note that the same spatial resolution must be chosen when comparing the numerically calculated exact and tight-binding band structures.

### Problem 5.9, Wannier Functions and Tight-Binding Band Structure

a)

$$\begin{aligned}\langle n'\boldsymbol{R}'|n\boldsymbol{R}\rangle &= \frac{1}{N}\sum_{\boldsymbol{k},\boldsymbol{k}'} e^{i\boldsymbol{k}'\boldsymbol{R}'} e^{-i\boldsymbol{k}\boldsymbol{R}} \langle\psi_{n'\boldsymbol{k}'}|\psi_{n\boldsymbol{k}}\rangle \\ &= \frac{1}{N}\sum_{\boldsymbol{k}} e^{i\boldsymbol{k}(\boldsymbol{R}'-\boldsymbol{R})}\delta_{nn'} = \delta_{\boldsymbol{R}\boldsymbol{R}'}\delta_{nn'}.\end{aligned}$$

b)

$$\begin{aligned}\varepsilon_n(\boldsymbol{k}) = \langle\psi_{n\boldsymbol{k}}|H|\psi_{n\boldsymbol{k}}\rangle &= \frac{1}{N}\sum_{\boldsymbol{R}\boldsymbol{R}'}\langle n\boldsymbol{R}|e^{-i\boldsymbol{k}\boldsymbol{R}} H e^{i\boldsymbol{k}\boldsymbol{R}'}|n\boldsymbol{R}'\rangle \\ &= \frac{1}{N}\sum_{\boldsymbol{R}\boldsymbol{R}'} e^{i\boldsymbol{k}(\boldsymbol{R}'-\boldsymbol{R})}\langle n\boldsymbol{R}|H|n\boldsymbol{R}'\rangle \\ &= \sum_{\boldsymbol{R}} e^{i\boldsymbol{k}\boldsymbol{R}}\langle n\boldsymbol{0}|H|n\boldsymbol{R}\rangle\end{aligned}$$

where in the last step the translational invariance of $H$ was used.

### Problem 5.10, Tight-Binding Band Structures

12 next-nearest-neighbor vectors for fcc structure:

$$\begin{aligned}\boldsymbol{\Delta} &= (\pm a/2, \pm a/2, 0), \quad (\pm a/2, 0, \pm a/2), \quad (0, \pm a/2, \pm a/2) \\ E(\boldsymbol{k}) &= E_0 + t\sum_{\boldsymbol{\Delta} n.n.} e^{-i\boldsymbol{k}\boldsymbol{\Delta}} \\ &= E_0 + t\big(e^{ik_xa/2}e^{ik_ya/2} + e^{ik_xa/2}e^{-ik_ya/2} + e^{-ik_xa/2}e^{ik_xa/2} \\ &\quad + e^{-ik_xa/2}e^{-ik_ya/2} + \ldots\big) \\ &= E_0 + 4t\Big(\cos\Big(k_x\frac{a}{2}\Big)\cos\Big(k_y\frac{a}{2}\Big) + \cos\Big(k_x\frac{a}{2}\Big)\cos\Big(k_z\frac{a}{2}\Big) \\ &\quad + \cos\Big(k_y\frac{a}{2}\Big)\cos\Big(k_z\frac{a}{2}\Big)\Big).\end{aligned}$$

Special points in the 1st Brillouin zone: $\Gamma = (0,0,0)$, $\mathrm{X} = \pi(1,0,0)$, $\mathrm{W} = \pi(1,\frac{1}{2},0)$, $\mathrm{L} = \pi(1/2,1/2,1/2)$, $\mathrm{K} = \pi(3/4,3/4,0)$.

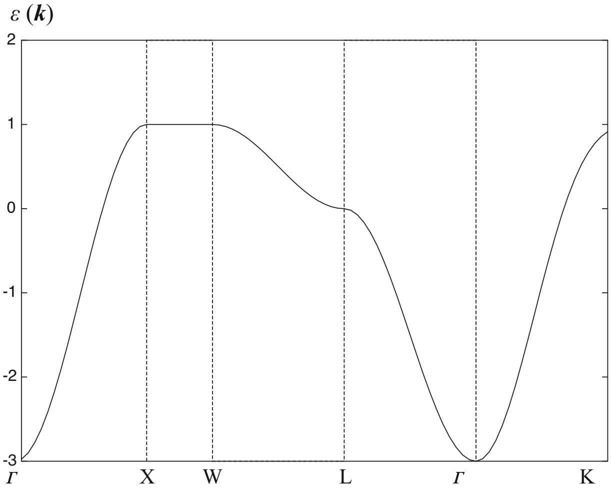

8 next nearest neighbors for bcc structure:

$$\begin{aligned}\boldsymbol{\Delta} &= (\pm a/2, \pm a/2, \pm a/2)\\ E(\boldsymbol{k}) &= E_0 + t\big(e^{ik_xa/2}e^{ik_ya/2}e^{ik_za/2} + e^{ik_xa/2}e^{ik_ya/2}e^{-ik_za/2}\\ &\qquad + e^{ik_xa/2}e^{-ik_ya/2}e^{ik_za/2} + e^{ik_xa/2}e^{-ik_ya/2}e^{-ik_za/2} + \ldots\big)\\ &= E_0 + 8t\cos\left(k_x\frac{a}{2}\right)\cos\left(k_y\frac{a}{2}\right)\cos\left(k_z\frac{a}{2}\right).\end{aligned}$$

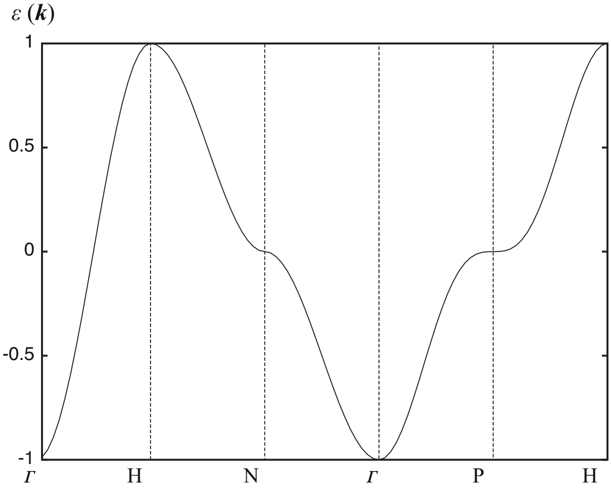

**Problem 5.11, Tight-Binding Model for 2-Dimensional Triangular Lattice**
The triangular lattice is spanned by the vectors $\boldsymbol{a}_1 = (1,0)$, $\boldsymbol{a}_2 = (1/2, \sqrt{3}/2)$ (lattice constant $a=1$). This results in the following nearest-neighbor tight-binding dispersion:

$$\begin{aligned}\varepsilon(\boldsymbol{k}) &= t \sum_{\boldsymbol{\Delta}} e^{i\boldsymbol{k}\boldsymbol{\Delta}}\\ &= t\Big(e^{ik_x} + e^{-ik_x} + e^{ik_x/2}e^{i\sqrt{3}k_y/2} + e^{ik_x/2}e^{-i\sqrt{3}k_y/2}\\ &\quad + e^{-ik_x/2}e^{i\sqrt{3}k_y/2} + e^{-ik_x/2}e^{-i\sqrt{3}k_y/2}\Big)\\ &= 2t\Big(\cos(k_x) + \cos(k_x/2)2\cos(\sqrt{3}k_y/2)\Big)\end{aligned}$$

because there are six nearest-neighbor vectors $\boldsymbol{\Delta} = (\pm 1, 0), (\pm 1/2, \pm\sqrt{3}/2)$.

Critical points of dispersion are determined by

$$\begin{aligned}\frac{\partial\varepsilon}{\partial k_x} &= 0 = -\sin(k_x) - \sin(k_x/2)\cos(\sqrt{3}k_y/2)\\ \frac{\partial\varepsilon}{\partial k_y} &= 0 = -\cos(k_x)\sin(\sqrt{3}k_y/2)\end{aligned}$$

in particular at $\boldsymbol{k}_1 = (k_x, k_y) = (0,0)$, $\boldsymbol{k}_2 = (k_x, k_y) = (4\pi/3, 0)$ (because for this $\sin(k_x) = -\sin(k_x/2)$) and $\boldsymbol{k}_3 = (\pi, \pi/\sqrt{3})$, $\boldsymbol{k}_4 = (0, 2\pi/\sqrt{3})$ with $\varepsilon(\boldsymbol{k}_1) = 3$, $\varepsilon(\boldsymbol{k}_2) = -1.5$, $\varepsilon(\boldsymbol{k}_3) = \varepsilon(\boldsymbol{k}_4) = -1$. At $\boldsymbol{k}_1, \boldsymbol{k}_2$ there are extrema, at $\boldsymbol{k}_3$ a saddle point of the dispersion.

The reciprocal lattice is spanned by the vectors $\boldsymbol{b}_1 = \frac{4\pi}{\sqrt{3}}(\sqrt{3}/2, 1/2)$ and $\boldsymbol{b}_2 = \frac{4\pi}{\sqrt{3}}(0, 1)$. The Brillouin zone is a hexagon, see sketch.

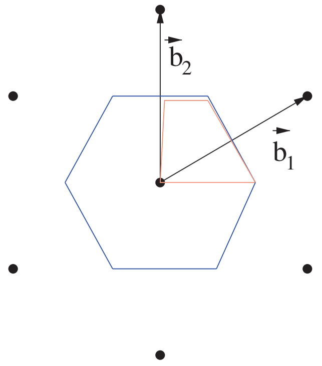

Along selected directions of the Brillouin zone, namely from $\boldsymbol{k}_1$ in $k_x$-direction to $\boldsymbol{k}_2$, from $\boldsymbol{k}_2$ via $\boldsymbol{k}_3$ to $(2\pi/3, 2\pi/\sqrt{3})$, from there to $(0, 2\pi/\sqrt{3}) = \boldsymbol{k}_4$ and from there back to the $\Gamma$ point (this corresponds to the red path through the Brillouin zone), the dispersion is shown below.

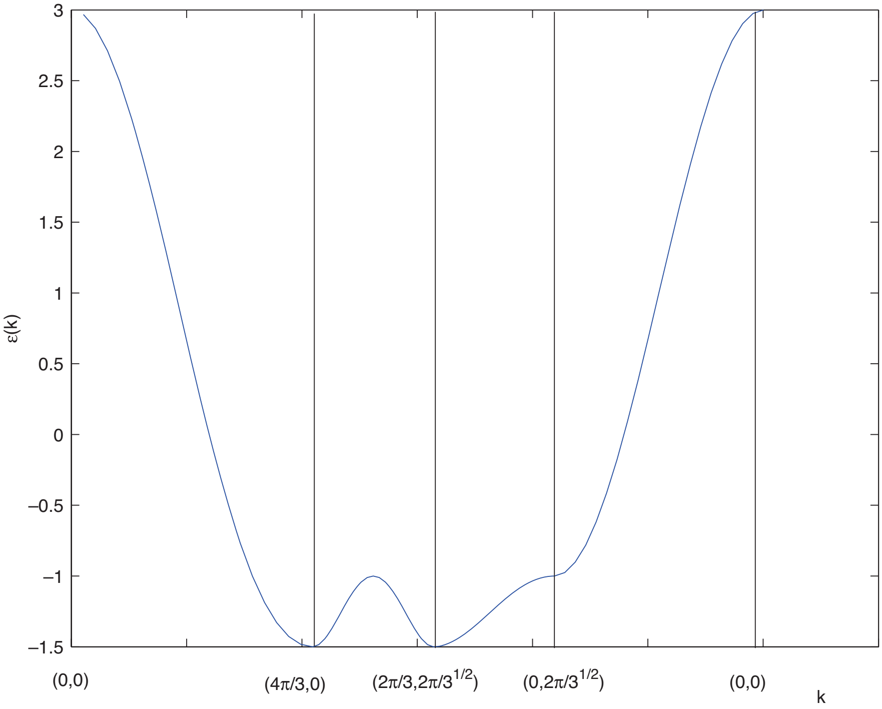

## Problem 5.12, Tight-Binding Model for Graphene

The tight-binding Hamiltonian operator can be represented as follows:

$$H = \sum_{\boldsymbol{R}} t\Big( c^{\dagger}_{\boldsymbol{R}} c_{\boldsymbol{R}+\boldsymbol{a}} + c^{\dagger}_{\boldsymbol{R}+\boldsymbol{a}} c_{\boldsymbol{R}} + c^{\dagger}_{\boldsymbol{R}+\boldsymbol{a}} c_{\boldsymbol{R}+\boldsymbol{a}_1} + c^{\dagger}_{\boldsymbol{R}+\boldsymbol{a}_1} c_{\boldsymbol{R}+\boldsymbol{a}} + c^{\dagger}_{\boldsymbol{R}+\boldsymbol{a}} c_{\boldsymbol{R}+\boldsymbol{a}_2} + c^{\dagger}_{\boldsymbol{R}+\boldsymbol{a}_2} c_{\boldsymbol{R}+\boldsymbol{a}} \Big).$$

The transition to the $\boldsymbol{k}$-representation is carried out by the unitary transformations

$$c^{\dagger}_{\boldsymbol{R}} = \frac{1}{\sqrt{N}} \sum_{\boldsymbol{k}} e^{i\boldsymbol{k}\boldsymbol{R}} c^{\dagger}_{A\boldsymbol{k}}, \quad c^{\dagger}_{\boldsymbol{R}+\boldsymbol{a}} = \frac{1}{\sqrt{N}} \sum_{\boldsymbol{k}} e^{i\boldsymbol{k}(\boldsymbol{R}+\boldsymbol{a})} c^{\dagger}_{B\boldsymbol{k}}.$$

This yields the Hamiltonian:

$$H = \frac{1}{N} \sum_{\boldsymbol{k},\boldsymbol{k}'} \sum_{\boldsymbol{R}} t e^{i(\boldsymbol{k}-\boldsymbol{k}')\boldsymbol{R}} \Big( e^{-i\boldsymbol{k}'\boldsymbol{a}} c^{\dagger}_{A\boldsymbol{k}} c_{B\boldsymbol{k}'} + e^{i\boldsymbol{k}\boldsymbol{a}} c^{\dagger}_{B\boldsymbol{k}} c_{A\boldsymbol{k}'} + e^{i\boldsymbol{k}\boldsymbol{a}} e^{-i\boldsymbol{k}'\boldsymbol{a}_1} c^{\dagger}_{B\boldsymbol{k}} c_{A\boldsymbol{k}'} + e^{i\boldsymbol{k}\boldsymbol{a}_1} e^{-i\boldsymbol{k}'\boldsymbol{a}} c^{\dagger}_{A\boldsymbol{k}} c_{B\boldsymbol{k}'} + e^{i\boldsymbol{k}\boldsymbol{a}} e^{-i\boldsymbol{k}'\boldsymbol{a}_2} c^{\dagger}_{B\boldsymbol{k}} c_{A\boldsymbol{k}'} + e^{i\boldsymbol{k}\boldsymbol{a}_2} e^{-i\boldsymbol{k}'\boldsymbol{a}} c^{\dagger}_{A\boldsymbol{k}} c_{B\boldsymbol{k}'} \Big).$$

Because of

$$\frac{1}{N} \sum_{\boldsymbol{R}} e^{i(\boldsymbol{k}-\boldsymbol{k}')\boldsymbol{R}} = \delta_{\boldsymbol{k},\boldsymbol{k}'}$$

,

$$H = \sum_{\boldsymbol{k}} \left( \gamma(\boldsymbol{k}) c^{\dagger}_{A\boldsymbol{k}} c_{B\boldsymbol{k}} + \gamma^*(\boldsymbol{k}) c^{\dagger}_{B\boldsymbol{k}} c_{A\boldsymbol{k}} \right)$$

$$\text{with} \quad \gamma(\boldsymbol{k}) = t\left(e^{-i\boldsymbol{k}\boldsymbol{a}} + e^{i\boldsymbol{k}(\boldsymbol{a}_1-\boldsymbol{a})} + e^{i\boldsymbol{k}(\boldsymbol{a}_2-\boldsymbol{a})}\right).$$

Diagonalization of a (trivial) $2*2$-matrix for each $\boldsymbol{k}$ yields the two bands (2 because of 2-atom basis)

$$\varepsilon_{\pm}(\boldsymbol{k}) = \pm|\gamma(\boldsymbol{k})| = \pm\sqrt{3 + 2\cos(\sqrt{3}k_y a) + 4\cos\left(\frac{3}{2}k_x a\right)\cos\left(\frac{\sqrt{3}}{2}k_y a\right)}$$

$$= \pm\sqrt{1 + \cos\left(\frac{\sqrt{3}}{2}k_y a\right)\left(\cos\left(\frac{\sqrt{3}}{2}k_y a\right) + 4\cos\left(\frac{3}{2}k_x a\right)\right)}.$$

The following Matlab commands can be used to graphically represent this dispersion:

```
clear all;
[X,Y]=meshgrid(-3:.1:3);
Z=3+2.*cos(sqrt(3)*Y)+4*cos(1.5*X).*cos(sqrt(3)*Y/2);
Z=sqrt(Z);
surf(X,Y,Z)
hold on;
surf(X,Y,-Z)
```

The result is shown below:

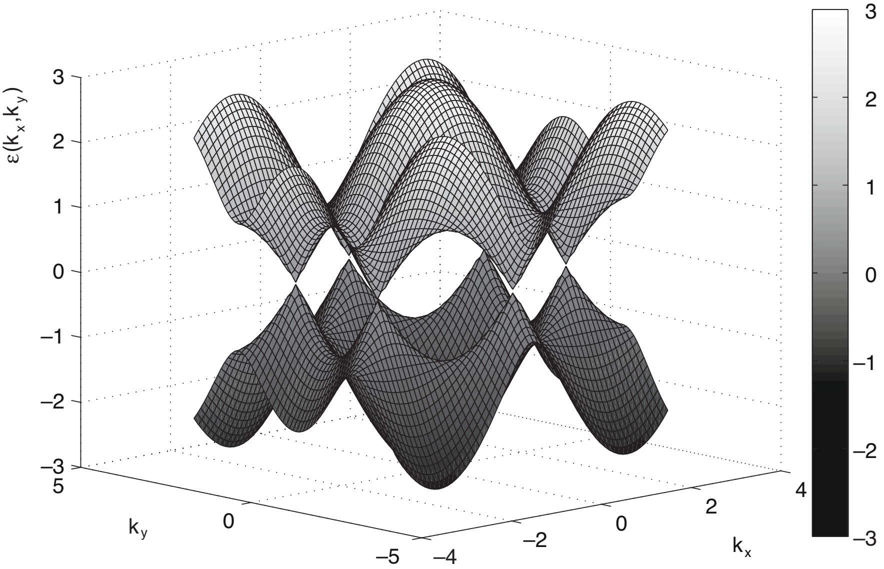

In particular, one recognizes that there are 6 points, namely just the corner points of the first Brillouin zone (K-points), at which the two bands touch and in whose vicinity there is a linear energy-momentum relation $E_k \sim |\boldsymbol{k}|$.

**Problem 5.13, Wannier Functions**

The periodic Bloch factors $u_{nk}(x)$ can be determined numerically as in Problem 5.4 by solving the effective Schrödinger equation (5.20). The Bloch functions according to (5.19) are then given by

$$\psi_{nk}(x) = \frac{1}{\sqrt{N}} e^{ikx} u_{nk}(x).$$

The Bloch functions are however not unique, but can contain an arbitrary phase factor $e^{i\phi_k}$; just as in the case of purely real functions the eigenstates are only uniquely determined up to the sign (i.e. a factor of $\pm 1$), they are in the complex only uniquely determined up to this phase factor. If the different Bloch functions now receive randomly chosen phase factors, the Wannier functions calculated according to definition

$$w_n(x - R) = \frac{1}{\sqrt{N}} \sum_k e^{-ikR} \psi_{nk}(x)$$

may not be localized around the lattice point $R$ at all. Therefore, the Bloch functions must first be "calibrated", i.e. suitable phase factors must be chosen. The simplest way[3] is to choose the phase factors for the different$k$ in such a way that they become real for the same$x_0$. We therefore determine from the numerically (with possibly still random phases) calculated$\psi_{nk}(x)$

$$e^{i\phi_k} = \frac{\psi_{nk}(x_0)}{|\psi_{nk}(x_0)|}.$$

Then the modified ("calibrated") Bloch functions

$$\tilde{\psi}_{nk}(x) = e^{-i\phi_k} \psi_{nk}(x)$$

fulfill especially for $x_0$

$$\tilde{\psi}_{nk}(x_0) = |\psi_{nk}(x_0)|,$$

they are therefore real for all$k$ at the same place$x_0$. With these calibrated Bloch functions one comes to localized Wannier functions.

```
clear;
im=1i;
x=zeros(400);
% n Zahl der Einheitszellen, ix*0.1 Gitterkonstante
```

---

[3] S. also Ilan Schnell, student work and diploma thesis, Univ. Bremen (1998/99).

```
ix=20;n=20;v0=-100;
% Lösung von (5.20) for each k on the unit cell
for nk=1:n
k(nk)=-pi+nk*2*pi/n;
kim=k(nk)*im;
h=zeros(ix,ix);
v=zeros(ix);
v(1)=v0; v(2)=v0; v(ix-1)=v0;v(ix)=v0;
for iix=1:ix
xx(iix)=iix*0.1;
h(iix,iix)=2+(v(iix)+k(nk)*k(nk))*0.01;
if iix > =2 h(iix,iix-1)=-1+kim*0.1; end
if iix < =ix-1 h(iix,iix+1)=-1-kim*0.1; end
end
h(1,ix)=-1+kim*0.1;
h(ix,1)=-1-kim*0.1;
[ev,ew]=eig(h);
for iix=1:ix
eps(nk,iix)=ew(iix,iix)/0.01;
u(nk,iix)=ev(iix,2);
end
end
% Energy-Eigenvalues (Bands) $\varepsilon_n(k)$ in eps(nk,iix)
% Determination of ungauged Bloch function
for nk=1:n
for nx=1:n
for iix=1:ix
jx=(nx-1)*ix+iix;
x(jx)=jx*0.1;
psi0(nk,jx)=exp(im*k(nk)*x(jx))*u(nk,iix)/sqrt(n);
end
end
end
% Gauging of Bloch function
for nk=1:n
cphas(nk)=psi0(nk,1)/abs(psi0(nk,1));
end
for nk=1:n
for jx=1:400
psi(nk,jx)=psi0(nk,jx)/cphas(nk);
end
end
figure(1); plot(k,eps(:,1),k,eps(:,2),k,eps(:,3))
figure(2); plot(x,psi(1,:))
% Determination of Wannier-Function
```

```
for jx=1:400
wann(jx)=0;
for nk=1:n
wann(jx)=wann(jx)+exp(-im*k(nk)*20)*psi(nk,jx)/sqrt(n);
end
end
% Solution of „atomic“ Problem:
h1=zeros(40,40);
v1=zeros(40);
v1(19)=v0; v1(20)=v0; v1(21)=v0;v1(22)=v0;
for iix=1:40
h1(iix,iix)=2+v1(iix)*0.01;
if iix >= 2 h1(iix,iix-1)=-1; end
if iix <= 39 h1(iix,iix+1)=-1; end
end
[ev1,ew1]=eig(h1);
for iix=1:400
atom(iix)=0;
end
for iix=1:40
atom(180+iix)=ev1(iix,2);
end
figure(3); plot(x,real(wann),x,atom)
```

Wannier function and "atomic" eigenstate for n = 20 with lattice constant $a = 1$:

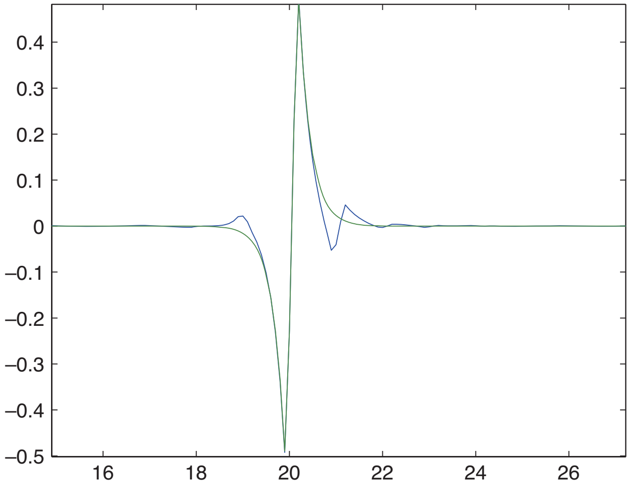

Wannier function and atomic eigenstate for $a = 2$:

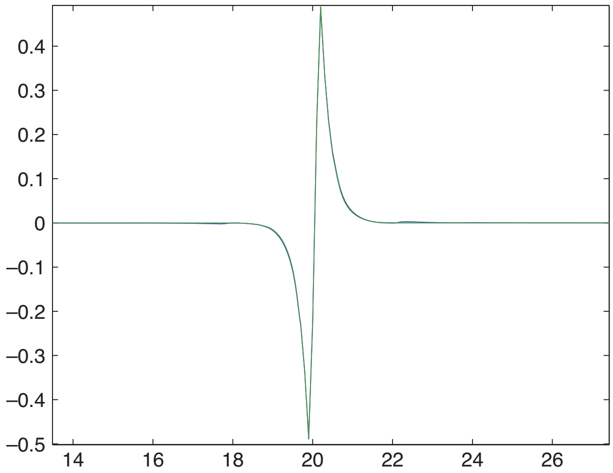

Because it works so well, a few more Wannier functions also for other values of $v_0$:

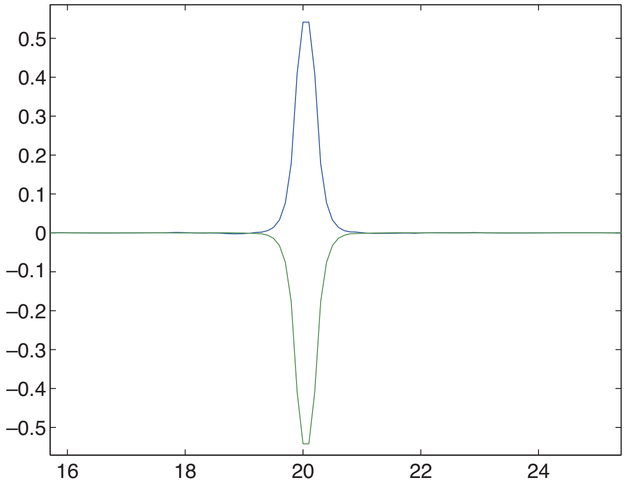

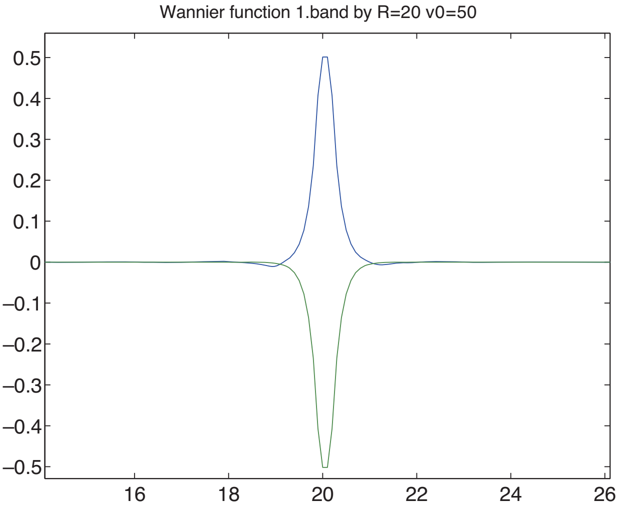

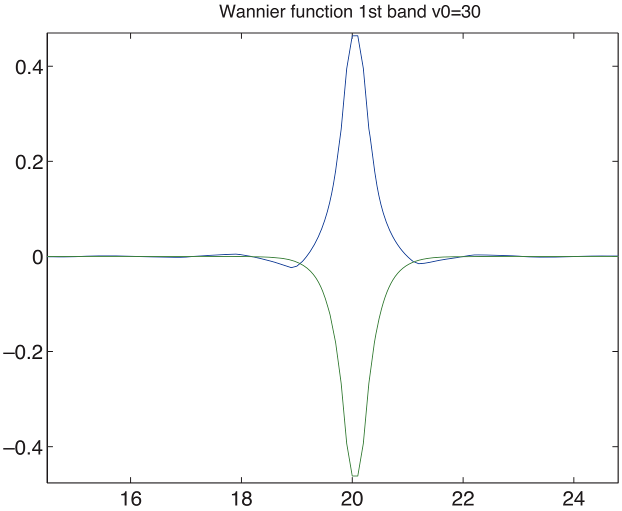

and for a stronger $v_0 = 300$, so that 3 bands correspond to bound states, Bloch function and Wannier function of the 3rd band:

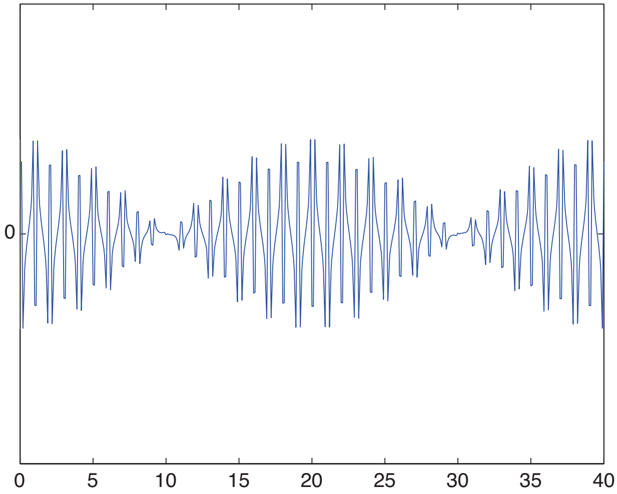

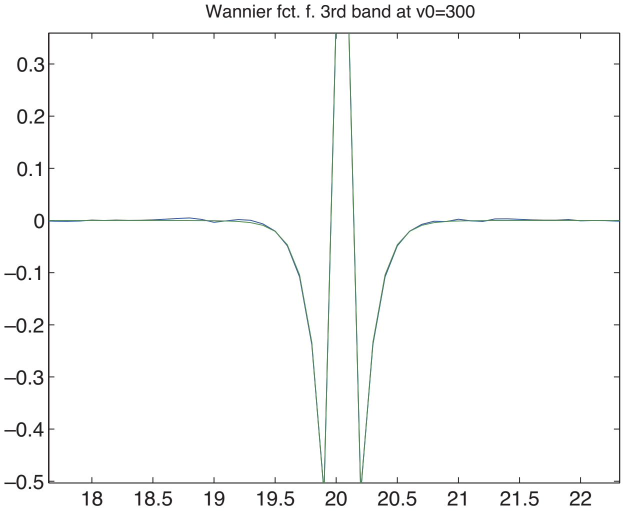

These well-localized Wannier functions therefore usually agree quite well with the atomic functions. They differ in particular in that they still have oscillations in the adjacent potential wells, which is necessary so that they are orthogonal to the Wannier functions localized around these wells. Orthonormality can also be checked numerically and agrees with an accuracy of $10^{-16}$.

## Problem 5.14, on the OPW Method

Matlab code for numerical solution:

```
clear all;v0=5;
for ix=1:200
     x(ix)=ix*0.1;
     v(ix)=0;
     for iy=1:200
          h(ix,iy)=0;
     end
end
for ix=1:200
     h(ix,ix)=2+v(ix)*0.01;
     ip1=ix+1;
     if ip1>200 ip1=ip1-200; end
     h(ix,ip1)=-1;h(ip1,ix)=-1;
end
[ev,ew]=eig(h);
for ix=1:200
     en0(ix)=ew(ix,ix)/0.01;
end
psi01=ev(:,1);psi02=ev(:,2);psi03=ev(:,3);psi04=ev(:,4);
psi05=ev(:,5);
for ix=95:105
     v(ix)=-v0;
end
for ix=1:200
     h(ix,ix)=2+v(ix)*0.01;
     ip1=ix+1;
     if ip1>200 ip1=ip1-200; end
     h(ix,ip1)=-1;h(ip1,ix)=-1;
end
[ev,ew]=eig(h);
for ix=1:200
     en1(ix)=ew(ix,ix)/0.01;
end
psi11=ev(:,1);psi12=ev(:,2);psi13=ev(:,3);psi14=ev(:,4);
psi15=ev(:,5);
figure(1);plot(x,psi11,x,psi12,x,psi13,x,psi14)
skp2=psi11'*psi02;skp3=psi11'*psi03;skp4=psi11'*psi04;
psi22=psi02-skp2*psi11;psi23=psi03-skp3*psi11;
psi24=psi04-skp4*psi11;
figure(2);plot(x,psi22,x,psi23,x,psi24)
```

```
psi11'*psi22
psi11'*psi24
figure(3);plot(x,psi12,x,psi22)
```

This program determines the exact eigenfunctions (plane waves) without attractive box potential on a finite interval [0, 20], on the other hand in the presence of a potential well of depth $v_0 = -5$. Then there is exactly one bound state with eigenenergy $E_0 = -2.73$. The eigenstates are shown in the following figure.

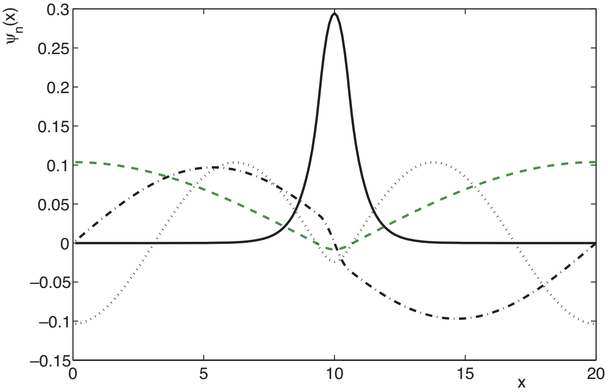

One recognizes the one bound (localized in the potential well) state ($\varphi_0(x) \equiv \psi_1(x)$) and the higher lying scattering states, which are extended over the whole system.

The OPW states constructed from the plane waves according to the equation given in the problem description or according to (5.126) are shown in the following figure:

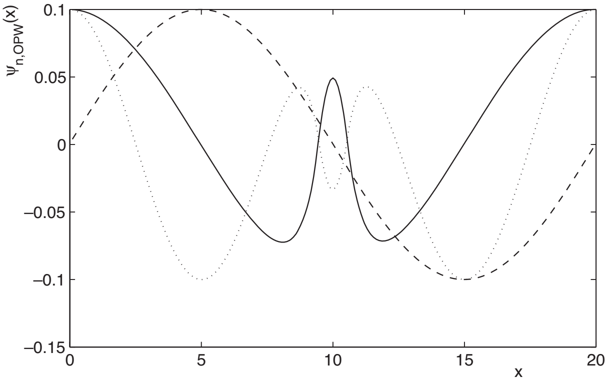

They are orthogonal to $|\varphi_0\rangle$, as it must be according to the construction, and therefore differ from the plane waves by structures in the area of the potential well.

However, they still differ significantly from the exact eigenstates, as the following comparison shows:

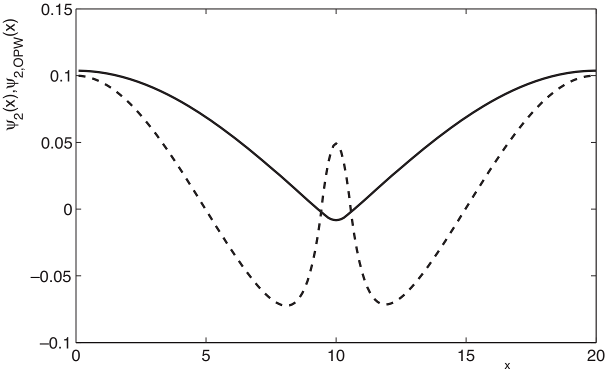

The OPW states are therefore not a good approximation to the exact scattering states for the example discussed here. Only for the energetically higher lying scattering states does the agreement become better. But then the difference to the simple plane wave is almost negligible.

**Problem 5.15, Density of states of (Quasi-)free Electrons**
For the density of states (per spin direction) one obtains according to (5.138) and analogously to the calculation in (5.143):

$$\rho_d(E) = \frac{1}{N}\sum_{\boldsymbol{k}} \delta\left(E - \frac{\hbar^2}{2m}k^2\right) = \frac{a^d}{(2\pi)^d}\int d^dk\,\delta\left(E - \frac{\hbar^2}{2m}k^2\right)$$

Then it follows for $d = 1, 2, 4$:

$$\begin{aligned}
\rho_1(E) &= \frac{a}{2\pi}2\int_{k>0} dk\,\delta\left(E - \frac{\hbar^2}{2m}k^2\right) = \frac{a}{\pi}\sqrt{\frac{m}{2\hbar^2}}\int_{y>0} dy\frac{1}{\sqrt{y}}\delta(E-y)\\
&= \frac{a}{\pi}\sqrt{\frac{m}{2\hbar^2}}\frac{1}{\sqrt{E}} \quad \text{for} \quad E > 0,\\
\rho_2(E) &= \frac{a^2}{4\pi^2}2\pi\int_{k>0} kdk\,\delta\left(E - \frac{\hbar^2}{2m}k^2\right) = \frac{a^2}{2\pi}\frac{m}{\hbar^2}\int_{y>0} dy\,\delta(E-y)\\
&= \frac{a^2}{2\pi}\frac{m}{\hbar^2} \quad \text{for} \quad E > 0,\\
\rho_4(E) &= \frac{a^4}{16\pi^2}2\pi^2\int_{k>0} dkk^3\,\delta\left(E - \frac{\hbar^2}{2m}k^2\right) = \frac{a^4}{8\pi^2}\frac{2m^2}{\hbar^4}\int_{y>0} dyy\,\delta(E-y)\\
&= \frac{a^4}{4\pi^2}\left(\frac{m}{\hbar^2}\right)^2 E \quad \text{for} \quad E > 0.
\end{aligned}$$

**Problem 5.16, Tight-Binding Density of States for fcc and bcc Lattices**

a) fcc structure:

$$\begin{aligned}\varepsilon(\boldsymbol{k}) &= -\cos(k_x)\cos(k_y) - \cos(k_x)\cos(k_z) - \cos(k_y)\cos(k_z)\\ \frac{\partial\varepsilon}{\partial\boldsymbol{k}} &= \big(\sin(k_x)\cos(k_y)\cos(k_z), \sin(k_y)\cos(k_x)\cos(k_z),\\ &\qquad \sin(k_z)\cos(k_x\cos(k_y)\big),\end{aligned}$$

critical points at:

$$\begin{aligned}&(0,0,0), (\pi,\pi,\pi), (0,0,\pi), (0,\pi,0), (\pi,0,0), (\pi,\pi,0),\\ &(\pi,0,\pi), (0,\pi,\pi), \left(\frac{\pi}{2},\frac{\pi}{2},\frac{\pi}{2}\right),\end{aligned}$$

corresponding critical energies with Van-Hove singularities at:

$$\varepsilon_1 = -3, \quad \varepsilon_2 = +1, \quad \varepsilon_3 = 0,$$

bcc structure:

$$\begin{aligned}\varepsilon(\boldsymbol{k}) &= -\cos(k_x)\cos(k_y)\cos(k_z)\\ \frac{\partial\varepsilon}{\partial\boldsymbol{k}} &= \big(\sin(k_x)\cos(k_y)\cos(k_z), \sin(k_y)\cos(k_x)\cos(k_z),\\ &\qquad \sin(k_z)\cos(k_x)\cos(k_y)\big).\end{aligned}$$

critical points at:

$$(0,0,0), (\pi,\pi,\pi), \left(\frac{\pi}{2},\frac{\pi}{2},\frac{\pi}{2}\right)$$

corresponding critical energies:

$$\varepsilon_1 = -1, \quad \varepsilon_2 = +1, \quad \varepsilon_3 = 0$$

b) Matlab code for nearest-neighbor tight-binding model on the bcc lattice (fcc analogous, use commented lines):

```
clear all;
ne=80;nq=100;
% for nearest-neighbor tight-binding model on % bcc lattice
%ne=120; nq=200;
% for nearest-neighbor tight-binding model on fcc lattice
de=4/ne;% for bcc
% de = 6/ne; % for fcc
rho=zeros(ne);
e=zeros(ne);
for ie=1:ne
   e(ie)=-2+ie*de; % bcc
   % e(ie)=-4+ie*de % fcc
```

```
end
n=0;
for ix=1:nq
    qx=ix*pi/nq;
    for iy=1:ix
        qy=iy*pi/nq;
        for iz=1:iy
            qz=iz*pi/nq;
            n=n+1;
    ee=-cos(qx)*cos(qy)*cos(qz);% bcc
        % ee=-cos(qx)*cos(qy)-cos(qx)*cos(qz)-cos(qy)*cos(qz);
        % fcc
            ie=ceil((ee+2)/de);% bcc
            % ie=ceil((ee+4)/de);% fcc
            rho(ie)=rho(ie)+1;
        end
    end
end
for ie=1:ne rho(ie)=rho(ie)/(de*n); end
plot(e,rho,'k-','Linewidth',2)
axis([-2 2 0 3])% bcc
% axis([-4 2 0 1.2]) % fcc
set(gca,'FontSize',16)
text(2.1,-.1,'E','FontSize',16)
text(-2.2,3.2,'\rho(E)','FontSize',16)% bcc
% text(-4.2,1.25,'\rho(E)','FontSize',16)% fcc
```

fcc density of states:

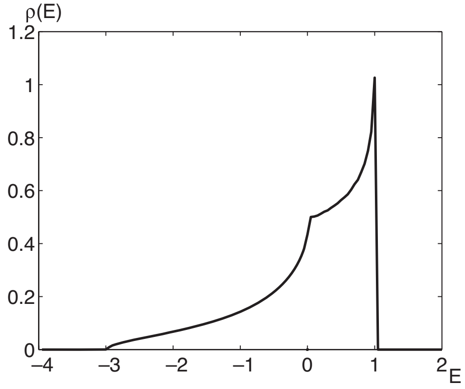

bcc density of states:

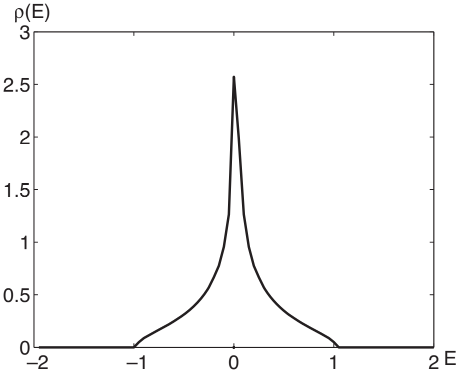

**Problem 5.17, Tight-Binding Density of States for Triangular Lattices and for Graphene**

For symmetry reasons, it is sufficient (because of the sixfold symmetry of the Brillouin zone) to carry out the numerical (discretized) ***k***-integration only over one sixth of the Brillouin zone in both cases. This is implemented in the following Matlab code for the simple tight-binding model on the triangular lattice by using the dispersion relation determined in Problem 5.11

```
clear;nm=1000;
for i=1:350
e(i)=-3+i*0.02;
rho(i)=0;
end
for ix=1:nm
kx=ix*2*pi/(3*nm);
for iy=1:ix
ky=sqrt(3)*iy*2*pi/(3*nm);
en=cos(kx)+2*(cos(0.5*kx)*cos(0.5*sqrt(3)*ky));
ie=ceil((en+3)/0.02);
rho(ie)=rho(ie)+1;
end
end
for ix=nm+1:2*nm
kx=ix*2*pi/(3*nm);
for iy=1:2*nm-ix
ky=sqrt(3)*iy*2*pi/(3*nm);
en=cos(kx)+2*(cos(0.5*kx)*cos(0.5*sqrt(3)*ky));
ie=ceil((en+3)/0.02);
rho(ie)=rho(ie)+1;
```

```
end
end
s=0;
rho=rho/(0.02*nm^2);
for i=1:350
s=s+rho(i)*0.02;
end
plot(e,rho)
```

This results in the following density:

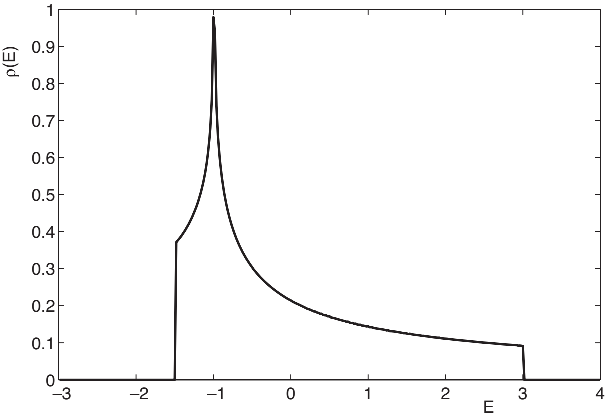

The characteristic jumps at the band edges and the logarithmic inner Van Hove singularity are clearly visible.

For graphene (2 atoms per elementary cell), the same program can be used essentially, except that for each ***k*** 2 energies (bands) exist according to problem 5.12:

```
clear;nm=1000;
for i=1:400
e(i)=-4+i*0.02;
rho(i)=0;
end
for ix=1:nm
kx=ix*2*pi/(3*nm);
for iy=1:ix
ky=sqrt(3)*iy*2*pi/(3*nm);
en=3+2*cos(sqrt(3)*ky)+4*cos(1.5*kx)*cos(0.5*sqrt(3)*ky);
en1=-sqrt(en);en2=sqrt(en);
ie1=ceil((en1+4)/0.02);ie2=ceil((en2+4)/0.02);
rho(ie1)=rho(ie1)+1;rho(ie2)=rho(ie2)+1;
end
end
```

```
for ix=nm+1:2*nm
kx=ix*2*pi/(3*nm);
for iy=1:2*nm-ix
ky=sqrt(3)*iy*2*pi/(3*nm);
en=3+2*cos(sqrt(3)*ky)+4*cos(1.5*kx)*cos(0.5*sqrt(3)*ky);
en1=-sqrt(en);en2=sqrt(en);
ie1=ceil((en1+4)/0.02);ie2=ceil((en2+4)/0.02);
rho(ie1)=rho(ie1)+1;rho(ie2)=rho(ie2)+1;
end
end
s=0;
rho=rho/(0.02*nm^2);
for i=1:400
s=s+rho(i)*0.02;
end
plot(e,rho)
```

This results in the density of states:

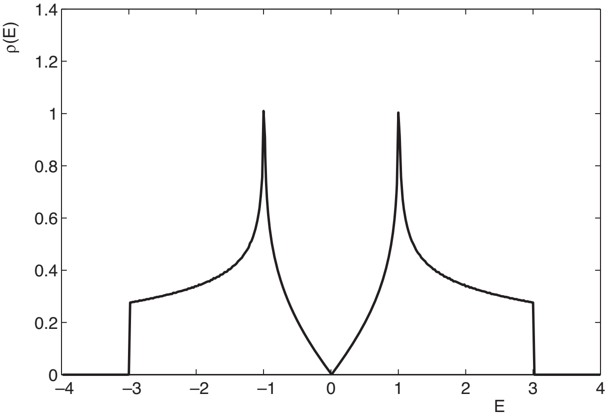

Here, too, the Van-Hove singularities characteristic of $d=2$ (jumps at the band edges and inner logarithmic) can be seen. Because of the linear dispersion vanishing at 0 (behavior of "massless Dirac fermions"), the density of states also vanishes linearly at this point. So there is no real band gap.

**Problem 5.18, Fermi Surface for Tight-Binding Bands**

The Fermi surfaces for a given dispersion relation $\varepsilon(\boldsymbol{k})$ and a given Fermi energy $E_F$ can relatively easily be plotted in three dimensions using the Matlab routine "isosurface". For this purpose, the values $\varepsilon(k_x, k_y, k_z)$ must be stored in a three-dimensional array for a given discretized three-dimensional $\boldsymbol{k}$-space grid. Then the Matlab command "isosurface $(k_x, k_y, k_z, \varepsilon, E)$" creates a three-dimensional plot of the surface on which $\varepsilon(\boldsymbol{k}) = E$ applies. As an example, an fcc lattice was selected for which the tight-binding dispersion is known from Problem 5.10 (and the density of states from Problem 5.16). With $4t = 1$ and $E_0 = 0$ there is a finite density of states on the interval $[-3, 1]$ and the Fermi energy must therefore fulfill $E_F \in [-3, 1]$.

The following is a Matlab code for plotting the Fermi surface with "isosurface". A cubic $\boldsymbol{k}$-space grid is given on a cube with edge length $2\pi$. In order to only display the Fermi surface in the area of the 1st Brillouin zone, it is first determined whether the given $\boldsymbol{k}$-points belong to the 1st Brillouin zone; for this purpose, the 14 reciprocal lattice vectors with components $r_j(i), j \in \{x, y, z\}, i \in \{1, \ldots, 14\}$) are determined for nearest and next-nearest neighbors and it is checked whether the given $\boldsymbol{k}$-point is closer to one of these points than to the origin. If they are (i.e. $not \in$ 1. Brillouin zone), the value of $\varepsilon(\boldsymbol{k})$ (or $v(ix, iy, iz)$ in the source code) is set to 1.5, which the Fermi energy cannot assume, so that points outside the 1st Brillouin zone cannot be considered in the Surface plot.

The Matlab source code is given below:

```
clear all;
x=-pi:.1:pi;
y=x;
z=x;
rx(1)=pi;ry(1)=pi;rz(1)=pi;
rx(2)=-pi;ry(2)=pi;rz(2)=pi;
rx(3)=pi;ry(3)=-pi;rz(3)=pi;
rx(4)=-pi;ry(4)=-pi;rz(4)=pi;
rx(5)=pi;ry(5)=pi;rz(5)=-pi;
rx(6)=-pi;ry(6)=pi;rz(6)=-pi;
rx(7)=pi;ry(7)=-pi;rz(7)=-pi;
rx(8)=-pi;ry(8)=-pi;rz(8)=-pi;
rx(9)=2*pi;ry(9)=0;rz(9)=0;
rx(10)=0;ry(10)=2*pi;rz(10)=0;
rx(11)=0;ry(11)=0;rz(11)=2*pi;
rx(12)=-2*pi;ry(12)=0;rz(12)=0;
rx(13)=0;ry(13)=-2*pi;rz(13)=0;
rx(14)=0;ry(14)=0;rz(14)=-2*pi;
for ix=1:63
for iy=1:63
for iz=1:63
r=sqrt(x(ix)^2+y(iy)^2+z(iz)^2);
v(ix,iy,iz)= -cos(x(ix))*cos(y(iy))-cos(x(ix))*cos(z(iz))-
             cos(y(iy))*cos(z(iz));
for i=1:14
ri=sqrt((x(ix)-rx(i))^2+(y(iy)-ry(i))^2+(z(iz)-rz(i))^2);
if ri<r v(ix,iy,iz)=1.5;end
end
end
```

```
end
end
isosurface(x,y,z,v,-2)
```

The plots show the results for $E_F = -2, E_F = -1, E_F = 0, E_F = 0.5$.

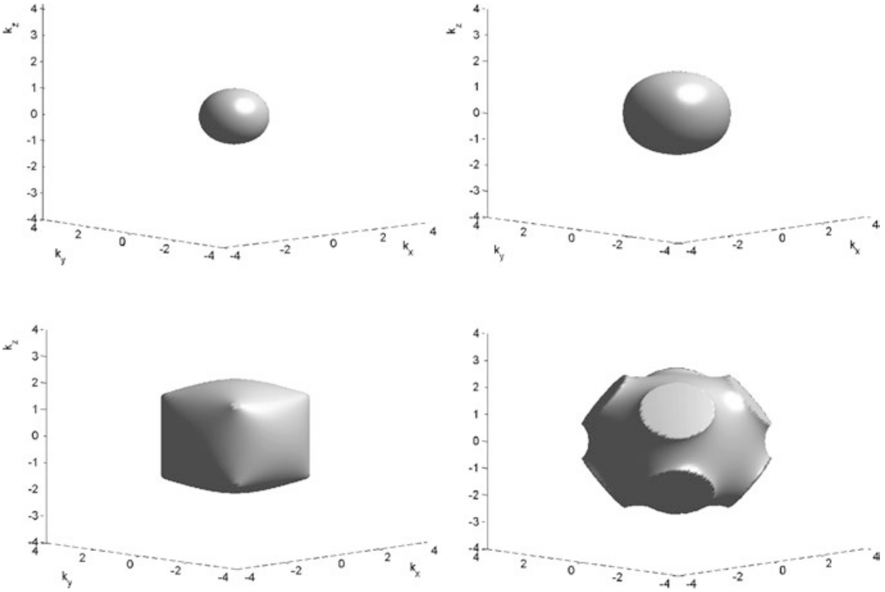

Only for $E_F = -2$ (Fermi energy near the lower edge of the band) is the Fermi surface approximately spherical, with increasing $E_F$ the cubic symmetry becomes noticeable, at $E_F = 0$ it is more cubical, for $E_F = 0.5$ (near the upper edge of the spectrum) "necks" to the neighboring Brillouin zones form. The empty (unoccupied) part of neighboring Brillouin zones (that is, the "hole states") are then surrounded by a spherical Fermi surface.

You can also use the program to display the Brillouin zone. If you set $E_F = 1$, all states of the first Brillouin zone are occupied, the Fermi surface must therefore coincide with the surface of the fcc Brillouin zone, as you can see in the following figure:

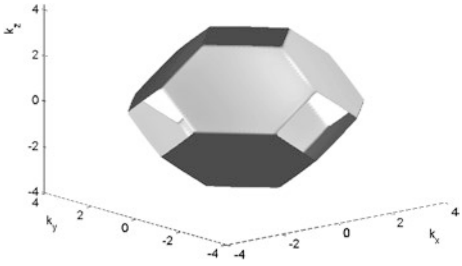

### Problem 5.19, Free Electrons in 2 Dimensions

Free electrons with dispersion

$$\varepsilon(\boldsymbol{k}) = \frac{\hbar^2 k^2}{2m} = \frac{\hbar^2}{2m}\left(k_x^2 + k_y^2\right)$$

in 2 dimensions.

a)

$$N = 2\sum_{k<k_F} 1 = 2\frac{F}{(2\pi)^2}\int_{k<k_F} d^k 1 = \frac{2F}{4\pi^2}2\pi\int_0^{k_F} kdk = \frac{F}{\pi}\frac{k_F^2}{2}$$

$$\text{therefore:}\quad k_F^2 = 2\pi\frac{N}{F} = 2\pi n,\quad E_F = \frac{\hbar^2 k_F^2}{2m} = \frac{\pi\hbar^2}{m}n$$

b)

$$\begin{aligned}\rho(E) &= \frac{1}{N}\sum_{\boldsymbol{k}\sigma}\delta\left(E - \frac{\hbar^2k^2}{2m}\right) = \frac{2F}{N4\pi^2}\int d^2k\delta\left(E - \frac{\hbar^2k^2}{2m}\right)\\ &= \frac{F}{\pi N}\int kdk\delta\left(E - \frac{\hbar^2k^2}{2m}\right) = \frac{Fm}{\pi\hbar^2N}\end{aligned}$$

The density of states is therefore constant for $E>0$.

c) Number of electrons per unit cell ($Z_e$)

$$\begin{aligned}Z_e &= \int dE\rho(E)f(E) = \frac{Fm}{\pi\hbar^2N}\int_0^\infty dEf(E)\\ &= \frac{Fm}{\pi\hbar^2N}k_BT\int_{-\mu/(k_BT)}^\infty dx\frac{1}{e^x+1} = \frac{Fm}{\pi\hbar^2N}k_BT\ln\left[1 + e^{\mu(T)/k_BT}\right].\end{aligned}$$

For $Z_e = 1$ (1 electron per elementary cell or $N$ electrons) one gets from a):

$$E_F = k_BT\ln\left[1 + e^{\mu(T)/k_BT}\right]$$

or

$$\begin{aligned}e^{\mu/k_BT} &= e^{E_F/k_BT} - 1 = e^{E_F/k_BT}\left(1 - e^{-E_F/k_BT}\right)\\ \mu(T) &= E_F + k_BT\ln(1 - e^{-E_F/k_BT}).\end{aligned}$$

d) According to (5.176), since the density of states $\rho(E)$ is constant:

$$\begin{aligned}u = U/N &= \int_0^\mu dEE\rho(E) + \frac{\pi^2}{6}(k_BT)^2\rho(\mu) = \frac{Fm}{\pi\hbar^2N}\left(\frac{\mu^2}{2} + \frac{\pi^2}{6}(k_BT)^2\right)\\ &= \frac{1}{2E_F}\left(\left[E_F + k_BT\ln\left(1 - e^{-E_F/k_BT}\right)\right]^2 + \frac{\pi^2}{3}(k_BT)^2\right)\\ &= \frac{E_F}{2}\left(1 - 2\frac{k_BT}{E_F}e^{-E_F/(k_BT)} + \frac{\pi^2}{3}\left(\frac{k_BT}{E_F}\right)^2\right).\end{aligned}$$

**Problem 5.20, Temperature Dependence of Chemical Potential and Internal Energy**

For $T=0$ it holds:

$$\int_0^{E_F} dE\sqrt{E} = \frac{2}{3}E_F^{3/2} = 1 \rightarrow \mu(T=0) = E_F = \left(\frac{3}{2}\right)^{\frac{2}{3}} = 1.31037$$

and

$$U(T=0) = E_0 = \int_0^{E_F} dEE\sqrt{E} = \frac{2}{5}E_F^{5/2} = 0.78622.$$

This can be used as a starting value for the calculation of $\mu(T)$ from

$$1 = \int_0^{\infty} dE\frac{\sqrt{E}}{e^{(E-\mu)/T}+1}$$

and $U(T)$ from

$$U(T) = \int_0^{\infty} dEE\frac{\sqrt{E}}{e^{(E-\mu)/T}+1}$$

In (numerical) practice, the upper integration limit can be replaced by a large value (e.g. 20), μ can be determined by the method of nested intervals. A Matlab program (with a very primitive numerical integration, namely simple summation after discretization) is printed below.

```
clear all;
t=0.01:0.01:3;
e=0:0.02:20;
rho=sqrt(e);
it=1;
mu(1)=1.31;mu3=mu(1);
s1=0;u(1)=0;
h1=(e-mu3)./t(it);
h1=exp(h1);
ferm=1./(h1+1);
for ie=1:1000
s1=s1+rho(ie)*ferm(ie)*0.02;u(1)=u(1)+rho(ie)*ferm(ie)*e
(ie)*0.02;
end
s(1)=s1;
for it=2:300
mu1=mu(it-1);mu2=mu1-0.1;
for iter=1:10
mu3=(mu1+mu2)/2;
h1=(e-mu3)/t(it);
h1=exp(h1);
```

```
ferm=1./(h1+1);
s1=0;u1=0;
for ie=1:1000
s1=s1+rho(ie)*ferm(ie)*0.02;
u1=u1+rho(ie)*ferm(ie)*e(ie)*0.02;
end
if s1<1 mu2=mu3; else mu1=mu3;end
end
mu(it)=mu3;s(it)=s1;u(it)=u1;
end
figure(1);plot(t,mu)
figure(2);plot(t,u)
```

The plots show the numerical results for $\mu(T)$ and $U(T)$ for $0<T<3$. It is clearly seen that the chemical potential decreases with increasing temperature, that for small $T$ there is a $T^2$-dependence, which for large $T$ transitions into an approximately linear $T$-behavior and that $\mu(T)$ becomes negative, here specifically for $T \approx 1.3$. The internal energy starts at the finite ground state energy $E_0 = 0.78622$, grows for small $T$ quadratically $\sim T^2$, which for large $T$ transitions into a linear $T$-behavior.

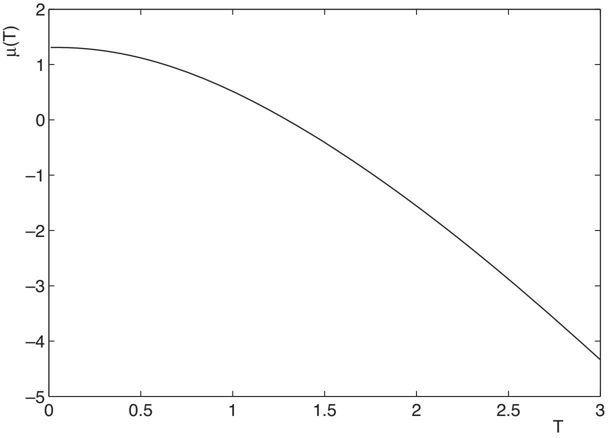

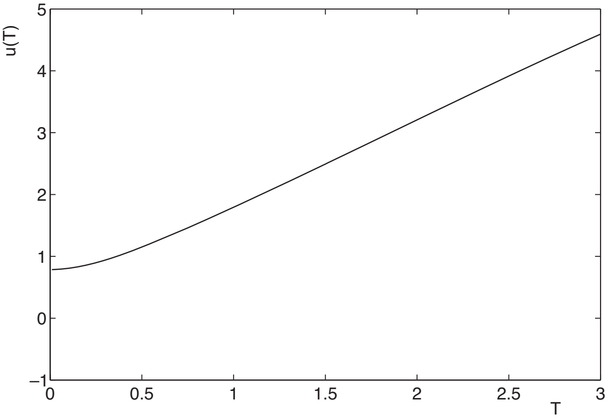

For large $T$ and thus $\mu \ll 0$ one can also estimate analytically:

$$\begin{aligned}1 &= \int_0^\infty dE \frac{\sqrt{E}}{e^{(E-\mu)/T}+1} \approx e^{\mu/T} \int_0^\infty dE \sqrt{E} e^{-E/T} \\ &= 2e^{\mu/T} T^{3/2} \int_0^\infty dx x^2 e^{-x^2} = e^{\mu/T} T^{3/2} \frac{\sqrt{\pi}}{2} \\ e^{\mu/T} &= \frac{2}{\sqrt{\pi}} T^{-3/2} \rightarrow \mu = T \ln \left( \frac{2}{\sqrt{\pi}} T^{-3/2} \right) = T \left( \ln \left( \frac{2}{\sqrt{\pi}} \right) - \frac{3}{2} \ln T \right)\end{aligned}$$

and

$$\begin{aligned}U(T) &= e^{\mu/T} \int_0^\infty dE E^{3/2} e^{-E/T} = 2e^{\mu/T} T^{5/2} \int_0^\infty dx x^4 e^{-x^2} \\ &= 2e^{\mu/T} T^{5/2} \frac{3}{8} \sqrt{\pi} = \frac{3}{2} T.\end{aligned}$$

This is nothing else but the result for the classical ideal gas. Even a Fermi gas approaches a classical ideal gas for large $T$ if $\mu$ becomes negative, but for electrons these are in practice unreachably large $T$.

**Exercise 5.21, Specific Heat of Semiconductors**

a) The step from (5.204) to (5.205) is clear if one neglects the second term in brackets in (5.204) with respect to the first (because the first is greater by a factor of $1/T$ at low $T$) and $\mu$ is replaced by $E_F$ In (5.205) if we set $E_F = \frac{1}{2}(E_c + E_v) = E_v + \frac{\Delta}{2} = E_c - \frac{\Delta}{2}$, we get:

$$c_V = \frac{e^{-\frac{\Delta}{2k_BT}}}{k_BT^2}\left(\int_0^{E_v} dEE\left(E - E_v - \frac{\Delta}{2}\right)\rho_v(E)e^{-\beta(E_v-E)}\right.$$
$$\left. + \int_{E_c}^{\infty} dEE\left(E - E_c + \frac{\Delta}{2}\right)\rho_c(E)e^{-\beta(E-E_c)}\right).$$

We set

$$\rho_v(E) = C_v\sqrt{E_v - E},\ \rho_c(E) = C_c\sqrt{E - E_c}, \quad \text{with}$$
$$C_{c,v} = \frac{V}{2\pi^2\hbar^3 N}(2m_{e,v})^{3/2}.$$

With the substitutions

$$x^2 = \frac{E_v - E}{k_BT},\ E = E_v - k_BTx^2,\ dE = -2k_BTxdx,\ \sqrt{E_v - E} = \sqrt{k_BT}x$$
$$x^2 = \frac{E - E_c}{k_BT},\ E = E_c + k_BTx^2,\ dE = 2k_BTxdx,\ \sqrt{E - E_c} = \sqrt{k_BT}x$$

it follows:

$$c_V = \frac{e^{-\frac{\Delta}{2k_BT}}}{k_BT^2}\left(C_v\int_0^{E_v/k_BT} 2k_BTxdx(E_v - k_BTx^2)\left(-k_BTx^2 - \frac{\Delta}{2}\right)\sqrt{k_BT}xe^{-x^2}\right.$$
$$\left. + C_c\int_0^{\infty} 2k_BTxdx(E_c + k_BTx^2)\left(k_BTx^2 + \frac{\Delta}{2}\right)\sqrt{k_BT}xe^{-x^2}\right)$$
$$c_V = \frac{e^{-\frac{\Delta}{2k_BT}}}{\sqrt{k_BT}}k_B\Delta(C_cE_c - C_vE_v)\int_0^{\infty} dxx^2e^{-x^2}$$
$$= \frac{e^{-\frac{\Delta}{2k_BT}}}{\sqrt{k_BT}}k_B\frac{V}{N}\Delta\frac{\sqrt{\pi}}{8\pi^2\hbar^3}\left((2m_e)^{3/2}E_c - (2m_v)^{3/2}E_v\right)$$
$$= \frac{e^{-\frac{\Delta}{2k_BT}}}{\sqrt{k_BT}}k_B\frac{V}{N}\Delta^2\left(\frac{m}{2\pi\hbar^2}\right)^{3/2}$$

where the latter equality only holds for equal valence and conduction band masses.

b) The density of states

$$\rho(E) = \begin{cases} \frac{1}{E_0} \text{ for } \quad 0 < E < E_0 \quad \text{and} \quad E_0 + \Delta < E < 2E_0 + \Delta \\ 0 \qquad\qquad\qquad\qquad\qquad \text{else} \end{cases}$$

is obviously symmetrical around $E_0 + \frac{\Delta}{2}$, therefore the Fermi energy is located there, and the chemical potential is T-independent, thus constant $\mu(T) = E_0 + \frac{\Delta}{2}$. For the specific heat one obtains:

$$\begin{aligned}
c_V &= \int dE\rho(E)E\frac{\partial f}{\partial T} \\
&= \int dEE\rho(E)\frac{E-\mu}{k_BT^2}\frac{1}{(e^{\beta(E-\mu)}+1)(e^{-\beta(E-\mu)}+1)} \\
&= \frac{1}{T}\int k_BTdx(\mu+k_BTx)\frac{x}{(e^x+1)(e^{-x}+1)}\rho(\mu+k_BTx) \\
&= \frac{2}{TE_0}(k_BT)^2\int_{\Delta/2k_BT}^{(E_0+\Delta/2)/2k_BT} dx\frac{x^2}{(e^x+1)(e^{-x}+1)} \\
&\approx \frac{2}{TE_0}(k_BT)^2\int_{\Delta/2k_BT}^{(E_0+\Delta/2)/2k_BT} dxx^2e^{-x} \\
&= \frac{2}{TE_0}(k_BT)^2(-x^2-2x-2)e^{-x}|_{\Delta/2k_BT}^{\infty} \\
&\approx \frac{2k_B^2T}{E_0}\left(\frac{\Delta}{2k_BT}\right)^2 e^{-\Delta/2k_BT} = \frac{\Delta^2}{2TE_0}e^{-\Delta/2k_BT}
\end{aligned}$$

in leading, non-vanishing order.

## 8.5 Solution to the Problems of Chap. 6

**Problem 6.1, One-Particle Operators in Occupation Number Representation ("2nd Quantization")**

The mentioned operators have the following form in 1. quantization:

$$\begin{aligned}
\boldsymbol{p} &= \sum_{i=1}^{N}\boldsymbol{p}_i \\
\rho(\boldsymbol{r}) &= \sum_{i=1}^{N}\delta(\boldsymbol{r}-\boldsymbol{r}_i) \\
\boldsymbol{j}(\boldsymbol{r}) &= \frac{1}{2m}\sum_{i=1}^{N}\left(\boldsymbol{p}_i\delta(\boldsymbol{r}-\boldsymbol{r}_i)+\delta(\boldsymbol{r}-\boldsymbol{r}_i)\boldsymbol{p}_i\right)
\end{aligned}$$

and are thus all one-particle operators. In 2nd quantization with respect to plane waves (as eigenstates of free particles in position representation) one obtains:

$$\begin{aligned}
\boldsymbol{p} &= \sum_{\boldsymbol{k}}\hbar\boldsymbol{k}c_{\boldsymbol{k}}^{\dagger}c_{\boldsymbol{k}} \\
\rho(\boldsymbol{r}) &= \frac{1}{V}\sum_{\boldsymbol{k}\boldsymbol{k}'}e^{i(\boldsymbol{k}'-\boldsymbol{k})\boldsymbol{r}}c_{\boldsymbol{k}}^{\dagger}c_{\boldsymbol{k}'} \\
\boldsymbol{j}(\boldsymbol{r}) &= \frac{1}{V}\frac{1}{2m}\sum_{\boldsymbol{k},\boldsymbol{k}'}e^{i(\boldsymbol{k}'-\boldsymbol{k})\boldsymbol{r}}(\boldsymbol{k}+\boldsymbol{k}')c_{\boldsymbol{k}}^{\dagger}c_{\boldsymbol{k}'}.
\end{aligned}$$

**Problem 6.2, 2-Level System and Occupation Number Representation**

a) In occupation number representation there are 4 (linear) independent states:

$$|0,0\rangle \ ; \ |1,0\rangle \ ; \ |0,1\rangle \ ; \ |1,1\rangle .$$

The Fock space is therefore 4-dimensional, the 2-particle Hilbert space 1-dimensional. As a Slater determinant, the 2-particle state is given by:

$$|1,1\rangle \quad \equiv \frac{1}{\sqrt{2}}\left(|\varphi_1\rangle^{(1)}|\varphi_2\rangle^{(2)} - |\varphi_2\rangle^{(1)}|\varphi_1\rangle^{(2)}\right).$$

b) It holds:

$$c_1^\dagger|0,0\rangle = |1,0\rangle \ ; \ c_2^\dagger|0,0\rangle = |0,1\rangle \ ; \ c_1^\dagger|1,0\rangle = 0 \ ; \ c_2^\dagger|1,0\rangle = -|1,1\rangle$$
$$c_1^\dagger|0,1\rangle = |1,1\rangle \ ; \ c_2^\dagger|0,1\rangle = 0 \ ; \ c_i^\dagger|1,1\rangle = 0.$$

In the transition to the matrix representation, the states correspond to column vectors:

$$|0,0\rangle \equiv \begin{pmatrix}1\\0\\0\\0\end{pmatrix} ; |1,0\rangle \equiv \begin{pmatrix}0\\1\\0\\0\end{pmatrix} ; |0,1\rangle \equiv \begin{pmatrix}0\\0\\1\\0\end{pmatrix} ; |1,1\rangle \equiv \begin{pmatrix}0\\0\\0\\1\end{pmatrix}.$$

Matrix representation of $c_i, c_i^\dagger$:

$$c_1^\dagger = \begin{pmatrix}0&0&0&0\\1&0&0&0\\0&0&0&0\\0&0&1&0\end{pmatrix}, \ c_2^\dagger = \begin{pmatrix}0&0&0&0\\0&0&0&0\\1&0&0&0\\0&-1&0&0\end{pmatrix},$$

$$c_1 = \begin{pmatrix}0&1&0&0\\0&0&0&0\\0&0&0&1\\0&0&0&0\end{pmatrix}, \ c_2 = \begin{pmatrix}0&0&1&0\\0&0&0&-1\\0&0&0&0\\0&0&0&0\end{pmatrix},$$

$$n_1 = c_1^\dagger c_1 = \begin{pmatrix}0&0&0&0\\0&1&0&0\\0&0&0&0\\0&0&0&1\end{pmatrix}, \ n_2 = c_2^\dagger c_2 = \begin{pmatrix}0&0&0&0\\0&0&0&0\\0&0&1&0\\0&0&0&1\end{pmatrix}.$$

c)

$$c_1^\dagger c_2^\dagger = \begin{pmatrix} 0&0&0&0 \\ 1&0&0&0 \\ 0&0&0&0 \\ 0&0&1&0 \end{pmatrix} \begin{pmatrix} 0&0&0&0 \\ 0&0&0&0 \\ 1&0&0&0 \\ 0&-1&0&0 \end{pmatrix} = \begin{pmatrix} 0&0&0&0 \\ 0&0&0&0 \\ 0&0&0&0 \\ 1&0&0&0 \end{pmatrix},$$

$$c_2^\dagger c_1^\dagger = \begin{pmatrix} 0&0&0&0 \\ 0&0&0&0 \\ 1&0&0&0 \\ 0&-1&0&0 \end{pmatrix} \begin{pmatrix} 0&0&0&0 \\ 1&0&0&0 \\ 0&0&0&0 \\ 0&0&1&0 \end{pmatrix} = \begin{pmatrix} 0&0&0&0 \\ 0&0&0&0 \\ 0&0&0&0 \\ -1&0&0&0 \end{pmatrix},$$

$$\to c_1^\dagger c_2^\dagger = -c_2^\dagger c_1^\dagger.$$

The other anti-commutation relations are analogous, consider in particular

$$c_1 c_1^\dagger = \begin{pmatrix} 0&1&0&0 \\ 0&0&0&0 \\ 0&0&0&1 \\ 0&0&0&0 \end{pmatrix} \begin{pmatrix} 0&0&0&0 \\ 1&0&0&0 \\ 0&0&0&0 \\ 0&0&1&0 \end{pmatrix} = \begin{pmatrix} 1&0&0&0 \\ 0&0&0&0 \\ 0&0&1&0 \\ 0&0&0&0 \end{pmatrix}$$

$$= \begin{pmatrix} 1&0&0&0 \\ 0&1&0&0 \\ 0&0&1&0 \\ 0&0&0&1 \end{pmatrix} - \begin{pmatrix} 0&0&0&0 \\ 0&1&0&0 \\ 0&0&0&0 \\ 0&0&0&1 \end{pmatrix} = 1 - c_1^\dagger c_1$$

and

$$\left(c_1^\dagger\right)^2 = \begin{pmatrix} 0&0&0&0 \\ 1&0&0&0 \\ 0&0&0&0 \\ 0&0&1&0 \end{pmatrix} \begin{pmatrix} 0&0&0&0 \\ 1&0&0&0 \\ 0&0&0&0 \\ 0&0&1&0 \end{pmatrix} = \begin{pmatrix} 0&0&0&0 \\ 0&0&0&0 \\ 0&0&0&0 \\ 0&0&0&0 \end{pmatrix} = 0.$$

d)

$$H = \varepsilon(c_1^\dagger c_1 + c_2^\dagger c_2) + t(c_1^\dagger c_2 + c_2^\dagger c_1) + U c_1^\dagger c_2^\dagger c_2 c_1 + J c_1^\dagger c_2^\dagger c_1 c_2$$

Matrix representation:

$$H = \begin{pmatrix} 0&0&0&0 \\ 0&\varepsilon&t&0 \\ 0&t&\varepsilon&0 \\ 0&0&0&2\varepsilon+U-J \end{pmatrix}.$$

The one-particle part can be diagonalized by transition to new eigenstates

$$|\psi_{1,2}\rangle = \frac{1}{\sqrt{2}}(|\varphi_1\rangle \pm |\varphi_2\rangle) \quad \text{with eigenenergies} \quad E_{1,2} = \varepsilon \pm t.$$

e) If one introduces the creators and annihilators $d_i, d_i^\dagger$ with respect to the one-particle eigenstates $|\psi_i\rangle$ of $H_0$, one has

$$H = \begin{pmatrix} 0 & 0 & 0 & 0 \\ 0 & \varepsilon - t & 0 & 0 \\ 0 & 0 & \varepsilon + t & 0 \\ 0 & 0 & 0 & 2\varepsilon + U - J \end{pmatrix}$$
$$= (\varepsilon - t)d_1^\dagger d_1 + (\varepsilon + t)d_2^\dagger d_2 + (U - J)d_1^\dagger d_2^\dagger d_2 d_1.$$

The new generators and annihilators $d_i, d_i^\dagger$ arise from the old $c_i, c_i^\dagger$ through the same canonical transformation as the one-particle eigenstates arise from the original one-particle eigenstates, that is,

$$d_i = \frac{1}{\sqrt{2}}(c_1 \pm c_2); \quad d_i^\dagger = \frac{1}{\sqrt{2}}(c_1^\dagger \pm c_2^\dagger).$$

By substituting the canonical transformation, one can—using the anti-commutation rules—directly transform the two versions of $H$ in 2 nd Quantization in e) and d) into each other.

**Problem 6.3, Wick's Theorem**

a) Since the Hamiltonian operator

$$H = \sum_\alpha \varepsilon_\alpha c_\alpha^\dagger c_\alpha$$

is diagonal, only diagonal elements with respect to this occupation number representation occur in the calculation of (grand-)canonical expectation values, so one must be in the initial state again after the action of the operator $c_{\alpha_1}^\dagger c_{\alpha_2}^\dagger c_{\alpha_3} c_{\alpha_4}$ in occupation number representation, so that there is a non-vanishing contribution to the expectation value. Therefore, the electrons that are "annihilated" must also be created, i.e. $\alpha_4 = \alpha_1$ and $\alpha_2 = \alpha_3$ must apply or $\alpha_4 = \alpha_2$ and $\alpha_1 = \alpha_3$. So one has

$$\langle c_{\alpha_1}^\dagger c_{\alpha_2}^\dagger c_{\alpha_3} c_{\alpha_4}\rangle = \langle n_{\alpha_1} n_{\alpha_2}\rangle \delta_{\alpha_1\alpha_4}\delta_{\alpha_2\alpha_3} - \langle n_{\alpha_1} n_{\alpha_2}\rangle \delta_{\alpha_1\alpha_3}\delta_{\alpha_2\alpha_4}.$$

Now it holds in the grand canonical ensemble for a one-particle Hamiltonian operator diagonal in occupation number representation:

$$\begin{aligned}
\langle n_{\alpha_2}\rangle &= \frac{1}{\sum_{\{n_\alpha\}} e^{-\beta\sum_\alpha n_\alpha(\varepsilon_\alpha-\mu)}} \sum_{\{n_\alpha\}} n_{\alpha_2} e^{-\beta\sum_\alpha n_\alpha(\varepsilon_\alpha-\mu)} \\
&= -k_BT\frac{\partial}{\partial\varepsilon_{\alpha_2}} \ln \sum_{\{n_\alpha\}} e^{-\beta\sum_\alpha n_\alpha(\varepsilon_\alpha-\mu)} \\
&= -k_BT\frac{\partial}{\partial\varepsilon_{\alpha_2}} \ln Z_{gk} = -k_BT\frac{\partial}{\partial\varepsilon_{\alpha_2}} \ln\left(\prod_\alpha (1+e^{-\beta(\varepsilon_\alpha-\mu)})\right) \\
&= -k_BT\frac{\partial}{\partial\varepsilon_{\alpha_2}} \sum_\alpha \ln(1+e^{-\beta(\varepsilon_\alpha-\mu)}) = -k_BT\frac{-\beta e^{-\beta(\varepsilon_{\alpha_2}-\mu)}}{(1+e^{-\beta(\varepsilon_{\alpha_2}-\mu)})} \\
&= \frac{1}{e^{\beta(\varepsilon_{\alpha_2}-\mu)}+1}.
\end{aligned}$$

This is just the derivation of the Fermi distribution from the grand canonical partition function. From the first equation one sees:

$$\begin{aligned}
-k_BT\frac{\partial}{\partial\varepsilon_{\alpha_1}}\langle n_{\alpha_2}\rangle &= -k_BT\frac{\partial}{\partial\varepsilon_{\alpha_1}}\left(\frac{\sum_{\{n_\alpha\}} n_{\alpha_2} e^{-\beta\sum_\alpha n_\alpha(\varepsilon_\alpha-\mu)}}{\sum_{\{n_\alpha\}} e^{-\beta\sum_\alpha n_\alpha(\varepsilon_\alpha-\mu)}}\right) \\
&= \frac{\sum_{\{n_\alpha\}} n_{\alpha_1} n_{\alpha_2} e^{-\beta\sum_\alpha n_\alpha(\varepsilon_\alpha-\mu)}}{\sum_{\{n_\alpha\}} e^{-\beta\sum_\alpha n_\alpha(\varepsilon_\alpha-\mu)}} \\
&\quad - \frac{\left(\sum_{\{n_\alpha\}} n_{\alpha_1} e^{-\beta\sum_\alpha n_\alpha(\varepsilon_\alpha-\mu)}\right)\left(\sum_{\{n_\alpha\}} n_{\alpha_2} e^{-\beta\sum_\alpha n_\alpha(\varepsilon_\alpha-\mu)}\right)}{\left(\sum_{\{n_\alpha\}} e^{-\beta\sum_\alpha n_\alpha(\varepsilon_\alpha-\mu)}\right)^2} \\
&= \langle n_{\alpha_1} n_{\alpha_2}\rangle - \langle n_{\alpha_1}\rangle\langle n_{\alpha_2}\rangle.
\end{aligned}$$

On the other hand, for $\alpha_1 \neq \alpha_2$:

$$\frac{\partial}{\partial\varepsilon_{\alpha_1}}\langle n_{\alpha_2}\rangle = \frac{\partial}{\partial\varepsilon_{\alpha_1}}\frac{1}{e^{\beta(\varepsilon_{\alpha_2}-\mu)}+1} = 0$$

So we find

$$\langle n_{\alpha_1} n_{\alpha_2}\rangle - \langle n_{\alpha_1}\rangle\langle n_{\alpha_2}\rangle = 0,$$

from which the claim follows.

b)

$$\begin{aligned}
\langle c^\dagger_{n_1} c^\dagger_{n_2} c_{n_3} c_{n_4}\rangle &= \sum_{\alpha_1}\sum_{\alpha_2}\sum_{\alpha_3}\sum_{\alpha_4} u^*_{n_1\alpha_1} u^*_{n_2\alpha_2} u_{n_3\alpha_3} u_{n_4\alpha_4} \langle c^\dagger_{\alpha_1} c^\dagger_{\alpha_2} c_{\alpha_3} c_{\alpha_4}\rangle \\
&= \sum_{\alpha_1}\sum_{\alpha_2}\sum_{\alpha_3}\sum_{\alpha_4} u^*_{n_1\alpha_1} u^*_{n_2\alpha_2} u_{n_3\alpha_3} u_{n_4\alpha_4} \left(\langle c^\dagger_{\alpha_1} c_{\alpha_4}\rangle\langle c^\dagger_{\alpha_2} c_{\alpha_3}\rangle - \langle c^\dagger_{\alpha_1} c_{\alpha_3}\rangle\langle c^\dagger_{\alpha_2} c_{\alpha_4}\rangle\right) \\
&= \langle c^\dagger_{n_1} c_{n_4}\rangle\langle c^\dagger_{n_2} c_{n_3}\rangle - \langle c^\dagger_{n_1} c_{n_3}\rangle\langle c^\dagger_{n_2} c_{n_4}\rangle.
\end{aligned}$$

**Problem 6.4, Interacting 2-Particle Model in One Dimension**

a) The one-dimensional one-particle Schrödinger equation is solved numerically

$$\left(-\frac{d^2}{dx^2} - 2V(|x|)\right)\varphi_i(x) = \varepsilon_i \varphi_i(x)$$

This results in the lowest (bound) energy eigenvalues (specifically for $\delta = 0.1$) $\varepsilon_1 = -19.0809$, $\varepsilon_2 = -2.6670$, $\varepsilon_3 = -1.7042$, $\varepsilon_4 = -0.8100$. The corresponding eigenfunctions $\varphi_i(x)$ are shown below.

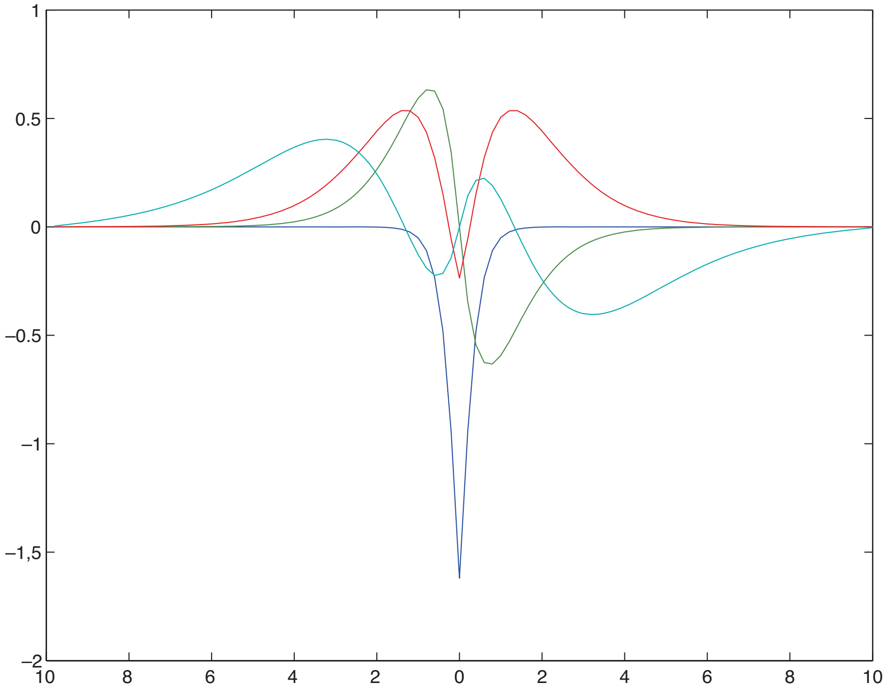

When only the lowest two states $i \in \{1, 2\}$ are considered, the Hamiltonian operator in 2nd quantization is

$$H = \sum_{i=1,2;\sigma} \varepsilon_i c^\dagger_{i\sigma} c_{i\sigma} + \frac{1}{2} \sum_{i_1,i_2,i_3,i_4=1,2;\sigma\sigma'} u_{i_1 i_2, i_3 i_4} c^\dagger_{i_1\sigma} c^\dagger_{i_2\sigma'} c_{i_3\sigma'} c_{i_4\sigma}$$

with the Coulomb matrix elements

$$u_{ij,kl} = \int dx \int dx' \varphi_i(x)\varphi_j(x')\varphi_k(x')\varphi_l(x) V(|x - x'|)$$

and $i, j, k, l \in \{1, 2\}$; in one dimension, all eigenfunctions can be chosen real. This leaves only 6 different Coulomb matrix elements:

$$\begin{aligned}
U_1 &= u_{11,11} = 10.4594, \quad U_2 = u_{22,22} = 3.2442, \\
V &= u_{12,21} = u_{21,12} = 2.6134, \\
J &= u_{12,12} = u_{21,21} = u_{22,11} = u_{11,22} = 0.3977, \\
X_1 &= u_{12,22} = u_{21,22} = u_{22,12} = u_{22,21} = 0 \\
= X_2 &= u_{21,11} = u_{12,11} = u_{11,21} = u_{11,12}.
\end{aligned}$$

Since the latter $X_{1,2}$ at least numerically vanish for the example discussed here, the many-particle Hamiltonian operator can be brought into the following form:

$$\begin{aligned}
H = {} & \sum_\sigma \left( \varepsilon_1 c^\dagger_{1\sigma} c_{1\sigma} + \varepsilon_2 c^\dagger_{2\sigma} c_{2\sigma} \right) + U_1 c^\dagger_{1\uparrow} c_{1\uparrow} c^\dagger_{1\downarrow} c_{1\downarrow} + U_2 c^\dagger_{2\uparrow} c_{2\uparrow} c^\dagger_{2\downarrow} c_{2\downarrow} \\
& + V \sum_{\sigma,\sigma'} c^\dagger_{1\sigma} c_{1\sigma} c^\dagger_{2\sigma'} c_{2\sigma'} + J \sum_{\sigma,\sigma'} c^\dagger_{1\sigma} c^\dagger_{2\sigma'} c_{1\sigma'} c_{2\sigma} \\
= {} & \varepsilon_1 c^\dagger_{1\uparrow} c_{1\uparrow} + \varepsilon_1 c^\dagger_{1\downarrow} c_{1\downarrow} + \varepsilon_2 c^\dagger_{2\uparrow} c_{2\uparrow} + \varepsilon_2 c^\dagger_{2\downarrow} c_{2\downarrow} \\
& + U_1 c^\dagger_{1\uparrow} c_{1\uparrow} c^\dagger_{1\downarrow} c_{1\downarrow} + U_2 c^\dagger_{2\uparrow} c_{2\uparrow} c^\dagger_{2\downarrow} c_{2\downarrow} + V (c^\dagger_{1\uparrow} c_{1\uparrow} c^\dagger_{2\downarrow} c_{2\downarrow} + c^\dagger_{1\downarrow} c_{1\downarrow} c^\dagger_{2\uparrow} c_{2\uparrow}) \\
& + J (c^\dagger_{1\uparrow} c^\dagger_{2\downarrow} c_{1\downarrow} c_{2\uparrow} + c^\dagger_{1\downarrow} c^\dagger_{2\uparrow} c_{1\uparrow} c_{2\downarrow}) \\
& + (V - J)(c^\dagger_{1\uparrow} c_{1\uparrow} c^\dagger_{2\uparrow} c_{2\uparrow} + c^\dagger_{1\downarrow} c_{1\downarrow} c^\dagger_{2\downarrow} c_{2\downarrow}) \\
& + J (c^\dagger_{1\uparrow} c^\dagger_{1\downarrow} c_{2\downarrow} c_{2\uparrow} + c^\dagger_{2\uparrow} c^\dagger_{2\downarrow} c_{1\downarrow} c_{1\uparrow}).
\end{aligned}$$

b) For antiparallel spins there are the following 4 2-particle states:

$$c^\dagger_{1\uparrow} c^\dagger_{1\downarrow} |0\rangle, \quad c^\dagger_{2\uparrow} c^\dagger_{2\downarrow} |0\rangle, \quad c^\dagger_{1\uparrow} c^\dagger_{2\downarrow} |0\rangle, \quad c^\dagger_{2\uparrow} c^\dagger_{1\downarrow} |0\rangle.$$

With respect to these states, the Hamiltonian operator has the following matrix representation:

$$H = \begin{pmatrix} 2\varepsilon_1 + U_1 & J & 0 & 0 \\ J & 2\varepsilon_2 + U_2 & 0 & 0 \\ 0 & 0 & \varepsilon_1 + \varepsilon_2 + V & J \\ 0 & 0 & J & \varepsilon_1 + \varepsilon_2 + V \end{pmatrix}.$$

This matrix has the eigenvalues

$$\begin{aligned}
E_{1,2} &= \frac{1}{2} \left( 2\varepsilon_1 + U_1 + 2\varepsilon_2 + U_2 \pm \sqrt{(2\varepsilon_1 + U_1 - 2\varepsilon_2 - U_2)^2 + 4J^2} \right) \\
E_{3,4} &= \varepsilon_1 + \varepsilon_2 + V \pm J.
\end{aligned}$$

Numerically, in particular:

$$E_1 = -27.7085, \quad E_3 = -19.5322, \quad E_4 = -18.7368, \quad E_2 = -2.0836.$$

For parallel spin-$z$-components there are only the two 2-particle states $c^\dagger_{1\uparrow} c^\dagger_{2\uparrow} |0\rangle,\ c^\dagger_{1\downarrow} c^\dagger_{2\downarrow} |0\rangle$, which are already eigenstates of $H$ with eigenenergies

$$E_{5,6} = \varepsilon_1 + \varepsilon_2 + V - J = E_3 = -19.5322.$$

The three eigenstates $c^\dagger_{1\uparrow}c^\dagger_{2\uparrow}|0\rangle$, $c^\dagger_{1\downarrow}c^\dagger_{2\downarrow}|0\rangle$, $\frac{1}{2}(c^\dagger_{1\uparrow}c^\dagger_{2\downarrow} - c^\dagger_{2\uparrow}c^\dagger_{1\downarrow})|0\rangle$ are degenerate with respect to the eigenvalue $E_3$ and form the triplet of states with total spin 1 (with spin-$z$-components $1, -1, 0$).

The ground state of this "one-dimensional helium atom" is therefore a singlet state ("para-helium") with ground state energy $E_1 = -27.7085$, the first excited state is the triplet state ("ortho-helium") with the energy $E_3 = -19.5322$.

In Hartree-Fock approximation, the effective Hamiltonian operator (under the assumption of diagonalization with respect to the same one-particle eigenstates)

$$\begin{aligned} H_{HF} = &\Big(\varepsilon_1 + U_1\langle c^\dagger_{1\downarrow}c_{1\downarrow}\rangle + (V-J)\langle c^\dagger_{2\uparrow}c_{2\uparrow}\rangle + V\langle c^\dagger_{2\downarrow}c_{2\downarrow}\rangle\Big)c^\dagger_{1\uparrow}c_{1\uparrow} \\ &+ \Big(\varepsilon_1 + U_1\langle c^\dagger_{1\uparrow}c_{1\uparrow}\rangle + (V-J)\langle c^\dagger_{2\downarrow}c_{2\downarrow}\rangle + V\langle c^\dagger_{2\uparrow}c_{2\uparrow}\rangle\Big)c^\dagger_{1\downarrow}c_{1\downarrow} \\ &+ \Big(\varepsilon_2 + U_2\langle c^\dagger_{2\downarrow}c_{2\downarrow}\rangle + (V-J)\langle c^\dagger_{1\uparrow}c_{1\uparrow}\rangle + V\langle c^\dagger_{1\downarrow}c_{1\downarrow}\rangle\Big)c^\dagger_{2\uparrow}c_{2\uparrow} \\ &+ \Big(\varepsilon_2 + U_2\langle c^\dagger_{2\uparrow}c_{2\uparrow}\rangle + (V-J)\langle c^\dagger_{1\downarrow}c_{1\downarrow}\rangle + V\langle c^\dagger_{1\uparrow}c_{1\uparrow}\rangle\Big)c^\dagger_{2\downarrow}c_{2\downarrow}. \end{aligned}$$

The energetically favorable 2-particle singlet state is again $c^\dagger_{1\uparrow}c^\dagger_{1\downarrow}|0\rangle$; for this $\langle c^\dagger_{1\sigma}c_{1\sigma}\rangle = 1$ and it results in the Hartree-Fock ground state energy (avoiding double counting!)

$$E_1^{HF} = 2\varepsilon_1 + U_1 = -27.7024,$$

thus a value that is only slightly higher than the true ground state energy.

For the triplet state $c^\dagger_{1\uparrow}c^\dagger_{2\uparrow}|0\rangle$, the Hartree-Fock approximation results in an energy

$$E_3^{HF} = \varepsilon_1 + \varepsilon_2 + V - J = -19.5322,$$

which is the exact result, since for this state $\langle c^\dagger_{i\uparrow}c_{i\uparrow}\rangle = 1$ and all other occupation numbers vanish.

**Problem 6.5, 1-Dimensional Helium Atom Model**

a) Matlab program for the numerical solution of this problem:

```
clear;
h=zeros(100,100);
h0=zeros(100,100);
v=zeros(100);
vhar=zeros(100);
eps=zeros(100);
for i=1:100
x(i)=-10+i*0.2;
v(i)=-4/(abs(x(i))+0.1);
end
```

```
for i=1:100
h0(i,i)=2+v(i)*0.04;
if i<=99 h0(i,i+1)=-1; end
if i>=2 h0(i,i-1)=-1; end
end
[ev,ew]=eig(h0);
ev(:,1)'*ev(:,1)
ev(:,1)'*ev(:,2)
for i=1:100
eps(i)=ew(i,i)/0.04;
end
eps(1)
eps(2)
u1111=0;u2222=0;u1221=0;u1212=0;
for i=1:100
for j=1:100
u1111=u1111+2*ev(i,1)^2*ev(j,1)^2/(abs(x(i)-x(j))+0.1);
u2222=u2222+2*ev(i,2)^2*ev(j,2)^2/(abs(x(i)-x(j))+0.1);
u1221=u1221+2*ev(i,1)^2*ev(j,2)^2/(abs(x(i)-x(j))+0.1);
u1212=u1212+2*ev(i,1)*ev(i,2)*ev(j,1)*ev(j,2)/
   (abs(x(i)-x(j))+0.1);
end
end
u1111
u2222
u1221
u1212
x1=2*eps(1)+u1111
x2=2*eps(2)+u2222;
en1=0.5*(x1+x2-sqrt((x1-x2)^2+4*u1212^2))
en2=eps(1)+eps(2)+u1221-u1212
en3=eps(1)+eps(2)+u1221+u1212
en4=0.5*(x1+x2+sqrt((x1-x2)^2+4*u1212^2))
figure(1); plot(x,ev(:,1),x,ev(:,2),x,ev(:,3),x,ev(:,4))
evh=ev;
for iter=1:15
for i=1:100
vhar(i)=0;
for j=1:100
vhar(i)=vhar(i)+2*evh(j,1)^2/(abs(x(i)-x(j))+0.1);
end
end
vg=v+vhar;
for i=1:100
h(i,i)=2+vg(i)*0.04;
```

```
if i<=99 h(i,i+1)=-1; end
if i>=2 h(i,i-1)=-1; end
end
[evh,ewh]=eig(h);
for i=1:100
epshf(i)=ewh(i,i)/0.04;
end
iter
ehf0=epshf(1)
end
hfpot11=0;hfpot22=0;hfpot12=0;
for i=1:100
hfpot11=hfpot11+evh(i,1)*evh(i,1)*vhar(i);
hfpot22=hfpot22+evh(i,2)*evh(i,2)*vhar(i);
hfpot12=hfpot12+evh(i,1)*evh(i,2)*vhar(i);
end
enhf1=2*epshf(1)-hfpot11
u1111=0;u2222=0;u1221=0;u1212=0;
for i=1:100
for j=1:100
u1111=u1111+2*evh(i,1)^2*evh(j,1)^2/(abs(x(i)-x(j))+0.1);
u2222=u2222+2*evh(i,2)^2*evh(j,2)^2/(abs(x(i)-x(j))+0.1);
u1221=u1221+2*evh(i,1)^2*evh(j,2)^2/(abs(x(i)-x(j))+0.1);
u1212=u1212+2*evh(i,1)*evh(i,2)*evh(j,1)*evh(j,2)/
   (abs(x(i)-x(j))+0.1);
end
end
u1111
u2222
u1221
u1212
enh011=evh(:,1)'*h0*evh(:,1)/0.04
enh022=evh(:,2)'*h0*evh(:,2)/0.04
enh012=evh(:,1)'*h0*evh(:,2)/0.04
enh021=evh(:,2)'*h0*evh(:,1)/0.04
x1=2*enh011+u1111;
x2=2*enh022+u2222;
enh1=0.5*(x1+x2-sqrt((x1-x2)^2+4*u1212^2))
enh2=eps(1)+eps(2)+u1221-u1212
enh3=eps(1)+eps(2)+u1221+u1212
enh4=0.5*(x1+x2+sqrt((x1-x2)^2+4*u1212^2))
figure(2); plot(x,evh(:,1),x,ev(:,1))
figure(3); plot(x,evh(:,2),x,ev(:,2))
```

The Hartree-Fock equations, which in this case reduce to the Hartree equations because the Fock term only acts between electrons of the same spin, but here the spin of the two electrons involved can be assumed to be different from the outset, can be solved by direct iteration. The lowest Hartee-Fock one-particle energies are given by:

$$\varepsilon_{HF1} = -9.5729.$$

This one-particle energy eigenvalue is of course much higher than the one-particle energy eigenvalue of the unperturbed Hamiltonian operator $H_0$, because the Hartree potential not only contains the attractive nuclear potential but also the repulsive contribution of the 2nd electron, the total effective one-particle potential is therefore less attractive. The Hartree one-particle ground state is accordingly slightly less localized than the one-particle ground state belonging to the unperturbed Hamiltonian operator $H_0$ $\phi_1(x)$, as can be seen in the following figure.

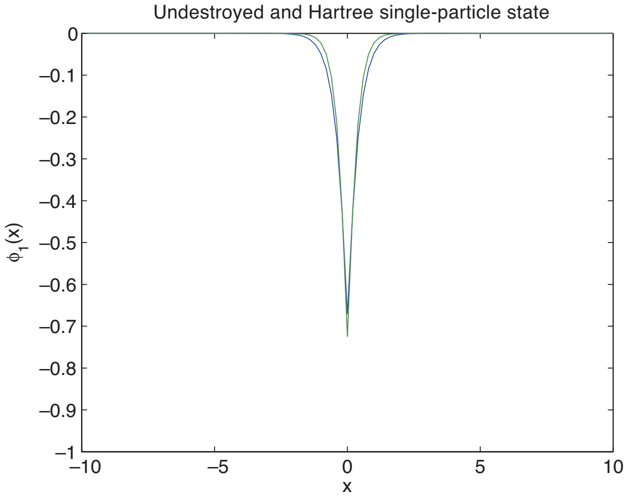

As the Hartree-Fock ground state energy, this results in

$$E_{HF0} = 2\varepsilon_{HF1} - \int dx \int dx' \frac{2|\phi_{HF1}(x)|^2 |\phi_{HF1}(x')|^2}{|x - x'| + \delta} = -28.3318,$$

which is energetically lower than the result from the 2nd quantization with respect to the eigenstates of $H_0$ from problem 6.4. Working in the Hartree single-particle basis is therefore more favorable than working in the single-particle eigenbasis of $H_0$.

b) Of course, the 2nd quantization can also be carried out with respect to the Hartree-Fock one-particle basis. If one restricts oneself, as in problem 6.4 only to the 2 lowest one-particle states, the Hamiltonian in 2nd quantization has the form

$$H = \sum_{i=1,2;\sigma} \varepsilon_i c^\dagger_{i\sigma} c_{i\sigma} + \frac{1}{2} \sum_{i_1,i_2,i_3,i_4=1,2;\sigma\sigma'} u_{i_1 i_2, i_3 i_4} c^\dagger_{i_1\sigma} c^\dagger_{i_2\sigma'} c_{i_3\sigma'} c_{i_4\sigma}$$

with

$$\varepsilon_i = \int dx \phi_{HFi}(x) \left( -\frac{d^2}{dx^2} - \frac{2}{|x| + \delta} \right) \phi_{HFi}(x)$$
$$u_{ij,kl} = \int dx \int dx' \phi_{HFi}(x) \phi_{HFj}(x') \phi_{HFk}(x') \phi_{HFl}(x) \frac{2}{|x - x'| + \delta}.$$

It turns out that the one-particle Hamiltonian is also approximately diagonal with respect to the Hartree-Fock one-particle states (non-diagonal elements of the order of $10^{-5}$) and that

$$\varepsilon_1 = -18.7589, \quad \varepsilon_2 = -1.9562, \quad u_{11,11} = 9.1860$$
$$u_{22,22} = 1.9355, \quad u_{12,21} = 1.2994, \quad u_{12,12} = 0.1086.$$

If one restricts oneself to these 2 lowest one-particle states and for antiparallel spins of the two electrons, the 2-particle Hilbert space becomes 4-dimensional again (cf. Problem 6.4) and one obtains as 2-particle eigenenergies

$$-28.3322, \quad -20.5571, \quad -20.3399, \quad -1.9764.$$

The ground state energy is therefore slightly lower than in simple Hartree-Fock calculation, but both are still about 2% lower than in the corresponding calculation in 2nd quantization with respect to the one-particle eigenstates of the non-interacting Hamiltonian $H_0$.

c) For given $Z \in [1, 2]$ one can determine $\varphi_Z(x)$ by (numerical) solution of the Schrödinger equation

$$\left( -\frac{d^2}{dx^2} - ZV(|x|) \right) \varphi_Z(x) = \varepsilon_{Z0} \varphi_Z(x).$$

Then one has to calculate the expectation value of the original 2-particle Hamilton operator with these $\varphi_Z(x)$. As an approximation for the ground state energy within the framework of this variation approach, one obtains:

$$E_0(Z) = 2 \int dx \varphi_Z(x) \left( -\frac{d^2}{dx^2} - 2V(|x|) \right) \varphi_Z(x)$$
$$+ \int dx \int dx' \frac{2|\varphi_Z(x)|^2 |\varphi_Z(x')|^2}{|x - x'| + \delta}.$$

$E_0(Z)$ is shown below; it obviously results in a minimum for $Z_0 \approx 1.55$ and the corresponding energy value, i.e. the approximation for the ground state energy within the framework of the approach, results in $E_0(Z_0) = -28.2844$, which is quite close to the Hartree-(Fock-)results from a) and b).

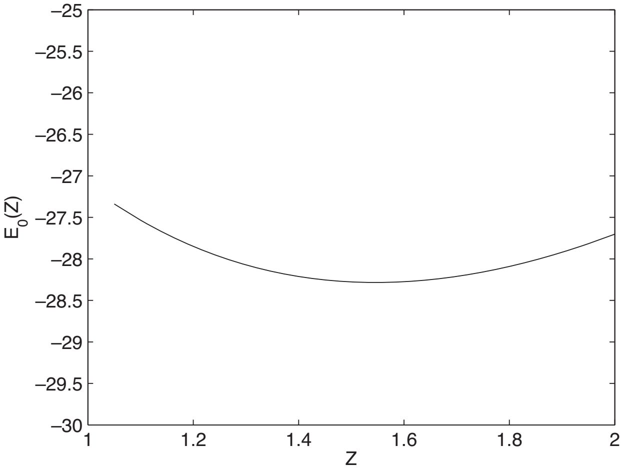

### Problem 6.6, Two-Site Hubbard Model

$$\begin{aligned} H = \varepsilon_0 &\Big( c_{1\uparrow}^\dagger c_{1\uparrow} + c_{1\downarrow}^\dagger c_{1\downarrow} + c_{2\uparrow}^\dagger c_{2\uparrow} + c_{2\downarrow}^\dagger c_{2\downarrow} \Big) \\ &+ t\Big( c_{1\uparrow}^\dagger c_{2\uparrow} + c_{1\downarrow}^\dagger c_{2\downarrow} + c_{2\uparrow}^\dagger c_{1\uparrow} + c_{2\downarrow}^\dagger c_{1\downarrow} \Big) \\ &+ U\Big( c_{1\uparrow}^\dagger c_{1\uparrow} c_{1\downarrow}^\dagger c_{1\downarrow} + c_{2\uparrow}^\dagger c_{2\uparrow} c_{2\downarrow}^\dagger c_{2\downarrow} \Big). \end{aligned}$$

a) The matrix representation of the two-site Hubbard model in the 4-dimensional subspace spanned by the states

$$c_{1\uparrow}^\dagger c_{1\downarrow}^\dagger |0\rangle, \quad c_{2\uparrow}^\dagger c_{2\downarrow}^\dagger |0\rangle, \quad c_{1\uparrow}^\dagger c_{2\downarrow}^\dagger |0\rangle, \quad c_{2\uparrow}^\dagger c_{1\downarrow}^\dagger |0\rangle$$

for spin-$z$ component 0 and particle number 2 is:

$$H = \begin{pmatrix} 2\varepsilon_0 + U & 0 & t & t \\ 0 & 2\varepsilon_0 + U & t & t \\ t & t & 2\varepsilon_0 & 0 \\ t & t & 0 & 2\varepsilon_0 \end{pmatrix}.$$

For this simple $4 * 4$-matrix one can guess eigenstates, namely

$$\begin{pmatrix} 1 \\ -1 \\ 0 \\ 0 \end{pmatrix}, \quad \begin{pmatrix} 0 \\ 0 \\ 1 \\ -1 \end{pmatrix}, \quad \begin{pmatrix} x \\ x \\ y \\ y \end{pmatrix}.$$

The first two column vectors are eigenstates to the eigenvalues $2\varepsilon_0 + U$ and $2\varepsilon_0$ , the 3rd ansatz leads to the 2-dimensional eigenvalue equation:

$$\begin{aligned}(2\varepsilon_0 + U)x + 2ty &= \lambda x\\ 2tx + 2\varepsilon_0 y &= \lambda y,\end{aligned}$$

which leads to the eigenvalues

$$\lambda = 2\varepsilon_0 + \frac{U}{2} \pm \sqrt{4t^2 + \frac{U^2}{4}}$$

Two more 2-particle eigenstates with parallel spin-$z$ component are given by $c^\dagger_{1\uparrow}c^\dagger_{2\uparrow}|0\rangle,\ c^\dagger_{1\downarrow}c^\dagger_{2\downarrow}|0\rangle$ with eigenvalues $2\varepsilon_0$.

In summary, one has 6 2-particle eigenvalues, namely

$$\begin{aligned}
E_1 &= 2\varepsilon_0 + \frac{U}{2} - \sqrt{4t^2 + \frac{U^2}{4}}\\
&\quad \text{with eigenstate} \quad \left[x\left(c^\dagger_{1\uparrow}c^\dagger_{1\downarrow} + c^\dagger_{2\uparrow}c^\dagger_{2\downarrow}\right) + y\left(c^\dagger_{1\uparrow}c^\dagger_{2\downarrow} + c^\dagger_{2\uparrow}c^\dagger_{1\downarrow}\right)\right]|0\rangle\\
E_2 &= 2\varepsilon_0 \quad \text{with eigenstate} \quad c^\dagger_{1\uparrow}c^\dagger_{2\uparrow}|0\rangle\\
E_3 &= 2\varepsilon_0 \quad \text{with eigenstate} \quad \frac{1}{\sqrt{2}}\left[c^\dagger_{1\uparrow}c^\dagger_{2\downarrow} - c^\dagger_{2\uparrow}c^\dagger_{1\downarrow}\right]|0\rangle\\
E_4 &= 2\varepsilon_0 \quad \text{with eigenstate} \quad c^\dagger_{1\downarrow}c^\dagger_{2\downarrow}|0\rangle\\
E_5 &= 2\varepsilon_0 + U \quad \text{with eigenstate} \quad \frac{1}{\sqrt{2}}\left[c^\dagger_{1\uparrow}c^\dagger_{1\downarrow} - c^\dagger_{2\uparrow}c^\dagger_{2\downarrow}\right]|0\rangle\\
E_6 &= 2\varepsilon_0 + \frac{U}{2} + \sqrt{4t^2 + \frac{U^2}{4}}\\
&\quad \text{with eigenstate} \quad \left[y\left(c^\dagger_{1\uparrow}c^\dagger_{1\downarrow} + c^\dagger_{2\uparrow}c^\dagger_{2\downarrow}\right) - x\left(c^\dagger_{1\uparrow}c^\dagger_{2\downarrow} + c^\dagger_{2\uparrow}c^\dagger_{1\downarrow}\right)\right]|0\rangle.
\end{aligned}$$

The dependence of the eigenenergies on $U$ is shown below for $2t = 1$ and $\varepsilon_0 = 0$.

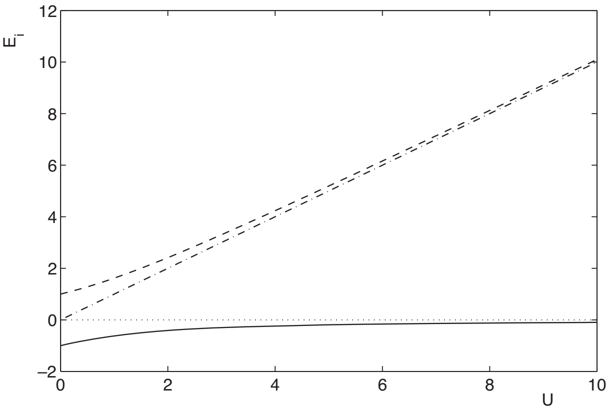

b) In Hartree-Fock approximation, the effective Hamiltonian operator is

$$\begin{aligned} H = &(\varepsilon_0 + U\langle c_{1\downarrow}^\dagger c_{1\downarrow}\rangle)c_{1\uparrow}^\dagger c_{1\uparrow} + (\varepsilon_0 + U\langle c_{1\uparrow}^\dagger c_{1\uparrow}\rangle)c_{1\downarrow}^\dagger c_{1\downarrow} \\ &+ (\varepsilon_0 + U\langle c_{2\downarrow}^\dagger c_{2\downarrow}\rangle)c_{2\uparrow}^\dagger c_{2\uparrow} + (\varepsilon_0 + U\langle c_{2\uparrow}^\dagger c_{2\uparrow}\rangle)c_{2\downarrow}^\dagger c_{2\downarrow} \\ &+ t\left(c_{1\uparrow}^\dagger c_{2\uparrow} + c_{1\downarrow}^\dagger c_{2\downarrow} + c_{2\uparrow}^\dagger c_{1\uparrow} + c_{2\downarrow}^\dagger c_{1\downarrow}\right). \end{aligned}$$

If the total particle number is 2, that is

$$\sum_{i=1,2,\sigma} \langle c_{i\sigma}^\dagger c_{i\sigma}\rangle = 2$$

holds, then, because of the equality of all 4 one-particle states,

$$\langle c_{i\sigma}^\dagger c_{i\sigma}\rangle = \frac{1}{2}$$

must hold. Then, for the two-particle ground state energy in Hartree-Fock approximation:

$$E_0^{HF} = 2\varepsilon_0 + \frac{U}{2} - 2t$$

which is obviously correct for very small $U$ (up to linear order in $U$), but not for larger $U$.

**Problem 6.7, Hartree-Fock Approximation for Two-Particle System**

Under the assumption that the one-particle wave functions $\phi_n, \phi_m$ are eigenfunctions of the one-particle Hamiltonian operator $h(r)$, it follows:

$$
\begin{aligned}
\langle\psi|H|\psi\rangle = {} & \frac{1}{2}\int dr_1\int dr_2(\phi_n^*(r_1)\phi_m^*(r_2)-\phi_m^*(r_1)\phi_n^*(r_2)) \\
& (h(r_1)+h(r_2)+v(r_1-r_2)) * (\phi_n(r_1)\phi_m(r_2)-\phi_m(r_1)\phi_n(r_2)) \\
= {} & \frac{1}{2}\Big(\int dr_1\phi_n^*(r_1)h(r_1)\phi_n(r_1)+\int dr_1\phi_m^*(r_1)h(r_1)\phi_m(r_1)+ \\
& +\int dr_2\phi_m^*(r_2)h(r_2)\phi_m(r_2)+\int dr_2\phi_n^*(r_2)h(r_2)\phi_n(r_2) \\
& +\int dr_1\int dr_2\phi_n^*(r_1)\phi_m^*(r_2)v(r_1-r_2)\phi_m(r_2)\phi_n(r_1) \\
& +\int dr_1\int dr_2\phi_m^*(r_1)\phi_n^*(r_2)v(r_1-r_2)\phi_n(r_2)\phi_m(r_1) \\
& -\int dr_1\int dr_2\phi_m^*(r_1)\phi_n^*(r_2)v(r_1-r_2)\phi_n(r_1)\phi_m(r_2) \\
& -\int dr_1\int dr_2\phi_n^*(r_1)\phi_m^*(r_2)v(r_1-r_2)\phi_m(r_1)\phi_n(r_2)\Big) \\
= {} & \int dr\phi_n^*(r)h(r)\phi_n(r)+\int dr\phi_m^*(r)h(r)\phi_m(r) \\
& +\int dr\int dr'\phi_n^*(r)\phi_m^*(r')v(r-r')\phi_m(r')\phi_n(r) \\
& -\int dr\int dr'\phi_m^*(r)\phi_n^*(r')v(r-r')\phi_m(r')\phi_n(r).
\end{aligned}
$$

Variation with respect to $\phi_n^*(r)$ under the condition $\int dr\phi_n^*(r)\phi_n(r)=1$ (i.e. normalization of $\phi_n(r)$), which is added to the energy functional to be minimized with a Lagrange multiplier $\varepsilon_n$, yields

$$
\begin{aligned}
h(r)\phi_n(r) & +\int dr'\phi_m^*(r')v(r-r')\phi_m(r')\phi_n(r) \\
& -\int dr'\phi_m^*(r')v(r-r')\phi_n(r')\phi_m(r)=\varepsilon_n\phi_n(r)
\end{aligned}
$$

the Hartree-Fock equation, an effective nonlinear Schrödinger equation for $\phi_n(r)$ and $\varepsilon_n$.

**Problem 6.8, Hartree Equations**

a) Under the assumption of the normalization of the one-particle wave functions $\phi_{n_j}(r)$, the expectation value of the $i$-th summand of the one-particle contribution results:

$$
\begin{aligned}
& \int dr_1\ldots\int dr_N\phi_{n_1}^*(r_1)\ldots\phi_{n_N}^*(r_N)h(r_i)\phi_{n_1}(r_1)\ldots\phi_{n_N}(r_N) \\
& =\int dr_i\phi_{n_i}^*(r_i)h(r_i)\phi_{n_i}(r_i).
\end{aligned}
$$

Accordingly, for a fixed $i \neq j$,

$$\int dr_1 \ldots \int dr_N \phi^*_{n_1}(r_1) \ldots \phi^*_{n_N}(r_N) v(r_i - r_j) \phi_{n_1}(r_1) \ldots \phi_{n_N}(r_N)$$
$$= \int dr_i \int dr_j \phi^*_{n_i}(r_i) \phi^*_{n_j}(r_j) v(r_i - r_j) \phi_{n_i}(r_i) \phi_{n_j}(r_j)$$

results, from which the claim of a) follows.

b) Variation with respect to a fixed $\phi^*_{n_k}(r)$ under the constraint of normali zation of the state leads to

$$h(r)\phi_{n_k}(r) + \sum_{j \neq k} \int dr' |\phi_{n_j}(r')|^2 v(r - r') \phi_{n_k}(r) = \varepsilon_{n_k} \phi_{n_k}(r),$$

(taking into account the fact that $k$ occurs twice in the double sum $i \neq j$: once as $i$, once as $j$).

**Problem 6.9, Homogeneous Electron Gas**

a)

$$\begin{aligned}
\frac{1}{V} \sum_{k', k' < k_F} \frac{1}{|k - k'|^2} &= \frac{1}{(2\pi)^2} \int_0^{k_F} dk' k'^2 \int_{-1}^{+1} \frac{du}{k^2 + k'^2 - 2kk'u} \\
&= \frac{1}{4\pi^2} \int_0^{k_F} dk' k'^2 \frac{1}{2kk'} \ln \frac{k^2 + k'^2 + 2kk'}{k^2 + k'^2 - 2kk'} = \frac{2\pi}{k} \int_0^{k_F} dk' k' \ln \left| \frac{k + k'}{k - k'} \right| \\
&= \frac{1}{4\pi^2 k} \left[ -\frac{1}{4} k'^2 + \frac{kk'}{2} + \frac{k'^2 - k^2}{2} \ln(k + k') + \frac{1}{4} k'^2 + \frac{kk'}{2} \right. \\
&\qquad \left. + \frac{k^2 - k'^2}{2} \ln(k - k') \right]_0^{k_F} \\
&= \frac{1}{4\pi^2 k} \left[ kk_F + \frac{k_F^2 - k^2}{2} \ln \frac{k + k_F}{k - k_F} + \frac{k^2}{2} \ln \frac{k + 0}{k - 0} \right] \\
&= \frac{k_F}{2\pi^2} \left[ \frac{1}{2} + \frac{1 - (k/k_F)^2}{4(k/k_F)} \ln \left| \frac{1 + k/k_F}{1 - k/k_F} \right| \right].
\end{aligned}$$

b)

$$\begin{aligned}
&\sum_{k < k_F} \frac{k_F^2 - k^2}{kk_F} \ln \left| \frac{k + k_F}{k - k_F} \right| \\
&\qquad = \frac{V}{2\pi^2 k_F} \int_0^{k_F} dk (k_F^2 k - k^3)(\ln(k_F + k) - \ln(k_F - k)) \\
&\qquad = \frac{V}{2\pi^2 k_F} \int_{-k_F}^{+k_F} dk (k_F^2 k - k^3) \ln(k_F + k) \\
&\qquad = \frac{V}{2\pi^2 k_F} \left[ \frac{k_F^2}{2} (k^2 - k_F^2) \ln(k_F + k) - \frac{k_F^2}{2} \frac{k^2}{2} + k_F^2 \frac{kk_F}{2} \right. \\
&\qquad\quad \left. - \frac{1}{4}(k^4 - k_F^4) \ln(k_F + k) + \frac{k^4}{16} - \frac{k_F k^3}{12} + \frac{k_F^2 k^2}{8} - \frac{k_F^3 k}{4} \right]_{-k_F}^{+k_F} \\
&\qquad = \frac{V}{2\pi^2 k_F} \left[ k_F^4 - \frac{k_F^4}{6} - \frac{k_F^4}{2} \right] = \frac{V}{6\pi^2} k_F^3.
\end{aligned}$$

**Problem 6.10, 1-Dimensional Homogeneous Electron Gas**
Hamilton operator in 1st quantization

$$H = \sum_{i=1}^{N_e} \left( \frac{p_i^2}{2m} + V(x_i) \right) + \frac{1}{2} \sum_{i \neq j} v(x_i - x_j)$$

$$\text{with} \quad V(x) = - \int dx' \frac{\rho(x')e^2}{|x - x'| + \delta}$$

as the attractive potential of the positive background charge $e\rho(x')$,

$$v(x_i - x_j) = \frac{e^2}{|x_i - x_j| + \delta}$$

(model for Coulomb interaction in one dimension). This is still generally valid if $\rho(x)$ denotes the particle density of the positive charges (ions), e.g. with $\rho(x) = \sum_i \delta(x - X_i)$ and the $X_i$ as one-dimensional lattice sites, this results in a one-dimensional periodic potential. In 2nd quantization one obtains generally with respect to plane waves $|k\rangle$ as one-particle basis:

$$H = \sum_{k\sigma} \varepsilon_k c_{k\sigma}^\dagger c_{k\sigma} + \sum_{k_1 k_2 \sigma} V_{k_1 k_2} c_{k_1\sigma}^\dagger c_{k_2\sigma} + \frac{1}{2} \sum_{k_1 k_2, k_3 k_4, \sigma\sigma'} u_{k_1 k_2, k_3 k_4} c_{k_1\sigma}^\dagger c_{k_2\sigma'}^\dagger c_{k_3\sigma'} c_{k_4\sigma}$$

with:

$$\begin{aligned}
V_{k_1 k_2} &= -\frac{1}{L} \int dx e^{-ik_1 x} \int dx' \frac{e^2 \rho(x')}{|x - x'| + \delta} e^{ik_2 x} \\
&= -\frac{1}{L} \int dx' \rho(x') \int dx e^{i(k_2 - k_1)(x - x')} \frac{e^2}{|x - x'| + \delta} e^{i(k_2 - k_1)x'} \\
&= -\frac{1}{L} \int dx' \rho(x') \int d\tilde{x} e^{i(k_2 - k_1)\tilde{x}} \frac{e^2}{|\tilde{x}| + \delta} e^{i(k_2 - k_1)x'} \\
&= -\frac{1}{L} \tilde{\rho}(k_2 - k_1) \tilde{v}(k_2 - k_1) \\
u_{k_1 k_2, k_3 k_4} &= \frac{1}{L^2} \int dx \int dx' e^{-ik1x - ik_2 x'} \frac{e^2}{|x - x'| + \delta} e^{ik_3 x' + ik_4 x} \\
&= \frac{1}{L^2} \int dx' e^{i(k_3 + k_4 - k_1 - k_2)x'} \int dx e^{i(k_4 - k_1)(x - x')} \frac{e^2}{|x - x'| + \delta} \\
&= \frac{1}{L} \delta_{k_3 - k_2, k_1 - k_4} \tilde{v}(k_4 - k_1) \\
\tilde{\rho}(q) &= \int dx e^{iqx} \rho(x) \ , \ \tilde{v}(q) = \int dx e^{iqx} v(x).
\end{aligned}$$

Thus:

$$H = \sum_{k\sigma} \varepsilon_k c^\dagger_{k\sigma} c_{k\sigma} - \frac{1}{L}\sum_{kq\sigma} \tilde{\rho}(q)\tilde{v}(q) c^\dagger_{k\sigma} c_{k+q\sigma}$$
$$+ \frac{1}{2L}\sum_{kk'q,\sigma\sigma'} \tilde{v}(q) c^\dagger_{k-q\sigma} c^\dagger_{k'+q\sigma'} c_{k'\sigma'} c_{k\sigma}.$$

Hartree-Fock decoupling results in:

$$H = \sum_{k\sigma} \varepsilon_k c^\dagger_{k\sigma} c_{k\sigma} - \frac{1}{L}\sum_{kq\sigma} \tilde{\rho}(q)\tilde{v}(q) c^\dagger_{k\sigma} c_{k+q\sigma}$$
$$+ \frac{1}{L}\sum_{kk'q,\sigma\sigma'} \tilde{v}(q) \langle c^\dagger_{k'+q\sigma'} c_{k'\sigma'}\rangle c^\dagger_{k-q\sigma} c_{k\sigma}$$
$$- \frac{1}{L}\sum_{kk'q,\sigma\sigma'} \tilde{v}(q) \langle c^\dagger_{k'+q\sigma'} c_{k\sigma}\rangle c^\dagger_{k-q\sigma} c_{k'\sigma'}.$$

For the operator of the electronic particle density, 1st quantization in position representation yields:

$$\hat{\rho}_e(x) = \sum_i \delta(x - x_i)$$
$$\rightarrow \text{ Fourier-Transform:} \quad \hat{\rho}_e(q) = \int dx e^{iqx} \hat{\rho}_e(x) = \sum_i e^{iqx_i}.$$

Thus in 2nd quantization:

$$\hat{\rho}_e(q) = \sum_{k_1 k_2 \sigma} \langle k_1 | e^{iqx} | k_2\rangle c^\dagger_{k_1\sigma} c_{k_2\sigma} = \sum_{k\sigma} c^\dagger_{k+q\sigma} c_{k\sigma}.$$

This results in the Hamilton operator in Hartree-Fock approximation:

$$H = \sum_{k\sigma} \varepsilon_k c^\dagger_{k\sigma} c_{k\sigma} - \frac{1}{L}\sum_{kq\sigma} \tilde{\rho}(q)\tilde{v}(q) c^\dagger_{k\sigma} c_{k+q\sigma}$$
$$+ \frac{1}{L}\sum_{kq,\sigma} \tilde{v}(q) \langle \hat{\rho}_e(q)\rangle c^\dagger_{k-q\sigma} c_{k\sigma} - \frac{1}{L}\sum_{kk'q,\sigma\sigma'} \tilde{v}(q) \langle c^\dagger_{k'+q\sigma'} c_{k\sigma}\rangle c^\dagger_{k-q\sigma} c_{k'\sigma'}.$$

If now the expectation value of the electronic particle density is equal to the particle density of the positive charge carriers, then the Fourier transforms are also equal and the 2nd and 3rd (Hartree) terms cancel each other out. Then the plane wave number $k$ is a good quantum number and the particle number expectation values are $k$- and spin-diagonal. This results in:

$$\begin{aligned} H &= \sum_{k\sigma} \varepsilon_k c^\dagger_{k\sigma} c_{k\sigma} - \frac{1}{L} \sum_{kk'\sigma} \tilde{v}(k-k') \langle c^\dagger_{k\sigma} c_{k\sigma} \rangle c^\dagger_{k'\sigma} c_{k'\sigma} \\ &= \sum_{k\sigma} \left( \varepsilon_k - \frac{1}{L} \sum_{k'} \tilde{v}(k'-k) \langle c^\dagger_{k'\sigma} c_{k'\sigma} \rangle \right) c^\dagger_{k\sigma} c_{k\sigma}. \end{aligned}$$

So the Hartree-Fock dispersion is given by:

$$\begin{aligned} \varepsilon_{HF}(k) &= \varepsilon(k) - \frac{1}{L} \sum_{k'} \tilde{v}(k'-k) \langle c^\dagger_{k'\sigma} c_{k'\sigma} \rangle \\ &= \frac{\hbar^2 k^2}{2m} - \frac{1}{2\pi} \int_{-k_F}^{k_F} dk' \tilde{v}(k'-k). \end{aligned}$$

A naive program for the calculation of the Fourier transforms of the one-dimensional model “Coulomb potential” $\tilde{v}(q)$ and the exchange integral (up to the Fermi momentum) is given below.

```
clear;
for iq=1:1000
q(iq)=0.01*iq;
v(iq)=0;
for ix=1:4000
x(ix)=ix*0.05;
v(iq)=v(iq)+0.1*cos(q(iq)*x(ix))/(x(ix)+0.1);
end
end
figure(1);plot(q,v)
for ik=1:300
k(ik)=0.01*ik;
eps(ik)=k(ik)^2;
epshf(ik)=0;
for ik1=1:100
ikk1=abs(ik1-ik);if ikk1 == 0 ikk1=1; end
ikk2=ik1+ik;
epshf(ik)=epshf(ik)+0.01*(v(ikk1)+v(ikk2))/(2*pi);
end
epsg(ik)=eps(ik)-epshf(ik);
end
figure(2);plot(k,epsg,k,eps)
figure(3);plot(k,epshf)
```

The following plots show results for the Fourier transform of the 1-dimensional Coulomb model potential, the analogue of the Lindhard function $F(q)$ and the Hartree-Fock dispersion $\varepsilon_{HF}(k)$.

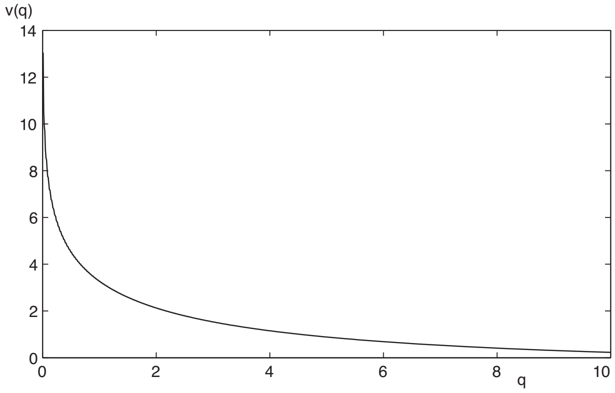

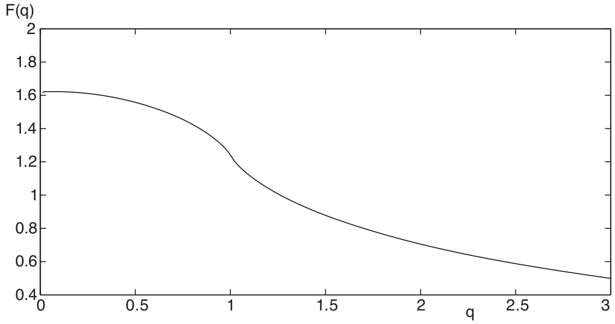

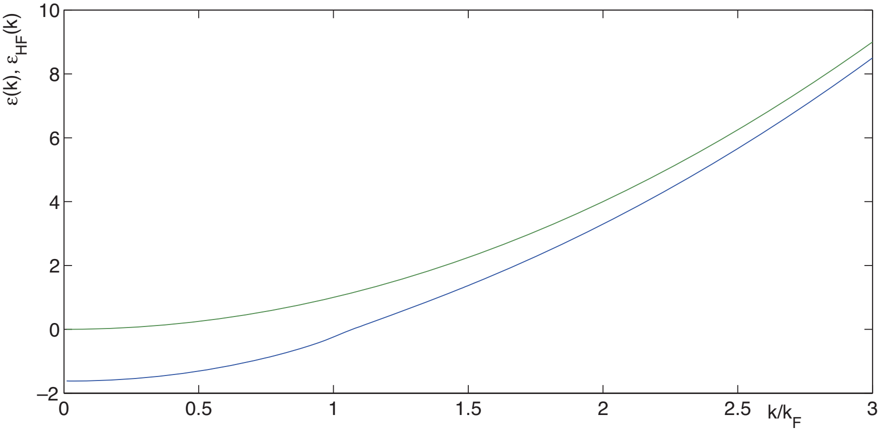

Qualitatively, therefore, all the properties known from the Hartree-Fock treatment of the 3-dimensional electron gas are reproduced, in particular the logarithmic singularities at the Fermi edge.

**Problem 6.11, Thomas-Fermi Approximation in Atomic Physics**

a) The Schrödinger equation for constant potential

$$\frac{\boldsymbol{p}^2}{2m}\psi_k(\boldsymbol{r}) + V_0\psi_k(\boldsymbol{r}) = E_k\psi_k(\boldsymbol{r})$$

has solutions

$$E_k = \frac{k^2}{2m} + V_0$$

with constant particle density

$$n_0 = \sum_{\boldsymbol{k}\sigma, k<k_F} 1 = \frac{1}{\pi^2}\int_0^{k_F} dkk^2 = \frac{1}{\pi^2}\frac{k_F^3}{3} = \frac{1}{3\pi^2}[2m(\varepsilon_F - V_0)]^{3/2}.$$

For at the location $\boldsymbol{r}$ approximately constant potential one therefore obtains as an approximation for the particle density at $\boldsymbol{r}$

$$n(\boldsymbol{r}) = \frac{1}{3\pi^2}[2m(\varepsilon_F - V(\boldsymbol{r}))]^{3/2}.$$

b) The atom is neutral, i.e. the total charge of the negative electron shell is equal in magnitude to the charge of the positive nucleus, outside the atom, where there is no electron density anymore and therefore $n(r) = 0$ also $V(r) = 0$ and therefore

$$\varepsilon_F = 0.$$

c) From (6.281) it follows by using $\nabla^2\frac{1}{|\boldsymbol{r}-\boldsymbol{r}'|} = -4\pi\delta(\boldsymbol{r}-\boldsymbol{r}')$:

$$\nabla^2 V(\boldsymbol{r}) = -4\pi e^2 n(\boldsymbol{r}) + 4\pi Z e^2\delta(\boldsymbol{r}).$$

If charge density and potential are spherically symmetric, one can use the Laplace operator in spherical coordinates here and obtains for $r>0$:

$$\frac{1}{r^2}\frac{d}{dr}\left(r^2\frac{dV(r)}{dr}\right) = 4\pi e^2 n(r) = \frac{4e^2}{3\pi}[-2mV(r)]^{3/2}.$$

d) With the given substitutions,

$$\begin{aligned}
\frac{dV(r)}{dr} &= \frac{Ze^2}{r^2}\Phi(x) - \frac{Ze^2}{r}\frac{d\Phi}{dx}\frac{dx}{dr} \\
\frac{d}{dr}\left(r^2\frac{dV}{dr}\right) &= \frac{d}{dr}\left(Ze^2\Phi(x) - Ze^2 r\frac{d\Phi}{dx}\frac{dx}{dr}\right) \\
&= Ze^2\left(\frac{d\Phi}{dx}\frac{dx}{dr} - \frac{d\Phi}{dx}\frac{dx}{dr} - r\frac{d^2\Phi}{dx^2}\left(\frac{dx}{dr}\right)^2\right) \\
&= -\frac{Z^{5/3}e^2}{b^2}r\frac{d^2\Phi}{dx^2}.
\end{aligned}$$

results. Therefore

$$\begin{aligned}
\frac{1}{r^2}\frac{d}{dr}\left(r^2\frac{dV(r)}{dr}\right) &= -\frac{Z^{5/3}e^2}{b^2}\frac{1}{r}\frac{d^2\Phi}{dx^2} = \frac{4e^2}{3\pi}\frac{(2m)^{3/2}e^3Z^{3/2}}{r^{3/2}}(\Phi(x))^{3/2}\\
-\frac{Z^{6/3}e^2}{b^3}\frac{1}{x}\frac{d^2\Phi}{dx^2} &= \frac{4}{3\pi}\frac{(2m)^{3/2}e^5Z^2}{b^{3/2}x^{3/2}}\Phi^{3/2}(x)\\
\frac{d^2\Phi}{dx^2} &= \frac{4}{3\pi}(2m)^{3/2}e^3b^{3/2}\frac{1}{\sqrt{x}}\Phi^{3/2}(x)\\
&= \frac{4}{3\pi}(2m)^{3/2}e^3\frac{1}{(2me^2)^{3/2}}\frac{3\pi}{4}\frac{1}{\sqrt{x}}\Phi^{3/2}(x)\\
&= \frac{1}{\sqrt{x}}\Phi^{3/2}(x).
\end{aligned}$$

e) The numerical solution of this nonlinear boundary value problem is not quite trivial, since a mapping to a simple matrix eigenvalue problem (after discretization) is not possible and there can be different solutions and solution branches. A simple integration with given initial values usually leads to a solution that does not fulfill the boundary condition on the other side. However, by varying the initial conditions, one can finally construct such a solution. A Matlab code containing a suitable initial condition is given below, the result for $\Phi(x)$ as well as Thomas-Fermi potential and electron density are shown below.

```
y1=zeros(1000);
y2=zeros(1000);
y3=zeros(1000);
x=zeros(1000);
x(1)=0.005;
dx=0.005;
y1(1)=1-1.47845*x(1);
y2(1)=-1.47845;
for i=1:999
x(i+1)=x(i)+dx;
y1(i+1)=y1(i) + dx * y2(i);
y2(i+1)=y2(i) + dx*y1(i) ^ 1.5/sqrt(x(i));
end
plot(x,y1,x,y2)
```

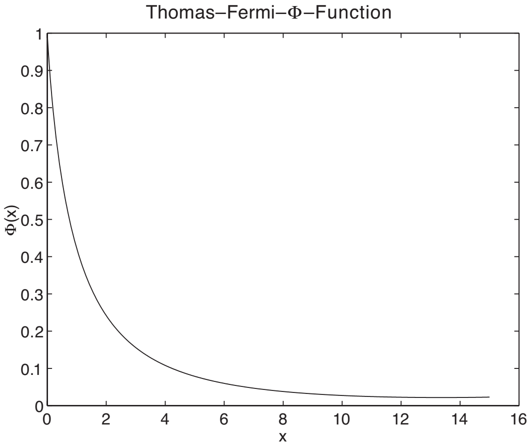
Thomas–Fermi–Φ–Function
Φ(x)
x
0
0.1
0.2
0.3
0.4
0.5
0.6
0.7
0.8
0.9
1
0
2
4
6
8
10
12
14
16

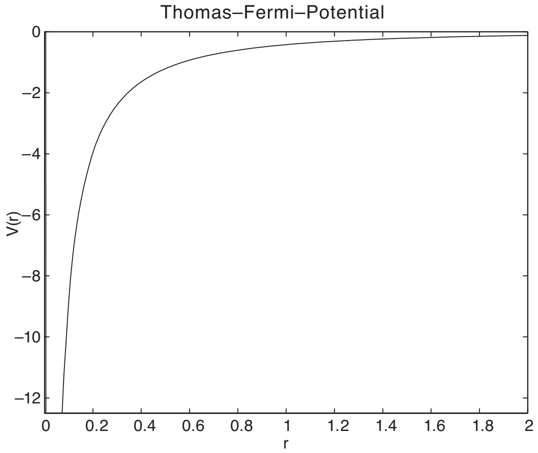
Thomas–Fermi–Potential
V(r)
r
0
−2
−4
−6
−8
−10
−12
0
0.2
0.4
0.6
0.8
1
1.2
1.4
1.6
1.8
2

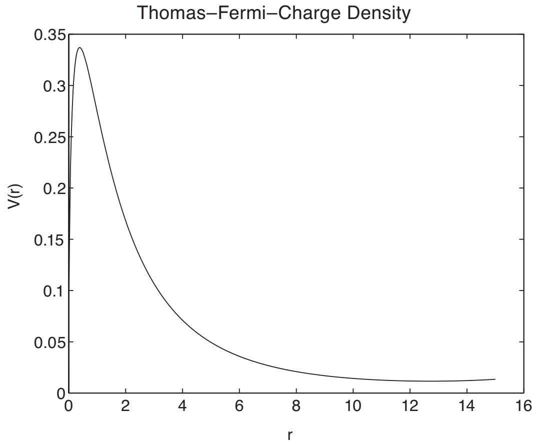
Thomas–Fermi–Charge Density
V(r)
r
0
0.05
0.1
0.15
0.2
0.25
0.3
0.35
0
2
4
6
8
10
12
14
16

### Exercise 6.12, Screening in One-Dimensional Electron Systems

a)

$$
\begin{aligned}
\chi(q) &= \frac{1}{L}\sum_k \frac{f(\varepsilon_k) - f(\varepsilon_{k+q})}{\varepsilon_k - \varepsilon_{k+q}} = \frac{1}{2\pi}\int dk \frac{f(\varepsilon_k) - f(\varepsilon_{k+q})}{k^2 - k^2 - 2kq - q^2} \\
&= \frac{1}{2\pi}\int dk \left( \frac{f(k^2)}{-2kq - q^2} - \frac{f((k+q)^2)}{-2kq - q^2} \right) \\
&= -\frac{1}{2\pi}\int_{-k_F}^{+k_F} \frac{dk}{2kq + q^2} + \frac{1}{2\pi}\int_{-k_F - q}^{k_F - q} \frac{dk}{2kq + q^2} \\
&= \frac{1}{4\pi q} \ln \frac{(-2k_F q + q^2)(2(k_F - q)q + q^2)}{(2k_F q + q^2)(2(-k_F - q)q + q^2)} = \frac{1}{2\pi q} \ln \frac{2k_F - q}{2k_F + q}.
\end{aligned}
$$

b) The k-integral can be calculated for small finite temperature $T = 0.0001$ using the Matlab program below.

```
clear;
for iq=1:40
q(iq)=0.2*iq;
chi(iq)=0;
k=-3*pi:.01:3*pi;
ek=k. ^ 2;
ekq=(k+q(iq)). ^ 2;
xek=(ek-3)./0.0001;
xekq=(ekq-3)./0.0001;
fek=0.5*(1.-tanh(0.5*xek));
fekq=0.5*(1.-tanh(0.5*xekq));
y=(fek-fekq)./(2*pi*(ek-ekq));
chi(iq)=trapz(k,y);
chi1(iq)=log(abs((2*sqrt(3)-q(iq))/(2*sqrt(3)+q(iq))))/
    (2*pi*q(iq));
end
plot(q,chi,q,chi1)
```

The plot shows the Lindhard susceptibility calculated numerically and analytically specifically for $\varepsilon_F = k_F^2 = 3$. There is no longer any difference between the numerical and analytical results, and the logarithmic singularity at $q = 2k_F = 2\sqrt{3}$ is evident.

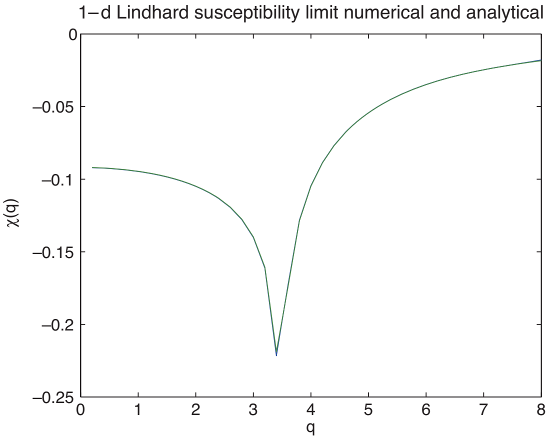

c) For the one-dimensional tight-binding band with dispersion $\varepsilon_k = -\cos(k)$ and Fermi energy $\varepsilon_F = 0$, the following, essentially identical program can be used:

```
clear;
for iq=1:80
q(iq)=+0.05*(iq-1)+eps;
chi(iq)=0;
k=-pi:.01:pi;
ek=-cos(k);
ekq=-cos(k+q(iq));
xek=(ek-0)./0.0001;
xekq=(ekq-0)./0.0001;
fek=0.5*(1.-tanh(0.5*xek));
fekq=0.5*(1.-tanh(0.5*xekq));
y=(fek-fekq)./(2*pi*(ek-ekq));
chi(iq)=trapz(k,y);
end
plot(q,chi)
```

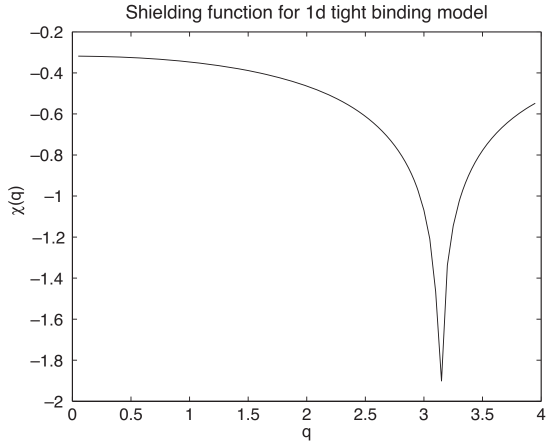

### Exercise 6.13, Generalized Lindhard Susceptibility for Semiconductors and Metals

The band structure with the first 3 bands is shown below for $v_0 = 50$. If the Fermi energy is in the gap between 2nd and 3rd band,

$$E_F = \frac{1}{2}(\varepsilon_2(0) + \varepsilon_3(0)) \approx 20.9.$$

applies. To model the metallic situation, one can choose $E_F \approx 10$ instead, because it apparently lies in the middle of the 2nd band. Then $\chi(q)$ can be calculated according to definition. The Matlab code is given below.

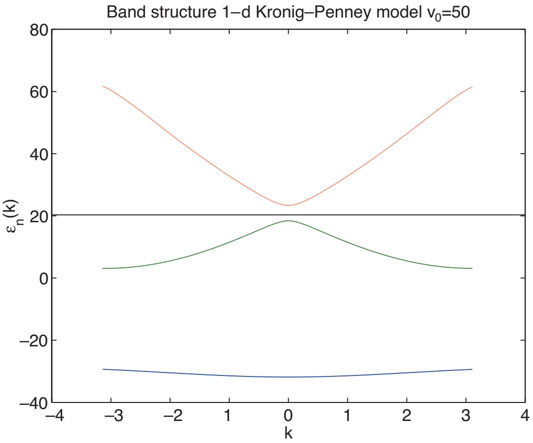

```
clear;
im=1i;
h=zeros(10,10);
v=zeros(10);
u=zeros(200,10,10);
psi=zeros(400);
for i=1:10
x(i)=i*0.1;
end
for i=1:4
v(i)=-50;
end
for ik=1:200
k(ik)=-pi+(ik-1)*2*pi/200;
kim=k(ik)*im;
for i=1:10
h(i,i)=+2+(v(i)+k(ik)^2)*0.01;
if i<=9 h(i,i+1)=-1+kim*0.1; end
if i>=2 h(i,i-1)=-1-kim*0.1; end
end
h(1,10)=-1-kim*0.1;
h(10,1)=-1+kim*0.1;
[ev,ew]=eig(h);
u(ik,:,:)=ev(:,:);
for iew=1:10
eps(ik,iew)=ew(iew,iew)/0.01;
end
end
figure(1); plot(k,eps(:,1),k,eps(:,2),k,eps(:,3))
figure(2); plot(x,u(99,:,5))
mue=0.5*(eps(101,3)+eps(101,2))
t=0.01;
for iq=1:70
q(iq)=iq*2*pi/200;
chi(iq)=0;
for n=1:3
for n1=1:3
for ik=1:200
ikq=ik+iq;
if ikq > 200 ikq=ikq-200; end
fermk=0.5*(1-tanh(0.5*(eps(ik,n)-mue)/t));
fermkq=0.5*(1-tanh(0.5*(eps(ikq,n1)-mue)/t));
mnn1=u(ikq,:,n1)*u(ik,:,n)';
chi(iq)=chi(iq)+(fermk-fermkq)*abs(mnn1)^2/
   (0.0001+eps(ik,n)-eps(ikq,n1));
```

```
end
end
end
mnn(iq)=abs(u(101+iq,:,3)*u(101,:,2)');
end
eps(101,3)
eps(101,2)
delta=eps(101,3)-eps(101,2)
figure(3); plot(q,chi)
```

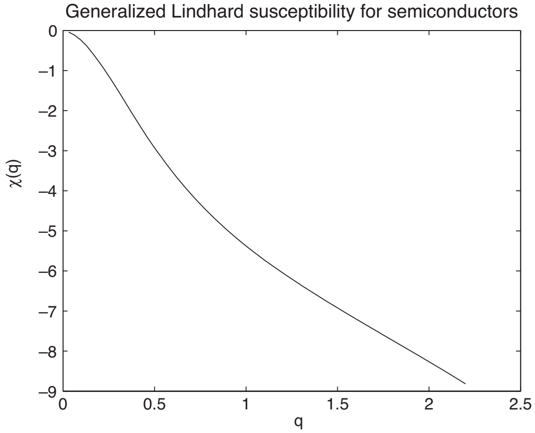

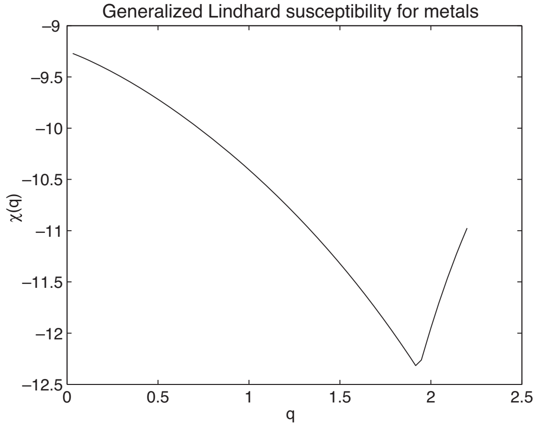

It can be seen that, in the case of the semiconductor, the condition $\chi(q) \to 0$ is satisfied for $q \to 0$, which leads to a constant dielectric constant, whereas for metals $\chi(q)$ remains finite for $q \to 0$, which is why the dielectric constant diverges for $q \to 0$, leading to a finite, Thomas-Fermi-type screening radius and thus a short-range screened Coulomb potential. In the metallic case, the behaviour characteristic of one dimension, known from Problem 6.12, is observed with a logarithmic singularity.

**Exercise 6.14, Excitons in One Dimension**
a) Ansatz:

$$H = \sum_k \varepsilon_v(k) v_k^\dagger v_k + \sum_k \varepsilon_c(k) c_k^\dagger c_k + \sum_{k,k',q} u_q v_{k+q}^\dagger c_{k'-q}^\dagger c_{k'} v_k$$

$$|\Phi_0\rangle = \prod_k v_k^\dagger |0\rangle \,,\; E_0 = \sum_k \varepsilon_v(k).$$

$$\begin{aligned}
|\Phi_1\rangle &= \sum_k a_k c_k^\dagger v_k |\Phi_0\rangle \\
H|\Phi_1\rangle &= \sum_k (E_0 + \varepsilon_c(k) - \varepsilon_v(k)) a_k c_k^\dagger v_k |\Phi_0\rangle \\
&\quad + \sum_{kk'k''q} a_k u_q v_{k'+q}^\dagger c_{k''-q}^\dagger c_{k''} v_{k'} c_k^\dagger v_k |\Phi_0\rangle \\
&= \sum_k (E_0 + \varepsilon_c(k) - \varepsilon_v(k)) a_k c_k^\dagger v_k |\Phi_0\rangle \\
&\quad - \sum_{kk'k''q} a_k u_q \underbrace{v_{k'} v_{k'+q}^\dagger \underbrace{c_{k''-q}^\dagger c_{k''} c_k^\dagger}_{\delta_{k''k} c_{k-q}} v_k}_{\delta_{k'+qk} v_k'} |\Phi_0\rangle .
\end{aligned}$$

It follows:

$$\begin{aligned}
H|\Phi_1\rangle &= \sum_k (E_0 + \varepsilon_c(k) - \varepsilon_v(k)) a_k c_k^\dagger v_k |\Phi_0\rangle - \sum_{kq} u_q a_k c_{k-q}^\dagger v_{k-q} |\Phi_0\rangle \\
&= \sum_k \left( (E_0 + \varepsilon_c(k) - \varepsilon_v(k)) a_k - \sum_q u_q a_{k+q} \right) c_k^\dagger v_k |\Phi_0\rangle = E|\Phi_1\rangle \\
\rightarrow & a_k (E_0 + \varepsilon_c(k) - \varepsilon_v(k) - E) - \sum_q u_q a_{k+q} = 0.
\end{aligned}$$

b)

$$u(x - x') = \begin{cases} u_0 & \text{for} \quad |x - x'| < a \\ 0 & \quad\text{else} \end{cases} .$$

Interaction matrix element $u_q$ for plane waves as a basis for both the valence and conduction band (additional, assumption, whose justification may be questionable):

$$\begin{aligned}
u_q &= \frac{1}{L^2}\int dx e^{-i(k+q)x}\int dx' e^{-i(k'-q)x'}u(x-x')e^{ik'x'}e^{ikx} \\
&= \frac{1}{L^2}\int dx \int dx' e^{iq(x'-x)}u(x-x') = \frac{1}{L^2}\int dx \int d\tilde{x} e^{iq\tilde{x}}u(\tilde{x}) \\
&= \frac{u_0}{L}\int_{-a}^{+a} dx' e^{iqx'} = \frac{u_0}{iqL}(e^{iqa}-e^{-iqa}) = \frac{2u_0\sin(qa)}{qL}.
\end{aligned}$$

c) Effective mass model for valence and conduction band near $k=0$:

$$\varepsilon_c(k) = \varDelta + \frac{\hbar^2k^2}{2m_c}, \quad \varepsilon_v(k) = -\frac{\hbar^2k^2}{2|m_v|}.$$

Then the eigenvalue equation (Schrödinger equation) in $k$-space results:

$$\frac{\hbar^2}{2m_r}k^2a_k - \sum_q \frac{2u_0\sin(qa)}{qL}a_{k+q} = (E-E_0-\varDelta)a_k = \tilde{E}_1 a_k$$

with $m_r$ as the reduced mass: $\frac{1}{m_r} = \frac{1}{m_c} + \frac{1}{|m_v|}$ and $\tilde{E}_1$ the excitation energy relative to the energy gap $\Delta$. This is apparently the Fourier transform of the Schrödinger equation in the attractive box potential $-u(x)$, which in position space reads:

$$-\frac{\hbar^2}{2m_r}\frac{d^2}{dx^2}\psi(x) - u(x)\psi(x) = \tilde{E}_1\psi(x)$$

Because if you insert the Fourier transforms $\psi(x) = \sum_k a_k e^{ikx}$, $u(x) = \sum_q u_q e^{-iqx}$ (where $u_q = \frac{1}{L}\int dx u(x)e^{iqx}$), the eigenvalue equation in $k$-space apparently reproduces itself.

In the following two Matlab programs are printed for the numerical solution in real space and in $k$-space; suitable dimensionless units are used so that $\frac{\hbar^2}{2m_r} = 1$, a finite system on the interval $[-8, 8]$ (i.e. system length $L=16$) and $a=1$. So that the plane waves $\frac{1}{\sqrt{L}}e^{ikx}$ form a basis, periodic boundary conditions must be assumed with $k = n\frac{2\pi}{L}$. In particular, in the following program , only 41 $k$-points are symmetrically chosen around $k=0$ and as the strength of the "Coulomb" potential $u_0 = 20$.

```
clear;
L=8;a=1;v0=20;nk=41;
h=zeros(nk,nk);
for ik=1:nk
k(ik)=-pi*(nk-1)/(4*L)+(ik-1)*2*pi/(2*L);
h(ik,ik)=k(ik)^2-v0/L;
end
for ik=1:nk-1
for ik1=ik+1:nk
q=(ik1-ik)*2*pi/(2*L);
```

```
h(ik,ik1)=-v0*sin(q)/(L*q);
h(ik1,ik)=h(ik,ik1);
end
end
[ev,ew]=eig(h);
for iew=1:nk
eigw(iew)=ew(iew,iew);
end
eigw(1)
eigw(2)
eigw(3)
eigw(4)
eigw(5)
eigw(6)
```

As the lowest 6 eigenvalues one obtains: $-18.3268, -13.3231, -4.7519, 0.0517,$ $0.1820$, $0.4629$, thus three bound states of negative excitation energy $\tilde{E}_1$, i.e. with less excitation energy than the energy gap $\Delta$.
Alternatively, the Schrödinger equation in real space can be solved by discretization; a Matlab program for this:

```
clear;
L=8;a=1;nm=1000;dx=2*L/nm;v0=20;
h=zeros(nm,nm);
for ix=1:nm
x(ix)=-L+ix*dx;
h(ix,ix)=2;
if abs(x(ix))<a h(ix,ix)=h(ix,ix)-v0*dx^2;end
ix1=ix+1;
if ix1>nm ix1=ix1-nm;end
h(ix,ix1)=-1;h(ix1,ix)=-1;
end
[ev,ew]=eig(h);
for iew=1:nm
eigw(iew)=ew(iew,iew)/dx^2;
end
eigw(1)
eigw(2)
eigw(3)
eigw(4)
eigw(5)
eigw(6)
```

delivers the results: $-18.3609, -13.5600, -6.1130, 0.0511, 0.1565, 0.4587$ with 1000 grid points, but with 40 grid points in space: $-18.5655, -14.5616,$

$-8.8378, -2.6798, 0.0488, 0.2056$, which is apparently not too good from the 2nd bound state on.
The solution of the Schrödinger equation (exciton equation) in $k$-space therefore is much easier than in real space, because with a much smaller matrix one already gets good results.

### Exercise 6.15, Excitons in a Spatially Limited System

$$V(x) = \begin{cases} -V_0 & \text{for} \quad |x| < L \\ 0 & \text{else} \end{cases}.$$

E.g. for $V_0 = 100$ and $L = 0.6$ the source code of a Matlab program for the calculation of the one-particle eigenstates $|\varphi_i\rangle$ and eigenvalues $\varepsilon_i$ and all Coulomb matrix elements $u_{ij,kl}$ for $i, j \in \{1, 2, 3, 4\}$ is given below:

```
clear;h=zeros(20,20);
for i=1:20
x(i)=-1+i*0.1;
v(i)=0;
if(abs(x(i))<0.6)v(i)=-100; end
end
for i=1:20
h(i,i)=2+v(i)*0.01;if i<20 h(i,i+1)=-1;h(i+1,i)=-1;end
end
[ev,ew]=eig(h);
for i=2:20
for j=1:i
if ew(i,i)<ew(j,j)
eh=ew(i,i);evh=ev(:,i);ew(i,i)=ew(j,j);ev(:,i)=ev(:,j);
ew(j,j)=eh;ev(:,j)=evh;end
end
end
for i=1:20
eigw(i)=ew(i,i)/0.01;
end
eigw
figure(1);plot(x,ev(:,1),x,ev(:,2),x,ev(:,3),x,ev(:,4))
for i=1:4
for j=1:4
for k=1:4
for l=1:4
u(i,j,k,l)=0;
for ix=1:20
for ix1=1:20
u(i,j,k,l)=u(i,j,k,l)+ev(ix,i)*ev(ix1,j)*ev(ix1,k)*ev(ix,l)/
   (abs(x(ix)-x(ix1))+0.05);
```

```
end
end
end
end
end
end
u(1,1,1,1)
u(2,2,2,2)
u(3,3,3,3)
u(4,4,4,4)
e0=2*eigw(1)+u(1,1,1,1)+2*eigw(2)+u(2,2,2,2)+4*u(1,2,2,1);
e1=2*eigw(1)+u(1,1,1,1)+eigw(2)+eigw(3)+2*u(1,2,2,1)+
   2*u(1,3,3,1)+u(2,3,3,2);
e2=2*eigw(1)+u(1,1,1,1)+2*eigw(3)+u(3,3,3,3)+4*u(1,3,3,1);
delte1=e1-e0
delte10=eigw(3)-eigw(2)
delte2=e2-e1
```

For the ground state with Coulomb interaction at $N=4$ one obtains

$$|\Phi_0\rangle = c^\dagger_{1\uparrow}c^\dagger_{1\downarrow}c^\dagger_{2\uparrow}c^\dagger_{2\downarrow}|0\rangle,$$

with $E_0 = 2\varepsilon_1 + u_{11,11} + 2\varepsilon_2 + u_{22,22} + 4u_{12,21}$. At least when neglecting the exchange interaction, the 1st excited state is given by

$$|\Phi_1\rangle = c^\dagger_{3\uparrow}c_{2\uparrow}|\Phi_0\rangle = c^\dagger_{1\uparrow}c^\dagger_{1\downarrow}c^\dagger_{3\uparrow}c^\dagger_{2\downarrow}|0\rangle$$

with energy

$$E_1 = 2\varepsilon_1 + u_{11,11} + \varepsilon_2 + \varepsilon_3 + 2u_{12,21} + 2u_{13,31} + u_{23,32}.$$

As excitation energy one thus obtains:

$$\Delta E = E_1 - E_0 = \varepsilon_3 - \varepsilon_2 + 2(u_{13,31} - u_{12,21}) + u_{23,32} - u_{22,22}.$$

This is generally smaller than the one-particle excitation energy $\Delta\varepsilon = \varepsilon_3 - \varepsilon_2$ (“energy gap”), in particular because $u_{23,32} < u_{22,22}$ applies. In this picture, a lowering of the excitation energy does not result from an attractive interaction between particleand “hole” but from the different Coulomb matrix elements between 2 electrons in the same states (or in the “valence band”) and between an electron in the “conduction band” and one in the “valence band”.

**Exercise 6.16, Commutators with Fermi Operators**
Clear after using fermion commutation rules.

## 8.6 Solution to Problems in Chap. 7

### Exercise 7.1, Fermion-Boson Model

$$H = \varepsilon c^\dagger c + M(b^\dagger + b)c^\dagger c + \omega b^\dagger b$$

a) $\underline{n_f = 0}$ :

$$H|n_f = 0, n_b\rangle = \omega n_b |n_f = 0, n_b\rangle.$$

The basis states are therefore eigenstates in the subspace to $n_f = 0$.
$\underline{n_f = 1}$ :

$$\begin{aligned} H|n_f = 1, n_b\rangle = (\varepsilon + \omega n_b)|n_f = 1, n_b\rangle + M\sqrt{n_b+1}|n_f = 1, n_b + 1\rangle \\ + M\sqrt{n_b}|n_f = 1, n_b - 1\rangle \\ \langle n_f = 1, n_b|H|n_f = 1, n_b\rangle = \varepsilon + \omega n_b \\ \langle n_f = 1, n_b + 1|H|n_f = 1, n_b\rangle = M\sqrt{n_b+1} \\ \langle n_f = 1, n_b - 1|H|n_f = 1, n_b\rangle = M\sqrt{n_b} \end{aligned}$$

b)

$$H = \varepsilon c^\dagger c + \omega\left(b^\dagger + \frac{M}{\omega}c^\dagger c\right)\left(b + \frac{M}{\omega}c^\dagger c\right) - \frac{M^2}{\omega}c^\dagger c c^\dagger c = \tilde{\varepsilon} c^\dagger c + \omega \tilde{b}^\dagger \tilde{b}$$

with $\tilde{\varepsilon} = \varepsilon - \frac{M^2}{\omega}$ and $\tilde{b} = b + \frac{M}{\omega}c^\dagger c$. This still satisfies the Bose commutation rules because they commute with $c^\dagger c$. Therefore, for the energy eigenvalues, the following is exactly true:

$$E_{n_f n_{\tilde{b}}} = \left(\varepsilon - \frac{M^2}{\omega}\right) n_f + \omega n_{\tilde{b}}.$$

c) A Matlab program for diagonalizing the Hamilton matrix from a) in the subspace to $n_f = 1$ is given below:

```
clear;npm=20;eps=1;omega=0.5;M=0.6;
for n=1:npm
h(n,n)=eps+(n-1)*omega;
if n<npm h(n,n+1) = sqrt(n)*M;h(n+1,n)=h(n,n+1);end
end
[ev,ew]=eig(h);
for n=1:npm
eigw(n)=ew(n,n);
end
for n=1:npm
```

```
eigw1(n)=eps-M*M/omega+(n-1)*omega;
end
eigw
eigw1
```

For $\varepsilon = 1, \omega = 0.5$, and a relatively large electron-phonon matrix element $M = 0.6$ and a maximum boson occupation number $n_{b\,max} \equiv npm = 20$, the following 20 eigenvalues are obtained numerically:
0.2800 0.7800 1.2800 1.7800 2.2800 2.7800 3.2800 3.7803 4.2828 4.7950 5.3345 5.9218 6.5707 7.2887 8.0834 8.9658 9.9537 11.0785 12.4015 14.0833,
whereas analytically
0.2800 0.7800 1.2800 1.7800 2.2800 2.7800 3.2800 3.7800 4.2800 4.7800 5.2800 5.7800 6.2800 6.7800 7.2800 7.7800 8.2800 8.7800 9.2800 9.7800.
It can be seen that the first 10 eigenvalues agree with sufficient accuracy, so that the artificial cut off only becomes noticeable only for the higher states, which may not play a role anyway (for example, at low enough temperatures), because they are not occupied. For a smaller $M = 0.1$, the following eigenvalues are obtained numerically:
0.9800 1.4800 1.9800 2.4800 2.9800 3.4800 3.9800 4.4800 4.9800 5.4800 5.9800 6.4800 6.9800 7.4800 7.9800 8.4800 8.9807 9.4902 10.0543 10.7949
and analytically
0.9800 1.4800 1.9800 2.4800 2.9800 3.4800 3.9800 4.4800 4.9800 5.4800 5.9800 6.4800 6.9800 7.4800 7.9800 8.4800 8.9800 9.4800 9.9800 10.4800.
For the smaller electron-phonon coupling, one therefore has agreement up to the 17th or 18th eigenvalue. One can therefore choose $n_{b\,max} = 12$ if one is only interested in the lowest 10 eigenvalues, etc.
The energy lowering of the fermion state without boson by $M^2/\omega$ found here as a consequence of the electron-phonon interaction corresponds precisely to the polaron discussed in Sect. 7.5 (as a new fermionic quasiparticle).

d) The fermionic one-particle Green function is given in spectral representation by

$$G_c(z) = \langle\langle c, c^\dagger \rangle\rangle_z$$
$$= \frac{1}{\mathcal{Z}} \sum_{n,m} \frac{\langle n|c|m\rangle\langle m|c^\dagger|n\rangle}{z + E_n - E_m} \left(e^{-\beta(E_n - N(n)\mu)} + e^{-\beta(E_m - N(m)\mu)}\right)$$
$$\text{where} \quad \mathcal{Z} = \sum_n e^{-\beta(E_n - N(n)\mu)}$$

is the grand canonical partition function, $|n\rangle$ the (many-particle) eigenstates, $\beta = 1/k_B T$ the inverse temperature, $z = E + i\delta$ a (complex) energy (frequency), and $N(n)$ the fermion number in state $|n\rangle$, and $\mu$ is the chemical potential. A Matlab program for calculating this one-particle Green function or spectral function according to the definition is given below:

```
clear;
nbm=20;nmges=2*nbm;eps=1;omega=0.5;M=0.1;temp=0.01;
for n=1:nmges
for m=1:nmges
h(n,m)=0;cp(n,m)=0;c(n,m)=0;
end
end
for n=1:nbm
h(n,n)=(n-1)*omega;
h(nbm+n,nbm+n)=eps+(n-1)*omega;
if n < nbm h(nbm+n,nbm+n+1)=M*sqrt(n);
h(nbm+n+1,nbm+n)=M*sqrt(n);end
cp(nbm+n,n)=1;c(n,nbm+n)=1;
end
h
[ev,ew]=eig(h);
for n=1:nmges
eigenw(n)=ew(n,n);
end
eigenw
zustds=0;
for n=1:nmges
for m=1:nmges
ccp(m,n)=ev(:,m)'*cp*ev(:,n);
cc(m,n)=ev(:,m)'*c*ev(:,n);
end
end
ccp;
cc;
nferm=ccp*cc;
index=0;
for n=1:nmges
if index < 1 & nferm(n,n) > 0 index=1;ngrund=n;end
end
ngrund
emue=eigenw(ngrund)+10*temp;
zustds=0;nfbes=0;
for n=1:nmges
exfact(n)=exp(-(eigenw(n)-nferm(n,n)*emue)/temp);
zustds=zustds+exfact(n);
nfbes=nfbes+nferm(n,n)*exfact(n);
end
zustds
```

```
nfbes=nfbes/zustds
for n=1:nmges
for m=1:nmges
ccc(m,n)=cc(n,m)*ccp(m,n)*(exfact(n)+exfact(m))/zustds;
eigwdiff(n,m)=eigenw(m)-eigenw(n);
end
end
ccc;
eigwdiff;
e=-20:.02:20;z=e+0.01i;s=0;fermi=1./(exp((e-emue)/temp)+1);
for ien=1:2001 g(ien)=0;
m=ngrund;
for n=1:nmges
for m=1:nmges
g(ien)=g(ien)+ccc(m,n)/(z(ien)-eigwdiff(n,m));
end
end
rhof(ien)=-imag(g(ien))/pi;
s=s+rhof(ien)*fermi(ien)*0.02;
end
s
plot(e,rhof)
```

The Fermi energy $\mu$ was chosen slightly above the one-fermion ground state energy, so that the fermion state is occupied.
Results for the spectral function for $\varepsilon = 1, \omega = 0.5, M = 0.1$ are shown in the following two plots for a lower temperature $T = 0.01$ (*left*) and a higher temperature $T = 1$(*right*).

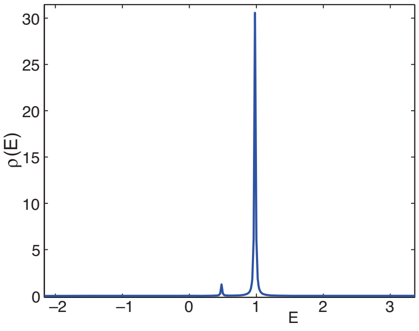

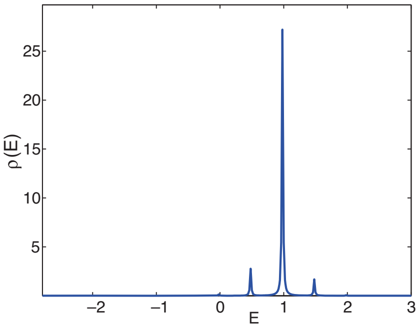

Without electron-phonon (boson) coupling, the spectral function would be a delta function at $\varepsilon = 1$. With this small electron-phonon coupling $M = 0.1$, the one-fermion ground state energy is slightly lowered to 0.98

(polaron effect, compare part c) of the problem), but there are also satellite peaks shifted exactly by phonon energies $\omega$, because in addition to the one-fermion ground state $|m\rangle$, basis states with more than one phonon contribute and there can therefore be transitions from the one-phonon state without fermion $|n\rangle$ with energy $E_n = \omega$ to the one-fermion ground state (peak at $E = E_n - E_m = 0.98 - 0.5 = 0.48$ in the spectral function). At higher temperatures (right image), higher one-fermion states also contribute, resulting in additional side peaks.

For a slightly larger value of the electron-phonon coupling $M=0.6$ the same is shown again in the following 2 figures, again for a low temperature $T=0.01$ (*left*) and a high temperature $T=1$ (*right*).

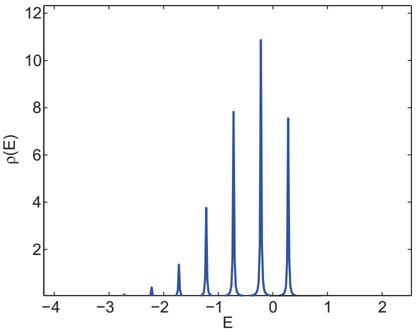

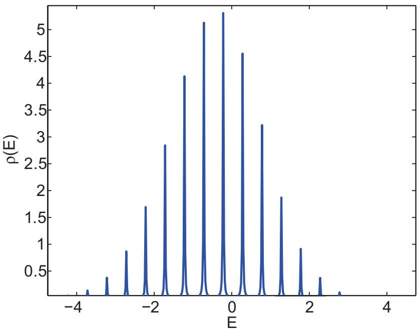

Here the one-fermion ground state is at $E_m = E_{n_f=1\, n_b=0} = 0.28$, see part c), where the top peak is in the left figure (corresponds to the excitation from the zero-phonon state without fermion with energy $E_n = E_{n_f=0\, n_b=0} = 0$ ). But excitations from higher zero-fermion states are also possible, which explains the satellite peaks.

## Task 7.2, Jaynes-Cummings Model

a)

$$H = \varepsilon_1 c_1^\dagger c_1 + \varepsilon_2 c_2^\dagger c_2 + \omega b^\dagger b + M(b^\dagger c_1^\dagger c_2 + b c_2^\dagger c_1)$$

There are only transitions from $2 \to 1$ under phonon emission and from $1 \to 2$ under phonon absorption. An obvious basis is given by $|n_1, n_2, n\rangle$ with $n_i \in \{1, 2\}$ as the fermionic occupation numbers and the phonon occupation number $n \in N$. The above electron-phonon (model) coupling then couples states $|0, 1, n\rangle$ with states $|1, 0, n+1\rangle$. It holds:

$$\langle 1, 0, n+1|H|0, 1, n\rangle = M\sqrt{n+1}.$$

Thus, only the following decoupled $2 * 2$-matrices have to be diagonalized:

$$\begin{pmatrix} \varepsilon_1 + (n+1)\omega & M\sqrt{n+1} \\ M\sqrt{n+1} & \varepsilon_2 + n\omega \end{pmatrix}$$

with the eigenvalues

$$E_{1,2,n} = \frac{\varepsilon_1 + \varepsilon_2 + (2n+1)\omega}{2} \pm \sqrt{\frac{(\varepsilon_2 - \omega - \varepsilon_1)^2}{4} + M^2(n+1)}.$$

In the case of resonance, $\omega = \varepsilon_2 - \varepsilon_1$ (phonon energy corresponds to energy difference of the electronic states) one obtains

$$E_{1,2,n} = \varepsilon_2 + n\omega \pm M\sqrt{n+1},$$

thus a splitting of the 2 degenerate levels with unperturbed eigenenergies $\varepsilon_1 + (n+1)\omega, \varepsilon_2 + n\omega$. But there is always (also in the interacting case) the eigenvalue $\varepsilon_1$ (undisturbed lower fermionic level without phonon). In addition, one can already see from this simple model that transitions are also possible if there is no resonance.

b) A Matlab program that deals with this model numerically is given below. As an additional numerical approximation, a maximum phonon (boson) number *nphm* is introduced (as in Problem 7.1). Furthermore, a chemical potential of the fermions $\mu = \frac{\varepsilon_1+\varepsilon_2}{2}$ was chosen such that the (average) fermion number is 1.

```
clear;
eps1=1;eps2=2;mu=1.5;omega=0.2;M=0.4;T=0.01;
nphm=10;nmax=4*nphm;
for n=1:nmax
for m=1:nmax
h(n,m)=0;
c1(n,m)=0;c2(n,m)=0;c1p(n,m)=0;c2p(n,m)=0;
end
end
for n=1:nphm
h(n,n)=(n-1)*omega;
h(nphm+n,nphm+n)=eps1+(n-1)*omega;
h(2*nphm+n,2*nphm+n)=eps2+(n-1)*omega;
h(3*nphm+n,3*nphm+n)=eps1+eps2+(n-1)*omega;
end
for n=1:nphm-1
h(2*nphm+n,nphm+n+1)=M*sqrt(n);h(nphm+n+1,2*nphm+n)=M*sqrt(n);
end
for n=1:nmax
for n=1:nphm
c1(n,nphm+n)=1;c1(2*nphm+n,3*nphm+n)=1;
c2(n,2*nphm+n)=1;c2(nphm+n,3*nphm+n)=-1;
c1p(nphm+n,n)=1;c1p(3*nphm+n,2*nphm+n)=1;
c2p(2*nphm+n,n)=1;c2p(3*nphm+n,nphm+n)=-1;
end
[ev,ew]=eig(h);
```

```
n1=c1p*c1;n2=c2p*c2;
for n=1:nmax
N(n)=ev(:,n)'*(n1+n2)*ev(:,n);
end
for i=1:nmax
eigen(i)=ew(i,i);enfact(i)=exp(-(eigen(i)-N(i)*mu)/T);
end
zstds=0;
for n=1:nmax
zstds=zstds+enfact(n);
end
n1erw=0;n2er=0;
for n=1:nmax
n1erw=n1erw+ev(:,n)'*n1*ev(:,n)*enfact(n);
n2erw=n2erw+ev(:,n)'*n2*ev(:,n)*enfact(n);
end
n1erw=n1erw/zstds
n2erw=n2erw/zstds
for ie=1:500
e(ie)=-1+ie*0.01;
z(ie)=e(ie)+0.001i;
g1(ie)=0;g2(ie)=0;
end
for m=1:nmax
enm=eigen(n)-eigen(m);
c1nm=ev(:,n)'*c1*ev(:,m);c1pmn=ev(:,m)'*c1p*ev(:,n);
c2nm=ev(:,n)'*c2*ev(:,m);c2pmn=ev(:,m)'*c2p*ev(:,n);
fact=(enfact(n)+enfact(m))/zstds;
g1=g1+(c1nm*c1pmn*fact)./(z+enm);
g2=g2+(c2nm*c2pmn*fact)./(z+enm);
end
end
plot(e,imag(g1))
```

Results for the $c_1$-electron spectral function are shown in the following plots (for $\varepsilon_1 = 1, \varepsilon_2 = 2, \omega = 0.2, M = 0.4$). Without the fermion-boson coupling, the spectral function would simply be a delta function at $\varepsilon_1$. Now, in addition to the main peak at $\varepsilon_1 = 1$, there are satellite peaks at relatively low temperatures $T=0.01$ (on the logarithmic scale) at about

$$\frac{\varepsilon_1 + \varepsilon_2 + \omega}{2} \pm \sqrt{\frac{(\varepsilon_2 - \varepsilon_1 - \omega)^2)}{4} + M^2} - \omega = 1.6 \pm 0.57 - 0.2$$
$$= \begin{cases} 0.83 \\ 1.97 \end{cases} .$$

These can be understood as the two possible one-particle excitations from the state with one phonon, while the main peak at $\varepsilon_1$ corresponds to the one-particle excitation without phonon.

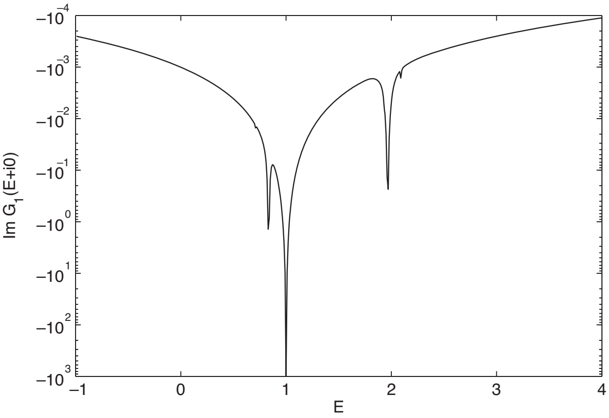

At higher temperatures ($T = 0.05$), more side peaks become noticeable, as the following figure shows:

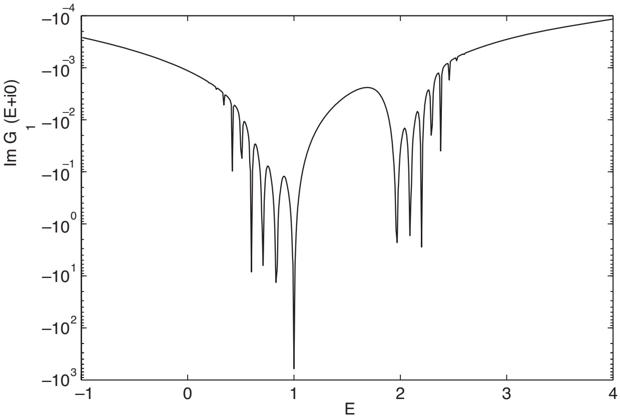

### Problem 7.3, 2-Fermion-Boson Model

The model is more realistic than the model from problem 7.2 in that it takes into account that each electronic transition can take place with both phonon emission and phonon absorption, and that the simple electron density also couples to phonons, ultimately because the displacements are the origin of the perturbation potential and the displacement is a linear combination of phonon creators and annihilators. But now all states are coupled to each other, the problem cannot be reduced to the problem of diagonalizing simple submatrices ($2 * 2$-matrix in problem 7.2). Numerically, it is not much more complex, because the Hilbert space and thus the Hamiltonian operator have the same dimension as in problem 7.2 b. There are only more non-vanishing matrix elements of the Hamiltonian operator with respect to the standard basis. With $M_1, M_2$ there are also more parameters that can be varied. The following lines have to be added to the Matlab code of problem 7.2 to populate the Hamiltonian matrix. All states (occupied by electrons) are coupled if the phonon number differs by 1.

```
h(nphm+n,nphm+n+1)=M1*sqrt(n);h(nphm+n+1,nphm+n)=M1*sqrt(n);
h(2*nphm+n,2*nphm+n+1)=M1*sqrt(n);h(2*nphm+n+1,2*nphm+n)=
    M1*sqrt(n);
h(3*nphm+n,3*nphm+n+1)=M1*sqrt(n);h(3*nphm+n+1,3*nphm+n)=
    M1*sqrt(n);
```

Two results are shown in the following figures, once for $M_2 = 0$, $M_1 = 0.1$ and once for $M_2 = 0.2, M_1 = 0.1$.

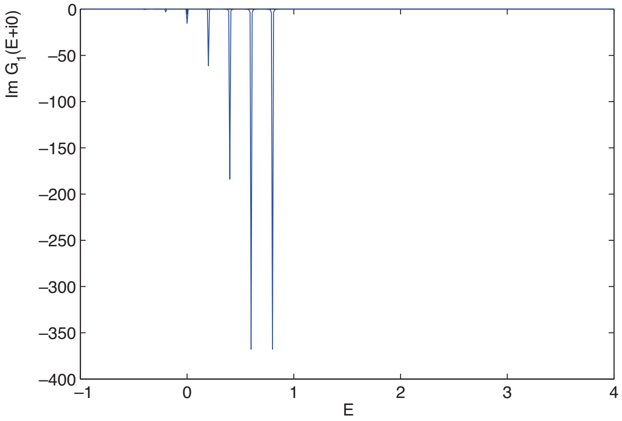

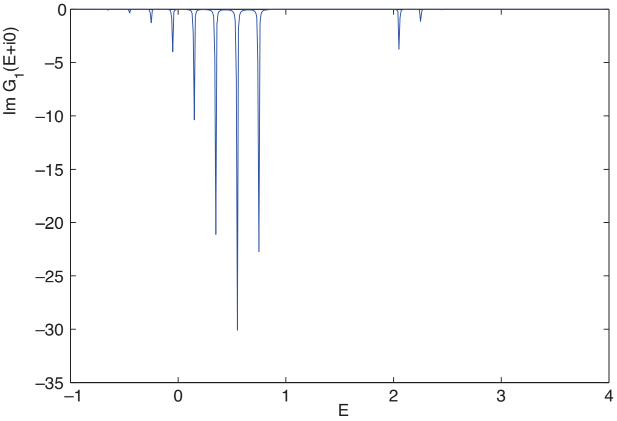

Now one observes in particular on the one hand a polaron shift and on the other hand various phonon satellite peaks.

# References

## General Textbooks on Theoretical Physics

1. W. Nolting: Theoretical Physics 1–9, Springer (2016–2018)
2. T. Fließbach: Lehrbuch zur Theoretischen Physik I–IV, Springer Spektrum bzw. Spektrum Akademischer Verlag (2008–2014)
3. F. Schwabl: Quantum Mechanics, Springer (2007)
4. F. Schwabl: Statistical Mechanics, Springer (2006)

## Textbooks on (experimental) solid state physics

5. C. Kittel : Introduction to Solid State Physics, 8th edition, Wiley (2004)
6. H. Ibach, H. Lüth: Solid-State Physics: An Introduction to Principles of Materials Science, Springer (2009)
7. R. Gross, A. Marx: Festkörperphysik, Oldenbourg-Verlag München (2012) (ISBN: 978-3486712940)

## Textbooks on Theoretical Solid State Physics

8. N. W. Ashcroft, N. D. Mermin: Solid State Physics, Cengage Learning; 1. Edition (1976)
9. O. Madelung: Introduction to Solid-State Theory, Springer Series in Solid-State Sciences, Heidelberg (1978)
10. J. Callaway: Quantum Theory of the Solid State, Student Edition, Academic Press, London 1976
11. H. Haken: Quantum Field Theory of Solids: An Introduction, North-Holland (1976)
12. W. A. Harrison: Solid State Theory, McGraw-Hill 1970 (Dover Publications 2012)
13. W. Jones, N. H. March: Theoretical Solid State Physics, Vol. 1, 2, Dover Publications 1985/86
14. C. Kittel: Quantum Theory of Solids, Wiley, 2nd Revised Edition (1987)
15. J. M. Ziman: Principles of the Theory of Solids, Cambridge University Press; 2 edition (1979)

© The Editor(s) (if applicable) and The Author(s), under exclusive license to
Springer-Verlag GmbH, DE, part of Springer Nature 2023
G. Czycholl, *Solid State Theory, Volume 1*,
https://doi.org/10.1007/978-3-662-66135-2

16. L. Valenta, J. Jäger: Festkörpertheorie. Eine Einführung, Wiley-VCH; 2. Auflage (1997)
17. U. Rößler: Solid State Theory. An Introduction, Springer, Berlin-Heidelberg, 2nd edition (2009)

## On the subject of symmetries and group-theoretical classification of crystals

18. Manfred Böhm: Symmetrien in Festkörpern. Gruppentheoretische Grundlagen und Anwendungen, Wiley-VCH (2002)
19. Wolfgang Ludwig, Claus Falter: Symmetries in Physics. Group Theory Applied to Physical Problems, Springer Series in Solid-State Sciences (1996)

## On the subject of the electronic band structure of solids

20. D. A. Papaconstantopoulos: Handbook of the Band Structure of Elemental Solids, Springer, 2nd ed. (2015)
21. V. A. Gubanov, A. I. Liechtenstein, A. V. Postnikov: Magnetism and the Electronic Structure of Crystals, Springer (1992, 2011)
22. H. L. Skriver: The LMTO Method: Muffin-Tin Orbitals and Electronic Structure, Springer Series in Solid-State Sciences, Vol. 41, (1984, 2011)

## On the topic of density functional theory and local density approximation

23. Eberhard Engel, Reiner M. Dreizler: Density Functional Theory: An Advanced Course, Springer (2011)
24. Helmut Eschrig: The Fundamentals of Density Functional Theory. Teubner Texte zur Physik, Vol. 32, (1996)